The Dissertation Committee for Eric Gregory Ekdale Certifies that this is the approved version of the following dissertation:

VARIATION WITHIN THE BONY LABYRINTH OF MAMMALS

Committee:

Timothy Rowe, Supervisor

Christopher J. Bell

James T. Sprinkle

Matthew W. Colbert

Zhe-Xi Luo

VARIATION WITHIN THE BONY LABYRINTH OF MAMMALS

by

Eric Gregory Ekdale, B.A.; M.S.

Dissertation

Presented to the Faculty of the Graduate School of

The University of Texas at Austin

in Partial Fulfillment

of the Requirements

for the Degree of

Doctor of Philosophy

The University of Texas at Austin

December 2009

Dedication

To my father, Tony, and sister, Joan, for their unyielding support and love.

Epigraph

"It is one of the most beautiful objects with which the anatomist is at all likely to meet…"

-Albert A. Gray (1907, p. 39), upon observing the inner ear of the yellow-faced baboon

Acknowledgements

I give the most sincere thanks to my advisor, Tim Rowe. Besides fulfilling the role of supervisor, Tim has been a mentor, and I look forward to calling him a life-long colleague. Chris Bell, who has been a second advisor to me in many ways, challenged me to think critically at every step of the way, which is a skill that I will carry with me throughout the rest of my career. Matt Colbert introduced me to the exciting world of computed tomography, and Jim Sprinkle, with whom I worked as a teaching assistant across several semesters, expanded my knowledge of paleontology beyond the vertebrate lineage. Zhe-Xi Luo added significant insight to my research through conversations concerning the mammalian ear and early mammal evolution, and he taught me the power of imagery in my dissertation.

The staff of The University of Texas High-Resolution X-ray CT facility (UTCT), an NSF-supported multi-user facility funded by NSF EAR-0345710, participated in hours of data collection and image processing, particularly Matt Colbert, Rich Ketcham, Jessie Maisano, Amy Balanoff, Alison Mote, and Rachel Racicot. All CT data utilized in the dissertation were collected at UTCT, except the data for *Trichechus manatus*, which was scanned for Tim Hullar at Washington University in St. Louis, MO. Funding for the scanning of specimens was provided by the Jackson

School of Geosciences at The University of Texas at Austin, the Texas Academy of Science, and the Paleontological Society.

Access to preexisting CT datasets were provided by Maria Chapala, Ashley Gosselin-Ildari, Tim Hullar, Chris Kirk, Ted Macrini, Mike Novacek, Sentiel Romel, Tim Rowe, Erik Sieffert, Nancy Simmons, and "Digital Morphology" (www.digimorph.org). Additional specimens that were CT scanned were provided by several individuals and institutions, including David Archibald and the members of the Uzbekistan/ Russian/ British/ American/ Canadian joint paleontological expedition, Kyzylkum Desert, Uzbekistan; Mike Novacek of the American Museum of Natural History, New York, NY; Tim Rowe and Lyn Murray of the Vertebrate Paleontology Laboratory, Texas Natural Science Center, Austin, TX; Jeff Saunders and Chris Widga of the Illinois State Museum, Springfield, IL; the Southwest Foundation for Biomedical Research in San Antonio, TX.

In addition to those mentioned above, there are numerous people who must be acknowledged. Surely, there are many names missing from the list. Christian George and Ryan Ewing instilled sanity when it was needed most. Jen Olori, Kerin Claeson, and Heather Ahrens put up with more than they could have ever imagined. Ted Macrini, Gabe Bever, and Chris Jass fostered my early academic ontogeny at UT. Other individuals that positively affected my education include Joey Carlin, Dave Dufeau, Sebastian Egberts, Murat Maga, Jeri Rodgers, Dennis Ruez, Nick Smith, Nina Triche, Jon Wagner, and Patrick Wheatley.

Lastly, my undying gratitude goes to my family, Tony and Joan. Their eternal love and support is the single reason I was able to wake up every morning, and to complete this major life accomplishment.

Variation within the bony labyrinth of mammals

Publication No._____

Eric Gregory Ekdale, Ph.D.

The University of Texas at Austin, 2009

Supervisor: Timothy Rowe

The morphological diversity of the external and internal surfaces of the petrosal bone, which contains the structures of the inner ear, across a broad range of therian mammals is documented, and patterns of variation across taxa are identified. One pattern of variation is the result of ontogenetic changes in the ear region, as described for the external surface morphology of a sample of isolated petrosal bones referred to Proboscidea from Pleistocene deposits in central Texas. The morphology of the aquaeductus Fallopii for passage of the greater petrosal branch of the facial nerve supports an ontogenetic explanation for some variation within the proboscidean sample, and a sequence of ossification surrounding the aquaeductus Fallopii is hypothesized. Further ontogenetic patterns are investigated using digital endocasts of the bony labyrinth (preserved on the internal surfaces of the petrosal) constructed from CT data across a growth series of the opossum *Monodelphis domestica*. Strong correlation between skull length and age is found, but from 27 days after birth onward, there is no correlation with age among most dimensions of the inner ear. Adult dimensions of several of the inner ear structures are achieved before the inner ear is functional in *M.*

domestica. Morphological variation within the inner ear of several eutherian mammals from the Cretaceous of Asia, including zhelestids from the Bissekty Formation of Uzbekistan, is described. The variation within the fossil sample is compared to that observed within extant species of placental mammals, and it is determined that the amount of variation within the Bissekty zhelestid population is within the range of that measured for extant species. Additional evolutionary and physiological patterns preserved within the walls of the bony labyrinth are identified through a high level anatomical comparison of the inner ear cavities across Placentalia as a whole. In particular, features of the inner ear support monophyly of Cetacea, Carnivora, Primatomorpha, and caviomorph Rodentia. The volumetric percentage of the vestibular apparatus (vestibule plus semicircular canals) of aquatic mammals is smaller than that calculated for terrestrial relatives of comparable body size. Thus, aspects of the bony labyrinth are both phylogenetically and physiologically informative.

Table of Contents

List of Tables

List of Figures

CHAPTER 1: INTRODUCTION TO THE EAR OF MAMMALS

The otic (ear) capsule is part of the special sensory system of the nervous system of vertebrates, and one of three major sensory capsules of the head, along with the optic (for vision) and olfactory (for smell) capsules. The function of the ear is two-fold – hearing and balance. The organs of hearing and balance within the ear of vertebrates are tiny structures. In humans, they are contained in cavities totaling only around 165 mm^3 in volume. Despite their small size, the organs of the ear are powerful. It is amazing that such minute structures can cause a myriad of problems from tinnitus to motion sickness to a general lack of balance. These reasons may explain why human beings are interested in the physiology and morphology of the ear region.

GROSS ANATOMY OF THE MAMMALIAN EAR

The generalized ear of mammals is partitioned into three sections – the outer, middle, and inner ears. The outer ear consists of the external pinna, which is prominent in most mammals, and it leads to the external auditory meatus and associated canal. The boundary between the external and middle ear is the tympanic membrane. The middle ear (tympanic) cavity is bounded dorsally by cranial elements, particularly the petrosal bone, and ventrally by an auditory bulla, which typically is ossified in extant mammals (see van der Klauuw, 1931; Novacek, 1977). The middle ear ossicles (malleus, incus, and stapes) are contained within the tympanic cavity, and they form a chain extending between the tympanic membrane and petrosal. The stapes articulates with a window in the petrosal called the fenestra vestibuli, which serves as one of two points of communication between the middle and inner ear cavities. The other opening is the fenestra cochleae, which is covered by a secondary tympanic membrane that accommodates expansion of

the inner ear space during changes in pressure. The petrosal itself separates the majority of the tympanic cavity from the cranial cavity.

The inner ear consists of a set of interconnected spaces within the petrosal known as the bony labyrinth (Figure 1.1), which contains a series of soft-tissue sacs and ducts, known as the membranous labyrinth. The membranous labyrinth is separated into an inferior division that includes the cochlear duct (containing the spiral organ of hearing) and saccule of the vestibule (containing receptors sensitive to linear motion), and a superior division that includes the utricle of the vestibule, the anterior, lateral, and posterior semicircular ducts and ampullae, and the common crus between the anterior and posterior ducts (all of which are involved with detecting rotational movement of the head). The osseous semicircular canals and cochlea of the bony labyrinth mirror the shape of the membranous ducts within, although the bony canals may not accurately reflect the size of the ducts (Curthoys et al., 1977b).

The bony cochlear canal is divided into the scala tympani that communicates with the fenestra cochleae, and the scala vestibuli that terminates at the fenestra vestibuli. The division is formed by a bony primary spiral lamina that curves along the modiolus (central bony pillar around which the cochlea coils) on the axial wall of the cochlea (Figure 1.1C-D). A secondary lamina often mirrors the primary lamina for a short distance on the opposing (radial) wall of the cochlea. The two laminae are connected by the basilar membrane (the laminae do not contact each other directly), upon which the spiral organ of hearing sits. The basilar membrane defines the tympanic wall of the membranous cochlear duct (also known as the scala media). The vestibular membrane crosses the width of the scala vestibuli to complete the cochlear duct at its vestibular edge. A small opening known as the helicotrema is situated at the apex of the cochlea, and it serves as a connection between the scalae tympani and vestibuli. The cochlear duct

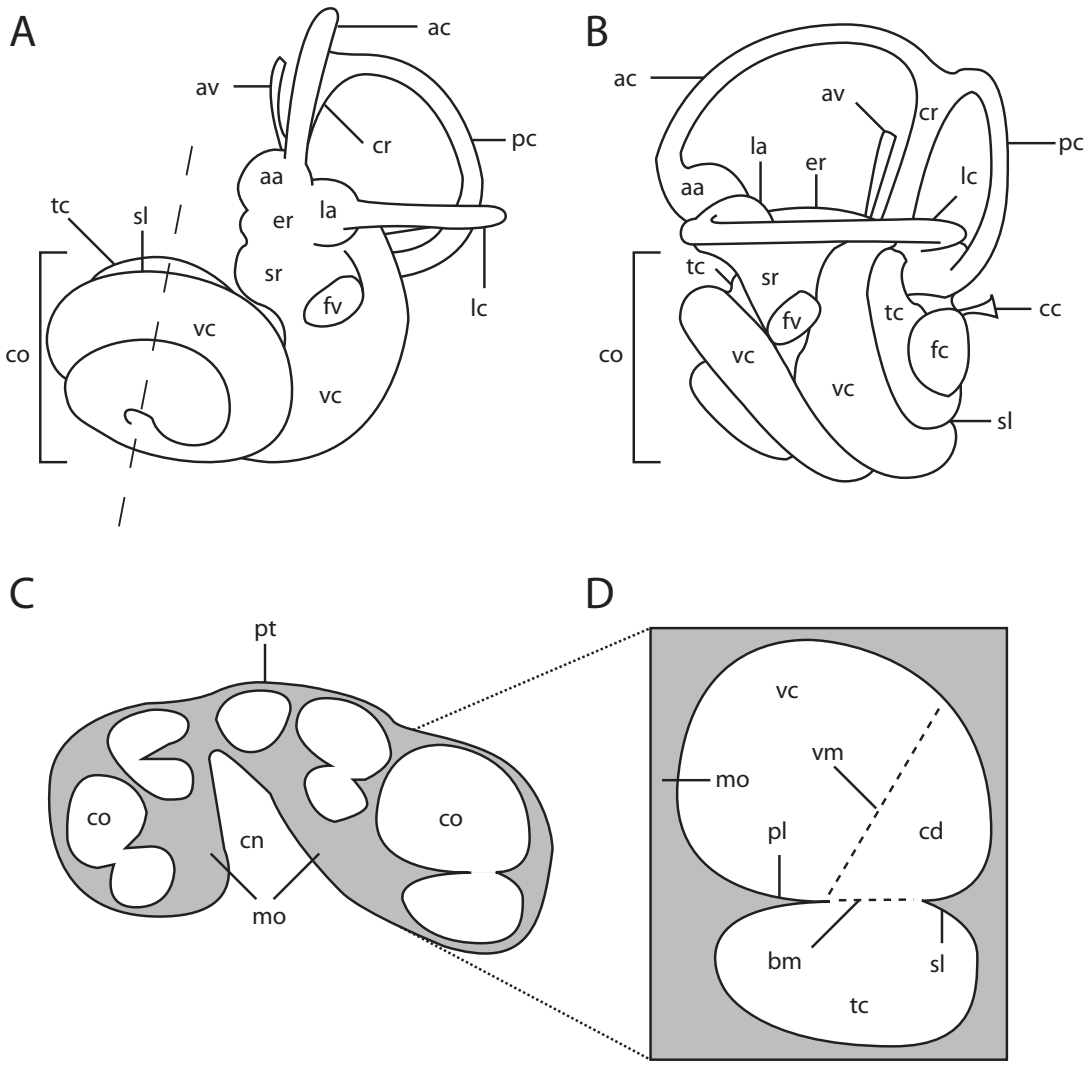

FIGURE 1.1. Gross anatomy of the inner ear. **A**, bony labyrinth in anterior view (dorsal towards top, medial towards left), where dashed line represents a slice through the cochlea presented in C of this figure; **B**, bony labyrinth in lateral view (dorsal towards top, anterior towards left); **C**, cross-section through entire cochlea (apex towards top) as indicated by dashed line in A; **D**, cross-section through cochlear canal and cochlear duct. **Abbreviations**: **aa**, anterior ampulla; **ac**, anterior semicircular canal; **av**, aqueduct of the vestibule (passage of endolymphatic duct); **bm**, basilar membrane; **cc**, canaliculus cochleae (passage of perilymphatic duct); **cd**, cochlear duct; **cn**, canal for cranial nerve VIII, within modiolus (axis); **co**, cochlea; **cr**, common crus; **er**, elliptical recess; **fc**, fenestra cochleae; **fv**, fenestra vestibuli; **la**, lateral ampulla; **lc**, lateral semicircular canal; **mo**, modiolus; **pa**, posterior ampulla; **pc**, posterior semicircular canal; **pl**, primary bony lamina; **pt**, petrosal bone; **sl**, secondary bony lamina; **sr**, spherical recess; **tc**, scala tympani of the cochlea; **vc**, scala vestibuli of the cochlea; **vm**, vestibular membrane.

is filled with endolymph, and the surrounding space, which includes both the scala tympani and scala vestibuli, is filled with perilymph. The perilymphatic duct exits the inner ear near the fenestra cochleae through a bony passage known as the canaliculus cochleae.

The bony vestibule is divided into the spherical recess inferiorly and the elliptical recess superiorly. The recesses correspond loosely to the saccule (spherical recess) and utricle plus semicircular ducts (elliptical recess), but the shapes of the membranous sacs are preserved minimally within the bony vestibule. The saccule, utricle, and semicircular ducts are filled with endolymph (exchange occurs between the cochlea and saccule at their junction), and perilymph fills the remainder of the space. Varying amounts of perilymph surround the semicircular ducts in different species (Gray, 1906, 1907, 1908), and the endolymphatic duct exits the inner ear from the medial edge of the labyrinths, passing through the bone and opening into the cranial cavity.

BIOLOGICAL SIGNIFICANCE OF THE EAR

Audition was the first function of the ear of humans to be recognized by early anatomists. The role of the ear in hearing was deduced from injuries to the temporal region of the head in ancient Egypt, as recorded in the Edwin Smith Surgical Papyrus (Hawkins, 2004), but the specific role that the cochlea itself played in the sense of hearing was not recognized until the mid 17th century AD, as reported by physician Thomas Willis (Hawkins, 2004). Sensations of orientation were attributed to the semicircular canals and vestibular system in the late 19th century (Dercum, 1879), and functional similarities of the canals and the lateral line system in fishes and amphibians were recognized at this time as well (Lee, 1898). Further advancements were made from

the middle of the 19th through early 20th centuries in comparative anatomy of broad samples of vertebrate species through dissections and histological sectioning (Retzius, 1884), corrosion casting (Hyrtl, 1845), and extraction of the intact membranous labyrinth from the surrounding bone (Gray, 1903, 1905, 1907), all of which added significant contributions to our understanding of the structure and function of the inner ear.

From a functional standpoint alone, the auditory and vestibular structures are significant agents in vertebrate biology. Hearing certainly played an important role in early tetrapod evolution, where newly terrestrial animals moved from detecting water-borne to air-borne sound waves (Manley, 1972; Clack, 2002). In the case of early mammals, which were hypothesized to be nocturnal (Kielan-Jaworowska et al., 2004), a reliance on non-visual senses to navigate the Mesozoic world would have been necessary. The hearing capabilities within Mammalia are varied, and mammals can hear in a great range of frequencies. Proboscideans are sensitive to very low frequencies (Payne et al., 1986; Poole et al., 1988), and cetaceans as a group can hear in both subsonic and ultrasonic ranges (Ketten, 1997). Microchiropteran bats use ultrasonic echolocation during prey capture (Simmons et al., 1979), and even tenrecs (Gould, 1965) and soricid lipotyphlans (Tomasi, 1979) are known to vocalize using ultrasonic noises.

Balance, and closely related equilibrium, was an important sense in vertebrate history as well. When tetrapods left an aquatic environment for land, they faced unique stability difficulties (Alexander, 2002), and the skeletons of tetrapods were well adapted to the new terrestrial lifestyle (Shubin et al., 2004; Boisvert, 2005). In fact, the vestibular end organs are similar in structure to, and likely derived from, the lateral line system of early gnathostomes (Lee, 1898). Balance is an integral aspect of vertebrate locomotion, and a broad range of mobility and agility is observed within Mammalia, from sure-footed

gazelles fleeing a sprinting cheetah, to sluggish koalas resting in eucalyptus trees (see Spoor et al., 2007).

However, the physiological capability of the inner ear is not the only significance possessed by the otic region. The potential that the inner ear region could be used to infer the evolutionary relationships of animals was not lost on late 19th and early 20th century otologists, particularly Albert Gray, who stated that "…the labyrinth must, of course, have some value when considering these relationships, just as have the teeth, the skeleton, and other parts of the body" (Gray, 1907, p. 2-3). This observation led to several systematic surveys of the external surface of the petrosal and middle ear cavities across a range of mammal taxa (Van Kampen, 1904; van der Klaauw, 1931; MacPhee, 1981), but broad phylogenetic surveys of the bony labyrinth are lacking.

Beyond the functional and phylogenetic significance of the ear region in extant taxa, the petrosal bone serves as a resource in understanding the phylogenetic relationships among extinct mammals. The petrosals are more robust and dense than other cranial elements, and the otic region is the sensory system that is best preserved in the fossil record, especially for mammals and their fossil relatives (e.g., Archibald, 1979; Quiroga, 1979; Miao, 1988). Therefore, the majority of sensory physiology information of fossil vertebrates revolves around the ear region, and the morphology of the inner ear is used to make functional (Spoor et al., 1994; Clack, 2002; Witmer et al., 2003; Alonso et al., 2004; Clarke, 2005) and phylogenetic (Hunt, 1987; Luo and Gingerich, 1999; Ekdale et al., 2004) interpretations of fossil taxa.

Given the functional and phylogenetic significance of the ear region, it is not surprising that the otic region is one of the most studied anatomical complexes. However, one aspect of the ear region that often is neglected involves gross morphological variation of the system (exceptions include the work of Caix and Outrequin, 1979; Muren et al.,

1986; Dimopolous and Muren, 1990). Observed variation can be the result of many factors. Perhaps the most obvious influence is physiology. Differently shaped semicircular canals may indicate different lifestyle habits (Georgi and Sipla, 2008). But other phenomena also may play a role, such as ontogeny, which has had a light treatment in published literature (Ryals et al., 1984; Jeffery and Spoor, 2004; Sánchez-Villagra and Schmelzle, 2007).

A final factor that has received little attention is the phylogenetic significance of the bony labyrinth, which can be presumed given that the external surface of the petrosal is informative. Potential phylogenetically useful features within the cochlea and vestibule were previously identified (Meng and Fox, 1995; Spoor and Zonneveld, 1998), but few broad taxonomic surveys have been completed with the sole intent of determining phylogenetic relationships based on morphology of the inner ear. The following chapters of this dissertation present the results of my investigations into the sources of variation observed within the inner ear cavities of mammals, ultimately placing the anatomy of the bony labyrinth into a phylogenetic context.

DISSERTATION OVERVIEW

Chapter 2 is focused on a description of an unparalleled sample of isolated petrosal bones referred to extinct elephantoid proboscideans from a Pleistocene cave deposit in central Texas. The inner ear of extinct elephantids is described for the first time, and variation observed on the external surface of the petrosal across the sample is discussed, namely completion of the floor of the bony aquaeductus Fallopii for branches of the facial nerve. The variation observed within the aqueductus Fallopii can be

explained by ontogenetic changes in the ear region, and an ossification sequence for the bone surrounding the facial nerve through the petrosal is identified in this fossil sample.

An investigation into morphological changes in the walls of the inner ear forming the bony labyrinth over maturation of the otic region in the extant marsupial *Monodelphis domestica* is provided in Chapter 3. A few dimensions of the semicircular canals are correlated to the maturity of an individual, but the majority of features examined are independent of age. The results of Chapter 3, along with published ontogenetic sequences of the otic region of humans (Jeffrey and Spoor, 2004) and rabbits (Hoyte, 1961) signify that researchers utilizing the anatomy of the inner ear probably do not need to be concerned with the maturity of an individual when using the bony labyrinth in phylogenetic or physiological studies (as long as the walls of the bony labyrinth are fully ossified).

Chapter 4 is a comparison of the bony labyrinths of fossil eutherian mammals from the Cretaceous, particularly zhelestids from Uzbekistan. Phylogenetic analyses place a monophyletic clade of zhelestid taxa from the Bissekty Formation either inside or outside crown Placentalia, and the position of the Bissekty zhelestid grouping on the mammalian tree plays a role in the timing of the origin of placentals. The morphology of the bony labyrinth of the Bissekty zhelestids is described in Chapter 4, contributing an essential body of knowledge to what is known about these taxonomically important mammals. In addition, variation within the fossil sample is identified and quantified. The degree of variation observed in the zhelestid sample is consistent with that observed in single extant mammal species. This result indicates that certain features thought to be important in phylogenetic and functional interpretations utilizing the ear region do not vary much within a species or among closely related taxa.

The final section, Chapter 5, includes a broad scale comparison of the bony labyrinths of placental mammals, where variation is observed and described across the sample. Correlations between dimensions of the inner ear are identified, as well as potential relationships between the morphology of the bony labyrinth and function. For example, the ratio of the radius of the arc formed by a semicircular canal to the body mass of the individual is significantly smaller in aquatic mammals than it is in their terrestrial relatives. In particular, the proportion that the vestibule and associated semicircular canals contributes to the overall volume of the bony labyrinth is distinctly smaller in Cetacea than that calculated for any other mammal. Although a reduced vestibular system in cetaceans may correlate to a fully aquatic lifestyle, the feature is reconstructed as a synapomorphy for Cetacea.

A secondary common crus between the lateral and posterior semicircular canals is ancestral for Theria, but lost in Placentalia (although a secondary crus is present in a small number of taxa). The cochlea of most crown placentals coils to a greater degree than that measured for Cretaceous eutherians (including the zhelestids from the Bissekty Formation of Uzbekistan), as is exemplified by the four turns observed in the cochlea of the guinea pig, *Cavia porcellus* (as opposed to the single coil observed in *Zalambdalestes* from the Cretaceous of Mongolia). In fact, the conical shape of the highly-coiled cochlea of the guinea pig is an attribute that only is observed within the inner ears of caviomorph rodents.

CHAPTER 2: MORPHOLOGY AND VARIATION IN THE PETROSAL OF EXTINCT ELEPHANTOIDEA (PROBOSCIDEA) FROM CENTRAL TEXAS

ABSTRACT

An unparalleled sample of isolated petrosal bones assigned to elephantoid Proboscidea was recovered from Pleistocene deposits in Friesenhahn Cave, Bexar County, TX. Morphology of the middle and inner ear of the elephantoids is described and variation within the sample is identified. The variations observed include the stapedial ratio, completeness of the aquaeductus Fallopii, and connection of the crista interfenestralis to the tympanohyal on the posterior aspect of the petrosal to form a foramen for passage of the stapedius muscle. The observed morphological differences may be the result of the taphonomic history of the specimens or else taxonomic differences as two species of proboscidean have been identified in the deposits of Friesenhahn Cave, but there are no unambiguous characters to distinguish between them. However, the morphology of the aquaeductus Fallopii supports an ontogenetic explanation for some variation, and a sequence of ossification surrounding the aquaeductus Fallopii, from the anterior end of the canal to the posterior, is hypothesized. A broad range of stapedial ratios is calculated across the sample, and this might have dramatic effect on how these characters apply to mammalian systematics.

INTRODUCTION

The otic region of mammals as preserved on and within the petrosal bone garners a great deal of interest in vertebrate morphology and physiology. The ear is one of the special sensory organs of the nervous system, and the structures of the inner ear serve two

functions: hearing and balance. The morphology of the bony walls of the middle ear cavity, which is preserved on the external surface of the petrosal, is phylogenetically informative for many mammal groups (e.g., Cifelli, 1982; Wible and Novacek, 1988; Hunt, 1989; Geisler and Luo, 1996), including elephants and their closest relatives (Fischer and Tassy, 1993). Furthermore, the petrosal bones are dense and robust relative to the rest of the skull, and they are readily preserved in the fossil record. Petrosal bones contribute significantly to our knowledge of Mesozoic mammal faunas, and the auditory region of early mammals and their relatives are among the best-preserved and most studied skeletal elements (Olson, 1944; Archibald, 1979; Quiroga, 1979; Miao, 1988). Because of this, the ear region provides paleontologists with many clues to the biology of early mammals and their relatives (Graybeal et al., 1989; Meng and Wyss, 1995).

Although the petrosal contribution to the middle ear cavity is well-studied and is used in a myriad of phylogenetic studies, thorough discussions of intraspecific morphological variation in the system within a species are lacking in paleontological literature (some variation discussed in Ekdale et al., 2004). Studies focusing upon variation within the ear region largely are restricted to biomedical studies of the physiology of the inner ear (e.g., Caix and Outrequin, 1979; Muren et al., 1986; Clark and Smith, 1993). Ontogeny, or the development of an individual from conception to ultimate death, is a significant source of variation in chordate anatomy (e.g., Wiens et al., 2005), and the ontogenetic development of the ear region has been described for several mammals (McCrady, 1938; Jeffrey and Spoor, 2004). Although ontogenetic variation can cause problems in phylogenetic analyses (Brinkman, 1988; Tykoski, 2005), ontogeny rarely is considered when scoring characters for phylogenetic analysis (see Brochu, 1996; Colbert and Rowe, 2008).

The purpose of the present study is two-fold. The first goal is to provide a thorough description of the ear region of the elephantoid proboscideans, which is lacking in the scientific literature, and to compare the ear of elephantoids to that of other proboscideans. Second, the sample provides a unique opportunity to study variation within the middle ear region of a population of extant proboscideans. In fact, very few studies have discussed variation within the middle ear region of any mammal species. The comparative morphology of mammoth and mastodon petrosals is discussed, and a hypothesized ontogenetic sequence is identified in the sample through an investigation of the variation expressed by the bones. The present discussion is the first account of an ontogenetic sequence identified for any fossil petrosal sample.

MATERIALS AND METHODS

Formation and history of Friesenhahn Cave

The examined petrosals were collected from Friesenhahn Cave in Central Texas (Graham, 1976). The cave, which is located north of San Antonio, Texas (Bexar County) on the eastern edge of the Edward's Plateau, is one of at least 37 caves on the plateau preserving Pleistocene faunas (Lundelius and Collins, 1999). The limestones of the Edward's Plateau are conducive to cave formation, and the caves are important from a paleontological perspective (Graham, 1976). Caves in general provide a sheltered environment that facilitates fossilization of vertebrate bones (George et al., 2007), and Friesenhahn Cave is the most studied cave preserving Pleistocene faunas on the Edward's Plateau, and the first cave of its kind in Central Texas to undergo a thorough excavation (see Evans, 1961).

The modern entrance of Friesenhahn Cave is a vertical shaft that formed around 10,000 years ago. An earlier entrance that was open 17,000-20,000 years ago, allowed for the rapid accumulation of vertebrate remains, including proboscideans (Graham, 1976). The largest bodied vertebrates recovered from the cave are extinct elephantoid proboscideans that are identifiable as *Mammut americanum* and *Mammuthus colombi* based on dentition (Graham, 1976). The Elephantoidea (group containing the ancestor of *Mammuthus* and *Mammut* and all of its descendents; Lambert and Shoshani, 1998) are represented in the cave by cranial (including isolated petrosals), dental, and postcranial material, with the majority of material assigned to *Mammuthus* by Graham (1976). An ontogenetic sequence of individuals represented by teeth, following the methods of Laws (1966), was recognized by Graham (1976). Given the paucity of adult proboscidean specimens in the cave (the oldest individual was estimated at four years old upon death; Graham, 1976), it is hypothesized that the carcasses of juvenile mammoths likely were dragged to the cave by carnivoran predators (Graham, 1976). That hypothesis is supported by large carnivoran tooth marks (attributed to *Homotherium serum*; Meade, 1961) observed on the postcrania of large herbivores found in the cave.

Petrosal specimens and identification

Sixty-five isolated petrosal bones assigned to *Mammuthus* by Graham (1976) are among the proboscidean specimens collected from Friesenhahn Cave. All of the petrosals are housed at the Vertebrate Paleontology Laboratory of the Texas Natural Science Center (TMM) in Austin, TX. The sample includes 37 right petrosals and 28 left petrosals, indicating a minimum number of 37 individuals. In all, the collection of petrosals provides an unprecedented opportunity to study the morphology of the ear

region of extinct proboscideans, upon which only a few studies have been focused (see Court, 1992b).

No criteria were given for the initial referral of the petrosals to Proboscidea (see identifications by Graham, 1976), although the decision to do so likely was based on the size of the bones. The petrosals are large, and because mammoths and mastodons are the largest bodied mammals recovered from the cave, it is reasonable to assume that the petrosals are in fact from proboscideans. Further examination of the specimens confirms the initial assessment through the identification of an apomorphic feature on the petrosals. The fenestra cochleae is confluent with the canaliculus cochleae to form a secondarily undivided perilymphatic foramen in all of the specimens examined here (Figure 2.1). Among Quaternary mammals (both extant and extinct), this feature is only observed in proboscideans and sirenians (Fischer, 1990; Court, 1994). Because sirenian material has never been recovered from any Pleistocene cave deposit on the Edward's Plateau (owing to the complete lack of Pleistocene marine deposits on the plateau), the referral of the petrosals to Proboscidea is accepted.

Within Proboscidea, the petrosals were referred to *Mammuthus* by Graham (1976). Again, no criteria were provided, but the referral likely was made based on the overabundance of *Mammuthus* material versus *Mammut*. Around 97% of proboscidean teeth from the cave (500 out of 513) were assigned to *Mammuthus* by Graham, but it is possible that one or more of the petrosals represent *Mammut*. In fact, by simple probability, two petrosals out of the sample should be *Mammut*. Based on the 13 teeth that Graham assigned to *Mammut*, there is a minimum number of three mastodon individuals, and a maximum number of 13.

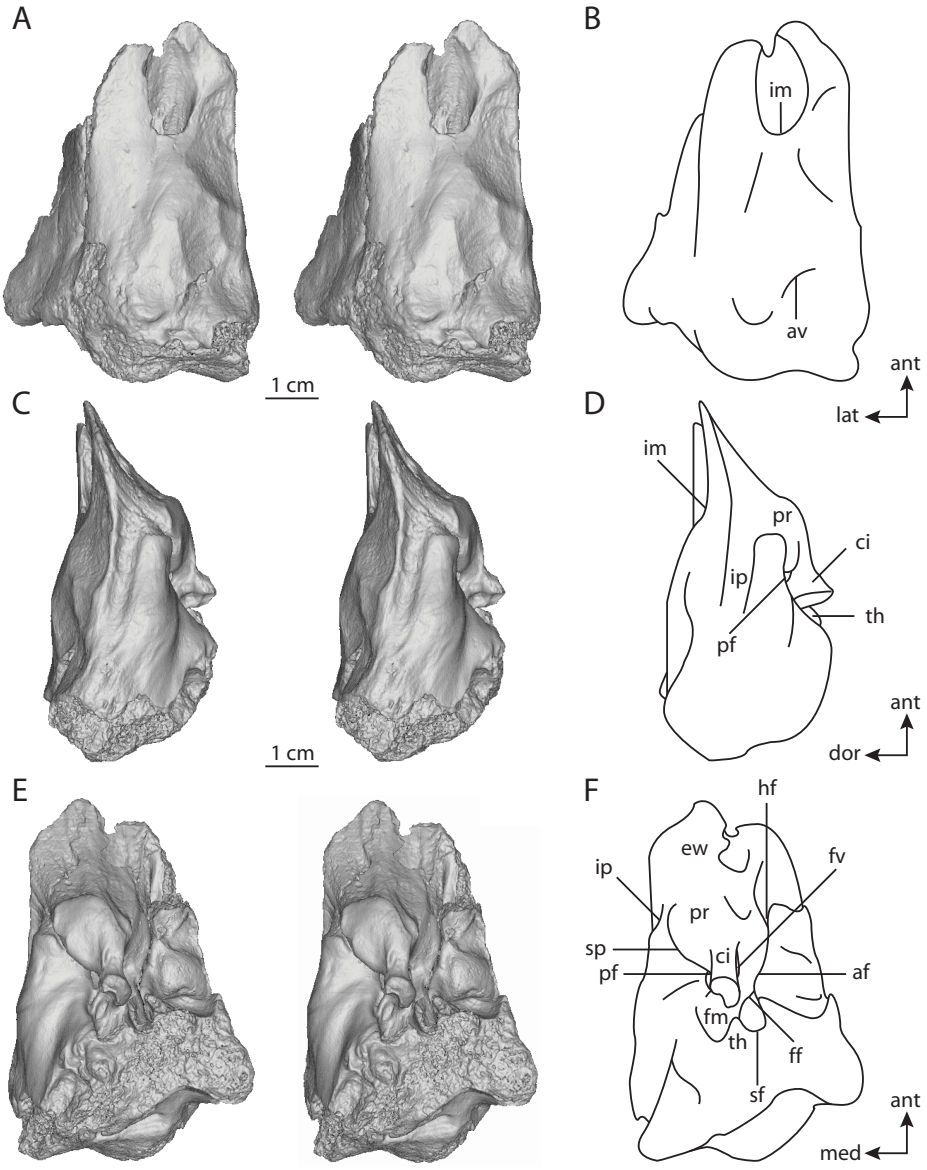

FIGURE 2.1. Three-dimensional CT reconstructions and labeled line drawings of petrosal of elephantoid from Friesenhahn Cave (TMM 933-950). **A-B**, cerebellar view; **C-D**, medial view; **E-F**, tympanic view. Abbreviations: **af** – floor of aqueductus Fallopii; **ant** – anterior; **av** – aquaeductus vestibuli; **ci** – crista interfenestralis; **dor** – dorsal; **ew** – epitympanic wing; **ff** – foramen faciale; **fm** – fossa musculus minor; **fv** – fenestra vestibuli; **hf** – hiaus Fallopii; **im** – internal auditory meatus; **ip** – sulcus for inferior petrosal sinus; **lat** – lateral; **med** – medial; **pf** – perilymphatic foramen; **pr** – promontorium; **sf** – sulcus facialis; **sp** – sulcus for perilymphatic duct; **th** – tympanohyal.

Unfortunately, there is no published information that discusses the anatomical differences between mammoth and mastodon petrosals, if any differences exist. An attempt is made here by comparing a sample of definitive *Mammut* petrosals collected from Pleistocene deposits from Boney Spring (BS) in the Western Ozark Highland, Missouri (housed at Illinois State Museum in Springfield, IL). Only proboscideans referred to *Mammut americanum* have been recovered from Boney Spring, so the taxonomic identity of this petrosal sample is more certain than that collected from Friesenhahn Cave. As is observed for Friesenhahn Cave, a growth series of proboscideans is identifiable in the fossil sample from Boney Spring (Saunders, 1977). Although the examination of the Friesenhahn Cave and Boney Spring samples is far from thorough, the comparison is a first attempt at investigating the ear regions of mammoths and mastodons, which may allow a finer identification of the petrosals from Friesenhahn Cave or other localities from which both mammoths and mastodons are known.

Computed tomography and measurement methods

The morphology of the bony labyrinth of the inner ear contained within the petrosal is described for the first time for Elephantoidea. The bony labyrinth of the inner ear is contained within cavities entirely surrounded by the petrosal bone itself. In order to observe the internal auditory structures, the surrounding bone must be removed. This is either accomplished through physical destruction of the bone, or it can be accomplished digitally through high-resolution X-ray computed tomography (CT), as was performed here. The only other data from the inner ear of extinct proboscideans comes from two Eocene taxa, *Moeritherium* and *Numidotherium* (Court, 1992b). Internal auditory structures of an elephantoid from Friesenhahn Cave were imaged using high resolution X-ray computed tomography (CT) at the University of Texas High-Resolution CT facility

(UTCT). A single petrosal (TMM 933-950) was CT scanned, and a digital endocast of the bony labyrinth of the inner ear was constructed in Amira 3.1 © computer software. The field of reconstruction for the CT scan was 53 mm, and each CT slice has a resolution of 1024 by 1024 pixels. The interpixel spacing (distance between pixels) is 0.052 mm, and the interslice spacing (between slices) is 0.13 mm. A total of 275 slices were collected through the petrosal. The digital endocast was compared to published reports of the inner ear of other proboscideans.

Anatomical terminology follows MacPhee (1981) for external petrosal anatomy, and Sisson and Grossman (1938) and Evans (1993) for internal anatomy. Methodologies for measurements of the inner ear follow Spoor and Zonneveld (1995) mostly, although two specific measurements, the stapedial ratio and coiling of the cochlea, follow Segall (1970) and a modified method of Geisler and Luo (1996) respectively. The stapedial ratio is an index of the shape of the footplate of the stapes that is calculated as the greatest length of the footplate divided by the greatest width perpendicular to the length. In the absence of the stapes, dimensions of the fenestra vestibuli were used as a proxy here (following Segall, 1970).

The method employed to obtain the number of turns completed by the cochlea follows the method utilized by Geisler and Luo (1996), and is comparable to that conceived by West (1985). Both methods orient the cochlea so the field of view points down the axis of rotation. A line is drawn from the center of the axis of rotation to a secondary landmark near the basal end of the cochlea, and the number of times that the cochlea crosses this line is counted as one half turn. An additional angle of rotation is added to this value if the cochlea passes beyond a half turn. The methods differ in their choice of a secondary landmark. One landmark that often is used is the point of inflection between the cochlea and vestibule (West, 1985). Although that method commonly is used

(e.g., Meng and Fox, 1995), the landmark at the inflection is arbitrary and difficult to locate. A different landmark is located at the proximal end of the basilar membrane (Geisler and Luo, 1996). The organ of hearing, which serves as the functional unit of the cochlea, rests on the basilar membrane in life. I used the proximal end of the basilar membrane as a landmark because it is more biologically appropriate (given the functional importance of the basilar membrane) and less ambiguous than the former (utilized by West, 1985).

ANATOMICAL OBSERVATIONS OF FRIESENHAHN CAVE PETROSALS

All of the petrosals from Friesenhahn Cave examined are isolated without any evidence of a tympanic bulla, nor any other cranial associations. Because of this, the orientations described here are only approximate. In general, the cerebellar (intercranial) surface of the petrosal faces dorsomedially and the tympanic surface is oriented ventrally when the petrosal is articulated with the rest of the skull (MacIntyre, 1972).

Cerebellar surface of petrosal

The cerebellar surface is slightly convex in all of the specimens, giving the petrosal an almost tubular appearance in this view (Figure 2.1A). There is no evidence of a subarcuate fossa, which holds a parafloccular lobe of the cerebellum in life in most mammals. Rather, the petrosal is inflated in the area where the fossa is located in other taxa. The opening of the internal auditory meatus is oriented towards the anterior apex of the petrosal rather than dorsomedially as is the case for most non-proboscidean mammals, and the opening is parallel to the long axis of the bone. The sulcus for the inferior petrosal sinus extends along the medial edge of the petrosal in an anterior-posterior direction (Figure 2.1A-2.1B). The fissure-like opening for the aquaeductus

vestibuli is positioned at the posterior end of the petrosal, posterolateral and dorsal to the posterior terminus of the sulcus for the inferior petrosal sinus.

Tympanic surface of petrosal

The anterior aspect of the tympanic surface is known as the promontorium, which houses the cochlea internally (Figure 2.1C). The bulbous promontorium is irregularly shaped with a distinct depression anteromedially. A broad epitympanic wing extends anteriorly from the promontorium. No sulci for the internal carotid or stapedial arteries are observed on the promontorium of any of the petrosals from Friesenhahn Cave.

The perilymphatic foramen (joining of the fenestra cochleae and canaliculus cochleae) is an irregular, pear-shaped opening on the posteromedial edge of the promontorium. The medial aspect of this opening leads to a depression that likely accommodated the perilymphatic duct in life.

The fenestra vestibuli on the posterolateral edge of the promontorium is round to oval in shape. Two specimens (TMM 933-950 and 933-951) preserve the footplate of the stapes was preserved for. The footplate of TMM 933-951 is preserved in articulation within the fenestra vestibuli, but the structure had come loose in TMM 933-950 and fallen through the fenestra and into the inner ear cavities. The footplate of TMM 933-950 was carefully removed with forceps and examined (Figure 2.2). The stapedial ratio of the stapes itself is slightly less than the ratio calculated for the fenestra vestibuli on the same specimen (1.7 versus 1.8). The range of stapedial ratios among the full petrosal sample is 1.4-2.1 (Table 1), with an average of 1.8 and a standard deviation of 0.1.

The footplate of the stapes of TMM 933-950 is concave outwards towards the crura, which are broken, and only their attachments to the footplate remain. Because there are bases for two crura, a stapedial foramen would have been present in a complete

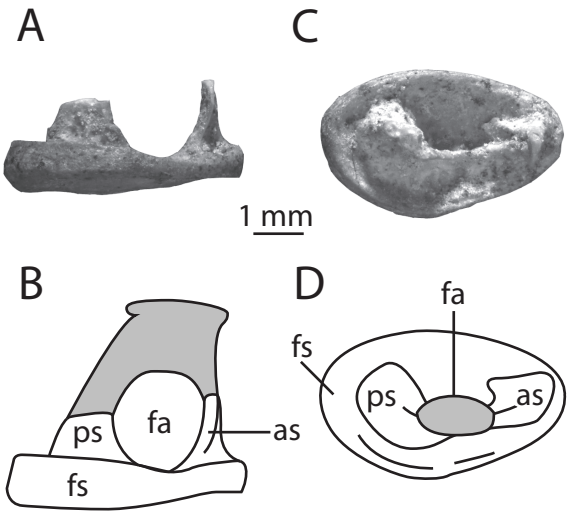

FIGURE 2.2. Photograph and line drawing if stapes of elephantoid from Friesenhahn Cave (TMM 933-950). **A-B**, lateral view, shaded area reconstructed in B; **C-D**, map view, shaded area reconstructed in D. Abbreviations: **as** – anterior crus of stapes; **fs** – footplate of stapes; **ps** – posterior crus of stapes.

TABLE 2.1. Variation observed among elephantoid petrosals from Friesenhahn Cave (Bexar County, Texas).

Specimen No.	Aquaeductus Fallopii	Stapedius Muscle Foramen	Stapedial Ratio
TMM 933-12	partial	-	1.7
TMM 933-69	-	-	1.6
TMM 933-166	partial	incomplete	1.6
TMM 933-414	-	complete	1.9
TMM 933-415	-	-	2.0
TMM 933-416	-	complete	1.8
TMM 933-507	partial	-	1.8
TMM 933-508	partial	-	1.9
TMM 933-548	partial	-	1.9
TMM 933-746	-	-	1.6
TMM 933-747	-	-	1.7
TMM 933-950	complete	-	1.8
TMM 933-951	complete	-	1.9
TMM 933-953	-	-	1.8
TMM 933-954	-	-	1.7
TMM 933-955	complete	complete	1.6
TMM 933-956	-	-	1.7
TMM 933-957	complete	-	2.1
TMM 933-959	-	-	1.7
TMM 933-1032	complete	incomplete	1.9
TMM 933-1033	-	-	2.0
TMM 933-1034	-	-	1.6
TMM 933-1035	partial	-	1.9
TMM 933-1036	complete	-	1.7
TMM 933-1078	-	-	1.9
TMM 933-1317	partial	-	1.7
TMM 933-1389	-	-	1.9
TMM 933-1489	partial	complete	1.9
TMM 933-1533	complete	-	1.7
TMM 933-1677	-	-	1.6
TMM 933-1678	-	-	1.7
TMM 933-1679	-	-	1.7
TMM 933-2032	-	-	1.8
TMM 933-2043	-	-	1.7
TMM 933-2044	-	-	1.9
TMM 933-2223	-	-	1.6
TMM 933-2248	-	-	1.6
TMM 933-2249	complete	-	1.4

TABLE 2.1. Continued.

Specimen No.	Aquaeductus Fallopii	Stapedius Muscle Foramen	Stapedial Ratio
TMM 933-2323	partial	complete	1.8
TMM 933-2414	partial	-	1.7
TMM 933-2415	-	-	1.8
TMM 933-2634	complete	complete	1.6
TMM 933-2635	-	-	1.7
TMM 933-2637	-	-	1.6
TMM 933-2638	-	-	1.8
TMM 933-2918	-	-	1.5
TMM 933-2920	-	-	1.8
TMM 933-2940	partial	-	1.9
TMM 933-3467	-	-	2.0
TMM 933-3468	-	-	1.7
TMM 933-3838	-	-	1.7
TMM 933-5732	-	-	2.0
TMM 933-5724	-	-	1.6
TMM 933-5733	-	-	1.7
TMM 933-5735	-	complete	1.6
TMM 933-5866	-	-	2.0
Average	-	-	1.8
Standard Deviation	-	-	0.1

stapes. The base of one crus is more robust than the other, and the overall shape of the footplate is not a perfect ellipse, but rather is egg-shaped, although it is more or less symmetrical along its long axis. When compared to the shape of the fenestra vestibuli, the narrow end of the footplate is the anteriormost end, with the robust crus directed posteriorly.

The aquaeductus Fallopii, a canal for transmission of branches of the facial nerve (cranial nerve VII), is positioned lateral to the promontorium. The ventral surface of the aquaeductus bears a distinct fissure where the medial and lateral walls of the floor meet in several specimens (Figs. 1.3, 3; Table 2.1). The ventral floor of the canal is incomplete with a gap between the medial and lateral aspects extending the entire length of the canal in most of the specimens (Figure 2.3A). The canal is partially complete in several specimens, having a noticeable gap between the posterior aspect of the medial and lateral contributions of the canal, but with the anterior end fused (Figure 2.3B). Many of these specimens are damaged near the aquaeductus Fallopii, but there is no observable damage in several of the specimens. Furthermore, the medial sheet underlying the aquaeductus Fallopii of TMM 933-548 bears a longitudinal groove along its lateral edge that likely was a facet for the lateral sheet, which is not preserved. The floor of the aquaeductus cochleae is complete in the remaining specimens (Figure 2.3C).

The sulcus facialis for the hyomandibular branch of the facial nerve extends posteriorly from the foramen faciale (Figure 2.1C). This groove curves along the posterolateral border of the promontorium. A complete stylomastoid foramen for passage of the facial nerve is not present in any of the specimens. A sigmoidal sulcus is observed on the ventral surface of the crista interfenestralis, which forms a robust process between

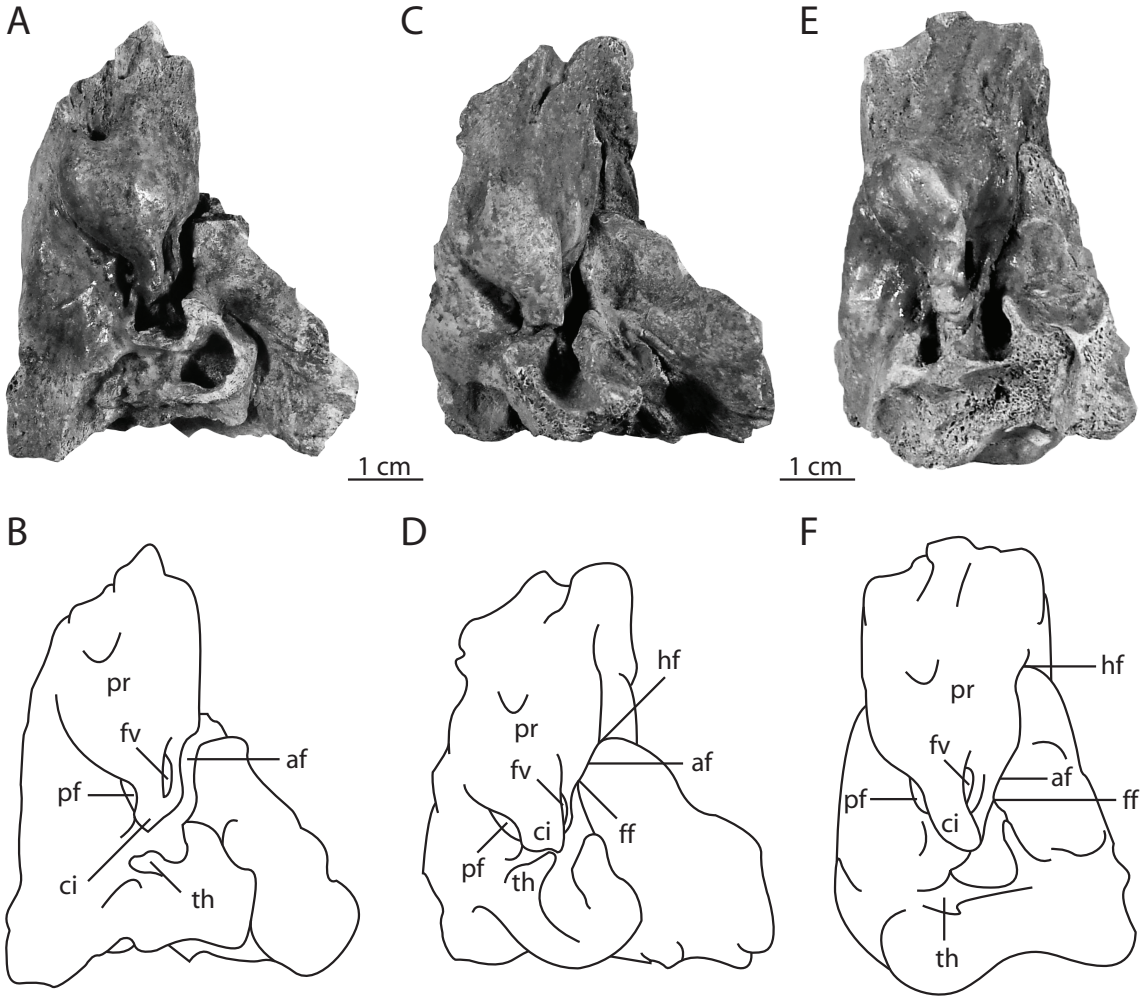

FIGURE 2.3. Variation within aquaeductus Fallopii of elephantoids from Friesenhahn Cave, petrosals in tympanic view. **A-B**, floor of canal incomplete (likely result of damage), both hiatus Fallopii and foramen faciale incomplete (TMM 933-1389); **C-D**, floor of canal partially complete, hiatus Fallopii complete, foramen faciale incomplete(TMM 933-166); **E-F**, floor of canal, hiatus Fallopii, and foramen faciale complete (TMM 933-2043). Abbreviations: **af** – aquaeductus Fallopii; **ci** – crista interfenestralis; **ff** – foramen faciale; **fv** – fenestra vestibuli; **hf** – hiatus Fallopii; **pf** – perilymphatic foramen; **pr** – promontorium; **th** - tympanohyal.

the foramina cochleae and vestibuli. This groove served as a facet for the tympanic bone that would form an auditory bulla in an articulated skull. The crista interfenestralis and tympanic bulla define the stylomastoid foramen in extant elephants (Eales, 1926), but because no bullae are preserved for the Friesenhahn petrosals, the stylomastoid foramen is incomplete in all specimens examined here.

Posteromedial to the crista interfenestralis is the fossa musculus minor for the stapedius muscle. A sulcus for the muscle extends between the fossa and the fenestra vestibuli. The crista interfenestralis on several of the petrosals contacts a process on the posterior aspect of the tympanic surface of the petrosal known as the tympanohyal. The connection between the ventral process of the crista interfenestralis and the tympanohyal is incomplete in most specimens (Figure 2.4A; Table 2.1), but when the crista interfenestralis and tympanohyal join, they form a foramen (Figure 2.4B; Table 2.1). In specimens such as TMM 933-2323, the sulcus for the stapedius muscle leads to the foramen, suggesting that the stapedius muscle passed through the foramen in life. The posterior region of the petrosal is damaged in the incomplete specimens; however, two exceptions are TMM 933-166 and 933-1032 wherein the crista interfenestralis and tympanohyal nearly touch, but do not contact one another. There is no apparent damage to account for the lack of contact in those specimens.

Inner ear

The bony labyrinth within the petrosal consists of the cochlea anteriorly and the vestibule with its semicircular canals posteriorly (Figure 2.5). The cochlea completes a little over two complete turns (765°) and is planispiral in shape. The diameter of the basal turn of the cochlea (13.7 mm) is more than twice as large as the height of the cochlear

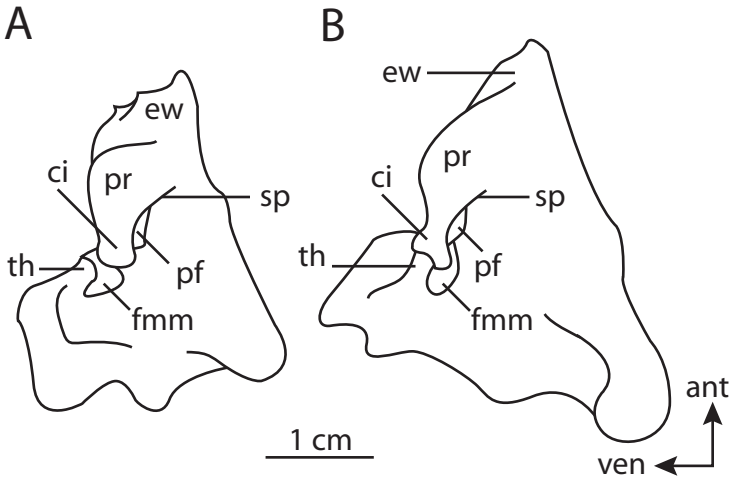

FIGURE 2.4. Foramen for stapedius muscle in elephantoids from Friesnehahn Cave, petrosals in medial view. **A**, crista interfenestralis and tympanohyal not connected, foramen for stapedius muscle incomplete (TMM 933-1932); **B**, crista interfenestralis and tympanohyal connected, foramen for stapedius complete (TMM 933-416). Abbreviations: **ant** – anterior; **ci** – crista interfenestralis; **ew** – epitympanic wing; **fmm** – fossa musculus minor; **pf** – perilymphatic foramen; **pr** – promontorium; **sp** – sulcus for perilymphatic duct; **th** – tympanohyal; **ven** – ventral.

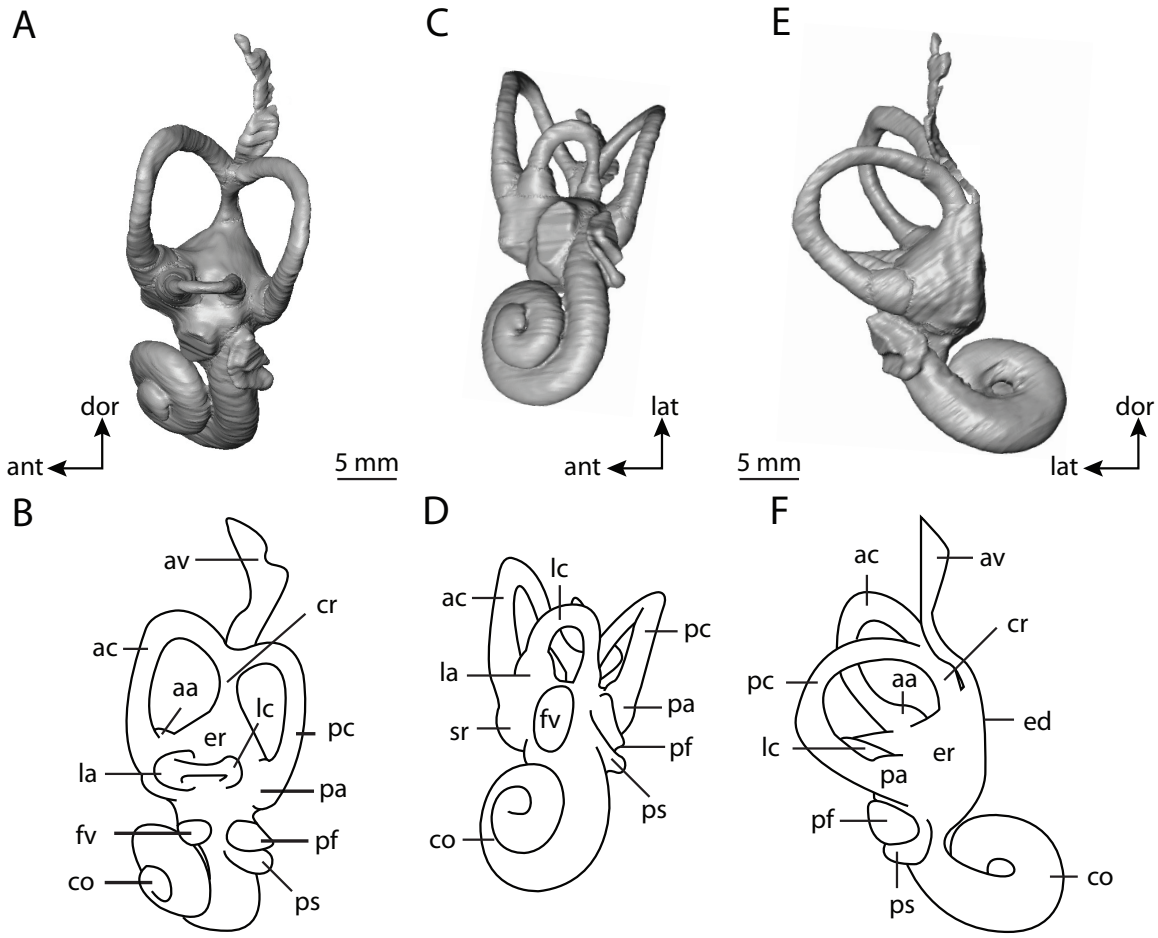

FIGURE 2.5. Digital endocast and labeled line drawing of bony labyrinth of inner ear of elephantoid from Friesenhahn Cave (TMM 933-950). **A-B**, lateral view; **C-D**, tympanic view; **E-F**, ventral view. Abbreviations: **aa** – anterior ampulla; **ac** – anterior semicircular canal; **av** – aquaeductus vestibuli; **cr** – crus commune; **co** – cochlea; **ed** – endolymphatic duct; **er** – elliptical recess; **fv** – fenestra vestibuli; **la** – lateral ampulla; **lc** – lateral semicircular canal; **ps** – out pocket for perilymphatic sac; **pa** – posterior ampulla; **pf** – perilymphatic foramen; **pc** – posterior semicircular canal; **sr** – recessus sphericus.

spiral (6.6 mm). The cochlea as a whole contributes only 30% of the total volume of the inner ear cavities (351 mm^3 out of 1145 mm^3 total). A curved out-pocketing for the perilymphatic sac is anteriorly adjacent to the fenestra cochleae. There is little to no development of a secondary bony labyrinth.

The medial edge of the fenestra vestibuli is the boundary between the cochlea and vestibule, with the fenestra vestibuli completely in the vestibule. The endocast of the vestibule has a sulcus that is laterally adjacent to the opening of the fenestra vestibuli. This sulcus represents a bony ridge on the outer wall of the vestibule, and defines the division between the spherical recess anteriorly, which houses the membranous saccule, and the larger elliptical recess for the membranous utricle posteriorly. The spherical recess communicates with the stapes via the fenestra vestibuli, and the recess is confluent with the cochlea anteriorly and the elliptical recess posteriorly. A groove on the dorsal wall of the spherical recess extends posteriorly. This groove, which is represented by a rounded ridge on the endocast, accommodates the endolymphatic duct in life. The groove extends towards the aquaeductus vestibuli, which opens ultimately onto the cerebellar surface of the petrosal.

The elliptical recess receives a total of six openings in addition to the opening into the spherical recess. Three of the openings are aligned along the border between the two recesses. They are, from medial to lateral, the posterior ampulla, medial limb of the lateral semicircular canal, and lateral ampulla. The opening for the anterior ampulla is laterally adjacent to the lateral ampulla, and the opening for the short and squat common crus is situated at the opposite end of the vestibule from the other four openings. The sixth and final orifice is for the aquaeductus vestibuli, dorsal to the common crus and at the terminus of the groove for the endolymphatic duct that begins in the spherical recess.

The lateral semicircular canal is the most planar of the three canals, and it opens into the vestibule, separate from the posterior canal and ampulla. The posterior and anterior semicircular canals join to form the crus commune. Among the three semicircular canals, the posterior is the largest and the lateral is the smallest in terms of arc radius of curvature (posterior = 5.51 mm, anterior = 4.99 mm, lateral = 2.67 mm, with an average semicircular canal radius = 4.39 mm; measured following the method outlined by Spoor and Zonneveld, 1995) and volume (posterior = 51.7 mm^3, anterior = 48.9 mm^3, lateral = 22.4 mm^3; measured in Amira ® software). However, the anterior canal is the longest of the three (anterior = 24.6 mm, posterior = 24.3 mm, lateral = 12.5 mm; ampullae not included, but length of the crus commune included for both anterior and posterior lengths).

The ratio of the length of a semicircular canal to the radius of the respective canal arc is thought to correlate to the rotational movement sensitivity of the head (Boyer and Georgi, 2007). The ratios of the length of the semicircular canals to the radius of curvature are similar for the anterior and lateral canals (anterior = 4.93, lateral = 4.70), but the ratio is lower for the posterior canal (4.41). The planes of the semicircular canals are not at right angles to one another. The plane of the anterior semicircular canal forms acute angles with the planes of the lateral and posterior canals (74° and 66° respectively), but the planes of the posterior and lateral canals form a slightly obtuse angle (92°). None of the canals are perfectly planar, although the lateral canal fits onto a single plane better than either of the other two canals.

ANATOMICAL OBSERVATIONS OF *MAMMUT* PETROSALS FROM BONEY SPRING

All of the petrosals examined from Boney Spring are isolated without any evidence of a tympanic bulla, as is observed in the sample from Friesenhahn Cave. The morphology of the definitive *Mammut* sample from Missouri does not differ significantly from that observed in the Friesenhahn elephantoid sample. For example, the subarcuate fossa is absent from the cerebellar surface of *Mammut*, and a secondarily undivided perilymphatic foramen is present on the tympanic surface of the petrosal. Out of the five petrosals examined, only one specimen (144cBS71) preserves an intact aquaeductus Fallopii. The ventral floor of the passage exhibits the partial condition in this specimen, where the floor is fused anteriorly, but is open at the posterior end near the fenestra vestibuli. Completion of the aqueductus could not be determined for the other four specimens (right and left petrosals of 56BS71 and right and left petrosals of 361BS71).

The tympanohyal is damaged in every specimen; thus the completion of the stapedius muscle foramen could not be determined. The sigmoid sulcus observed on the ventral surface of the crista interfenestralis of the petrosals from Friesenhahn Cave is observed on the petrosals from Boney Spring, excepting the left petrosal of 361BS71. A groove for the perilymphatic duct extends medially from the undivided perilymphatic foramen in the Boney Spring petrosals, as is observed for the sample collected from Friesenhahn Cave. No stapedial footplates are preserved for the Boney Spring petrosals, but the stapedial ratio was estimated for three of the five petrosals examined (average is 1.9 with a range of 1.9-2.0).

DISCUSSION

Comparison with other Proboscidea

Apart from *Moeritherium* and *Numidotherium* (Court and Jaeger, 1991; Court, 1992b, 1994), there is little information concerning the ear region of fossil proboscideans. The petrosal is fused solidly to the skull in extant proboscideans as well as in *Mammuthus* and *Mammut* specimens examined at the University of Texas at Austin. The bony bulla covering the tympanic cavity, along with the massive size of proboscidean skulls, makes the otic region of proboscideans difficult to study. Nonetheless, the isolated petrosals of Elephantoidea individuals preserved in Friesnehahn Cave allow comparisons among other proboscidean taxa.

The external petrosal surface of the elephantoids from Friesenhahn Cave agrees in many respects with the ear regions of other non-elephantoid proboscideans. The most obvious similarity is the confluence of the fenestra cochleae and canaliculus cochleae into a common perilymphatic foramen. This structure also is observed in extant elephants, and in fossils as early as the Eocene (Court, 1994), although separate in the Eocene proboscidean *Numidotherium* (Court, 1992b, 1994). An undivided perilymphatic foramen was hypothesized to be an adaptation for low frequency hearing by Court (1994). It was demonstrated previously that extant elephants are specialized for low frequency hearing (Payne et al., 1986; Poole et al., 1988). Given that an undivided perilymphatic foramen is present in the Friesenhahn elephantoids, one might hypothesize that extinct elephantoids were capable of hearing in low frequencies. However, a more thorough study of the bony labyrinths of extinct proboscideans and the closest extant relatives of elephants (Sirenia; Bininda-Emonds et al., 2007) is necessary to assess the auditory capabilities of Elephantoidea as a whole in a sufficient manner.

Although a groove for the perilymphatic duct is medial to the perilymphatic foramen in *Mammut* from Boney Spring and the elephantoids from Friesenhahn Cave, such a sulcus is absent in the extant elephant *Loxodonta* (Fischer and Tassy, 1993) and the extinct proboscidean *Moeritherium* (Court, 1994). The sulcus for the perilymphatic duct is present in the extant sirenian *Trichechus* (Fischer and Tassy, 1993), but the groove is considered to have derived independently in both taxa (for further discussion, see Court and Jaeger, 1991; Court, 1994).

Another feature shared by the elephantoids from Friesenhahn Cave and other proboscideans, namely *Mammut* from Boney Spring, *Moeritherium* (Court, 1994) and *Elephas* (TMM M-6445), is the absence of the subarcuate fossa on the cerebellar surface of the petrosal. A well-developed subarcuate fossa is associated with coordination of head and eye movement, and even agility, if only indirectly (Jeffry and Spoor, 2006). Extant elephants have low agility ('medium slow' as coded by Spoor et al., 2007), which agrees with the absence of the subarcuate fossa. The subarcuate fossa was lost in Proboscidea by the Eocene epoch (as exemplified by *Moeritherium*; Court, 1994) suggesting that fossil proboscideans were not agile either.

Only the footplate of the stapes is preserved completely for the elephantoid specimens from Friesenhahn Cave, but enough remains to compare to the stapes of extant elephants. The broken pieces of the crura on the stapes indicate that the stapes was perforated with a foramen, a condition seen in most mammals that possess a proximal stapedial artery (Novacek and Wyss, 1986a; Wible, 1987). The stapes of the modern elephant is perforated (Blair, 1710-1712b) as in the elephantoid proboscideans from Friesenhahn Cave, suggesting that the proximal stapedial artery was present in these taxa. However, a proximal stapedial artery is not described for any living proboscidean (at least such a vessel was not mentioned by Blair, 1710-1712a, b, 1717-1719, Watson,

1874, or Eales, 1926). Furthermore, a sulcus for the stapedial artery is absent on the promontorium of the Friesenhahn Cave and Boney Spring proboscideans. There is an apparent contradiction since the stapedial foramen supports reconstruction of a proximal stapedial artery through the ear region of Elephantoidea, but absence of a sulcus for the stapedial artery medial to the fenestra vestibuli indicates an absence of the vessel.

There are two hypotheses for the reconstruction of the stapedial artery system within the ear region of *Mammuthus*. First, the stapedial foramen developed in the complete absence of a proximal stapedial artery. This accounts for absence of the sulcus for the artery, as well as the lack of identification of the vessel in published accounts of the elephant middle ear. Such a condition is observed in Cetacea where the proximal stapedial artery is absent (Wible, 1987), but the stapes possesses a small foramen (the 'massive-microperforate' condition of Novacek and Wyss, 1986a).

A second hypothesis is that a proximal stapedial artery was present, penetrating the stapes, but it did not leave a sulcus on the promontorium, and the vessel has remained unreported. For the second scenario to be accepted, the proximal stapedial artery must occur in at least one other species of mammal without leaving a trace on the petrosal, which is observed in some lipotyphlans and bats (Wible, 1987). The stapes of either *Mammuthus* or *Mammut* (it is unclear for which species the stapedial footplate is preserved) likely was the typical bicrurate form, as it is in *Elephas*, and the lack of a proximal stapedial artery in published descriptions of the ear region of elephants would be the result of the difficulty in studying the otic system of Proboscidea. In fact, descriptions of the otic vasculature in proboscideans are superficial. There is a great need for a thorough investigation of the circulation pattern across the elephant basicranium. Until such a study is completed, the presence or absence of a proximal stapedial artery for Elephantoidea remains unresolved.

Several studies that were focused on the ear region of proboscideans discuss the morphology of the bony labyrinth of the inner ear (Blair, 1717-1719; Hyrtl, 1845; Court, 1992b). Although not a description of otic morphology per se, the supplemental information provided by Spoor et al. (2007) included dimensions of inner ear structures for the extant elephant species, *Loxodonta africana* and *Elephas maximus*. Those published measurements form a basis for a comparative discussion of the inner ear of extinct and extant proboscideans.

The radii of the semicircular canals of the elephantoid from Friesenhahn Cave are closer to those reported for extant *Loxodonta* than for *Elephas* (Table 2; Spoor et al., 2007). A positive correlation between the radius of curvature of the anterior canal and afferent sensitivity of that canal was found by Yang and Hullar (2007). Their results indicated that the sensitivity of the anterior canal was higher than that of the smaller lateral canal within an individual, as well as between the canals of different mammal species. This result caused them to conclude that canals with larger radii are more sensitive than those with smaller radii. However, mammals with large body sizes tend to have large canal arc radii (see Spoor et al., 2007). If the specimen for which the bony labyrinth was studied is *Mammuthus*, then the data for proboscideans reported here confirms this, because *Mammuthus* and *Loxodonta* have both larger body masses (Christiansen, 2004) and larger canal radii than *Elephas*.

The two coils of the cochlea of the elephantoid from Friesenhahn Cave is similar to what is observed in *Elephas* (Hyrtl, 1845). However, the cochlea of an unidentified extant elephant completed over three coils, as reconstructed by Blair (1717-1719). The number of coils completed by the cochlea can vary within a species (see Chapter 3), but there are no reports of variations greater that 360° (see also Chapters 3-4, for further discussion of inner ear variation). Although the morphology of the petrosals potentially

represents taxonomic variation, these differences more likely are artefactual. Hyrtl examined casts of the inner ear cavities, whereas Blair filed the bone to expose the structures. Casting of the bony labyrinth (e.g., Hyrtl, 1945) would provide a more precise reconstruction of the cochlea, but the possibility that the cochlea of extant elephants varies to such an extent has yet to be confirmed.

As with the elephantoid from Friesenhahn Cave, the cochlea of extant *Elephas maximus* (personal observation of CT data of TMM M-6445, *Elephas maximus* at http://digimorph.org) and the Eocene fossil *Numidotherium koholense* (Court, 1992b) are planispiral. Both *Numidotherium* and TMM 933-950 share similar ratios between the height of the cochlea and maximum width of the basal turn (0.52 and 0.48). In contrast, the same ratio is much higher in the Eocene proboscidean *Moeritherium* (0.79; Court, 1992b). This index of the shape of the cochlea might reflect functional aspects of the ear region. Gosselin-Ildari (2006) found a positive correlation between the index and both low frequency limits and best frequency achieved by the cochlea. If Gosselin-Ildari's correlations are correct, then *Moeritherium* would have had both a higher low frequency limit, as well as a higher best frequency, than either *Numidotherium* or the elephantoid from Friesenhahn Cave.

There is little to no development of a secondary lamina in the Friesenhahn Cave elephantoid, unlike the well-developed lamina that extends throughout the basal turn in *Numidotherium* (Court, 1992b, fig. 2). The secondary lamina supports the basilar membrane, which in turn supports the spiral organ of Corti for hearing. The width of the basilar membrane can be determined by measuring the gap between the secondary lamina on the outer wall of the bony labyrinth, and the primary lamina that juts into the cochlear cavity from the modiolus (central axis of the cochlea). The size of the gap between laminae is significant, because the width of the basilar membrane is correlated to auditory

TABLE 2.2. Semicircular canal radii of curvature (in mm) for extant elephants and elephantoid from Friesenhahn Cave.

Radius	*Elephas*	*Loxodonta*	Elephantoid	Radius Average
Anterior	4.0	5.2	5.0	4.7
Lateral	2.8	3.6	2.7	3.0
Posterior	4.1	5.5	5.5	5.0
Species Average	3.6	4.8	4.4	4.3

function (Fleischer, 1976). For example, the basilar membrane of microchiropteran bats that echolocate is narrower through the basal turn of the cochlea (Ramprashad et al., 1979) than in mammals sensitive to low frequencies, such as elephants (Payne et al., 1986; Poole et al., 1988). The absence of the secondary lamina and presence of the secondarily undivided perilymphatic foramen supports the sensitivity to low frequency vibrations by the proboscideans from Friesenhahn Cave.

Variation within the ear region

Although the external surfaces of the petrosals are similar across the Friesenhahn Cave sample, there are minor anatomical variations. This variation includes connection of the crista interfenestralis to the tympanohyal to form a foramen for the stapedius muscle, completion of the ventral floor of the aquaeductus Fallopii, and the shape of the fenestra vestibuli (stapedial ratio). The variations may be the result of one or several factors. The taphonomic history of the specimens both before and after burial is one possibility. Phylogenetic variation also is possible, because remains of two proboscidean species were recovered from the cave. Lastly, ontogenetic variations given that a growth series of individuals was identified based on teeth, and individual variation (in the absence of phylogeny and ontogeny) are other potential sources. Each type of variation is discussed below in the context of the morphological features that vary within the Friesenhahn Cave petrosal sample.

Taphonomy is an important concept in paleontology, and data that are lost as a result of post-mortem degradation of fossil specimens can be both extreme and frustrating (e.g., Lawrence, 1968). All of the petrosals in the sample from Friesenhahn Cave show taphonomic damage to some extent. Because the petrosal is so solidly fused to the rest of

the cranium in mammoths, the skulls of the young elephants found in the cave would have to be greatly fragmented in order to isolate the petrosals. In fact, no complete skulls of *Mammuthus* or *Mammut* were recovered from the cave.

The lack of complete skulls might be a result of predation following the hypothesis that Friesenhahn was a carnivoran den (Graham, 1976). Although there is no direct evidence of predation on the petrosal bones themselves, tooth marks were observed on many of the long bones in the cave, and the cranial elements may have fragmented as individuals of *Homotherium* gnawed on skulls. A second more likely hypothesis for the fragmentation of skulls is damage via compaction of sediments after the elephant remains were buried. The skulls of mammoths, mastodons, and extant elephants are quite delicate, with a high degree of pneumaticity. But as stated earlier, the petrosals are dense and lend themselves well to preservation. It is credible that only petrosals and jaw fragments with teeth would be preserved, as this is a phenomenon that is observed in many mammal faunas (Archibald, 1979).

Variation among the stapedial ratios cannot be explained by taphonomic destruction since the measurement was calculated only for those specimens with complete fenestrae vestibuli. Taphonomy does account for the majority of the variation observed for the foramen for the stapedius muscle, with noticeable damage is observed in most cases where the crista interfenestralis does not meet the tympanohyal on the posterior aspect of the petrosal. However, the region is undamaged in TMM 933-166 and 933-1032, where the foramen is not closed. Thus, taphonomy cannot account for the observed variation.

The ventral floor of the aquaeductus Fallopii is broken in most of the specimens, but a few specimens, including TMM 933-548, appear to be undamaged in the vicinity of the canal. The longitudinal groove that spans the length of the medial portion of the floor

of the canal likely is a facet for a missing lateral edge that would have completed the canal. The floor of the aquaeductus is thin, but finished edges on the sheets are easily discernable from broken edges.

Phylogenetic differences between the gross anatomy of molars of *Mammuthus* and *Mammut* are well documented, and remains of both *Mammuthus* and *Mammut* were found in Friesenhahn Cave. Although the vast majority of identifiable specimens (teeth) were referred to *Mammuthus* by Graham (1976), one or more petrosals might represent *Mammut*, and the variation observed might be taxonomic. In fact, the partial condition of the aquaeductus Fallopii is the only feature that varies in the Friesenhahn Cave sample that also is observed in the sample of *Mammut* petrosals from Boney Spring. However, the condition is only observed in one specimen. No other specimen from Boney Spring preserves this region of the petrosal intact.

Nonetheless, the partial condition may be a distinguishing feature of the petrosal of *Mammut*. The partial condition is observed within 57% (12 out of 21 specimens preserving the region intact) of the elephantoid petrosals from Friesenhahn Cave. If the partial condition is unique to *Mammut* (at the very least when comparing *Mammut* and *Mammuthus*), then at least 12 out of the 65 petrosals (18%), but as many as 37 petrosals (57%) recovered from Friesenhahn Cave represent *Mammut*. Such a figure does not agree with the relative abundance based on numbers of molars, where the vast majority of molars (500 out of 513, or 97%) are identifiable as *Mammuthus*. A more likely scenario is that the variation between partial and complete aquaeducti will be uncovered in a larger sampling of *Mammut* petrosals, and that mammoth and mastodon fossils cannot be distinguished based on petrosal characters alone. However, in order to fully test this hypothesis, a large sample of definitively *Mammuthus* and definitively *Mammut* (greater than the sample from Boney Spring that was examined here) is needed. Until such a study

is accomplished, the least inclusive taxon that can be identified for any Friesenhahn Cave petrosal sample is Elephantoidea, yet this may change as additional proboscidean taxa are included in anatomical comparisons.

The completion of the stapedial muscle foramen could not be determined for *Mammut* from Boney Spring, so whether the variation identified in the Friesenhahn Cave sample is taxonomic in nature is inconclusive. The average stapedial ratio is slightly larger for *Mammut* than the Friesenhahn Cave sample (1.9 versus 1.8), but the range falls within that calculated for the Friesenhahn Cave elephantoids. This would be expected if there are multiple mastodons in the Friesenhahn fossil sample, but there is no clear indication if there is a difference in stapedial ratios between *Mammut* and *Mammuthus*. Until stapedial ratios are calculated for a large sampling of definitive mastodons and mammoths, the taxonomic nature of the stapedial ration among elephantoids remains inconclusive.

Ontogenetic variation may explain some variation observed in the sample, including that for the aquaeductus Fallopii. A growth series of mammoths is recognized in Friesenhahn Cave based on dental and postcranial material (Graham, 1976), and it is reasonable to expect the petrosals to have come from individuals of different maturities. Furthermore, all the petrosals likely are from juveniles because no adult mammoth teeth were recovered from the cave.

In order to ascertain whether or not the observed variation is related to the maturity of an individual, there must be some way to determine the relative maturities of the petrosals. Evidence suggests that dimensions of the inner ear of mammals do not change significantly once the bony walls are ossified (Hoyte, 1961; Ekdale, 2005), but such is not the case with the external surface of the petrosal, which expands externally via accretionary growth of bone (Chapters 3-4; Hoyte, 1961). However, there is no

correlation between overall size of the petrosals in the sample and any of the variation observed. Overall size of petrosals is affected by breakage, especially in the sample from Friesenhahn Cave, so using size would not be a reliable indicator of maturity.

The best candidate for ontogenetic variation is the aquaeductus Fallopii, provided that the variation is not the result of taxonomy (which is unlikely; see above). The embryological development of the aquaeductus is undocumented for proboscideans, but a published account of the skull of a fetal African elephant (Eales, 1926) sheds light onto the ossification of the elephant otic region. A similar groove extending the length of the ventral floor of the aquaeductus Fallopii was observed in the fetal skull (Eales, 1926, pl. 9; Fig. 2.6). The aquaeductus was not fully ossified in the fetus, and the groove formed a seam between the bony petrosal medially and a cartilaginous wing that extended to the squamosal laterally. Further evidence from the ontogeny of the ear region of the gray short-tailed opossum, *Monodelphis domestica*, where the lateral aspect of the petrosal is the last part of the ear region to ossify (Clark and Smith, 1993), agrees with Eales' observation in *Loxodonta*. If the lateral portion of the ventral floor of the canal of a juvenile mammoth was not ossified completely upon death, an incomplete (Figure 2.3A) or partially complete aquaeductus (Figure 2.3B) would be preserved in the fossil record.

If one was to assume that completion of the ventral floor of the aqueductus Fallopii is the result of variations in maturity, then the petrosals from Friesenhahn Cave can be divided into two maturity stages based on aquaeductus development – an immature canal versus a mature canal. The incomplete state illustrated in Figure 2.3A is the result of damage to the bone. However, the specimens that possess a partially complete aquaeductus Fallopii (Figure 2.3B) represent an immature stage. In all of these partially complete specimens, the aquaeductus is enclosed anteriorly, but not posteriorly. Assuming the specimens represent immature stages, then ossification of the ventral

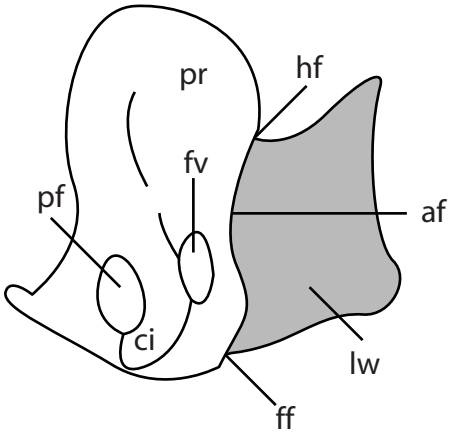

FIGURE 2.6. Diagram of petrosal of fetal elephant (redrawn from Eales, 1926). Abbreviations: **af** – aquaeductus Fallopii; **ci** – crista interfenestralis; **ff** – foramen faciale; **fv** – fenestra vestibuli; **hf** – hiatus Fallopii; **lw** – lateral wing (shaded), cartilaginous in fetal elephant; **pf** – perilymphatic foramen; **pr** – promontorium.

aspect of the floor of the aquaeductus Fallopii begins at the anterior edge of the canal and continues posteriorly. As stated above, 57% of the petrosals within the sample have the partial, or immature state (see Table 2.1).

Variation in the stapedius muscle foramen might have an ontogenetic basis as well. One hypothesis is that the petrosals in which the foramen is not complete (Figure 2.4A) are less mature than individuals with a complete foramen (Figure 2.4B). There is no correlation between a complete connection of the crista interfenestralis and tympanohyal and a complete aquaeductus Fallopii because the stapedius muscle foramen is complete regardless of completion of the aquaeductus Fallopii. This would suggest that the crista interfenestralis and tympanohyal ossify together earlier in ontogeny than the medial and lateral portions of the aquaeductus Fallopii. Interestingly, the stapedius muscle foramen is incomplete in TMM 933-166 and 933-1032, however the aquaeductus Fallopii is partially complete in TMM 933-166, while the floor of the canal is complete in TMM 933-1032, causing ambiguity. The closure of the foramen for the stapedius muscle could be ontogenetic in nature, but it would have to ossify out of sequence with the aquaeductus Fallopii. Ontogenetic sequence polymorphism may be a fairly common phenomenon (see Colbert and Rowe, 2008).

The broad range in stapedial ratios is not correlated with size of the petrosals, nor with the ontogenetic sequence based on the maturity of the aquaeductus Fallopii. That is, the ratios of immature petrosals are neither more nor less elliptical than the ratios of the bones with mature canals. In fact, both the minimum (1.4) and maximum (2.1) ratios were calculated for specimens with complete canals.

The variation in the stapedius muscle foramen and the stapedial ratio cannot be explained by taphonomy or ontogeny, and variation in both structures is inconclusive for taxonomy. The two specimens in which the crista interfenestralis and tympanohyal do not

meet to form the foramen for the stapedius muscle may instead reflect individual variation. Likewise, the variation observed in the stapedial ratio appears to be intraspecific variation that is not explained by maturity.

Marsupials tend to have more circular stapedial footplates with ratios below 1.8 when compared to placentals, which tend to have ratios at or above 1.8 (Segall, 1970). With a few exceptions, the pattern of the ratio has held for extinct and extant therians (marsupials plus placentals). Because of this, the ratio is used to distinguish isolated marsupial and placental petrosals (see Archibald, 1979; Wible et al., 2001; Ekdale et al., 2004), and the ratio is used in phylogenetic analyses (Wible, 1990; Rougier et al., 1998; Archibald et al., 2001; Ladevèze, 2007). However, those studies did not take variation of the ratio into account. The rounded average stapedial ratio for the sample from Friesenhahn Cave is 1.8, which agrees with the values for placental mammals that Segall (1970) calculated. However, when the range observed within the entire Friesenhahn sample is considered, the ratios span both sides of Segall's cut-off (1.4-2.1; Table 1). In fact, the proportion of specimens with ratios below 1.8 versus above 1.8 is 30:27, nearly 1:1 (note that the ratio was not calculated for every specimen, only for those that have the complete fenestra).

The observed range of variation casts doubt on the validity of using the stapedial ratio to distinguish between placental and marsupial taxa. If identification of the elephantoid petrosals from Friesenhahn Cave were based solely on the stapedial ratio, then half of the specimens would be identified as marsupials, and half as placentals. Broad ranges of ratios have been reported for other taxa, including *Monodelphis domestica* (Chapter 3) and the Cretaceous eutherian *Kulbeckia kulbecke* (Ekdale et al., 2004). In fact, a much greater range is observed in *Kulbeckia* than in the elephantoid petrosal sample from Friesenhahn Cave (which likely contains two taxa). How the range

in stapedial ratios of the Friesenhahn petrosals compares with ratios in modern elephant populations is unknown.

The ratios reported here (as well as in Ekdale et al., 2004) were calculated using the fenestra vestibuli as a proxy. Ideally the stapes would fit snugly into the fenestra vestibuli in life. Stapes are unknown for *K. kulbecke*, but stapedial footplates were recovered for *Mammuthus* (as described above). Perhaps the dimensions of the fenestra vestibuli do not serve as an accurate proxy for dimensions of the stapedial footplate. The footplate of the stapes is held into the fenestra vestibuli by an annular ligament, so the footplate must be smaller than the fenestra. Indeed, the ratios differ when using the fenestra vestibuli versus the actual footplate in TMM 933-950 (1.8 versus 1.7, respectively), but the difference in these values is within one standard deviation of the mean (0.1). Furthermore, the stapes of TMM 933-951 does, in fact, fit tightly in the fenestra vestibuli. Blair (1717-1719) observed the same in the extant elephant. Nonetheless, no thorough investigations comparing ratios between the footplate of the stapes and the respective fenestra vestibuli have been published for any mammal taxon, and such a study is beyond the scope of this paper.

CONCLUSIONS

The sample of elephantoid proboscidean petrosals collected form Friesenhahn Cave is significant for several reasons. First, there is a poor representation of isolated proboscidean petrosals in the fossil record. That such a large sample of proboscidean petrosals exists from Friesenhahn Cave is a testament to the importance of that locality. Furthermore, the petrosal is solidly fused to the skull in extant proboscideans, as well as in *Mammuthus* and *Mammut*. Together with the presence of a bony bulla covering the

tympanic cavity in mature petrosals, as well as the massive size of elephant skulls, the otic region of proboscideans is a difficult region to study. The Friesenhahn sample provides an opportunity to study an important region of fossil proboscidean skulls that otherwise is unavailable.

The further significance of the petrosal sample is that a unique growth series is identified for the first time from a collection of fossil petrosals using data from the aquaeductus Fallopii. If variations observed in other elements besides the petrosal coincide with one of the two maturity stages identified from Friesenhahn Cave, then that information can be used to construct an ontogenetic sequence between elements within an individual, and expand our knowledge of the biology of fossil mammals. The possibility that the variation is the result of multiple taxa in the sample exists, although this phenomenon is not likely given the discrepancy between the frequencies of variable states and taxonomic frequencies within molar samples.

Lastly, the sample from Friesenhahn Cave exhibits a broad range of stapedial ratios, a measurement that often is used in phylogenetic analyses. Given that this measurement is variable, not only in the elephantoids from Friesenhahn Cave and Boney Spring, but also select Mesozoic taxa, it seems inappropriate for the stapedial ratio to be used to distinguish metatherian and eutherian petrosals. In fact, the general systematic utility of the ratio among all mammals is questionable. Likewise, the measurement should not be used for phylogenetic analyses unless treated as a continuous character to account for variation and large samples are examined and measured before character scoring in an analysis.

CHAPTER 3: POSTNATAL ONTOGENETIC VARIATION IN THE BONY LABYRINTH OF *MONODELPHIS DOMESTICA* (MAMMALIA: MARSUPIALIA)

ABSTRACT

Ontogeny, or the development of an individual from conception to death, is a major source of variation in vertebrate morphology. All anatomical systems are affected by ontogeny, and knowledge of the ontogenetic history of these systems is important to understand when formulating biological interpretations of evolutionary history and physiology. The present study is focused on how variation affects the bony labyrinth across a growth series of an extant mammal. Digital endocasts of the bony labyrinth were constructed using CT data across an ontogenetic sequence of *Monodelphis domestica*, an important experimental animal. Various aspects of the labyrinth were measured, including angles between the semicircular canals, number of turns of the cochlea, volumes of inner ear constituents, as well as linear dimensions of semicircular canals. There is a strong correlation between skull length and age, but from 27 days after birth onward, there is no correlation with age among most of the inner ear measurements. Exceptions are the height of the arc of the lateral semicircular canal, the angular deviation of the lateral canal from planarity, the length of the slender posterior semicircular canal, and the length of the canaliculus cochleae. Adult dimensions of several of the inner ear structures, such as the arcs of the semicircular canals, are achieved before the inner ear is functional, and the non-ontogenetic variation in the bony labyrinth serves as an important source for behavioral, physiological, and possibly phylogenetic information.

INTRODUCTION

Variation is a phenomenon that affects all morphological systems. Phenotypic variation is the result of many factors, including phylogenetic history, gender, geography, and ontogeny. Ontogeny, or the development of an individual from conception to death, is a major source of variation that has garnered much attention in scientific literature. Ontogenetic variation is a special problem for systematists, particularly paleontologists, when only one specimen or a small sample of specimens of a taxon is known, which can lead to vexing systematic problems (Brinkman, 1988; Tykoski, 2005; Wiens et al., 2005). For example, two specimens that differ slightly in morphology might represent two separate taxa, or they might represent different ontogenetic stages of a single species, or the variation might indicate any of a series of other possibilities (see Bever, 2006). Because of this, the effect of ontogenetic transformations on anatomy should be taken into consideration when scoring states of morphological characters for phylogenetic analyses.

All morphological systems are affected by ontogenetic variation at some level. The fully formed bony labyrinth of the inner ear, as preserved within the internal cavities of the petrosal bone of mammals, often is considered immune to ontogenetic change, because the petrosal ossifies and matures early in development in humans (Jeffery and Spoor, 2004). This is not to say that the mammalian bony labyrinth does not exhibit variation throughout ontogeny. The auditory system undergoes profound and pronounced ontogenetic transformations, but it quickly achieves mature morphologies that appear to remain stable through the remainder of the life of an individual, if only for select placentals including humans (Jeffery and Spoor, 2004) and rabbits (Hoyte, 1961). In contrast, the majority of other systems, such as the long bones of the vertebrate limb, experience a more prolonged ontogeny relative to the inner ear and teeth. Given the rapid

maturation of the mammalian ear region, as well as the prevalence of ear regions in the fossil record (the petrosal is among the densest elements in the body), the otic region is special and important to vertebrate paleontologists. In fact, petrosals are common elements preserved in Mesozoic mammal faunas (Archibald, 1979).

If the fully ossified bony labyrinth does not change throughout postnatal ontogeny, then the maturity of a specimen would not need to be known in order to make biological interpretations of behavior or phylogeny, using the ossified inner ear. The results of recent studies included information from the bony labyrinth that has been used by researchers to investigate bipedalism in fossil hominids (Spoor et al., 1994, 1996), evolutionary relationships among early humans (Hublin et al., 1996), aquatic adaptations in cetaceans (Spoor et al., 2002), and behaviors in extinct dinosaurs (Rogers, 1998, 1999) where the relative maturity of individuals was not ascertained.

The middle ear region of mammals, as preserved on the external surface of the petrosal, is a widely used source of phylogenetic information. This region is useful for the inference of evolutionary relationships within and among major groups of mammals, including Carnivora (Bugge, 1978; Hunt, 1987, 1989), Cetacea (Geisler and Luo, 1996; Luo and Gingerich, 1999), Chiroptera (Wible and Davis, 2000; Wible and Novacek, 1988), Primates (Harvati and Weaver, 2006; MacPhee, 1981; Wible and Martin, 1993), and even some of the earliest mammals (Archibald, 1979; Ekdale et al., 2004; Ladevèze, 2004; MacIntyre, 1972; Meng and Fox, 1995; Wible, 1990; Wible et al., 2001). However, mammalian systematists often are unable to evaluate the complex structures of the inner ear, such as the cochlea, vestibule, and semicircular canals, because these structures are surrounded completely by bone and are difficult to observe. Thus, the degree of ontogenetic variation within the inner ear is unknown for most mammals.

Natural endocasts of the inner ear chambers are known (Court, 1992b; Kielan-Jaworowska, 1984; Meng and Wyss, 1995), but preservation of such fossils in the rock record is rare. In the absence of such exceptional preservation, removal of the surrounding bone therefore is necessary in order to observe the bony labyrinth. Historically, access to the inner ear cavities was granted through serial sectioning or dissolution of bone (Gray, 1907, 1908; Luo and Marsh, 1996; Novacek, 1986; West, 1985). More recently, the advent of high-resolution X-ray computed tomography (CT) has allowed observation of the internal cranial structures and description of the cranial osteology of vertebrate taxa (Bever et al., 2005; Maisano et al., 2002; Rowe et al., 1995, 1997; Spoor and Zonneveld, 1995; Tykoski et al., 2002; Hullar and Williams, 2006).

Computed tomography was used here in order to investigate changes following the onset of ossification of the bony labyrinth across an ontogenetic series of *Monodelphis domestica*, which is a species of marsupial mammal that is important for experimental biomedical research (Fadem et al., 1982; Macrini, 2004). *Monodelphis* commonly is used in clinical studies (e.g., Eugenín and Nicholls, 1997; Kusewitt et al., 1999; Wang et al., 2003; Halpern et al., 2005), and knowledge of the ear benefits future studies of the auditory system of mammals.

The development of the inner ear of the closely related species *Didelphis virginiana* is well documented (e.g., Larsell et al., 1935; McCrady, 1938), and both *D. virginiana* and *M. domestica* share similar chronologies in skeletal maturation (although both species exhibit different rates of growth; Rowe, 1996, 1997). Because of this, information about the maturation of the inner ear of *D. virginiana* likely is similar in relative timing to that of *M. domestica*. At birth, the inner ear of *D. virginiana* is clearly recognizable (Larsell et al., 1935: fig. 3, stage 35), but it is still immature in form. The anterior, lateral, and posterior semicircular canals are present as complete tubes, but they

are not as large as those of adults. The cochlea completes one half of a turn at birth, and will eventually complete two and a quarter turns (Larsell et al., 1935).

Ossification of the bony labyrinth has not begun at birth, and the petrosal bone itself is one of the last endochondral bones to begin ossification in *M. domestica*, around postnatal day 12 (Clark and Smith, 1993). Ossification of the petrosal of *M. domestica* begins in three ossification centers around the developing cochlea, and the bone surrounding the cochlea is fully ossified by day 25. Expansion of ossification of the cochlear cartilage and ossification of the postparietal into the region of the semicircular canals triggers the onset of ossification of the canalicular cartilage (Clark and Smith, 1993). Ossification of the region of the semicircular canals is underway by day 20, and the bony walls of the semicircular canals are the first to ossify, followed by the spaces between them.

The petrosal of *M. domestica* is not fully ossified by day 30, but the only unossified portions are part of the styloid process and the lateral wall of the subarcuate fossa, which houses a petrosal lobule of the paraflocculus of the cerebellum. The styloid process does not contribute to the morphology of the bony labyrinth within the petrosal bone, but the subarcuate fossa is defined by the semicircular canals. The development of the bony semicircular canals versus the subarcuate fossa is not entirely independent in primates (Jeffery and Spoor, 2006), but the influence that subarcuate fossa ossification has on the dimensions and orientation of the fully ossified semicircular canals is unknown.

Beyond anatomy, the development of auditory and vestibular physiological responses in *M. domestica* is well documented (Aitkin et al., 1997; Reimer, 1996). The inner ear of *M. domestica* is not functional at birth, because the middle ear cavity is filled with fluid until 26 days after birth, and the external auditory meatus does not open until

28-30 days postnatal (Aitkin et al., 1997). Pouch young of *D. virginiana* respond to vestibular stimuli before acoustic reflexes are observed (Larsell et al., 1935), and the same may be the case for *M. domestica* (given similarities in skeletal development between the two species), although such a relationship between the physiological responses has yet to be determined for *M. domestica*. Evoked auditory responses can be detected in *M. domestica* at 28 days after birth, and adult hearing thresholds are achieved by day 39 (Reimer, 1996).

The ontogeny of hearing in *M. domestica* follows a similar pattern observed in placental mammals of similar size, allowing *M. domestica* to be used as a generalized model for physiological investigations of the inner ear of therian mammals (Reimer, 1996). The morphology of the membranous labyrinth of *D. virginiana* (Larsell et al., 1935) develops in a similar fashion to that of *Mus musculus* (Morsli et al., 1998), further suggesting that the ontogenetic pattern of the inner ear of didelphids (to which both *Monodelphis* and *Didelphis* belong) also may afford insights into the developmental morphology of placentals.

MATERIALS AND METHODS

Eleven whole dried skulls of *Monodelphis domestica* representing different ages (absolute numbers of postnatal days) were scanned at The University of Texas High-Resolution X-ray CT facility (UTCT). All specimens were born and raised in captivity under controlled conditions at the Southwest Foundation for Biomedical Research in San Antonio, TX, where exact numbers of postnatal days were recorded. Once CT scanned, the specimens were accessioned into the Vertebrate Paleontology Laboratory (Austin, TX) recent mammal collection (TMM M). The specimens used for this study range in age

from 27 to 465 days after birth. Day 27 was chosen as the earliest age, because the bony labyrinth itself likely is to be fully ossified by that time.

The specimens used are TMM M 7595 (day 27), 8261 (day 27), 8265 (day 27), 7536 (day 48), 8266 (day 56), 7539 (day 57), 7542 (day 75), 8267 (day 76), 7545 (day 90), 8268 (day 90), and 8273 (day 465). One additional individual (TMM M 7599), a fully mature retired breeder from the colony, was used in this study, although the exact age of the individual is unknown. That specimen (TMM M 7599) was not used to ascertain age-related changes, but rather it was used for morphological comparisons with the rest of the specimens in the sample. Scan data for many of these specimens are publicly available at the website entitled 'Digital Morphology: a National Science Foundation Library at the University of Texas at Austin' (http://digimorph.org/specimens/Monodelphis_domestica/whole/). Table 3.1 includes scanning parameters used for each specimen.

The inner ear cavities were digitally segmented into constituent parts (cochlea; vestibule; anterior, lateral, and posterior semicircular canals; anterior, lateral and posterior ampullae; common crus) by isolating voxels on individual CT slices that define the anatomical structure of interest. These segmented data can be rendered as a 3-dimensional digital endocast of the segmented structure, which provides easy observation of inner ear structures. Segmentation, visualization, and measurement of digital endocasts was performed in the computer programs VG Studio Max 1.2© (Volume Graphics) and Amira 3.1©. Anatomical terminology follows Evans (1993) and Spoor and Zonneveld (1995).

Numerous angular and linear measurements, as well as indices describing various aspects of the digital endocasts, were made in Amira software, and volumetric measurements were made in both VG Studio Max and Amira. Measurement methods and

TABLE 3.1. CT scanning parameters for specimens of *Monodelphis domestica*. The specific parameters employed during the scanning and post-scanning image processing for each specimen is provided here. Definitions of parameters are as follows: **Spec. #** – specimen number, catalogued as TMM M; # **Slices** – number of CT slices through the inner ear collected in the coronal (original) slice plane; **Interslice** – interslice spacing, the distance between consecutive slices (mm); **Field Rec.** – field of reconstruction, dimensions of individual CT slice (mm); **Interpixel** – interpixel spacing, vertical and horizontal dimensions of individual pixel measured by dividing field of reconstruction by resolution (mm); **Resolution** – number of pixels in CT image, either 512 X 512 pixels, or 1024 X 1024 pixels.

Spec. #	# Slices	Interslice	Field Rec.	Interpixel	Resolution
7595	116	0.0371	10.8	0.0211	512
8261	69	0.0483	16.5	0.0161	1024
8265	108	0.0338	13.0	0.0127	1024
7536	81	0.0625	14.0	0.0273	512
8266	119	0.0355	17.0	0.0166	1024
7539	76	0.0676	14.9	0.0291	512
7542	96	0.0608	17.9	0.035	512
8267	91	0.048	22.0	0.0215	1024
7545	81	0.0682	19.0	0.0371	512
8268	109	0.048	22.0	0.0215	1024
8273	61	0.117	55.65	0.0543	1024
7599	151	0.09	23.0	0.0449	512

indices calculated largely follow those used by Spoor and Zonneveld (1995, 1998), and Jeffery and Spoor (2004), many of which were used previously to formulate interpretations of mammalian systematics and the physiology of the inner ear. A detailed explanation of each measurement is provided in the following section.

Definitions and exploration of measurements

Angular Measurements

Most of the angles considered in this study are thought to be important to inner ear physiology, such as planar relationships between semicircular canals (Calabrese and Hullar, 2006), as well as the evolutionary relationships of mammals, such as coiling of the cochlea (Ekdale et al., 2004; Graybeal et al., 1989; Rougier et al., 1998). The degree of coiling completed by the cochlea is calculated to investigate if the number of cochlear turns increases as the bony labyrinth matures after the onset of ossification. The coiling of the cochlea often is used to separate therian mammals from non-therian mammals, including monotremes and non-mammalian synapsids (Graybeal et al., 1989), and cochlear coiling, in conjunction with the length of the cochlear canal, is related to audible frequencies (West, 1985). To measure the number of turns of the coil, the cochlea is viewed from above, perpendicular to the axis of rotation. A line is drawn from the junction of the primary and secondary bony laminae at the base of the cochlea (following Geisler and Luo, 1996) to the center of the axis of rotation. Each time that the cochlea crosses this line is counted as one half turn. An additional value is added to this – an angle measured from the line drawn through the axis of rotation to the apical tip of the cochlear canal – in order to determine the total number of degrees completed by the cochlea.

The deviations of semicircular canals away from the orthogonal planes of the skull are calculated and reported in several physiological studies (e.g., Calabrese and Hullar, 2006; Hullar and Williams, 2006). The orientation of canals might signify that a vertebrate is more sensitive to certain movements of the head, such as pitch or roll (Hullar and Williams, 2006). Orthogonal planes in the published studies are defined by landmarks across a complete skull, so the orthogonality of the planes of canals cannot be determined for isolated petrosals (which often is the case with fossils). Nonetheless, the angles between the planes are measured here. If the angles between the canals changes across ontogeny, then the orientation of the canals with respect to the orthogonal planes of the skull changes also. Orientations of the canals are measured as the angle between the planes of two canals, when both planes are perpendicular to the field of view (Figure 3.1a-c). The plane of a canal is fit to points at the center of the lumen at the midpoint of the arc, as well as the aperture of the canal into the ampulla at one end, and vestibule at the other.

The plane of the lateral semicircular canal is used to measure the angle between the canal and the cochlea. It often is assumed that mammals hold their heads so that the lateral semicircular canal is parallel to Earth horizontal (de Beer, 1947), but such is not always the case (see Hullar, 2006, for a review). The angle is measured in the same manner as the orientations of the three canals, where the plane of the cochlea intersects three points equally spaced through the basal turn of the cochlear canal (Figure 3.1d).

Measurement of angular deviation of a canal from its plane was made following modified protocols outlined by Calabrese and Hullar (2006) and Hullar and Williams (2006). The dimension is calculated by determining the maximum linear deviation achieved by the center of the lumen of the canal when the plane of the canal is oriented parallel to the horizon (Figure 3.1e). Partial angles of deviation are determined trigonometrically using

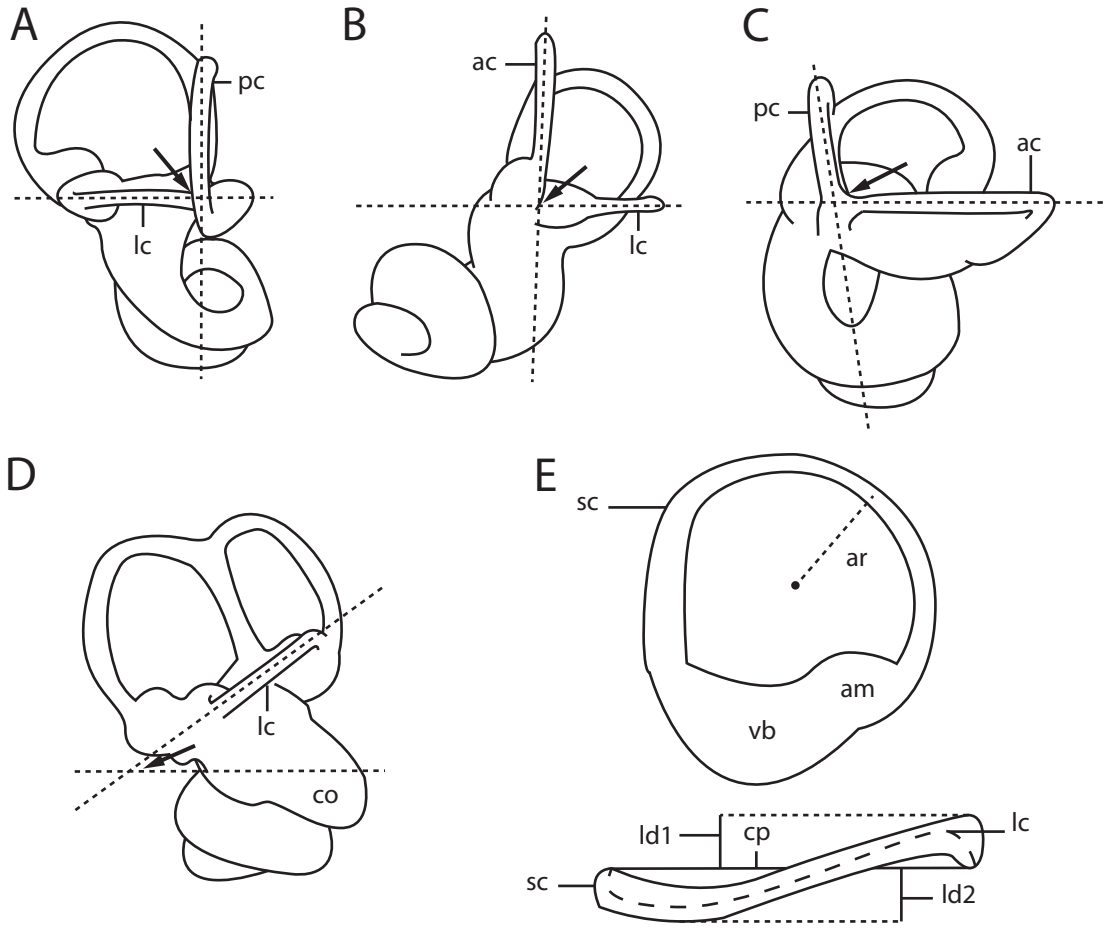

FIGURE 3.1. Graphical depiction of angular measurements between semicircular canals and cochlea. **A**, planes of posterior and lateral canals; **B**, planes of anterior and lateral canals; **C**, planes of anterior and posterior canals; **D**, planes of basal turn of cochlea and lateral canal; **E**, semicircular canal in profile and viewed with plane parallel to horizon. Arrows indicate angle measured. Abbreviations: **ac** – anterior semicircular canal; **am** – ampulla; **ar** – arc radius of curvature; **co** – cochlea; **cp** – plane of semicircular canal; **lc** – lateral semicircular canal; **ld** – linear deviation of canal from plane; **pc** posterior semicircular canal; **sc** – semicircular canal; **vb** – vestibule.

the linear deviations and the arc radius of curvature of the semicircular canal (described below with other linear measurements). The total angular deviation, reported here, is the sum of the two partial deviations.

Linear Measurements

The measurements made on digital endocasts are reported in millimeters, and they include total length of the labyrinth, radius of the arcs of the semicircular canals, diameters of the canal lumen, and lengths of the semicircular and cochlear canals, the canaliculus cochleae (for the perilymphatic duct), and the aquaeductus vestibuli (for the endolymphatic duct).

The total length of the bony labyrinth is a linear measure of size of the entire series of inner ear cavities (following Jeffery and Spoor, 2004). The length is measured as the greatest distance from the posterior-most point at the center of the lumen of the posterior semicircular canal to the center of the lumen of the outer bend of the basal turn of the cochlea.

Linear measurements of the size of the cochlear spiral follow the method proposed by Gosselin-Ildari (2006). The width of the cochlea is measured as the greatest distance from the ventral edge of the fenestra cochleae to the outer wall of the outer curve of the basal turn of the cochlea (Figure 3.2). The height of the cochlea is measured from the top of the spiral to the level of the dorsal edge of the fenestra cochleae, perpendicular to the width and parallel to the plane of the basal turn of the cochlea.

The radius of curvature of the arc of the semicircular canals ("R" of Jones and Spells 1963) is correlated to both sensitivity of the canal, as well as agility of the animal. For animals of similar body size, larger canals are more sensitive (Hullar and Williams, 2006) and are indicative of a more maneuverable and agile animal (Spoor et al., 2007).

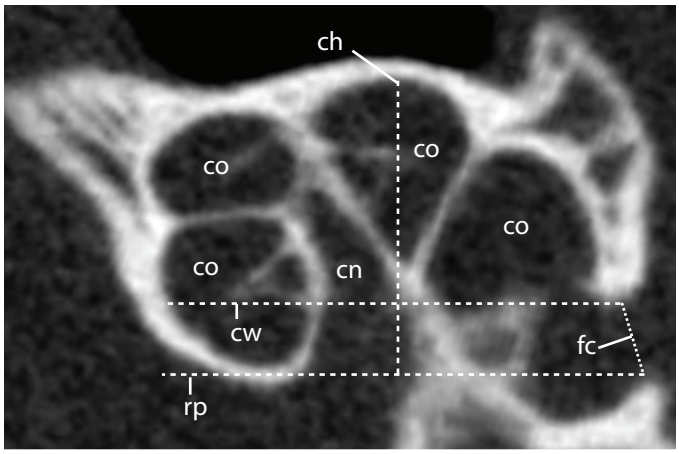

FIGURE 3.2. Cross-section through midline of the cochlea displaying the measurements for height and width of the spiral of the cochlea. Abbreviations: **ch** – height of spiral of cochlea; **co** – cochlear canal; **cw** – width of spiral of cochlea; **fc** – fenestra cochleae; **cn** – canal for cochlear branch of cranial nerve VIII within the modiolus; **rp** – reference plane for measuring height of spiral of cochlea.

The arc radius of a canal is half the average of the height and width of the arc. The height of the anterior semicircular canal is measured as the greatest distance from the wall of the vestibule to the center of the lumen of the canal, perpendicular to the plane of the lateral canal. The height of the posterior semicircular canal is measured parallel to the plane of the lateral canal from the center of the lumen of the common crus to the center of the lumen of the posterior limb of the canal. The height of the lateral canal is measured as the greatest distance from the wall of the vestibule to the center of the lumen of the canal. The widths for all of the canals are perpendicular to the respective heights, and measured from the center of the lumen of opposing limbs.

Dynamic responses of the semicircular canals also are dependent on the radius of the membranous semicircular duct within the bony canal (Hullar, 2006). There is not a 1:1 size correlation between the bony and membranous labyrinth (Curthoys et al., 1977a, b; Igarashi, 1967), so the radius of the membranous duct cannot be determined in the absence of soft tissues (such is the case with fossils). The diameter of the bony canals is a common measurement taken, and diameters for *M. domestica* are reported here, but they should not be used as proxies for the diameters of the membranous ducts.

The lengths of the slender semicircular canals, defined as the unampullated portion of the canals, relates to sensitivity of rotations by the head (Boyer and Georgi, 2007). The canal lengths were measured using the SplineProbe tool in the Amira software, wherein anchor points were placed at varying intervals at the center of the lumen of the canal. The length of the cochlear canal was measured in the same manner, with the starting point at the junction of the primary and secondary laminae.

Volumetric Measurements

Planar boundaries were maintained as much as possible between cavities and the separation between the cochlea and vestibule was made at the medial border of the fenestra vestibuli. The entirety of the fenestra itself was included within the vestibule. The canaliculus cochleae and aquaeductus vestibuli were included in the volumes of the cochlea and vestibule, respectively.

Indices and Ratios

Several indices and ratios were calculated from the linear measurements described above. Partial volumes of specific segments were calculated by dividing the volume of the segment (e.g., cochlea) by the total volume of the bony labyrinth. The majority of the remaining indices describe the aspect ratios of the arcs of the semicircular canals (which might signify agility in locomotion; see Hullar, 2006) and the cochlea, which is related to auditory capabilities (Gosselin-Ildari, 2006). The aspect ratios are calculated as respective height over width.

The stapedial ratio is a value that often is used to distinguish marsupials from placentals in systematic studies. Segall (1970) defined the ratio as the greatest height versus width of the footplate of the stapes, and he concluded that marsupials tended towards a more circular fenestra, and that placentals tended towards a more elliptical fenestra. Subsequently, the ratio has been used in phylogenetic systematic analyses (Archibald et al., 2001; Rougier et al., 1998; Wible et al., 2007).

RESULTS

The basic shape of the bony labyrinth of *Monodelphis domestica* remains constant over the ontogenetic series studied (Figure 3.3). The specific measurements described

above were plotted over number of postnatal days in order to investigate whether specific dimensions are correlated with maturity. Correlations between the measurements were calculated from these graphs, and any correlations equaling 0.70 or above are considered to be strong. There is no clear correlation between most of the angular dimensions measured and age (Table 3.2), although the total angular deviation of the lateral semicircular canal (r=0.72) expresses a strong correlation with the number of postnatal days. The oldest *M. domestica* specimens tend to have lateral semicircular canals that deviated above the canal plane to a greater degree than younger individuals.

Another measurement that is correlated strongly with age is the height of the arc of the lateral semicircular canal (r=0.80), although the width (r=0.25), length (r=0.55), and arc radius of curvature (r=0.54) are not (Table 3.3). The correlation between the length of the slender lateral semicircular canal and age is not considered strong under the parameters of the current study (r=0.67), but it is close. The coefficient of correlation likely will change with an increase in sampling of individuals.

A strong correlation is observed between age and the length of the posterior semicircular canal (r=0.79). In short, the posterior canal increases in length through the age sequence studied, even though the volume and radius of curvature of the canal do not. The length of the anterior semicircular canal is not correlated with age.

The length of the canaliculus cochleae also shows a positive correlation to age, (r=0.86; Table 3.4). This bony tube for the perilymphatic duct increases in length as the bony labyrinth matures. The canaliculus cochleae is included in the segmentation of the cochlea, and therefore its volume is included in the cochlear volume. Despite the strong correlation of the length of the canaliculus cochleae, the overall volume of the cochlea is correlated with age only weakly (perhaps as a result of grouping the volume of the canaliculus cochleae with that of the cochlea).

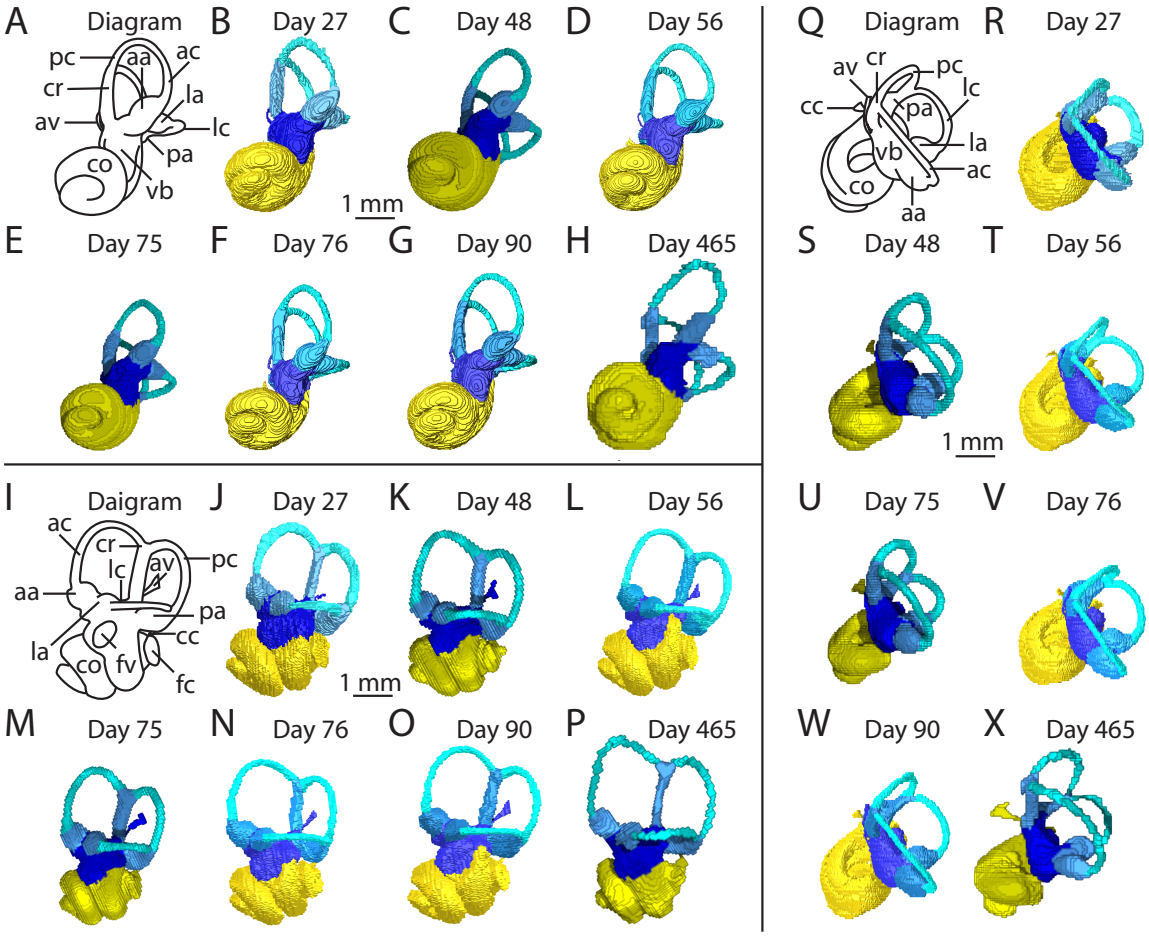

FIGURE 3.3. Comparison of endocasts of the bony labyrinths of *Monodelphis domestica* across ontogenetic ages in ventral (**A**-**H**), lateral (**I**-**P**), and posterior views (**Q**-**X**). **A**, **I**, **Q** – line drawing of bony labyrinth major features identified; **B**, **J**, **R** – TMM M 8265 (day 27); **C**, **K**, **S** – TMM M 7536 (day 48); **D**, **L**, **T** – TMM M 8266 (day 56); **E**, **M**, **U** – TMM M 7542 (day 75); **F**, **N**, **V** – TMM M 8267 (day 76); **G**, **O**, **W** – TMM M 8268 (day 90); **H**, **P**, **X** –TMM M 8273 (day 465). Anterior is towards bottom in **A**-**P**, lateral towards right in **A**-**H**, and **Q**-**X**, dorsal towards right in **I**-**P**, and ventral towards bottom in **Q**-**X**. Abbreviations: **aa** – anterior ampulla; **ac** – anterior semicircular canal; **av** aquaeductus vestibuli; **cc** – canaliculus cochleae; **cr** – common crus; **co** – cochlea; **fc** – fenestra cochleae; **fv** – fenestra vestibuli; **la** – lateral ampulla; **lc** – lateral semicircular canal; **pa** – posterior ampulla; **pc** – posterior semicircular canal; **vb** – vestibule.

TABLE 3.2. Angular measurements of the bony labyrinth across an ontogenetic series of *Monodelphis domestica*. Measurements expressed in degrees, except for number of turns. Abbreviations: **ac**, anterior semicircular canal; **co** – cochlea; **lc** – lateral semicircular canal; **pc** – posterior semicircular canal; **r** – coefficient of correlation, calculated from measurement over number of days, strong correlations italicized.

Specimen	Plane Angles			Deviation			Cochlea		
(# Days)	ac-lc	ac-pc	lc-pc	ac	lc	pc	co-lc	Coiling	Turns
TMM M-7597 (27)	88.5	88.0	86.5	4.60	5.30	8.30	33.7	682	1.90
TMM M-8261 (27)	77.9	88.0	91.9	6.90	0.00	6.00	37.9	606	1.70
TMM M-8265 (27)	84.4	103	95.5	15.2	2.50	6.80	34.3	604	1.7
TMM M-7536 (48)	88.9	89.1	80.0	25.1	3.00	8.20	62.5	658	1.8
TMM M-8266 (56)	87.1	100	86.6	12.1	7.00	3.80	47.9	665	1.9
TMM M-7539 (57)	80.9	90.0	83.9	0.00	0.00	7.80	55.9	671	1.9
TMM M-7542 (75)	87.6	95.9	98.7	20.1	3.80	8.70	57.7	658	1.8
TMM M-8267 (76)	88.9	90.1	85.9	10.9	6.10	11.8	30.2	621	1.7
TMM M-7545 (90)	91.6	100	91.4	14.5	9.20	5.50	52.9	685	1.9
TMM M-8268 (90)	96.2	102	91.0	17.3	5.80	3.20	23.0	638	1.8
TMM M-8273 (465)	73.7	83.0	87.0	15.3	12.2	3.80	65.6	650	1.8
r	0.52	0.19	0.10	0.03	*0.72*	0.39	0.46	0.07	0.07

TABLE 3.3. Linear measurements of the semicircular canals across an ontogenetic series of *Monodelphis domestica*. Measurements expressed in millimeters. Abbreviations: **ASC** – anterior semicircular canal; **d** – diameter of canal; **h** – height of canal; **l** – length of canal; **LSC** – lateral semicircular canal; **PSC** – posterior semicircular canal; **R** – arc radius; **r** – coefficient of correlation, calculated from measurement over number of days, strong correlations italicized; **Spec.** – specimen number (TMM M); **w** – width of canal.

Spec. (#	ASC					LSC					PSC				
Days)	l	h	w	R	d	l	h	w	R	d	l	h	w	R	d
7597 (27)	3.99	1.55	1.9	0.86	0.20	5.52	1.12	1.17	0.57	0.27	3.16	1.42	1.41	0.71	0.26
8261 (27)	3.18	1.8	2.02	0.96	0.21	1.91	1.08	1.21	0.57	0.24	2.92	1.39	1.64	0.76	0.18
8265 (27)	4.23	1.96	1.94	0.97	0.29	2.45	0.94	1.22	0.54	0.25	3.42	1.27	1.65	0.73	0.22
7536 (48)	4.58	1.68	2.04	0.93	0.19	2.85	1.15	1.08	0.56	0.19	3.95	1.45	1.45	0.81	0.24
8266 (56)	4.39	1.95	2.02	0.99	0.19	2.87	1.21	1.47	0.67	0.19	3.79	1.40	1.40	0.76	0.19
7539 (57)	4.35	1.80	2.02	0.96	0.21	2.51	1.03	0.99	0.51	0.19	3.69	1.39	1.40	0.73	0.22
7542 (75)	4.38	1.76	1.99	0.94	0.23	2.62	1.14	1.25	0.60	0.22	3.66	1.54	1.54	0.76	0.25
8267 (76)	4.4	1.85	2.09	0.99	0.17	2.84	1.21	1.44	0.66	0.19	3.85	1.44	1.67	0.78	0.22
7545 (90)	4.62	1.85	1.95	0.95	0.17	2.88	1.21	1.34	0.64	0.25	3.98	1.48	1.48	0.77	0.27
8268 (90)	4.68	2.19	2.14	1.08	0.17	2.56	1.15	1.37	0.63	0.20	4.17	1.56	1.75	0.83	0.20
8273 (465)	4.95	2.02	2.16	1.04	0.23	3.08	1.41	1.3	0.70	0.20	4.62	1.53	1.53	0.82	0.24
r	0.55	0.40	0.62	0.51	0.15	0.55	*0.80*	0.25	0.54	0.30	*0.73*	0.50	0.34	0.52	0.15

TABLE 3.4. Linear measurements of the cochlea and other morphological structures across an ontogenetic series of *Monodelphis domestica*. Measurements expressed in millimeters. Abbreviations: **Aq. Vest.** – aquaeductus vestibuli; **Coch. Can.** – canaliculus cochleae; **h** – height; **l** – length; **Labyr.** – bony labyrinth; **r** – coefficient of correlation, calculated from measurement over number of days, strong correlations italicized; **w** – width.

Specimen	Cochlea			Can. Coc.	Aq. Vest.	Labyr.	Skull
(# Days)	l	h	w	l	l	l	l
7597 (27)	5.08	1.4	2.21	0.29	0.83	3.91	18.4
8261 (27)	4.20	1.71	1.92	0.18	-	3.21	NA
8265 (27)	5.19	1.50	2.42	0.22	0.84	3.41	NA
7536 (48)	5.37	1.38	2.33	0.32	0.87	3.38	23.8
8266 (56)	5.37	1.39	2.42	0.57	0.84	3.42	26.3
7539 (57)	5.09	1.10	2.10	0.32	0.82	3.36	26.4
7542 (75)	4.83	1.53	2.49	0.62	1.12	3.28	29.3
8267 (76)	5.8	1.66	2.44	0.56	0.96	3.43	31.0
7545 (90)	5.22	1.36	2.34	0.46	0.85	3.43	31.0
8268 (90)	5.57	1.56	2.51	0.58	1.29	3.56	34.2
8273 (465)	4.44	1.45	2.14	1.02	-	3.57	40.5
r	0.37	0.02	0.17	*0.86*	0.52	0.60	*0.71*

No strong correlations were observed between age and partial or total volumes within the bony labyrinth (Table 3.5). The highest coefficient of correlation was calculated for volume of the lateral semicircular canal (r=0.67), which is close to, but does not meet, the criterion for being considered a strong correlation. Likewise, none of the ratios or indices expressed a strong correlation with age.

Additional correlations also were found among the inner ear dimensions themselves. For example, there is a correlation between the length of the inner ear and the radius of the arcs of the three semicircular canals (anterior, r=0.86; lateral, r=0.72; posterior, r=0.73). All of these values increase as the length of the inner ear becomes larger. The total length of the bony labyrinth also is correlated with the length of the skull (r=0.74), which in turn is correlated with number of postnatal days (r=0.71; measurements in Table 3.6). Although there is a strong link between the lengths of the inner ear and skull, the inner ear length does not correlate with age (r=0.60), as is the case with the skull.

The lengths of each canal also correlate with the respective radii of curvature (anterior, r=0.72; lateral, r=0.74; posterior, r=0.87), so that canals with large arc radii of curvature have long slender canal lengths. An additional strong correlation is observed between the aspect ratio of the anterior semicircular canal and the radius of its arc (r=0.76), but there is no observed correlation between the radius of the arc of any semicircular canal and its respective volume. Nor is a single canal more voluminous in every specimen. Either the anterior or posterior semicircular canal expressed the highest volume (each canal with the highest value in 5 of the 11 specimens). Unlike the volume, however, the anterior semicircular canal had the longest arc radius in every individual examined (see Table 3.3).

TABLE 3.5. Volumes of compartments within the bony labyrinth across an ontogenetic series of *Monodelphis domestica*. Measurements expressed in cubic millimeters. Abbreviations: **aa** – anterior ampulla; **ac** – anterior; **Crus** – common crus; **la** – lateral ampulla; **lc** – lateral; **pa** – posterior ampulla; **pc** – posterior; **r** – coefficient of correlation, calculated from measurement over number of days; **SC** – semicircular canals.

Specimen	Cochlea	SC			Ampullae			Crus	Vestibule	Total
(# Days)		ac	lc	pc	aa	la	pa			
7597 (27)	2.23	0.08	0.06	0.06	0.16	0.14	0.23	0.08	0.68	3.73
8261 (27)	2.42	0.07	0.06	0.08	0.16	0.13	0.25	0.09	0.82	4.07
8265 (27)	2.92	0.08	0.06	0.08	0.2	0.12	0.27	0.08	0.95	4.76
7536 (48)	2.46	0.08	0.05	0.07	0.13	0.19	0.11	0.11	0.75	3.94
8266 (56)	2.59	0.06	0.05	0.09	0.16	0.11	0.18	0.09	0.8	4.14
7539 (57)	1.98	0.06	0.07	0.05	0.16	0.12	0.26	0.1	0.72	3.5
7542 (75)	2.33	0.08	0.05	0.07	0.15	0.11	0.22	0.15	0.88	4.05
8267 (76)	2.4	0.08	0.06	0.08	0.2	0.14	0.28	0.1	0.83	4.18
7545 (90)	2.41	0.08	0.06	0.08	0.14	0.12	0.23	0.12	0.71	3.94
8268 (90)	2.51	0.07	0.04	0.07	0.19	0.14	0.25	0.1	0.82	4.19
8273 (465)	2.55	0.07	0.03	0.05	0.12	0.11	0.15	0.09	0.69	3.85
r	0.12	0.33	0.67	0.52	0.48	0.3	0.42	0.12	0.39	0.6

TABLE 3.6. Volume percentages and ratios calculated for the bony labyrinth across an ontogenetic series of *Monodelphis domestica*. Abbreviations: **aa** – anterior ampulla; **ac** – anterior semicircular canal; **cr** – common crus; **co** – cochlea; **la** – lateral ampulla; **lc** – lateral semicircular canal; **pa** – posterior ampulla; **pc** – posterior semicircular canal; **r** – coefficient of correlation, calculated from measurement over number of days; **vb** – vestibule.

Specimen	% Volume									Aspect Ratios				STR
(# Days)	aa	ac	cr	co	la	lc	pa	pc	vb	ac	lc	pc	co	
7597 (27)	4.35	2.09	2.23	59.90	3.78	1.53	6.23	1.53	1.83	81.50	96.20	101	63.40	1.5
8261 (27)	3.99	1.80	2.13	59.40	3.26	1.43	6.08	5.85	2.01	89.20	89.10	84.60	89.10	1.4
8265 (27)	4.23	1.71	1.67	61.30	2.52	1.27	5.69	1.73	1.99	101	77.50	77.10	62.00	1.7
7536 (48)	3.37	2.00	2.66	62.40	4.87	1.17	2.74	1.70	1.91	82.20	107	81.40	59.20	1.5
8266 (56)	3.86	1.53	2.28	62.60	2.77	1.17	4.40	2.10	1.93	96.40	82.50	84.80	57.40	1.7
7539 (57)	4.60	1.60	2.74	56.50	3.40	1.94	7.28	1.37	2.06	88.70	104	90.00	52.40	1.5
7542 (75)	3.73	1.90	3.76	57.70	2.79	1.11	5.54	1.71	2.18	88.60	91.10	101	61.50	1.5
8267 (76)	4.84	1.86	2.41	57.40	3.37	1.38	6.79	2.02	1.99	88.50	84.10	85.80	68.00	1.6
7545 (90)	3.50	1.93	3.00	61.30	3.00	1.52	5.79	1.90	1.81	94.70	90.10	92.40	58.10	1.5
8268 (90)	4.42	1.66	2.53	59.90	3.25	1.00	5.95	1.72	1.96	102	83.90	88.80	62.10	1.5
8273 (465)	3.22	1.69	2.21	66.10	2.91	0.86	3.90	1.20	1.79	93.70	108	88.70	67.80	1.3
r	0.49	0.23	0.06	0.64	0.21	0.53	0.37	0.59	0.45	0.16	0.48	0.05	0.07	0.61

The aspect ratios of the semicircular arcs are not correlated with age, and neither is the aspect ratio of the cochlea (Table 3.6). There is not a strong relationship between maturity and volume, and the percentages that the various chambers of the inner ear contribute to the bony labyrinth do not follow a pattern of change across ontogeny.

DISCUSSION

It is not surprising that there is a strong correlation between the length of the skull and age, nor should it be surprising that there is a correlation between the length of the inner ear and size of certain components such as the radii of the arcs of the semicircular canals. Yet the results reveal that there is little appreciable change in the bony labyrinth once ossification has spread through the otic region. One exception appears to be some of the dimensions of the lateral and posterior semicircular canals.

The length of the posterior canal increases after birth, which is not the case for any other features of this canal. The correlation between age and posterior canal length does not necessarily signify an ontogenetic lengthening of the membranous canal, because there is not an exact relationship between size of the bony semicircular canal and the membranous duct within it. At one extreme, the cross-sectional area of the membranous posterior semicircular duct is only 7% of the cross-sectional area of the bony canal (Curthoys et al., 1977b). Although there is a correlation between the length of the posterior canal and maturity, the strength of the correlation likely will decrease as more individuals are added to the sample. Because different aspects of the semicircular canals are correlated with age, the three canals develop in different fashions. In fact, ossification of the canals is not synchronous in humans (Jeffrey and Spoor, 2004), and the

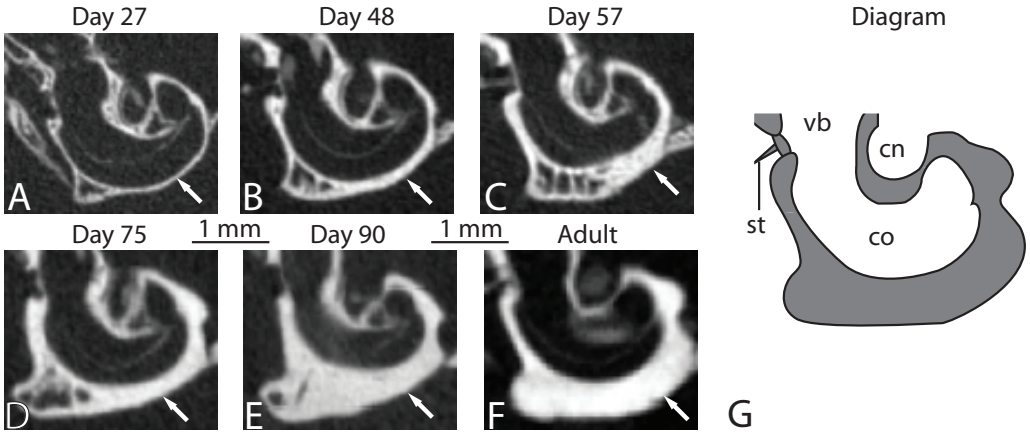

FIGURE 3.4. CT slices through the cochlea of *Monodelphis domestica*. **A**, axial slice #45 of TMM M 7595 (day 27); **B**, axial slice #34 of TMM M 7536 (day 48); **C**, axial slice #71 of TMM M 7539 (day 57); **D**, axial slice #40 of TMM M 7542 (day 75); **E**, axial slice #35 of TMM M 7545 (day 90); **f** axial slice #70 of TMM M 7599 (adult); **G**, generalized diagram through cochlea. White arrow points to tympanic surface of bony promontorium. Abbreviations: **co** – cochlea; **cn** – canal for cochlear branch of cranial nerve VIII; **st** – stapes within fenestra vestibuli; **vb** – vestibule.

membranous canals of *Didelphis* are formed at different times, with the lateral canal the last of the three to fully develop (Larsell et al., 1935).

Although there are few morphologic changes among structures inside of the petrosal across the growth series, there is a correlation between age and features on the external surface of the petrosal. For example, the facial nerve canal of elephantoid proboscideans exhibits ontogenetic variation (Chapter 2), and the length of the canaliculus cochleae, which connects the inner ear and the cranial cavity, increases over age in *M. domestica* (r=0.86). The petrosal grows via accretion of bone on external surface of the petrosal (Figure 3.4), and the canaliculus cochleae elongates in order to connect the inner ear and endocranial cavities.

Although most of the measurements taken in this study did not show a correlation with the maturity of the individual, ranges of variation were observed in every dimension. Measurements with varying values are not significant phenomena given that variation is a natural occurrence, but differences in certain measurements used in phylogenetic studies were observed, which has significant implications for the assessment of the evolutionary relationships of mammals.

One measurement that is thought to be phylogenetically informative in mammalian systematics (Rougier et al., 1998; Segall, 1970) is the stapedial ratio. Marsupials possess a stapedial ratio less than 1.8 (Segall, 1970), whereas the ratio for placentals is above 1.8 (although some eutherians are an exception; see also Ekdale et al., 2004, and Wible et al., 2001). Indeed, the average stapedial ratio for *M. domestica* (1.5) falls within the range for marsupials, but there is a range of variation in the ratio (1.3-1.7; Table 3.6), related in part to changes in the width of the fenestra vestibuli (which has a measurement range spanning 0.20 mm versus the span of 0.06 mm for the height). The stapedial ratio itself is not strongly correlated with age (r=0.61), nor does any *M.*

domestica individual possess a ratio in the placental range of Segall (1970), but the variation that is observed suggests that the use of the measurement could be problematic. It appears that the ratio varies in many taxa, not just *M. domestica*. For example, large ratios are reported for two Cretaceous mammal taxa (Ekdale et al., 2004), as well as a sampling of elephantoid petrosals collected from Pleistocene deposits (Chapter 2).

The coiling of the cochlea is another character that was used previously in phylogenetic analyses (e.g., Archibald et al., 2001; Rougier et al., 1998). The cochlea is a more-or-less straight tube in non-mammalian synapsids, and slightly curved (but not coiled) in modern monotremes (Graybeal et al., 1989). No therian mammal (Theria is the group containing the most recent common ancestor of marsupials and placentals, plus all of the descendants of that ancestor) possesses a cochlea that is coiled less than 360° (Meng and Fox, 1995), except for a few potential exceptions known for extinct forms. One of these exceptions is the Cretaceous eutherian *Uchkudukodon nessovi*, the cochlea of which is coiled at least 270°, but certainly does not complete an entire revolution (McKenna et al., 2000).

A cochlea coiled at or just under 360° might separate crown placental mammals from their closest fossil eutherian relatives. The cochlea of zalambdalestids, a Cretaceous group of mammals, which may fall outside of crown Placentalia (Wible et al., 2005, 2007), completes around one turn (Chapter 4; Kielan-Jaworowska, 1984). *Uchkudukodon nessovi* likely is outside of Placentalia as well. Broad ranges in cochlear coiling has tremendous implications for this hypothesis, especially because the variation of cochlear coiling in *M. domestica* spans 81°, nearly a full quarter of a turn (at the moment, it is unclear what the range of cochlear coiling is in other taxa).

The state of coiling in *U. nessovi* provides an example of the ambiguity to which variation can lead. The cochlea of *U. nessovi* may not coil 360°, or perhaps there is a

range in this measurement (similar to that observed in *M. domestica*) that might span the 360° boundary. If the latter is true, the cochleae of some *U. nessovi* individuals might complete a full coil while the cochleae of different individuals do not. Variation in the otic system can affect the results of phylogenetic analyses (depending on the observed state in the specimen used to score the data matrix). Although the maturity of the individual should not affect scoring of the cochlear coiling, the character does vary among individuals, and the variation should be considered when scoring matrices.

The relationships among the three semicircular canals in *M. domestica* agree with observations made on other vertebrates. The degree to which the anterior semicircular canal deviates from the plane of the canal is greater than the values for either the lateral or posterior semicircular canals (Figure 3.5). That is to say, the anterior canal is less planar than the other two, with an average total deviation of 12.9° versus 5.0° and 6.7° (for the lateral and posterior semicircular canals, respectively), which is a pattern that also is observed in laboratory mice (Calabrese and Hullar, 2006). Further, the radius of the arc of the anterior semicircular canal is the greatest of the three arcs in *M. domestica* and in various other mammals as well, including rodents, carnivorans, and primates (Blanks et al., 1972, 1975; Calabrese and Hullar, 2006; Curthoys et al., 1975; Hullar, 2006; Muren et al., 1986; Spoor and Zonneveld, 1998). The results of many studies (e.g., Calabrese and Hullar, 2006; Hullar, 2006; Hullar and Williams, 2006; Spoor et al., 2007) support the hypothesis that the radius of curvature of the semicircular canals is related to locomotor agility. Because these features of the inner ear are not correlated with age, the eventual behavior associated with labyrinthine anatomy emerges after the morphology is established in *M. domestica*.

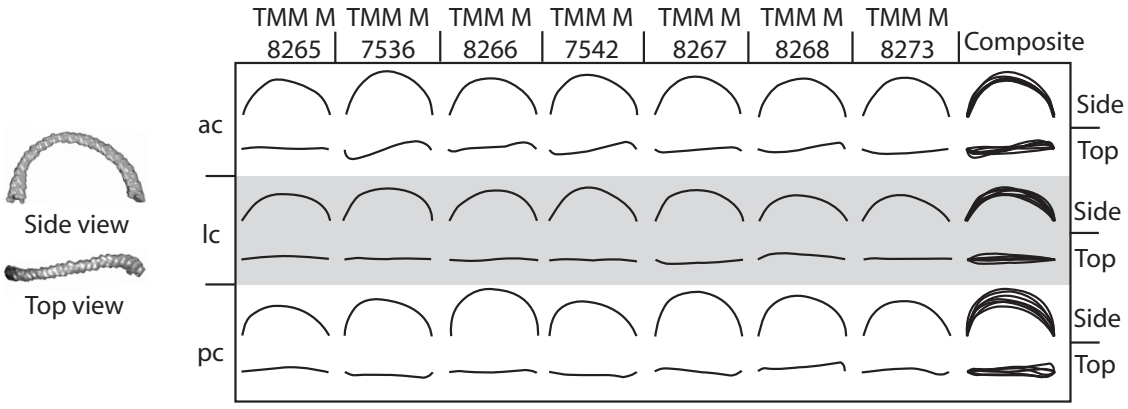

FIGURE 3.5. Comparison of the shape of the semicircular canals of *Monodelphis domestica*. An endocast of a semicircular canal is on the left, and the chart on the right includes lines drawn through the lumen of the three semicircular canals of various *M. domestica* individuals. Side view is a view perpendicular to the plane of the semicircular canal. Top view is a view parallel to the plane of the semicircular canal. The ampulla associated with the respective semicircular canal is to the right in all views. Angular deviations of specific canals reported in Table 3.2. Abbreviations: **ac** – anterior semicircular canal; **lc** – lateral semicircular canal; **pc** – posterior semicircular canal.

The variation and correlations reported here may be influenced by several additional factors. For instance, males tend towards larger bodies than females in *M. domestica* (Macrini, 2004), but the opossum sample examined here is inadequate for determining sexual dimorphism in the inner ear of *M. domestica*. Another factor affecting the observed range of variation is an artifact of specimen sampling. With the addition of more individuals, the correlation of these measurements might decrease, or else new correlations may be recovered. Future studies focused on the otic region of *M. domestica* will further elucidate the causes of variation exhibited by the inner ear

CONCLUSION

The results reported above contribute to the first reconstruction of the bony labyrinth of *Monodelphis domestica*, a biomedically important marsupial mammal, which is consistent with the anatomy and variation observed in placental mammals (Hullar and Williams, 2006; Spoor et al., 2007). The results also demonstrate that, first, taxonomists and functional anatomists need not worry about the maturity of individuals when dealing with most metrics of the inner ear of didelphid marsupials (although the implication might be indicative of a broader taxonomic pattern as there is little postossification change in the bony labyrinth of rabbits; Hoyte, 1961) as long as the bony labyrinth is ossified. In several cases, the adult form precedes the onset of function of the system. Second, there is noticeable intraspecific variation that is not related to ontogeny. The variation may be the result of one or any combination of several factors, and observed variation could influence greatly the results of physiological and phylogenetic studies.

Although most of the dimensions are immune to ontogenetic changes once the walls of the labyrinth have ossified, the variation observed within the inner ear of *M.*

domestica is an important biological phenomenon that cannot be ignored. Systematic biologists have made implicit assumptions that the inner ear is invariant throughout ontogeny. Most measurements do not vary throughout ontogeny, but there is a broad range of variation in inner ear morpholology within a single species. Without further investigation into the variation within a species, use of measurements, such as the stapedial ratio and coiling of the cochlea, in phylogenetic analyses is ill-advised.

Nonetheless, the majority of shape and size variation observed within the bony labyrinth of *M. domestica* indicate intraspecific variation, regardless of ontogenetic age, as opposed to ontogenetic trends in morphologic change. Much like the adult teeth in mammals, once the petrosal is ossified, its internal morphology does not change. The morphology of the system is locked in place before the animal achieves mature hearing or locomotor potential. Unlike teeth, however, the inner ear does not wear as it is being used. Barring any major pathology, the bony labyrinth should retain the same morphology throughout the life of the animal. Therefore, the petrosal of a juvenile is as valuable in interpreting behavior, physiology, and possibly phylogeny as is the petrosal from an elderly individual.

CHAPTER 4: THE BONY LABYRINTH OF ZHELESTIDS (MAMMALIA: EUTHERIA) AND OTHER MESOZOIC MAMMALS

ABSTRACT

Zhelestids are a group of eutherian mammals from the Late Cretaceous. High resolution X-ray computed tomography was used to image the bony labyrinths of zhelestid petrosals and to construct digital endocasts of the inner ear. The endocasts were used to measure aspects of the inner ear that are behaviorally and phylogenetically significant, including cochlear coiling, the radii of curvature of semicircular canal arcs, and canal planarity.

The morphology of the labyrinth of zhelestids agrees with that of other extinct eutherians, including *Kulbeckia kulbecke*, *Ukhaatherium nessovi*, and *Zalambdalestes lechei*. Features of the labyrinth of zhelestids include a cochlea with one and a half turns and a secondary common crus. Although isolated petrosals likely represent multiple species because several species of zhelestids are recognized based on dental characters, the degree of variation within the considered zhelestid petrosal sample is comparable to that observed in extant species. Planarities of individual semicircular canals were the most variable measurements. Coiling of the cochlea and arc radii of the semicircular canals do not vary significantly in the specimens examined. Presence of the secondary common crus and a cochlea with one and a half turns or less are plesiomorphic features of the ear of eutherians. The morphology of the bony labyrinth does not suggest any phylogenetic affinities of zhelestids, but the anatomy described will be useful for future studies of the evolution and physiology of the ear of mammals.

INTRODUCTION

The end of the Cretaceous witnessed massive extinctions of numerous animal groups (Raup and Sepkoski, 1982; Sheehan and Fastovsky, 1992), yet several dominant life forms on the planet today originated during the Cretaceous, or shortly after the Cretaceous-Tertiary boundary. Other major organisms are thought to have crossed the boundary into the Cenozoic, including angiosperms (Boulter et al., 1998), birds (Cracraft, 1986; Cooper and Penny, 1997; Clarke et al., 2005), and mammals (Hedges et al., 1996; Kumar and Hedges, 1998; Bininda-Emonds et al., 2007).

One group of mammals that plays an important role in the origin of placentals is a paraphyletic group of eutherians from the Late Cretaceous of Laurentia (Kielan-Jaworowska et al., 2004) known as zhelestids. Although zhelestids have been recovered from Europe (Pol et al., 1992; Gheerbrant and Astibia, 1994) and North America (Lillegraven, 1976; Fox, 1989; Cifelli, 1990), they are best known from Asia, particularly from the Bissekty Formation in the Kyzylkum Desert of Uzbekistan (Nessov, 1985, 1993; Nessov et al., 1998). Zhelestids contribute a rich biota to the Bissekty local fauna, where at least four, but as many as six species of zhelestids are recognized among other eutherian taxa (Archibald and Averianov, 2005, 2007).

The group "Zhelestidae" (sensu Averianov and Archibald, 2005) is paraphyletic (see Wible et al., 2007), although the named zhelestid taxa recovered from the Bissekty Formation (*Aspanlestes aptap*, *Parazhelestes mynbulakensis*, *P. robustus*, and *Zhelestes temirkazyk*; Kielan-Jaworowska et al., 2004; Archibald and Averianov, 2005, 2007) form an unnamed clade to the exclusion of other eutherian taxa (second analysis of Archibald et al., 2001; Wible et al., 2007). Because the petrosal bones referred to zhelestids were collected from the Bissekty Formation, the fossil ear regions likely represent one or more of the species within the Bissekty zhelestid group. When speaking of zhelestids in the

present chapter, I am referring only to those taxa from the Bissekty local fauna that form a monophyletic group to the exclusion of all other taxa, some of which previously were grouped within "Zhelestidae" (e.g., *Eozhelestes*).

Like most Mesozoic mammals, the Bissekty zhelestids are represented predominately by teeth (Archibald and Averianov, 2005), but other skeletal elements, including postcrania (Chester et al., 2007, 2008) and petrosal bones (Ekdale et al., 2004), have been referred to zhelestids as a group, although not to individual species. The petrosals themselves are of particular interest, given the importance of the ear region in evolutionary studies of mammals (e.g., Cifelli, 1982; Hunt, 1987; Norris, 1994). The petrosals were referred to zhelestids based on relative abundance, size, and anatomy (see Ekdale et al., 2004), and although none of the fossil petrosals were assigned to individual zhelestid species recognized in the Bissekty local fauna, they were used in conjunction with teeth in phylogenetic analyses exploring the relationships among Cretaceous eutherian taxa and members of extant placental clades (Archibald et al., 2001; Wible et al., 2007).

The phylogenetic affinities of the Bissekty zhelestid clade to other Mesozoic mammals are contentious. The teeth of many zhelestids appear derived (Nessov et al., 1998; Archibald et al., 2001), but the petrosals referred to Bissekty Formation zhelestids retain features that are considered ancestral for therians, such as the prootic canal (Ekdale et al., 2004). Using primarily data from teeth, competing hypotheses either include all Bissekty zhelestid taxa as stem members of archaic ungulate lineages within crown Placentalia (Archibald, 1996; Nessov et al., 1998; Archibald et al., 2001), or else exclude zhelestid taxa from Placentalia altogether (Wible et al., 2007). In the latter case, zhelestids occupy basal positions on the eutherian phylogeny. A final hypothesis that has

not been proposed is an inclusion of some zhelestid taxa within Placentalia, such as the Bissekty clade, with an exclusion of other non-Bissekty zhelestids.

Because information from dental material and the middle ear region of the Bissekty zhelestids has yielded conflicting results, additional data may provide crucial information concerning the relationship among zhelestids and other eutherians, both extinct and extant. Toward an ultimate goal of resolving the positions of the Bissekty zhelestids, I herein describe new details of the inner ear of these mammals. The external morphology of the petrosals is well described (Ekdale et al., 2004), but a thorough description of the internal cavities of the petrosal is lacking. The inner ear is difficult to study, because the structures are contained in cavities that are completely surrounded by bone. With the use of high resolution X-ray computed tomography (CT), the bony labyrinth is easily observed. Computed tomographic data was incorporated in investigations of several previous studies focused on the inner ear of a variety of extinct mammals (Luo and Ketten, 1991; Luo and Eastman, 1995; Hublin et al., 1996; Hurum, 1998; Spoor et al., 2002), and the sample of zhelestid petrosals from the Bissekty Formation provides a unique opportunity to study the auditory and vestibular anatomy of these enigmatic mammals.

Despite the difficulty in observing the bony labyrinth, the anatomy of the inner ear was used previously to make physiological interpretations about fossil taxa, including pterosaurs (Witmer et al., 2003), dinosaurs (Alonso et al., 2004; Clarke, 2005), multituberculates (Miao, 1988; Meng and Wyss, 1995), early therians (Meng and Fox, 1995), primates (Spoor et al., 1994, 1996), bats (Simmons et al., 2008), and cetaceans (Fleischer, 1976; Geisler and Luo, 1996; Luo and Marsh, 1996; Spoor et al., 2002). Furthermore, certain aspects of the bony labyrinth are phylogenetically informative for

early humans (Hublin et al., 1996) and higher taxonomic levels (e.g., the cochlea differs between therian and nontherian mammals; Rowe, 1986, 1988; Luo and Ketten, 1991).

Although additional work is needed to clarify the affinities of zhelestids, the goal of the present paper is not to place the Bissekty zhelestids on a phylogenetic tree, nor is it an attempt to assign isolated petrosal specimens to specific zhelestid taxa diagnosed by dental morphology. Rather, the goal is to describe a novel body of data for zhelestids and other Cretaceous eutherian taxa. The described anatomy will prove beneficial to future studies investigating the phylogenetic and physiological implications of the inner ear, and the variation observed across the zhelestid sample initiates a discussion of variation and variability within an anatomical system that often is assumed to be morphologically conservative. Variation within the inner ear of mammals is discussed in clinical literature (Caix and Outrequin, 1979; Dimopoulos and Muren, 1990), and the phenomenon of morphological variation may affect phylogenetic hypotheses in significant ways.

Institutional Abbreviations

PSS-MAE, Collections of Joint Paleontological and Stratigraphic Section of the Geological Institute, Mongolian Academy of Science, Ulaanbaatar – American Museum of Natural History, New York; **TMM M**, Texas Natural Science Center recent mammal collections, Vertebrate Paleontology Laboratory; **URBAC**, Uzbekistan/ Russian/ British/ American/ Canadian joint paleontological expedition, Kyzylkum Desert, Uzbekistan, specimens in the Institute of Zoology, Tashkent; **ZIN C.**, Systematic Collections, Zoological Institute, Russian Academy of Sciences, Saint Petersburg, Russia.

MATERIALS AND METHODS

Computed Tomography Methods

Seven isolated petrosals assigned to zhelestids from the Late Cretaceous Bissekty Formation of Uzbekistan were CT scanned at the University of Texas High Resolution X-ray CT facility (UTCT). A complete list of specimens scanned for this study, along with the parameters used during scanning and post-scanning image processing, is provided in Appendix 1.

The bony labyrinths of the Bissekty zhelestids were digitally segmented into the constituent parts of the inner ear (e.g., cochlea and vestibule) in order to calculate partial volumes for the inner ear cavities. Segmentation is accomplished by isolating the voxels on CT slices that define the anatomical structure of interest (such as the anterior semicircular canal). Individual CT slices are 'stacked', and the extracted volume of the selected voxels is visualized as a 3-dimensional (3D) endocast that can be studied and measured. Segmentation and endocast extractions were performed in the computer programs VG Studio Max 1.2 © (Volume Graphics) and Amira 3.1 ©. The bony channels for the cochlear and vestibular aquaeducts were included in the segments of the cochlea and vestibule respectively. Canals for branches of cranial nerve VIII were not segmented, nor were they included in any measurement. Planar boundaries between the components were maintained as much as possible. The medial border of the fenestra vestibuli (oval window) was used as the divider between the cochlea and vestibule, with the entirety of the opening within the vestibule.

Measurement Methods

Several angular, linear, and volumetric measurements were made using the Amira software. Most of these measurements are used to interpret physiology and evolutionary relationships of a wide variety of mammals. Dimensions of the structures of the bony labyrinth were measured on the endocasts, and the inner ear morphology of the Bissekty zhelestids was compared to original observations and published information about other Cretaceous eutherians, namely the Mesozoic eutherians *Ukhaatherium nessovi*, *Kulbeckia kulbecke*, and *Zalambdalestes lechei* (see Appendix 1 for specimens and scanning parameters). Two skulls of *Zalambdalestes* were examined, for which two petrosals each are preserved (four labyrinths total). However, PSS-MAE 130 is damaged through the left petrosal, and portions of the left labyrinth of that specimen are missing. The four labyrinths of *Zalambdalestes* were treated independently, as though they were from isolated elements like the zhelestid sample. This allows me to explore cranial asymmetry between right and left bony labyrinths from the same skull.

Measurement methodologies follow those conceived by Fleischer (1976) and Spoor and Zonneveld (1995), unless otherwise noted. Anatomical terminology of the bony labyrinth follows Sisson and Grossman (1938) and Evans (1993), and orientation terminology within the cochlea follows Fleischer (1976).

Measurements of the cochlea involve the degree of coiling completed by the canal, as well as gross length of the canal and widths of internal cochlear structures (Figure 4.1). The degree of coiling completed by the cochlea is calculated following two separate methods, one modified from that proposed by West (1985), and the other a method employed by Geisler and Luo (1996). The two methods are the same operationally, although they utilize different landmarks (Figure 4.1A). Both methods draw a line from the axis of rotation to a secondary landmark at the base of the cochlea

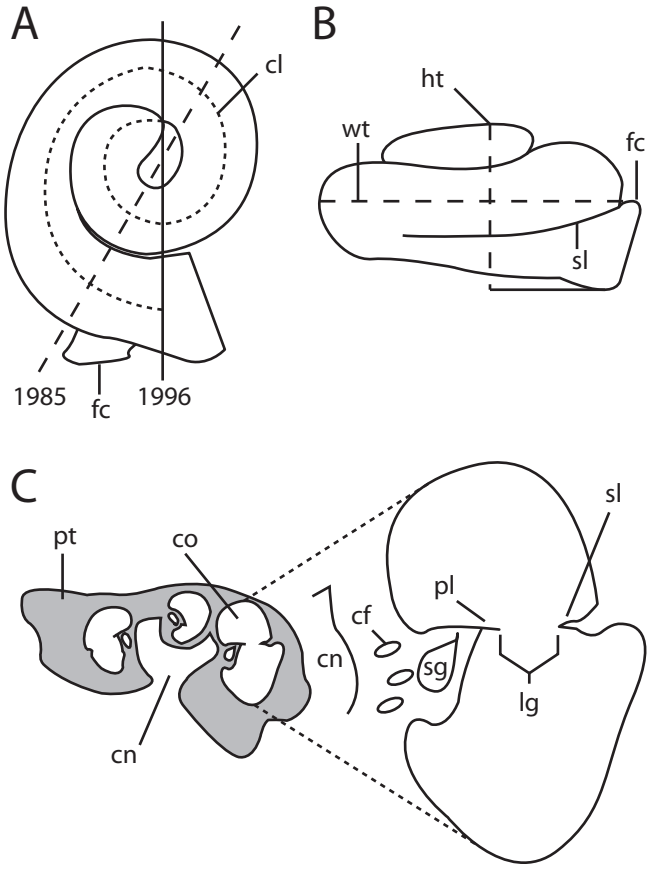

FIGURE 4.1. Diagrams of measurements of cochlear dimensions. **A**, cochlea in vestibular view with straight lines used to count number of turns that intersect axis of rotation (at intersection of lines) and secondary landmarks of West (1985) and Geisler and Luo (1996); **B**, cochlea in profile to measure height and width of cochlear spiral. **C**, cross section through cochlea with expanded view of cochlear canal. **Abbreviations**: **1985**, dashed line intersecting land mark of West (1985); **1996**, solid line intersecting landmark of Geisler and Luo (1996); **cf**, foramina within cribriform plate for nerves connecting cranial nerve VIII and spiral ganglion; **cl**, dashed line representing length of cochlea, approximating length of basilar membrane; **cn**, canal for cochlear branch of cranial nerve VIII; **co**, cochlea; **fc**, fenestra cochleae; **ht**, height of cochlear spiral; **lg**, laminar gap between primary and secondary bony laminae; **pl**, primary bony lamina; **pt**, petrosal bone; **sg**, canal for spiral ganglion; **sl**, secondary bony lamina; **wt**, width of cochlear spiral.

near the fenestra cochleae when the cochlea is in vestibular ('map') view. The number of times that the cochlea crosses this line is counted and multiplied by 180° to provide a gross value of cochlear coiling. An additional value is added to this product – an angle measured between the line drawn through the cochlea and a line drawn from the center of the axis of rotation to the most apical point of the cochlear canal. This second angle falls on a plane parallel to the field of view (perpendicular to the axis of the cochlea). The total measurement of coiling of the cochlea is expressed both as number of degrees and total number of turns (total number of degrees divided by 360°).

The secondary landmark used by West (1985) is the point of inflection of the cochlea near the vestibule, which at times is very close to the fenestra cochleae. Most subsequent researchers used West's landmark to measure the coiling of the cochlea (e.g., Wible et al., 2001). However, the exact point of inflection is somewhat arbitrary, especially if the inflection is a continuous curve, rather than a sharp angle. The landmark used by Geisler and Luo (1996) is at the beginning of the laminar gap, or the space between the bony primary and secondary laminae on the axial and radial walls of the cochlear canal respectively (Figure 4.1A, C). The basilar membrane, upon which the organ of hearing sits in life, occupies the laminar gap. Because the membrane and associated organ of hearing is the functional unit of the cochlea, it is more appropriate biologically to start measuring the coiling of the cochlea at the beginning of this functional unit, rather than a more arbitrary inflection in the canal. Nevertheless, many researchers followed the method proposed by West (1985), so measurements obtained using that method are reported here for comparative purposes alongside measurements following the method of Geisler and Luo. Only the measurements following Geisler and Luo (1996) are discussed in the text.

The width of the cochlea is a linear measure of the size of the basal turn of the cochlea, and the height of the cochlea is a measure of the overall height of the cochlear spiral (following Gosselin-Ildari, 2006). Both measurements fall on the plane that intersects all points along the axis of cochlear rotation and the center of the fenestra cochleae. The width of the cochlea is measured as the greatest distance from the vestibular edge (closest to the apex of the spiral) of the fenestra cochleae to the radial wall on the opposite side of the basal turn of the cochlear canal (Figure 4.1B). This measurement is parallel to the plane of the basal turn of the cochlea. The height of the cochlea is measured as the greatest vertical distance (perpendicular to width) from the level of the most tympanal edge of the fenestra cochleae to the vestibular-most wall of the cochlear spiral (within the apical turn). The aspect ratio of the profile of the cochlea, calculated as the height over the width, may correlate to auditory ability (Gosselin-Ildari, 2006).

The overall length of the cochlear canal extends from the beginning of the laminar gap (landmark used for measuring number of turns in the cochlea following Geisler and Luo, 1996) to the apical most point of the canal, as measured with the SplineProbe tool in the Amira software (Figure 4.1A). The length of the canal approximates the length of the basilar membrane, which West (1985) argued is related to audible frequencies.

Multiple measurements were made for structures within the cochlear canal (following Fleischer, 1976). These include the width of primary and secondary laminae, laminar gap between the laminae, and diameter of the spiral nerve ganglion canal within the primary lamina (Figure 4.1). The measurements were taken on two perpendicular planes, each of which bisects the cochlea across the axis of rotation, which is exemplified by the section through the cochlea of URBAC 03-39 depicted in Figure 4.1C. One plane intersects the point at which the basilar membrane begins (same landmark used for

measuring coiling of the cochlea following Geisler and Luo, 1996), as well as the axis of rotation. The second plane is perpendicular to the first, and measurements were taken from cross-sections at each quarter turn throughout the length of the cochlea on both of the planes. The width of the laminar gap was measured as the distance between the primary and secondary laminae as long as both structures were present, and between the primary lamina and the radial wall of the canal when the secondary lamina was absent (the secondary lamina does not extend the entire length of the cochlea).

The internal cochlear measurements were used for graphical reconstructions of the widths of the internal cochlear structures, following a method conceived by Guild (1921), and later modified by Schuknecht (1953) and Wever et al. (1971 a, b). Such reconstructions previously were drawn for multiple species of fossil and extant cetaceans (Luo and Eastman, 1995; Geisler and Luo, 1996; Luo and Marsh, 1996). The widths of the internal structures (laminar gap in particular) are related to inner ear function, and the type of diagrams described here allow accurate observation of the relative proportions of the two bony cochlear laminae. The longitudinal and transverse diameters of the basal turn are constrained in these 'cochlear maps'. Because parts of the apical turns of the cochlea (beyond the basal turn) obstruct the basal turn in vestibular view, the turns beyond the basal turn are distorted in the illustrations to allow observation of the cochlea in its entirety.

One additional measurement of the cochlea is the angle between the basal turn of the cochlea and the lateral semicircular canal. The lateral canal is parallel to the horizon when an animal is at rest as evidenced by X-radiographs of several mammals (de Beer, 1947). Although right and left lateral canals are not always symmetrical within the same skull (Caix and Outrequin, 1979), the angle between the cochlea and lateral canal provides a rough estimate of the angle of the cochlea to the horizon. The average plane of

the cochlea intersects points at the center of the lumen of the basal turn of the cochlear canal, and the plane of the lateral canal fits to points at the center of the lumen at the midpoint of the canal and the entry points of the canal into the vestibule.

Measurements of the vestibular apparatus, which includes the semicircular canals, include angles between the planes of the canals, the angular deviation of each canal from its average plane, the arc radius of curvature of each canal, and the length of the slender canals (i.e., the course of the canal that does not include the ampulla, sensu Boyer and Georgi, 2007; Figure 4.2). Angles between the planes of the three semicircular canals are measured with both planes perpendicular to the field of view. The average plane of a canal is fit to points at the center of the lumen at the midpoint of the arc of the canal, and the entry points of the canal into its ampulla at one end and vestibule at the other. The common crus is included with the paths of both the anterior and posterior semicircular canals, and the posterior ampulla is included with the path of the lateral semicircular canal when a secondary common crus is present.

The slender canal is defined as the course of the canal that does not include the ampullated portion (sensu Boyer and Georgi, 2007). The lengths of the three slender semicircular canals were measured in the Amira software using the SplineProbe tool in the same fashion used to calculate the length of the cochlear canal, and the curved line created by the tool passes through he center of the lumen of the canal (Figure 4.2A).

The radius of curvature of a semicircular canal (‘R’ of Jones and Spells, 1963) describes the size of the arc completed by the canal, following Spoor and Zonneveld (1995). The radius is calculated as half the average of the height and width of the canal arc (Figure 4.2A-B). The height of the anterior canal is measured as the greatest distance from the wall of the vestibule to the center of the lumen of the canal, perpendicular to the plane of the lateral semicircular canal. The height of the posterior canal is measured as

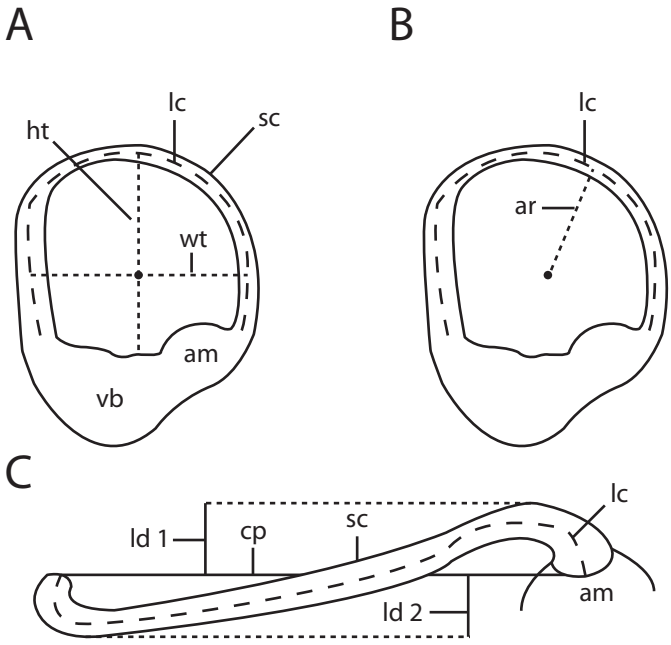

FIGURE 4.2. Diagrams of measurements of semicircular canal dimensions. **A**, semicircular canal in profile displaying height and width of arc and length of slender canal; **B**, semicircular canal in profile displaying radius of arc; **C**, semicircular canal viewed when plane is parallel to horizon (solid line behind canal), displaying linear deviations of canal from its plane. Total angular deviation equals the arcsine of linear deviation 1 over radius plus arcsine of linear deviation 2 over radius. **Abbreviations**: **am**, ampulla; **ar**, arc radius of curvature ('R' of Jones and Spells, 1963); **cp**, plane of semicircular canal; **ht**, height of semicircular canal arc; **lc**, length of slender (unampullated) semicircular canal; **ld**, linear deviation of semicircular canal from its plane; **sc**, semicircular canal; **vb**, vestibule; **wt**, width of semicircular canal arc.

the greatest distance from the center of the lumen of the posterior limb of the canal to the center of the lumen of the common crus, parallel to the plane of the lateral semicircular canal. The height of the lateral canal is measured as the greatest distance from the wall of the vestibule to the center of the lumen of the canal. The widths for all canal arcs are measured as the greatest distance between the center of the lumen in opposing limbs of the canal, and perpendicular to the height of the respective canal.

The total angular deviation of a semicircular canal from its respective average plane is calculated using trigonometry and two linear measurements of the canal (adapted from Calabrese and Hullar, 2006, and Hullar and Williams, 2006). The linear measures of the canal are the arc radius of curvature of the canal and the linear deviation of the canal from the plane. The linear deviation is measured when the plane is perpendicular to the field of view (Figure 4.2C). The maximum distance between the center of the lumen of the canal and the average plane are measured on both sides of the plane. The angular deviation of the canal on each side of the plane is calculated as the arcsine of the linear deviation divided by the arc radius of curvature. The total angular deviation is the sum of the angular deviations on both sides of the plane.

Variation Methods

Because multiple species of zhelestids are recognized based on teeth recovered from the same deposits as the petrosals within the Bissekty Formation, any variation in the measurements described above for the Bissekty zhelestids might reflect species-level differences. In order to explore whether or not the variation observed within the zhelestid sample is any greater or less than that observed within a single species, endocasts were constructed for multiple individuals of the extant placentals *Dasypus novemcinctus* and

Tadarida brasiliensis, as well as the extant marsupial *Monodelphis domestica* (see Appendix 1). Although *Monodelphis* is not a eutherian mammal, the ontogeny of the inner ear within didelphid marsupials is similar to the ontogeny of the auditory region in placental mammals (Larsell et al., 1935; Reimer, 1996; Morsli et al., 1998). Because of this, the patterns observed in *M. domestica* can be compared to that of other therian mammals.

The coefficient of variation (CV) was calculated in order to visualize and compare amounts of variation among the various taxa listed in Appendix 1. The value is reported as a percentage of the standard deviation with respect to the arithmetic mean. A CV is a standardized value, and it can be compared between systems with different units, as well as significantly different means. Because the coefficient is a ratio of standard deviation to mean, high CV value indicates a high degree of variation in the measurement under question. A CV of 100 indicates that the standard deviation is equal to the mean.

BONY LABYRINTH OF ZHELESTIDS

The inner ear of mammals contains a series of connected soft tissue ducts and sacs that together embody the membranous labyrinth that is housed in the bony canals and cavities of the bony labyrinth. The membranous labyrinth is divided into an inferior division that includes the membranous cochlear duct and saccule of the vestibule, and a superior division that includes the utricle of the vestibule, the three membranous semicircular ducts (anterior, posterior, and lateral) with their respective ampullae, and the common crus between the anterior and posterior semicircular ducts. The bony semicircular canals and cochlea of the bony labyrinth approximate the shape of the membranous ducts, although not necessarily the size (see Curthoys et al., 1977b). The

bony vestibule is divided into an inferior spherical recess and superior elliptical recess (see Figure 4.3). The spherical and elliptical recesses loosely correspond to the saccule and utricle respectively, but there is little of the shape and size of the membranous vestibule preserved within the bony vestibular cavity (as opposed to divisions observed within the bony labyrinths of non-mammalian amniotes; Georgi and Sipla, 2008). Unfortunately, the membranous labyrinth is not preserved in the fossils, so all information gleaned from the inner ear of extinct mammals, such as zhelestids, is derived from the bony labyrinth by necessity. Volumes of the cochlea, vestibule, and bony labyrinth as a whole is presented in Table 4.1.

Cochlear Canal

Dimensions of the bony cochlear canal (housing the membranous cochlear duct) are presented in Table 4.2. The cochlea of the Bissekty zhelestids communicates with the middle ear cavity via the fenestra cochleae, which is located near the basal end of the bony cochlear canal (Figure 4.3). A curved groove within the bony cavity is situated internal to the fenestra cochleae. The groove is expressed as an outpocketing on the endocast, and it likely accommodated the perilymphatic sac in life, because it leads into the bony channel for the perilymphatic duct known as the canaliculus cochleae. The canaliculus opens onto the external surface of the petrosal dorsomedial to the fenestra cochleae. Further discussion and orientation of the canaliculus cochleae was provided by Ekdale et al. (2004).

The cochlea contributes 60% of the total volume of the inner ear cavity. Table 4.1 includes a list of volumes of the cochlea and vestibule for Bissekty zhelestids. The cochlear canal itself is coiled and it invariably turns medioventrally from the fenestra

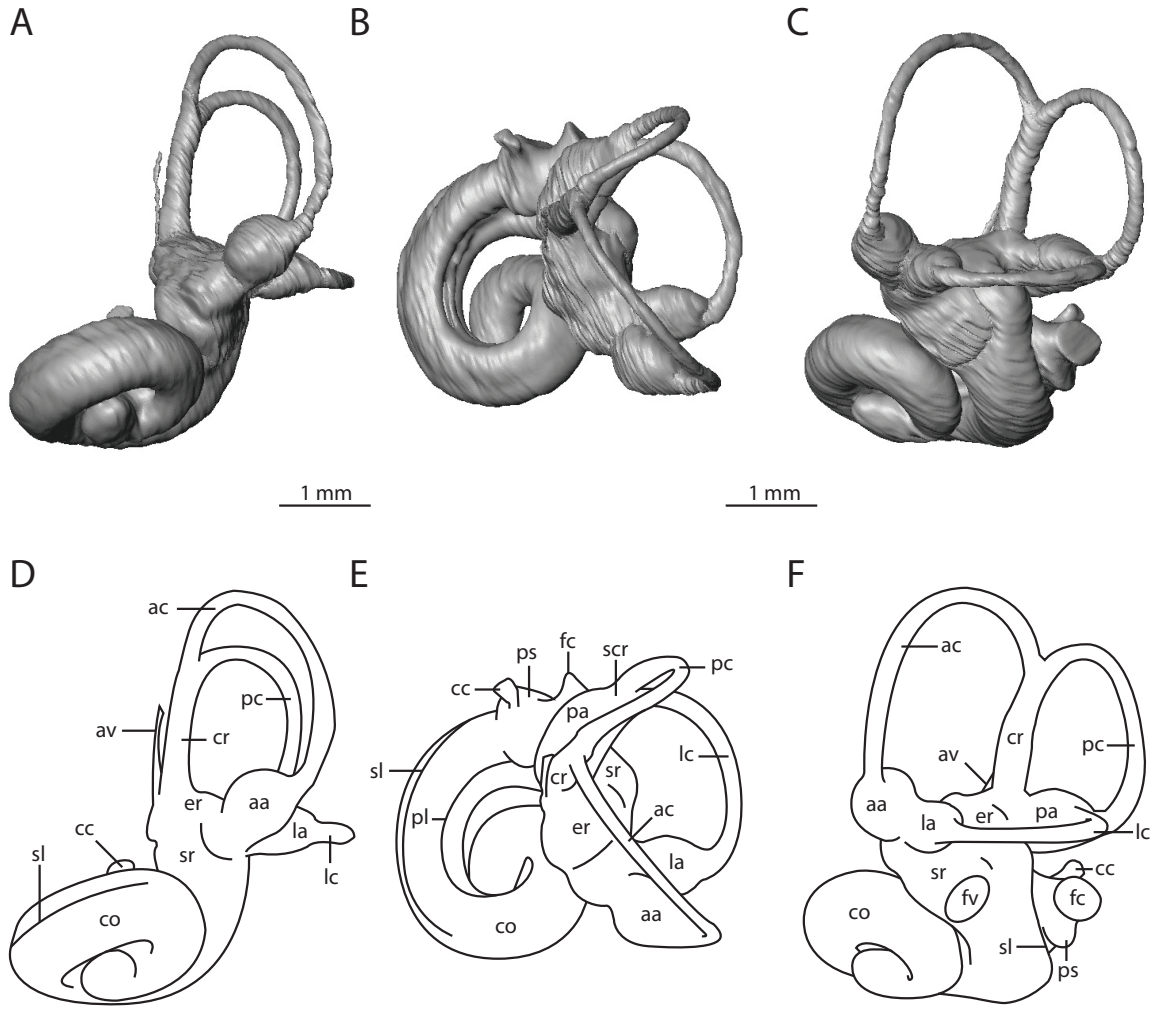

FIGURE 4.3. Endocast of left zhelestid bony labyrinth (URBAC 03-39). Orientations are approximated because petrosals are isolated from the cranium. **A-C**, digital endocasts; **D-F**, line drawings of labyrinth with labels; **A** and **D**, anterior view with dorsal towards top and lateral towards right; **B** and **E**, dorsal view with posterior towards top and lateral towards right; **C** and **F**, lateral view with dorsal towards top and posterior towards right. **Abbreviations**: **aa**, anterior ampulla; **ac**, anterior semicircular canal; **av**, aquaeductus vestibuli; **cc**, canaliculus cochleae; **co**, cochlea; **cr**, common crus; **er**, elliptical recess of vestibule; **fc**, fenestra cochleae; **fv**, fenestra vestibuli; **la**, lateral ampulla; **lc**, lateral semicircular canal; **pa**, posterior ampulla; **pc**, posterior semicircular canal; **pl**, primary bony lamina; **ps**, outpocketing for perilymphatic sac; **scr**, secondary common crus; **sl**, secondary bony lamina; **sr**, spherical recess of vestibule.

TABLE 4.1. Volume of the cochlea, vestibule (including semicircular canals and ampullae), and entire bony labyrinth for zhelestids and other selected Cretaceous eutherians listed in Appendix 1. Only specimens with a complete cochlea and vestibular apparatus are reported. Dashes indicate measurements unavailable on account of poor preservation of the specimen. Values expressed in mm^3.

Specimen	Cochlea	Vestibule	Total
Zhelestid			
URBAC 99-73	5.59	-	-
URBAC 03-39	3.65	2.02	5.67
URBAC 04-233	3.75	3.14	6.89
Zhelestid Average	4.15	2.58	6.28
Kulbeckia kulbecke			
URBAC 98-113	0.667	-	-
URBAC 00-16	3.51	-	-
URBAC 02-56	3.13	-	-
URBAC 04-36	3.07	2.30	5.37
Kulbeckia Average	2.59	2.3	5.37
Ukhaatherium nessovi			
PSS-MAE 110	1.23	0.943	2.17
Zalambdalestes lechei			
PSS-MAE 108 - left	2.31	3	5.59
PSS-MAE 108 - right	2.47	3.05	5.52
PSS-MAE 130 - left	3.44	3.65	7.09
PSS-MAE 130 - right	3.41	-	-
Zalambdalestes Average	2.91	3.23	6.07

TABLE 4.2. Dimensions and orientations of the cochlea of zhelestids and other Cretaceous eutherians. Coiling follows West (1985; C-85) and Geyser and Luo (1996; C-96), expressed in degrees. Number of turns calculated from coiling following Geisler and Luo (1996). Length, height, and width expressed in millimeters. Angle refers to angle between the cochlea and plane of the lateral semicircular canal, expressed in degrees.

Specimen	C-85	C-96	# Turns	Length	Height	Width	Angle
Zhelestid							
URBAC 99-02	498	532	1.5	4.40	1.27	2.84	32.2
URBAC 99-41	505	531	1.5	4.57	1.15	2.98	34.4
URBAC 99-73	567	596	1.7	5.45	1.60	2.91	-
URBAC 03-39	511	545	1.5	5.17	1.37	3.01	31.8
URBAC 04-233	532	547	1.5	5.08	1.33	3.05	36.2
ZIN C. 85511	500	523	1.5	4.78	1.55	2.81	40.9
ZIN C. 85512	514	540	1.5	5.05	1.22	2.96	28.5
Zhelestid Average	518	545	1.5	4.93	1.36	2.94	34.0
Kulbeckia kulbecke							
URBAC 98-113	385	390	1.1	2.94	0.770	1.84	16.4
URBAC 00-16	464	487	1.4	4.52	1.29	2.96	16.0
URBAC 02-56	429	460	1.3	4.53	1.34	2.86	5.54
URBAC 04-36	427	448	1.2	4.46	1.28	2.87	10.3
Kulbeckia Average	426	446	1.2	4.11	1.17	2.63	12.1
Ukhaatherium nessovi							
PSS-MAE 110	371	380	1.1	2.77	0.830	2.40	6.63
Zalambdalestes lechei							
PSS-MAE 108 - lt	360	365	1.0	3.35	0.920	2.84	10.1
PSS-MAE 108 - rt	360	382	1.1	3.27	0.960	2.94	11.4
PSS-MAE 130 - lt	340	350	0.97	3.49	1.19	2.81	19.2
PSS-MAE 130 - rt	360	376	1.0	3.47	1.18	3.17	13.1
Zalambdalestes Average	355	368	1.0	3.40	1.06	2.94	13.5

cochleae. The cochlea of the zhelestids completes nearly 1.5 turns on average (518º), which is a slightly larger value than previous estimates made using damaged specimens (Ekdale et al., 2004). The average length of the cochlea is 4.93 mm. The cochlear canal as a whole is planispiral in profile, and the average aspect ratio of the cochlea (height versus width) is 46.3. An osseous wall separates the basal and apical turns of the cochlear spiral, as illustrated in Figure 4.1C. The cochlea is inflected near the confluence of the cochlear canal and vestibule, lateral to the fenestra cochleae. The plane of the basal turn of the cochlea is not parallel to the plane of the lateral semicircular canal in zhelestids, but rotated ventrally 34°.

In life, the spiral organ of hearing rests upon a soft tissue structure known as the basilar membrane, which is supported by a bony primary spiral lamina on the axial surface of the cochlear curve, and either a secondary lamina or the wall of the canal on the radial surface of the curve (Figure 4.1C). Within the primary lamina is a canal for the ganglion of the spiral nerve. The CT scan slices reveal a cribriform plate between the canal for the spiral ganglion and the canal for the auditory branch of cranial nerve VIII, which is housed within the modiolus (bony axis) of the cochlea (Figure 4.1C). The cribriform plate is perforated with numerous foramina for branches of the auditory nerve leading into the spiral nerve ganglion.

The widths of the primary and secondary bony laminae, laminar gap, and spiral ganglion canal at each quarter turn are listed in Table 4.3. The primary spiral lamina extends along the inside of the coil for most of the length of the cochlea, as is illustrated in the graphical reconstructions provided in Figure 4.4. The lamina is broadest at the base of the cochlea and it decreases gradually before disappearing near the tip of the canal. Likewise, the diameter of the canal for the spiral nerve ganglion, which is surrounded by

TABLE 4.3. Dimensions of internal structures of the cochlea at each quarter turn of coiled canal for zhelestids and other Cretaceous eutherians. Measurements for *Zalambdalestes lechei* only taken for the right labyrinth of PSS-MAE 108 and left labyrinth of PSS-MAE 130 on account of poor preservation. Internal structures not preserved in CT scans of *Ukhaatherium nessovi*. Dashes signify absence of the structure in that turn of cochlea. Measurements expressed in millimeters.

	Cochlea turns				
	1/4	2/4	3/4	4/4	5/4
Zhelestid					
Primary lamina width	0.25	0.22	0.19	0.15	0.13
Secondary lamina width	0.11	0.06	0.04	-	-
Laminar gap width	0.45	0.46	0.48	0.51	0.54
Diameter of spiral ganglion canal	0.18	0.13	0.13	0.11	0.09
Kulbeckia kulbecke					
Primary lamina width	0.32	0.29	0.28	0.28	-
Secondary lamina width	0.1	0.05	0.03	-	-
Laminar gap width	0.28	0.35	0.37	0.47	-
Diameter of spiral ganglion canal	0.19	0.19	0.19	-	-
Zalambdalestes lechei					
Primary lamina width	0.40	0.35	0.26	-	-
Secondary lamina width	0.06	-	-	-	-
Laminar gap width	0.38	0.43	0.50	0.48	-
Diameter of spiral ganglion canal	0.21	0.16	0.13	-	-

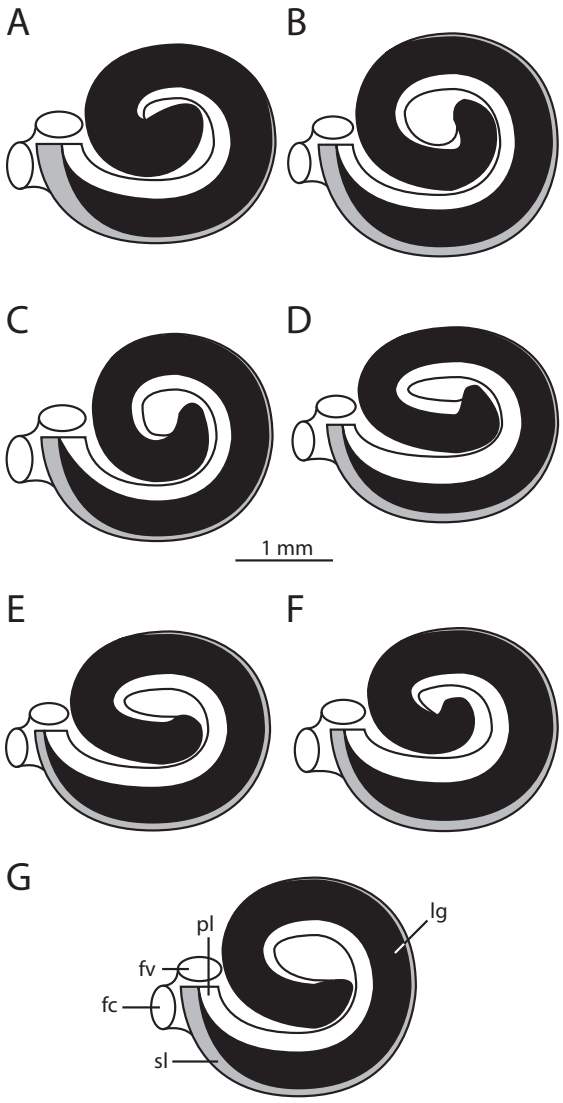

FIGURE 4.4. Graphic reconstructions of internal structures of the cochlea of zhelestid specimens following methods of Guild (1921), Schuknecht (1953), and Wever et al. (1971 a, b). Internal structures are poorly preserved for URBAC 99-41, and the cochlea is not reconstructed for that specimen. **A**, URBAC 99-02; **B**, URBAC 99-73; **C**, URBAC 03-39; **D**, URBAC 04-233; **E**, ZIN C. 85511; **F**, ZIN C. 85512; **G**, Average across sample with labels. Orientations of **B**, **C**, **E**, and **F** reversed for comparison. Longitudinal and transverse diameters of basal turn conserved, in each image, but apical turn distorted to allow observation of complete canal. **Abbreviations**: **fc**, fenestra cochleae; **fv**, fenestra vestibuli; **lg**, laminar gap (black band); **pl**, primary bony labyrinth (white band); **sl**, secondary bony labyrinth (gray band).

the primary lamina, is largest near the base of the cochlea and tapers similarly before it disappears near the apical terminus of the primary lamina (Table 4.3).

The secondary bony lamina is present in the zhelestid inner ear, but the osseous ridge, which is expressed on the endocast as a groove along the outside surface of the cochlea (Figure 4.3), does not extend much beyond 1/2 to 3/4 of the basal turn of the cochlea (Table 4.3). The basilar membrane would attach to the radial wall of the canal after the secondary lamina disappears within the last half or quarter of the basal turn to the apex of the cochlea. As with the primary lamina, the secondary lamina is broadest at the base of the cochlea and diminishes rapidly before it disappears.

The laminar gap is less than 0.5 mm at the base of the cochlea in all of the zhelestids examined, and it widens towards the apex (as the primary and bony laminae decrease in width; Figure 4.4). The widening of the laminar gap is punctuated within individual specimens, rather than a continuous increase to the end of the canal. However, when the laminar gap is averaged across the zhelestid sample, there is a continuous increase in width (Table 4.3).

Vestibule and Semicircular Canals

The vestibule is partially divided in the Bissekty zhelestids into the small spherical recess and the larger elliptical recess, where the spherical is continuous with the cochlea and communicates with the middle ear cavity via the fenestra vestibuli (Figure 4.3). The elliptical recess is mediolaterally extended with two lateral and three medial openings. The lateral openings are for the lateral and anterior ampullae, with the opening for the lateral ampulla closer to the spherical recess and fenestra vestibuli. Those openings are located in a separate depression within the elliptical recess (that depression

appears as an outpocketing of the vestibule in the endocast). The three openings that penetrate the opposite wall of the vestibule are entrances into the posterior ampulla, common crus, and the much smaller opening for the aquaeductus vestibuli posterodorsal to the common crus. A secondary common crus that connects the lateral and posterior semicircular canals to the posterior ampulla is observed in the zhelestid labyrinth, and there is no separate opening into the vestibule for the lateral semicircular canal (Figure 4.3).

The planes of the semicircular canals form approximately right angles with each other, and although none of the canals fit perfectly on a single plane, the average total angular deviation of the canals from their planes is not great (Table 4.4). The radius of curvature of the anterior semicircular canal is larger than the radii of the lateral and posterior canals in all of the zhelestid labyrinths examined, and the radius of the lateral canal arc was always the smallest (Table 4.5). The same pattern was observed for the length of the slender canal.

COMPARISON WITH CRETACEOUS EUTHERIANS

Eutheria is an inclusive group that contains crown Placentalia, plus all taxa more closely related to Placentalia than to crown Marsupialia. The overall morphology of the inner ear of zhelestids from the Bissekty Formation is the same as that observed in extant placental mammals, as well as Mesozoic eutherians that may or may not be members of crown Placentalia, namely *Kulbeckia kulbecke*, *Ukhaatherium nessovi*, and *Zalambdalestes lechei* (Figure 4.5). However, there are differences among the Cretaceous taxa examined (Tables 4.1-4.55). For example, the cochleae of the zhelestids coil to a

TABLE 4.4. Orientations of the semicircular canals for zhelestids and selected Cretaceous eutherians. **Abbreviations**: **A**, anterior semicircular canal; **A-L**, angle between planes of anterior and lateral semicircular canals; **A-P**, angle between planes of anterior and posterior semicircular canals; **L**, lateral semicircular canal; **L-P**, angle between lateral and posterior semicircular canals; **lt**, left labyrinth; **P**, posterior semicircular canal; **rt**, right labyrinth. Canal plane angles and angular deviations expressed in degrees. Canal lengths and arc radii expressed in millimeters. Measurements not reported for URBAC 98-113 (*Kulbeckia kulbecke*) because little more than the cochlea is preserved. Only anterior canal complete in URBAC 99-73 (zhelestid). Definitions of measurements in text.

Specimen	Angles			Deviations		
	A-L	A-P	L-P	A	L	P
Zhelestid						
URBAC 99-02	88.9	102	94.3	9.44	5.95	15.3
URBAC 99-41	85.1	98.1	97.3	17.0	12.1	28.0
URBAC 99-73	-	-	-	-	-	-
URBAC 03-39	102	90.8	84.7	11.6	2.92	17.3
URBAC 04-233	86.0	94.3	88.9	17.5	2.88	8.90
ZIN C. 85511	88.7	107	97.1	-	11.0	-
ZIN C. 85512	82.2	88.5	96.1	8.75	6.43	6.66
Zhelestid Average	88.8	96.8	93.1	12.9	6.88	15.2
Kulbeckia kulbecke						
URBAC 00-16	87.6	90.0	86.7	-	2.52	5.51
URBAC 02-56	65.6	77.5	90.1	-	3.06	-
URBAC 04-36	86.6	84.8	92.0	11.1	2.52	4.67
Kulbeckia Average	79.9	79.9	89.6	11.1	2.70	5.09
Ukhaatherium nessovi						
PSS-MAE 110	88.8	105	88.4	8.22	6.21	9.92
Zalambdalestes lechei						
PSS-MAE 108 (lt)	71.6	85.8	83.4	7.90	4.75	6.21
PSS-MAE 108 (rt)	82.1	91.9	82.8	6.85	4.88	6.20
PSS-MAE 130 (lt)	86.3	91.6	89.4	7.33	9.33	8.14
PSS-MAE 130 (rt)	84.0	91.5	86.6	1.23	-	-
Zalambdalestes Average	81.0	93.6	85.6	5.83	6.32	6.85

TABLE 4.5. Orientations of the semicircular canals for zhelestids and selected Cretaceous eutherians. **Abbreviations**: **A**, anterior semicircular canal; **L**, lateral semicircular canal; **lt**, left labyrinth; **P**, posterior semicircular canal; **rt**, right labyrinth. Canal plane angles and angular deviations expressed in degrees. Canal lengths and arc radii expressed in millimeters. Measurements not reported for URBAC 98-113 (*Kulbeckia kulbecke*) because little more than the cochlea is preserved. Only anterior canal complete in URBAC 99-73 (zhelestid). Definitions of measurements in text.

Specimen	Arc Radii			Lengths		
	A	L	P	A	L	P
Zhelestid						
URBAC 99-02	1.16	0.773	0.865	5.69	3.63	4.70
URBAC 99-41	1.09	0.758	0.888	5.25	3.31	4.83
URBAC 99-73	1.22	-	-	6.71	-	-
URBAC 03-39	1.19	0.785	0.865	5.87	3.38	4.53
URBAC 04-233	1.18	0.795	0.840	5.72	3.41	4.49
ZIN C. 85511	1.15	0.838	0.925	-	3.60	-
ZIN C. 85512	1.18	0.803	0.863	5.54	3.58	4.55
Zhelestid Average	1.17	0.792	0.864	5.80	3.49	4.62
Kulbeckia kulbecke						
URBAC 00-16	-	0.910	0.936	-	4.07	4.63
URBAC 02-56	-	0.937	-	-	4.03	-
URBAC 04-36	1.19	0.910	0.983	5.70	3.72	4.47
Kulbeckia Average	1.19	0.919	0.960	5.70	3.94	4.55
Ukhaatherium nessovi						
PSS-MAE 110	0.837	0.739	0.694	3.81	3.16	3.39
Zalambdalestes lechei						
PSS-MAE 108 (lt)	1.45	1.21	1.20	7.13	5.33	5.75
PSS-MAE 108 (rt)	1.51	1.18	1.20	7.14	5.17	6.18
PSS-MAE 130 (lt)	1.49	1.23	1.20	6.53	5.09	5.61
PSS-MAE 130 (rt)	1.40	-	-	6.86	-	-
Zalambdalestes Average	1.21	1.20	1.21	6.92	5.20	5.85

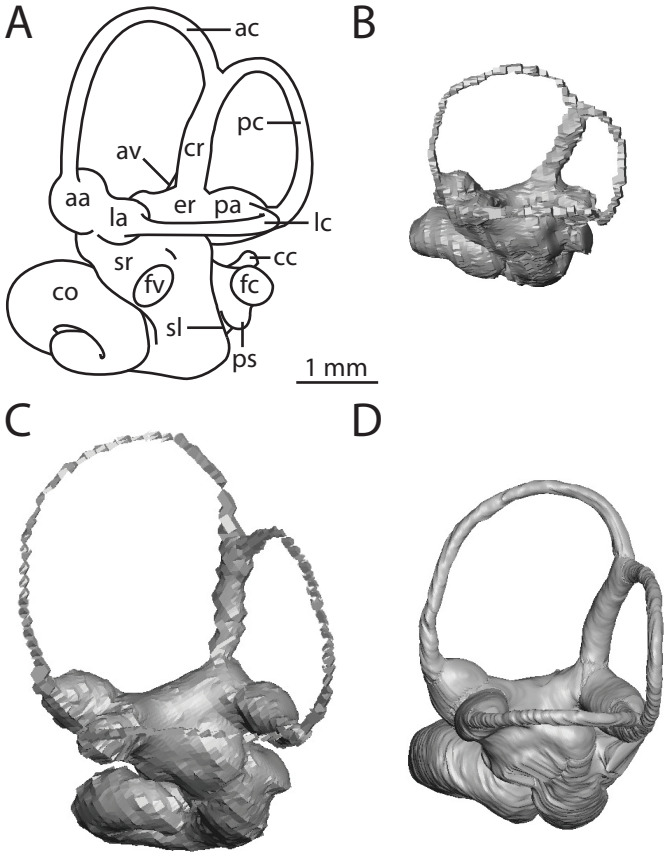

FIGURE 4.5. Bony labyrinths of Cretaceous eutherians listed in Appendix 1 in lateral view. **A**, line drawing of zhelestid (URBAC 03-39); **B**, *Ukhaatherium nessovi* (PSS-MAE 110); **C**, *Zalambdalestes lechei* (PSS-MAE 108), right labyrinth reversed for comparison; **D**, *Kulbeckia kulbecke* (URBAC 04-36), reversed for comparison. Blocky appearance of PSS-MAE 110 and 108 indicative of smaller data size (512 vs. 1024) and datasets with fewer slices through labyrinth (see Appendix 1). **Abbreviations**: **aa**, anterior ampulla; **ac**, anterior semicircular canal; **av**, aquaeductus vestibuli; **cc**, canaliculus cochleae; **co**, cochlea; **cr**, common crus; **er**, elliptical recess of vestibule; **fc**, fenestra cochleae; **fv**, fenestra vestibuli; **la**, lateral ampulla; **lc**, lateral semicircular canal; **pa**, posterior ampulla; **pc**, posterior semicircular canal; **ps**, groove for perilymphatic sac; **sl**, secondary bony lamina; **sr**, spherical recess of vestibule.

greater degree than what is observed in *Ukhaatherium* and *Zalambdalestes*, both of which have cochleae that complete only a single coil following the measurement method of Geisler and Luo (1996). The cochlea of *Kulbeckia* coils more than *Ukhaatherium* and *Zalambdalestes*, but not as much as zhelestids. The degree of coiling observed within *Z. lechei* agrees with the single complete turn reported for a natural endocast of the inner ear from the Cretaceous of Mongolia (Kielan-Jaworowska, 1984). However, the left cochlea of PSS-MAE 130 (*Zalambdalestes*) completes less than one turn, even though the right ear of the same individual coils over 360°. The right ear of that particular specimen is damaged having a fracture that traverses the vestibule in the CT data, but the cochlea appears to be intact.

The extent of the bony secondary lamina in *Kulbeckia* is similar to that in zhelestids, but the secondary lamina only is prolonged past the first quarter turn in *Zalambdalestes* (Table 4.3). The internal cochlear structures were not preserved well enough in *Ukhaatherium* to appear on the CT scans with a resolution sufficient to permit reliable measurements. The primary lamina extends past the fifth quarter in at least one *Kulbeckia* specimen (URBAC 02-56), which is the condition that is observed in most of the Bissekty zhelestid labyrinths. The laminar gap between the primary and secondary bony laminae is narrowest at the base of the cochlea in all of the taxa examined, and the width of the membrane increases towards the apex. However, the gap increases at a faster rate in *Kulbeckia* and *Zalambdalestes* than it does in zhelestids (see Table 4.3).

The cochleae of all of the Mesozoic eutherians are planispiral in profile, and the smallest height-to-width ratio was observed in the left cochlea of PSS-MAE 108 (*Zalambdalestes*; calculated from measurements in Table 4.2), although the ratio in *Ukhaatherium* (34.6) is similar to PSS-MAE 108 (32.4-32.7), and less than what is observed in the other *Zalambdalestes* specimen (36.2-42.3).

The rotation of the plane of the basal turn of the cochlea from the plane of the lateral semicircular canal is greater in every zhelestid labyrinth than it is in any of the other Cretaceous specimens studied. The least amount of rotation of the basal plane of the cochlea was observed in the bony labyrinth of URBAC 02-56 (*Kulbeckia*), followed by *Ukhaatherium*. Among the non-zhelestids, the highest degree of rotation (19.2°) was observed in the left ear of PSS-MAE 130 (*Zalambdalestes*), compared to the least amount of rotation in any zhelestid specimen (28.5°), which was ZIN C. 85511.

The gross morphology of the vestibular apparatus is in general accordance among all of the Cretaceous eutherians listed in Appendix 1, including zhelestids. The secondary crus was observed in every specimen, and the radius of curvature and length of the anterior semicircular canal always was the largest of the three canals within any single labyrinth. However, some minute differences among the sample were detected in specific dimensions of the inner ear. For example, the planes of the semicircular canals of zhelestids are closer to 90° than any of the other Cretaceous taxa. The planes of the anterior and posterior semicircular canals form the greatest angle between any canal planes in *Ukhaatherium* (105°), but the planes between the lateral canal and both the anterior and posterior canals of *Ukhaatherium* are near 90° (89 and 88° respectively).

MORPHOLOGICAL VARIATION

Variation was observed among all measurements taken on the Bissekty zhelestid sample, as well as among the *Kulbeckia kulbecke* specimens and between the two *Zalambdalestes lechei* individuals used in this study (Tables 4.1-4). In fact, the two skulls of *Zalambdalestes* exhibit cranial asymmetry having dramatically different dimensions and orientations between right and left labyrinths within a single skull.

Although variation was observed in the measurement data, there was no variation in the presence or absence of structures. For instance, the secondary common crus was present in every Cretaceous petrosal for which that particular region of the labyrinth was preserved. Further, the cochlea had a complete coil in almost every specimen (the only exception being the left ear of PSS-MAE 130, although the opposing ear completes over one full turn), even if to differing extents, and the canal always curved medially from the fenestra vestibuli.

Coefficients of variation were not calculated for every measurement, but rather those that commonly are reported in literature. The highest CV for each measurement is italicized in Table 4.6, in which reports the CV values for cochlear dimensions and orientations of the semicircular canals are summarized. No single extant species expressed the most variation (highest CV value) for all of the measurements, although patterns are observed among the data. For example, the majority of high CV values were calculated for *Monodelphis domestica*. Zhelestids as a whole did not have the highest CV value for any measurement, and the variation within the labyrinth dimensions of zhelestids falls within the range of a single species (based on the extant sample).

Coiling of the cochlea expressed relatively low levels of variation across the sampled taxa, especially the CV calculated for *Dasypus novemcinctus*. The most variation in cochlear coiling, as well as in length of the cochlear canal (basilar membrane) was observed in *Kulbeckia*.

The arc radius of curvature of the semicircular canals expressed relatively low amounts of variation. The CV of the arc radius of the lateral canal was less than 10.0% in all of the specimens studied. Likewise, the angles between the average planes of the three semicircular canals expressed low-level CV values. The same is not the case for the angular deviation of the canals, where these coefficients expressed the highest degree of

TABLE 4.6. Coefficients of variation (CV) for measurements of labyrinth dimensions of Cretaceous eutherians (including zhelestids) and selected extant taxa listed in Appendix 1. Coefficient calculated as standard deviation divided by mean and multiplied by 100 (reported as percentage). Largest CV for each measurement is italicized. **Abbreviations**: **A**, anterior semicircular canal; **A-L**, angle between planes of anterior and lateral semicircular canals; **A-P**, angle between planes of anterior and posterior semicircular canals; **C-L**, angle between planes basal turn of cochlea and lateral semicircular canal; **L**, lateral semicircular canal; **LP**, angle between lateral and posterior semicircular canals; **P**, posterior semicircular canal.

Specimen	Cochlea		
	Coiling	Length	C-L
Zhelestid	4.42	7.43	9.19
Kulbeckia kulbecke	*9.17*	*19.0*	4.96
Zalambdalestes lechei	3.80	3.07	29.9
Dasypus novemcinctus	0.923	5.69	4.10
Monodelphis domestica	4.38	9.15	*31.6*
Tadarida brasiliensis	1.15	4.97	6.41
	Plane Angles		
	A-L	A-P	L-P
Zhelestid	7.79	7.22	5.53
Kulbeckia kulbecke	*15.5*	3.43	8.59
Zalambdalestes lechei	8.02	3.26	3.58
Dasypus novemcinctus	14.5	*7.55*	*12.8*
Monodelphis domestica	7.43	7.30	6.02
Tadarida brasiliensis	7.08	6.22	4.32
	Deviations		
	A	L	P
Zhelestid	32.4	55.5	55.1
Kulbeckia kulbecke	-	13.3	8.32
Zalambdalestes lechei	53.1	41.2	16.4
Dasypus novemcinctus	22.0	21.6	20.0
Monodelphis domestica	55.6	*98.3*	38.2
Tadarida brasiliensis	*60.8*	86.4	*82.3*
	Length		
	A	L	P
Zhelestid	8.52	3.89	3.06
Kulbeckia kulbecke	-	4.83	2.50
Zalambdalestes lechei	4.12	2.39	5.04
Dasypus novemcinctus	6.97	3.89	3.06
Monodelphis domestica	*10.6*	*11.9*	*12.6*
Tadarida brasiliensis	6.27	4.82	4.45

TABLE 4.6. (Continued)

Specimen	Arc Radii		
	A	L	P
Zhelestid	3.66	3.49	3.33
Kulbeckia kulbecke	-	1.72	3.45
Zalambdalestes lechei	3.15	2.29	0.112
Dasypus novemcinctus	*7.70*	5.53	*6.36*
Monodelphis domestica	6.00	*9.58*	4.81
Tadarida brasiliensis	2.28	5.68	4.13

variation among the coefficients that were calculated. In particular, the angular deviation of the lateral semicircular canal of *Monodelphis* was nearly the maximum amount (over 98%).

DISCUSSION

Morphological variation is a natural occurrence to which no anatomical system is immune. Structures of the inner ear that express variation pertain to function of the cochlea and vestibular apparatus, and other structures have been used to assert broad evolutionary patterns concerning the history of mammal lineages through deep time. Before anatomy of the otic region can be used to interpret physiology and/or phylogeny, the issue of variation must adequately be explored.

Variation Considerations

The observed variation within the Bissekty zhelestid labyrinth could be the result of several factors, including ontogeny, phylogeny, or individual variation. While the external surface of the petrosal exhibits ontogenetic variation, as exemplified by a growth series of petrosals referred to Elephantoidea (Proboscidea; Chapter 2), dimensions of the internal surface of the petrosal (bony labyrinth) do not change significantly once the walls of the labyrinth are ossified early in ontogeny (Chapter 3). Accordingly, variation within the inner ear of zhelestids is not the result of differences in maturity of individuals examined.

The isolated petrosals of zhelestids were collected from the same horizons within the Bissekty Formation as teeth that represented different zhelestid taxa, and it is likely that the zhelestid petrosals represent more than one of the Bissekty species. The

coefficient of variation (CV) was calculated to compare amounts of variation among individual extant species and zhelestids. If the CV values of zhelestids are higher than those for extant species, then it is possible that the variation observed in the zhelestid labyrinths reflects multiple species within the sample (see Cope and Lacy, 1995; Carrasco, 1998).

The amount of variation observed within the Bissekty zhelestid inner ears is no greater than that in the original observations of the extant species *Dasypus novemcinctus*, *Monodelphis domestica*, and *Tadarida brasiliensis*. The variation observed in the extant sample parallels that calculated from measurements of additional placental species reported elsewhere (published taxa and literature sources are listed in Appendix 2). Although the variation within the bony labyrinth of zhelestids is within the range of extant species, this does not necessarily signify that all of the petrosals are the same species, or even a particular higher taxon. Although several previous workers documented variation within the inner ear of single species (e.g., Muren et al., 1986), no study has attempted to determine strictly at which taxonomic level the inner ear varies. To what degree the arc radius of curvature varies at the generic level, or at the ordinal level for that matter, is unknown.

The results of this variation study are significant for one important reason. Although the morphology of the inner ear varies (which is not significant in and of itself), the variation does not appear to be great within a species for the most part (keeping in mind that only three species were evaluated). Variation does not pose a problem when using measurements, such as the arc radius of a semicircular canal or the angles between two canals, to make behavioral interpretations of extinct mammal species. However, the planarity of single canals is a variable feature. The total angular deviation may not be much, but the variation of this measure is considerably high. The physiological

significance of canals that deviate from a single plane is not well known, but such deviation likely affects the sensitivity of the canals. Whatever correlation the deviation a canal from its plane has with physiology should be approached with caution, especially given that the standard deviation of the lateral canal varies almost as much as possible within *Monodelphis*; there is little room for the planarity of the lateral canal to vary any more than it already does. Fortunately, the other dimensions described here can be used for physiology and evolutionary studies without much issue.

Physiological Considerations

The arc radius of a semicircular canal is positively correlated to the afferent sensitivity of the canal (Yang and Hullar, 2007). That is, semicircular canals with large arc radii are more sensitive than those with smaller radii. The largest canals among the Cretaceous sample were observed in *Zalambdalestes lechei*, signifying that that species possessed the most sensitive canals. Absolute size of canals might relate to overall body size (larger species have larger canal radii; Spoor et al., 2007), but the average total volume of the bony labyrinth of the two *Zalambdalestes* specimens (6.31 mm^3) is nearly identical to that of the Bissekty zhelestids (6.28 mm^3). Large canals not only are correlated to afferent sensitivity, but agile animals tend to have larger canals than slower animals (Spoor et al., 2007).

Based on variable molar sizes in zhelestids (Nessov et al., 1998), body size is thought to vary among zhelestid taxa. In order to eliminate size from the comparison, a ratio was taken between the arc radius of each canal over the total labyrinth volume, which may exhibit a correlation to body mass (preliminary unpublished data). The ratios are presented in Table 4.7. If the size of the semicircular canal arc is related to locomotor

ability, and total volume of the bony labyrinth is correlated to body size, then a higher ratio would signify a 'fast' animal under the system developed by Spoor et al. (2007). The ratio of arc radius to inner ear volume indeed is larger for *Zalambdalestes* than for zhelestids, suggesting that *Zalambdalestes* would have been a much more agile animal. In fact, the highest ratios were observed in *Ukhaatherium nessovi*, suggesting that this animal was the most agile, even though its arc radii were the smallest (*Ukhaatherium* likely is the smallest Cretaceous eutherian included in the present study).

The vertical (anterior and posterior) semicircular canals of aquatic species of non-mammalian amniotes tend to have lower canal aspect ratios than closely related terrestrial species (Georgi and Sipla, 2008). Although the Bissekty zhelestids are not hypothesized as aquatic animals, it is worth comparing the morphology in question with these potential correlations. The aspect ratios of the vertical canals are similar among all of the Cretaceous taxa considered in the present report in that none of the taxa have canals with drastically smaller aspect ratios (Table 4.7). Although this result might suggest that all of the Cretaceous species were terrestrial (or else all aquatic), the correlation observed by Georgi and Sipla (2008) was found for closely related species. Among the Cretaceous sample, *Kulbeckia* and *Zalambdalestes* share the closest ancestry, but neither species has vertical canals with noticeably low aspect ratios.

The aspect of the cochlea in profile (height divided by width) plays a role in the sense of hearing. A positive correlation between the ratio and both best frequency and low frequency limit was recovered by Gosselin-Ildari (2006). In short, mammals with planispiral cochleae have lower frequency limits. All of the Cretaceous labyrinths possessed nearly planispiral cochleae, which suggests that the hearing ability was similar among these taxa. A low aspect ratio likely is plesiomorphic for Eutheria, although a low

TABLE 4.7. Ratios between dimensions of semicircular canals. Volume is total volume of bony labyrinth. Canal aspect ratio calculated as height of arc over width. Length is calculated for the slender canal. **Abbreviations**: **A**, anterior semicircular canal; **L**, lateral semicircular canal; **P**, posterior semicircular canal.

Taxon	Radius/Volume			Aspect Ratio			Radius/Length		
	A	L	P	A	L	P	A	L	P
Zhelestid	0.191	0.127	0.137	94.7	74.6	88.5	4.96	4.40	5.15
Kulbeckia kulbecke	0.221	0.169	0.183	102	96.5	102	4.80	4.29	4.75
Ukhaatherium nessovi	0.382	0.341	0.320	94.0	94.6	90.0	4.55	4.28	4.88
Zalambdalestes lechei	0.247	0.204	0.204	108	87.7	97.5	4.77	4.36	4.53

ratio might be a result of the low degree of coiling. Both *Zalambdalestes* and *Ukhaatherium* have cochleae that complete only a single turn, which might result in a smaller aspect ratio. However, a broader sampling of taxa is needed before a correlation between the aspect ratio of the cochlea in profile and coiling of the cochlea can be determined.

The ratio of the slender canal length over arc radius was computed by Boyer and Georgi (2007) in order to investigate changes in frequency ranges transduced from head movements in three Tertiary eutherians, *Aphronorus orieli*, *Eoryctes melanus*, and *Pantolestes longicaudus*. The values that Boyer and Georgi calculated are similar to those measured for the Cretaceous sample here (Table 4.7), although the significance of this measure and any role that it plays in the locomotor behavior of mammals is yet to be determined.

Phylogenetic Considerations

The number of turns completed by the cochlea is a character that commonly is used in phylogenetic analyses incorporating Mesozoic mammals (e.g., Rougier et al., 1998; Archibald et al., 2001). Among the Cretaceous fossils examined here, the cochlea completes around one and a half turns (in zhelestids) or less (in the remaining taxa). This value is consistent with those reported for other Mesozoic eutherians, including those collected from the Bug Creek Anthills of Montana (Meng and Fox, 1995), which complete one and a half turns, as well as the natural endocast of *Zalambdalestes* described by Kielan-Jaworowska (1984), which completes a single coil. Other Cretaceous eutherians for which the morphology of the inner ear is known include *Prokennalestes trofimovi* (~360°; Wible et al., 2001), and *Uchkudukodon nessovi* (reassigned from

Daulestes nessovi by Archibald and Averianov, 2006), which completes slightly less than 360° (McKenna et al., 2000).

Interestingly, one labyrinth of *Zalambdalestes* fails to complete a single coil, as well (left labyrinth of PSS MAE-130). Although the variation is not great (low CV values) for coiling of the cochlea, variation is observed. If the average degree of coiling for a species is 360° and the coiling varies, some individual cochleae will fall below the average. Only a single cochlea of *Uchkudukodon* is described, but it can be hypothesized that other cochleae of *Uchkudukodon* would complete more than 360°. However, this hypothesis cannot be tested until additional petrosals are referred to *Uchkudukodon*.

Despite the variation, the degree of coiling observed within Cretaceous eutherians is significantly less than that of in most extant eutherians. No single cochlea with fewer than two turns was reported by West (1985), and cochleae with two or more coils were observed in the majority of the placentals examined by Gray (1906, 1907, 1908). The exceptions Gray noted mainly include lipotyphlans, a pipistrelle bat, a porpoise, and a manatee, in all of which the cochlea coils between 1.5 and 1.75 turns.

A single turn in the cochlea is plesiomorphic for Eutheria (Meng and Fox, 1995), and the data from the current study support this hypothesis. But coiling beyond one turn likely developed more than once within the placental lineage. The phylogenetic affinities of zhelestids are contentious, but the most recent and thorough phylogenetic analysis that incorporated zhelestids (Wible et al., 2007) placed zhelestids near the bottom of the eutherian tree. Given the topology recovered by Wible et al. (2007), a cochlea coiled to 540° and above would have evolved at least twice within Eutheria – once with the Bissekty zhelestids, and a second time within Placentalia.

In addition to the coiling of the cochlea, the secondary common crus between the lateral and posterior semicircular canals is a plesiomorphic structure for Eutheria (Meng

and Fox, 1995). The structure was observed in all of the Mesozoic taxa examined here, as well as in the eutherians examined by Meng and Fox (1995). The secondary crus was figured for *Prokennalestes* by Wible et al. (2001:fig. 2), although the structure is not labeled in the figure, nor discussed in the text. A secondary common crus is not reported for *Uchkudukodon* (McKenna et al., 2000), but the specimen is broken along the posterior aspect of the lateral semicircular canal. Within Placentalia, a secondary common crus is observed in several species of *Canis* and *Felis* (Hyrtl, 1845), *Eumetopias jubatus*, and *Orycteropus afer* (personal observation), but is absent in most members of the crown. The structure was lost, possibly multiple times, within Placentalia.

Whether or not the membranous lateral and posterior semicircular ducts themselves were joined in the Cretaceous taxa is unclear. Joining of the ducts is not uncommon within Mammalia. For example, the ducts fuse to form a membranous secondary common crus in *Trichosurus* (Gray, 1908). However, the presence of an osseous secondary common crus does not necessarily indicate that the membranous ducts are joined, because the posterior and lateral ducts are separate in *Canis* (Gray, 1907; Evans, 1993) despite the presence of a bony secondary common crus (Evans, 1993; personal observation). A similar state was observed in the marsupial *Caluromys philander* (Sánchez-Villagra and Schmelzle, 2007).

The measurements of the *Kulbeckia* specimen URBAC 98-113 are considerably smaller than the other specimens referred to the same species (also discussed by Ekdale et al., 2004). Two size morphs based on dentition were identified within *Kulbeckia* (Archibald and Averianov, 2003). The difference in size, as hypothesized by Archibald and Averianov, is the result of either sexual dimorphism or else a second, smaller species of *Kulbeckia*. Changes through ontogeny is not a likely source of the observed differential in size, because there is no correlation between most dimensions of the inner

ear and maturity of the individual once the bony labyrinth is ossified (for further discussion, see Chapter 3). Alternatively, URBAC 98-113 might represent *Uchkudukodon*. The size of the petrosal is consistent with that of *Uchkudukodon* (McKenna et al., 2000), but the morphology is consistent with that of the other petrosals referred to *Kulbeckia* (Ekdale et al., 2004). Specifically, *Uchkudukodon* possesses a distinct groove for the transpromontorial artery on the tympanic surface of the petrosal (McKenna et al., 2000, fig. 8). Such a sulcus is absent in URBAC 98-113, as well as the petrosals of other zalambdalestids, including *Zalmbdalestes* (Wible et al., 2004, fig. 37).

CONCLUSIONS

The results of this study support the hypothesis of the ancestral morphology that the bony labyrinth of eutherians includes a low degree of coiling (less than one and a half turns, with the zhelestids having a higher degree of coiling of any identified Cretaceous eutherian) and a secondary common crus. The results also indicate the generalities and low degree of variation among Cretaceous eutherian taxa. Although the debate on placental origins cannot be addressed, the data support a few functional interpretations of the ear of Cretaceous eutherians. The cochleae of Cretaceous eutherians were not specially derived for particularly high or low frequency hearing, as determined from the structure of the cochlear spiral. *Zalambdalestes* and *Ukhaatherium* likely were more agile animals than the Bissekty zhelestids, because they possessed relatively large semicircular canal arcs for the size of their labyrinths.

Whether Placentalia originated within the Mesozoic or Cenozoic era, the inner ear experienced a diversification of morphologies and physiologies after the end of the Cretaceous, as reflected in the great diversity of ear anatomy and function among extant

placentals. Combination of the results detailed here with future research into the ear regions of extinct eutherians, both inside and outside crown Placentalia, as well as from both sides of the Cretaceous-Tertiary boundary, may clarify eutherian relationships, and significantly increase our knowledge of the evolution of the senses of balance and hearing of placental mammals.

CHAPTER 5: THE BONY LABYRINTH OF PLACENTAL MAMMALS

ABSTRACT

The morphological diversity of the bony labyrinth of the inner ear (contained within the petrosal bone) across a broad range of placental mammal taxa is documented, and patterns of variation among the taxa are identified. Comparisons were made using digital endocasts constructed using high-resolution X-ray computed tomography (CT) imagery. The descriptions are organized taxonomically, covering the major placental clades within Afrotheria, Xenarthra, Laurasiatheria, and Euarchontoglires, wherein linear, angular, and volumetric dimensions were measured for the endocasts. The size of the bony labyrinth is correlated to the overall body mass of individuals, where large bodied mammals have absolutely longer and more voluminous inner ear cavities. The arc radius of curvature averaged over the three semicircular canals is not correlated with agility as has been hypothesized elsewhere, but the ratio between the average arc radius and body mass of aquatic species is substantially lower than the ratios of related terrestrial taxa. Additionally, the volume percentage of the vestibular apparatus of aquatic mammals tends to be less than that calculated for terrestrial species. A significantly reduced vestibule is unique to Cetacea among cetartiodactyls, and a cochlear spiral that is taller than it is wide likely is a synapomorphy for caviomorph rodents, a low position of the plane of the lateral semicircular canal compared to the posterior canal in Cetacea and Carnivora, the lateral semicircular canal enters the vestibule at its posterior end in Placentalia and into the posterior ampulla in Cetacea and Carnivora, and the cochlea has

a low aspect ratio in Primatomoprha. Thus, aspects of bony labyrinth morphology appear to be phylogenetically informative.

INTRODUCTION

The vertebrate otic region, which functions in hearing via the cochlea as well as balance and equilibrium via the vestibule and semicircular canals, is one of the most intensively studied sensory systems. The external morphology of the petrosal bone, which surrounds the delicate structures of the inner ear, is a common source of characters used in phylogenetic analyses (e.g., Geisler and Luo, 1998; Rougier et al., 1998; Archibald et al., 2001; Ladevèze, 2004; Wible et al., 2007). Because petrosals preserve readily in the fossil record (see Archibald, 1979), the otic region is a valuable resource for paleontologists when making biological inferences about extinct mammals (Fleischer, 1976; Spoor et al., 1994; Meng and Wyss, 1995; Witmer et al., 2003; Alonso et al., 2004; Clarke, 2005).

The internal cavities within the petrosal comprise the bony labyrinth of the inner ear, including the cochlea anteroventrally and the vestibular apparatus (with semicircular canals) posterodorsally. The dimensions of inner ear structures are correlated to the physiological capabilities of the otic region, including both hearing and balance. Ratios between measurements of the cochlea are related to auditory frequency limits (Gosselin-Ildari, 2006; Manoussaki et al., 2006, 2008; Gosselin-Ildari and Kirk, 2007; Kirk and Gosselin-Ildari, 2009), which correlate with vocalization and social behavior, and the dimensions of the semicircular canals relate to the sensitivity of the canals (Yang and Hullar, 2007), which may in turn correlate to agility and locomotor behaviors (Spoor et al., 2002, 2007; Georgi and Sipla, 2008).

The labyrinth of the inner ear is difficult to study because the inner ear structures are completely surrounded by bone, and removal of this bone is necessary in order to observe the inner ear cavities (Figure 5.1). The structures of the inner ear can be exposed via dissolution of the surrounding bone (Gray, 1907, 1908; West, 1985) or through serially sectioning the petrosal (Luo and Marsh, 1996; Novacek, 1986). Alternatively, non-destructive techniques, such as high resolution X-ray computed tomography (CT), can be used to digitally image the internal cavities of the petrosal bone (Georgi and Sipla, 2008; Spoor and Zonneveld, 1995; Witmer et al., 2003).

Morphology of the inner ear is phylogenetically informative at both more- and less-inclusive taxonomic levels. For example, the cochlea completes at least one complete 360° turn in living therian mammals, but less in monotremes (Gray, 1908; Rowe, 1988). The bony labyrinth of Mesozoic therians exhibit ancestral morphologies, such as a fusion of the posterior and lateral semicircular canals to form a secondary common crus, which is lost in several clades within crown Theria (Meng and Fox, 1995; Chapter 4). Within Primates, dimensions of the semicircular canals differ between the great apes and other primates (Spoor and Zonneveld, 1998). Further phylogenetic information can be found in the cochleae of squamate reptiles (Shute and Bellairs, 1953; Schmidt, 1964; Miller, 1966a, b, 1968).

Given the functional and phylogenetic importance of this region of the skull, it is surprising that broad comparisons of the inner ear of mammals are lacking (the most notable exceptions are the works of Gray, 1906, 1907, and 1908). Furthermore, most authors, owing to the functional division between the cochlea and vestibular apparatus, decouple the structural continuity within the labyrinth. Functional studies therefore are restricted either to the cochlea and the sense of hearing (Fleisher, 1976; Ramprashad et al., 1979; West, 1985; Manley, 2000; Manoussaki et al., 2008), or to the vestibular

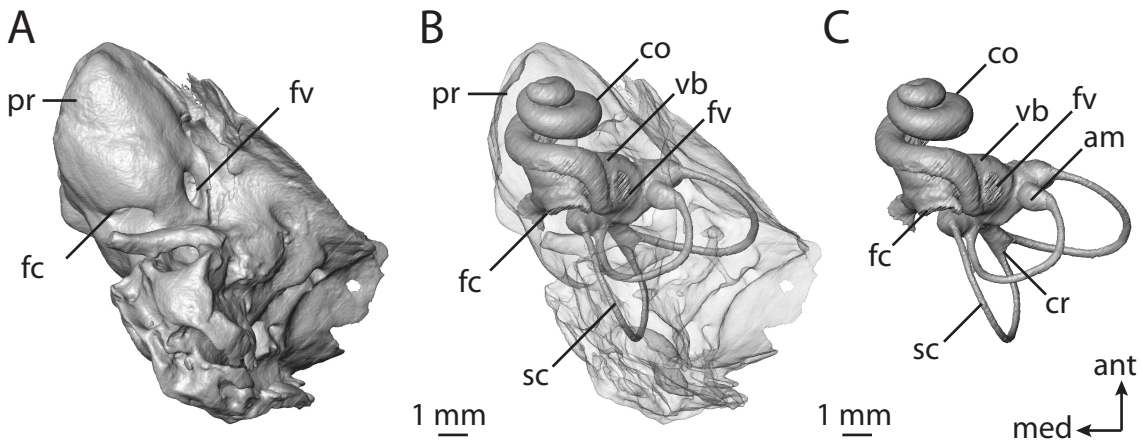

FIGURE 5.1. Petrosal of *Dasypus novemcinctus* (TMM M-1885) within which sits endocast of bony labyrinth. **A**, tympanic view of petrosal bone; **B**, bone rendered semi-transparent to reveal bony labyrinth; **C**, endocast of bony labyrinth. Abbreviations: **am**, ampulla; **ant**, anterior direction (approximate); **co**, cochlea; **cr**, common crus; **fc**, fenestra cochleae; **fv**, fenestra vestibuli; **med**, medial direction (approximate); **pr**, promontorium; **sc**, semicircular canal; **vb**, vestibule.

apparatus and the sense of balance (Jones and Spells, 1963; Blanks et al., 1975; Hullar and Williams, 2006; Spoor et al., 2007). Rarely is the labyrinth considered as a whole and compared across a large number of species. Such a comparison for the bony labyrinth of placental mammals is provided here, along with potential functional and phylogenetic considerations.

Systematic Context

As a point of departure for comparison, the bony labyrinth of a marsupial, *Didelphis virginiana*, is described. The opossum is considered in many respects to retain ancestral morphologies for Theria (Gaudin and Biewener, 1992; Vaughn et al., 2000; Nilsson et al., 2003; Beck et al., 2008; however, see Clemens, 1968), and didelphids hold a basal position on the marsupial phylogeny (Springer et al., l998; Bininda-Emonds et al, 2007). Moreover, *Didelphis* commonly is used as a marsupial outgroup in phylogenetic analyses investigating placental relationships (e.g., Geisler and Luo, 1998; O'Leary and Uhen, 1999; Amrine-Madsen et al., 2003; Asher, 2007). Whereas certain aspects of the cranial morphology of the opossum are apomorphic (e.g., reduced pterygoids), comparisons of the bony labyrinth suggest the otic morphology largely is plesiomorphic (see Wible, 2003).

From *Didelphis*, descriptions of the labyrinths of eutherians (which includes crown Placentalia and all extinct therians more closely related to Placentalia than its extant sister taxon, Marsupialia) are arranged taxonomically following the relationships recovered for Mesozoic non-placental eutherians by Wible et al. (2007), and the relationships recovered for extant placentals by Bininda-Emonds et al. (2007).

A composite tree following the results of both studies is illustrated in Figure 5.2. The relationships proposed by Wible et al. (2007) and Bininda-Emonds et al. (2007) were based on an extensive taxonomic sampling, and therefore are used here. The relationships recovered by Bininda-Emonds et al. (2007) were presented as a supertree (see Sanderson et al., 1998) of 2622 published source tree topologies that included 4,510 out of 4,554 (99%) of mammal species recognized. The resulting supertree is the most comprehensive phylogeny of extant mammals produced thus far. Likewise, the phylogeny produced by Wible et al. (2007) is the most recent study to include the largest combination of eutherian taxa both within and outside of crown Placentalia.

The descriptions of the bony labyrinths of crown placental mammals begin with Afrotheria, and follow in order with Xenarthra, Laurasiatheria, and Euarchontoglires (Figure 5.2). The descriptions are organized taxonomically within these major divisions to allow the reader skip ahead to the account of the species in which he or she is interested (see Table 5.1 for a list of species examined).

MATERIALS AND METHODS

Specimens

At least one representative of the major clades of placental mammals recovered by the phylogenetic analyses of Bininda-Emonds et al. (2007) was selected (Figure 5.2) based on availability of specimens at the Texas Natural Science Center Recent mammal collection at the University of Texas at Austin, as well as available CT imagery from "Digital Morphology: a National Science Foundation Digital Library at The University of Texas at Austin" (www.digimorph.org). The specimens used in this study are listed in Table 5.1, along with institutional abbreviations. Anatomical terminology follows Sisson

FIGURE 5.2. Cladogram of Theria including taxa considered. Relationships follow Bininda-Emonds et al. (2007) and Wible et al. (2007). Nodes: **A**, Theria; **B**, Eutheria; **C**, *Ukhaatherium*+Zalambdalestidae+Placentlia; **D**, Zalambdalesidae+Placentalia; **E**, Zalambdalestidae; **F**, Placentalia; **G**, Afrotheria; **H**, Afrosoricida+*Macroscelides*; **I**, Afrosoricida; **J**, Paenungulata; **K**, *Procavia*+*Trichechus*; **L**, Boreoeutheria; **M**, Laurasiatheria; **N**, Ungulata+Fera+Chiroptera; **O**, Ungulata; **P**, Cetartiodactyla; **Q**, *Sus*+Cetacea; **R**, Cetacea; **S**, Ferae; **T**, Carnivora; **U**, Caniformia; **V**, Chiroptera; **W**, Microchiroptera; **X**, *Rhinolophus*+*Tadarida*; **Y**, Eulipotyphla; **Z**, Euarchonoglires; **a**, Glires; **b**, Rodentia; **c**, Lagomorpha; **d**, Primatomorpha; **e**, Primates.

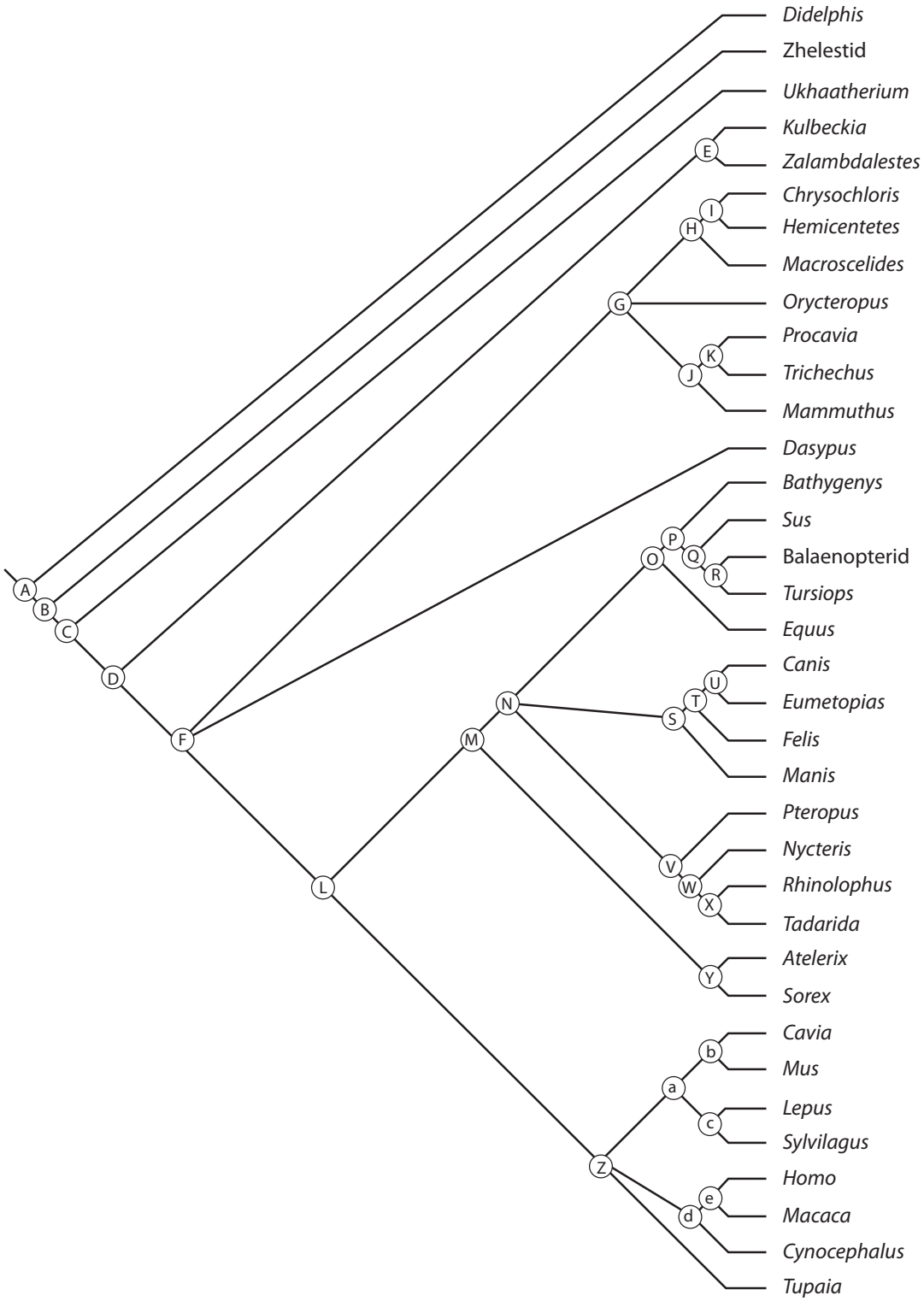
Didelphis
Zhelestid
Ukhaatherium
Kulbeckia
Zalambdalestes
Chrysochloris
Hemicentetes
Macroscelides
Orycteropus
Procavia
Trichechus
Mammuthus
Dasypus
Bathygenys
Sus
Balaenopterid
Tursiops
Equus
Canis
Eumetopias
Felis
Manis
Pteropus
Nycteris
Rhinolophus
Tadarida
Atelerix
Sorex
Cavia
Mus
Lepus
Sylvilagus
Homo
Macaca
Cynocephalus
Tupaia
A
B
C
D
E
F
G
H
I
J
K
L
M
N
O
P
Q
R
S
T
U
V
W
X
Y
Z
a
b
c
d
e

TABLE 5.1. Taxa examined and scanning parameters[a]

Taxon[b]	Slices	Space	FR	Pixel	Size
Marsupialia					
Didelphis virginiana (TMM M-25527)	111	0.132	61	0.0596	1024
Eutheria					
Kulbeckia kulbecke (URBAC 04-36)	387	0.016	14.9	0.0146	1024
Ukhaatherium nessovi (PSS-MAE 110)	59	0.080	15	0.0290	512
Zalambdalestes lechei (PSS-MAE 108)	66	0.113	24.5	0.0479	512
Zhelestid (URBAC 03-39)	536	0.016	14.9	0.0146	1024
Afrotheria					
Afrosoricida					
Chrysochloris sp. (AMNH 82372)	85	0.050	31	0.0303	1024
Hemicentetes semispinosum (AMNH 100837)	56	0.067	48	0.0469	1024
Macroscelidea					
Macroscelides proboscideus (AMNH 161535)	151	0.055	22.5	0.0220	1024
Tubulidentata					
Orycteropus afer (AMNH 51909)	136	0.202	95	0.0930	1024
Hyracoidea					
Procavia capensis (TMM M-4351)	180	0.799	70	0.0683	1024
Sirenia					
Trichechus manatus (MSW 03156)[c]	229	0.300	80	0.1563	512
Proboscidea					
Elephantoidea (TMM 933-950)	275	0.134	53	0.0518	1024
Xenarthra					
Dasypus novemcinctus (TMM M-152)	494	0.291	25	0.0244	1024
Laurasiatheria					
Ceatartiodactyla					
Bathygenys reevesi (TMM 40209-198)	149	0.141	64	0.0625	1024
Sus scrofa (TMM M-2689)	601	0.033	31	0.0303	1024
Balaenopteridae (TMM 42958-35)	1131	0.072	64.8	0.0633	1024
Tursiops truncatus (SDSNH 21212)	346	0.128	40	0.0391	1024
Perissodactyla					
Equus caballus (TMM M-171)	645	0.115	54	0.0567	1024
Carnivora					
Canis familiaris (TMM M-150)	92	0.144	68	0.0664	1024
Eumetopias jubatus (TMM M-171)	645	0.115	54	0.0527	1024
Felis catus (TMM M-968)	627	0.033	31	0.0303	1024
Pholidota					
Manis tricuspis (AMNH 53896)	101	0.116	35.5	0.0347	1024
Chiroptera					
Pteropus lyelli (AMNH 237593)	188	0.447	41	0.0400	1024

TABLE 5.1. (Continued)

Nycteris grandis (AMNH 268369)	70	0.072	67	0.0654	1024
Rhinolophus ferrumequinum (AMNH 245591)	45	0.097	44	0.0430	1024
Tadarida brasiliensis (TMM M-3030)	380	0.010	9.9	0.0097	1024
Eulipotyphla					
Atelerix albiventris (uncatalogued)	68	0.082	65	0.0635	1024
Sorex monticolus (uncatalogued)[d]	130	0.265	12	0.0117	1024
Euarchontoglires					
Rodentia					
Cavia porcellus (TMM M-7283)	728	0.038	29.4	0.0287	1024
Mus musculus (TMM M-3196)	84	0.044	12.6	0.0246	512
Lagomorpha					
Lepus californicus (TMM M-7500)	114	0.144	67	0.0654	1024
Sylvilagus floridanus (TMM M-2689)	325	0.034	30	0.0293	1024
Primates					
Maraca emulate (TMM M-5987)	1121	0.033	31	0.0303	1024
Homo sapiens (UT Teach Coll)	636	0.027	24.84	0.0272	1024
Dermoptera					
Cynocephalus volans	350	0.028	22	0.0215	1024
Scandentia					
Topeka glass (TMM M-2256)	537	0.038	59	0.0576	1024

[a] Definitions of parameters are as follows: FR, field of reconstruction refers to the dimensions of an individual CT slice, expressed in millimeters; Pixel, interpixel spacing, or vertical and horizontal dimensions of an individual pixel, expressed in millimeters, and calculated as FR/Size; Size, number of pixels in a CT slice, either 512X512 or 1024X1024 pixels; Slices, number of CT slices through the ear collected in the coronal (original) slice plane; Space, interslice spacing, or distance between consecutive slices, expressed in millimeters.

[b] Taxonomy and systematic arrangement follows Bininda-Emonds et al. (2007) and Wible et al. (2007). Institutional abbreviations: AMNH, American Museum of Natural History, New York; MSW, Mortality South West; PSS-MAE, Collections of Joint Paleontological and Stratigraphic Section of the Geological Institute, Mongolian Academy of Science, Ulaanbaatar – American Museum of Natural History, New York; SDSNH, San Diego Society of Natural History, San Diego, CA; TMM, Texas Natural Science Center, Austin, TX; URBAC, Uzbekistan/ Russian/ British/ American/ Canadian joint paleontological expedition, Kyzylkum Desert, Uzbekistan, specimens in the Institute of Zoology, Tashkent.

[c] This specimen was the 156th Mortality South West in 2003, collected by S. Rommel at University of North Carolina Wilmington.

[d] Specimen information at http://digimorph.org/specimens/Sorex_monticolus/whole/

and Grossman (1938) and Evans (1993), and orientation terminology of the cochlea follows Fleischer (1976) as depicted in Figure 5.3A-B.

Whenever possible, isolated petrosal bones were scanned to maximize the resolution of the CT imagery (CT methods described below). The left petrosal was examined for each taxon, with a few exceptions, for consistency. Although cranial asymmetry is known within the ear region (Caix and Outrequin, 1979), the physiological significance of such asymmetry is poorly understood. Images of the bony labyrinth are reversed in figures in the cases where right petrosals were used instead of elements from the left side of the skull for easy visual comparison.

All specimens were presumed mature, although no rigorous assessment of maturity was done. Although the external surface of the petrosal changes through accretionary growth, there is evidence that the structures of the inner ear do not change significantly once the walls of the bony labyrinth have ossified (Hoyte, 1961; Chapter 3). Based on those studies, the maturity of individuals used in this study should not affect the observed morphology. Because post-ossification changes in the bony labyrinth only have been investigated for the rabbit (Hoyte, 1961) and the marsupial *Monodelphis domestica* (Chapter 3), but not all of Mammalia, the overall consistency of this pattern among all therian mammal species cannot be assessed. Such a survey is beyond the scope of the current study, and it is assumed that any variation in the mature and fully ossified bony labyrinths used in the following comparisons does not affect the observation of characters at the gross morphological level.

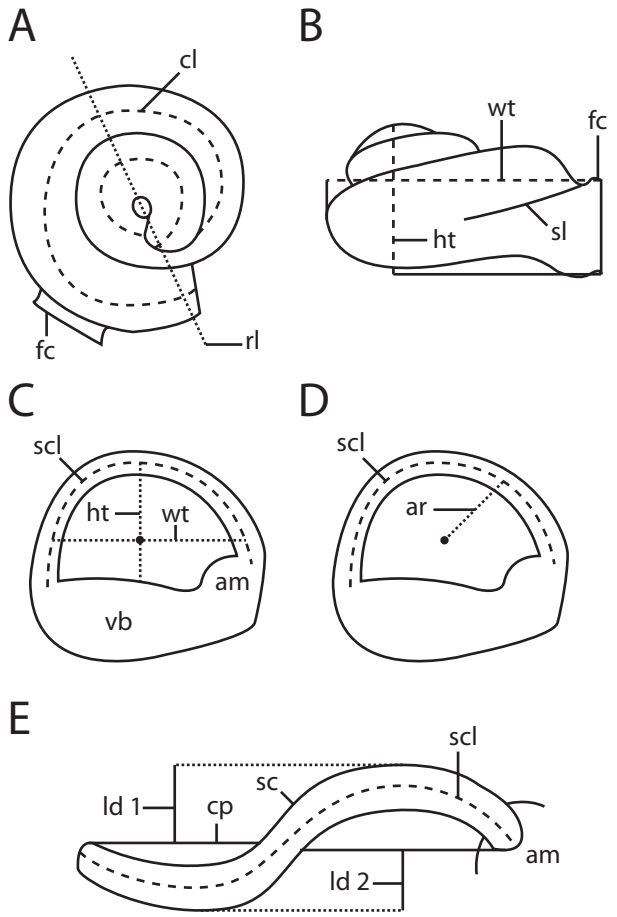

FIGURE 5.3. Measurement methods employed. **A**, coiling of cochlea; **B**, height and width of cochlea used for calculation of aspect ratio; **C**, height, width, and length of semicircular canal; **D**, arc radius of curvature calculated from height and width of arc; **E**, linear deviation of semicircular canal, used with arc radius of curvature to calculate angular deviation. Abbreviations: **am**, ampulla; **ar**, semicircular canal arc radius of curvature; **cl**, length of cochlear canal; **cp**, plane of semicircular canal; **fc**, fenestra cochleae; **ht**, height; **ld**, linear deviation of semicircular canal from its plane; **rl**, reference line for measuring coiling of cochlea; **sc**, semicircular canal; **scl**, slender semicircular canal length; **sl**, secondary bony lamina; **vb**, vestibule; **wt**, width.

Computed Tomography Methods

Digital imagery obtained through computed tomography (CT) was employed to observe the internal chambers of the petrosal that constitute the bony labyrinth. The majority of the specimens used for this study were scanned at the University of Texas High-resolution X-ray CT facility (UTCT) in Austin, TX. The only specimen not scanned at UTCT was *Trichechus manatus* (MSW 03156), which was scanned at Washington University in Saint Louis, MO. Parameters for CT scanning and post-scanning image processing are provided in Table 5.1.

Resolution of the CT data was not uniform among the datasets, in terms of the number of voxels per slice (512 X 512 versus 1024 X 1024), interslice spacing, field of reconstruction (which affects the size of individual voxels), as well as the number of slices through the bony labyrinth (listed in Table 5.1). Differences in data resolution not only affect the appearance of the bony labyrinth (see digital endocasts in Figures 5.4-5.69), but minute structures may not appear on low-resolution datasets (see the anatomical descriptions of the afrosoricid *Hemicentetes* and the carnivoran *Canis* discussed below). Canals with diameters that are less than the size of a pixel may not be observed, and there is a chance that the CT scanner will miss a structure smaller than the interslice spacing. Furthermore, differences in dataset resolution can affect the values of measurements in a significant manner (see Gosman and Ketcham, 2009). The absolute number of slices through the ear region (ranging from 45 for the bat *Rhinolophus ferrumequinum* to 1131 for a fossil balaenopterid whale) seems to have the most dramatic effect on the data presented here.

The bony labyrinths were digitally segmented from the CT imagery into the various partitions of the inner ear (e.g., cochlea and vestibule) in order to calculate partial

volumes of the osseous cavities, as well as create a 3-dimensional representation of the osseous inner ear cavities. Segmentation was performed in the computer software packages VGStudio Max 1.2 © (Volume Graphics, 2004) and Amira 3.1 © (Mercury Computer Systems, 2003). The process of segmentation was achieved by isolating individual voxels that represent a particular anatomical feature of interest on 2-dimensional CT slices (in this case, the spaces within the petrosal). A series of individual CT slices were "stacked", and the isolated voxels were extracted from the surrounding bone to create a 3-dimensional endocast of the segmented structure. The bony channels for the vestibular and cochlear aqueducts were included in the segments of the cochlea and vestibule respectively. The canals for branches of cranial nerve VIII were not segmented. The boundaries between the components were kept as planar as possible. The medial border of the fenestra vestibuli was used as the dividing line between the cochlea and vestibule, where the entire fenestra is included within the segmented vestibule. Thresholding during segmentation (determining the air to bone boundary) was accomplished visually, modified from the half-maximum height protocol (HMH) of Coleman and Colbert (2007).

Standard orientation of the bony labyrinth as a whole is not trivial or straightforward. The endocasts constructed for this study are oriented with the plane of the lateral semicircular canal parallel to the horizon. Such an orientation was selected because the lateral semicircular canal usually is held horizontal when the animal is in a state of alertness (de Beer, 1947). Although the lateral canal is not parallel to the earth-horizon at all times in every animal (Hullar, 2006), a standard position is used in the present study for comparative purposes. Anterior view is oriented down a line connecting the ampullar aperture of the lateral semicircular canal and the vestibular aperture of the posterior limb of the lateral canal (or vestibular aperture of the posterior ampulla if the

canal does not open directly into the vestibule at its posterior end). The labyrinth is oriented with respect to this anterior position in all other views.

Measurement Methods

Methodologies for various measurements follow Fleisher (1976), Spoor and Zonneveld (1995), Geisler and Luo (1996), and Jeffery and Spoor (2004). Angular, linear, and volumetric measurements were made in the Amira software. The measurements made on the digital endocasts, as well as ratios calculated from the measurements, have been used to interpret the physiology and evolutionary relationships in a wide variety of vertebrate species. Many of the measurements are depicted graphically in Figure 5.3.

The total volume of the bony labyrinth is calculated here as a measure of overall size of the inner ear. Volumes are calculated for individual compartments within the internal cavities, including the cochlea, vestibule, and semicircular canals. In addition, the linear length of the bony labyrinth was measured as the greatest distance from the center of the lumen at the posteriormost point of the posterior semicircular canal to the center of the lumen at the anteriormost point along the basal turn of the cochlea (Jeffery and Spoor, 2004).

Dimensions of the cochlea include the total degrees of coiling completed by the canal, as well as the length of the cochlear spiral and widths of internal cochlear structures. In order to calculate the degree of coiling exhibited by the cochlea (following modified methods of West, 1985, and Geisler and Luo, 1996), the endocast of the cochlear canal is positioned in vestibular ("map") view, down the axis of rotation (Figure 5.3A). A line is drawn from the axis of rotation to a point at the base of the cochlea, between the fenestrae cochleae and vestibuli (round and oval windows respectively). The

number of times that the cochlea crosses the line are counted and multiplied by 180° in order to calculate a gross value of cochlear coiling. Added to this product is an additional angle measured between the line drawn through the cochlea and a second line drawn from the axis of rotation to the apex (most distal point) of the cochlear canal. The total measurement of coiling of the cochlea is expressed both in degrees as well as total number of turns (calculated as total degrees divided by 360°).

A shape index (aspect ratio) of the cochlear spiral was calculated by dividing the height of the spiral by the width of the basal turn (Gosselin-Ildari, 2006). The width of the basal turn (which has the largest diameter of all turns in the cochlea) is measured as the greatest distance from the vestibular edge (closest to the apex of the spiral) of the fenestra cochleae to the radial (outside) wall on the opposite side of the basal turn of the cochlea, parallel to the plane of the basal turn of the cochlea (Figure 5.3B). The height of the cochlea is measured as the greatest distance from the level of the most tympanal edge of the fenestra cochleae to the vestibular-most wall of the cochlear spiral (within the apical turn), perpendicular to the width. The aspect ratio of the cochlea in profile may correlate with frequency limits (Gosselin-Ildari, 2006). A high aspect ratio is considered to be above 0.55, following observations of “flattened” and “sharp-pointed” cochleae by Gray (1907, 1908), where “flattened” cochleae have an aspect ratio 0.55 and below.

The total length of the cochlear canal from base to apex was measured using the SplineProbe tool in the Amira software. In order to measure this, a curved line is fit to points within the lumen of the cochlea at the center of the laminar gap (the space between the primary and secondary bony spiral laminae that support the basilar membrane and spiral organ of hearing in life). The endpoints of the line are at the base of the laminar gap (where the primary and secondary lamina converge) and the apex (most distal point) of the canal. The length of the cochlear canal approximates the length of the soft-tissue

basilar membrane, upon which the spiral organ of hearing sits, which may correlate to audible frequencies (West, 1985).

The orientation of the cochlea with respect to the vestibule is quantified as the angle between the planes of the basal turn of the cochlea and the lateral semicircular canal. Often it is assumed that an alert animal will hold its head so that the lateral semicircular canal is held parallel to the horizon (de Beer, 1947), although such is not always the case with all species (see review provided by Hullar, 2006). The plane of the basal turn of the cochlea intersects points at the center of the lumen of the basal turn, and the plane of the lateral canal fits to points at the center of the lumen at the two ends of the canal, as well as the midpoint of the arc. The angle is measured while the bony labyrinth is oriented in the Amira software so that the intersection of the two planes is perpendicular to the field of view.

Dimensions of the semicircular canals include the angles between the planes of the canals, the angular deviation of each canal from its average plane, the arc radius of curvature of each canal, diameter of the canal lumen, and the length and volume of the slender canal (unampullated course). The angle between two semicircular canals is measured when the intersection of the planes is perpendicular to the field of view. The planes of the canals intersect a point at the midpoint of the canal arc, as well as the entry of the canal into its respective ampulla at one end and the vestibule at the other.

The lengths of the slender semicircular canals are measured using the SplineProbe tool in the Amira software, similar to the method used for measuring the length of the cochlear canal, where the curved line intersects points at the center of the lumen across the slender course of the canal. The slender canal is defined as the course of the semicircular canal that does not include the ampulla (Boyer and Georgi, 2007). The common crus is included with the slender paths of both the anterior and posterior

semicircular canals, and the posterior ampulla is included in the path of the lateral semicircular canal when the posterior limb of the lateral semicircular canal does not enter the vestibule directly.

The radius of curvature of a semicircular canal (the dimension "R" of Jones and Spells, 1963, and Spoor and Zonneveld, 1995) is calculated as half the average between the height and width of the canal arc (Figures 5.3C and 5.3D). The specific methods to measure the height and width of the semicircular canal arc are adapted from Spoor and Zonneveld (1995), and the measurements are taken on the digital endocasts in the Amira software using the line measuring tool with the 3-dimensional capability enabled. The height of the lateral semicircular canal is measured as the greatest distance from the wall of the vestibule to the center of the lumen of the canal. The height of the anterior and width of the posterior semicircular canals are measured when the lateral canal is viewed parallel to the horizon, where the height of the anterior semicircular canal arc is measured as the greatest distance from the wall of the vestibule to the center of the lumen of the canal, and the width of the posterior canal is measured as the greatest distance between the center of the lumen of the posterior limb of the canal and the center of the lumen of the common crus.

The total angular deviation of a semicircular canal from its respective plane is calculated trigonometrically using two linear measurements of the canal (adapted from Calabrese and Hullar, 2006, and Hullar and Williams, 2006). The linear measures utilized in the calculation of angular deviation are the arc radius of curvature of the canal and total linear deviation of the canal from its plane (Figure 5.3E). The total linear deviation is measured when the plane of the semicircular canal is perpendicular to the field of view in the Amira software using the line measurement tool with the 2-dimensional capability enabled. The greatest distance from the center of the lumen to the plane of the canal is

measured on both sides of the plane. Partial angular deviations are calculated as the arcsine of the partial linear deviation divided by the arc radius of curvature. The total angular deviation is the sum of the two partial angular deviations.

Substantial deviation of a semicircular canal from its plane is defined here as any ratio of the total linear deviation over the cross-sectional diameter at the midpoint of the semicircular canal being greater than 1. In short, if the total linear deviation of a canal from its plane is greater than the diameter of the canal in cross-section, the deviation is considered significant, in a non-statistical sense. The measure of significant deviation is arbitrary and does not have any basis in the physiology of the semicircular canal system. The functional implications of non-planar semicircular canals are poorly understood, and the significance values are intended to emphasize the phenomenon of non-planarity, rather than to make any functional interpretations at this time.

The sagittal labyrinthine index, which is defined as the percentage of the width of the posterior semicircular canal arc below the plane of the lateral semicircular canal (Spoor and Zonneveld, 1995), quantifies the relative positions of the lateral and posterior semicircular canals. High sagittal labyrinthine indices separate the great apes from other primates (Spoor and Zonneveld, 1998), and the index might be useful in the phylogenetic assessment of other mammal groups.

Two additional indices are ratios that might relate to aquatic habitat and locomotion. Specifically, the ratio of the slender canal length over arc radius (Boyer and Georgi, 2007), as well as the aspect ratio (height over width) of the arcs of the vertical (anterior and posterior) semicircular canals (Georgi and Sipla, 2008) distinguish aquatic species from their terrestrial ancestors. These ratios were calculated for the present sample.

The stapedial ratio describes the shape of the footplate of the stapes (Segall, 1970), which contacts the inner ear spaces via the fenestra vestibuli. Marsupial mammals tend towards circular fenestrae with ratios below 1.8, whereas the fenestrae of placentals are more elliptical. In absence of the stapedial footplate, the dimensions of the fenestra vestibuli can be used. Although the footplate of the stapes is held in place by an annular ligament, the stapes articulates tightly with the fenestra (personal observation). The fenestra vestibuli is expressed on the digital endocasts, and the stapedial ratio is calculated as the greatest distance along the long axis of the fenestra, divided by the greatest distance measured along the short axis, perpendicular to the first measurement.

To ascertain whether the dimensions of the inner ear are correlated to overall body size of the animal, specific measurements were plotted over body mass (all data logarithmically transformed using the natural log) and the coefficient of correlation ("r") was calculated. Any coefficient greater than or equal to 0.7 is considered significant. If the body mass of the specimen examined was not known, an average was calculated from Silva and Downing (1995) for most non-human taxa (data for *Eumetopias jubatus* from Loughlin et al., 1987), and values from Ogden et al. (2004) were used for *Homo sapiens*. Body mass data are unavailable for the two fossils (*Bathygenys reevesi* and Balaenopteridae). Further, a body mass was not used for *Canis familiaris* given the broad range of body masses observed in domestic dogs (Galvão, 1947; Heusner, 1991). Further correlations were investigated between dimensions of the cochlea, as well as dimensions of the semicircular canals.

Ancestral states, both continuous and discrete, for the hypothetical common ancestors of the clades pictured in Figure 5.2 were reconstructed in the computer program Mesquite (Maddison and Maddison, 2008). Although discrete character states of ancestors were reconstructed using the parsimony method in the Mesquite software, the

maximum likelihood method was utilized for continuous characters (following Martins, 1999). Characters that were traced across the cladogram are (1) entry of the lateral semicircular canal into a secondary common crus, the posterior ampulla, or the vestibule, (2) largest semicircular canal arc among the anterior, lateral, and posterior canals, (3) aspect ratio of the cochlear spiral in profile, (4) degree of cochlear coiling, and (5) contribution (percentage) of the volume of the cochlea to the entire labyrinth.

RESULTS –ANATOMICAL COMPARISONS

The osseous cavities that constitute the bony labyrinth of the inner ear contain a series of membranous sacs and ducts that embody the membranous labyrinth. The membranous labyrinth consists of the cochlear duct and saccule of the vestibule within a ventral division of the labyrinth, and the utricle of the vestibule, along with the three semicircular ducts with their respective ampullae and the common crus within a dorsal division.

Theria

Theria includes the most recent common ancestor of extant marsupials (such as *Didelphis virginiana*, which is used to represent Marsupialia) and extant placentals (such as *Homo sapiens*) and all of the descendents of that ancestor. The bony labyrinth of the hypothetical therian ancestor possessed a secondary common crus formed between the lateral and posterior semicircular canals (see the labyrinth of *Didelphis* in Figure 5.4-5.5), which likely was inherited from a much more distant mammalian ancestor (Ruf et al., 2009).

The plane of the lateral canal is positioned low with respect to the ampullar entrance of the posterior canal so that the area of the arc of the posterior canal is not

FIGURE 5.4. Bony labyrinth of *Didelphis virginiana*. **A**, stereopair and labeled line drawing of digital endocast in anterior view; **B**, stereopair and labeled line drawing of digital endocast in dorsal view; **C**, stereopair and labeled line drawing of digital endocast in lateral view; **D**, line drawing of cochlea viewed down axis of rotation to display degree of coiling; **E**, line drawing of cochlea in profile; **F**, vestibular apparatus displaying secondary common crus. Abbreviations: **aa**, anterior ampulla; **ac**, anterior semicircular canal; **ant**, anterior direction; **av**, bony channel for aqueduct of vestibule; **cc**, canaliculus cochleae for aqueduct of cochlea; **co**, cochlea; **cr**, common crus; **dor**, dorsal direction; **er**, elliptical recess of vestibule; **fc**, fenestra cochleae; **fv**, fenestra vestibuli; **la**, lateral ampulla; **lc**, lateral semicircular canal; **med**, medial direction; **pa**, posterior ampulla; **pc**, posterior semicircular canal; **pl**, primary bony lamina; **pos**, posterior direction; **ps**, outpocketing for perilymphatic sac; **scr**, secondary common crus; **sl**, secondary bony lamina; **sr**, spherical recess of vestibule; **vb**, vestibule.

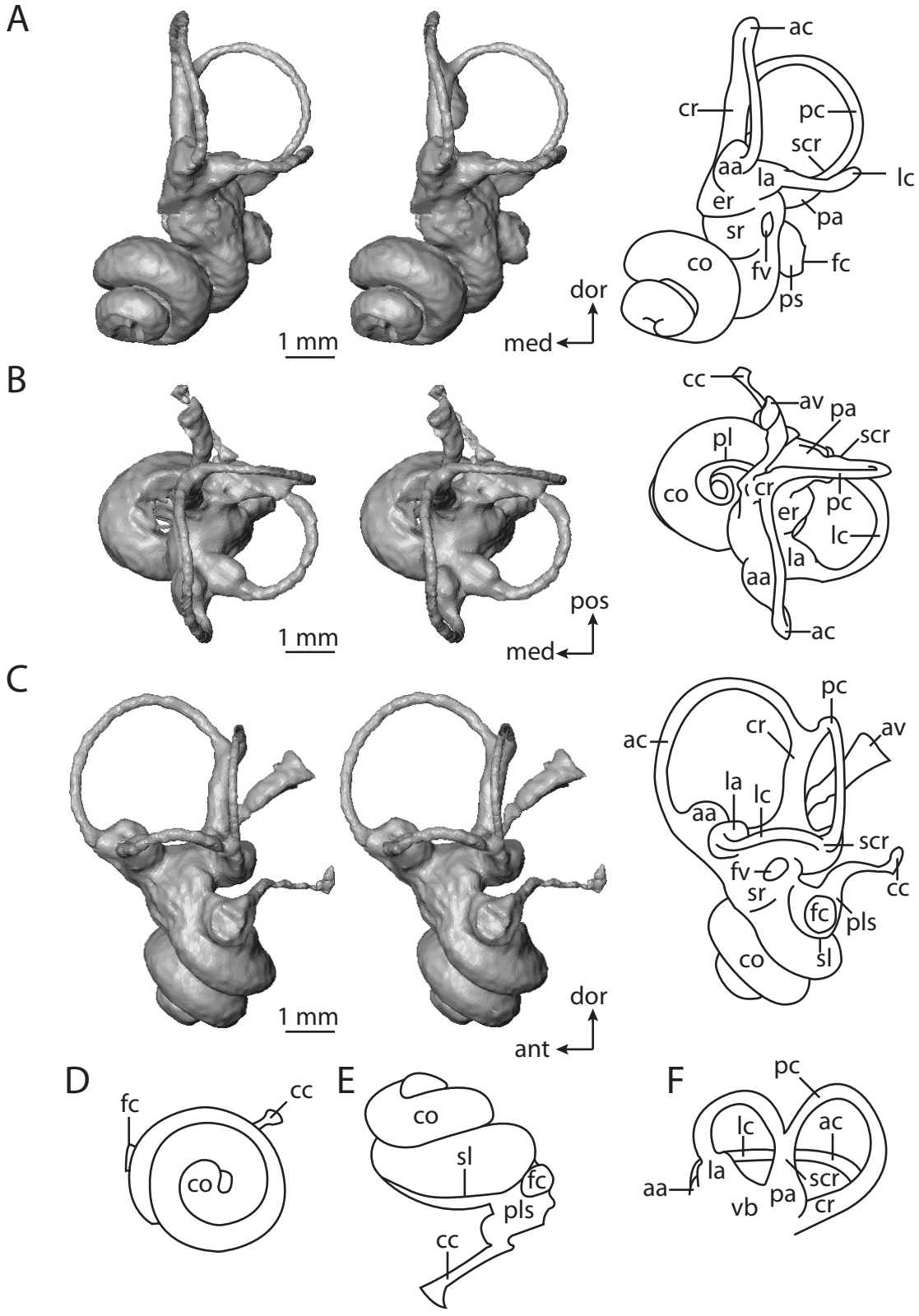
A
1 mm
dor
med
ac
cr
pc
scr
aa
la
lc
er
pa
sr
co
fv
fc
ps
B
1 mm
pos
med
cc
av
pa
pl
scr
co
cr
er
pc
lc
la
aa
ac
C
1 mm
dor
ant
pc
ac
cr
av
la
lc
aa
scr
fv
sr
cc
fc
pls
co
sl
D
fc
cc
co
E
co
sl
fc
pls
cc
F
pc
lc
ac
aa
la
scr
vb
pa
cr

FIGURE 5.5. Original CT slices through ear region of *Didelphis virginiana*. Numbers refer to specific CT slices. Abbreviations: **aa**, anterior ampulla; **ac**, anterior semicircular canal; **av**, bony channel for aqueduct of vestibule; **cc**, canaliculus cochleae; **cn**, canal for cranial nerve VIII; **co**, cochlea; **cr**, common crus; **dor**, dorsal direction; **fc**, fenestra cochleae; **fn**, canal for cranial nerve VII; **fv**, fenestra vestibuli; **la**, lateral ampulla; **lat**, lateral direction; **lc**, lateral semicircular canal; **pa**, posterior ampulla; **pc**, posterior semicircular canal; **pl**, primary bony lamina; **pos**, posterior direction; **pr**, promontorium housing cochlea; **scr**, secondary common crus; **sl**, secondary bony lamina; **sr**, spherical recess of vestibule.

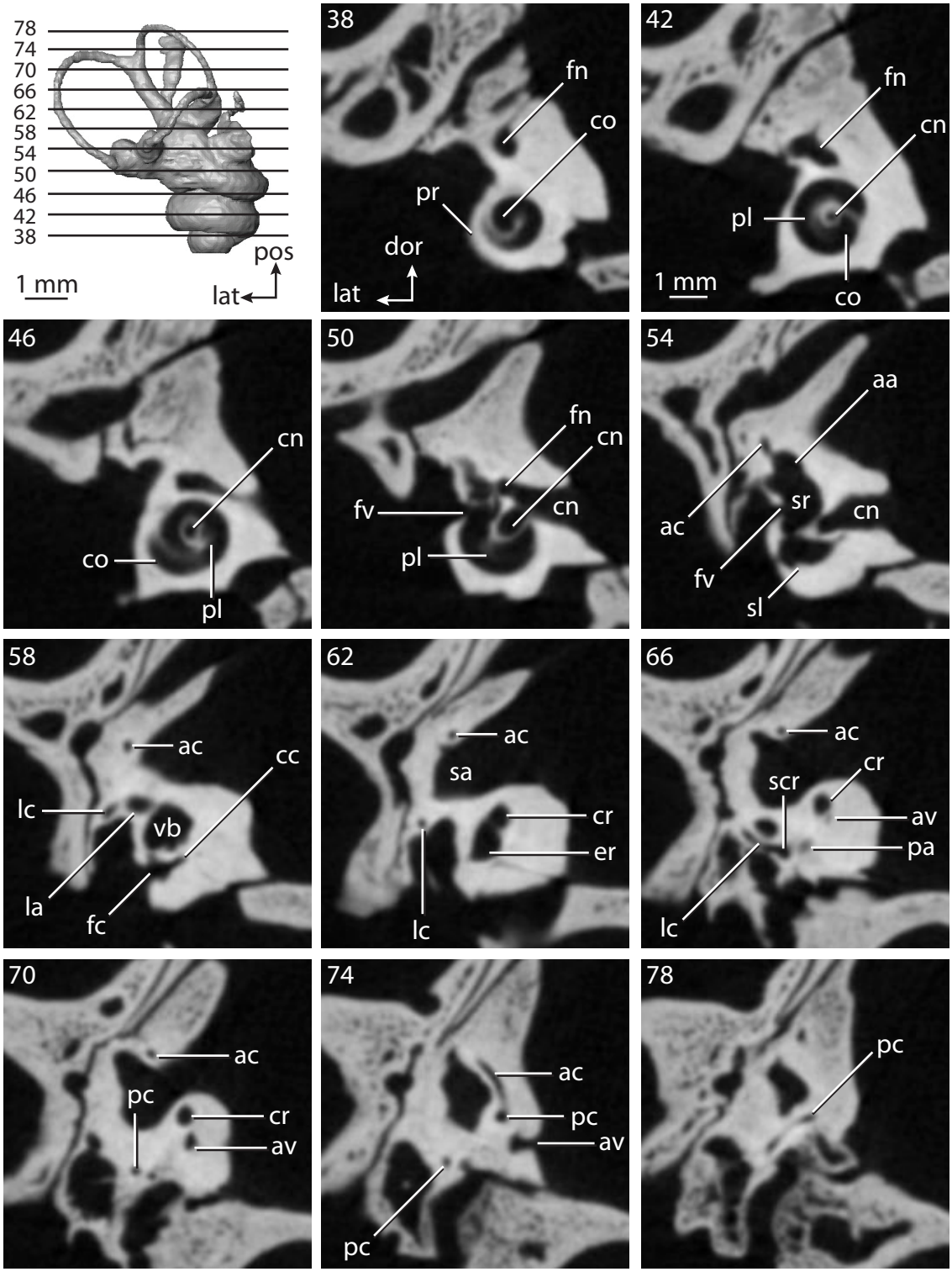
78
74
70
66
62
58
54
50
46
42
38
pos
lat
1 mm
38
fn
co
pr
dor
lat
42
fn
cn
pl
co
1 mm
46
cn
co
pl
50
fn
cn
fv
cn
pl
54
aa
ac
sr
cn
fv
sl
58
ac
cc
lc
vb
la
fc
62
ac
sa
cr
er
lc
66
ac
cr
scr
av
pa
lc
70
ac
pc
cr
av
74
ac
pc
av
pc
78
pc

divided by the lateral canal in anterior view, as it is in most extant placentals (e.g., *Chrysochloris* or *Sylvilagus*). As observed in most mammal species, the arc of the anterior semicircular canal is the largest among the three canals. The cochlea completed a 685° coil (nearly two turns) and contributed 66% of the total inner ear volume. The aspect ratio of the cochlea of the ancestral therian is reconstructed as low, although the aspect ratio in *Didelphis* (0.62) is higher than that calculated for basal taxa along the eutherian lineage. The ancestor of Theria likely possessed a cochlea with a low aspect ratio given the close similarities between basal metatherian and eutherian labyrinths (see Meng and Wyss, 1995), and the ancestral state is reconstructed as such.

Marsupialia

The structure of the inner ear of *Didelphis virginiana* is described for comparison with the inner ear structures of crown placentals and their Mesozoic eutherian relatives. Dimensions of the bony labyrinth as a whole of *Didelphis* (and all other taxa) are provided in Table 5.2. Dimensions of the cochlea are provided in Table 5.3, and dimensions and orientations of the semicircular canals are reported in Tables 5.4-5.6.

Didelphis is a common animal in North America, despite it being the only North American marsupial. The body mass of the specimen used (TMM M-2517) is 2.8 kg (see Table 5.2), which is on the higher end of the mass range of the species (1.6-3.1 kg; Silva and Downing, 1995). The bony labyrinth of *D. virginiana* is 5.15 mm in total length, and the cochlea contributes 68.7% of the total volume of the inner ear (8.30 out of 12.1 mm^3), which is close to that calculated for the ancestral therian (66.0%). The cochlear spiral is high in profile, with an aspect ratio of 0.62 (height equals 2.28 mm and width equals 3.68 mm). The cochlea completes nearly two and a quarter turns (790.7°), and the length of

TABLE 5.2. Body mass, skull length, and dimensions of the entire bony labyrinth of placentals[a]

Taxon[b]		Body Mass	Skull Length	Bony Labyrinth Volume	Bony Labyrinth Length
Marsupialia					
	Didelphis	2800.00	106.65	12.08	5.15
Eutheria					
	Kulbeckia	NA	NA	5.37	4.73
	Ukhaatherium	NA	NA	2.17	3.57
	Zalambdalestes	NA	NA	6.07	5.31
	Zhelestid	NA	NA	6.28	4.51
Afrotheria					
	Chrysochloris	44.40	23.85	4.11	3.93
	Elephantoidea	NA	NA	1145.18	26.00
	Hemicentetes	110.00	30.61	2.78	4.08
	Macroscelides	38.40	32.26	9.19	4.31
	Orycteropus	60000.00	245.48	107.32	14.95
	Procavia	3800.00	75.87	19.36	8.50
	Trichechus	500000.00	NA	621.04	19.29
Xenarthra					
	Dasypus	4753.75	NA	26.48	8.06
Laurasiatheria					
	Atelerix	866.38	38.13	4.58	5.46
	Balaenopteridae	NA	NA	1075.51	19.67
	Bathygenys	NA	90.71	29.83	7.40
	Canis	NA	87.10	31.36	8.10
	Equus	258324.32	530.00	165.16	16.52
	Eumetopias	735000.00	NA	138.60	13.71
	Felis	3407.86	NA	45.78	8.91
	Manis	4500.00	75.05	28.53	6.66
	Nycteris	29.27	27.80	2.13	3.39
	Pteropus	435.00	65.23	7.01	6.19
	Rhinolophus	17.21	24.28	5.89	3.76
	Sorex	6.07	16.90	0.81	2.81
	Sus	88285.71	240.00	61.86	9.95
	Tadarida	12.13	NA	3.86	3.22
	Tursiops	179500.00	543.02	167.98	10.08
Euarchontoglires					
	Cavia	728.00	67.80	22.22	7.13

TABLE 5.2. (Continued)

Taxon[b]		Body Mass	Skull Length	Bony Labyrinth Volume	Bony Labyrinth Length
	Cynocephalus	1000.00	NA	20.32	7.17
	Homo	8000.00	NA	164.73	16.31
	Lepus	2350.00	94.37	24.26	7.39
	Macaca	4667.50	NA	41.64	11.23
	Mus	15.48	20.81	1.47	2.71
	Sylvilagus	1160.00	68.70	11.32	5.82
	Tupaia	131.15	49.60	9.83	6.67

[a] Body mass expressed in grams; Skull and bony labyrinth length expressed in millimeters; bony labyrinth volume expressed in cubic millimeters.
[b] Specimens used listed in Table 5.1. Taxonomy follows Bininda-Emonds et al. (2007) and Wible et al. (2007). Values for *Kulbeckia*, *Zalambdalestes*, and the Zhelestid are averages (reported in Chapter 4).

TABLE 5.3. Dimensions and orientations of the cochlea of placentals[a]

Taxon[b]	Volume	Coiling	2° Lamina	Length	Aqueduct	Ratio	Angle
Marsupialia							
Didelphis	8.30	790.7	427.0	7.54	1.68	0.62	19.6
Eutheria							
Kulbeckia	2.59	446.0	208.7	4.93	0.60	0.44	12.1
Ukhaatherium	1.23	380.0	76.8	2.77	0.36	0.35	6.63
Zalambdalestes	2.91	368.0	95.3	3.40	0.48	0.36	13.5
Zhelestid	4.15	545.0	197.7	4.93	0.37	0.46	34.0
Afrotheria							
Chrysochloris	2.93	1191.0	301.0	6.65	0.45	0.63	41.9
Elephantoidea	350.66	765.0	NA	32.45	NA	0.42	48.5
Hemicentetes	1.39	540.0	240.3	3.79	.28	.38	18.4
Macroscelides	6.59	720.0	334.0	7.11	0.58	0.80	25.1
Orycteropus	59.31	709.0	390.0	14.86	4.82	0.45	31.9
Procavia	9.24	1363.0	190.0	14.97	1.21	0.72	45.4
Trichechus	441.63	407.0	NA	22.46	NA	0.55	27.7
Xenarthra							
Dasypus	17.48	816.3	383.0	11.21	1.17	0.63	17.9
Laurasiatheria							
Atelerix	2.28	623.7	240.0	4.99	0.77	0.69	53.8
Balaenopteridae	973.91	886.0	238.0	53.02	3.65	0.48	23.2
Bathygenys	16.17	667.0	NA	8.51	NA	0.32	26.8
Canis	20.72	1156.0	104.0	13.85	2.08	0.64	20.8
Equus	84.33	911.3	153.0	22.08	11.33	0.41	37.9
Eumetopias	74.17	795.4	249.0	19.25	4.16	0.68	31.6
Felis	31.12	1092.0	243.0	16.77	3.60	0.69	45.8
Manis	14.00	863.0	NA	9.64	2.85	0.54	20.3
Nycteris	1.42	801.0	316.0	6.66	0.66	0.61	47.2
Pteropus	4.13	656.0	335.0	7.66	0.73	0.61	36.2
Rhinolophus	5.24	1115.0	935.0	11.57	0.59	0.63	5.5
Sorex	0.37	493.0	179.0	2.52	0.23	0.47	9.41
Sus	36.25	1340.0	NA	22.89	2.64	0.71	23.8
Tadarida	2.80	751.6	659.0	6.95	0.12	0.52	29.2
Tursiops	157.11	661.0	396.0	24.01	6.47	0.47	21.3
Euarchontoglires							
Cavia	12.26	1457.0	195.0	13.42	2.52	1.29	35.1

TABLE 5.3. (Continued)

Taxon[b]	Volume	Coiling	2° Lamina	Length	Aqueduct	Ratio	Angle
Cynocephalus	9.83	953.7	65.4	12.20	0.90	0.50	34.6
Homo	71.49	889.0	22.2	22.49	10.86	0.36	62.4
Lepus	13.07	693.0	147.0	8.80	1.34	0.64	40.6
Macaca	20.96	1088.0	81.0	16.94	3.53	0.48	47.8
Mus	0.86	627.7	327.0	3.87	0.17	0.62	10.8
Sylvilagus	6.26	816.8	200.0	8.75	1.05	0.71	40.3
Tupaia	5.43	1125.0	220.0	10.51	0.66	0.66	28.9

[a] Measurement methodologies provided in text: Volume, total volume of cochlear canal, expressed in cubic millimeters; Coiling, the total degrees completed by the cochlea; 2° Lamina, extension of secondary lamina through cochlea, expressed in degrees; Length; length of canal, expressed in millimeters; Aqueduct, length of cochlear aqueduct, expressed in millimeters; Ratio, aspect ratio calculated as height of spiral over width; Angle, formed between basal turn of cochlea and lateral semicircular canal, expressed in degrees.

[b] Specimens used listed in Table 5.1. Taxonomy follows Bininda-Emonds et al. (2007) and Wible et al. (2007). Values for *Kulbeckia*, *Zalambdalestes*, and the Zhelestid are averages (reported in Chapter 4).

TABLE 5.4. Dimensions of vestibular elements and orientations of semicircular canals[a]

Taxon[b]	Aqueduct Length	Stapedial Ratio	Labyrinth Index	Semicircular Canal Angles		
				Ant-Lat	Ant-Post	Lat-Post
Marsupialia						
Didelphis	2.58	1.6	0.0	109.0	102.0	104.0
Eutheria						
Kulbeckia	1.24	2.0	0.0	79.9	79.9	89.6
Ukhaatherium	NA	1.5	0.0	88.8	105.0	88.4
Zalambdalestes	1.74	1.7	0.0	81.0	93.6	85.6
Zhelestid	1.06	1.6	0.0	88.8	96.8	93.1
Afrotheria						
Chrysochloris	0.37	2.8	21.7	65.6	86.9	96.7
Elephantoidea	13.90	1.6	0.0	66.3	73.7	92.6
Hemicentetes	NA	1.6	4.1	79.3	87.9	87.0
Macroscelides	2.08	1.9	32.7	100.0	90.7	95.7
Orycteropus	8.25	1.8	0.0	78.5	91.9	87.4
Procavia	3.39	2.1	44.9	87.4	112.0	86.3
Trichechus	12.30	1.6	0.0	52.2	84.9	77.5
Xenarthra						
Dasypus	2.63	1.7	23.0	62.4	67.7	87.3
Laurasiatheria						
Atelerix	NA	1.8	26.4	82.2	91.7	92.1
Balaenopteridae	3.83	1.5	0.0	71.6	105.0	75.6
Bathygenys	NA	NA	45.2	86.0	99.6	91.3
Canis	NA	1.3	0.0	80.4	101.0	89.1
Equus	11.70	1.7	10.5	84.7	93.3	90.1
Eumetopias	2.26	1.5	0.0	79.7	105.0	90.6
Felis	3.77	1.9	13.1	76.8	91.4	96.7
Manis	2.45	1.7	20.5	77.0	84.8	88.6
Nycteris	NA	1.0	0.0	85.9	112.0	94.9
Pteropus	1.62	1.8	29.7	84.9	98.3	90.4
Rhinolophus	1.40	1.4	38.3	79.9	104.0	87.9
Sorex	1.58	1.7	11.9	75.3	89.6	89.3
Sus	3.18	1.3	16.5	82.8	96.0	87.9
Tadarida	1.42	2.0	22.1	74.7	98.4	98.4
Tursiops	2.23	1.4	0.0	52.2	84.9	77.5
Euarchontoglires						
Cavia	3.82	2.9	25.3	77.2	105.0	85.5

TABLE 5.4. (Continued)

Taxon[b]	Aqueduct Length	Stapedial Ratio	Labyrinth Index	Semicircular Canal Angles		
				Ant-Lat	Ant-Post	Lat-Post
Cynocephalus	1.80	2.0	30.8	92.2	90.0	91.8
Homo	5.47	3.0	55.8	98.9	100.0	89.8
Lepus	3.71	1.7	32.4	84.2	94.0	88.6
Macaca	3.76	2.5	50.1	83.1	100.0	89.0
Mus	1.28	1.9	25.8	88.8	94.4	95.6
Sylvilagus	2.08	1.5	33.9	92.7	97.5	77.9
Tupaia	2.61	2.6	13.1	82.3	106.0	102.0

[a] Measurement methodologies provided in text: Aqueduct Length, expressed in millimeters; Stapedial Ratio, height of fenestra vestibuli over width; Labyrinth Index, sagittal labyrinthine index (Spoor and Zonneveld, 1995); Semicircular Canal Angles, formed between planes of canals, expressed in degrees.
[b] Specimens used listed in Table 5.1. Taxonomy follows Bininda-Emonds et al. (2007) and Wible et al. (2007). Values for *Kulbeckia*, *Zalambdalestes*, and the Zhelestid are averages (reported in Chapter 4).

TABLE 5.5. Linear dimensions of the semicircular canals[a]

Taxon[b]	Radius			Length			Lumen Diameter		
	Ant	Lat	Post	Ant	Lat	Post	Ant	Lat	Post
Marsupialia									
Didelphis	1.46	0.88	1.23	8.24	5.07	7.53	0.26	0.30	0.28
Eutheria									
Kulbeckia	1.19	0.92	0.96	5.70	3.94	4.55	0.18	0.20	0.20
Ukhaatherium	0.84	0.74	0.69	3.81	3.16	3.39	0.17	0.13	0.15
Zalambdalestes	1.46	1.21	1.20	6.92	5.20	5.85	0.19	0.17	0.18
Zhelestid	1.17	0.79	0.86	5.80	3.49	4.62	0.19	0.19	0.19
Afrotheria									
Chrysochloris	1.10	0.67	0.71	4.71	2.62	3.60	0.15	0.18	0.16
Elephantoidea	4.99	2.67	5.51	24.57	12.50	24.28	1.85	1.69	1.77
Hemicentetes	1.10	0.68	0.89	4.96	2.44	4.79	0.13	0.15	0.09
Macroscelides	1.32	1.05	1.02	5.61	4.21	5.22	0.19	0.20	0.20
Orycteropus	3.10	3.27	3.50	15.40	16.40	18.86	0.58	0.53	0.55
Procavia	1.99	1.79	2.18	10.23	7.65	10.68	0.21	0.33	0.27
Trichechus	4.30	4.46	3.54	17.30	14.20	16.53	0.51	0.52	0.51
Xenarthra									
Dasypus	1.64	1.60	1.92	9.69	7.38	11.30	0.22	0.23	0.23
Laurasiatheria									
Atelerix	1.24	0.88	1.22	5.88	3.67	5.80	0.16	0.15	0.15
Balaenopteridae	2.54	2.11	1.92	10.65	8.54	9.46	0.32	0.51	0.41
Bathygenys	1.91	1.52	1.79	9.72	7.11	10.02	0.44	0.33	0.38
Canis	1.73	1.57	1.43	8.58	7.08	7.37	0.31	0.35	0.33
Equus	3.62	3.55	3.50	17.35	14.30	18.63	0.51	0.45	0.48
Eumetopias	3.00	3.13	2.86	12.99	14.80	14.08	0.38	0.53	0.45
Felis	1.92	1.68	1.91	8.78	7.48	9.39	0.26	0.26	0.26
Manis	1.46	1.06	1.66	6.59	3.71	7.03	0.55	0.62	0.59
Nycteris	0.97	0.87	0.79	4.34	3.40	4.36	0.12	0.14	0.13
Pteropus	1.57	1.28	1.35	6.86	5.86	7.03	0.17	0.24	0.20
Rhinolophus	0.83	0.69	0.74	3.52	3.21	3.90	0.07	0.09	0.08
Sorex	0.65	0.48	0.63	3.20	1.63	3.42	0.12	0.14	0.13
Sus	2.50	2.08	2.18	12.14	8.04	10.65	0.42	0.39	0.41
Tadarida	0.85	0.73	0.74	3.90	3.26	3.59	0.15	0.17	0.16
Tursiops	1.19	1.36	0.84	4.14	4.61	4.35	0.27	0.25	0.26
Euarchontoglires									
Cavia	1.88	1.57	1.63	9.01	6.49	8.18	0.21	0.29	0.25

TABLE 5.5. (Continued)

Taxon[b]	Radius			Length			Lumen Diameter		
	Ant	Lat	Post	Ant	Lat	Post	Ant	Lat	Post
Cynocephalus	1.93	1.47	1.70	9.93	6.99	8.38	0.27	0.37	0.32
Homo	2.94	2.35	3.10	13.55	10.30	14.73	0.92	0.86	0.89
Lepus	2.34	1.66	1.69	11.45	6.86	8.10	0.27	0.26	0.26
Macaca	2.70	2.47	2.54	12.79	10.60	13.05	0.33	0.50	0.41
Mus	0.78	0.60	0.67	3.86	2.48	3.60	0.15	0.15	0.15
Sylvilagus	1.86	1.29	1.44	8.98	5.65	7.38	0.12	0.24	0.18
Tupaia	1.73	1.44	1.50	9.24	7.85	8.07	0.18	0.22	0.20

[a] Measurement methodologies provided in text; expressed in millimeters.
[b] Specimens used listed in Table 5.1. Taxonomy follows Bininda-Emonds et al. (2007) and Wible et al. (2007). Values for *Kulbeckia*, *Zalambdalestes*, and the Zhelestid are averages (reported in Chapter 4).

TABLE 5.6. Deviations and aspect ratios of the semicircular canals[a]

Taxon	Linear			Angular			Ratio[c]		
	Ant	Lat	Post	Ant	Lat	Post	Ant	Lat	Post
Marsupialia									
Didelphis	0.22	0.38	0.00	8.62	23.70	0.00	0.97	0.79	1.08
Eutheria									
Kulbeckia	0.23	0.04	0.09	11.10	2.70	5.09	1.02	0.97	1.02
Ukhaatherium	0.06	0.04	0.12	8.22	6.21	9.92	0.94	0.95	0.90
Zalambdalestes	0.08	0.13	0.14	5.83	6.32	6.85	1.08	0.88	0.98
Zhelestid	0.23	0.11	0.23	12.90	6.88	15.20	0.95	0.75	0.89
Afrotheria									
Chrysochloris	0.13	0.00	0.23	6.81	0.00	18.90	1.32	1.01	0.91
Elephantoidea	1.60	0.14	1.36	18.50	3.01	14.30	0.72	1.31	1.10
Hemicentetes	0.18	0.07	0.10	9.41	5.90	6.48	0.88	0.93	0.72
Macroscelides	0.26	0.06	0.24	11.40	3.27	13.50	0.91	0.75	0.82
Orycteropus	1.06	0.41	0.70	19.70	7.21	11.50	0.81	1.03	1.28
Procavia	0.27	0.18	0.23	7.79	5.78	6.06	0.68	0.72	0.79
Trichechus	0.59	0.69	0.00	7.86	8.87	0.00	0.91	0.89	1.19
Xenarthra									
Dasypus	0.37	0.50	0.26	13.00	18.10	7.76	0.58	0.96	1.16
Laurasiatheria									
Atelerix	0.23	0.29	0.31	10.60	18.90	14.60	0.87	0.99	0.97
Balaenopteridae	0.40	0.20	0.53	9.03	5.44	15.90	0.91	0.39	1.21
Bathygenys	0.27	0.21	0.42	8.10	7.92	13.50	0.86	0.99	0.95
Canis	0.18	0.14	0.27	5.98	5.10	10.80	0.82	1.01	0.98
Equus	0.14	0.29	0.35	2.22	4.68	5.74	0.93	1.15	1.04
Eumetopias	0.04	0.89	0.47	0.76	16.40	9.45	0.96	1.24	1.18
Felis	0.15	0.13	0.00	4.48	4.43	0.00	0.77	1.04	1.01
Manis	0.17	0.00	0.21	6.69	0.00	7.25	0.76	0.82	0.93
Nycteris	0.07	0.10	0.31	4.14	6.61	22.70	0.91	0.71	0.95
Pteropus	0.28	0.32	0.11	10.20	14.30	4.67	0.94	0.97	0.85
Rhinolophus	0.12	0.05	0.18	8.31	4.14	13.90	0.83	0.46	0.98
Sorex	0.09	0.00	0.23	7.94	0.00	21.20	1.63	0.88	0.72
Sus	0.00	0.08	0.10	0.00	2.20	2.63	0.78	0.83	0.74
Tadarida	0.03	0.06	0.00	2.03	4.69	0.00	0.81	0.58	0.91
Tursiops	0.00	0.21	0.00	0.00	8.86	0.00	0.95	0.96	1.60
Euarchontoglires									
Cavia	0.62	0.43	0.86	19.10	15.80	30.70	0.75	0.49	0.99

TABLE 5.6. (Continued)

Taxon	Linear			Angular			Ratio[c]		
	Ant	Lat	Post	Ant	Lat	Post	Ant	Lat	Post
Cynocephalus	0.45	0.09	0.09	13.40	3.51	3.04	0.82	0.85	1.05
Homo	0.99	0.29	0.68	19.50	7.08	12.70	0.86	0.85	1.08
Lepus	0.16	0.06	0.32	3.92	2.07	10.90	0.86	0.87	0.81
Macaca	1.23	0.33	0.52	26.40	7.68	11.80	0.87	0.89	0.98
Mus	0.18	0.02	0.04	13.30	1.90	3.43	0.67	0.92	0.75
Sylvilagus	0.16	0.12	0.62	4.95	5.34	25.30	0.97	0.84	0.94
Tupaia	0.69	0.21	0.28	23.10	8.41	10.80	0.85	0.71	0.96

[a] Measurement methodologies provided in text; linear deviations expressed in millimeters; angular deviations expressed in degrees.
[b] Specimens used listed in Table 5.1. Taxonomy follows Bininda-Emonds et al. (2007) and Wible et al. (2007). Values for *Kulbeckia*, *Zalambdalestes*, and the Zhelestid are averages (reported in Chapter 4).
[c] Aspect ratio, calculated as height of canal arc divided by width.

the canal is 7.54 mm. The vestibular wall of the cochlea is expanded behind the fenestra cochleae to accommodate the perlimphatic sac. The bony canaliculus cochleae for the aqueduct of the cochlea extends 1.68 mm from the swelling in the cochlea as a straight tube.

The plane of the basal turn of the cochlea is rotated ventrally and anteriorly from the plane of the lateral semicircular canal by 19.6°. The basal end of the cochlea is inflected at the junction between the cochlea and the spherical recess of the vestibule. The fenestra vestibuli, in which the stapes sits, is rounded in shape, with a width versus height (stapedial) ratio of 1.6.

The division between the spherical and elliptical recesses within the bony vestibule is not distinct in *Didelphis*, although the swelling of the spherical recess is observed in anterior view of the labyrinth. The elliptical recess is bowed slightly medially. The anterior and posterior ends of the elliptical recess are penetrated by two large openings each, with the anterior (medial) and lateral (lateral) ampullae in the anterior aspect and the common crus and posterior ampulla at the posterior extremity (the opening for the common crus is medial to that of the posterior ampulla. The lateral semicircular canal does not possess a separate opening into the vestibule. Rather, the posterior limb of the lateral canal joins with the lateral limb of the posterior canal to form a secondary common crus. Presence of the secondary crus in *Didelphis* is a plesiomorphic condition inherited from the ancestor of Theria.

The bony channel for the vestibular aqueduct exits the vestibule ventral and anterior to the vestibular aperture of the common crus. The aqueduct extends dorsally and posteriorly, crossing the common crus in medial view, as a slender and straight tube before widening as it curves medially and becomes flattened. The channel for the vestibular aqueduct is more robust than the canaliculus cochleae, and the vestibular

aqueduct is over one and a half times longer than the cochlear aqueduct (2.58 mm versus 1.68 mm).

The planes of all three semicircular canals form obtuse angles with one another, particularly between the anterior and lateral canals (109°). The plane of the posterior canal forms an angle of 104° with the plane of the lateral canal, and 102° with the anterior. The posterior canal fits onto a single plane. However, both the anterior and lateral canals deviate from their average plane (8.24° and 5.07° respectively). The course of the anterior semicircular canal diverges medially at its midpoint, and the lateral canal is sigmoid when viewed with its plane parallel to the horizon. Although the total angular deviation of the anterior semicircular canal plane is greater than that calculated for the lateral canal, the anterior canal does not deviate significantly from its plane (ratio of the total linear deviation over canal diameter equals 0.85), whereas the deviation exhibited by the lateral canal is significant (ratio equals 1.29).

The anterior canal is the largest of the three, in terms of slender canal length (8.24 mm; 5.07 mm and 7.53 mm for the lateral and posterior respectively) and arc radius (1.46 mm; 0.93 mm and 1.23 mm for lateral and posterior respectively). However, the cross-sectional diameter of the lumen of the lateral semicircular canal (0.30 mm) is greater than either the anterior (0.26 mm) or posterior (0.24 mm) canals. The arcs of the anterior and posterior approach circularity (aspect ratios are 0.97 for the anterior arc and 1.08 for the posterior arc), although the arc of the lateral semicircular canal is lower (0.79), being relatively wider than either the anterior or posterior canal arcs. The ratio of the slender semicircular canal length over arc radius of curvature calculated for the posterior canal is greatest among the three canals (6.11; ratios for anterior and lateral canals are 5.63 and 5.47 respectively).

Compared to the reconstructions for the therian ancestor, the bony labyrinth of *Didelphis* retains several plesiomorphic therian characters, namely the presence of the secondary common crus and a relatively larger anterior semicircular canal compared to the lateral and posterior canals (see Meng and Fox, 1995; Chapter 4). A third character that likely is ancestral for therians, or at least eutherians, is a cochlea that is coiled to around 360°. However, the cochlea is derived for *Didelphis* in this regard, as it completes over two turns (Table 5.3). Lastly, the position of the lateral semicircular canal of *Didelphis* is similar to that of Cretaceous eutherians (Chapter 4) in that the lateral canal does not divide the space enclosed by the posterior canal in anterior view, a condition that is observed in many placentals, including the golden mole *Chrysochloris* (see below).

Eutheria

Eutheria is defined as the most recent common ancestor of crown Placentalia and all taxa more closely related to Placentalia than to Marsupialia (the marsupial mammals). a brief overview of the labyrinth of *Kulbeckia kulbecke* is provided here as a representative of non-placental Mesozoic eutherians (which are thought to exhibit the ancestral condition for Eutheria, if not Theria; Chapter 4), although data from three additional non-placental eutherian taxa were used to reconstruct hypothetical ancestral states. The non-placental eutherian taxa that were examined are from the Cretaceous of Asia, and they include a representative of a monophyletic group of zhelestids from the Bissekty Formation of Uzbekistan (see Chapter 4), *Kulbeckia kulbecke* (also from Uzbekistan), *Ukhaatherium nessovi*, and *Zalambdalestes lechei* (the latter two taxa from Mongolia). The relationships depicted for these taxa in Figure 5.2 follow Wible et al. (2007), and more thorough descriptions of the bony labyrinths of these taxa are provided

elsewhere (Chapter 4). The gross morphology of the non-placental taxa does not vary significantly among the taxa examined, and the values of measurements for *Kulbeckia* are averages across a sample of four petrosals reported in Chapter 4 of this dissertation. The bony labyrinth of *Kulbeckia* is illustrated in Figures 5.6-5.7.

The total length of the bony labyrinth of *Kulbeckia* is 4.73 mm (labyrinth length could only be measured for two specimens, URBAC 00-16 and URBAC 04-36), and the cochlea contributes 48.2% of the total volume of the inner ear (2.59 out of 5.37 mm^3). The contribution of the cochlea to the entire bony labyrinth is noticeably less in *Kulbeckia* than in *Didelphis*. Likewise, both the aspect ratio of the cochlear spiral (0.44) and the degree of coiling of the cochlea (446°) are smaller in *Kulbeckia* than in *Didelphis*. The spiral length of the cochlear canal of *Kulbeckia* is 4.11 mm. The canaliculus cochleae extends for 0.60 mm from a swelling of the cochlea near the fenestra cochleae.

The plane of the basal turn of the cochlea is rotated from the plane of the lateral semicircular canal by an average of 12.1° in *Kulbeckia*. The basal end of the cochlea is inflected before it joins the spherical recess of the vestibule near the fenestra vestibuli (average stapedial ratio of 1.9; Ekdale et al., 2004). The spherical and elliptical recesses are distinguished by a constriction of the vestibule lateral to the fenestra vestibuli.

As was observed in *Didelphis*, the posterior and lateral semicircular canals fuse to form a secondary common crus, which in turn empties into the posterior ampulla. The common crus between the anterior and posterior semicircular canals is situated medial to the posterior ampulla. The bony channel for the vestibular aqueduct was observed anteromedial to the common crus in two *Kulbeckia* specimens (URBAC 00-16 and 04-36), extending for an average of 1.24 mm.

The planes of the lateral and posterior semicircular canals almost form a right angle (89.6°), but the angles that each of these canals form with the anterior canal are

FIGURE 5.6. Bony labyrinth of *Kulbeckia kulbecke*. **A**, stereopair and labeled line drawing of digital endocast in anterior view; **B**, stereopair and labeled line drawing of digital endocast in dorsal view; **C**, stereopair and labeled line drawing of digital endocast in lateral view; **D**, line drawing of cochlea viewed down axis of rotation to display degree of coiling; **E**, line drawing of cochlea in profile. Abbreviations: **aa**, anterior ampulla; **ac**, anterior semicircular canal; **ant**, anterior direction; **cc**, canaliculus cochleae for aqueduct of cochlea; **co**, cochlea; **cr**, common crus; **dor**, dorsal direction; **er**, elliptical recess of vestibule; **fc**, fenestra cochleae; **fv**, fenestra vestibuli; **la**, lateral ampulla; **lc**, lateral semicircular canal; **med**, medial direction; **pa**, posterior ampulla; **pc**, posterior semicircular canal; **pl**, primary bony lamina; **pos**, posterior direction; **scr**, secondary common crus; **sl**, secondary bony lamina; **sr**, spherical recess of vestibule.

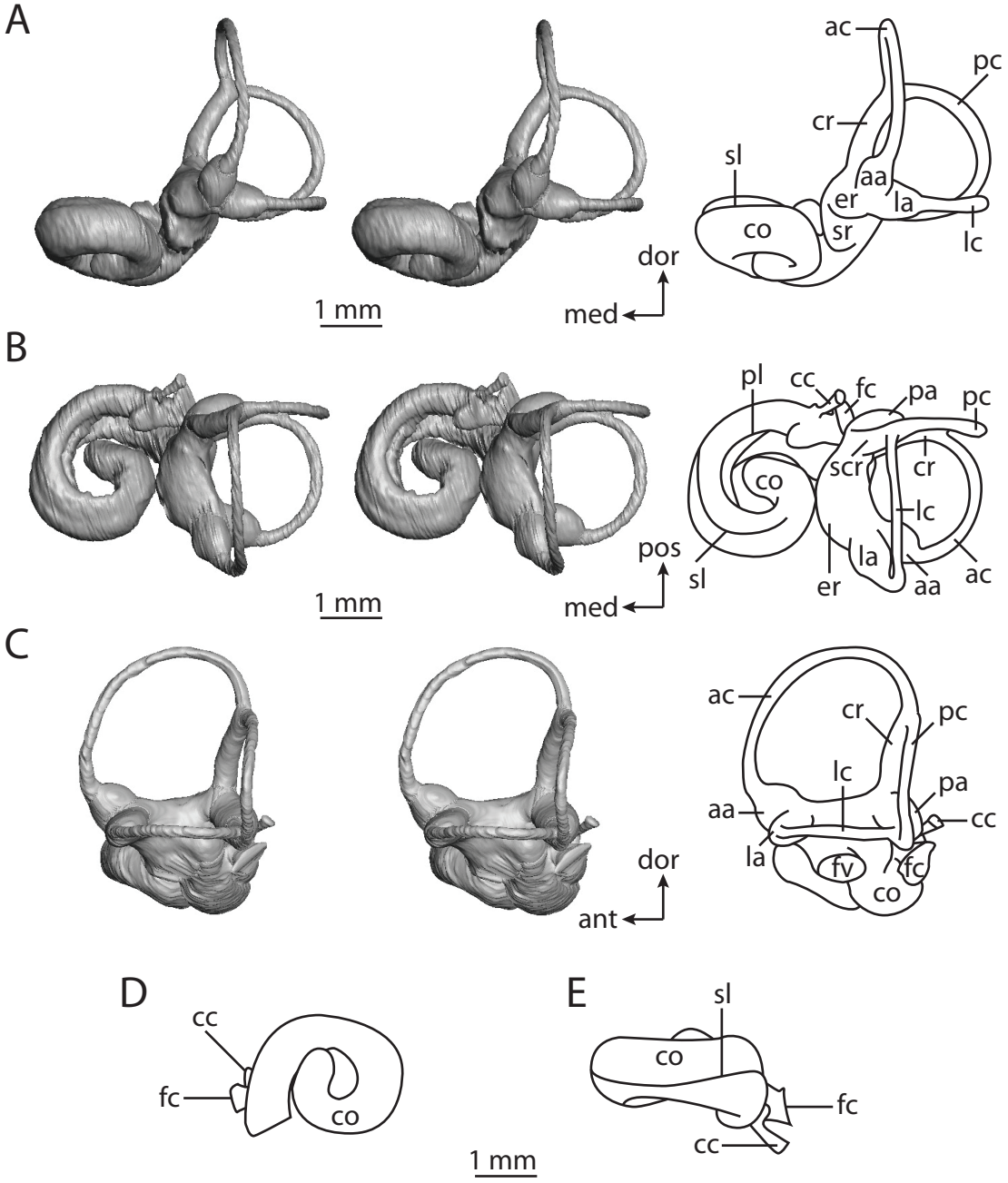
A
ac
pc
cr
sl
aa
er
la
co
sr
lc
dor
med
1 mm
B
pl
cc
fc
pa
pc
scr
cr
co
lc
pos
sl
la
er
aa
ac
med
1 mm
C
ac
cr
pc
lc
pa
aa
cc
la
fv
fc
co
dor
ant
D
cc
fc
co
E
sl
co
fc
cc
1 mm

FIGURE 5.7. CT slices through ear region of *Kulbeckia kulbecke*. Numbers refer to specific CT slices. Abbreviations: **aa**, anterior ampulla; **ac**, anterior semicircular canal; **ant**, anterior direction; **cn**, canal for cranial nerve VIII; **co**, cochlea; **cr**, common crus; **fc**, fenestra cochleae; **fn**, canal for cranial nerve VII; **fv**, fenestra vestibuli; **la**, lateral ampulla; **lc**, lateral semicircular canal; **med**, medial direction; **pa**, posterior ampulla; **pc**, posterior semicircular canal; **pl**, primary bony lamina; **pr**, promontorium housing cochlea; **sa**, subarcuate fossa; **scr**, secondary common crus; **sg**, canal for spiral ganglion within primary bony lamina; **sl**, secondary bony lamina; **ven**, ventral direction.

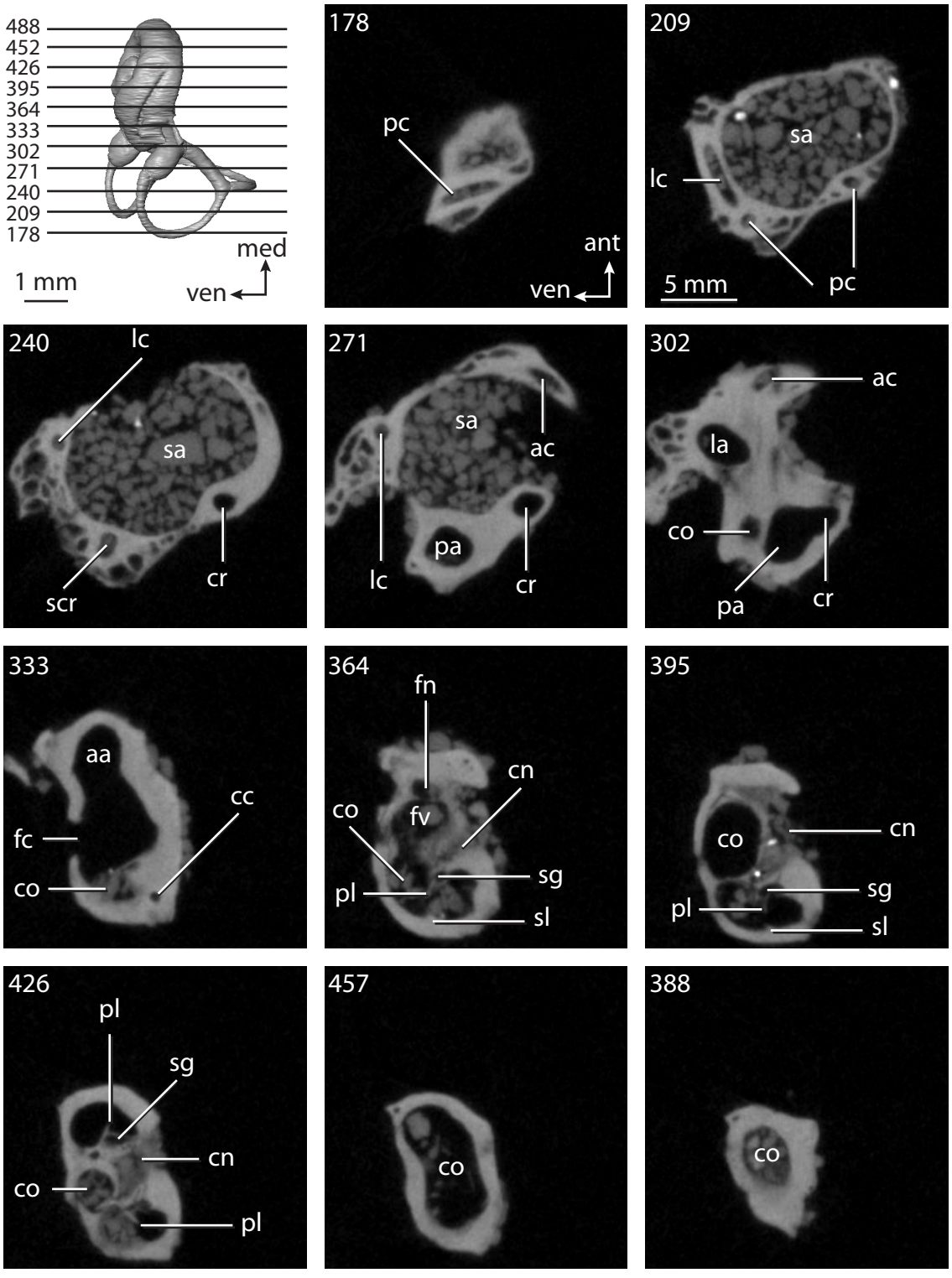
488
452
426
395
364
333
302
271
240
209
178
med
1 mm
ven
178
pc
ant
ven
209
sa
lc
5 mm
pc
240
lc
sa
scr
cr
271
sa
ac
lc
pa
cr
302
ac
la
co
pa
cr
333
aa
cc
fc
co
364
fn
cn
co
fv
pl
sg
sl
395
co
cn
pl
sg
sl
426
pl
sg
cn
co
pl
457
co
388
co

acute (79.9° for both). The anterior semicircular canal deviates the most from its plane (11.1°), and the lateral canal is the most planar (deviation of 2.70°; posterior canal deviates by 5.09°). Only the anterior canal deviates from its plane by a significant amount.

The anterior semicircular canal is the largest in terms of radius (1.19 mm; 0.92 mm and 0.96 mm for lateral and posterior respectively) and slender canal length (5.70 mm; 3.94 mm and 4.55 mm for lateral and posterior respectively). However, the lateral canal is the largest in terms of cross-sectional diameter (0.20 mm; 0.18 mm and 0.19 mm for anterior and posterior respectively). The aspect ratios of the anterior and posterior semicircular canals are identical (1.02) with arcs that are higher than they are wide. In contrast, the arc of the lateral semicircular canal is wider than it is high (ratio equals 0.97). The ratio of the slender anterior semicircular canal length over arc radius of curvature (4.80) is the largest ratio calculated among the three canals, although the ratio for the posterior canal is close to that of the anterior (4.75; ratio for lateral canal is 4.29).

The inner ear morphology of *Kulbeckia* and the other Mesozoic taxa, as well as *Didelphis*, were used to reconstruct the ancestral states of Eutheria. The bony labyrinth of the ancestor of Eutheria retained the ancestral therian conditions in all respects. The lateral semicircular canal formed a secondary common crus with the posterior canal, the plane of the lateral canal was low compared to the ampullar entrance of the posterior semicircular canal, the arc of the anterior semicircular canal was the largest among the three semicircular canals, and the aspect ratio of the cochlea was low (below 0.55). All ancestors at the nodes leading to crown Placentalia retained the ancestral eutherian states for all discrete characters.

The contribution of the ancestral eutherian cochlea to the total inner ear volume was 64%, which was less than that reconstructed for Theria (66%), and the percentage

decreased through time (59% for the most recent common ancestor of *Ukhaatherium* and Placentalia; 56% for the most recent common ancestor of Zalambdalestidae, which includes *Kulbeckia* and *Zalambdalestes*, and Placentalia). The contribution of the cochlea of the ancestral zalambdalestid was 51%.

The ancestral eutherian cochlea completed 580°, which was less than that reconstructed as the ancestral therian condition (685°). The most recent common ancestor of *Ukhaatherium* and Placentalia completed 510°, whereas the cochlea of the ancestor of Zalambdalestidae and Placentalia completed 570°. The ancestral condition of the cochlea reconstructed for Zalambdalestidae was 461°.

Placentalia

Placentalia includes the most recent common ancestor of extant placental mammals (e.g., *Hemicentetes semispinosum*, *Dasypus novemcinctus*, and *Homo sapiens*) plus all of its descendants. Placentalia is divided into the three major lineages Afrotheria, Xenarthra, and Boreoeutheria, which in turn is divided into Laurasiatheria and Euarchontoglires (Murphy et al., 2001b; Bininda-Emonds et al., 2007).

Entry of the lateral semicircular canal directly into the vestibule in absence of a secondary common crus is the single unambiguous otic synapomorphy for Placentalia, which is a condition not found outside of the crown (at least within Eutheria). The vast majority of placental taxa lack a secondary common crus (only exceptions among sampled taxa are *Orycteropus afer* and *Canis familiaris*). The cochlea of the ancestor of placental mammals completes 738° (over two turns), which is almost one half turn greater than the cochlea of the most recent common ancestor of Placentalia and

Zalambdalestidae (570°). The volumetric contribution of the cochlea to the entire labyrinth (58%) is less than that of the ancestral eutherian (64%).

The arc of the anterior semicircular canal is the largest among the three canal arcs, which is retained from the ancestor of Theria. The reconstructed states of both the position of the plane of the lateral semicircular canal compared to the ampullar entrance of the posterior canal and the aspect ratio of the cochlea in profile are equivocal owing to variation in the position of the lateral canal within Afrotheria and variation in the shape of the cochlear spiral in both Afrotheria and Boreoeutheria.

Afrotheria

Afrotheria is a clade of placentals endemic to Africa that includes the groups Afrosoricida (tenrecs and golden moles), Macroscelidea (elephant shrews), Tubulidentata (aardvark), Hyracoidea (hyraxes), Sirenia (dugongs and manatees), and Proboscidea (elephants). Monophyly of Afrotheria is controversial, primarily because it was not recognized in classical morphological studies of placentals, whether based on strict cladistic methodologies or not (Gregory, 1910; Simpson, 1945; McKenna, 1975; Novacek, 1986; Novacek and Wyss, 1986b; Novacek et al., 1988; Novacek, 1992a, b, 1993; McKenna and Bell, 1997). Monophyletic Afrotheria (including the afrosoricids and macroscelids) was first proposed by Springer et al. (1997), although the first use of the name “Afrotheria” was by Stanhope et al. (1998).

The earliest support for Afrotheria as a whole was restricted to molecular evidence (Springer et al., 1997; Stanhope et al., 1998; Springer et al., 1999; Madsen et al., 2001; Murphy et al., 2001a; van Dijk et al., 2001). Although more recent morphological evidence has been proposed to support the clade (Asher, 2001; Mess and

Carter, 2006; Sánchez-Villagra et al., 2007; Seiffert, 2007), strict morphological analyses fail to recover afrotherian monophyly (Asher et al., 2003; Wible et al., 2007).

The members of Afrotheria studied here are *Macroscelides proboscideus* (Macroscelidea), *Orycteropus afer* (Tubulidentata), a fossil elephantoid proboscidean (either *Mammut* or *Mammuthus*; see Chapter 2), *Trichechus manatus* (Sirenia), *Procavia capensis* (Hyracoidea), and the two afrosoricids *Chrysochloris* sp. (Chrysochloridae) and *Hemicentetes semispinosum* (Tenrecidae). There is a broad range in body mass among these taxa (Table 5.2), from 44 grams in *Chrysochloris* (Silva and Downing, 1995) to upwards of 8,000 kg in extinct elephantoids (Christiansen, 2004). Likewise, the inner ear cavities vary in size. The overall volume of the bony labyrinth within Afrotheria ranges from 4.11 mm^3 in *Chrysochloris* to 26.0 mm^3 in the fossil elephantoid. Dimensions of the bony labyrinths of afrotherians are provided in Table 5.2. Dimensions of the cochlea are provided in Table 5.3, and dimensions and orientations of the semicircular canals are reported in Tables 5.4-5.6.

Afrotheria often is placed as the sister taxon to all other placentals (e.g., Murphy et al., 2001a, b), although the results of Bininda-Emonds et al. (2007) include Afrotheria in a basal polytomy with Xenarthra and a clade comprised of the remaining placentals. Three major lineages are included within Afrotheria, which are Tubulidentata (aardvarks), Paenungulata (hyraxes, manatees, and elephants), and a clade including Macroscelidea (elephant shrews) and Afrosoricida (golden moles and tenrecs). The three major lineages are placed include these lineages within a polytomy at the base of Afrotheria (see Bininda-Emonds et al., 2007; Figure 5.2).

The bony labyrinth of the ancestor of Afrotheria retained the ancestral morphology of Placentalia in that the lateral semicircular canal entered into the vestibule directly and the arc of the anterior semicircular canal was the greatest among the three

canal arcs. The reconstructed states of the position of the lateral semicircular canal compared with the posterior canal, as well as the aspect ratio of the cochlea, are equivocal. The states reconstructed for all of the nodes within Afrotheria are identical to that of the afrotherian ancestor, except the state for the largest semicircular canal arc is equivocal for the clade consisting of *Procavia* and *Trichechus* (the posterior arc is largest for *Procavia* and the lateral is largest for *Trichechus*; see below).

The volumetric contribution of the cochlea to the total labyrinthine volume of the ancestral afrotherian was 56.0%, which was close to that reconstructed for the ancestor of Placentalia (58.0%). The ancestral cochlear contribution of the paenungulate clade consisting of *Procavia* and *Trichechus* was the same as that of the afrotherian ancestor (56.0%), although the contribution of the cochlea of the ancestor of Paenungulata was almost ten percent less (48.0%). Contributions of 63.0% and 64.0% were reconstructed for the ancestors of Afrosoricida and the more inclusive clade that also includes Macroscelidea, respectively. The ancestral afrotherian cochlea coiled 751°, which was greater than the ancestral placental condition, but less than the values reconstructed for the nodes within Afrotheria (768° for the clade consisting of Afrosoricida and Macroscelides; 833° for Afrosoricida; 790° for Paenungulata; 853° for the clade consisting of *Procavia* and *Trichechus*).

Afrosoricida

The group Afrosoricida contains Tenrecidae (tenrecs) and Chrysochloridae (golden moles). Although traditional classifications (e.g., Simpson, 1945) group tenrecids and chrysochlorids with other insectivorous mammals, such as the lipotyphlans *Erinaceus* (hedgehog) and *Sorex* (shrew), the results of more recent molecular studies (e.g., Springer et al., 1997; Stanhope et al., 1998), ally Tenrecidae and Chrysochloridae

with other placentals within the clade of African endemic mammals Afrotheria. Each afrosoricid group is represented by a single taxon, *Chrysochloris* sp. (Chrysochloridae) and *Hemicentetes semispinosum* (Tenrecidae).

The bony labyrinths of *Chrysochloris* and *Hemicentetes* differ in several ways, one of which is absolute size (Figures 5.8-5.11), where the former tends to be smaller than the latter (also observed in body mass where *Chrysochloris* sp. is 44.4 grams and *H. semispinosum* is 110 grams; Silva and Downing, 1995). For example, the labyrinth is 4.08 mm long in *Hemicentetes*, and 3.93 mm in *Chrysochloris*. However, the volume of the bony labyrinth is smaller in *Hemicentetes* (2.78 mm^3) than in *Chrysochloris* (4.11 mm^3).

The cochlear canal is not only longer in *Chrysochloris* (6.65 mm versus 3.79 mm), but the spiral also completes a greater degree of coiling (1191° or 3.3 turns versus 540° or 1.5 turns). The absolute volume of the cochlea is larger in *Chrysochloris* (2.93 mm^3 versus 1.39 mm^3 in *Hemicentetes*), and the proportion of the total labyrinth volume is greater in *Chrysochloris* (71.3%) than in *Hemicentetes* (49.9%).

The cochlea is more planispiral in *Hemicentetes* (aspect ratio of 0.38) than it is in *Chrysochloris* (aspect ratio of 0.63). The second turn of the cochlea in *Chrysochloris* is nearly equal in diameter to the basal turn, and obscures most of the basal turn when the cochlea is viewed tympanally (from down the axis of rotation), although the apical turn nearly fits within the arc of the basal turn of the cochlea of *Hemicentetes*. The plane of the basal turn of the cochlea of *Hemicentetes* also is rotated less from the plane of the lateral semicircular canal than it is in *Chrysochloris* (18.4° versus 41.9°).

The bony canaliculus cochleae for the aqueduct of the cochlea is shorter in *Hemicentetes* (0.28 mm versus 0.45 mm in *Chrysochloris*), and the cochlea is expanded

FIGURE 5.8. Bony labyrinth of *Chrysochloris* sp. **A**, stereopair and labeled line drawing of digital endocast in anterior view; **B**, stereopair and labeled line drawing of digital endocast in dorsal view; **C**, stereopair and labeled line drawing of digital endocast in lateral view; **D**, line drawing of cochlea viewed down axis of rotation to display degree of coiling; **E**, line drawing of cochlea in profile. Abbreviations: **aa**, anterior ampulla; **ac**, anterior semicircular canal; **ant**, anterior direction; **co**, cochlea; **cr**, common crus; **dor**, dorsal direction; **er**, elliptical recess of vestibule; **fc**, fenestra cochleae; **fv**, fenestra vestibuli; **la**, lateral ampulla; **lc**, lateral semicircular canal; **med**, medial direction; **pa**, posterior ampulla; **pc**, posterior semicircular canal; **pl**, primary bony lamina; **pos**, posterior direction; **ps**, outpocketing for perilymphatic sac; **sr**, spherical recess of vestibule.

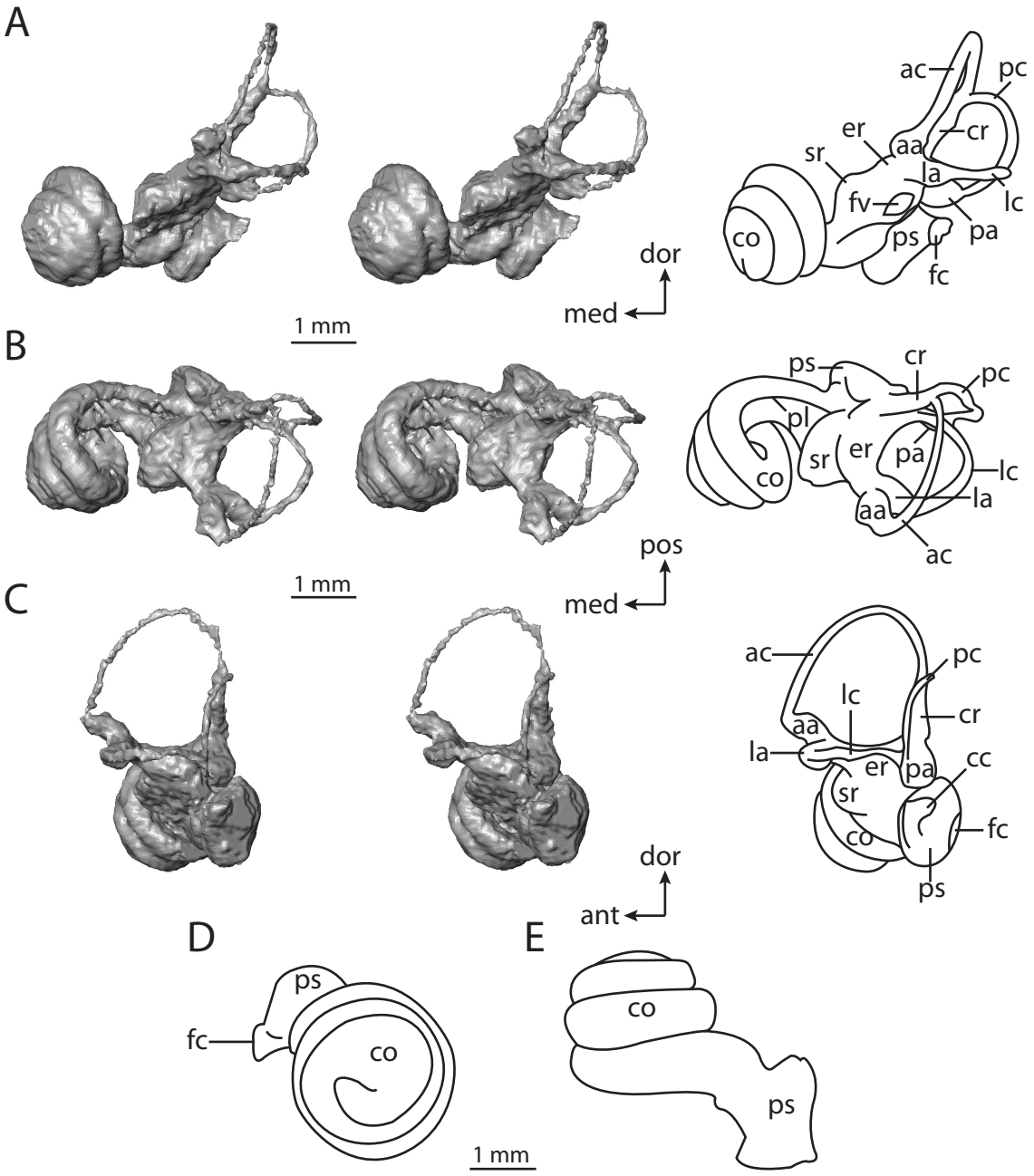
A
ac
pc
er
cr
sr
aa
la
fv
lc
co
ps
pa
fc
dor
med
1 mm
B
ps
cr
pc
pl
sr
er
pa
lc
co
la
aa
ac
pos
med
1 mm
C
ac
pc
lc
cr
aa
la
er
pa
cc
sr
fc
co
ps
dor
ant
D
ps
fc
co
1 mm
E
co
ps

FIGURE 5.9. CT slices through ear region of *Chrysochloris* sp. Numbers refer to specific CT slices. Abbreviations: **aa**, anterior ampulla; **ac**, anterior semicircular canal; **cn**, canal for cranial nerve VIII; **co**, cochlea; **cr**, common crus; **dor**, dorsal direction; **er**, elliptical recess of vestibule; **fn**, canal for cranial nerve VII; **fv**, fenestra vestibuli; **la**, lateral ampulla; **lc**, lateral semicircular canal; **med**, medial direction; **pc**, posterior semicircular canal; **pl**, primary bony lamina; **pos**, posterior direction; **sr**, spherical recess of vestibule; **st**, stapes within fenestra vestibuli; **vb**, vestibule.

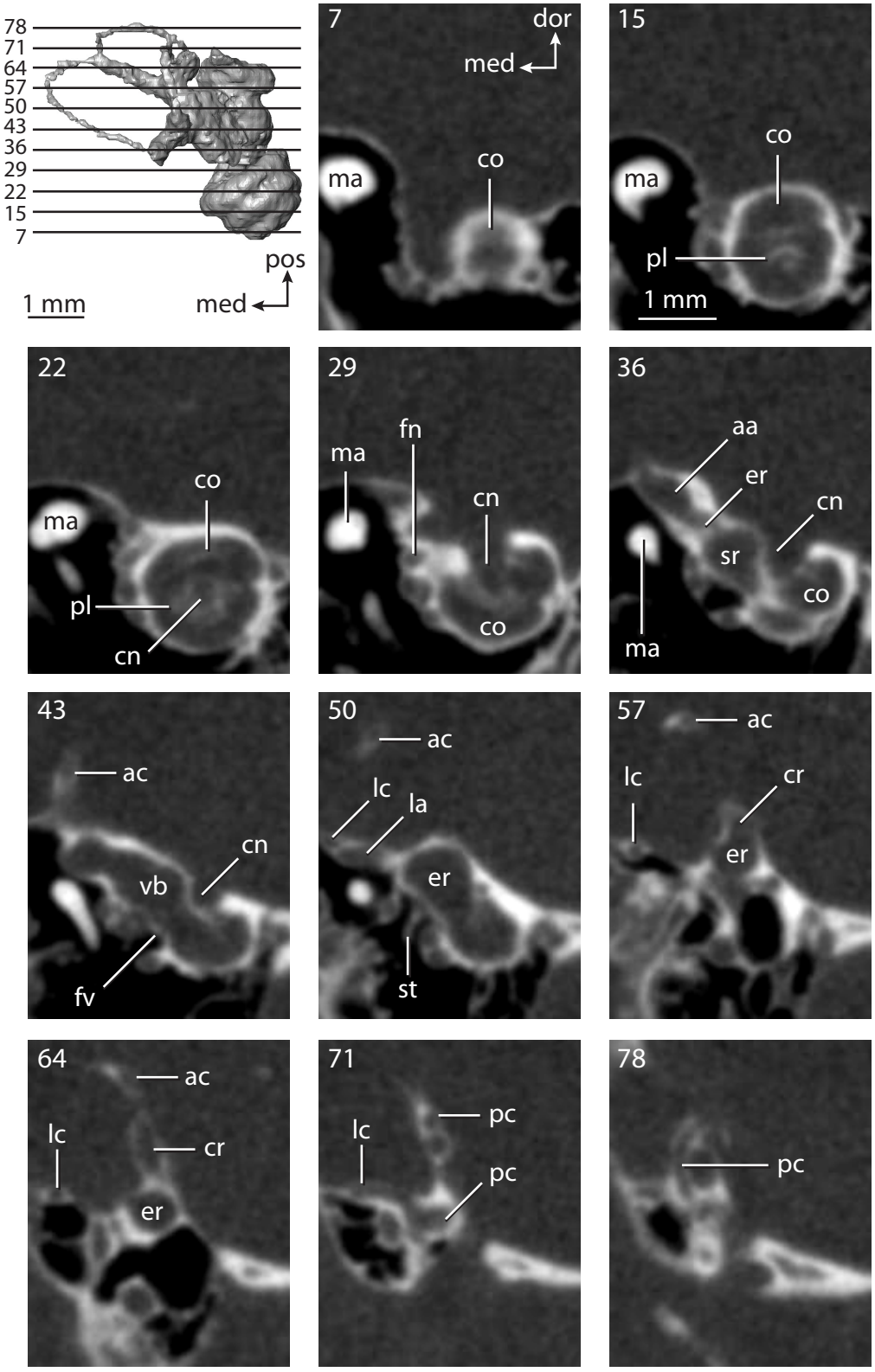
78
71
64
57
50
43
36
29
22
15
7
pos
med
1 mm
7
dor
med
ma
co
15
co
ma
pl
1 mm
22
co
ma
pl
cn
29
fn
ma
cn
co
36
aa
er
cn
sr
co
ma
43
ac
cn
vb
fv
50
ac
lc
la
er
st
57
ac
lc
cr
er
64
ac
lc
cr
er
71
pc
lc
pc
78
pc

FIGURE 5.10. Bony labyrinth of *Hemicentetes semispinosum*. **A**, stereopair and labeled line drawing of digital endocast in anterior view; **B**, stereopair and labeled line drawing of digital endocast in dorsal view; **C**, stereopair and labeled line drawing of digital endocast in lateral view; **D**, line drawing of cochlea viewed down axis of rotation to display degree of coiling; **E**, line drawing of cochlea in profile. Abbreviations: **aa**, anterior ampulla; **ac**, anterior semicircular canal; **ant**, anterior direction; **cc**, canaliculus cochleae; **co**, cochlea; **cr**, common crus; **dor**, dorsal direction; **er**, elliptical recess of vestibule; **fc**, fenestra cochleae; **fv**, fenestra vestibuli; **la**, lateral ampulla; **lc**, lateral semicircular canal; **med**, medial direction; **pa**, posterior ampulla; **pc**, posterior semicircular canal; **pos**, posterior direction; **ps**, outpocketing for perilymphatic sac; **sl**, secondary bony lamina; **sr**, spherical recess of vestibule.

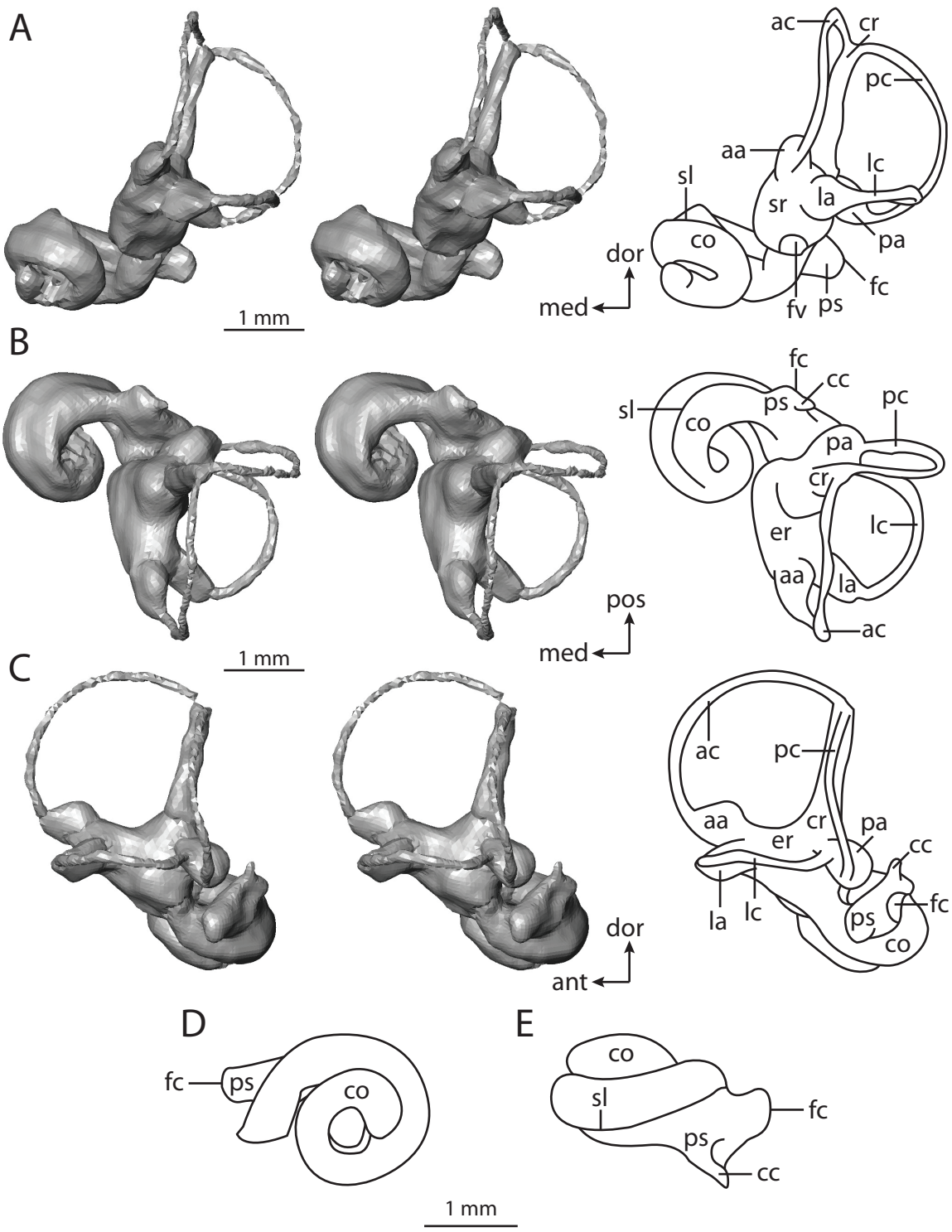
A
ac
cr
pc
aa
lc
sl
sr
la
pa
co
dor
med
fc
fv
ps
1 mm
B
fc
cc
ps
pc
sl
co
pa
cr
er
lc
aa
la
ac
pos
med
1 mm
C
ac
pc
aa
cr
pa
er
cc
fc
la
lc
ps
co
dor
ant
D
fc
ps
co
E
co
sl
fc
ps
cc
1 mm

FIGURE 5.11. CT slices through ear region of *Hemicentetes semispinosum*. Numbers refer to specific CT slices. Abbreviations: **aa**, anterior ampulla; **ac**, anterior semicircular canal; **co**, cochlea; **cr**, common crus; **dor**, dorsal direction; **er**, elliptical recess of vestibule; **fn**, canal for cranial nerve VII; **la**, lateral ampulla; **lc**, lateral semicircular canal; **med**, medial direction; **pa**, posterior ampulla; **pc**, posterior semicircular canal; **pos**, posterior direction; **sa**, subarcuate fossa; **vb**, vestibule.

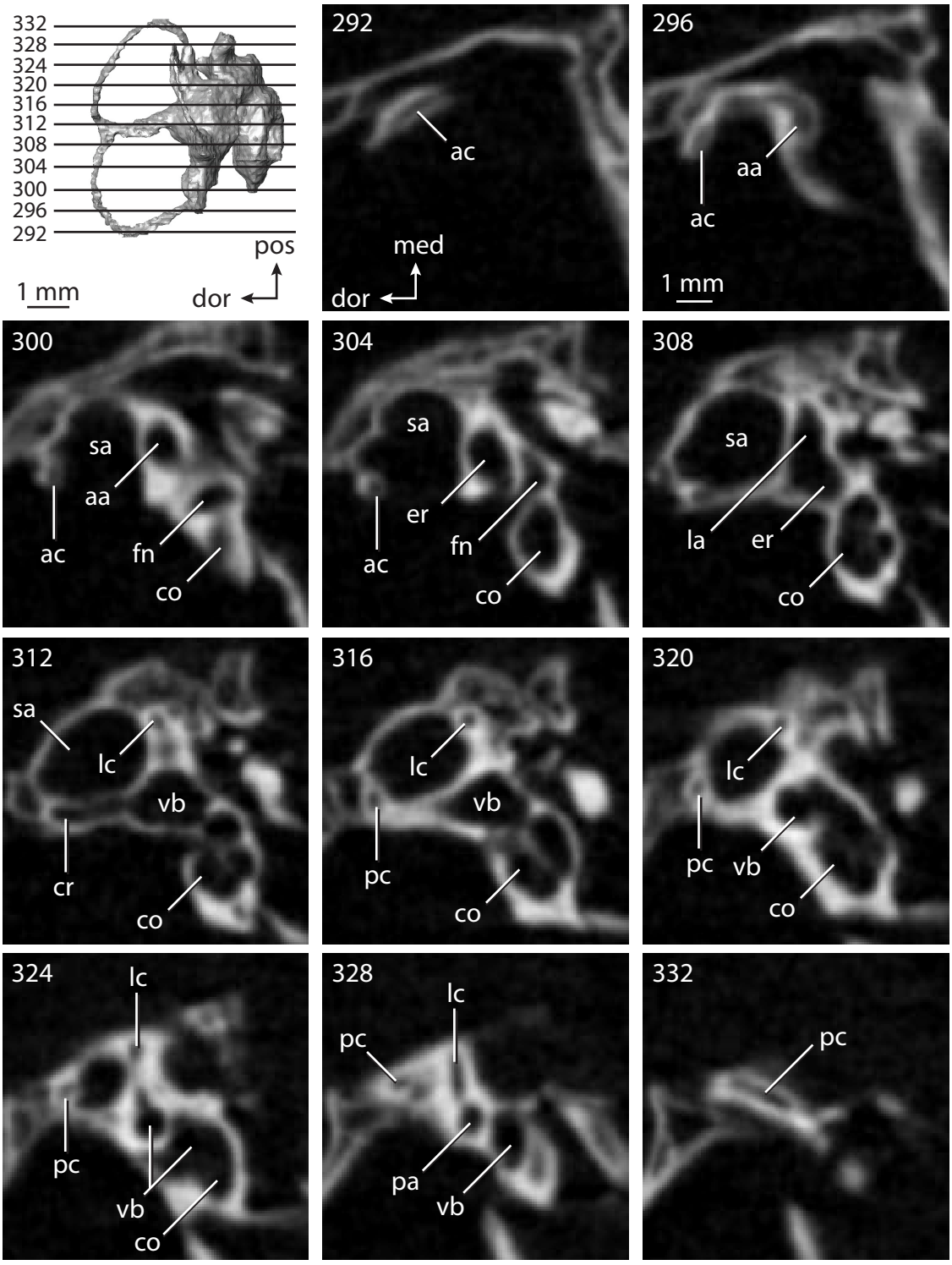
332
328
324
320
316
312
308
304
300
296
292
pos
dor
1 mm
292
ac
med
dor
296
aa
ac
1 mm
300
sa
aa
ac
fn
co
304
sa
er
ac
fn
co
308
sa
la
er
co
312
sa
lc
vb
cr
co
316
lc
vb
pc
co
320
lc
pc
vb
co
324
lc
pc
vb
co
328
lc
pc
pa
vb
332
pc

behind the fenestra cochleae in *Chrysochloris* for the perilymphatic sac in both afrosoricid species. The swelling hooks posteriorly before the canaliculus cochleae exits the cochlea, and the canaliculi of these taxa are not as delicate as that observed in *Didelphis*. The fenestra vestibuli is more oval in *Chrysochloris*, with a stapedial ratio of 2.8. The ratio is 1.6 in *Hemicentetes*.

The spherical and elliptical recesses are distinguishable within the vestibule of *Chrysochloris*, where the former projects anteriorly towards the cochlea. As a whole, the spherical recess is ovoid in shape. The elliptical recess is smaller than the spherical recess in *Chrysochloris*, and forms a gently curved tube with openings for the semicircular canal system in dorsal view. Each end of the tube is extended into a chamber dorsally, and each extension is expressed as a short pedestal in the endocast. The anterior and posterior ampullae open into the anterior chamber of the elliptical recess. The posterior chamber is penetrated by three major apertures, which lead to the posterior ampulla, the common crus, and the posterior limb of the lateral semicircular canal. The latter of these apertures opens into the vestibule near the anterodorsal edge of the opening for the posterior ampulla.

The recesses are less distinguishable in *Hemicentetes*, and the vestibule forms a continuous cavity, albeit irregular in shape. The vestibule of *Hemicentetes* is penetrated by four major openings only, as opposed to five in *Chrysochloris*. The openings into the vestibule of *Hemicentetes*, in addition to the junction of the vestibule and cochlea, lead to the ampullae of the three semicircular canals, as well as the common crus. As in *Didelphis*, the posterior limb of the lateral semicircular canal does not have its own aperture into the vestibule in *Hemicentetes*, as is the case with *Didelphis*. However, the lateral canal of *Hemicentetes* does not join with the posterior semicircular canal to form a secondary common crus which is observed in the opossum,; rather the lateral canal

empties into the posterior ampulla. A groove on the anterior wall of the posterior ampulla that presumably accommodated the membranous lateral semicircular duct in life extends from the lateral semicircular canal to the vestibule. Such a condition suggests the lateral duct is separate from the membranous posterior ampulla in this species, although such cannot be determined with certainty through examination of the bony labyrinth alone.

No trace of the bony channel for the vestibular aqueduct was observed in the CT slices of *Hemicentetes*. The aqueduct likely is present (there is no record of any mammal lacking this structure) but likely is small and too narrow to be captured on the CT imagery. The channel for the aqueduct is observed in CT data of *Chrysochloris*, in which the channel exits the elliptical recess medial to the common crus. An indistinct groove for the endolymphatic duct along the medial wall of the elliptical recess (expressed as a ridge on the endocast) extends from the channel for the vestibular aqueduct to the junction between the elliptical and spherical recesses.

The planes of the semicircular canals do not form right angles with one another in either afrosoricid species examined. In *Chrysochloris*, the largest angle was measured between the posterior and lateral canals (96.7°), and the smallest was measured between the anterior and lateral canals (65.6°). The angle between the anterior and posterior semicircular canal planes is 86.9°. The widest angle measured in *Hemicentetes* is between the anterior and posterior canals (87.9°), which not only is the largest angle between two semicircular canals in either taxon, but it is also the closest angle to 90° in the labyrinths of either *Chrysochloris* or *Hemicentetes*. The smallest angle in *Hemicentetes* is between the posterior and lateral canals (79.3°), and the angle between the anterior and lateral semicircular canals in this species is 87.0°.

The anterior canal is the largest of all semicircular canals in terms of volume, slender canal length, and arc radius for both afrosoricid taxa included in the present study

(0.031 mm^3, 4.71 mm, and 1.10 mm respectively in *Chrysochloris*; 0.37 mm^3, 4.96 mm, and 1.10 mm respectively in *Hemicentetes*). Likewise, the lateral semicircular canal was the smallest in both species in at least slender canal length and arc radius (2.62 mm and 0.67 mm respectively for *Chrysochloris*; 4.69 mm and 1.38 mm respectively for *Hemicentetes*).

Not only is the anterior semicircular canal the largest among all of the canals, it has the highest aspect ratio in *Chrysochloris* (1.32 versus 0.88 in *Hemicentetes*), indicating that the height of the arc is larger in proportion to the width than it is in other canals. The height of the lateral semicircular canal arc is nearly equal to the width of that arc in *Chrysochloris* (ratio of 1.01), and nearly so in *Hemicentetes* (ratio of 0.93). The posterior canal arc has a ratio of 0.91 in *Chrysochloris*, and 0.72 in *Hemicentetes*. In fact, the aspect ratio of the posterior canal arc is the lowest among all of the canals between the two species. The ratios between the length of a slender semicircular canal and the radius of its arc for *Chrysochloris* are 4.30 for the anterior canal, 3.89 for the lateral canal, and 5.07 for the posterior canal. A similar pattern is observed in *Hemicentetes* where the posterior semicircular canal has the highest canal length to arc radius ratio (5.41), and the lateral canal has the lowest (3.59; ratio for anterior canal equals 4.52).

The angular deviation of the anterior and lateral semicircular canals from their planes in *Chrysochloris* are less than that observed for the same canals in *Hemicentetes*, although the lateral semicircular canal of *Chrysochloris* is the only planar canal between the taxa (the total angular deviation of the lateral canal in *Hemicentetes* is 5.90°). The least planar canal in *Chrysochloris* is the posterior (18.9°; 6.48 ° in *Hemicentetes*), and the posterior is the only canal to deviate substantially from its plane in *Chrysochloris* (ratio of the total linear deviation over cross-sectional diameter of the posterior canal is 1.31; ratio for the anterior canal is 0.87). Both the anterior and posterior canals of

Hemicentetes deviate substantially from their planes (ratios are 1.38 and 1.11 respectively), although the ratio is only 0.47 for the lateral semicircular canal. The anterior semicircular canal of *Hemicentetes* deviates from its plane by a total of 9.4°, whereas the same canal deviates by 6.8° in *Chrysochloris*.

Lastly, the plane of the lateral semicircular canal is high with respect to the posterior canal in both *Chrysochloris* and *Hemicentetes* to an extent that it divides the space enclosed by the arc of the posterior semicircular canal into dorsal and ventral sections when the labyrinth is oriented in anterior view. Within Afrotheria, a similar condition is observed in *Macroscelides* and *Procavia* as described below. The sagittal labyrinthine index (following Spoor and Zonneveld, 1995) of *Chrysochloris* is 21.7 and 4.1 in *Hemicentetes*, both of which are lower than the other afrotherians exhibiting this feature of the bony labyrinth (see below). The labyrinthine index of *Hemicentetes* is smaller than that calculated for any other mammal in this study (in which the lateral canal divides the space enclosed by the posterior canal arc when the labyrinth is in anterior view).

The bony labyrinths of both afrosoricid taxa retain the ancestral placental condition in that the lateral semicircular canal does not form a secondary common crus (although the canal opens into the posterior ampulla rather than the vestibule in *Hemicentetes*), and the anterior semicircular canal has the greatest radius among the three canals. Although the cochlea of *Chrysochloris* exhibits a great degree of coiling (over three complete turns at 1191°; Table 5.3), the coiling in *Hemicentetes* (540° or 1.5 turns) is only slightly greater than the average calculated for zhelestids from the Bissekty Formation (518° or 1.4 turns; Chapter 4), and nearly 200° (over one half turn) less than the ancestral placental condition.

Both *Hemicentetes* and *Chrysochloris* are derived with respect to the ancestral eutherian condition in the placement of the lateral semicircular canal that visually divides the space enclosed by the posterior semicircular canal when the labyrinth is in anterior view. Such a condition is not observed in *Didelphis* or any Mesozoic eutherian, including *Kulbeckia* as described above (also see Chapter 4 of this dissertation).

Macroscelidea

Macroscelidea contains the elephant shrews or sengis. The phylogenetic affinities of Macroscelidea are contentious, although the analyses of Bininda-Emonds et al. (2007), as well as other molecular studies (e.g., Springer et al., 1998; Murphy et al., 2001a) group macroscelideans inside Afrotheria. Within Afrotheria, Macroscelides holds a sister relationship with Afrosoricida (Bininda-Emonds et al., 2007).

Only one species of Macroscelidea (*Macroscelides proboscideus*) was examined in the present study (Figures 5.12-5.13). The average body mass of *Macroscelides* (38.4 grams) is less than either afrosoricid taxon examined (44.4 grams for *Chrysochloris* sp. and 110 grams for *Hemicentetes semispinosum*; mass for *Chrysochloris* is an average across the genus because the species of *Chrysochloris* used is unknown) as reported by Silva and Downing (1995). However, the dimensions of the bony labyrinth of *Macroscelides* tend to be intermediate between the afrosoricids. The volume of the combined inner ear cavities in Macroscelides is 9.19 mm^3 (4.11 mm^3 for *Chrysochloris*; 2.78 mm^3 for *Hemicentetes*) and the labyrinth is 4.31 mm in length (3.93 mm for *Chrysochloris*; 4.08 mm for *Hemicentetes*). Likewise, the skull length of the *Macroscelides* specimen (32.26 mm) is intermediate between *Chrysochloris* (23.85 mm) and *Hemicentetes* (30.61 mm).

FIGURE 5.12. Bony labyrinth of *Macroscelides proboscideus*. **A**, stereopair and labeled line drawing of digital endocast in anterior view; **B**, stereopair and labeled line drawing of digital endocast in dorsal view; **C**, stereopair and labeled line drawing of digital endocast in lateral view; **D**, line drawing of cochlea viewed down axis of rotation to display degree of coiling; **E**, line drawing of cochlea in profile. Abbreviations: **aa**, anterior ampulla; **ac**, anterior semicircular canal; **ant**, anterior direction; **av**, bony channel for aqueduct of vestibule; **cc**, canaliculus cochleae for aqueduct of cochlea; **co**, cochlea; **cr**, common crus; **cv**, canal for cochlear vein; **dor**, dorsal direction; **er**, elliptical recess of vestibule; **fc**, fenestra cochleae; **fv**, fenestra vestibuli; **la**, lateral ampulla; **lc**, lateral semicircular canal; **med**, medial direction; **pa**, posterior ampulla; **pc**, posterior semicircular canal; **pl**, primary bony lamina; **pos**, posterior direction; **ps**, outpocketing for perilymphatic sac; **sl**, secondary bony lamina; **sr**, spherical recess of vestibule.

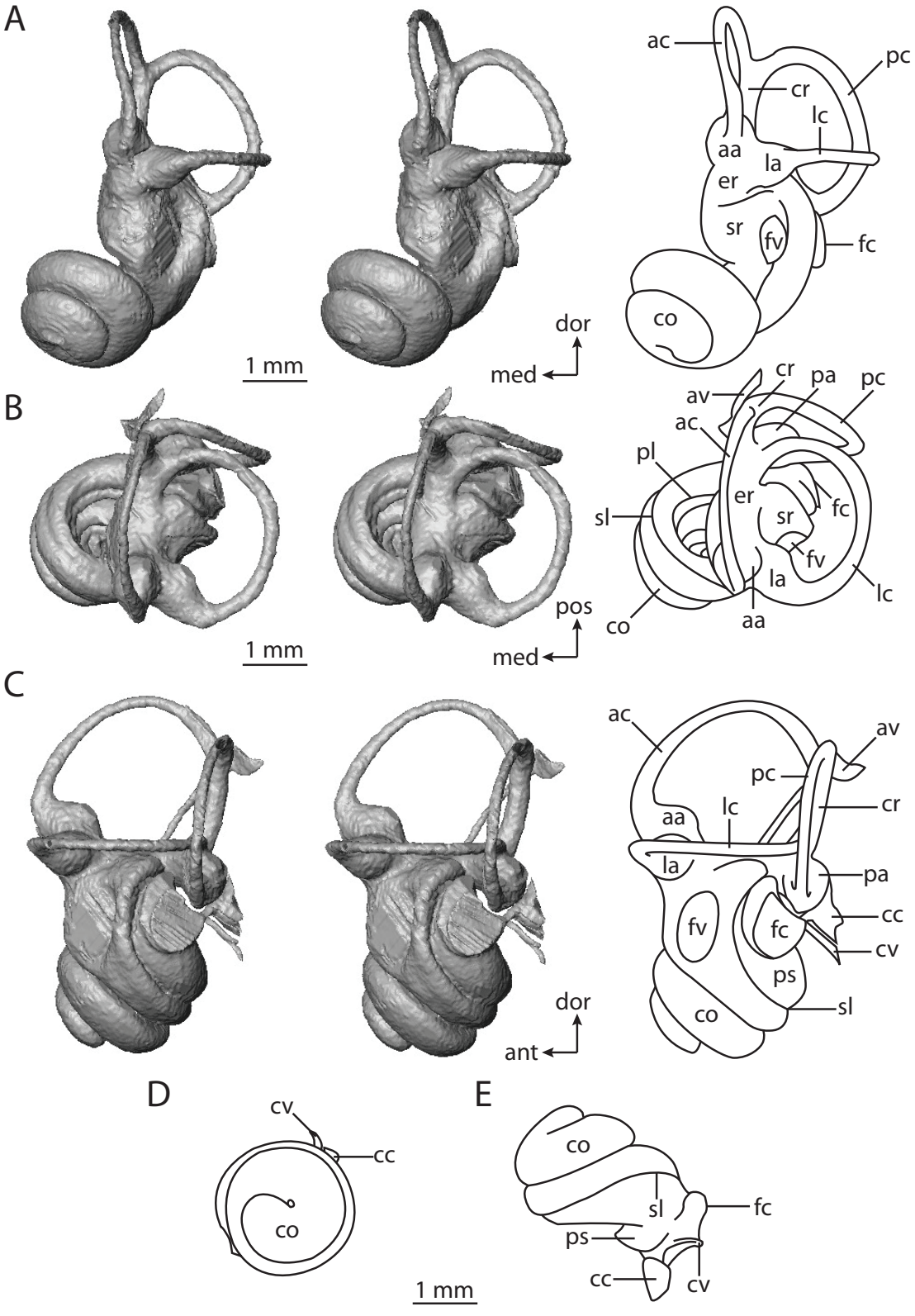
A
ac
pc
cr
lc
aa
la
er
sr
fv
fc
co
dor
med
1 mm
B
cr
pa
pc
av
ac
pl
er
sl
sr
fc
fv
la
lc
co
aa
pos
med
1 mm
C
ac
av
pc
cr
lc
aa
la
pa
cc
fv
fc
cv
ps
co
sl
dor
ant
D
cv
cc
co
E
co
sl
fc
ps
cc
cv
1 mm

FIGURE 5.13. CT slices through ear region of *Macroscelides proboscideus*. Abbreviations: **aa**, anterior ampulla; **ac**, anterior semicircular canal; **av**, bony channel for aqueduct of vestibule; **cc**, canaliculus cochleae; **cn**, canal for cranial nerve VIII; **co**, cochlea; **cr**, common crus; **dor**, dorsal direction; **er**, elliptical recess of vestibule; **fc**, fenestra cochleae; **la**, lateral ampulla; **lc**, lateral semicircular canal; **med**, medial direction; **pa**, posterior ampulla; **pc**, posterior semicircular canal; **pl**, primary bony lamina; **pos**, posterior direction; **sa**, subarcuate fossa; **sl**, secondary bony lamina; **sr**, spherical recess of vestibule; **st**, stapes within fenestra vestibuli.

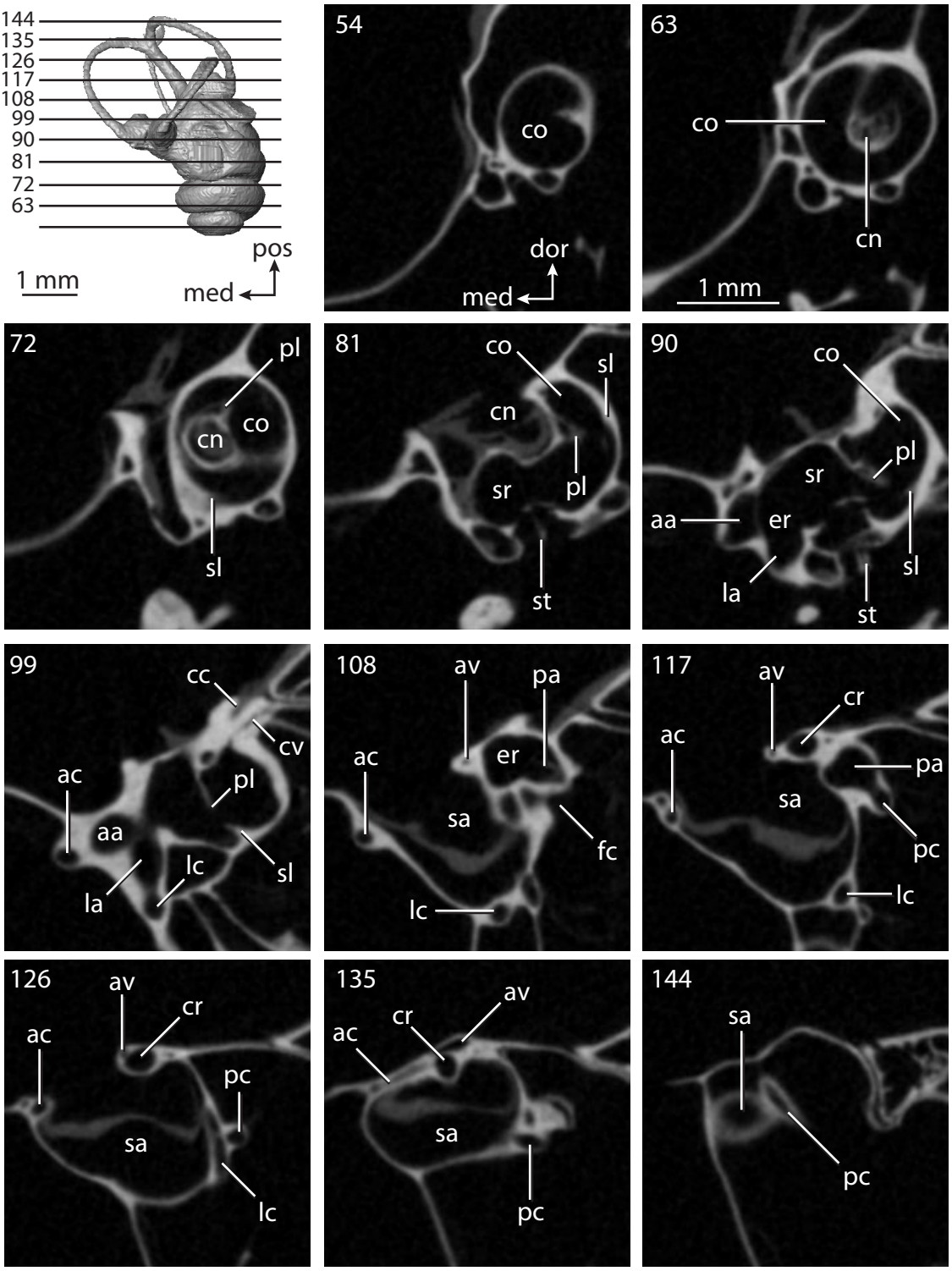
144
135
126
117
108
99
90
81
72
63
1 mm
pos
med
54
co
dor
med
63
co
cn
1 mm
72
pl
co
cn
sl
81
co
sl
cn
sr
pl
st
90
co
pl
sr
aa
er
la
sl
st
99
cc
cv
ac
pl
aa
lc
la
sl
108
av
pa
ac
er
sa
fc
lc
117
av
cr
ac
pa
sa
pc
lc
126
av
cr
ac
pc
sa
lc
135
av
cr
ac
sa
pc
144
sa
pc

The cochlea of *Macroscelides* contributes 71.3% of the total volume of the inner ear (6.59 mm^3 out of 9.19 mm^3; Figure 5.4). This proportion is almost identical to that of *Chrysochloris*. Furthermore, the cochlea of *Macroscelides* not only has a higher aspect ratio than *Hemicentetes* (0.80 versus 0.38; ratio of *Chrysochloris* is 0.63), but the ratio in *Macroscelides* is higher than that calculated for any other afrotherian examined in this study. The second turn of the cochlea in *Macroscelides* sits upon the basal whorl, as is observed in *Chrysochloris*, but not *Hemicentetes*. The cochlear spiral of *Macroscelides* completes two whorls (720°), and the total length of the canal is 7.11 mm.

The secondary bony lamina for the basilar membrane is well developed on the radial wall of the basal turn of the cochlea (expressed as the distinct groove on the endocast), and is prolonged beyond three quarter turns of the basal whorl, but ends before the basal whorl is complete. The secondary lamina curves sharply at the basal end of the cochlear canal, between the fenestrae cochleae and vestibuli, the latter of which has an aspect ratio of 1.9 (similar to that observed in *Hemicentetes*). The plane of the basal turn of the cochlea deviates from that of the lateral semicircular canal by 25.1° in *Macroscelides*, which is greater than *Hemicentetes* (18.4°), but not as great as *Chrysochloris* (41.9°).

A triangular outpocketing for the perilymphatic sac that leads to two bony canals is situated medial to the fenestra cochleae. One of these canals is situated ventral to the other. The dorsal canal extending from the triangular outpocketing is the bony canaliculus cochleae for the aqueduct of the cochlea, and the ventral channel transmits a cochlear vein in life (which is observed traveling with the membranous aqueduct of various mammal species; Gray, 1907, 1908). The ventral canal for the cochlear vein is more delicate than the canaliculus cochleae, and forms a straight tube that widens slightly before it opens on the medial surface of the petrosal. Unlike the canal for the cochlear

vein, the canaliculus cochleae widens rapidly as it extends away from the cochlea, forming a pyramid shaped conduit for the aqueduct of the cochlea. The canaliculus cochleae is 0.58 mm in length, which is larger than the channel in either *Chrysochloris* (0.45 mm) or *Hemicentetes* (0.51 mm). The canaliculus is more easily observed in the CT scans of *Macroscelides* than in the data of afrosoricids, also.

The division between the spherical and elliptical recesses is not well defined in *Macroscelides*, although there is a slight constriction in the vestibule lateral to the fenestra vestibuli. The elliptical recess of the vestibule is not curved in *Macroscelides*, but the chamber contains five major openings, as also is observed in the bony labyrinth of *Chrysochloris*, for the common crus, ampullae of the semicircular canals, and a separate opening for the posterior limb of the lateral semicircular canal near the vestibular aperture of the posterior ampulla.

The bony channel for the aqueduct of the vestibule exits the spherical recess anterior to the common crus at a greater distance than it does in *Didelphis*. The channel is a straight tube of uniform diameter across most of its length (2.08 mm, which is significantly longer than the canaliculus cochleae at 0.58 mm) until it turns posterolaterally and flattens into a fissure-like chamber before opening onto the endocranial surface of the petrosal (near the union of the posterior and anterior semicircular canals at the apex of the common crus).

The semicircular canals form gentle curves, and the planes of the anterior and posterior canals nearly form a right angle (90.7°). The planes of the lateral and other two semicircular canals form obtuse angles (95.7° between lateral and posterior; 100° between lateral and anterior). None of the semicircular canals fit onto a single plane, particularly the anterior canal where a significant deviation of 26.4° was measured (ratio of total linear deviation over cross-sectional diameter is 1.37). The posterior canal is the

most planar of the three (total deviation equals 5.9°; lateral canal deviates 7.7°), although the deviation of the posterior canal is significant, whereas the deviation of the lateral canal is not (ratios of linear deviation to canal diameter are 1.36 and 0.30 respectively).

The anterior semicircular canal is the longest of the three canals (5.61 mm; lateral equals 4.21 mm; posterior equals 5.22 mm), and the radius of the anterior canal arc (1.32 mm) is larger than either the lateral (1.05 mm) or posterior (1.02 mm) arc canals. However, the cross-sectional diameter of the lumen of the posterior canal is larger than the anterior canal (0.47 mm versus 0.33 mm), although the largest diameter was measured for the lateral canal (0.50 mm).

The ratio of the slender canal length over arc radius is greatest for the posterior semicircular canal (5.10). The ratio for the anterior canal is 4.24, and the ratio for the lateral canal is 4.00. The aspect ratio of the anterior semicircular canal arc (0.91; height equals 2.51 mm; width equals 2.77 mm) is higher than the ratio of the arcs of either the lateral (0.75; height equals 1.81 mm; width equals 2.40 mm) or posterior canal (0.82; height equals 1.85 mm; width equals 2.25 mm). This result signifies that the arc of the anterior semicircular canal approaches a perfect circle more so than the other canal arcs.

The plane of the lateral semicircular canal is positioned high with respect to the posterior semicircular canal in *Macroscelides* so that the lateral canal divides the space enclosed by the posterior semicircular canal arc when the bony labyrinth is viewed anteriorly. The sagittal labyrinthine index for *Macroscelides* is 32.7, which is greater than that measured for *Chrysochloris*. A high index indicates a more dorsal position of the lateral semicircular canal.

Although *Macroscelides* holds a sister relationship with afrosoricids in the supertrees reconstructed by Bininda-Emonds et al. (2007), there are no unambiguous otic synapomorphies uniting the clade. The lateral semicircular canal is derived relative to the

ancestral eutherian state in that it takes a high position relative to the posterior canal, as is observed in *Chrysochloris* and *Hemicentetes*. The afrosoricids and *Macroscelides* lack secondary common crura, which are present in Cretaceous eutherians (Meng and Fox, 1995; Chapter 4). Absence of a secondary common crus is derived for Placentalia, and therefore a feature that the clade consisting of Macroscelidea and Afrosoricida inherited from its placental ancestor. The anterior semicircular canal is the largest in terms of radius, indicating that the bony labyrinth of *Macroscelides* retains the ancestral therian condition in this regard.

Tubulidentata

Only one extant species, *Orycteropus afer*, contributes to the group Tubulidentata (aardvarks), although two additional genera of aardvarks (*Leptorycteropus* and *Myorycteropus*) were present during the Neogene of sub-Saharan Africa (Holroyd and Mussell, 2005). Morphology does not support any strong systematic placement of Tubulidentata within Eutheria, either placing it either in a basal polytomy with most placental lineages (Novacek, 1986; Novacek and Wyss, 1986b) or with weak associations to ungulates (Novacek, 1992b; Shoshani and McKenna, 1998). Molecular evidence suggests a close relationship between aardvarks some ungulates (Miyamoto and Goodman, 1986), particularly Paenungulata (de Jong et al., 1981), which includes Hyracoidea, Sirenia, and Proboscidea (sensu Simpson, 1945). Both Tubulidentata and Paenungulata are included within Afrotheria, although the relationships among these taxa within the African clade are ambiguous (Springer et al., 1997; Eizirik et al., 2001; Murphy et al., 2001 a, b; Murata et al., 2003; Bininda-Emonds et al., 2007).

The average body mass of *Orycteropus afer* is significantly greater than any of the other afrotherians described thus far (50.5 kg; Silva and Downing, 1995), and the

mass of the specimen used in this study (AMNH 51909) is above the species average (60 kg). The large body size of *Orycteropus* is reflected in the bony labyrinth of the inner ear (total volume equals 107 mm^3; total length equals 14.95 mm^3).

The cochlea of *Orycteropus* contributes a similar volumetric proportion (55.4%; volume equals 59.3 mm^3) to that calculated for the ancestor of Afrotheria (56.0%), and the spiral of the cochlea is fairly flat (Figure 5.14; aspect ratio of 0.45; height equals 4.23 mm; width equals 9.49 mm). The cochlea completes nearly two turns (709°), but the diameter of the second whorl is smaller than the basal turn (Figure 5.15), and therefore does not obscure the basal turn when the cochlea is viewed down the axis of rotation. The total length of the canal is 14.86 mm.

The basal plane of the cochlea is rotated by 31.9° from the plane of the lateral semicircular canal. The fenestra cochleae opens into the tympanic cavity at the end of a short stalk. A groove is situated behind the fenestra cochleae (expressed on the endocast as a curved ridge) that leads to the bony canaliculus cochleae. The canaliculus, which accommodates the aqueduct of the cochlea in life, is developed in *Orycteropus* as a slightly curved tube that widens at the tip. The curve of the 4.82 mm long canaliculus is best observed in medial view. The secondary lamina that supports the basilar membrane in life extends between one half and three quarters of the basal turn of the cochlear canal.

A gentle constriction of the vestibule lateral to the fenestra vestibuli (stapedial ratio of 1.8) divides the spherical and elliptical recesses, although the elliptical recess within the vestibule of *Orycteropus* is not divided into anterior and posterior chambers as is observed within the labyrinth of *Chrysochloris*. One striking feature of the vestibular apparatus of *Orycteropus* is that the lateral and posterior semicircular canals are joined to form a secondary common crus, a structure that is present in *Didelphis* (Figure 5.4). The secondary common crus is flattened, and bony ridges (expressed as thin grooves on the

FIGURE 5.14. Bony labyrinth of *Orycteropus afer*. **A**, stereopair and labeled line drawing of digital endocast in anterior view; **B**, stereopair and labeled line drawing of digital endocast in dorsal view; **C**, stereopair and labeled line drawing of digital endocast in lateral view; **D**, line drawing of cochlea viewed down axis of rotation to display degree of coiling; **E**, line drawing of cochlea in profile. Abbreviations: **aa**, anterior ampulla; **ac**, anterior semicircular canal; **ant**, anterior direction; **av**, bony channel for aqueduct of vestibule; **cc**, canaliculus cochleae for aqueduct of cochlea; **co**, cochlea; **cr**, common crus; **dor**, dorsal direction; **er**, elliptical recess of vestibule; **fc**, fenestra cochleae; **fv**, fenestra vestibuli; **la**, lateral ampulla; **lc**, lateral semicircular canal; **med**, medial direction; **pc**, posterior semicircular canal; **pl**, primary bony lamina; **pos**, posterior direction; **ps**, outpocketing for perilymphatic sac; **scr**, secondary common crus; **sl**, secondary bony lamina; **sr**, spherical recess of vestibule.

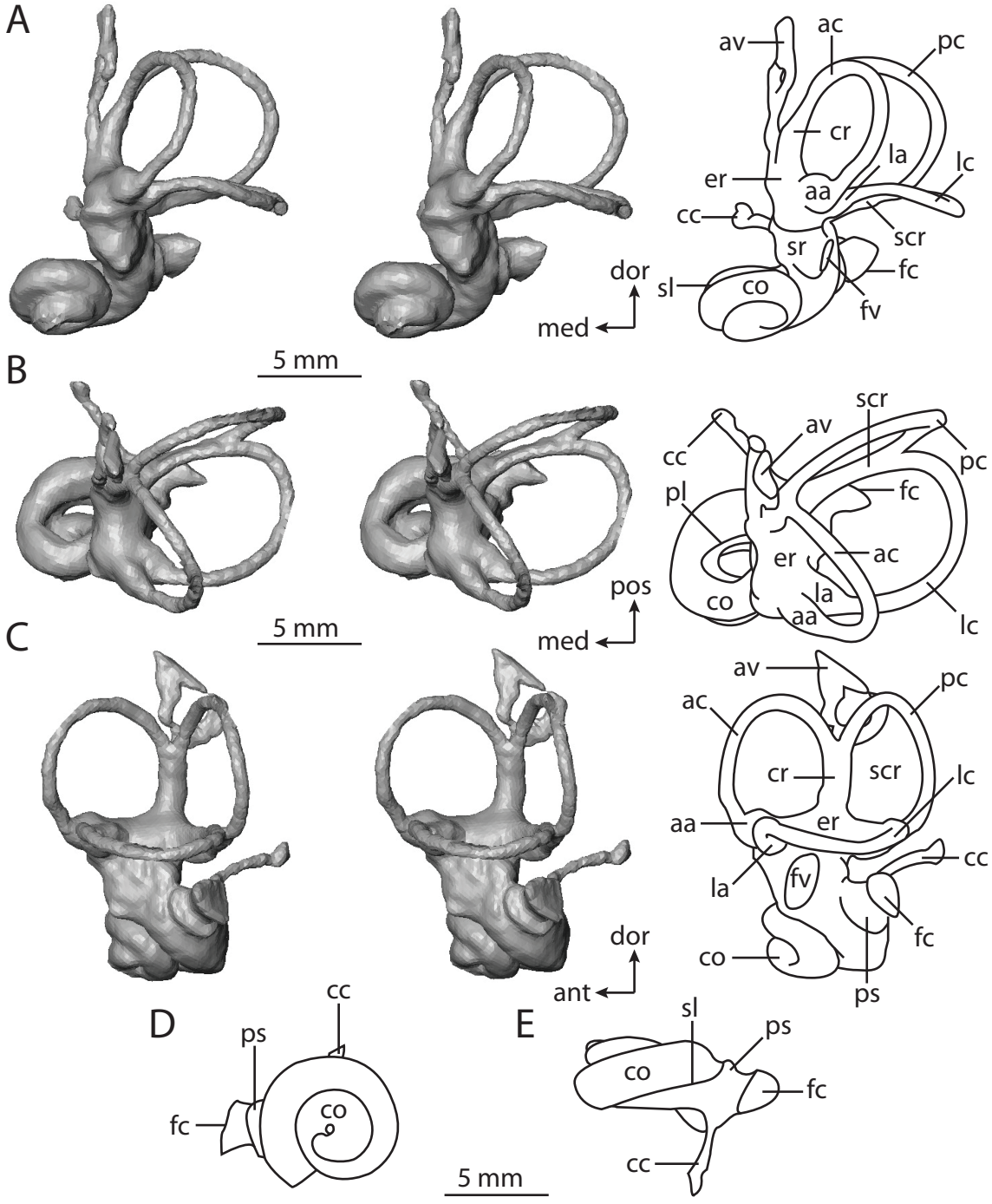
A
av
ac
pc
cr
la
lc
er
aa
cc
scr
sr
fc
dor
sl
co
fv
med
5 mm
B
scr
av
cc
pc
pl
fc
er
ac
pos
co
la
aa
lc
med
5 mm
C
av
pc
ac
cr
scr
lc
aa
er
cc
la
fv
fc
co
ps
dor
ant
D
cc
ps
fc
co
E
sl
ps
co
fc
cc
5 mm

FIGURE 5.15. CT slices through ear region of *Orycteropus afer*. Abbreviations: **aa**, anterior ampulla; **ac**, anterior semicircular canal; **av**, bony channel for aqueduct of vestibule; **cc**, canaliculus cochleae; **cn**, canal for cranial nerve VIII; **co**, cochlea; **cr**, common crus; **dor**, dorsal direction; **fc**, fenestra cochleae; **fn**, canal for cranial nerve VII; **fv**, fenestra vestibuli; **la**, lateral ampulla; **lc**, lateral semicircular canal; **med**, medial direction; **pa**, posterior ampulla; **pc**, posterior semicircular canal; **pl**, primary bony lamina; **pos**, posterior direction; **scr**, secondary common crus; **sl**, secondary bony lamina; sr, spherical recess of vestibule; **vb**, vestibule.

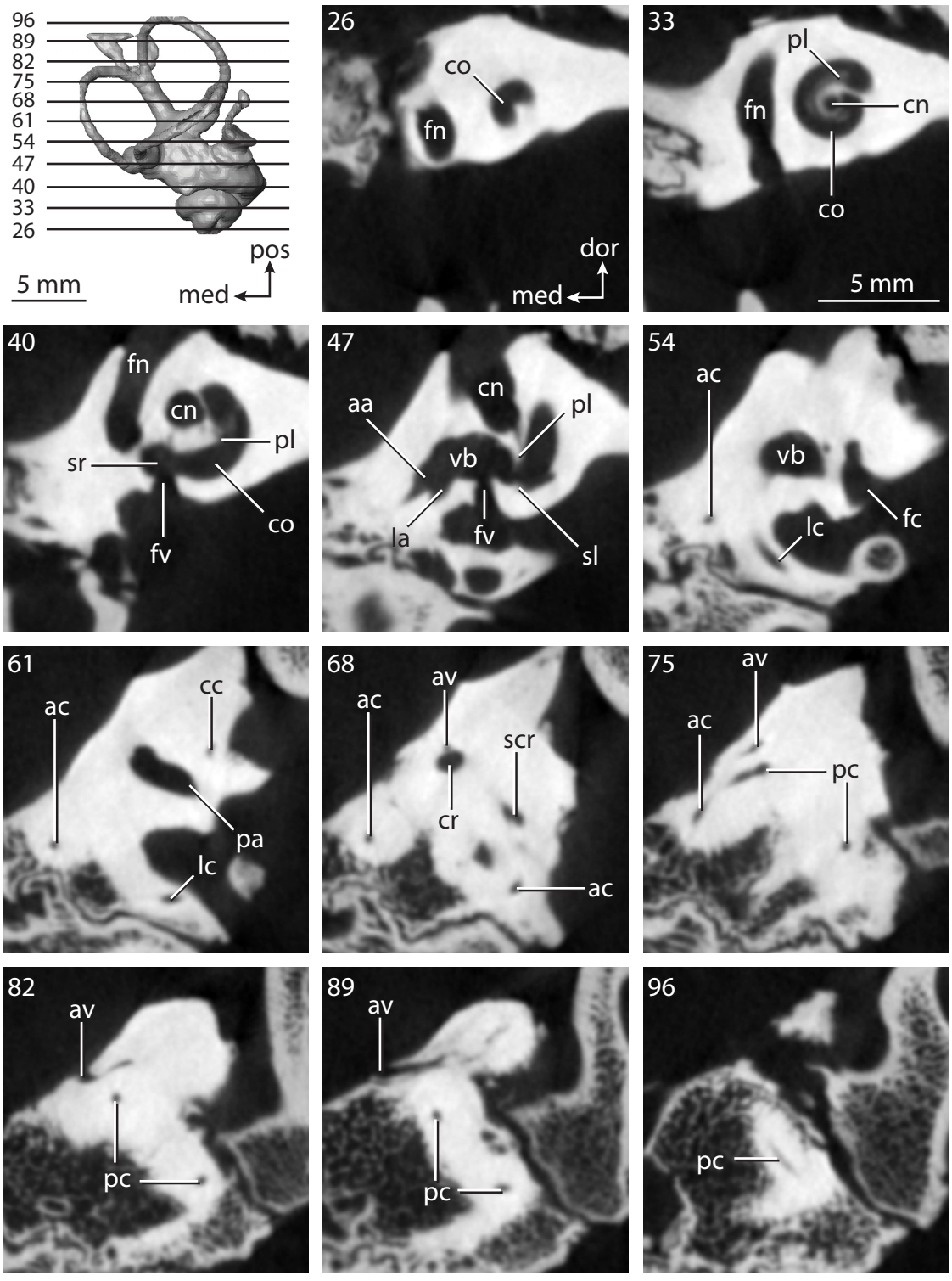
96
89
82
75
68
61
54
47
40
33
26
pos
5 mm
med
26
co
fn
dor
med
33
pl
fn
cn
co
5 mm
40
fn
cn
pl
sr
co
fv
47
cn
aa
pl
vb
la
fv
sl
54
ac
vb
fc
lc
61
ac
cc
pa
lc
68
av
ac
scr
cr
ac
75
av
ac
pc
82
av
pc
89
av
pc
96
pc

endocast) divide the crus into a section for the lateral semicircular canal anteriorly, and the posterior canal posteriorly, although the two sections are continuous.

The primary common crus between the anterior and posterior canals in *Orycteropus* appears squat in relation to the semicircular canal arcs when compared to the labyrinth of *Macroscelides proboscideus* (Figure 5.12). The bony channel for the aqueduct of the vestibule exits medial to the vestibular aperture for the common crus. The 8.25 mm long channel forms a straight tube for a little over half of its length, whereupon it bifurcates into an anterior and a posterior projection. The anterior projection is wider than the posterior. The bifurcation of the channel for the aqueduct of the vestibule is unique to *Orycteropus* among all of the mammals considered in this study. No mammal observed by Gray (1907, 1908) possessed a bifurcated membranous aqueduct, and it is unlikely that the aqueduct of *Orycteropus* is forked, although the membranous labyrinth of the species is poorly known (the aardvark was not among the species examined by Gray).

The planes between the anterior and posterior semicircular canals approach a right angle (91.9°), and the angle between the posterior and lateral canals are not far from 90°, either (87.4°). The angle between the anterior and lateral semicircular canal planes is noticeably acute (78.5°). The lateral semicircular canal is the most planar among the three with a total angular deviation of 7.2° and a ratio of the total linear deviation over cross-sectional diameter of the canal of 0.78. The anterior canal deviates most from its plane, at 19.7°, while the posterior canal deviates a total of 11.5° from its plane. The deviation of both the anterior and posterior semicircular canals are significant with ratios of linear deviation over canal diameter of 1.82 and 1.06 respectively.

The posterior semicircular canal is larger than the anterior and lateral in terms of slender canal length (18.86 mm; anterior equals 15.40 mm; lateral equals 16.44 mm),

diameter of canal in cross-section (0.66 mm; anterior equals 0.58; lateral equals 0.53), and arc radius of curvature (3.50 mm; anterior equals 3.10 mm; lateral equals 3.27 mm). This pattern is not observed in the afrosoricids, nor in *Macroscelides*, where the anterior canal tends to be the largest. The dimensions of the anterior semicircular canal of *Orycteropus* are the smallest among the three canals, including the aspect ratio of the anterior semicircular canal arc (0.81). The arc of the lateral semicircular canal approaches a perfect circle, with an aspect ratio of 1.03, and the height of the posterior semicircular canal arc is greater than the width (aspect ratio equals 1.28). The ratio between the slender semicircular canal length and arc radius for the anterior, lateral, and posterior semicircular canals are 4.96, 5.03, and 5.39 respectively.

The bony labyrinth of *Orycteropus* possesses two features that are observed in *Kulbeckia* and other Cretaceous eutherians (Meng and Fox, 1995; Chapter 4), which are the secondary common crus and the low position of the lateral semicircular canal relative to the posterior canal. Such plesiomorphic features support a basal position of Tubulidentata within Afrotheria, as reconstructed by Eizirik et al. (2001) and Malia et al. (2002), and are not inconsistent with the relationships recovered by Bininda-Emonds et al. (2007), in which Tubulidentata is placed in a basal polytomy within Afrotheria.

If *Orycteropus* is the sister taxon to all other afrotherians, then absence of the secondary common crus (or separate openings for the lateral and posterior semicircular canals into the vestibule) might be a synapomorphy uniting the remaining afrotheres. However, the absence of the secondary common crus is reconstructed as a synapomorphy for all of Placentalia based on the phylogeny used here (Figure 5.2). Thus, the presence of the secondary crus is an autapomorphy for *Orycteropus*. It is interesting, however, that the bony labyrinth of *Orycteropus* possesses a few apomorphies (when compared to stem

eutherians). For example, the cochlea completes over one and a half turns (almost two), and the posterior semicircular canal has the largest radius, rather than the anterior canal.

Hyracoidea

A close relationship between Hyracoidea (hyraxes) and ungulates, particularly either Perissodactyla or Tethytheria (Sirenia + Proboscidea), is a classical hypothesis. Although some morphological data support a sister relationship between Hyracoidea and Perissodactyla (Owen, 1848; McKenna, 1975; Fischer and Tassy, 1993), the majority of morphological (Novacek, 1986; Novacek and Wyss, 1986b; Shoshani, 1986; Novacek 1992a, b; Rasmussen et al., 1990) and molecular data (Shoshani, 1986; Stanhope et al., 1998; Springer et al., 1999; Murphy et al., 2001a, b; van Dijk et al., 2001; Bininda-Emonds et al., 2007) support a pairing of Hyracoidea and Tethytheria within the group Paenungulata. The results of most phylogenetic analyses recover a sister relationship between Hyracoidea and a monophyletic Tethytheria, but the results of a few recent analyses, including the supertree constructed by Bininda-Emonds et al. (2007), support a closer relationship between Hyracoidea and Sirenia, rendering Tethytheria paraphyletic.

A digital endocast of *Procavia capensis* was constructed (Figure 5.16) to examine the labyrinth of Hyracoidea. *Procavia* is a little larger than a house cat in overall body mass (3.8 kg; Silva and Downing, 1995). The total length of the bony labyrinth of the hyrax is 8.50 mm, and the total volume of the inner ear cavities is 19.34 mm^3, of which the cochlea contributes 47.7% (9.22 mm^3). The percentage of volume of the bony labyrinth that is made up by the cochlea is relatively low among the afrotherians investigated, although larger than that of the elephantoid (the cochlea of which comprises 30.6 %, as described below).

FIGURE 5.16. Bony labyrinth of *Procavia capensis*. **A**, stereopair and labeled line drawing of digital endocast in anterior view; **B**, stereopair and labeled line drawing of digital endocast in dorsal view; **C**, stereopair and labeled line drawing of digital endocast in lateral view; **D**, line drawing of cochlea viewed down axis of rotation to display degree of coiling; **E**, line drawing of cochlea in profile. Abbreviations: **aa**, anterior ampulla; **ac**, anterior semicircular canal; **ant**, anterior direction; **av**, bony channel for aqueduct of vestibule; **cc**, canaliculus cochleae for aqueduct of cochlea; **co**, cochlea; **cr**, common crus; **dor**, dorsal direction; **er**, elliptical recess of vestibule; **fc**, fenestra cochleae; **fv**, fenestra vestibuli; **la**, lateral ampulla; **lc**, lateral semicircular canal; **med**, medial direction; **pa**, posterior ampulla; **pc**, posterior semicircular canal; **pl**, primary bony lamina; **pos**, posterior direction; **ps**, outpocketing for perilymphatic sac; **sl**, secondary bony lamina; **sr**, spherical recess of vestibule.

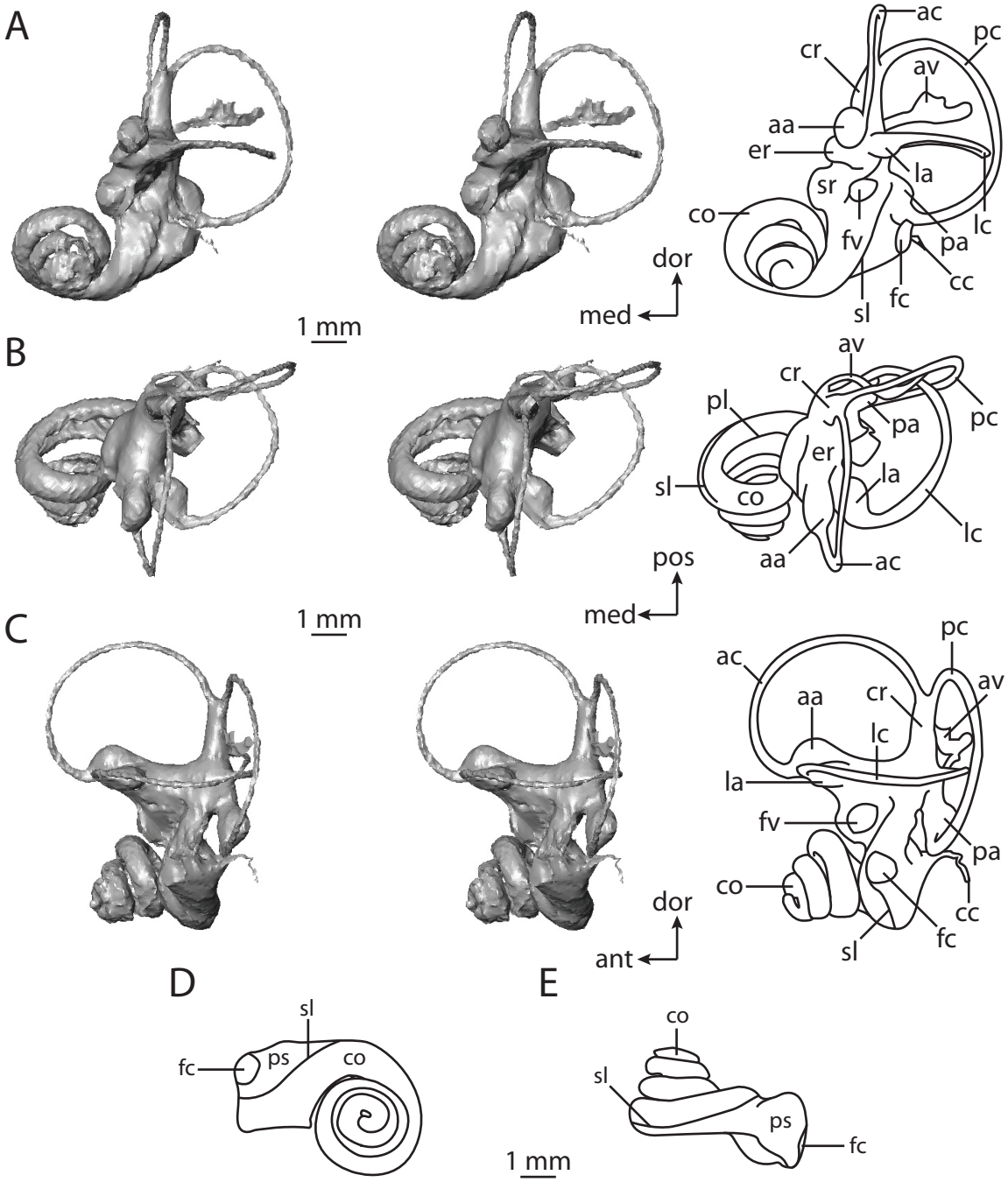
A
ac
pc
cr
av
aa
er
la
sr
co
lc
fv
pa
dor
cc
med
fc
sl
1 mm
B
av
cr
pl
pc
pa
er
sl
la
co
lc
pos
aa
ac
med
1 mm
C
pc
ac
av
aa
cr
lc
la
fv
pa
co
dor
cc
ant
fc
sl
D
E
sl
co
fc
ps
co
sl
ps
fc
1 mm

The aspect ratio of the cochlear spiral is 0.72, which is large when compared to most of the other afrotherians examined, although the aspect ratio of *Macroscelides proboscideus* is larger (0.80). However, the overall shape of the cochlea is different between *Procavia* and *Macroscelides*. Whereas the apical turn sits upon the basal turn of the cochlea in *Macroscelides*, the apical turns of *Procavia* fit within the arc formed by the basal turn. Such morphology gives the cochlea of *Procavia* a conical appearance, rather than the cylindrical shape of *Macroscelides* and *Chrysochloris*.

The cochlea of *Procavia* completes over three and three quarters turns (1363°), a greater degree than in any other afrotherian. The secondary lamina of *Procavia* (Figure 5.17) is not as well developed as the structure is in *Macroscelides*, and only extends a short distance past the first half of the basal turn of the cochlea. The plane of the basal turn deviates from that of the lateral canal by 45.4°, which is greater than all other afrotherians except the elephantoid (48.5°). The degree of rotation exhibited by the cochlea might be a synapomorphy for Paenungulata, although the cochlea of *Trichechus* only deviates from the plane of the lateral canal by 27.7°. The bony canaliculus cochleae for transmission of the cochlear aqueduct (1.21 mm) is very slender and is not observed easily in the CT slices, having a maximum diameter of a single pixel (around 0.07 mm) at several points along its path. The canaliculus is not a straight tube, but rather hooks laterally. The canaliculus cochleae exits the bony labyrinth from a bulge posteromedial to the fenestra cochleae.

The spherical recess of the vestibule is distinguished easily from the elliptical recess particularly at the anterior aspect of the vestibule, dorsal to the fenestra vestibuli (stapedial ratio is 2.1). Despite its name, the spherical recess is ovoid in shape. However, the elliptical recess is much more elongated, and it gently curves laterally. The anterior end of the elliptical recess opens into the anterior and lateral ampullae, and the posterior

FIGURE 5.17. CT slices through ear region of *Procavia capensis*. Abbreviations: **aa**, anterior ampulla; **ac**, anterior semicircular canal; **av**, bony channel for aqueduct of vestibule; **cn**, canal for cranial nerve VIII; **co**, cochlea; **cr**, common crus; **dor**, dorsal direction; **fc**, fenestra cochleae; **fn**, canal for cranial nerve VII; **fv**, fenestra vestibuli; **la**, lateral ampulla; **lc**, lateral semicircular canal; **med**, medial direction; **pa**, posterior ampulla; **pc**, posterior semicircular canal; **pl**, primary bony lamina; **pos**, posterior direction; **vb**, vestibule; **ven**, ventral direction.

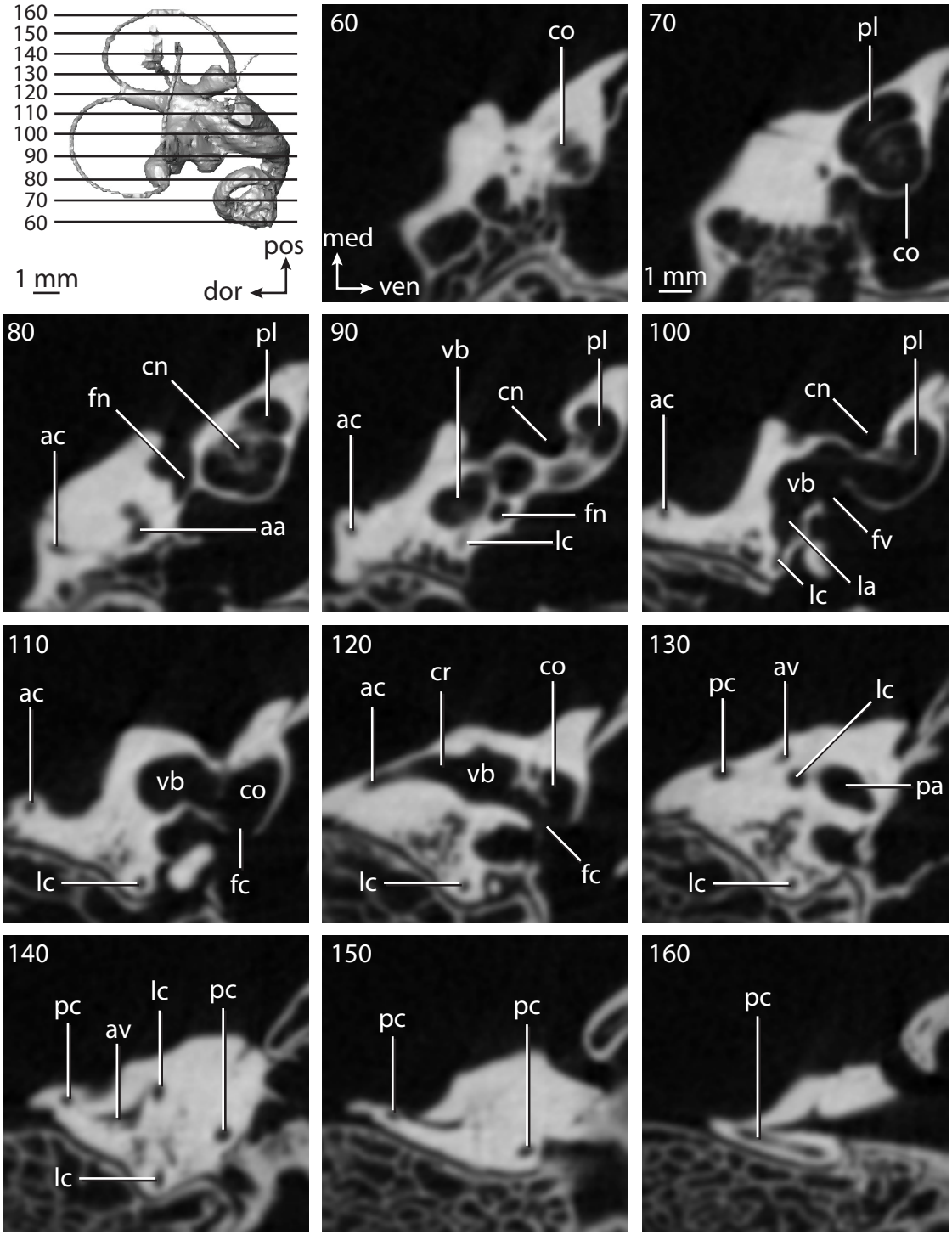
160
150
140
130
120
110
100
90
80
70
60
pos
dor
1 mm
60
co
med
ven
70
pl
co
1 mm
80
pl
cn
fn
ac
aa
90
vb
pl
cn
ac
fn
lc
100
pl
ac
cn
vb
fv
la
lc
110
ac
vb
co
lc
fc
120
ac
cr
co
vb
lc
fc
130
pc
av
lc
pa
lc
140
pc
av
lc
pc
lc
150
pc
pc
160
pc

end of the recess leads to the vestibular apertures of the posterior ampulla, common crus, and posterior limb of the lateral semicircular canal. The lateral canal enters the vestibule closer to the common crus than it does to the posterior ampulla, which causes the lateral semicircular canal to divide the space enclosed by the arc of the posterior semicircular canal into dorsal and ventral regions in anterior view. The sagittal labyrinthine index for *Procavia* is 44.9, which is over twice that observed in *Chrysochloris* (21.7), and greater than that in *Macroscelides* (32.7).

The bony channel for the aqueduct of the vestibule exits medial and ventral to the vestibular aperture of the common crus, and it is 3.39 mm in length, almost three times longer than the canaliculus cochleae. The channel curves laterally along the posterior border of the base of the common crus, but the aqueduct does not cross the rise of the common crus when the bony labyrinth is viewed medially. The channel for the aqueduct is a uniformly subcircular tube in cross-section, until it flares and flattens into a fissure nearly on the plane of the posterior semicircular canal arc.

The greatest angle between the planes of two semicircular canals in *Procavia* was measured between the anterior and posterior canals (112°). The angle between the anterior and lateral canals is almost as acute as the angle between the lateral and posterior canals is obtuse (87.4° and 94.9° respectively). No canal fits onto a single plane in *Procavia*, although the angular deviation is not great for any canal. The anterior canal shows the largest angular deviation of a canal from its plane (7.79°), although this is not much different than the deviations of the lateral (5.78°) and posterior canals (6.06°). Even so, only the deviation of the anterior canal is considered significant, with the ratio of total linear deviation of the anterior canal over the cross-sectional diameter of the canal equaling 1.28 (ratios for the lateral and posterior canals are 0.54 and 0.88 respectively).

As in *Orycteropus afer*, the posterior semicircular canal of *Procavia* is the most voluminous (0.41 mm^3), as well as the longest of the three canals (10.68 mm). The arc radius of curvature of the posterior semicircular canal arc is greater for the posterior canal (2.18 mm) than for either the anterior (1.99 mm) or lateral semicircular canals (1.79 mm). The slender anterior canal of *Procavia* is 10.24 mm long, whereas the length of the slender lateral canal is 7.65 mm. Both the anterior and lateral semicircular canals have a volume of 0.37 mm^3 each. Among afrotherians, the posterior canal is the largest only in *Procavia* and *Orycteropus* and is a potential synapomorphy uniting the two taxa. A sister relationship between aardvarks and hyraxes has not been proposed, although Hyracoidea has been placed in a polytomy along with Tubulidentata and Sirenia (sister taxon to polytomy is Proboscidea; de Jong et al., 1981).

The arcs of the three semicircular canals are wider than they are high, and the aspect ratio of the arcs of the anterior and lateral canals are similar (0.68 and 0.72 respectively). The aspect ratio of the posterior semicircular canal arc is higher at 0.79. The ratio of the slender canal length over semicircular canal arc radius is greatest for the anterior canal, at 5.14 (lateral equals 4.28; posterior equals 4.90).

There is no unambiguous support for paenungulate monophyly in the bony labyrinth. Hyraxes retain the ancestral placental condition in that the secondary common crus is absent, but are derived from the placental ancestor in that the posterior canal is largest in terms of arc radius, rather than the anterior canal. Among the remaining afrotherians, only *Orycteropus* shares the condition of having the largest arc in the posterior semicircular canal. The labyrinth of *Procavia* is derived from the ancestral eutherian condition in that the lateral semicircular canal is positioned dorsal with respect to the ampullar entrance of the posterior semicircular canal.

Sirenia

Dugongs and manatees comprise the clade Sirenia. Sirenia and Cetacea are the two exclusively aquatic groups of extant mammals (the other is Cetacea), although they are not closely related despite similar lifestyles and superficial resemblances, such as a fusiform body and short neck. Rather, there is a closer connection between Sirenia and Proboscidea, which is a relationship that has been recognized for several centuries (Linnaeus, 1758; Simpson, 1945; McKenna, 1975).

Monophyly of Tethytheria, which is the clade that includes Sirenia, Proboscidea, as well as the extinct groups Desmostylia, "Anthrocobunidae", and Embrithopoda (McKenna, 1975; Gheerbrant et al., 2005), is supported by more recent morphological (Novacek, 1986; Novacek and Wyss, 1986b; Court, 1990; Fischer and Tassy, 1993) and molecular evidence (Lavergne et al., 1996; Murphy et al., 2001a). However, the results of a few recent molecular analyses (Murphy et al., 2001b; Amrine-Madsen et al., 2003; Bininda-Emonds et al., 2007) refute tethytherian monophyly, while still recovering a close relationship between Sirenia and Proboscidea within Paenungulata.

The Florida manatee, *Trichechus manatus*, represents Sirenia. The manatee has an average species body mass of 500 kg (Silva and Downing, 1995), and this is reflected in the total length of the bony labyrinth (19.29 mm) of the *Trichechus* specimen used, as well as in total volume of the inner ear cavities (1069.4 mm^3).

The most notable feature observable on the digital endocast of *Trichechus* is the absence of the bony canaliculus cochleae for transmission of the aqueduct of the cochlea (Figure 5.18). Rather, the canaliculus and fenestra cochleae are fused to form an undivided perilymphatic foramen, which is unique to Sirenia and Proboscidea among extant mammals. Although the three living species of manatees and the dugong possess an undivided perlymphatic foramen, the bony canaliculus cochleae is separate from the

FIGURE 5.18. Bony labyrinth of *Trichechus manatus*. **A**, stereopair and labeled line drawing of digital endocast in anterior view; **B**, stereopair and labeled line drawing of digital endocast in dorsal view; **C**, stereopair and labeled line drawing of digital endocast in lateral view; **D**, line drawing of cochlea viewed down axis of rotation to display degree of coiling; **E**, line drawing of cochlea in profile. Abbreviations: **aa**, anterior ampulla; **ac**, anterior semicircular canal; **ant**, anterior direction; **av**, bony channel for aqueduct of vestibule; **co**, cochlea; **cr**, common crus; **dor**, dorsal direction; **fv**, fenestra vestibuli; **la**, lateral ampulla; **lc**, lateral semicircular canal; **med**, medial direction; **pa**, posterior ampulla; **pc**, posterior semicircular canal; **pf**, perilymphatic foramen; **pl**, primary bony lamina; **pos**, posterior direction; **vb**, vestibule.

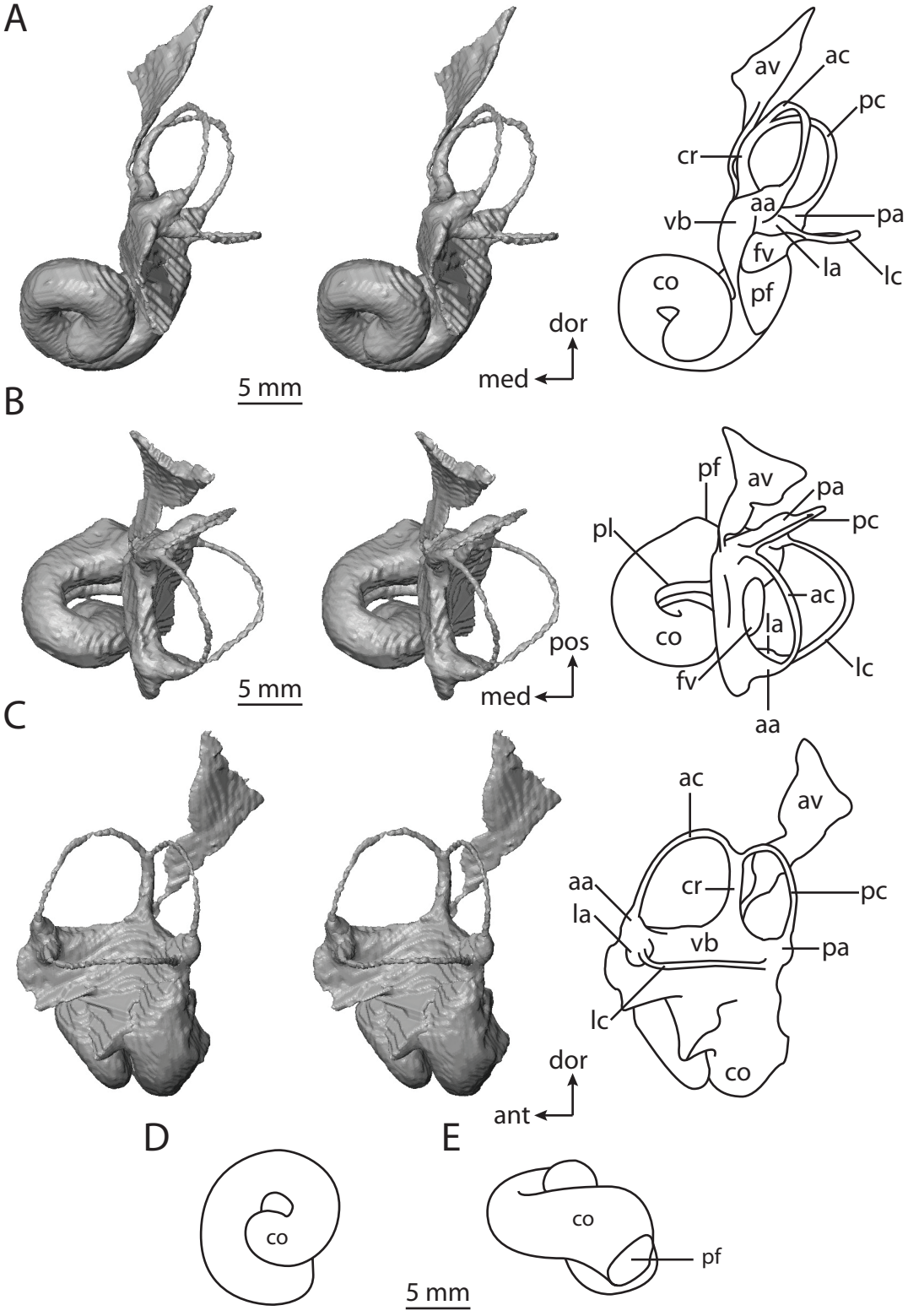
A
av
ac
pc
cr
aa
vb
pa
fv
la
lc
co
pf
dor
med
5 mm
B
pf
av
pa
pc
pl
ac
la
co
lc
fv
aa
pos
med
5 mm
C
ac
av
aa
cr
pc
la
vb
pa
lc
co
dor
ant
D
co
E
co
pf
5 mm

fenestra cochleae in the Eocene sirenian *Prorastamus*, suggesting that the undivided perilymphatic foramen either evolved independently in Sirenia and Proboscidea (Court, 1990, 1992a), or a reversal in the Eocene sirenian.

The cochlea is large (441.6 mm^3) with respect to the entire bony labyrinth, contributing 71.1% of the entire labyrinthine volume. Although this is a greater contribution than the cochleae of either the ancestral afrotherian (56.0%) or paenungulate (48.0%), the dimension is not much different than the volumetric percentages calculated for *Chrysochloris* sp. (71.3%) and *Macroscelides proboscideus* (71.7%). However, the aspect ratio of the spiral of the cochlea (0.55) is lower in *Trichechus* than in either *Chrysochloris* (0.63) or *Macroscelides* (0.80). The cochlea of *Trichechus* completes just over a single turn (407°), which is less than any other afrotherian examined, and almost a complete turn lower than that calculated for the ancestor of Afrotheria (751°). A low degree of coiling may be a synapomorphy for Sirenia, given that a similar degree of coiling is observed in the fossil *Hydrodamalis gigas* (Kaiser, 1974). The length of the canal from the base to the apex in *Trichechus* is 22.46 mm, and the plane of the basal turn of the cochlea deviates from that of the lateral semicircular canal by 27.7°. As in proboscideans, the secondary lamina is not present in *Trichechus* (Figure 5.19).

The fenestra vestibuli has an aspect (stapedial) ratio of 1.6, which signifies a less elliptical window than other afrotherians. The spherical recess of the vestibule, which communicates with the tympanic cavity via the fenestra vestibuli, is poorly developed, and not distinguishable from the elliptical recess. In fact, the vestibule as a whole is mediolaterally compressed as can be seen when the bony labyrinth is in anterior view. The thickest part of the vestibule is at the anterior end, where a slight laterodorsal projection leads to the anterior and lateral ampullae. The ampullae of the semicircular

FIGURE 5.19. CT slices through ear region of *Trichechus manatus*. Abbreviations: **ac**, anterior semicircular canal; **av**, bony channel for aqueduct of vestibule; **cn**, canal for cranial nerve VIII; **co**, cochlea; **cr**, common crus; **dor**, dorsal direction; **fv**, fenestra vestibuli; **la**, lateral ampulla; **lat**, lateral direction; **lc**, lateral semicircular canal; **med**, medial direction; **pa**, posterior ampulla; **pc**, posterior semicircular canal; **pf**, perilymphatic foramen; **pl**, primary bony lamina; **pos**, posterior direction; **vb**, vestibule; **ven**, ventral direction.

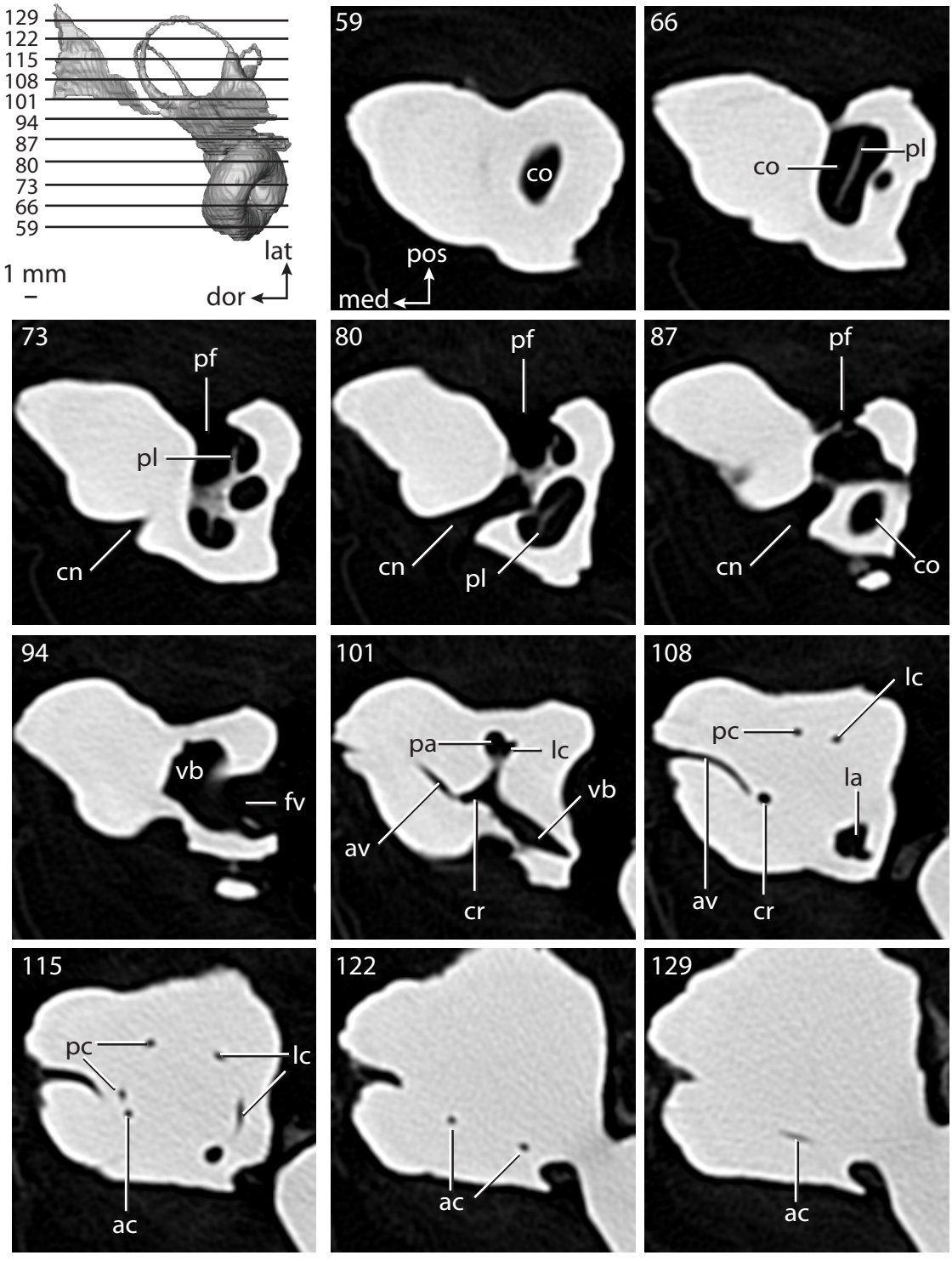
129
122
115
108
101
94
87
80
73
66
59
lat
1 mm
dor
59
co
pos
med
66
co
pl
73
pf
pl
cn
80
pf
cn
pl
87
pf
cn
co
94
vb
fv
101
pa
lc
vb
av
cr
108
lc
pc
la
av
cr
115
pc
lc
ac
122
ac
129
ac

canals are proportionately smaller in *Trichechus* than in other taxa examined, such as *Macroscelides* and *Procavia*.

Apertures for the posterior ampulla, common crus, and the posterior limb of the lateral semicircular canal are situated at the posterior end of the vestibule, with the common crus as the medial-most opening. The bony channel for the aqueduct of the vestibule exits the bony labyrinth ventromedial to the vestibular aperture of the common crus. The channel for the aqueduct extends from the vestibule as a round tube for a very short distance before opening into a broad fissure that flares posterodorsally. The bony channel is 12.33 mm in length, which is nearly two thirds as long as the total length of the bony labyrinth (19.29 mm).

The vestibular aperture of the lateral semicircular canal opens near the base of the posterior ampulla in *Trichechus*, similar to the state observed in *Macroscelides*. However, the lateral canal enters the vestibule lateral and ventral to the posterior ampulla in *Trichechus*, which is on the opposite side of the posterior ampulla from *Macroscelides* and other taxa where the opening for the canal is well separated from the ampulla, such as *Procavia*. Even in *Orycteropus*, where the lateral and posterior canals fuse to form a secondary common crus, the lateral canal is situated dorsal and slightly medial to the posterior canal. The morphology observed in *Trichechus* places the plane of the lateral semicircular canal relatively low on the vestibule.

All of the planes of the semicircular canals of *Trichechus* form acute angles with each other. The angle between the planes of the anterior and lateral semicircular canals (52.2°) is the smallest angle measured between any two canals in any afrotherian specimen. Within *Trichechus*, the only canals that approach a right angle are the anterior and posterior canals (84.9°). The angle between the posterior and lateral semicircular canal planes is 77.5°. The posterior semicircular canal does not deviate from its plane,

and the anterior canal is more planar than the lateral canal, with total angular deviations of 7.86° and 8.87° respectively. The deviations exhibited by both the anterior and lateral semicircular canals are significant (ratios of total linear deviation over cross-sectional diameter are 1.17 and 1.33 respectively).

No single semicircular canal within the bony labyrinth of *Trichechus* is the greatest in all dimensions measured. The radius of the arc of the lateral semicircular canal (4.46 mm) is the larger than the arc of the posterior canal by nearly a millimeter (3.54 mm), but only slightly larger than the arc of the anterior canal (4.30 mm). Both the diameter of the lumen of the lateral semicircular canal (0.52 mm), as well as the volume of the canal (2.5 mm^3) are the largest among the three canals (dimensions for the anterior canal equal 0.51 mm and 2.3 mm^3; dimensions for the posterior canal equal 0.50 mm and 1.8 mm^3). However, the length of the slender canal of the lateral semicircular canal (14.20 mm) is noticeably smaller than both the anterior (17.31 mm) and posterior (16.53 mm) semicircular canals.

The posterior limbs of the anterior and lateral semicircular canals form steeper slopes than the anterior limbs. Although the anterior canal is curved along its entire course, the anterior limb of the lateral canal is flattened, giving the arc of the canal an angular appearance at its midpoint, before the posterior limb curves gradually to meet the vestibule. The arc of the posterior semicircular canal is noticeably higher than the other two canals, with an aspect ratio of 1.18. The aspect ratio of the anterior canal arc is 0.91, which is similar to that of the lateral canal (0.89). The ratio of the slender canal length over semicircular canal arc radius is greatest for the posterior canal (4.67), followed by the anterior canal (4.02). The ratio for the lateral canal equals 3.18.

Although the results of several recent molecular analyses, including those of Bininda-Emonds et al. (2007), do not support the monophyly of Tethytheria, the structure

of the inner ear supports a sister relationship between Sirenia and Proboscidea among the paenungulates. Notable labyrinthine features that are shared by Sirenia and Proboscidea within Paenungulata are a low position of the lateral semicircular canal compared to the posterior canal (the lateral canal is high in *Procavia*), and a low cochlear spiral. The large radius of the lateral semicircular canal is an autapomorphy for *Trichechus* compared to all other afrotherians. The bony labyrinth of *Trichechus* retains the ancestral placental condition of the lateral semicircular canal opening directly into the vestibule in the absence of a secondary common crus.

Proboscidea

The bony labyrinth of a specimen of he extinct elephantoid was described elsewhere (Chapter 2), but for the sake of comparison, a brief overview of the inner ear anatomy of Proboscidea is provided here. Not only are proboscideans the largest afrotherians, as is reflected in the volume (1145.2 mm^3) and length (26.00 mm) of the inner ear, they are the largest extant terrestrial mammal. Because the species of the proboscidean used for this study is not known with certainty (see Chapter 2), the body mass of the individual could not be estimated. Extant Proboscidea is not a taxonomically diverse clade, with no more than three species (Wilson and Reeder, 2005; Reeder et al., 2007), but proboscidean diversity was much greater throughout the Tertiary period (McKenna and Bell, 1997).

As mentioned in the description of the bony labyrinth of the sirenian *Trichechus manatus*, the canaliculus cochleae for the cochlear aqueduct is absent in the elephantoid (Figure 5.20), which is an apomorphic condition for Tethytheria. Rather, both the elephantoid and *Trichechus* share a secondarily undivided perilymphatic foramen in lieu of a fenestra cochleae (although this condition may have an independent derivation in

FIGURE 5.20. Bony labyrinth of the fossil elephantoid proboscidean. **A**, stereopair and labeled line drawing of digital endocast in anterior view; **B**, stereopair and labeled line drawing of digital endocast in dorsal view; **C**, stereopair and labeled line drawing of digital endocast in lateral view; **D**, line drawing of cochlea viewed down axis of rotation to display degree of coiling; **E**, line drawing of cochlea in profile. Abbreviations: **aa**, anterior ampulla; **ac**, anterior semicircular canal; **ant**, anterior direction; **av**, bony channel for aqueduct of vestibule; **co**, cochlea; **cr**, common crus; **dor**, dorsal direction; **er**, elliptical recess of vestibule; **fv**, fenestra vestibuli; **la**, lateral ampulla; **lc**, lateral semicircular canal; **med**, medial direction; **pa**, posterior ampulla; **pc**, posterior semicircular canal; **pf**, perilymphatic foramen; **pos**, posterior direction; **ps**, outpocketing for perilymphatic sac; **sr**, spherical recess of vestibule; **vb**, vestibule.

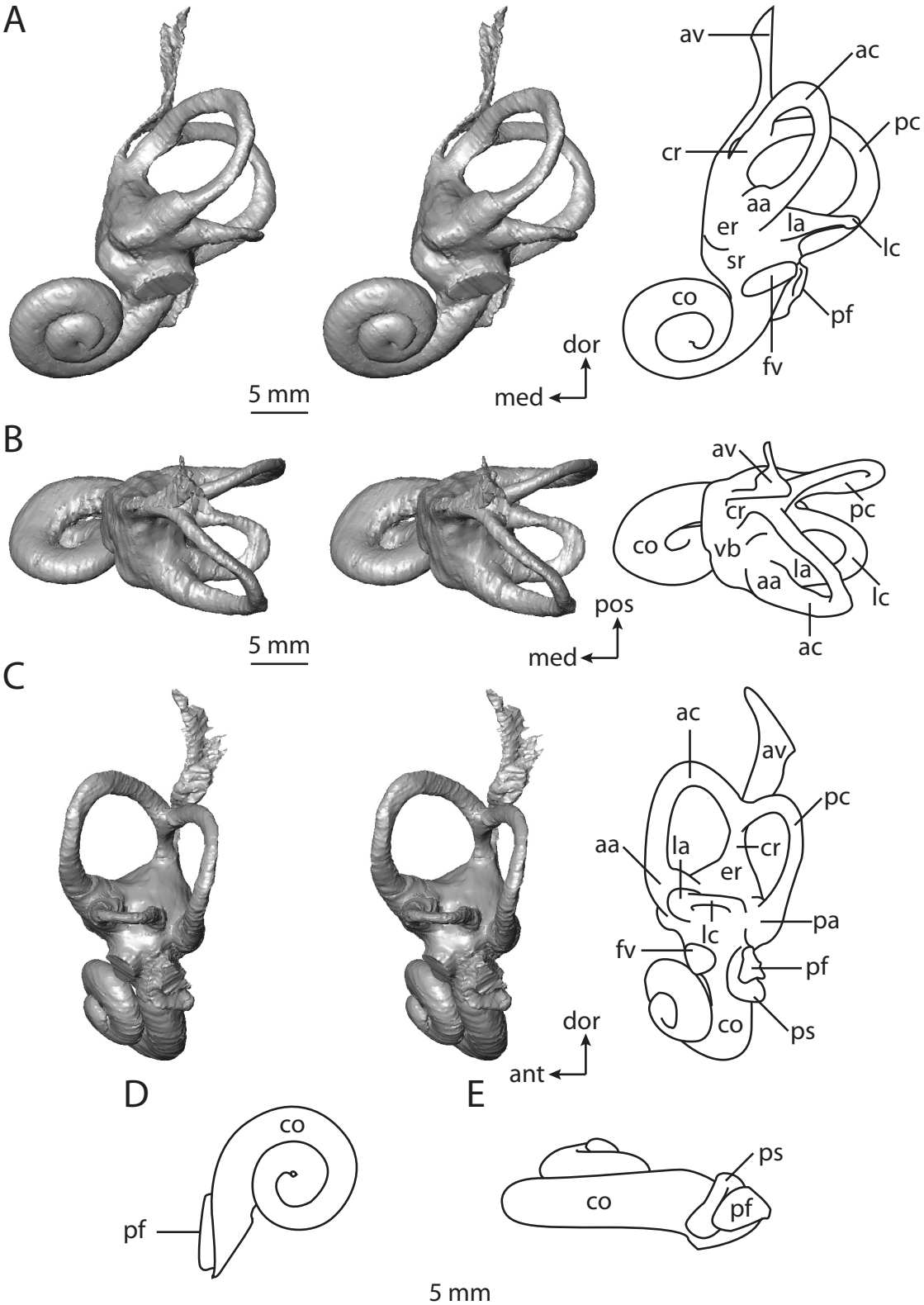
A
av
ac
pc
cr
aa
er
la
lc
sr
co
pf
fv
dor
med
5 mm
B
av
cr
pc
co
vb
aa
la
lc
ac
pos
med
5 mm
C
ac
av
pc
aa
la
cr
er
pa
lc
fv
pf
co
ps
dor
ant
D
co
pf
E
ps
co
pf
5 mm

both clades; see Court 1990, 1992a). The stapedial ratio measured from the fenestra vestibuli of the elephantoid is 1.60, which is similar to that calculated for *Trichechus* (1.64). A round fenestra also is characteristic of the extinct embrythopod *Arsinotherium*, which is closely related to Tethytheria (McKenna and Bell, 1997; Gheerbrant et al., 2005), if not within Tethytheria itself as the sister taxon of Proboscidea (Court, 1992a).

The cochlea of the elephantoid completes a little over two whorls (765°) and contributes only 30.6% of the total volume of the inner ear, which is the smallest contribution observed among the afrotherian sample investigated. Although the total volume of the inner ear is greater in the elephantoid than any of the other afrotherians, the volume of the cochlea (350.7 mm^3) is less than that measured for *Trichechus* (441.6 mm^3). The secondary lamina is not developed in Proboscidea (Figure 5.21), and the cochlea is fairly planispiral in the elephantoid with an aspect ratio of 0.42. The only other afrotherian to have a lower aspect ratio is *Hemicentetes* (0.38). The aspect ratios of the cochleae of the other paenungulates are greater than that of the elephantoid (*Trichechus* is 0.55 and *Procavia* is 0.72).

The vestibular aperture of the posterior limb of the lateral semicircular canal is situated anterior to the posterior ampulla in the elephantoid. The bony channel for the aqueduct of the vestibule leaves the vestibule medial to the common crus, and the aqueduct extends 13.94 mm before exiting the petrosal via a fissure on the endocranial surface of the bone. The posterior limb of the lateral semicircular canal enters the vestibule separately from the posterior ampulla.

The angle between the planes of the basal turn of the cochlea and the lateral semicircular canal is greater for the elephantoid (48.5°) than any other afrotherian. The most acute angle between the planes of two semicircular canals is between the anterior and lateral canals (66.3°), and the most obtuse angle was measured between the posterior

FIGURE 5.21. CT slices through ear region of the fossil elephantoid proboscidean. Abbreviations: **aa**, anterior ampulla; **ac**, anterior semicircular canal; **av**, bony channel for aqueduct of vestibule; **cn**, canal for cranial nerve VIII; **co**, cochlea; **cr**, common crus; **dor**, dorsal direction; **fn**, canal for cranial nerve VII; **fv**, fenestra vestibuli; **la**, lateral ampulla; **lat**, lateral direction; **lc**, lateral semicircular canal; **pc**, posterior semicircular canal; **pf**, perilymphatic foramen; **pos**, posterior direction; **vb**, vestibule.

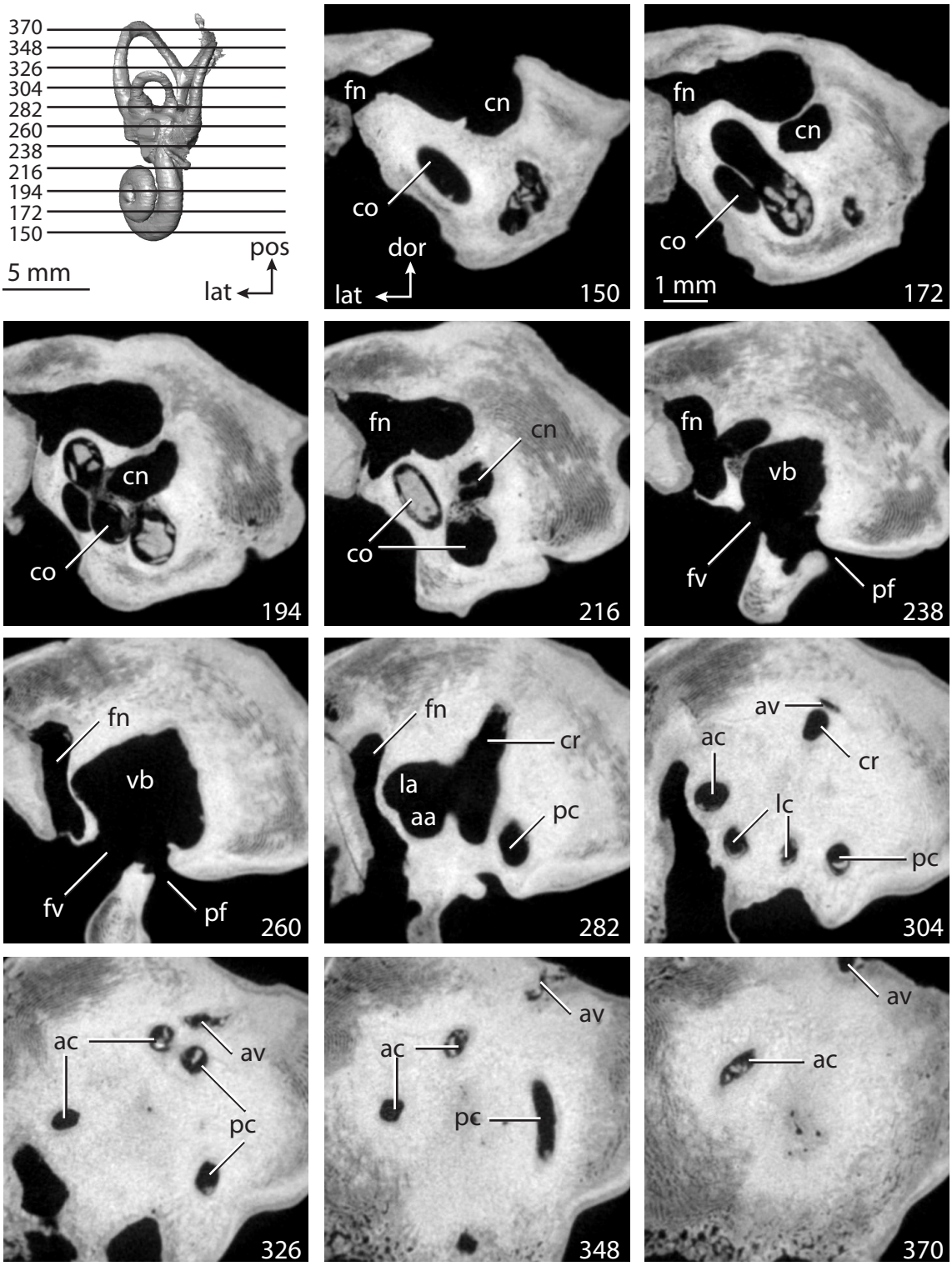
370
348
326
304
282
260
238
216
194
172
150
5 mm
pos
lat
fn
cn
co
dor
lat
150
fn
cn
co
1 mm
172
cn
co
194
fn
cn
co
216
fn
vb
fv
pf
238
fn
vb
fv
pf
260
fn
cr
la
aa
pc
282
av
ac
cr
lc
pc
304
ac
av
pc
326
av
ac
pc
348
av
ac
370

and lateral canals (92.6°). The angle between the planes of the anterior and posterior semicircular canals is 73.7°. Although the canals deviate from their planes, the deviation is not significant (ratio of total linear deviation over cross-sectional area for the anterior canal equals 0.87; lateral canal equals 0.08; posterior canal equals 0.71). The total angular deviations of the anterior, lateral, and posterior semicircular canals are 18.5°, 3.0°, and 14.3° respectively.

The arc radius of the posterior semicircular canal (5.51 mm) is larger than both the anterior (4.99 mm) and lateral canals (2.67 mm), as is the diameter of the posterior canal in cross-section (1.91 mm; anterior equals 1.85 mm; lateral equals 1.69 mm). However, the length of the slender canal of the anterior semicircular canal (24.57 mm) is greater than either the posterior (24.28 mm) or lateral canals (12.54 mm).

The arcs of the lateral and posterior semicircular canals are higher than they are wide in the elephantoid with aspect ratios of 1.31 and 1.10 respectively. The aspect ratio of the arc of the lateral semicircular canal is less (0.72). The ratios between the length of the slender canal and arc radius of the anterior canal is 4.93, which is the largest ratio among the three canals, and 4.41 for the posterior canal, which is the smallest value. The ratio for the lateral canal is 4.70.

The bony labyrinth of the elephantoid retains the primitive eutherian morphology observed in *Kulbeckia*, although the mammoth inner ear is derived in the absence of the secondary common crus. There are no unambiguous characters within the bony labyrinth to support monophyly of Tethytheria to the exclusion of all other afrotherians, although among the paenungulates, both the elephantoid and *Trichechus* share a flattened cochlea and a low position of the lateral semicircular canals (which are both the ancestral condition for Eutheria), although the ancestral paenungulate state for both of these characters is equivocal.

Xenarthra

There are two major groups of xenarthrans, the armadillos and extinct glyptodonts that belong to Cingulata, and the anteaters and sloths, which make up the clade Pilosa (McKenna and Bell, 1997). Xenarthra often occupies a basal position in placental mammal phylogenies reconstructed using both morphological (e.g., Novacek and Wyss, 1986b) and molecular (e.g., Murphy et al., 2001a, b) analyses.

A close relationship between Xenarthra and Pholidota (pangolins) within a group called Edentata has been proposed (as recently as the mid-1980's by Novacek, 1986) based on morphology, but such anatomical similarities, which include adaptations for a fossorial lifestyle and a reduction in teeth, are considered homoplastic in more recent phylogenetic analyses, including Bininda-Emonds et al. (2007). The validity of Edentata as a natural grouping was discussed by Rose et al. (2005). Further, nearly all molecular analyses group Pholidota with other placental clades separate from Xenarthra (e.g., Miyamoto and Goodman, 1986; Honeycutt and Adkins, 1993; Springer et al., 1997; Shoshani and McKenna, 1998; Liu et al., 2001; Murphy et al., 2001a, b; van Dijk et al., 2001; Amrine-Madsen et al., 2003; Bininda-Emonds, 2007; one exception is McKenna, 1992, which recovers a sister relationship between Xenarthra and Pholidota).

The nine-banded armadillo, *Dasypus novemcinctus*, which is the only xenarthran found in the United States, represents Xenarthra in this study. *Dasypus* as a genus is known from the Pliocene to Recent in North, Central, and South America (McKenna and Bell, 1997), and *D. novemcinctus* itself has the largest biogeographical distribution of any xenarthran species (McBee and Baker, 1982).

Intraspecific variation within the inner ear of *D. novemcinctus* was discussed in Chapter 4, and a more thorough description of the bony labyrinth of this species is provided here (Figures 5.22-5.23). Dimensions of the bony labyrinth of *Dasypus* are

FIGURE 5.22. Bony labyrinth of *Dasypus novemcinctus*. **A**, stereopair and labeled line drawing of digital endocast in anterior view; **B**, stereopair and labeled line drawing of digital endocast in dorsal view; **C**, stereopair and labeled line drawing of digital endocast in lateral view; **D**, line drawing of cochlea viewed down axis of rotation to display degree of coiling; **E**, line drawing of cochlea in profile. Abbreviations: **aa**, anterior ampulla; **ac**, anterior semicircular canal; **ant**, anterior direction; **av**, bony channel for aqueduct of vestibule; **cc**, canaliculus cochleae for aqueduct of cochlea; **co**, cochlea; **cr**, common crus; **dor**, dorsal direction; **er**, elliptical recess of vestibule; **fc**, fenestra cochleae; **fv**, fenestra vestibuli; **la**, lateral ampulla; **lc**, lateral semicircular canal; **med**, medial direction; **pa**, posterior ampulla; **pc**, posterior semicircular canal; **pos**, posterior direction; **ps**, outpocketing for perilymphatic sac; **sl**, secondary bony lamina; **sr**, spherical recess of vestibule.

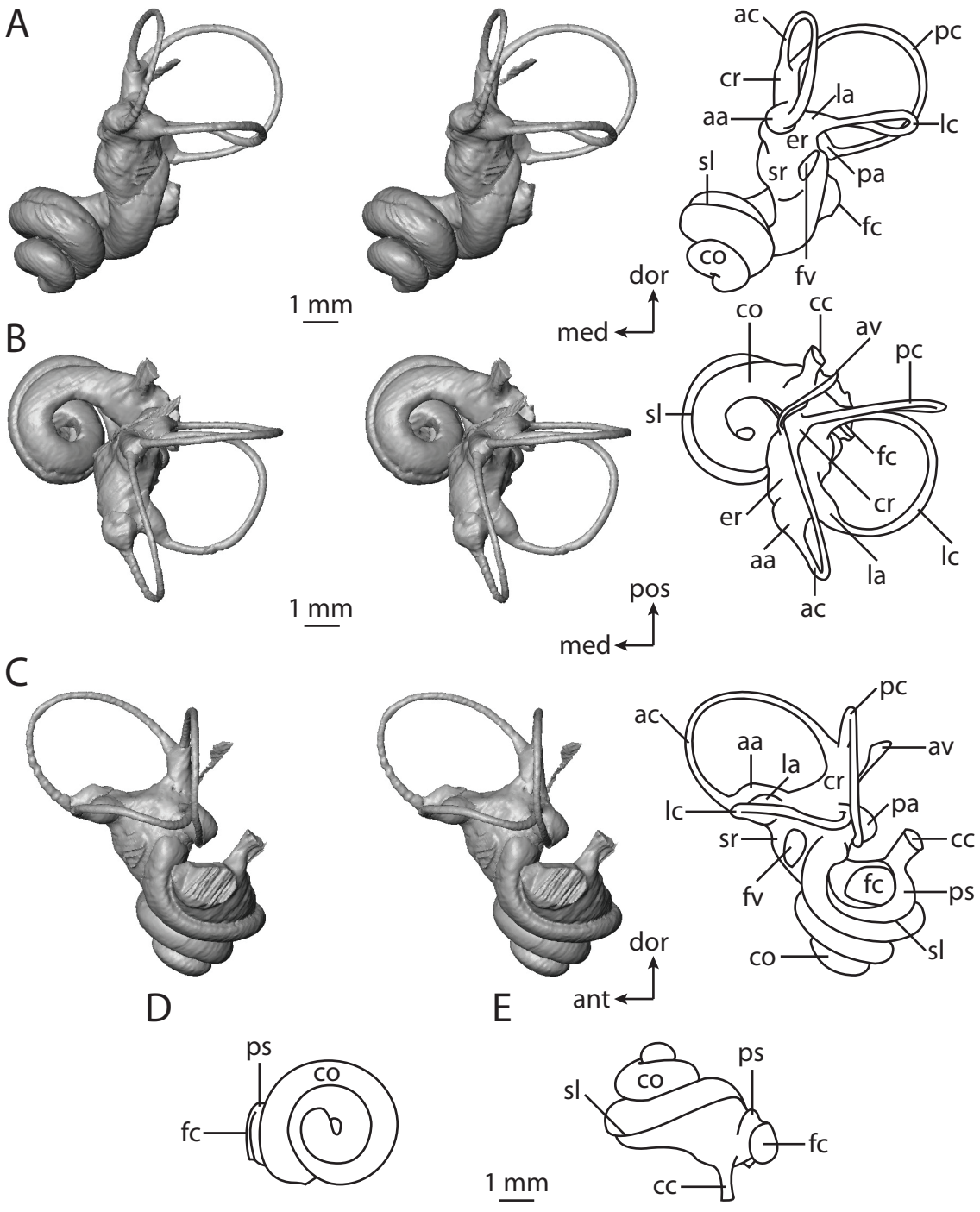
A
ac
pc
cr
la
aa
lc
er
sl
sr
pa
fc
co
fv
dor
med
1 mm
B
co
cc
av
pc
sl
fc
cr
er
aa
la
lc
ac
pos
med
1 mm
C
pc
ac
aa
av
la
cr
lc
pa
sr
cc
fv
fc
ps
co
sl
dor
ant
D
ps
co
fc
E
ps
co
sl
fc
cc
1 mm

FIGURE 5.23. CT slices through ear region of *Dasypus novemcinctus*. Abbreviations: **aa**, anterior ampulla; **ac**, anterior semicircular canal; **av**, bony channel for aqueduct of vestibule; **cc**, canaliculus cochleae; **cf**, foramina within cribriform plate; **cn**, canal for cranial nerve VIII; **co**, cochlea; **cr**, common crus; **dor**, dorsal direction; **fc**, fenestra cochleae; **fn**, canal for cranial nerve VII; **fv**, fenestra vestibuli; **la**, lateral ampulla; **lc**, lateral semicircular canal; **med**, medial; **pc**, posterior semicircular canal; **pl**, primary bony lamina; **pos**, posterior direction; **sl**, secondary bony lamina; **vb**, vestibule.

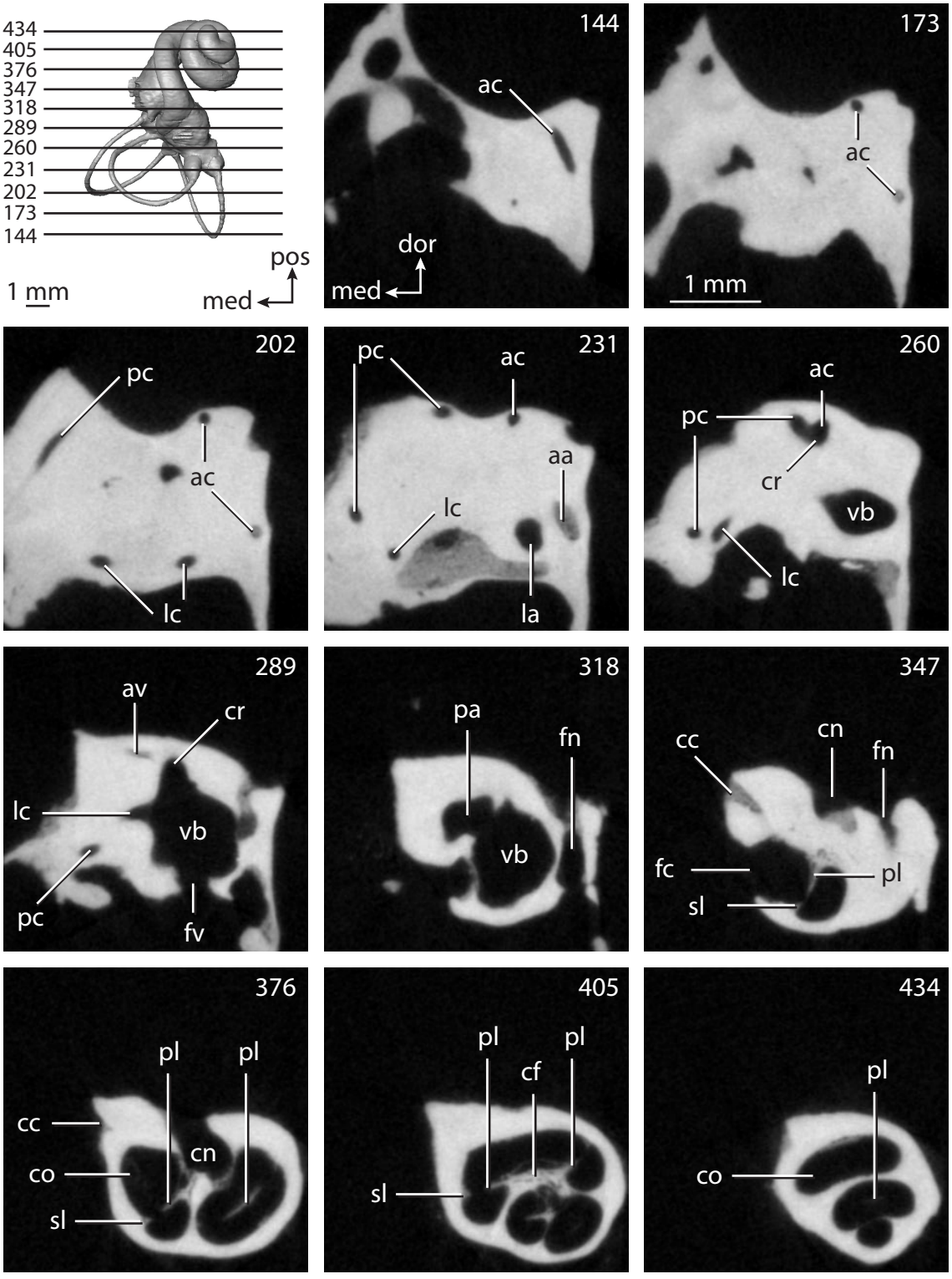
434
405
376
347
318
289
260
231
202
173
144
1 mm
pos
med
144
ac
dor
med
173
ac
1 mm
202
pc
ac
lc
231
pc
ac
aa
lc
la
260
ac
pc
cr
vb
lc
289
av
cr
lc
vb
pc
fv
318
pa
fn
vb
347
cc
cn
fn
fc
pl
sl
376
pl
pl
cc
cn
co
sl
405
pl
pl
cf
sl
434
pl
co

provided in Table 5.2. The total length of the bony labyrinth is 8.06 mm, and the volume of the combined inner ear cavities is 26.48 mm^3. The cochlea itself contributes 17.48 mm^3 (see Table 5.3) to the volume of the bony labyrinth (66.0%), which is larger than that reconstructed for the ancestors of both Placentalia (58.0%) and Afrotheria (56.0%). Further dimensions of the cochlea are provided in Table 5.3, and dimensions and orientations of the semicircular canals are reported in Tables 5.4-5.6. Average body mass for the species is 4.8 kg (Silva and Downing, 1995).

The cochlea completes nearly two and a quarter turns (816.3°), and the total length of the cochlear canal is 11.21 mm. The diameters of the apical whorls of the cochlea are smaller than the basal turn of the cochlea (unlike the condition observed in *Macroscelides*), although the successive whorls sit upon the basal turn (Figure 5.22). The aspect ratio of the cochlear spiral in profile is 0.63, which is the same that was calculated for the afrosoricid *Chrysochloris*.

As was observed within the cochlea of *Macroscelides*, the secondary bony lamina is well developed in *Dasypus* (Figure 5.23), and the structure extends past the basal turn (383.1°). The lamina is expressed as the distinct groove along the radial wall of the digital endocast. The secondary lamina curves around the dorsal border of the fenestra cochleae, and it defines the posterior border of an inflation of the scala vestibuli between to the fenestra cochleae and fenestra vestibuli (stapedial ratio equals 1.74). Medial to the fenestra cochleae, an outpocketing of the scala tympani for the perilymphatic duct leads to a robust canaliculus cochleae for transmission of the aqueduct of the cochlea (1.17 mm in length).

The angle between the plane of the basal turn of the cochlea and the lateral semicircular canal is low for *Dasypus* (17.9°) when compared to other taxa that are

described above. The angle is 18.4° in *Hemicentetes*, but the cochlea deviates from the plane of the lateral canal to a greater degree in all other taxa discussed so far.

The spherical recess of the vestibule is distinguishable from the elliptical recess as the former bulges medially toward the axis of rotation of the cochlea. The anterior and lateral ampullae open into a small anterior chamber of the elliptical recess (expressed on the endocast as a short pedestal). The posterior limb of the lateral semicircular canal opens into the vestibule dorsal to the posterior ampulla, which gives the lateral canal a high position with respect to the rest of the vestibule. The lateral canal divides the space enclosed by the arc of the posterior semicircular canal when the labyrinth is in anterior view, and the sagittal labyrinthine index is 23.0. This index is slightly larger than that calculated for *Chrysochloris* (21.7).

The common crus appears stout with respect to the arcs of the semicircular canals. The bony channel for the aqueduct of the vestibule exits the labyrinth from a triangular excavation on the medial wall of the spherical recess, medioventral to the common crus. The canal for the aqueduct of the vestibule is longer than the canaliculus cochleae (2.63 mm versus 1.17 mm), but is a more delicate structure overall. The aqueduct only crosses the base of the common crus on its posterodorsal course.

All of the semicircular canal planes of *Dasypus* form acute angles with each other, although the angle between the planes of the posterior and lateral canals approaches a right angle (87.3°). The plane of the anterior semicircular canal forms an angle of 62.4° with the plane of the lateral canal, and an angle of 67.7° with the plane of the posterior canal. The posterior semicircular canal is the most planar of the three, with a total angular deviation of 7.8° from its plane, and the lateral canal is the least planar (18.1°). The angular deviation of the anterior semicircular canal from its plane is 13.0°, and the ratio

of the total linear deviation over cross-sectional diameter is significant for all three canals (anterior is 1.68; lateral is 2.13; posterior is 1.18).

The posterior semicircular canal is the largest of the three canals in terms of slender canal length (11.30 mm; anterior equals 9.69 mm; lateral equals 7.38 mm) and arc radius of curvature (1.92 mm; anterior equals 1.64 mm; lateral equals 1.60 mm). However, the diameter of the lumen of the lateral semicircular canal (0.24 mm) is greater than either the anterior or posterior canal (each with a diameter of 0.22 mm).

The area enclosed by the arc of the anterior semicircular canal is elliptical, as expressed by the aspect ratio of the arc (0.58), whereas the area enclosed by the arc of the posterior semicircular canal is circular (aspect ratio equals 0.96). The aspect ratio of the arc of the lateral semicircular canal is 1.16, signifying that the height of the arc is greater than the width. The ratio of the length of the slender semicircular canal over the arc radius is 5.91 for the anterior semicircular canal, 4.63 for the lateral semicircular canal, and 5.88 for the posterior semicircular canal.

The bony labyrinth of *Dasypus* is derived in all respects to that of the ancestral eutherian, but retains the direct vestibular entry of the lateral semicircular canal from its placental ancestor. The plane of the lateral canal is high relative to the ampullar entry of the posterior canal, which is derived with respect to Eutheria, but the ancestral placental condition is unknown. Furthermore, the posterior semicircular canal of *Dasypus* is largest in terms of arc radius, rather than the anterior canal arc, and the aspect ratio of the cochlear spiral is high, giving the cochlea a “sharp-pointed” appearance. Although the labyrinth of *Dasypus* is derived with respect to the eutherian ancestral condition, there are no unambiguous characters within the labyrinth to support a closer relationship between Xenarthra and either Afrotheria or Boreoeutheria. The cochlea of *Dasypus* coils to a greater degree than the ancestor of Placentalia (816.3° versus 738.2°), and the cochlea

contributes a larger percentage of the total inner ear volume than the placental ancestor (66.0% versus 58.0%).

Boreoeutheria

The non-afrotherian and non-xenarthran placentals, or Boreoeutheria, are divided into two sister clades, the Euarchontoglires and Laurasiatheria (Figure 5.2). The lateral semicircular canal of the ancestral boreoeutherian entered the vestibule directly without forming a secondary common crus with the posterior semicircular canal (a state inherited from the placental ancestor), and the arc of the anterior semicircular canal was the largest among the three arcs, which is a state retained from the therian ancestor. The plane of the lateral semicircular canal was positioned high compared to the ampullar opening of the posterior semicircular canal, which is derived from the ancestors of both Theria and Eutheria, although the state in the placental ancestor is unknown. A high position of the lateral canal in Boreoeutheria is shared with *Dasypus*, which might support a sister relationship between Xenarthra and Boreoeutheria, but the ancestral state in Afrotheria could not be reconstructed unequivocally. Owing to variation of the aspect ratio of the cochlear spiral within Laurasiatheria and Euarchontoglires, the condition for the ancestor of Boreoeutheria is equivocal between the high and low conditions.

The degree of coiling of the ancestor of Boreoeutheria (815.4°) is almost identical to that of *Dasypus* (816.3°), both of which are greater than that reconstructed for Afrotheria (751.3°). Such a degree of coiling might support a Xenarthra plus Boreoeutheria pairing. However, the volumetric contribution of the cochlea to the entire labyrinth of Boreoeutheria (55%) nearly is identical that reconstructed for Afrotheria (56%), both of which are less than that calculated for *Dasypus* (66%).

Laurasiatheria

Laurasiatheria encompasses a great diversity of placental mammals in terms of body size, ranging from the smallest extant mammal, the hog-nosed bat (*Craseonycteris thonglongyai*) at around 2 g, to the largest, the blue whale (*Balaenoptera musculus*) at around 150000 kg (Silva and Downing, 1995). Some laurasiatherians are specialized for efficient cursoriality, such as the cheetah (*Acinonyx jubatus*) or Thomson's gazelle (*Eudorcas thomsoni*), while others are adapted for fossorial lifestyles, such as the European mole (*Talpa europaea*). Furthermore, volant bats and fully aquatic cetaceans are included within Laurasiatheria. As a whole, the clade Laurasiatheria is composed of Cetartiodactyla (represented here by *Sus scrofa*, *Bathygenys reeves*, *Tursiops truncatus*, and an extinct member of Balaenopteridae), Perissodactyla (represented by *Equus caballus*), Carnivora (represented by *Canis familiaris*, *Eumetopias jubatus*, and *Felis catus*), Chiroptera (represented by *Pteropus lyelli*, *Nycteris grandis*, *Rhinolophus ferrumequinum*, and *Tadarida brasiliensis*), and Eulipotyphla (represented by *Atelerix albiventris* and *Sorex monticolus*). Dimensions of the bony labyrinths of laurasiatheres are provided in Table 5.2. Dimensions of the cochlea are provided in Table 5.3, and dimensions and orientations of the semicircular canals are reported in Tables 5.4-5.6.

Most character states reconstructed for the ancestral laurasiatherian were retained from its boreoeutherian ancestor. That is, the lateral semicircular canal entered directly into the vestibule without forming a secondary common crus, the arc of the anterior semicircular canal has the greatest radius, and the plane of the lateral semicircular canal was high compared to the junction of the posterior canal and its ampulla. The state of the aspect ratio of the cochlea was reconstructed as equivocal, as was calculated for Boreoeutheria. The ancestral degree of coiling of the cochlea of Laurasiatheria (751.0°) was less than that reconstructed for Boreoeutheria (815.4°), but the contribution of the

cochlea to the entire labyrinthine volume of Laurasiatheria (55%) was similar to that of the boreoeutherian ancestor (56%).

The relationships within Boreoeutheria that were recovered by Bininda-Emonds et al. (2007) place Chiroptera in a polytomy with Ungulata (Cetartiodactyla plus Perissodactyla) and Ferae (Carnivora and Pholidota). The states reconstructed for the bony labyrinth of the most recent common ancestor of this polytomy were the same as those calculated for the ancestor of Laurasiatheria. That is, the lateral semicircular canal entered the vestibule directly in the absence of a secondary common crus, the plane of the lateral canal was high compared to the ampullar entry of the posterior semicircular canal, and the arc of the anterior semicircular canal was the largest among the three canal arcs. The ancestral degree of coiling for the ungulate-feran-chiropteran polytomy was 815.1°, which was similar to that of the ancestral boreoeutherian condition (815.4°), and the cochlea contributed 56.0% of the total labyrinthine volume, which also was inherited from the ancestor of Boreoeutheria (50.0%).

Systematic analyses of mammals based on morphology (Novacek, 1986, 1992a, b; McKenna and Bell, 1997) group cetartiodactyls (although separated into monophyletic Artiodactyla with the exclusion of Cetacea) and perissodactyls in a group called Ungulata along with Sirenia, Hyracoidea, and Proboscidea (and often Tubulidentata). Ungulate monophyly has been brought into question by more recent molecular results that not only separate hyracoids, sirenians, proboscideans, and tubulidentates from the perissodactyls, artiodactyls, and cetaceans into Afrotheria (as discussed above), but some recover a close relationship between the cetartiodactyls and perissodactyls with a Carnivora+Pholidota clade (Liu et al., 2001; Murphy et al., 2001a), and at times placing Perissodactyla as the sister taxon to the Carnivora+Pholidota grouping (Springer et al., 1997; Stanhope et al., 1998; Murphy et al., 2001b). However, most molecular analyses, including those of

Bininda-Emonds et al (2007), recover a Perissodactyla+Cetartiodactyla clade, whether Cetacea falls within Artiodactyla or not (e.g., Honeycutt and Adkins, 1993; Madsen et al., 2001).

The only state reconstructed for the ungulate ancestor that differs from that of the ancestor of Boreoeutheria was the aspect ratio of the cochlea, which was low in the ancestor of Ungulata. The state of the boreoeutherian cochlea was equivocal, although the aspect ratio of the cochlea was low in the ancestral therian. The bony labyrinth of the ancestor of Ungulata had a lateral semicircular canal that opened into the vestibule directly (retained from the placental ancestor), a position of the plane of the lateral canal high compared to the posterior canal (retained from the boreoeutherian ancestor), and an anterior semicircular canal arc as the largest of the three arcs (retained from the therian ancestor). The ancestral coiling of the cochlea of Ungulata was 857.4°, which was greater than that reconstructed for the ancestor of the ungulate-feran-chiropteran polytomy (815.1°), and the ancestral ungulate cochlea contributed 55.0% of the total labyrinthine volume, which was a value retained from the boreoeutherian ancestor (55.0%).

The ancestor of Ferae (Carnivora plus Pholidota as supported by the results of numerous analyses; Murphy et al., 2001a, b; Amrine-Madsen et al., 2003; Bininda-Emonds et al., 2007) retained labyrinthine morphology similar to the most recent common ancestor of Ungulata, Ferae, and Chiroptera. The lateral semicircular canal entered the vestibule directly in absence of a secondary common crus, the anterior semicircular canal arc was the largest among the three arcs, and the lateral canal was positioned high compared to the ampullar opening of the posterior semicircular canal. The aspect ratio of the cochlea was equivocal, but the ancestral feran cochlea coiled 888.2° and contributed 56.0% of the total labyrinthine volume. The volumetric contribution of the cochlea of Ferae was retained from the boreoeutherian ancestor, but

the degree of coiling was greater than that reconstructed for its ancestors within Boreoeutheria.

There are no unambiguous otic synapomorphies that support any relationships between Ungulata, Ferae, and Chiroptera. Ancestral states reconstructed for the ancestors of clades within Ungulata, Ferae, and Chiroptera, as well as the ancestral states for Chiroptera as a whole, are provided in separate sections below.

Terrestrial Cetartiodactyla

The origins of Cetacea were mired in controversy in the past (see Gingerich, 2005, for a brief historical review of cetacean systematics), but most evidence supports a close relationship between cetaceans and even-toed ungulates (traditionally classified as Artiodactyla). Both morphology (McKenna and Bell, 1997; Geisler and Luo, 1998; O'Leary, 1999; O'Leary and Geisler, 1999; O'Leary and Uhen, 1999; Thewissen and Madar, 1999; Geisler, 2001; Gingerich et al., 2001; Thewissen et al., 2001; Theodor and Foss, 2005) and molecules (Boyden and Gemeroy, 1950; Graur and Higgins, 1994; Gatesy et al., 1996; Ursing and Arnason, 1998; Gatesy et al., 1999; Kleineidam et al., 1999; Madsen et al., 2001; Murphy et al., 2001a, b; Bininda-Emonds et al., 2007) have been used to suggest a common origin for cetaceans and their terrestrial hoofed relatives. Although a large amount the genetic data support a nesting of Cetacea within Artiodactyla, only recently have such relationships found support from morphology (Naylor and Adams, 2001; Geisler and Uhen, 2003; Geisler and Theodor, 2009). Because the name Cetartiodactyla is commonly used in scientific literature, including those studies that include Cetacea within Artiodactyla (e.g., Bininda-Emonds et al., 2007), the name Cetartiodactyla is used throughout the remainder of the present paper.

The terrestrial members of Cetartiodactyla (non-cetacean even-toed ungulates) are divided into the three major extant groups, which are Suiformes (pigs and hippos), Tylopoda (camels and llamas), and Ruminantia (deer and cows) (Theodor et al., 2005). The extinct oreodont *Bathygenys reevesi* and its closest relative in the sample, the extant pig *Sus scrofa*, represent the terrestrial cetartiodactyls here.

Oreodonts (classified under Tylopoda by Theodor et al., 2005) are common members of the North American mammal biota during the Tertiary (MacFadden and Morgan, 2003). *Bathygenys reevesi* itself is a small oreodont from the Airstrip and Little Egypt local faunas in the Trans-Pecos region of Texas (Wilson, 1971), and inclusion of the ear region of this taxon extends the temporal range of the placental sample into the Oligocene (Prothero and Emry, 2004). Preservation of the ear region in the skull of *Bathygenys* was such that the matrix filling the inner ear cavities appears very similar to the bone in the CT scans. Because of this, small structures, such as the bony channels for the aqueducts for the cochlea and vestibule, are not visible in the digital imagery. Furthermore, the boundaries of the fenestrae cochleae and vestibuli are ill defined, and measurements, such as the stapedial ratio calculated from the dimensions of the fenestra vestibuli, were not taken. However, the gross anatomy of the bony labyrinth of *Bathygenys* was segmented (Figures 5.24-5.25) and described here along with *Sus scrofa* (Figures 5.26-5.27).

The bony labyrinth of *Sus* is larger than the labyrinth of *Bathygenys*, both in terms of the length of the inner ear (9.95 mm versus 7.40 mm), as well as the gross volume of the inner ear cavities (61.86 mm^3 versus 29.83 mm^3). Overall, *Sus* is a larger animal than *Bathygenys*, given that the length of the skull of *Sus* (240.00 mm) is over two and a half times greater than that measured for *Bathygenys* (90.71 mm). The body mass of

FIGURE 5.24. Bony labyrinth of *Bathygenys reevesi*. **A**, stereopair and labeled line drawing of digital endocast in anterior view; **B**, stereopair and labeled line drawing of digital endocast in dorsal view; **C**, stereopair and labeled line drawing of digital endocast in lateral view; **D**, line drawing of cochlea viewed down axis of rotation to display degree of coiling; **E**, line drawing of cochlea in profile. Abbreviations: **aa**, anterior ampulla; **ac**, anterior semicircular canal; **ant**, anterior direction; a**v**, bony channel for aqueduct of vestibule; **co**, cochlea; **cr**, common crus; **dor**, dorsal direction; **fc**, fenestra cochleae; **la**, lateral ampulla; **lc**, lateral semicircular canal; **med**, medial; pa, posterior ampulla; **pc**, posterior semicircular canal; **pos**, posterior direction; **sr**, spherical recess of vestibule.

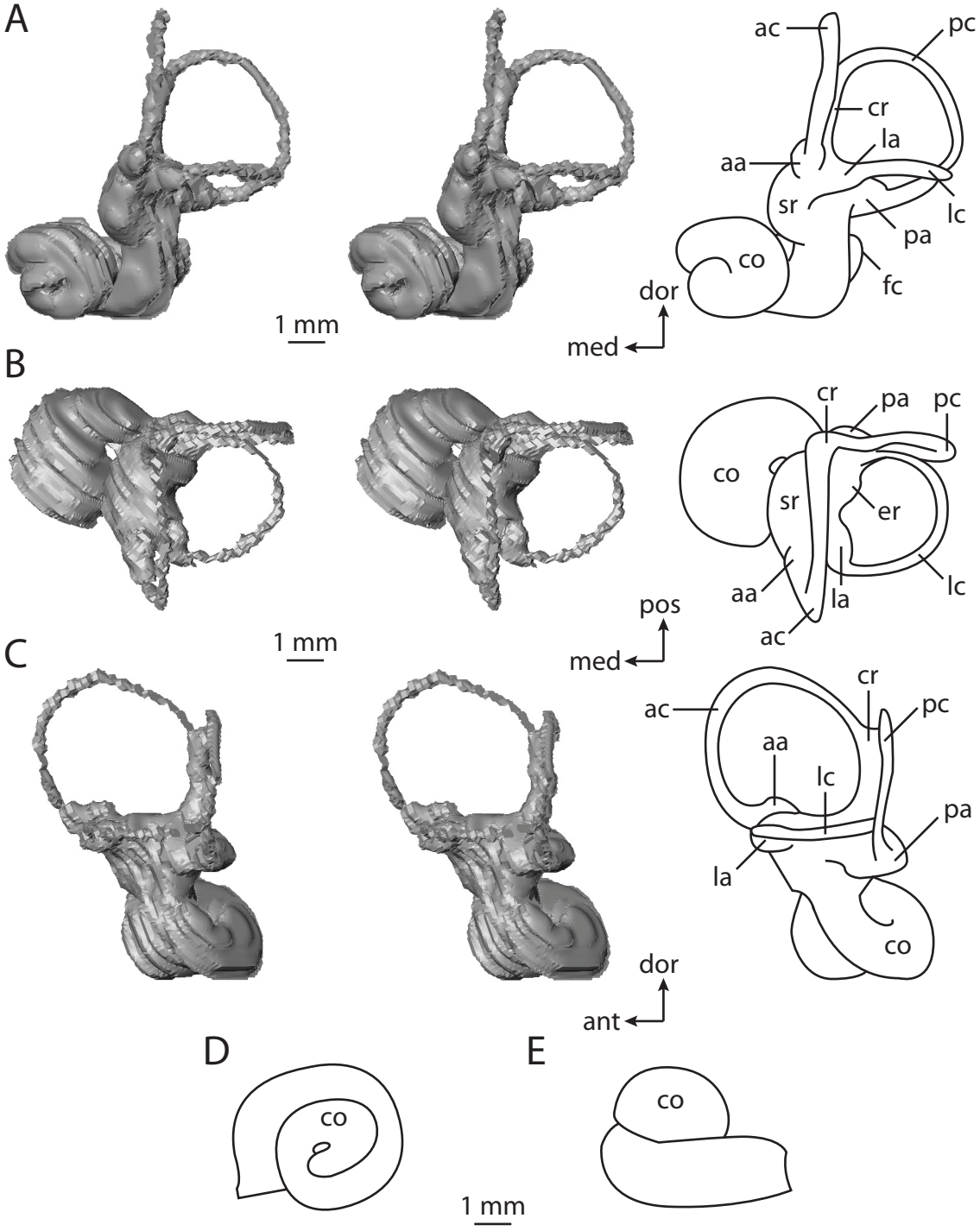
A
ac
pc
cr
la
aa
sr
lc
pa
co
fc
dor
med
1 mm
B
cr
pa
pc
co
sr
er
aa
la
lc
ac
pos
med
1 mm
C
cr
ac
pc
aa
lc
pa
la
co
dor
ant
D
co
E
co
1 mm

FIGURE 5.25. CT slices through ear region of *Bathygenys reevesi*. Abbreviations: **aa**, anterior ampulla; **ac**, anterior semicircular canal; **co**, cochlea; **cr**, common crus; dor, dorsal direction; **la**, lateral ampulla; **lc**, lateral semicircular canal; **med**, medial; **pa**, posterior ampulla; **pc**, posterior semicircular canal; **pos**, posterior direction; **vb**, vestibule.

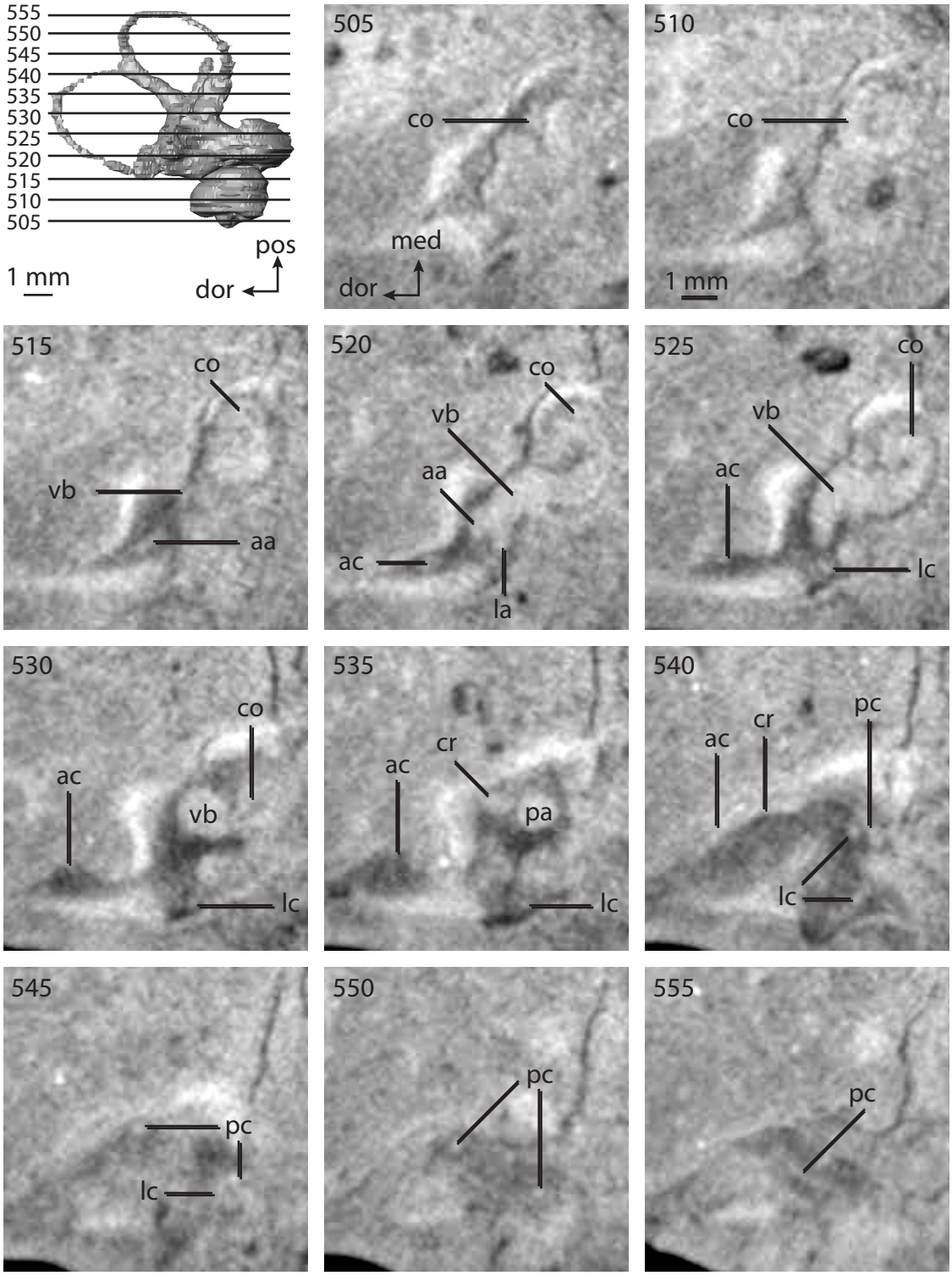
555
550
545
540
535
530
525
520
515
510
505
pos
1 mm
dor
505
co
med
dor
510
co
1 mm
515
co
vb
aa
520
co
vb
aa
ac
la
525
co
vb
ac
lc
530
co
ac
vb
lc
535
cr
ac
pa
lc
540
pc
cr
ac
lc
545
pc
lc
550
pc
555
pc

FIGURE 5.26. Bony labyrinth of *Sus scrofa*. **A**, stereopair and labeled line drawing of digital endocast in anterior view; **B**, stereopair and labeled line drawing of digital endocast in dorsal view; **C**, stereopair and labeled line drawing of digital endocast in lateral view; **D**, line drawing of cochlea viewed down axis of rotation to display degree of coiling; **E**, line drawing of cochlea in profile. Abbreviations: **aa**, anterior ampulla; **ac**, anterior semicircular canal; **ant**, anterior direction; **av**, bony channel for aqueduct of vestibule; **cc**, canaliculus cochleae; **co**, cochlea; **cr**, common crus; **dor**, dorsal direction; **er**, elliptical recess; **fc**, fenestra cochleae; **fv**, fenestra vestibuli; **la**, lateral ampulla; **lc**, lateral semicircular canal; **med**, medial; **pa**, posterior ampulla; **pc**, posterior semicircular canal; **pos**, posterior direction; **ps**, outpocketing for the perilymphatic sac.

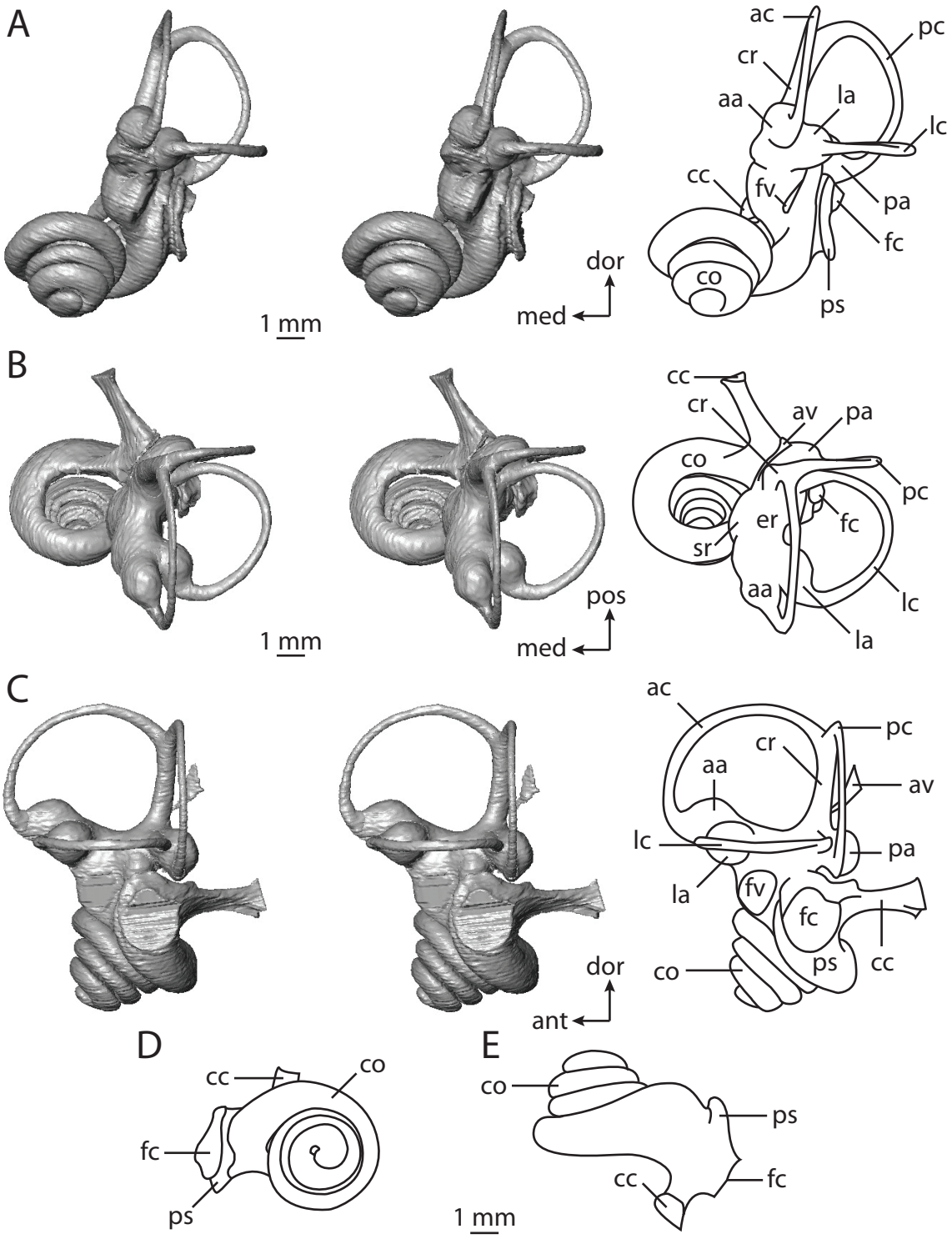
A
1 mm
dor
med
ac
pc
cr
aa
la
lc
cc
fv
pa
fc
co
ps
B
1 mm
pos
med
cc
cr
av
pa
co
pc
er
fc
sr
aa
lc
la
C
dor
ant
ac
pc
cr
aa
av
lc
pa
la
fv
fc
co
ps
cc
D
cc
co
fc
ps
E
co
ps
cc
fc
1 mm

FIGURE 5.27. CT slices through ear region of *Sus scrofa*. Abbreviations: **aa**, anterior ampulla; **ac**, anterior semicircular canal; **av**, bony channel for aqueduct of vestibule; **ca**, canal for vasculature through petrosal; **cc**, canaliculus cochleae; **cf**, foramina within cribriform plate; **cn**, canal for cranial nerve VIII; **co**, cochlea; **cr**, common crus; **dor**, dorsal direction; **fc**, fenestra cochleae; **fn**, canal for cranial nerve VII; **iam**, internal auditory meatus; **la**, lateral ampulla; **lat**, lateral direction; **lc**, lateral semicircular canal; **pa**, posterior ampulla; **pc**, posterior semicircular canal; **pl**, primary bony lamina; **pos**, posterior direction; **sa**, subarcuate fossa; **sr**, spherical recess of vestibule; **st**, stapes within fenestra vestibuli; **vn**, canal for vestibular branch of cranial nerve VIII.

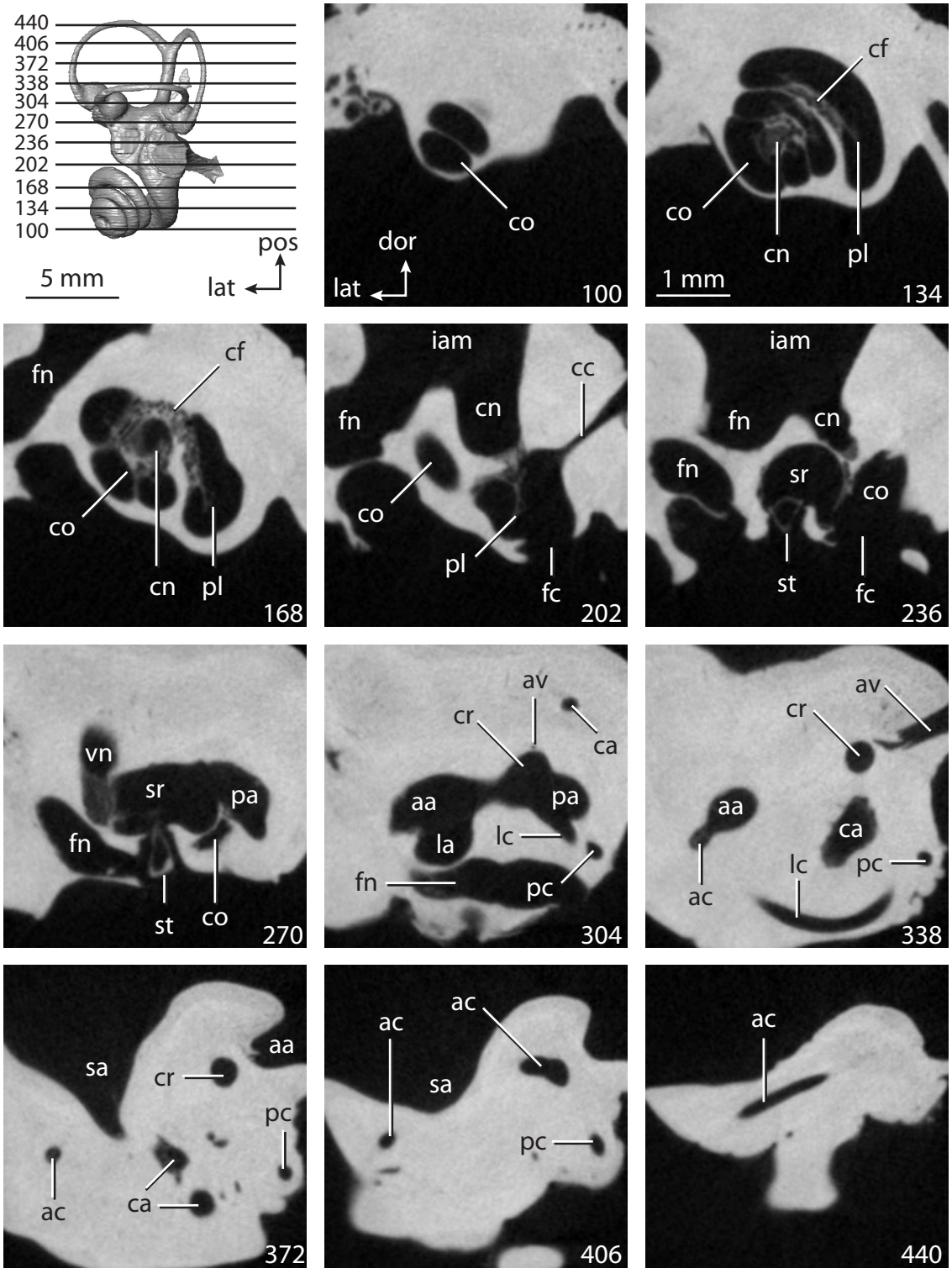
440
406
372
338
304
270
236
202
168
134
100
pos
5 mm
lat
co
dor
lat
100
cf
co
cn
pl
1 mm
134
fn
cf
co
cn
pl
168
iam
cc
fn
cn
co
pl
fc
202
iam
fn
cn
fn
sr
co
st
fc
236
vn
sr
pa
fn
st
co
270
av
cr
ca
aa
pa
la
lc
fn
pc
304
av
cr
aa
ca
lc
pc
ac
338
sa
aa
cr
pc
ac
ca
372
ac
ac
sa
pc
406
ac
440

Bathygenys was not estimated, but the average body mass of *Sus* is 88 kg (Silva and Downing, 1995).

Although the cochlea of *Sus* is more voluminous (36.25 mm^3) than the cochlea of *Bathygenys* (16.17 mm^3), the structure contributes a similar amount to the total volume of the bony labyrinth in both species (54.2% in *Bathygenys*; 58.6% in *Sus*). However, this is the only similarity between the cochleae of the two taxa. The cochlear canal is significantly longer (22.89 mm) and coils to a much greater degree (1274°) in *Sus* than is observed in *Bathygenys* (canal is 8.51 mm long; canal coils 665°). Furthermore, the cochlear spiral of *Sus* has a much higher aspect ratio (0.71) than the cochlea of *Bathygenys* (0.32). The aspect ratio of the cochlea of *Bathygenys* is similar the ratio calculated for *Hemicentetes semispinosum* (0.38). The apical whorl of the cochlea of *Bathygenys* sits upon the basal turn, although the diameter of the apical whorl is smaller than the basal, as can be seen when the cochlea is in vestibular view.

The shape of the cochleae of *Sus* and *Procavia* are strikingly similar (Figure 5.16). The aspect ratios calculated for the cochlear spirals are identical between the two taxa, and both spirals form a pyramid-like structure, where the apical whorls do not sit directly upon the basal whorl, but rather fit within the basal turn when the cochlea is in vestibular view. The diameters of the second and third turns are similar, so that the third whorl shields most of the second from view when the cochlea is viewed down the axis of rotation.

Preservation of the bony labyrinth of *Bathygenys* was such that presence or absence of a secondary bony lamina within the cochlea could not be determined (Figure 5.25). However, the CT scans through the ear region of *Sus* (Figure 5.27) demonstrate that the secondary lamina was not present in the cochlea of the pig. The scala tympani of *Sus* is expanded posterodorsal to the fenestra cochleae, and a very robust bony

canaliculus cochleae projects posteromedially from the excavation. The canaliculus is triangular in cross-section and 2.64 mm in length. As stated above, the canaliculus cochleae was not observed for *Bathygenys*, owing to preservation of the fossil specimen. The canaliculus cochleae likely was present in the taxon, given that the structure is observed in all other cetartiodactyls examined here and elsewhere (e.g., Gray, 1907), as well as most placental taxa.

The angles formed between the planes of the basal turn of the cochlea and the lateral semicircular canal are not much different between *Bathygenys* (26.8°) and *Sus* (23.8°). The degree of angular deviation observed in these taxa is similar to that measured in the elephant shrew, *Macroscelides proboscideus* (25.1°). The stapedial ratio could not be measured for *Bathygenys*, but a ratio of 1.28 was calculated for *Sus*. The spherical recess of the vestibule, through which the labyrinth communicates with the middle ear cavity via the fenestra vestibuli and stapes, is well defined in *Sus*. The recess in the pig is a sphere that is bisected, and the fenestra vestibuli is situated on the cut surface. The spherical recess cannot be distinguished from the elliptical recess in *Bathygenys*, where the vestibule is developed as a continuous yet irregularly shaped cavity.

The elliptical recess of the vestibule of *Sus* is elongate, with a stout anterior projection that is expressed as a pedestal for the anterior and lateral ampullae on the digital endocast. A similar projection is observed in the vestibule of *Bathygenys*. All three ampullae in *Sus* are rounded, teardrop-shaped excavations within the vestibule. The posterior limb of the lateral semicircular canal opens directly into the vestibule dorsal to the posterior ampulla in both cetartiodactyls. Because of this, the lateral canal divides the space enclosed by the arc of the posterior semicircular canal when either labyrinth is viewed anteriorly. The sagittal labyrinthine index is nearly the same for *Bathygenys* (17.4) as it is for *Sus* (16.5).

The bony channel for the aqueduct of the vestibule is not observed in *Bathygenys,* but the channel is a thin canal in *Sus* that exits the vestibule ventromedial and slightly anterior to the vestibular aperture of the common crus. The channel for the aqueduct of the vestibule is expressed on the endocast as a fine thread before expanding as the aqueduct opens into a fissure near the endocranial surface of the petrosal. Although the channel for the aqueduct of the vestibule is more delicate than the canaliculus cochleae for the aqueduct of the cochlea, the vestibular channel is slightly longer, with a length of 3.18 mm (as opposed to 2.64 mm for the canaliculus cochleae).

Although the specific measured values of the angles between the planes of the three semicircular canals are different for *Sus* and *Bathygenys*, the basic pattern is the same for both of these species. For example, the angle between the planes of the anterior and posterior semicircular canals is the greatest for both *Bathygenys* (99.6°) and *Sus* (96.0°), and the angle between the anterior and lateral canals is the smallest (*Bathygenys* equals 86.0°; *Sus* equals 82.8°). The angles between the planes of the posterior and lateral semicircular canals are the closest to 90° for both *Bathygenys* (91.3°) and *Sus* (87.9°).

The semicircular canals of *Sus* are more planar (fit better onto a single plane) than the canals of *Bathygenys*. In fact, the anterior semicircular canal is perfectly planar in *Sus*, whereas the anterior canal deviates from its plane by a total of 8.10°. The posterior canal is the least planar of the three for both taxa, where it deviates from its plane by 2.63° in the labyrinth of *Sus* and by 13.5° in *Bathygenys*. The lateral semicircular canal of *Sus* deviates from its plane by a total of 2.20° and the lateral canal of *Bathygenys* deviates by 7.92°. Only the posterior semicircular canal of *Bathygenys* is considered significant (ratio of total linear deviation over cross-sectional diameter is 1.23 versus 0.61 for anterior and 0.64 for lateral; ratios for anterior, lateral, and posterior canals of *Sus* are 0.00, 0.20, and 0.24 respectively).

A similar pattern is observed in the radius of the semicircular canal arcs, as well as in the cross-sectional diameter of the canals. That is, the radius of the anterior semicircular canal arc is the largest in both *Sus* (2.50 mm; lateral equals 2.08 mm; posterior equals 2.18 mm) and *Bathygenys* (1.91 mm; lateral equals 1.52 mm; posterior equals 1.79 mm). The diameter of the lumen of the anterior semicircular canal is greater than the other two canals in both *Sus* (0.42 mm; lateral equals 0.36 mm; posterior equals 0.42 mm) and *Bathygenys* (0.44 mm; lateral equals 0.33 mm; posterior equals 0.34 mm). However, this pattern is not observed universally across all dimensions of the semicircular canals. For example, the slender canal length of the anterior semicircular canal is the greatest in *Sus* (12.14 mm; lateral equals 8.04 mm; posterior equals 10.65 mm), but the posterior canal is the longest in *Bathygenys* (10.01 mm; anterior equals 9.72 mm; posterior equals 7.11 mm).

The aspect ratio of the lateral semicircular canal is the greatest in both *Bathygenys* (0.99) and *Sus* (0.83), although the aspect ratio of the anterior canal was the smallest in *Bathygenys* (0.86; *Sus* equals 0.78), whereas the aspect ratio of the posterior canal was the smallest in *Sus* (0.74; *B. reevesi* equals 0.95). The ratio between the slender canal length and arc radius for the posterior semicircular canal was the greatest for both *Bathygenys* (5.59; anterior equals 5.08; lateral equals 4.68) and *Sus* (4.89; anterior equals 4.86; lateral equals 3.87).

The bony labyrinth of the ancestor of Cetartiodactyla was similar to that reconstructed for the ancestor of Ungulata. The lateral semicircular canal opened into the vestibule directly in absence of a secondary common crus, the arc of the anterior semicircular canal was the largest among the three, the lateral semicircular canal was positioned high compared to the posterior canal, and the aspect ratio of the cochlea was low. The cochlea of Cetartiodactyla coiled to a lesser degree than Ungulata (845.8°

versus 857.4°), but the cochlear canal contributed a greater percentage to the overall labyrinthine volume (59% versus 55%).

The labyrinths of the two terrestrial cetartiodactyls retain the ancestral cetartiodactyl condition of the anterior canal possessing the largest arc radius. The cochlea of *Bathygenys* is flattened (low aspect ratio), which is the ancestral condition, although the cochlea of *Sus* has a high profile. Both labyrinths retain the ancestral cetartiodactyl condition of the high position of the lateral semicircular canal as compared to the posterior canal, and a vestibular entrance of the lateral canal, rather than formation of a secondary common crus.

Although the cladogram presented in Figure 5.2 (modified from the supertree of Bininda-Emonds et al., 2007, with additional cetartiodactyl information from Theodor et al., 2005) depicts a closer relationship between *Sus* and Cetacea, there are no unambiguous otic synapomorphies supporting this relationship. Both *Sus* and *Bathygenys* share a high position of the lateral semicircular canal that is absent in Cetaceans (discussed in the following section), but this state was ancestral for crown Placentalia as a whole. Nonetheless, the most recent common ancestor of *Sus* and Cetacea possessed a bony labyrinth with the lateral semicircular canal opening directly into the vestibule, the anterior semicircular canal arc with the largest radius among the three canals, a high position of the lateral semicircular canal compared to the posterior canal, and a low aspect ratio of the cochlea in profile. The ancestral cochlear coiling of *Sus* and Cetacea was 1013.1°, and the contribution of the cochlea to the entire labyrinth is 67.0%.

Cetacea

With the exception of Sirenia (the bony labyrinth of which was described above in the Afrotheria section), cetaceans are the only fully aquatic extant mammals. Two

major cetacean clades recognized are the baleen whales, or Mysticeti, which includes the largest living mammal (*Balaenoptera musculus*), and the toothed whales, Odontoceti, which includes porpoises and dolphins such as *Tursiops truncatus*. The bony labyrinth of the bottlenose dolphin *Tursiops* is described, along with the labyrinth of a fossil member of Balaenopteridae (Mysticeti).

The bony labyrinth of the extinct balaenopterid (Figures 5.28-5.29) is larger than that of *Tursiops* (Figures 5.30-5.31). The anterior-posterior length of the mysticete inner ear is 19.67 mm (*Tursiops* equals 10.01 mm), and the gross volume of the inner ear cavities of the mysticete is 1075.51 mm^3 (*Tursiops* equals 167.98 mm^3). The greater dimensions of the mysticete labyrinth likely reflects body size differences between balaenopterids and *Tursiops*, with the average body mass of most mysticete species being several orders of magnitude greater than that of the bottlenose dolphin (Silva and Downing, 1995). Average body mass for *Tursiops* is 179.5 kg, whereas the smallest extant balaenopterid is 4,000 kg (*Balaenoptera acutorostrata*; Silva and Downing, 1995).

The cochlea of the balaenopterid is larger than *Tursiops* in all dimensions, including volume (973.91 mm^3 versus 157.11 mm^3), cochlear canal length (53.02 mm versus 24.01 mm), degree of coiling (886° versus 661°), and even aspect ratio, although to a lesser extent (0.48 versus 0.47). The volumetric contribution of the cochlea of towards the total inner ear volume is greater for *Tursiops* (93.5%) than for the balaenopterid (90.6%), although the value for the balaenopterid is exceptionally high. The significant contribution of the total volume by the cochlea is higher for the two cetacean taxa than any other mammal investigated here, including the afrotherians *Chrysochloris, Macroscelides*, and *Trichechus* (each with a cochlear contribution around 71-72%). The other extreme is the cochlea of the elephantoid, which only contributes 30.6% of the total volume of the bony labyrinth.

FIGURE 5.28. Bony labyrinth of fossil Balaenopteridae. **A**, stereopair and labeled line drawing of digital endocast in anterior view; **B**, stereopair and labeled line drawing of digital endocast in dorsal view; **C**, stereopair and labeled line drawing of digital endocast in lateral view; **D**, line drawing of cochlea viewed down axis of rotation to display degree of coiling; **E**, line drawing of cochlea in profile. Abbreviations: **aa**, anterior ampulla; **ac**, anterior semicircular canal; **ant**, anterior direction; **cc**, canaliculus cochleae for aqueduct of cochlea; **co**, cochlea; **cr**, common crus; **dor**, dorsal direction; **fc**, fenestra cochleae; **fv**, fenestra vestibuli; **la**, lateral ampulla; **lc**, lateral semicircular canal; **med**, medial direction; **pa**, posterior ampulla; **pc**, posterior semicircular canal; **pl**, primary bony lamina; **pos**, posterior direction; **ps**, outpocketing for perilymphatic sac; **sl**, secondary bony lamina; **sr**, spherical recess of vestibule.

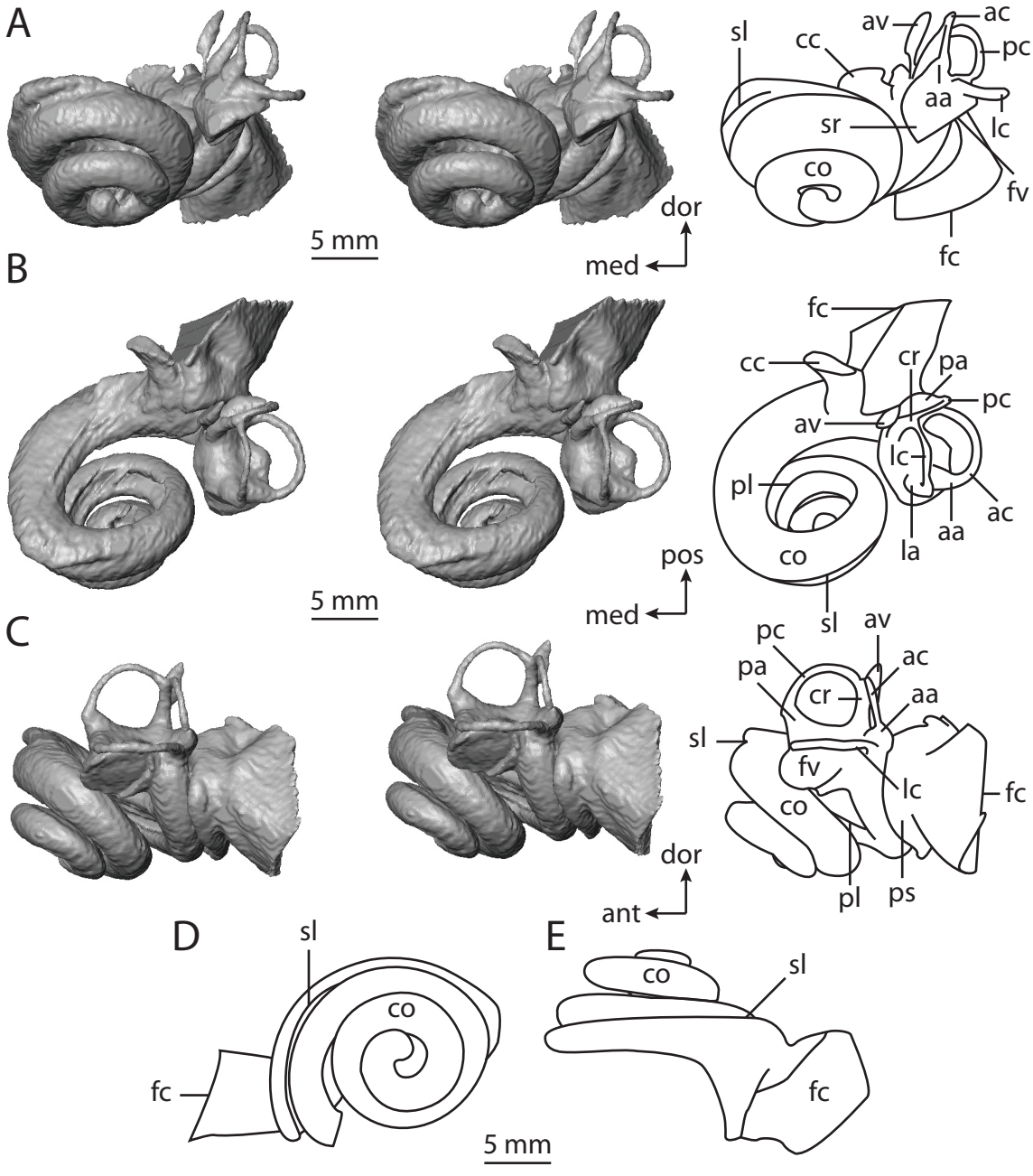
A
sl
cc
av
ac
pc
aa
sr
lc
co
fv
fc
5 mm
dor
med
B
fc
cc
cr
pa
pc
av
lc
pl
ac
aa
la
co
sl
5 mm
pos
med
C
pc
sl
av
pa
ac
cr
aa
sl
fv
lc
fc
co
pl
ps
dor
ant
D
sl
co
fc
5 mm
E
co
sl
fc

FIGURE 5.29. CT slices through ear region of fossil Balaenopteridae. Abbreviations: **aa**, anterior ampulla; **ac**, anterior semicircular canal; **av**, bony channel for aqueduct of vestibule; **cc**, canaliculus cochleae; **cf**, foramina within cribriform plate; **cn**, canal for cranial nerve VIII; **co**, cochlea; **dor**, dorsal direction; **fc**, fenestra cochleae; **fn**, canal for cranial nerve VII; **la**, lateral ampulla; **lc**, lateral semicircular canal; **med**, medial direction; **pa**, posterior ampulla; **pc**, posterior semicircular canal; **pl**, primary bony lamina; **pos**, posterior direction; **sg**, canal for spiral ganglion within primary bony lamina; **sl**, secondary bony lamina; **st**, stapes within fenestra vestibuli; **vb**, vestibule; **vn**, canal for vestibular branch of cranial nerve VIII.

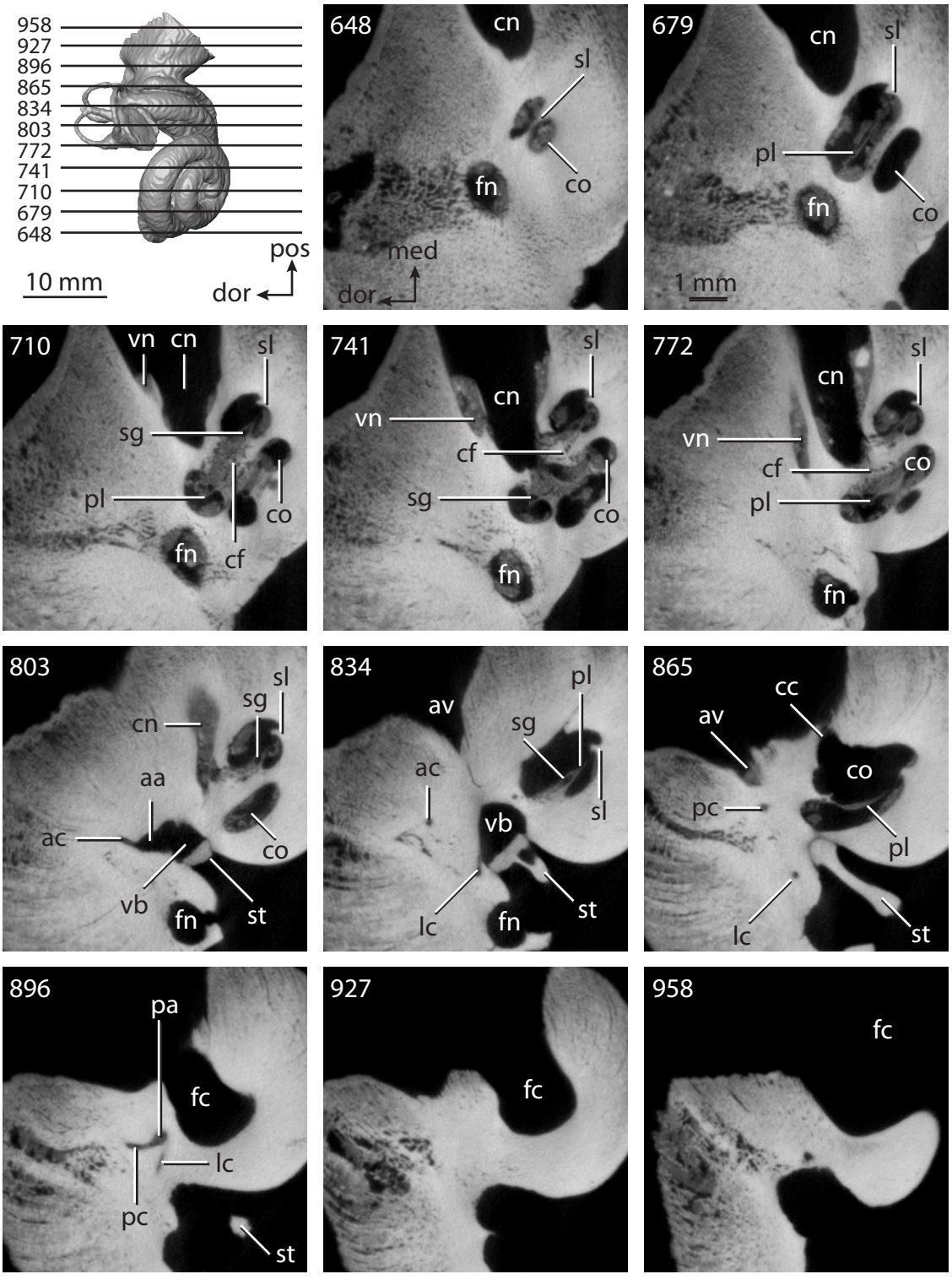
958
927
896
865
834
803
772
741
710
679
648
10 mm
pos
dor
648
cn
sl
fn
co
med
dor
679
cn
sl
pl
fn
co
1 mm
710
vn
cn
sl
sg
pl
co
fn
cf
741
sl
cn
vn
cf
sg
co
fn
772
sl
cn
vn
cf
co
pl
fn
803
sl
sg
cn
aa
ac
co
vb
fn
st
834
pl
av
sg
ac
sl
vb
lc
fn
st
865
cc
av
co
pc
pl
lc
st
896
pa
fc
lc
pc
st
927
fc
958
fc

FIGURE 5.30. Bony labyrinth of *Tursiops truncatus*. **A**, stereopair and labeled line drawing of digital endocast in anterior view; **B**, stereopair and labeled line drawing of digital endocast in dorsal view; **C**, stereopair and labeled line drawing of digital endocast in lateral view; **D**, line drawing of cochlea viewed down axis of rotation to display degree of coiling; **E**, line drawing of cochlea in profile. Abbreviations: **aa**, anterior ampulla; **ac**, anterior semicircular canal; **ant**, anterior direction; **cc**, canaliculus cochleae for aqueduct of cochlea; **co**, cochlea; **cr**, common crus; **dor**, dorsal direction; **fc**, fenestra cochleae; **fv**, fenestra vestibuli; **la**, lateral ampulla; **lc**, lateral semicircular canal; **med**, medial direction; **pa**, posterior ampulla; **pc**, posterior semicircular canal; **pl**, primary bony lamina; **pos**, posterior direction; **ps**, outpocketing for perilymphatic sac; **sl**, secondary bony lamina.

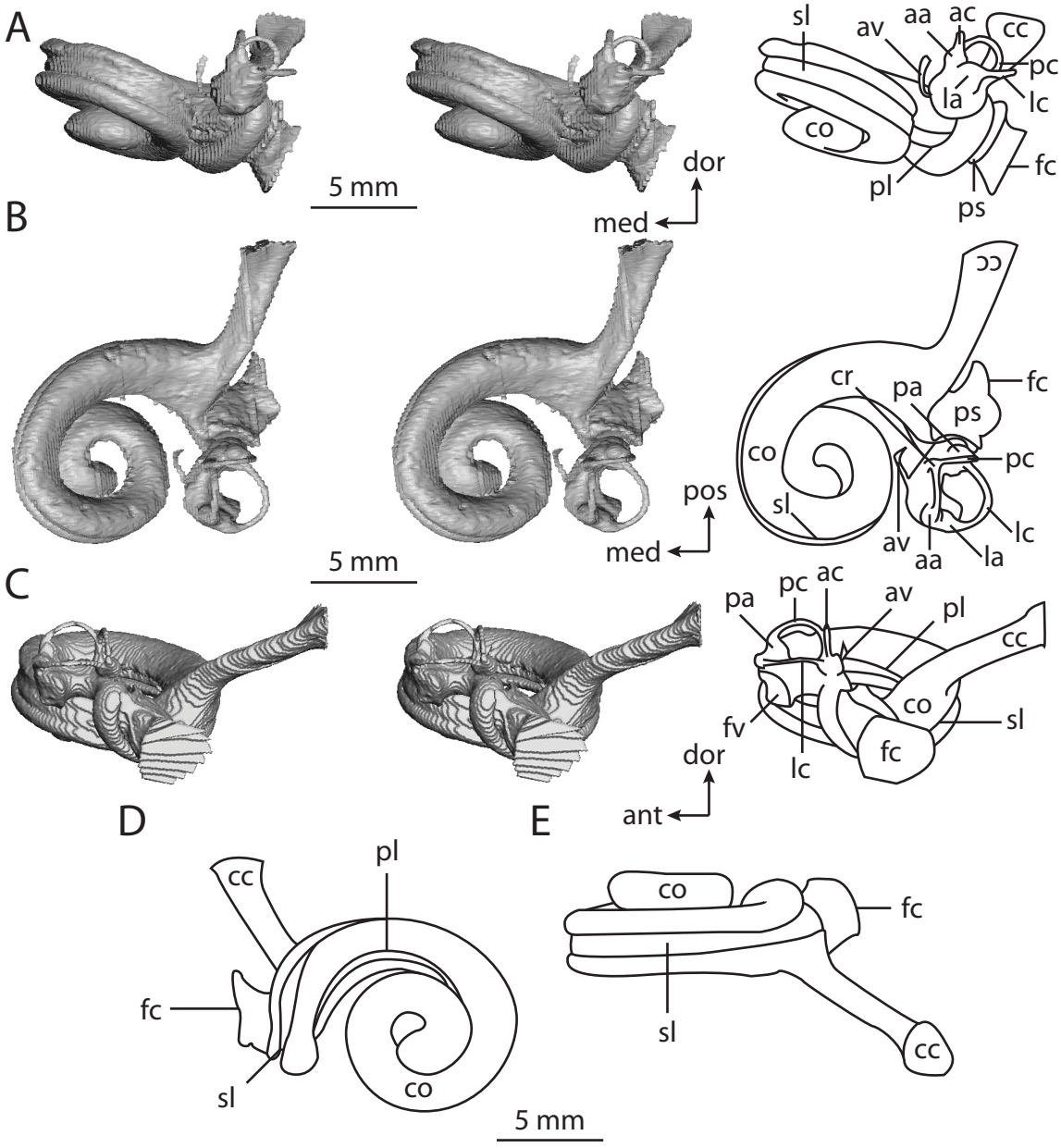
A
B
C
D
E
5 mm
5 mm
5 mm
dor
med
pos
med
dor
ant
sl
av
aa
ac
cc
pc
la
lc
co
fc
pl
ps
cr
pa
ps
pa
pc
ac
av
pl
cc
fv
co
sl
lc
fc
cc
pl
fc
sl
co
co
fc
sl
cc

FIGURE 5.31. CT slices through ear region of *Tursiops truncatus*. Abbreviations: **ac**, anterior semicircular canal; **ant**, anterior direction; **av**, bony channel for aqueduct of vestibule; **cf**, foramina within cribriform plate; **cn**, canal for cranial nerve VIII; **co**, cochlea; **dor**, dorsal direction; **fn**, canal for cranial nerve VII; **iam**, internal auditory meatus; **la**, lateral ampulla; **lat**, lateral direction; **lc**, lateral semicircular canal; **med**, medial direction; **pl**, primary bony lamina; **sg**, canal for spiral ganglion within primary bony lamina; **sl**, secondary bony lamina; **st**, stapes within fenestra vestibuli; **vb**, vestibule.

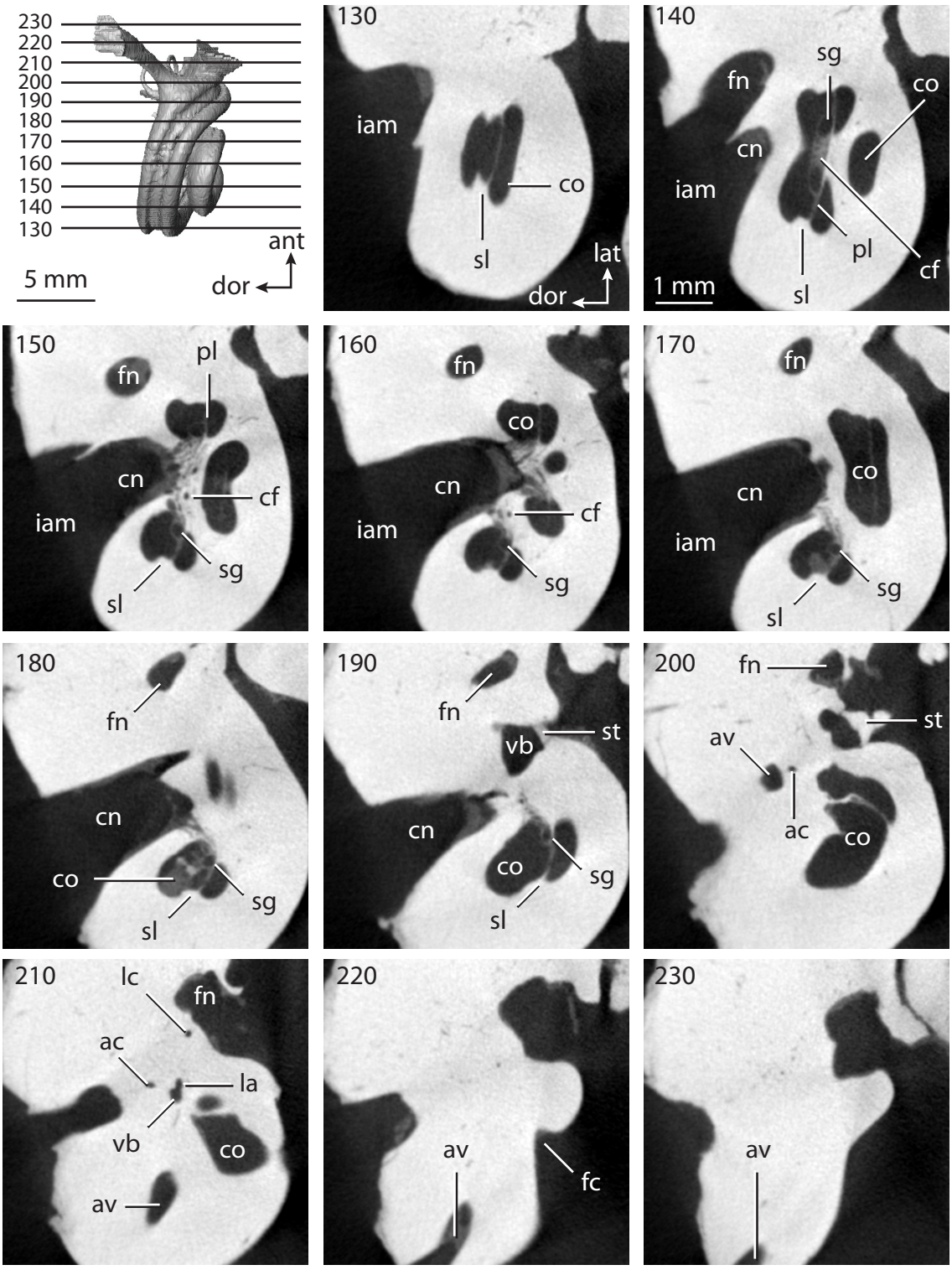
230
220
210
200
190
180
170
160
150
140
130
ant
5 mm
dor
130
iam
co
sl
lat
dor
140
sg
fn
co
cn
iam
pl
cf
sl
1 mm
150
pl
fn
cn
cf
iam
sg
sl
160
fn
co
cn
cf
iam
sg
170
fn
co
cn
iam
sg
sl
180
fn
cn
co
sg
sl
190
fn
st
vb
cn
co
sg
sl
200
fn
st
av
ac
co
210
lc
fn
ac
la
vb
co
av
220
av
fc
230
av

As is evident with the aspect ratios reported above, the cochleae of both cetaceans are planispiral, and the apical turns of the cochlea are smaller in diameter than the basal whorl. A well-developed secondary bony lamina is present in both labyrinths (Figures 5.29, 5.31), extending from a point anterior to the fenestra cochleae for a considerable distance along the radial wall of the cochlear canal. The secondary lamina, which is expressed as a distinct groove on the endocast, is present for around two thirds of the basal turn (238°) in the balaenopterid, but it persists for a short distance beyond the basal turn in *Tursiops* (396°).

An anteriorly oriented excavation of the cochlea (expressed as a flange on the endocast) is immediately basal to the apical terminus of the secondary bony lamina in the balaenopterid. A similar structure is observed in the reconstruction of the inner ear of the extinct mysticete *Herpetocetus* (Geisler and Luo, 1996), and it might be characteristic of the Mysticeti. Such an extension of the cochlea is not observed in *Tursiops* or any other mammal studied here. The anterior excavation is distinct, but it is not deep enough to give the cochlea an elliptical outline when viewed vestibularly.

The bony canaliculus for the aqueduct of the cochlea is significantly longer in *Tursiops* (6.47 mm) than in the balaenopterid (3.83 mm). The canaliculus of *Tursiops* is roughly triangular in cross-section, whereas the bony passage is flattened. The scala tympani is not inflated near the proximal end of the canaliculus cochleae posterior to the fenestra cochleae in *Tursiops*, but a groove (expressed as a ridge on the endocast) extends from the canaliculus cochleae for a short distance on the tympanal surface of the cochlea in the balaenopterid. The angle between the planes of the basal turn of the cochlea and lateral semicircular canal for the balaenopterid (23.2°) and *Tursiops* (21.3°) are similar to the angles measured for the terrestrial cetartiodactyls *Bathygenys* (26.8°) and *Sus* (23.8°).

The fenestra vestibuli is separated from the fenestra cochleae by a great distance in both cetacean taxa. This likely is the result of a flexure near the junction of the cochlea and vestibule. This cochlear hook is a common feature in the inner ear of cetaceans, primarily odontocetes (Fleischer, 1976; Luo and Eastman, 1995; Luo and Marsh, 1996). The stapedial ratios, as calculated from the fenestra vestibuli, are more circular in both cetacean taxa (1.52 for the balaenopterid; 1.44 for *Tursiops*) than the ratios calculated for other placental mammals.

The entire vestibular apparatus of the cetacean bony labyrinth is significantly smaller than that of other taxa. This is expressed not only in the imagery of the endocasts, but also in the volumetric measurements (cochlea of *Tursiops* contributes around 93% of the volume, so vestibular apparatus contributes 7%). The vestibule of *Tursiops* is bowed medially with the fenestra vestibuli opening through an anterior excavation of the cavity. The vestibule is not curved in the balaenopterid, and the spherical recess is small and is distinguished from the elliptical recess by a gentle constriction behind the fenestra vestibuli. A similar constriction is observed in *Tursiops*, but the connection between the anterior aspect of the spherical recess and the cochlea is not distinguishable.

An extension of the elliptical recess adjacent to the constriction between the vestibular compartments leads to the lateral and posterior ampulla. The posterior limb of the lateral semicircular canals of both cetacean taxa do not have separate openings into the vestibule. Rather, the lateral canal empties into the posterior ampulla just above the vestibular aperture of the ampulla (a secondary common crus is not present in either taxon). The bony channel for the aqueduct of the vestibule exits the bony labyrinth near the medial edge of the vestibular aperture of the common crus in the balaenopterid. The passage in this taxon is expressed as fine thread that extends 3.65 mm to the endocranial aperture of the aqueduct. The vestibular aperture for the channel for the aqueduct of the

vestibule of *Tursiops* is separated from the common crus by a relatively greater distance than it is in the balaenopterid. In medial view, the massive cochlea shields the channel in *Tursiops*, but is best observed when the bony labyrinth is oriented dorsally.

The angle between the planes of the anterior and posterior semicircular canals is obtuse in both *Tursiops* (97.6°) and the balaenopterid (105°), but the remaining canal plane angles are acute. The lowest angles for each cetacean were measured between the anterior and lateral canals (balaenopterid equals 71.6°; *Tursiops* equals 75°). Overall, the semicircular canals of *Tursiops* fit onto single planes (the anterior and posterior canals are planar). The only canal of *Tursiops* that does not fit onto a single plane, the lateral semicircular canal, deviates from its plane by a total of 8.86°, although this degree is not significant (ratio of total linear deviation over cross-sectional diameter is 0.85). The angular deviations of the anterior (9.0°) and posterior (15.9°) semicircular canals of the balaenopterid are significant (ratio of anterior is 1.27; posterior is 1.56), but the lateral semicircular canal of the balaenopterid deviates from its plane by 5.4°, which is not significant (ratio is 0.39).

An identical pattern is observed between the balaenopterid and *Tursiops* when the semicircular canal arc radii are compared. The radius of the anterior canal arc is the largest in both taxa (2.45 mm in the balaenopterid; 1.19 mm in *Tursiops*), and the radius of the posterior arc is the smallest (1.92 mm in the balaenopterid; 0.84 mm in *Tursiops*). The radius of curvature of the lateral semicircular canal arc is 2.11 mm in the balaenopterid and 1.36 mm in *Tursiops*. A common pattern is not observed in any of the other dimensions of the semicircular canals. The slender canal length of the anterior semicircular canal of the balaenopterid is the greatest (10.65 mm; lateral equals 8.54 mm; posterior equals 9.46 mm), although the lateral canal is the longest in *Tursiops* (4.61 mm; anterior equals 4.14 mm; posterior equals 4.35 mm). The diameter of the lumen is

greatest in the lateral semicircular canal in the balaenopterid (0.51 mm; anterior equals 0.32 mm; posterior equals 0.34 mm), whereas the diameters of the anterior and posterior canals are equal (0.27 mm) and larger than the value taken for the lateral canal (0.25 mm) in *Tursiops*.

The aspect ratio of the posterior semicircular canal is greatest in both *Tursiops* (1.60) and the balaenopterid (1.21). The aspect ratio of the lateral semicircular canal is the smallest in the balaenopterid (0.39; anterior equals 0.91), and the ratio of the of the anterior canal is the smallest in *Tursiops* (0.95), although it is not much different than that of the lateral canal (0.96). The largest ratio between the length of any slender canal and arc radius of curvature among the cetaceans examined was calculated for the posterior semicircular canal of *Tursiops* (5.17). The ratio calculated for the posterior canal of the balaenopterid was the largest among the three canals in this specimen as well (4.94). Although the ratio calculated for the posterior canal of *Tursiops* was larger than that of the balaenopterid, the ratios for the anterior (4.19) and lateral (4.05) semicircular canals were larger than those calculated for *Tursiops* (3.47 and 3.38 respectively).

The bony labyrinth of the ancestral cetacean lacked a secondary common crus formed between the lateral and posterior semicircular canal, as did the ancestor of Cetartiodactyla, but the cetacean labyrinth was derived from the ancestral cetartiodactyl condition in that the lateral canal opened into the posterior ampulla, rather than into the vestibule directly. Although this state is a synapomorphy for Cetacea within Cetartiodactyla, the lateral canal also opens into the posterior ampulla in Perissodactyla, Scandentia, some Carnivora, and some Chiroptera (see below). A second otic synapomorphy that separates Cetacea from the terrestrial cetartiodactyls is a low position of the plane of the lateral semicircular canal compared to the ampullar entrance of the

posterior semicircular canal. The state is derived with respect to the ancestral cetartiodactyl condition, and it is a reversal to the ancestral therian state.

Additional states reconstructed for the ancestor of Cetacea include the anterior semicircular canal arc as the greatest among the three arcs, and a low aspect ratio for the cochlear spiral in profile. The coiling of the cochlea of the ancestral cetacean (853.4°) was retained from the ungulate ancestor (857.4°), but the contribution of the ancestral cetacean cochlea to the total labyrinthine volume was greater than that calculated for Ungulata (84.0% versus 55.0%). The high contribution of the cochlea to the total volume distinguishes Cetacea from other members of Cetartiodactyla.

Perissodactyla

The odd-toed ungulates that make up extant Perissodactyla are divided into Equidae (horses), Tapiridae (tapirs), and Rhinocerotidae (rhinoceroses). Monophyly of Perissodactyla is well supported (Gregory, 1910; Simpson, 1945; McKenna and Bell, 1997; Cao et al., 1999; Norman and Ashley, 2000; Bininda-Emonds et al., 2007), as is a sister taxon relationship between Tapiridae and Rhinocerotidae within the group (Radinsky, 1964; Cao et al., 1999; Norman and Ashley, 2000; Murphy et al., 2001a, b; Hooker, 2005; Bininda-Emonds et al., 2007). Only the modern horse, *Equus caballus*, was available for examination. Imagery of the inner ear and an endocast of the bony labyrinth is presented in Figures 5.32-5.33.

The total volume of the inner ear cavities of *Equus* (165.16 mm^3) is similar to that of the dolphin, *Tursiops truncatus* (167.98 mm^3). This is also reflected in the length of the skull, where the skull of *Equus* (530.00 mm) is slightly shorter than that of *Tursiops* (543.02 mm). However, the total length of the inner ear is larger in *Equus* (16.52 mm)

FIGURE 5.32. Bony labyrinth of *Equus caballus*. **A**, stereopair and labeled line drawing of digital endocast in anterior view; **B**, stereopair and labeled line drawing of digital endocast in dorsal view; **C**, stereopair and labeled line drawing of digital endocast in lateral view; **D**, line drawing of cochlea viewed down axis of rotation to display degree of coiling; **E**, line drawing of cochlea in profile. Abbreviations: **aa**, anterior ampulla; **ac**, anterior semicircular canal; **ant**, anterior direction; **av**, bony channel for aqueduct of vestibule; **cc**, canaliculus cochleae for aqueduct of cochlea; **co**, cochlea; **cr**, common crus; **cv**, canal for cochlear vein; **dor**, dorsal direction; **er**, elliptical recess of vestibule; **fc**, fenestra cochleae; **fv**, fenestra vestibuli; **la**, lateral ampulla; **lc**, lateral semicircular canal; **med**, medial direction; **pa**, posterior ampulla; **pc**, posterior semicircular canal; **pl**, primary bony lamina; **pos**, posterior direction; **ps**, outpocketing for perilymphatic sac; **sr**, spherical recess of vestibule.

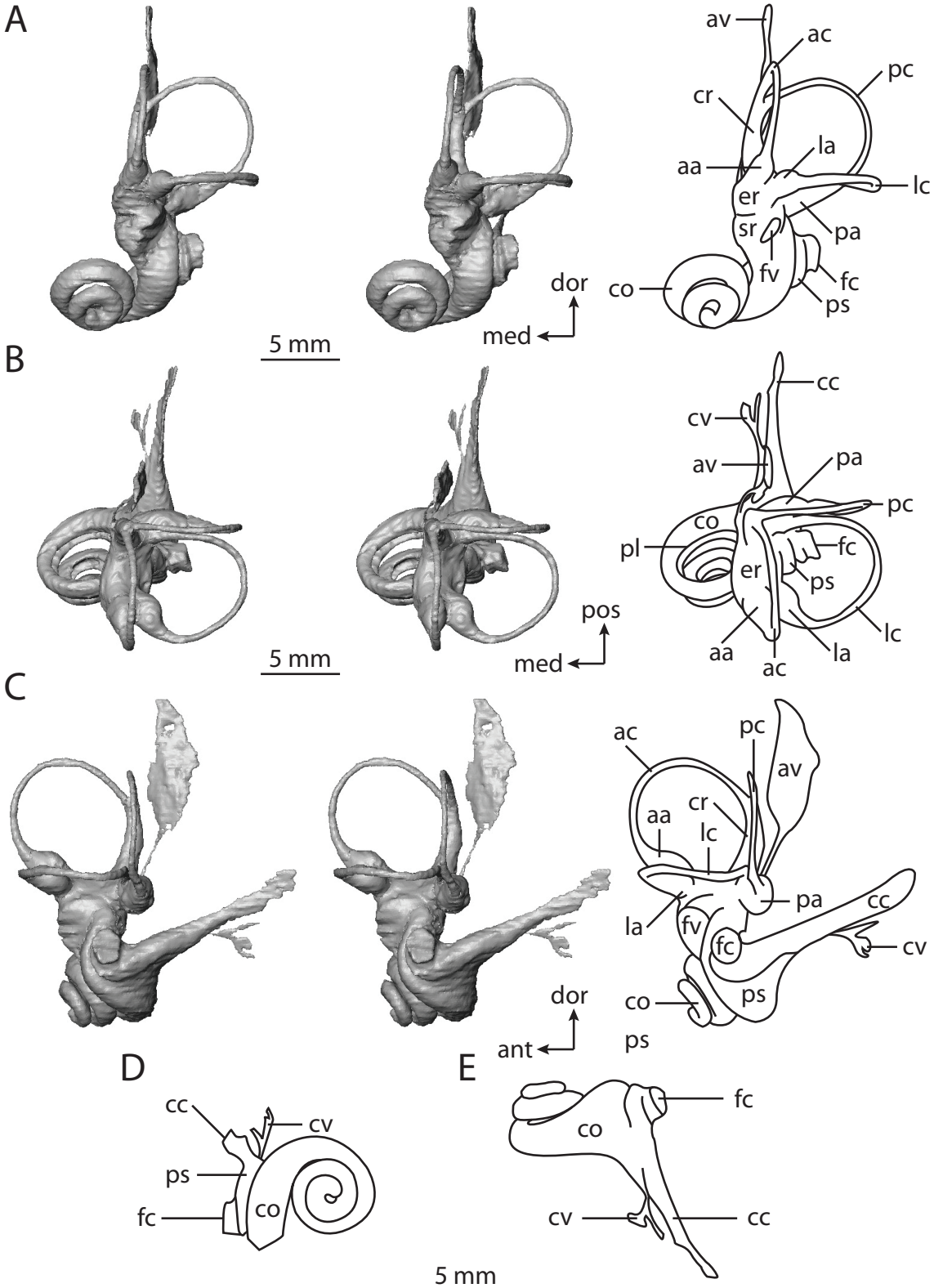
A
av
ac
pc
cr
la
aa
lc
er
sr
pa
fv
fc
co
ps
dor
med
5 mm
B
cc
cv
av
pa
pc
co
pl
fc
er
ps
lc
aa
ac
la
pos
med
5 mm
C
ac
pc
av
cr
aa
lc
pa
cc
la
fv
fc
cv
co
ps
ps
dor
ant
D
cc
cv
ps
fc
co
E
fc
co
cv
cc
5 mm

FIGURE 5.33. CT slices through ear region of *Equus caballus*. Abbreviations: **ac**, anterior semicircular canal; **av**, bony channel for aqueduct of vestibule; **cc**, canaliculus cochleae for aqueduct of cochlea; **cn**, canal for cranial nerve VIII; **co**, cochlea; **cr**, common crus; **dor**, dorsal direction; **er**, elliptical recess of vestibule; **fc**, fenestra cochleae; **fn**, canal for cranial nerve VII; **fv**, fenestra vestibuli; iam, internal auditory meatus; **la**, lateral ampulla; **lc**, lateral semicircular canal; **med**, medial direction; **pa**, posterior ampulla; **pc**, posterior semicircular canal; **pl**, primary bony lamina; **pos**, posterior direction; **ps**, outpocketing for perilymphatic sac; **st**, stapes that has fallen into vestibule; **vb**, vestibule; **vn**, canal for vestibular branch of cranial nerve VIII.

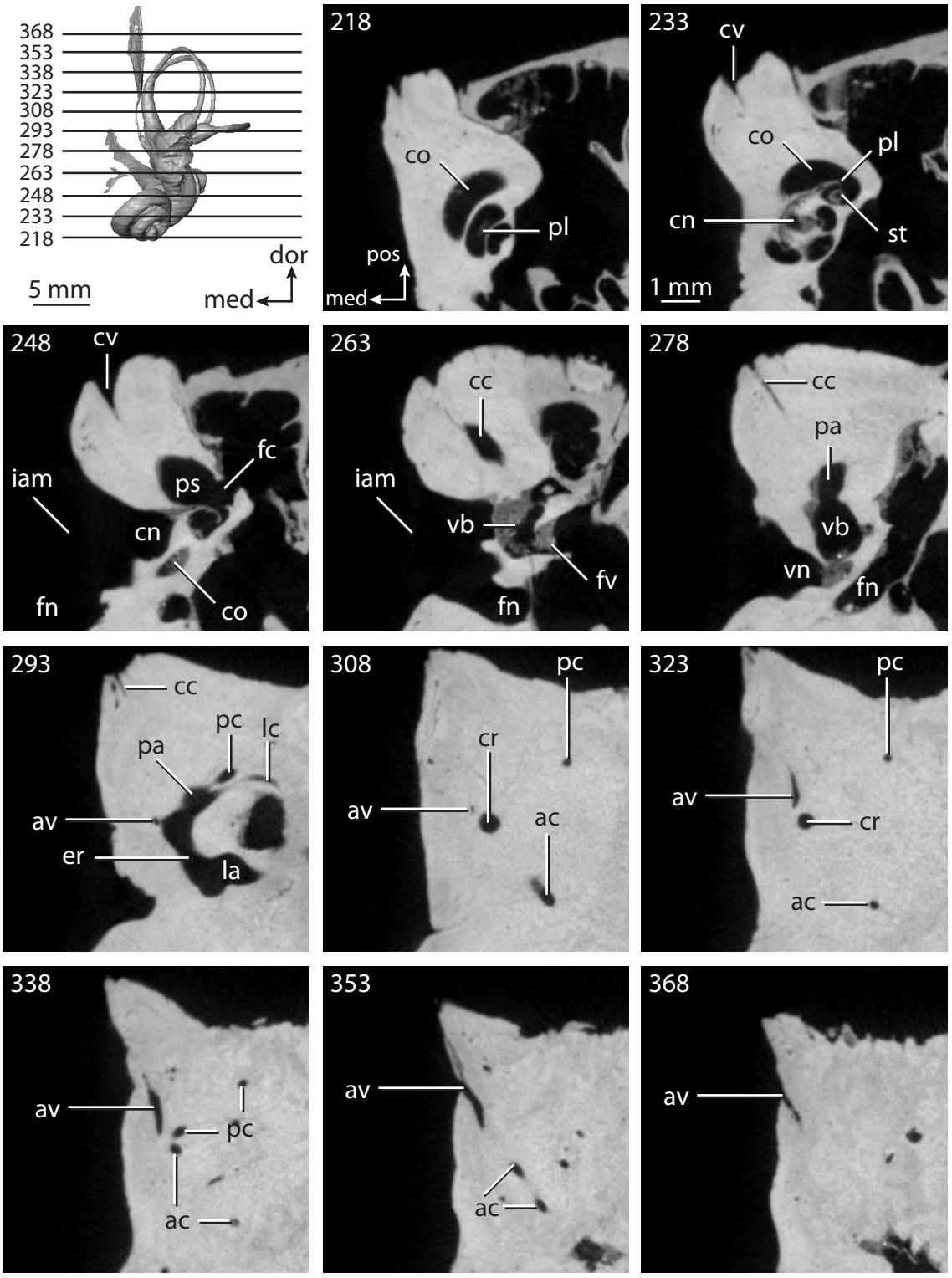
368
353
338
323
308
293
278
263
248
233
218
5 mm
dor
med
218
co
pl
pos
med
233
cv
co
pl
cn
st
1 mm
248
cv
fc
iam
ps
cn
co
fn
263
cc
iam
vb
fv
fn
278
cc
pa
vb
vn
fn
293
cc
pc
lc
pa
av
er
la
308
pc
cr
av
ac
323
pc
av
cr
ac
338
av
pc
ac
353
av
ac
368
av

than it is in *Tursiops*, and the horse has a greater average body mass (258.3 kg versus 179.5 kg; Silva and Downing, 1995).

Although the total volume of the bony labyrinth of *Equus* is similar to that in *Tursiops*, the cochlea of the horse is only half the volume of the cochlea of the dolphin (84.33 mm^3 versus 157.11 mm^3). Because of this, the cochlea's total volumetric contribution of *Equus* (51.1%) is significantly less than that of *Tursiops* (93.5%), but rather is more in line with the percentage calculated for the terrestrial cetartiodactyl *Bathygenys reevesi* (54.2%).

Each turn of the cochlea, of which there are two and a half (900°), is separated from the adjacent whorls (Figure 5.32). The cochlea of *Equus* has an aspect ratio of 0.41, which is similar to that calculated for the elephantoid (0.42) and *Orycteropus afer* (0.45).

The total length of the cochlear canal of *Equus* is 22.08 mm. This value is similar to that measured in the cochlea of *Sus* (22.89 mm), and even *Tursiops* (24.01 mm), despite the fact that the volume of the cochlea of the horse falls in between the dolphin (157.11 mm^3) and pig (36.25 mm^3).

A bony secondary lamina, which extends around two fifths of the basal turn (153°), is observed in *Equus* (Figure 5.33). The scala tympani is expanded into a wedge shaped excavation leading to the straight canaliculus cochleae for the aqueduct of the cochlea posterior to the fenestra cochleae. The canaliculus narrows towards its terminus, and flattens into a fissure near its external aperture, although it retains robusticity along its course. The bony passage is 11.33 mm in length, which is the longest canaliculus measured for any taxon described here (Table 5.3). A short and delicate secondary passage, likely for a vein, exits the medial side of the canaliculus near the midpoint of the bony channel for the aqueduct.

The angle between the planes of the basal turn of the cochlea and the lateral semicircular canal in *Equus* is 37.9°, and the stapedial ratio, measured from dimensions of the fenestra vestibuli, is 1.7. The spherical and elliptical recesses are separated by a constriction of the vestibule ventral to the ampullae of the semicircular canals. The constriction forms a bony ring (expressed as a wide sulcus on the endocast) surrounding the vestibule. The bony ring sits on a plane that nearly is parallel with that of the lateral semicircular canal. The elliptical recess is elongate, and it slightly bows medially, away from the arc of the lateral semicircular canal.

The anterior and lateral ampullae open into a slight excavation at the anterior end of the elliptical recess. At the posterior end of the recess, the posterior limb of the lateral semicircular canal opens into the posterior ampulla, immediately anterolateral to the vestibular aperture of the ampulla. Because of this, the lateral semicircular canal does not have its own opening into the vestibule (also observed in both cetaceans, *Hemicentetes*, and other taxa, including the tree shrew, some carnivorans, and some bats, as described below). Additionally, the plane of the canal is high relative to other vestibular constituents. The elevated lateral semicircular canal divides the space enclosed by the posterior semicircular canal arc when the endocast of the bony labyrinth is viewed posteriorly, and the sagittal labyrinthine index of *Equus* is 10.50. This is the smallest index calculated for any mammal described thus far in the paper, in which the plane of the lateral canal takes a high position.

A groove (expressed on the endocast as a low ridge) extends from the dorsomedial edge of the spherical recess to the vestibular aperture of the bony channel for the aqueduct of the vestibule, which is situated ventral and medial to the vestibular aperture of the common crus. The channel is developed as a very delicate thread for half of its length in *Equus*, extending posteriorly and crossing the base of the common crus

when the endocast of the bony labyrinth is viewed medially. The distal half of the channel is broad and flattened, indicating that the aqueduct enters a fissure before exiting on the endocranial surface of the petrosal. The total length of the bony channel for the aqueduct of the vestibule is 11.66 mm, which is a bit larger than the length of the canaliculus cochleae (11.33 mm).

The planes of the posterior and lateral semicircular canals of *Equus* roughly form a right angle with one another (90.1°), and the angle between the planes of the posterior and anterior canals only is slightly obtuse (93.3°). The angle between the anterior and lateral semicircular canal planes is 84.7°. The semicircular canals themselves are fairly planar, especially the anterior canal, which deviates from an average plane by a total of 2.22° (the total angular deviation of the lateral and posterior canals for their planes are 4.68° and 5.74° respectively). The degree of deviation is not significant for any canal, where the ratios of total linear deviation over cross-sectional diameter of the canal for the anterior, lateral, and posterior canals are 0.27, 0.64, and 0.70 respectively.

Both the slender canal length (18.63 mm) and radius of canal arc (3.83 mm) of the posterior semicircular canal are the greatest among these dimensions measured for the three canals of *Equus*. The lateral semicircular canal exhibited the smallest value of these two dimensions, where the slender canal length is 14.28 mm (versus 17.35 mm for the anterior) and the arc radius is 3.55 mm (versus 3.62 mm for the anterior). The largest canal lumen diameter in cross-section was measured for the anterior semicircular canal (0.51 mm; lateral equals 0.45 mm; posterior 0.50 mm), and the largest volume was measured for the lateral semicircular canal (2.57 mm^3; anterior equals 2.19 mm^3; posterior equals 2.32 mm^3).

The aspect ratios of the anterior and lateral semicircular canal arcs are similar (0.95 and 0.96 respectively), and both are lower than the aspect ratio of the posterior

canal (1.60). The high aspect ratio of the posterior semicircular canal indicates that the height of the canal arc is greater than the width. The greatest ratio of slender canal length to arc radius was calculated for the posterior semicircular canal (5.17), and the ratio for the anterior (3.46) and lateral (3.38) semicircular canals are not significantly different.

The cochlear spiral of *Equus* possesses the ancestral ungulate state of a low aspect ratio, giving the cochlea a flattened appearance. The pattern of semicircular canal arc radii in *Equus*, with the largest radius being the anterior, is inherited from its boreoeutherian ancestor, although the entry of the lateral semicircular canal into the posterior ampulla is derived and shared with Cetacea. The high position of the lateral semicircular canal with respect to the ampullar opening of the posterior canal is retained from the ancestor of Boreoeutheria.

Carnivora

Extant carnivorans belong to two phylogenetically distinct clades, Caniformia (dogs, bears, raccoons, weasels, and pinnipeds) and Feliformia (cats, hyenas, mongooses, and viverrids). Monophyly of Pinnipedia (within Caniformia) has been questioned in the past (McLaren, 1960; Tedford, 1976), although most recent data are in support of a single origin for seals, sealions, and walruses (Wyss, 1987; Bininda-Emonds et al., 1999; Flynn and Wesley-Hunt, 2005; Bininda-Emonds et al., 2007). Most, if not all, carnivoran classifications include pinnipeds with dogs and dog-like animals (Simpson, 1945; McKenna and Bell, 1997; Flynn and Wesley-Hunt, 2005).

The carnivorans examined here include two common terrestrial species (*Canis familiaris* and *Felis catus*), as well as the aquatic Stellar sea lion, *Eumetopias jubatus* (Pinnipedia). The sea lion is a much larger animal, with an average body mass of 735 kg (Loughlin et al., 1987), than either the cat (3.4 kg; Silva and Downing, 1995) or dog

(upwards of 31 kg; Galvão, 1947). The number of CT slices obtained through the ear regions of *Felis* (627 slices) and *Eumetopias* (498 slices) are is significantly greater than the number obtained for *Canis* (92 slices). Because of this, the imagery through the ear region of *Canis* is of a lower resolution than that of *Felis* and *Eumetopias*, and minute features of the inner ear of the dog are not discernable (such as the bony channel for the aqueduct of the cochlea). The inner ear of *Canis* is imaged in Figures 5.34-5.35, the inner ear of *Eumetopias* is depicted in Figures 5.36-5.37, and that of *Felis* in Figures 5.38-5.39.

The total volume of the inner ear cavities of the *Canis* specimen used in this study (31.36 mm^3) is less than that computed for both the *Felis* (45.78 mm^3) and *Eumetopias* specimens (138.60 mm^3). In fact, the volume of the cochlea of the cat is 31.12 mm^3, which nearly is the volume of the bony labyrinth of the dog as a whole. The specimen of *Canis* used is from a small dog (a Chihuahua), which might explain the size difference. Even so, the percent of the total inner ear volume that is the cochlea is similar between the two terrestrial carnivorans, as the cochlea of *Felis* contributes 68.0% of the volume, and the cochlea of *Canis* contributes 66.1% (volume of cochlea equals 20.72 mm^3). The cochlea of *Eumetopias* contributes less to the labyrinth (53.5%; cochlear volume equals 74.17 mm^3). Similarly, the length of the inner ear cavity of the dog (8.10 mm) is not much different than that measured for the cat (8.91 mm) and the length of the bony labyrinth of *Eumetopias* is substantially greater (13.71 mm) than either of the other species.

The length of the cochlear canal in *Eumetopias* (19.25 mm) is greater than either the dog (13.85 mm) or the cat (16.76 mm), and the cochlea of the dog completes a greater degree of coiling (1155.6°) than the cat (1091.8°) and especially the sea lion (795.4°). A secondary bony lamina is observed extending along the radial wall of the cochlea in all three taxa, although the lamina persists for a greater relative distance in *Eumetopias*

FIGURE 5.34. Bony labyrinth of *Canis familiaris*. **A**, stereopair and labeled line drawing of digital endocast in anterior view; **B**, stereopair and labeled line drawing of digital endocast in dorsal view; **C**, stereopair and labeled line drawing of digital endocast in lateral view; **D**, line drawing of cochlea viewed down axis of rotation to display degree of coiling; **E**, line drawing of cochlea in profile. Abbreviations: **aa**, anterior ampulla; **ac**, anterior semicircular canal; **ant**, anterior direction; **cc**, canaliculus cochleae for aqueduct of cochlea; **co**, cochlea; **cr**, common crus; **dor**, dorsal direction; **er**, elliptical recess of vestibule; **fc**, fenestra cochleae; **fv**, fenestra vestibuli; **la**, lateral ampulla; **lc**, lateral semicircular canal; **med**, medial direction; **pa**, posterior ampulla; **pc**, posterior semicircular canal; **pl**, primary bony lamina; **pos**, posterior direction; **scr**, secondary common crus; **sl**, secondary bony labyrinth; **sr**, spherical recess of vestibule.

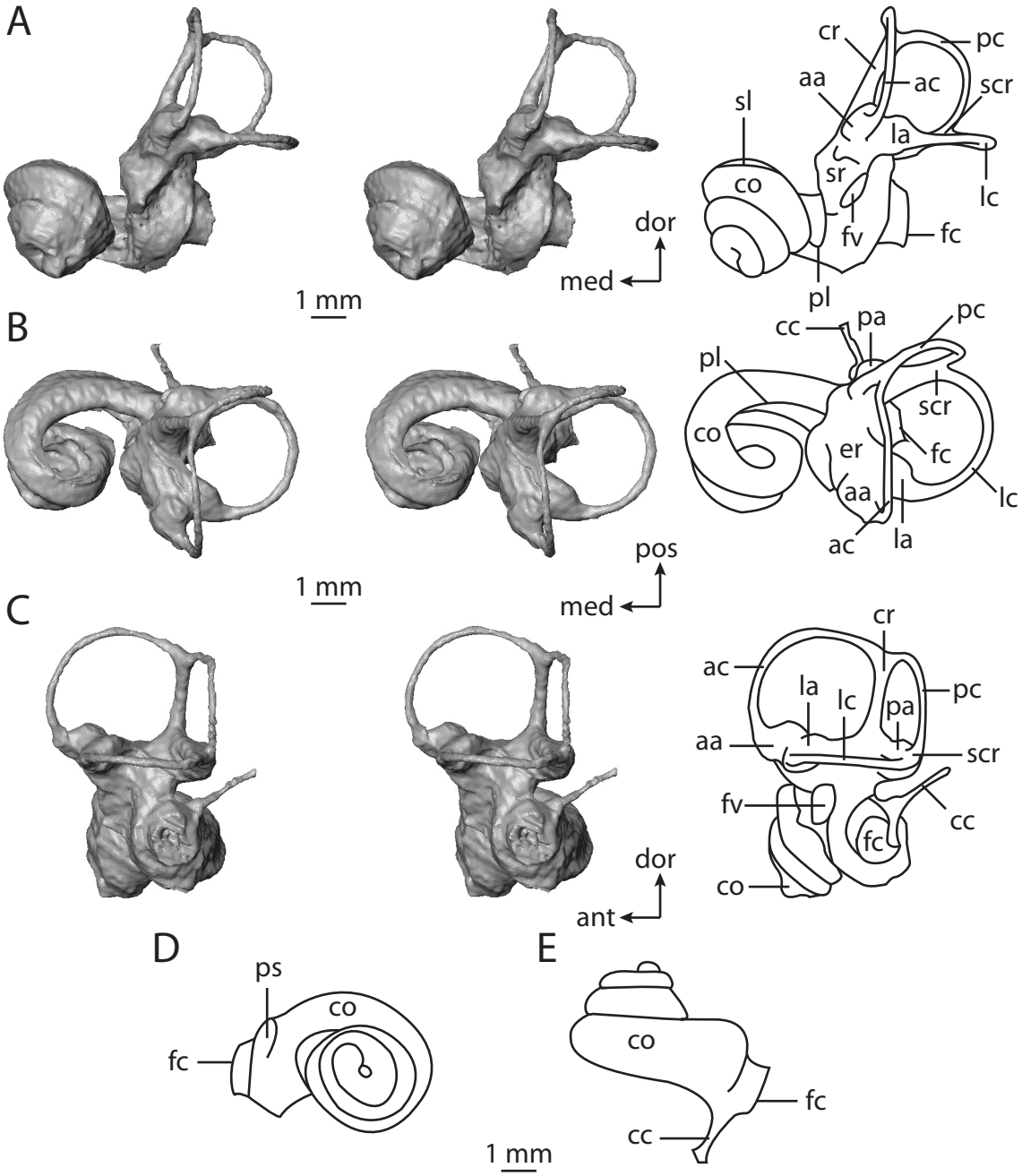
A
cr
pc
aa
ac
scr
sl
la
sr
co
lc
fv
fc
pl
dor
med
1 mm
B
cc
pa
pc
pl
scr
co
er
fc
aa
lc
ac
la
pos
med
1 mm
C
cr
ac
la
lc
pc
pa
aa
scr
fv
cc
fc
co
dor
ant
D
ps
co
fc
E
co
fc
cc
1 mm

FIGURE 5.35. CT slices through ear region of *Canis familiaris*. Abbreviations: **aa**, anterior ampulla; **ac**, anterior semicircular canal; **cc**, canaliculus cochleae for aqueduct of cochlea; **cn**, canal for cranial nerve VIII; **co**, cochlea; **cr**, common crus; **dor**, dorsal direction; **fc**, fenestra cochleae; **fn**, canal for cranial nerve VII; **fv**, fenestra vestibuli; **iam**, internal auditory meatus; **la**, lateral ampulla; **lat**, lateral direction; **lc**, lateral semicircular canal; **pa**, posterior ampulla; **pc**, posterior semicircular canal; **pl**, primary bony lamina; **pos**, posterior direction; **scr**, secondary common crus; **sg**, canal for spiral ganglion within primary bony lamina; **st**, stapes within fenestra vestibuli; **vb**, vestibule.

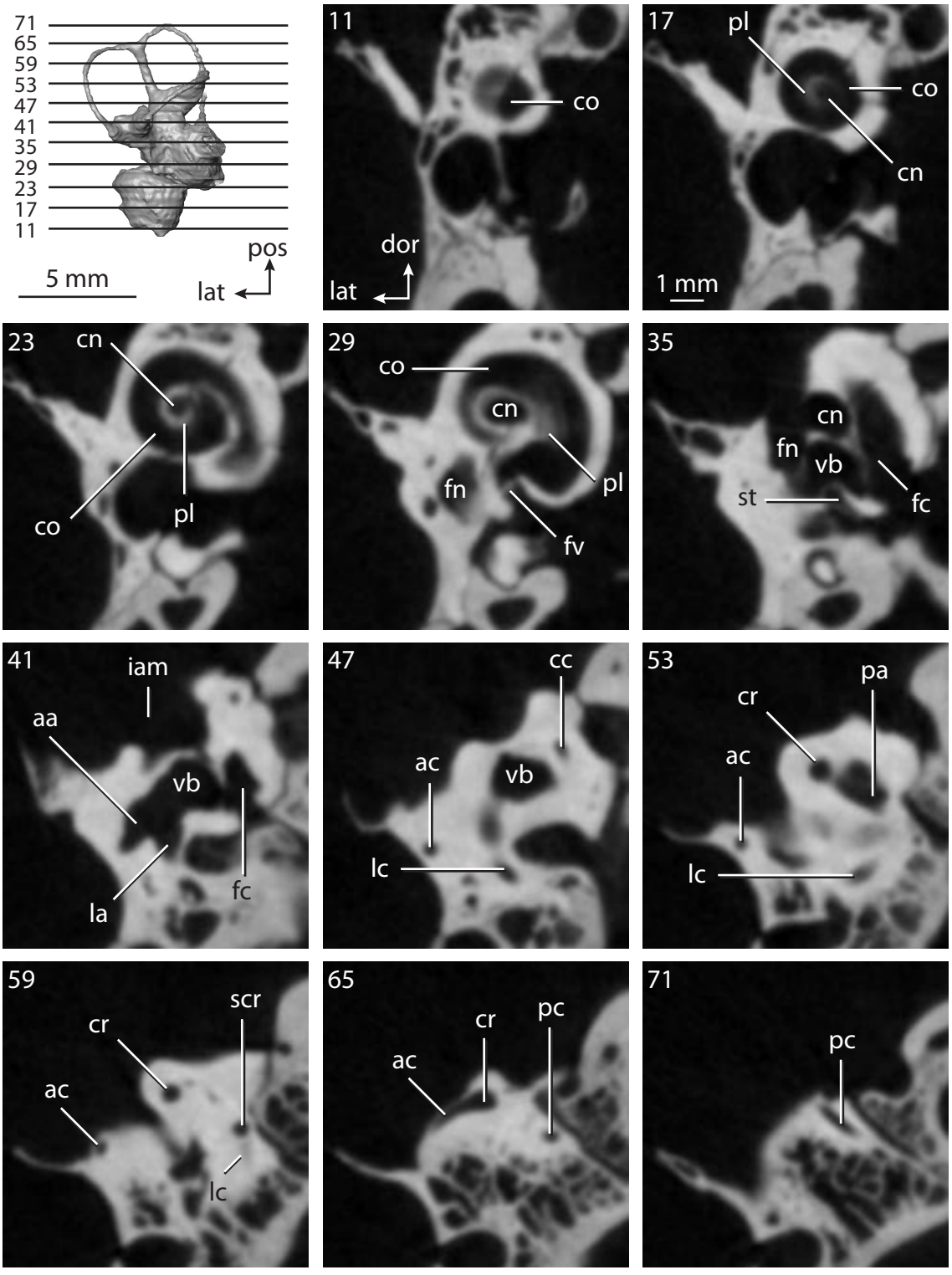
71
65
59
53
47
41
35
29
23
17
11
5 mm
pos
lat
11
co
dor
lat
17
pl
co
cn
1 mm
23
cn
co
pl
29
co
cn
fn
pl
fv
35
cn
fn
vb
st
fc
41
iam
aa
vb
la
fc
47
cc
ac
vb
lc
53
pa
cr
ac
lc
59
scr
cr
ac
lc
65
cr
pc
ac
71
pc

FIGURE 5.36. Bony labyrinth of *Eumetopias jubatus*. **A**, stereopair and labeled line drawing of digital endocast in anterior view; **B**, stereopair and labeled line drawing of digital endocast in dorsal view; **C**, stereopair and labeled line drawing of digital endocast in lateral view; **D**, line drawing of cochlea viewed down axis of rotation to display degree of coiling; **E**, line drawing of cochlea in profile. Abbreviations: **aa**, anterior ampulla; **ac**, anterior semicircular canal; **ant**, anterior direction; **av**, bony channel for aqueduct of vestibule; **cc**, canaliculus cochleae for aqueduct of cochlea; **co**, cochlea; **cr**, common crus; **dor**, dorsal direction; **fc**, fenestra cochleae; **fv**, fenestra vestibuli; **la**, lateral ampulla; **lc**, lateral semicircular canal; **med**, medial direction; **pa**, posterior ampulla; **pc**, posterior semicircular canal; **pl**, primary bony lamina; **pos**, posterior direction; **ps**, outpocketing for perilymphatic sac; **sl**, secondary bony labyrinth; **sr**, spherical recess of vestibule.

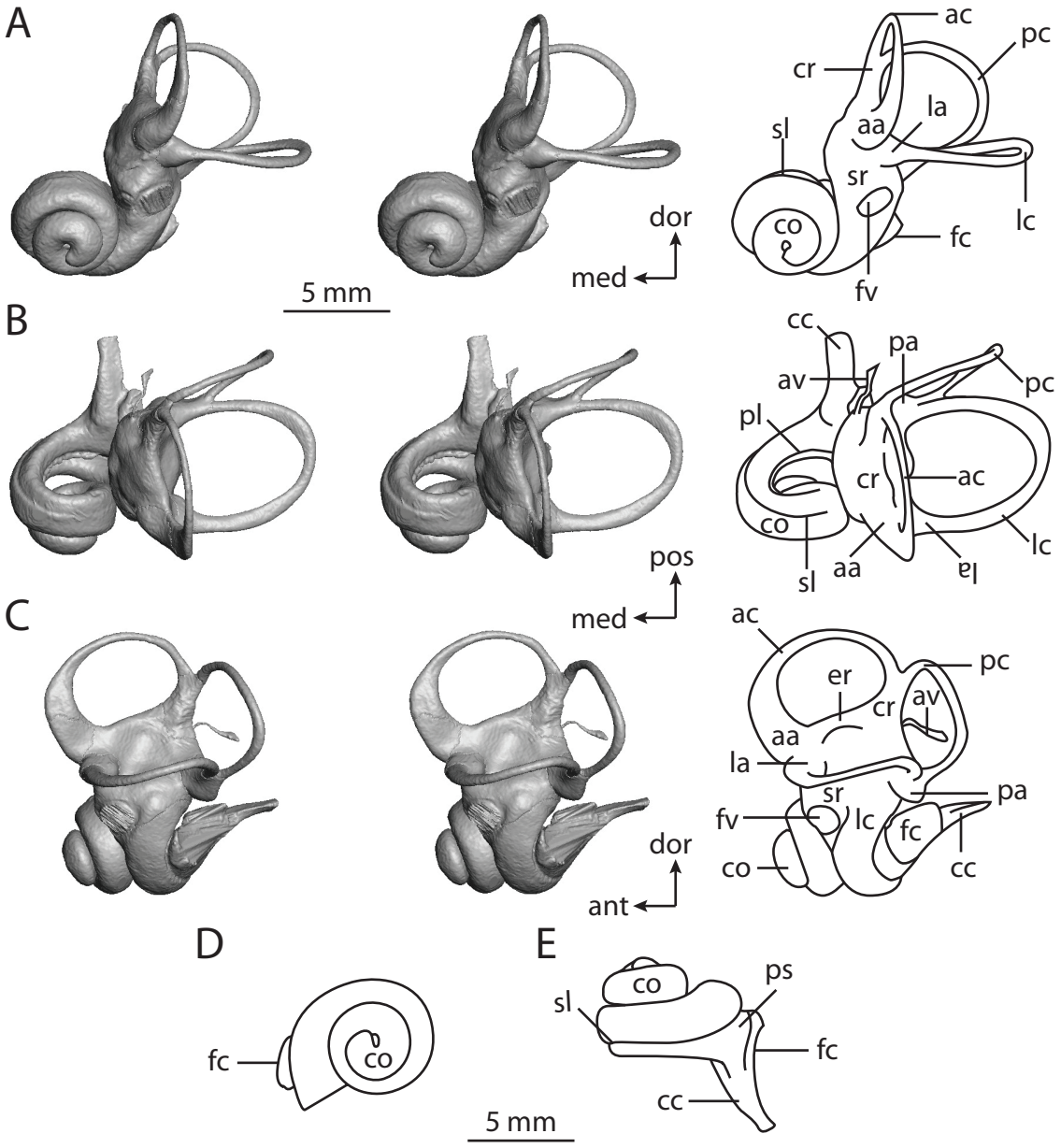
A
ac
pc
cr
la
sl
aa
sr
lc
co
fc
fv
dor
med
5 mm
B
cc
pa
av
pc
pl
cr
ac
co
lc
sl
aa
la
pos
med
C
ac
pc
er
cr
av
aa
la
sr
pa
fv
lc
fc
co
cc
dor
ant
D
fc
co
E
co
ps
sl
fc
cc
5 mm

FIGURE 5.37. CT slices through ear region of *Eumetopias jubatus*. Abbreviations: **aa**, anterior ampulla; **ac**, anterior semicircular canal; **av**, bony channel for aqueduct of vestibule; **cf**, foramina in cribriform plate; **cn**, canal for cranial nerve VIII; **co**, cochlea; **cr**, common crus; **dor**, dorsal direction; **er**, elliptical recess; **fc**, fenestra cochleae; **fn**, canal for cranial nerve VII; **fv**, fenestra vestibuli; **la**, lateral ampulla; **lat**, lateral direction; **lc**, lateral semicircular canal; **pa**, posterior ampulla; **pc**, posterior semicircular canal; **pl**, primary bony lamina; **pos**, posterior direction; **sg**, canal for spiral ganglion within primary bony lamina; **sl**, secondary bony lamina; **sr**, spherical recess of vestibule; **st**, stapes fallen into vestibule; **vn**, canal for vestibular branch of cranial nerve VIII.

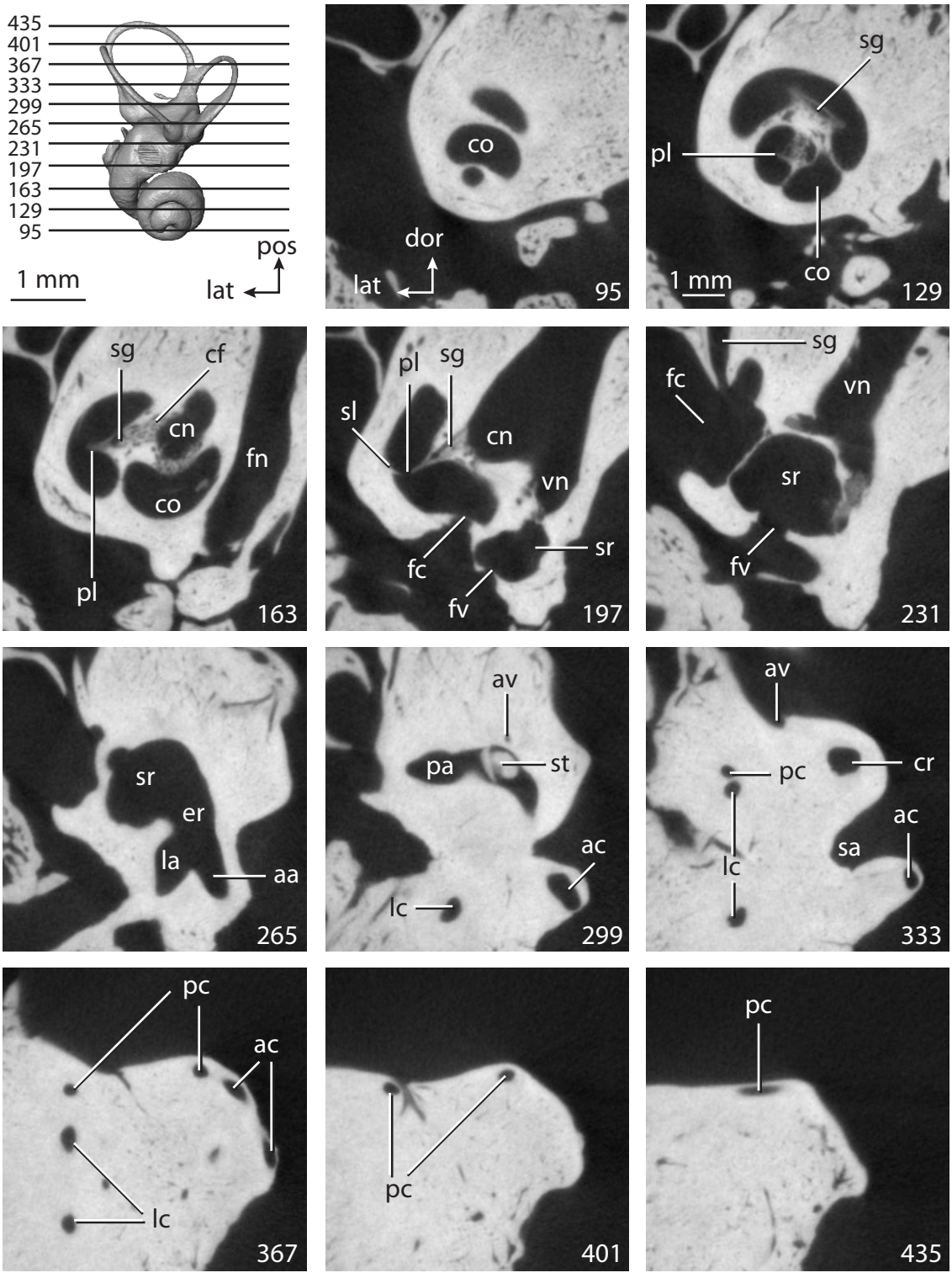
435
401
367
333
299
265
231
197
163
129
95
pos
1 mm
lat
co
dor
lat
95
sg
pl
1 mm
co
129
sg
cf
cn
fn
co
pl
163
pl
sg
sl
cn
vn
fc
sr
fv
197
sg
fc
vn
sr
fv
231
sr
er
la
aa
265
av
pa
st
ac
lc
299
av
pc
cr
ac
sa
lc
333
pc
ac
lc
367
pc
401
pc
435

FIGURE 5.38. Bony labyrinth of *Felis catus*. **A**, stereopair and labeled line drawing of digital endocast in anterior view; **B**, stereopair and labeled line drawing of digital endocast in dorsal view; **C**, stereopair and labeled line drawing of digital endocast in lateral view; **D**, line drawing of cochlea viewed down axis of rotation to display degree of coiling; **E**, line drawing of cochlea in profile. Abbreviations: **aa**, anterior ampulla; **ac**, anterior semicircular canal; **ant**, anterior direction; **av**, bony channel for aqueduct of vestibule; **cc**, canaliculus cochleae for aqueduct of cochlea; **co**, cochlea; **cr**, common crus; **dor**, dorsal direction; **er**, elliptical recess of vestibule; **fc**, fenestra cochleae; **fv**, fenestra vestibuli; **la**, lateral ampulla; **lc**, lateral semicircular canal; **med**, medial direction; **pa**, posterior ampulla; **pc**, posterior semicircular canal; **pl**, primary bony lamina; **pos**, posterior direction; **ps**, outpocketing for perilymphatic sac; **sl**, secondary bony labyrinth; **sr**, spherical recess of vestibule.

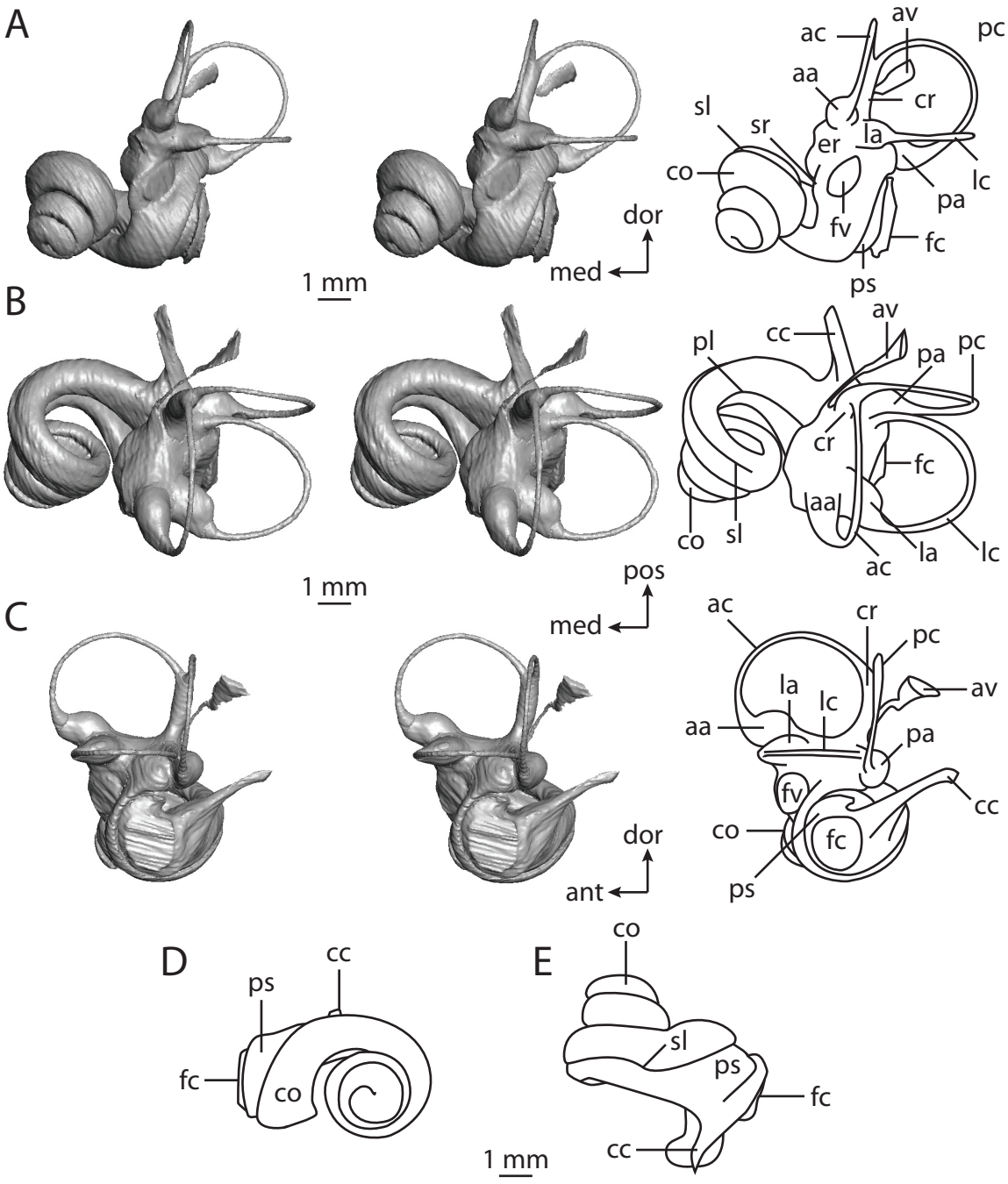
A
av
ac
pc
aa
cr
sl
sr
la
er
co
lc
pa
fv
fc
ps
dor
med
1 mm
B
av
pl
cc
pa
pc
cr
fc
laa
co
sl
la
lc
ac
pos
med
1 mm
C
ac
cr
pc
la
lc
av
aa
pa
fv
cc
co
fc
ps
dor
ant
D
cc
ps
fc
co
E
co
sl
ps
fc
cc
1 mm

FIGURE 5.39. CT slices through ear region of *Felis catus*. Abbreviations: **aa**, anterior ampulla; **ac**, anterior semicircular canal; **av**, bony channel for aqueduct of vestibule; **cc**, canaliculus cochleae for aqueduct of cochlea; **cf**, foramina in cribriform plate; **cn**, canal for cranial nerve VIII; **co**, cochlea; **cr**, common crus; **dor**, dorsal direction; **fc**, fenestra cochleae; **fn**, canal for cranial nerve VII; **fv**, fenestra vestibuli; **hf**, hiatus Fallopii for exit of greater petrosal nerve; **la**, lateral ampulla; **lat**, lateral direction; **lc**, lateral semicircular canal; **pa**, posterior ampulla; **pc**, posterior semicircular canal; **pl**, primary bony lamina; **pos**, posterior direction; **sg**, canal for spiral ganglion within primary bony lamina; **sl**, secondary bony lamina; **sr**, spherical recess of vestibule; **vb**, vestibule.

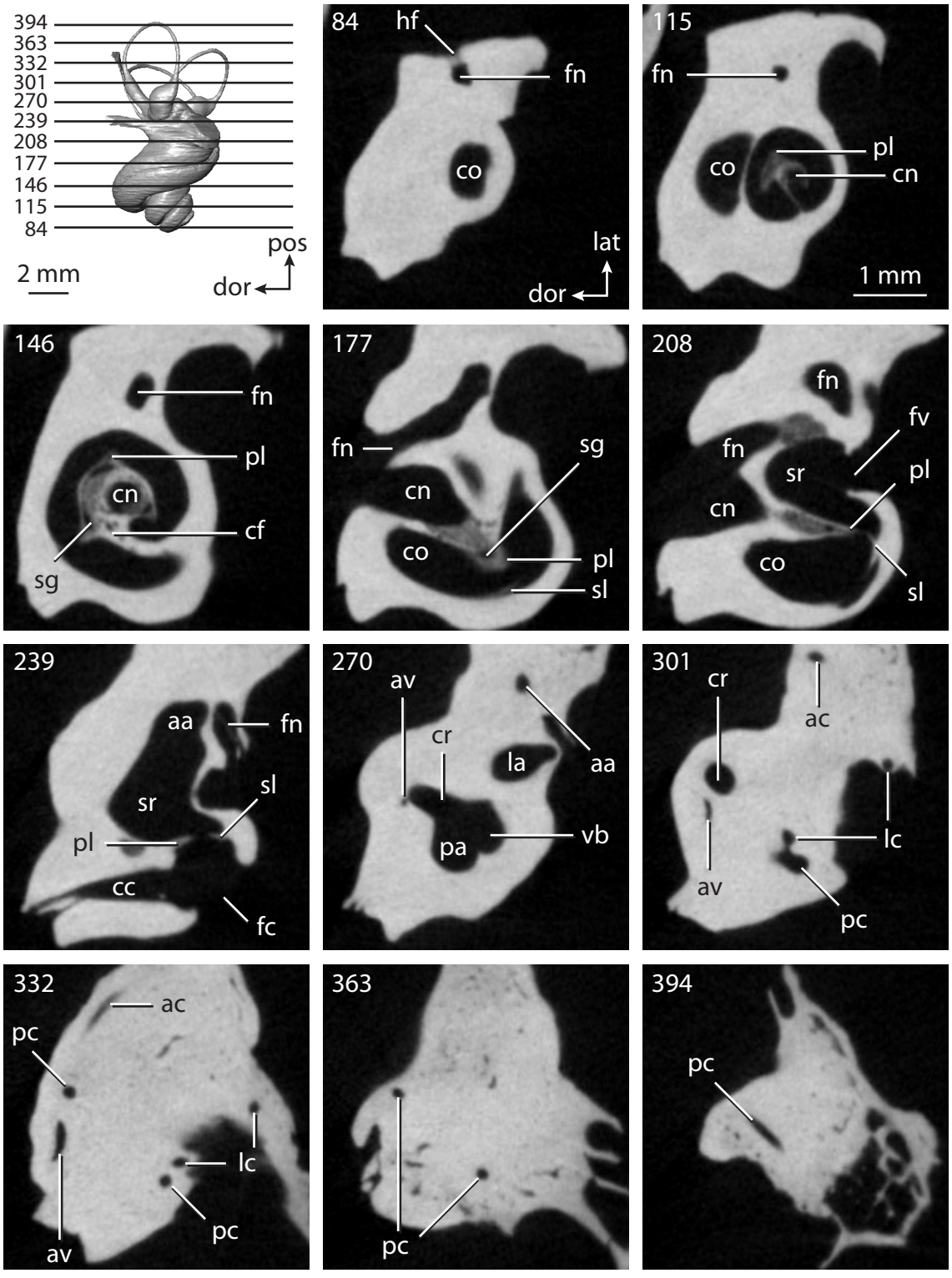
394
363
332
301
270
239
208
177
146
115
84
2 mm
pos
dor
84
hf
fn
co
lat
dor
115
fn
pl
co
cn
1 mm
146
fn
pl
cn
cf
sg
177
fn
sg
cn
co
pl
sl
208
fn
fv
fn
sr
pl
cn
co
sl
239
aa
fn
sl
sr
pl
cc
fc
270
av
cr
la
aa
pa
vb
301
cr
ac
lc
av
pc
332
ac
pc
lc
pc
av
363
pc
394
pc

(248.6°) and *Felis* (242.6°) than what was measured for *Canis* (104.0°). The aspect ratios of the cochleae of carnivorans are high relative to other species described above. The ratio of the cat (0.69) is higher than that of the dog (0.64), and the ratio calculated for the sea lion is intermediate (0.68). Other species with high aspect ratios include *Sus* and *Macroscelides* (ratios around 0.71 for both taxa).

The basal whorl of each carnivoran cochlea is separated from the apical turns, where the apical turns fit within the arc created by the basal turn when the cochlea is in vestibular view. The apical turns sit upon one another in all three taxa, but each successive whorl is smaller than the turn immediately basal to it, forming a pointed cone beyond the basal whorl. The scala tympani is expanded posterior to the fenestra cochleae in all carnivoran taxa. The expansion of the scala tympani leads to the bony canaliculus cochleae for the aqueduct of the cochlea. The canaliculus is longer and more robust in *Felis* (3.60 mm) than in *Canis* (2.08 mm), although the longest canaliculus was measured for *Eumetopias* (4.16 mm).

The angle between the planes of the basal turn of the cochlea and the lateral semicircular canal in *Canis* (20.8°) is similar to that measured for the cetaceans (21.3° in *Tursiops*; 23.2° in the balaenopterid) and *Sus* (23.8°). However, the angle is greater in *Felis* (45.8°), being more similar to the hyrax, *Procavia capensis* (45.4°), than to the dog. The angle formed between the cochlea and lateral canal of *Eumetopias* (31.6°) is intermediate between the dog and cat, most closely resembling *Orycteropus* (31.9°). The scalae tympani and vestibuli bend around the dorsal border of the fenestra cochleae in the carnivorans. The fenestra vestibuli of *Felis* is elliptical (stapedial ratio equals 1.9), although the fenestra of *Canis* is distinctly more circular (ratio equals 1.3). The fenestra vestibuli of *Eumetopias* is intermediate between the other carnivorans (1.7).

The spherical recess of the vestibule is separated from the elliptical recess by a constriction of the vestibule in the carnivoran species. The elliptical recess is gently curved, forming a secondary excavation at its anterior end for the vestibular apertures of the anterior and lateral ampullae in *Canis* and *Felis*, but not in *Eumetopias*. Rather, the elliptical recess of *Eumetopias* is concave laterally. The anterior excavation of the elliptical recess of the vestibule in both *Canis* and *Felis* is expressed as a pedestal for the ampullae in the digital endocasts. The anterior ampulla of *Eumetopias* forms a teardrop-shaped structure, although the lateral ampulla is deflated and dorsoventrally compressed in this taxon.

The bony channel for the aqueduct of the vestibule was not observed in *Canis*, owing to the inadequate resolution of the CT data. The structure is observed in both *Eumetopias* and *Felis*, in which the bony channel opens ventral to the medial edge of the vestibular aperture of the common crus in both taxa, and bends laterally along its course. As is the case in many of the species described here, the channel for the aqueduct ends in a flattened fissure. The length of the channel is longer in *Felis* (3.77 mm) than that measured for *Eumetopias* (2.26 mm).

The posterior limb of the lateral semicircular canal opens into the posterior ampulla, rather than the vestibule itself, dorsal to the anterior edge of the vestibular aperture of the posterior ampulla in *Felis*. The position of the lateral semicircular canal in *Felis* is high relative to the other vestibular components. When the endocast of the bony labyrinth of *Felis* is viewed anteriorly, the lateral canal crosses the space enclosed by the posterior semicircular canal (sagittal labyrinthine index equals 13.1). The lateral semicircular canal of *Canis* is situated in a lower position than in *Felis*, and the plane of the canal does not cross the space enclosed by the posterior canal in anterior view. The lateral semicircular canal of *Eumetopias* empties into the posterior ampulla, as in the cat,

but the plane of the canal does not take a high position in the sea lion as it does in the cat. In this manner, the vestibular apparatus of *Eumetopias* appears more similar to *Canis* among the carnivorans examined here.

As in the cat and sea lion, the posterior limb of the lateral semicircular canal does not open into the vestibule in *Canis*. Unlike the other taxa, the lateral canal of *Canis* does not open into the posterior ampulla directly either, but rather the lateral canal is fused with the posterior semicircular canal to form a secondary common crus. A secondary crus is developed in the aardvark (*Orycteropus afer*) and also in non-placental mammals.

The greatest angle between the planes of any two semicircular canals in *Eumetopias* was measured between the anterior and posterior semicircular canals (105°). The angle between the canals is also obtuse in *Canis* (101°). The angle between the anterior and posterior canals in *Felis* is closer to a right angle (91.4°), although the posterior and lateral semicircular canal planes nearly are perpendicular in *Canis* (89.1°) and *Eumetopias* (90.6°). The angle between the planes of the posterior and lateral semicircular canals of *Felis* is 96.7°, which is the greatest angle between any two canals in the cat. The angle between the anterior and lateral semicircular canals is 80.4° in *Canis*, 79.7° in *Eumetopias*, and 76.8° in *Felis*.

The lateral semicircular canal is the least planar of the three canals in *Eumetopias*, with a total angular deviation of 16.4°. In fact, the lateral canal of *Eumetopias* is the least planar of any semicircular canal measured for any carnivoran specimen examined here (4.4° for *Felis*; 5.1° for *Canis*). The posterior semicircular canal of *Canis* is the least planar of its three canals, with a total angular deviation from the plane of the canal of 10.8°. However, the posterior canal of *Felis* does not deviate from its plane in any significant manner, but the total angular deviation calculated for the posterior canal of *Eumetopias* is 9.5°. The deviation of the anterior canal is smaller in *F. catus* (4.5°) than

in *Canis* (6.0°), but not by much. The anterior semicircular canal of *Eumetopias* deviates by a miniscule amount (0.8°). None of the canals in either of the terrestrial species deviate significantly from their respective planes. The ratios of the total linear deviation over cross-sectional diameter of the anterior, lateral, and posterior semicircular canals of *Canis* are 0.59, 0.40, and 0.94 respectively, and the ratios for the same canals in *Felis* are 0.57, 0.51, and 0.00 (planar). The anterior canal of *Eumetopias* does not deviate from its plane significantly (linear deviation to lumen diameter ratio equals 0.11), although the lateral and posterior semicircular canals of the sea lion deviate by a substantial amount (ratio of lateral equals 1.70; posterior equals 1.15).

The semicircular canals of both terrestrial taxa form graceful curves along their courses. As with most dimensions within the bony labyrinth, the semicircular canals of *Felis* are larger than the canals of *Canis*, although a common pattern across the canal arc radii is observed in both taxa. Namely, the radius of the arc of the anterior semicircular canal is the greatest for both *Canis* (1.73 mm; lateral equals 1.57 mm; posterior equals 1.43 mm) and *Felis* (1.92 mm; lateral equals 1.68 mm; posterior equals 1.91 mm). However, the lateral semicircular canal is the largest in terms of radius in *Eumetopias* (3.13 mm; anterior equals 3.00 mm; posterior equals 2.86 mm).

The posterior semicircular canal of the cat is the longest of all of the canals in this species (9.39 mm), and the lateral canal is the shortest (7.48 mm; posterior equals 8.78 mm). Likewise, the lateral semicircular canal of *Canis* is the shortest of its canals (7.08 mm), but its anterior canal is the longest (8.57 mm), rather than its posterior canal (7.34 mm) as was observed in *Felis*. Unlike the terrestrial carnivorans, the lateral canal of *Eumetopias* is the longest (14.70 mm; anterior equals 12.99 mm; posterior equals 14.08 mm). The lateral semicircular canal of *Canis* may be the shortest of the three canals in this species, but the lumen of the lateral canal has the greatest cross-sectional diameter in

the dog (0.35 mm; anterior equals 0.31 mm; posterior equals 0.29mm). Similarly, the lateral canal has the greatest diameter in *Eumetopias*. All of the canals of *Felis* were equal in cross-sectional diameter (0.26 mm).

The aspect ratio of the arc of the lateral semicircular canal is highest in both *Canis* (1.01) and *Felis* (1.04), and the aspect ratio is the smallest for the anterior canal arc for both species (0.82 and 0.77 respectively). The aspect ratio of the posterior semicircular canal arc is 0.98 for *Canis* and 1.01 for *Felis*. The aspect ratios of all three canal arcs are larger in *Eumetopias* than those measured for the terrestrial carnivorans (anterior equals 0.96; lateral equals 1.24; posterior equals 1.18). The ratio of the slender canal length over arc radius of the posterior semicircular canal was the greatest among the three canals in *Canis* (5.14; anterior equals 4.97; lateral equals 4.45), *Eumetopias* (4.92; anterior equals 4.33; lateral equals 4.72), and *Felis* (4.93; anterior equals 4.57; lateral equals 4.45).

Two labyrinthine characters are synapomorphies for Carnivora within Ferae. The first is the higher aspect ratio of the carnivoran cochlea in profile that gives the cochlear spiral the "sharp-pointed" condition described by Gray (1907, 1908). The second synapomorphy is the entrance of the lateral canal into the posterior ampulla, which is observed in *Eumetopias* and *Felis*. The secondary common crus observed in *Canis* is an apomorphic reversal to the ancestral therian condition, and it also is observed in *Orycteropus* among crown placentals. The ancestral coiling of the cochlea of Carnivora is over a quarter of a turn greater than that reconstructed for the ancestor of Ferae (986.5° versus 888.2°), and the carnivoran cochlea contributes 5% more to the total labyrinthine volume than that of the feran ancestor (61% versus 56%).

A single character from the bony labyrinth, reversal to a low position of the lateral semicircular canal in relation to the ampullar entrance of the posterior canal, is optimized as a synapomorphy for Caniformia. The lateral canal of *Felis* is positioned high, which is

derived from the ancestral eutherian condition, but is plesiomorphic for Carnivora as a whole. The low position of the lateral canal is a reversal for Caniformia. The lateral semicircular canal enters the posterior ampulla in the ancestral caniform (even though a secondary common crus is present in *Canis*), and the arc of the anterior semicircular canal is the largest of the three canal arcs (even though the lateral canal arc is the largest in *Eumetopias*). The ancestral labyrinth of Caniformia possesses a cochlea with a high aspect ratio that coiled 979.3° and contributed 60% of the total labyrinthine volume.

Pholidota

Although extant species of pangolins are known only from Africa and Asia, fossils of Pholidota have been recovered from Tertiary deposits of Europe and North America (McKenna and Bell, 1997; Rose et al., 2005). Pangolins have not contributed greatly to the mammalian biota throughout time (Rose et al., 2005), nor is Pholidota a taxonomically diverse group at present, with only eight species recognized within the single genus *Manis* (Reeder et al., 2007).

The gross volume of the inner ear cavities of the pangolin, *Manis tricuspis*, examined in this study (28.53 mm^3) is similar to that of *Bathygenys reevesi* (29.83 mm^3), *Dasypus novemcinctus* (26.48 mm^3), and *Canis familiaris* (31.36 mm^3). Likewise, the lengths of the bony labyrinth are not vastly different (6.66 mm for *Manis*; 7.40 mm for *Bathygenys*; 8.06 mm for *Dasypus*; 8.10 mm for *Canis*). The overall body size of *Manis* is similar to *Dasypus* (4.5 versus 4,8 k; Silva and Downing, 1995), which is reflected in the dimensions of the inner ear. The volume of the cochlea in *Manis* is 14.00 mm^3, which is 49.1% of the total volume of the bony labyrinth. The cochlear contribution measured in *Manis* is closer to that calculated for *Bathygenys* (54.2%) than *Canis* (66.1%).

The cochlea completes over two and one third turns (863°), and the length of the canal is 9.64 mm. The aspect ratio of the cochlear spiral is 0.54, and the apical whorls of the cochlea sit upon the basal turn, rather than fit within the basal turn (Figure 5.40) as is observed in cetaceans. A secondary bony lamina is not developed within the cochlea of *Manis* (Figure 5.41), and the angle between the plane of the basal turn of the cochlea and the lateral semicircular canal is 20.3°. The secondary lamina also is absent in the terrestrial cetartiodactyls *Bathygenys* and *Sus*.

The scala tympani of the cochlea is expanded internal to the fenestra cochleae. The excavation of the scala tympani leads to a robust canaliculus cochleae for the aqueduct of the cochlea. The canaliculus is oriented dorsally and takes a straight course as it extends to the external surface of the petrosal (2.85 mm in length). The external aperture for the aqueduct of the cochlea is shared by a second canal, which empties into the lateral aspect of the canaliculus cochleae proximal to the midpoint of the canaliculus. The second canal is not straight. The canal opens lateral to the canaliculus cochlea and hooks dorsally to join the canaliculus. A curved canal that fuses to the canaliculus cochleae is not observed in any other mammal.

A slight constriction of the vestibule dorsal to the fenestra vestibuli (stapedial ratio of 1.7 calculated from fenestra) is the only separation between the spherical and elliptical recesses. Otherwise, the vestibule is a single and undivided unit. The bony channel for the aqueduct of the vestibule exits the vestibule medial to the vestibular opening of the short and stout common crus. The 2.45 mm long channel terminates in a spatulate shaped fissure.

The posterior limb of the lateral semicircular canal opens into the vestibule anterodorsal to the vestibular aperture of the posterior ampulla. Because the lateral canal empties directly into the vestibule at its posterior end, there is not a secondary common

FIGURE 5.40. Bony labyrinth of *Manis tricuspis*. **A**, stereopair and labeled line drawing of digital endocast in anterior view; **B**, stereopair and labeled line drawing of digital endocast in dorsal view; **C**, stereopair and labeled line drawing of digital endocast in lateral view; **D**, line drawing of cochlea viewed down axis of rotation to display degree of coiling; **E**, line drawing of cochlea in profile. Abbreviations: **aa**, anterior ampulla; **ac**, anterior semicircular canal; **ant**, anterior direction; **av**, bony channel for aqueduct of vestibule; **cc**, canaliculus cochleae for aqueduct of cochlea; **co**, cochlea; **cr**, common crus; **dor**, dorsal direction; **er**, elliptical recess of vestibule; **fc**, fenestra cochleae; **fv**, fenestra vestibuli; **la**, lateral ampulla; **lc**, lateral semicircular canal; **med**, medial direction; **pa**, posterior ampulla; **pc**, posterior semicircular canal; **pl**, primary bony lamina; **pos**, posterior direction; **ps**, outpocketing for perilymphatic sac; **sr**, spherical recess of vestibule.

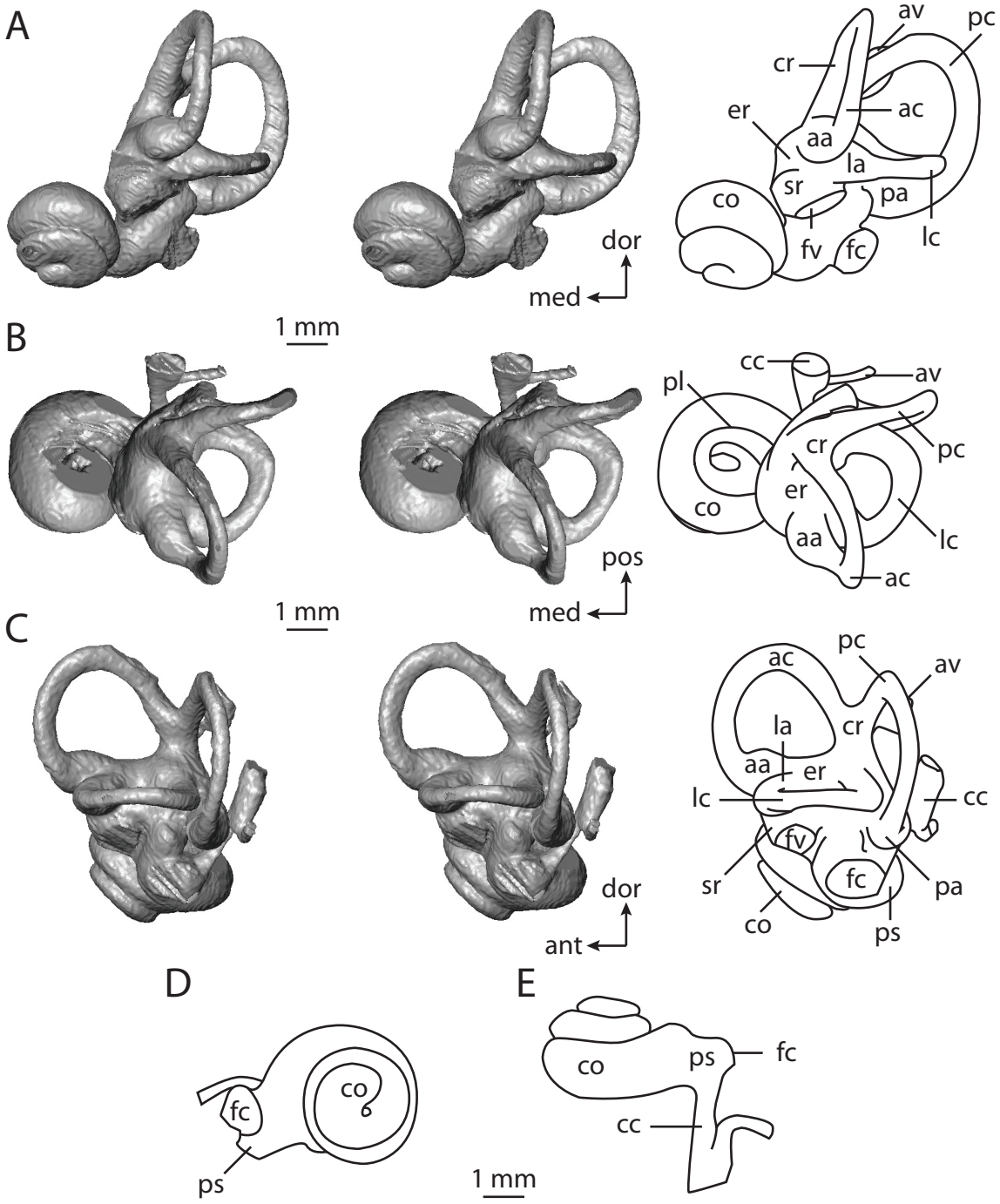
A
av
pc
cr
er
ac
aa
la
sr
pa
co
fv
fc
lc
dor
med
1 mm
B
cc
av
pl
cr
pc
er
co
aa
lc
ac
pos
med
1 mm
C
pc
ac
av
la
cr
aa
er
lc
cc
fv
sr
fc
pa
co
ps
dor
ant
D
co
fc
ps
E
co
ps
fc
cc
1 mm

FIGURE 5.41. CT slices through ear region of *Manis tricuspis*. Abbreviations: **aa**, anterior ampulla; **ac**, anterior semicircular canal; **av**, bony channel for aqueduct of vestibule; **cc**, canaliculus cochleae for aqueduct of cochlea; **cn**, canal for cranial nerve VIII; **co**, cochlea; **dor**, dorsal direction; **fc**, fenestra cochleae; **fn**, canal for cranial nerve VII; **fv**, fenestra vestibuli; **iam**, internal auditory meatus; **la**, lateral ampulla; **lat**, lateral direction; **lc**, lateral semicircular canal; **med**, medial direction; **pa**, posterior ampulla; **pc**, posterior semicircular canal; **pl**, primary bony lamina; **pos**, posterior direction; **sr**, spherical recess of vestibule; **vb**, vestibule; **vn**, canal for vestibular branch of cranial nerve VIII.

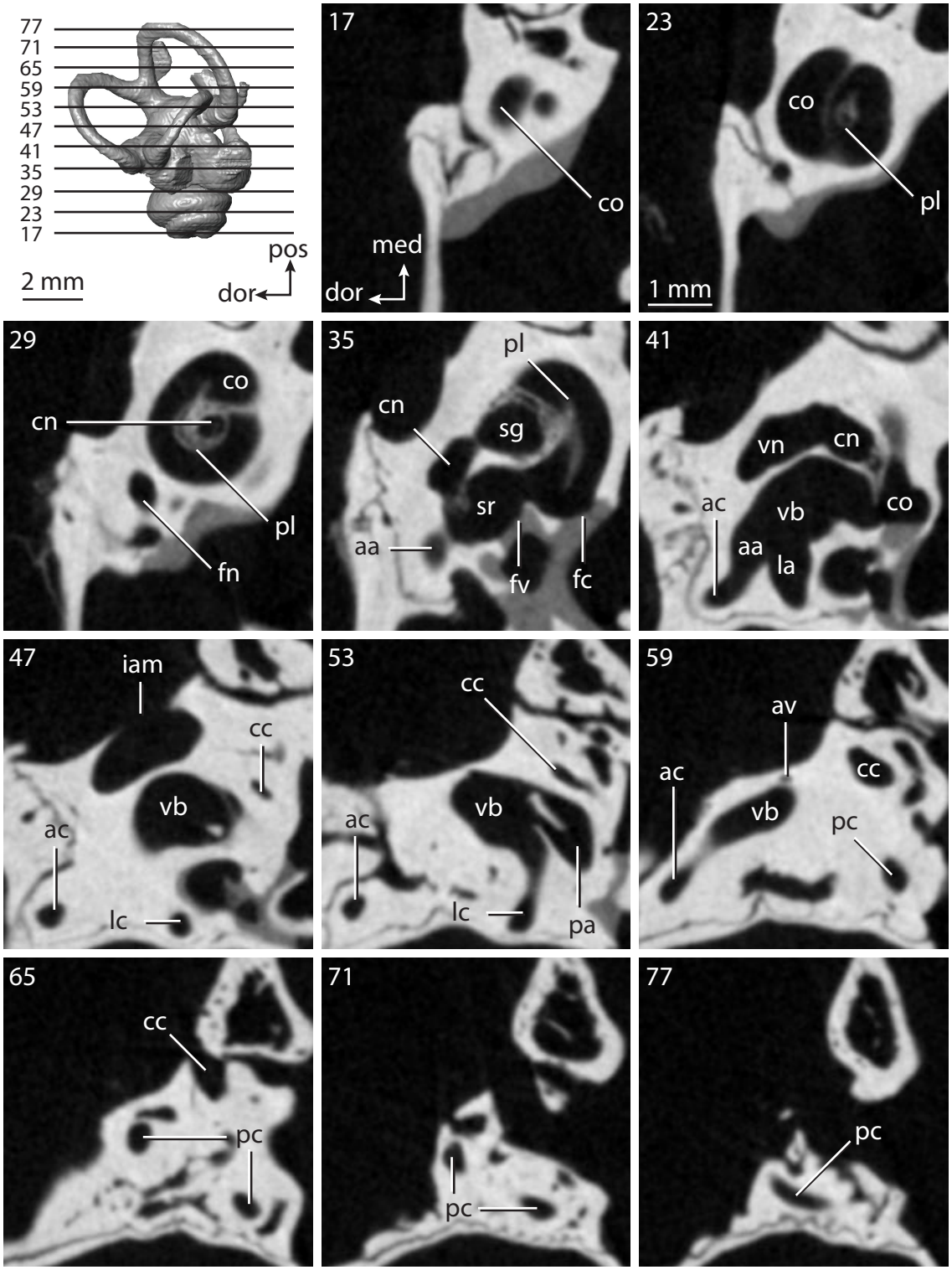
77
71
65
59
53
47
41
35
29
23
17
pos
dor
2 mm
17
co
med
dor
23
co
pl
1 mm
29
co
cn
pl
fn
35
pl
cn
sg
sr
aa
fv
fc
41
vn
cn
ac
vb
co
aa
la
47
iam
cc
vb
ac
lc
53
cc
vb
ac
lc
pa
59
av
ac
cc
vb
pc
65
cc
pc
71
pc
77
pc

crus between the lateral and posterior semicircular canals. The position of the plane of the lateral semicircular canal, intersecting points along the lumen of the canal, is high relative to the rest of the vestibular elements, and the sagittal labyrinthine index of *Manis* is 20.5. The three semicircular canals are especially thick relative to the size of the labyrinth, including the lateral canal, which makes the high position of the canal plane difficult to observe.

The angle between the planes of the posterior and lateral semicircular canals approach a right angle (88.6°), and the other angles between canal planes are acute (anterior-lateral equals 77.0°; anterior-posterior canal equals 84.8°). The lateral semicircular canal of *Manis* does not deviate from its average plane by any significant degree, and the total angular deviations of the anterior (6.7°) and posterior (7.3°) are not great. The degrees of deviation measured for both the anterior and posterior semicircular canals are not significant (ratios of total linear deviation over cross-sectional diameter are 0.31 and 0.40 respectively).

As stated above, the semicircular canals of *Manis* are thick relative to the total size of the bony labyrinth. As a comparison, the total length of the bony labyrinth of *Manis* (6.66 mm) is not much less than that of the oreodont *Bathygenys* (7.40), although the cross-sectional diameter of the anterior, lateral, and posterior semicircular canals of the pangolin (0.55 mm, 0.62 mm, and 0.52 mm respectively) are substantially greater than that measured for the oreodont (0.44 mm, 0.33 mm, and 0.34 mm for the same canals). However, a similar pattern is not observed in the slender semicircular canal lengths and radii of the semicircular canal arcs, which are smaller in *Manis* than *Bathygenys*. The radii of the anterior, lateral, and posterior semicircular canals of *Manis* are 1.46 mm, 1.06 mm, and 1.66 mm respectively (radii for *Bathygenys* are 1.91 mm, 1.52 mm, and 1.79 mm), and the lengths of the canals are 6.59 mm, 3.71 mm, and 7.03

mm for the anterior, lateral, and posterior canals (lengths for *Bathygenys* are 9.72 mm, 7.11 mm, and 10.01 mm).

The lowest aspect ratio of a semicircular canal arc was calculated for the anterior canal (0.76). The ratio for the lateral semicircular canal arc is 0.82, and a ratio of 0.93 was computed for the posterior arc. The ratio of the slender canal length to the arc radius is largest for the anterior semicircular canal (4.52). The ratio for the posterior canal is 4.23, and the ratio for the lateral canal in *Manis* is 3.49.

The bony labyrinth of *Manis* inherited a direct entry of the lateral semicircular canal into the vestibule from the ancestral placental, and the high position of the plane of the lateral semicircular canal compared to the posterior canal is retained from the ancestor of Boreoeutheria. The low aspect ratio of the cochlea observed in *Manis* is the same as that reconstructed for the ancestor of Eutheria. Because the state of the cochlea could not be reconstructed for the ancestor of Placentalia, the condition in *Manis* is either a primitive retention or a secondary reversal. The arc of the posterior semicircular canal of *Manis* is the largest among the three arcs, which is derived relative to both the ancestor of Boreoeutheria, as well as the most recent common ancestor of Pholidota and Carnivora (for which the anterior arc is the largest).

There are no unambiguous synapomorphies within the inner ear that support an exclusive Carnivora plus Pholidota clade (Ferae). The ancestor of the clade retained features that were present in the ancestor of Placentalia, including entry of the lateral semicircular canal into the vestibule directly, and an anterior semicircular canal arc that was the largest among the three arcs (also present in the ancestor of Theria). The plane of the lateral semicircular canal of the ancestor of Ferae was high compared to the ampullar entrance of the posterior canal, which was the state reconstructed for the ancestor of

Boreoeutheria. The state of the aspect ratio of the cochlea was equivocal as reconstructed for the feran ancestor.

Megachiroptera

Chiroptera (bats) is the only group of truly volant mammals, and with over 1,000 species, it forms the second most speciose group of mammals (second only to rodents). Bats traditionally are separated into Megachiroptera, which includes non-echolocating bats and potentially one group of echolocators (see below), and Microchiroptera, which only includes echolocating bats. The results of several recent molecular studies support a closer relationship between Pteropidae (of which *Pteropus lyelli* is used as a representative; Figures 5.42-5.43) and the echolocating Rhinolophidae (of which *Rhinolophus ferrumequinum* was examined here) than between Rhinolophidae and other echolocating bats, which are represented here by the Nycteridae species *Nycteris grandis* and the Molossidae species *Tadardia brasiliensis* (Teeling et al., 2000, 2005; Simmons et al., 2008). However, the results of Bininda-Emonds et al. (2007) separates Pteropidae as the sister taxon to all other bats. Because the morphological descriptions of the bony labyrinth are organized based on the relationships recovered by Bininda-Emonds et al. (2007) in the present study, description of the inner ear of *Rhinolophus* is included with *Nycteris* and *Tadarida*.

Pteropus includes the bats with the largest body sizes (Silva and Downing, 1995), and the average body mass of *Pteropus lyelli* (435 g) is an order of magnitude larger than that of the microchiroperan species examined (see Table 5.2). The total length of the bony labyrinth (Figure 5.42) of *Pteropus* is 6.19 mm, and the gross volume of the inner ear cavities is 7.01 mm^3. The cochlea contributes 58.9% of the total labyrinthine volume (4.13 mm^3). The cochlear canal is 7.66 mm in length, and completes over one and three

FIGURE 5.42. Bony labyrinth of *Pteropus lyelli*. **A**, stereopair and labeled line drawing of digital endocast in anterior view; **B**, stereopair and labeled line drawing of digital endocast in dorsal view; **C**, stereopair and labeled line drawing of digital endocast in lateral view; **D**, line drawing of cochlea viewed down axis of rotation to display degree of coiling; **E**, line drawing of cochlea in profile. Abbreviations: **aa**, anterior ampulla; **ac**, anterior semicircular canal; **ant**, anterior direction; **av**, bony channel for aqueduct of vestibule; **cc**, canaliculus cochleae for aqueduct of cochlea; **co**, cochlea; **cr**, common crus; **dor**, dorsal direction; **er**, elliptical recess of vestibule; **fc**, fenestra cochleae; **fv**, fenestra vestibuli; **la**, lateral ampulla; **lc**, lateral semicircular canal; **med**, medial direction; **pa**, posterior ampulla; **pc**, posterior semicircular canal; **pl**, primary bony lamina; **pos**, posterior direction; **ps**, outpocketing for perilymphatic sac; **sa**, subarcuate fossa; **sg**, canal for spiral ganglion within primary lamina; **sl**, secondary bony lamina; **sr**, spherical recess of vestibule; **st**, stapes within fenestra vestibuli.

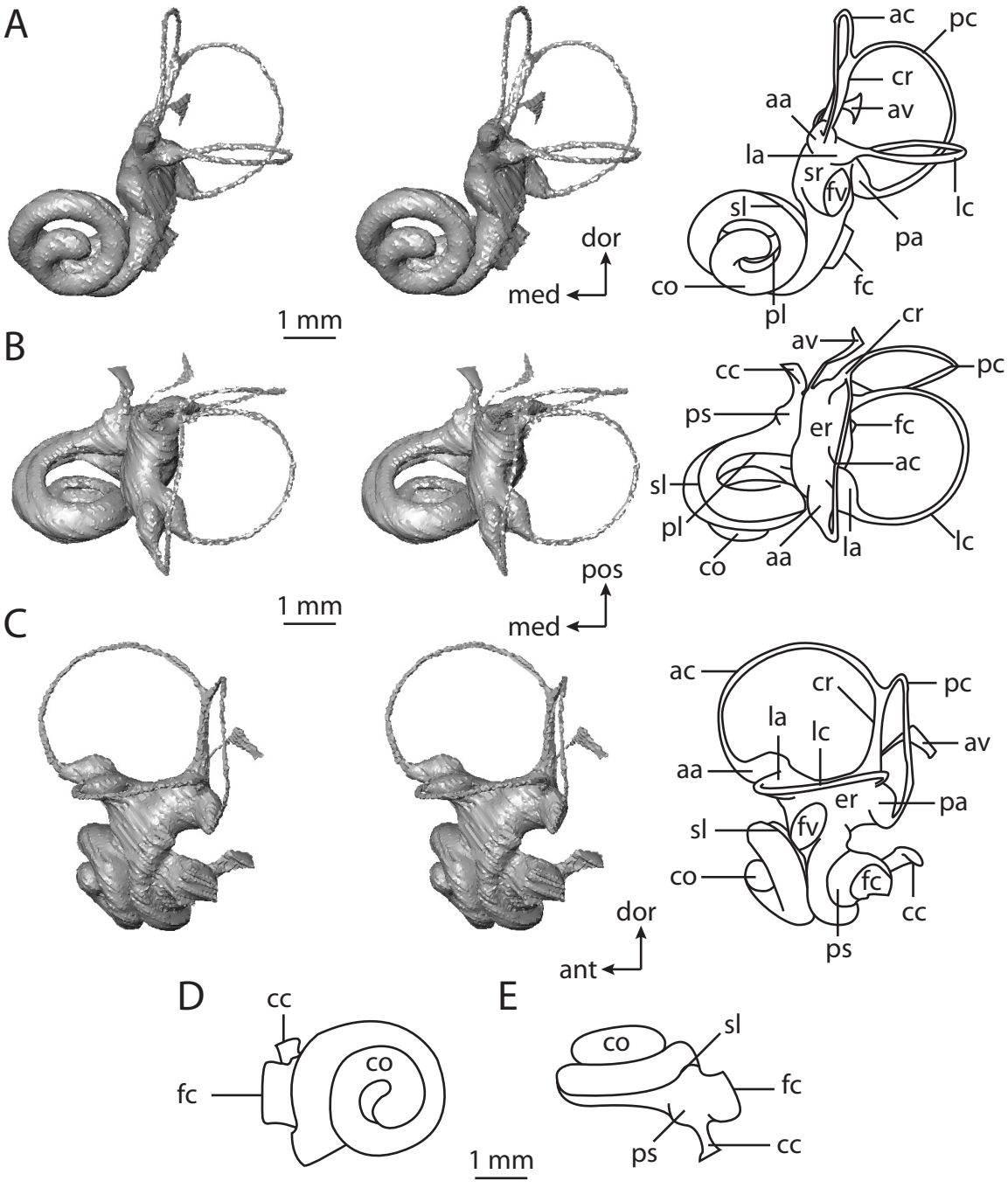
A
ac
pc
cr
aa
av
la
sr
fv
lc
sl
pa
dor
med
co
fc
pl
1 mm
B
cr
av
cc
pc
ps
er
fc
ac
sl
pl
lc
co
aa
la
pos
1 mm
med
C
ac
cr
pc
la
lc
av
aa
er
pa
sl
fv
co
fc
cc
ps
dor
ant
D
cc
co
fc
E
co
sl
fc
ps
cc
1 mm

FIGURE 5.43. CT slices through ear region of *Pteropus lyelli*. Abbreviations: **aa**, anterior ampulla; **ac**, anterior semicircular canal; **av**, bony channel for aqueduct of vestibule; **cn**, canal for cranial nerve VIII; **co**, cochlea; **cr**, common crus; **dor**, dorsal direction; **er**, elliptical recess; **fc**, fenestra cochleae; **fn**, canal for cranial nerve VII; **la**, lateral ampulla; **lc**, lateral semicircular canal; **med**, medial direction; **pa**, posterior ampulla; **pc**, posterior semicircular canal; **pl**, primary bony lamina; **pos**, posterior direction; **sr**, spherical recess of vestibule.

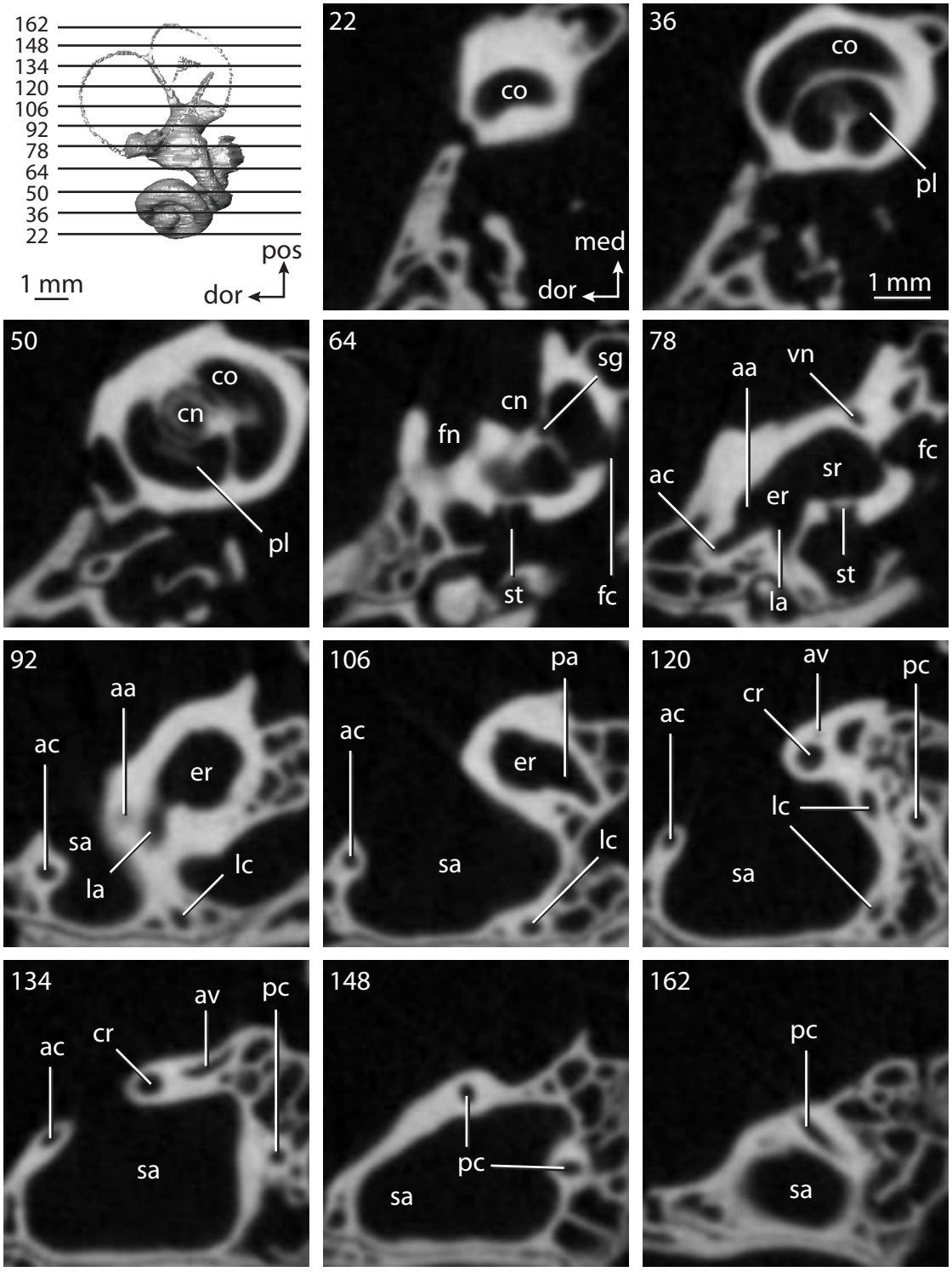
162
148
134
120
106
92
78
64
50
36
22
pos
1 mm
dor
22
co
med
dor
36
co
pl
1 mm
50
co
cn
pl
64
sg
cn
fn
st
fc
78
aa
vn
fc
ac
sr
er
st
la
92
aa
ac
er
sa
la
lc
106
pa
ac
er
sa
lc
120
av
pc
cr
ac
lc
sa
134
av
pc
cr
ac
sa
148
pc
sa
162
pc
sa

quarters turns (656°). The secondary bony lamina is present (Figure 5.43) and persists for nearly the entire basal turn (335°).

The aspect ratio of the cochlea in *Pteropus* is 0.61, and the cochlear canal itself appears narrow compared to the labyrinth as a whole. The apical turnings of the cochlea fit within the basal whorl when the cochlea is viewed down its axis of rotation. The angle between the planes of the basal turn of the cochlea and the lateral semicircular canal is 36.2°, and the stout and straight canaliculus cochleae for the aqueduct of the cochlea is 1.62 mm in length.

The stapedial ratio of *Pteropus*, as measured from the fenestra vestibuli, is 1.8. The spherical and elliptical recesses are undivided, although an excavation is present at the anterior end of the vestibule, which is expressed as a pedestal for the anterior and lateral ampullae on the endocast. The common crus and semicircular canals are delicate and form graceful curves in *Pteropus*. The bony channel for the aqueduct of the vestibule exits the inner ear cavities medial to the vestibular aperture of the common crus. The channel, which is 0.73 mm in length, extends posteriorly before terminating in a triangular-shaped fissure. The posterior limb of the lateral semicircular canal enters the vestibule dorsal to the vestibular aperture of the posterior ampulla, giving the plane of the lateral semicircular canal a relatively high position. The sagittal labyrinthine index of *Pteropus* is 29.7.

The planes of the posterior and lateral semicircular canals essentially form a right angle (90.4°), while the angle between the anterior and lateral canals is acute (84.9°) and the angle between the anterior and posterior canal is obtuse (98.3°). None of the semicircular canals fit on a single plane, although the total angular deviation of the posterior canal (4.7°) is not significant (ratio of total linear deviation over cross-sectional diameter is 0.52). On the other hand, the anterior (10.3°) and lateral (14.3°) semicircular

canals of *Pteropus* deviate from their average planes by a significant amount (ratios of linear deviation over canal diameter are 1.63 and 1.35 respectively).

The radius of the arc of the anterior semicircular canal (1.57 mm) is greater than that measured for the lateral (1.28 mm) and posterior canals (1.35 mm). This differs from the other dimensions of the semicircular canals in *Pteropus*. For example, the slender canal length of the posterior semicircular canal (7.03 mm) is greater than either the anterior (6.86 mm) or lateral canal (5.86 mm). Although the lateral semicircular canal is the smallest of the three in terms of slender canal length and arc radius, the cross-sectional diameter of the lateral canal (0.24 mm) is greater than that measured for either the anterior (0.17 mm) or posterior semicircular canal (0.21 mm).

The aspect ratio of the lateral semicircular canal arc of *Pteropus* is the highest among the three canals (0.97; anterior equals 0.94; posterior equals 0.85). The high ratio of the lateral semicircular canal arc indicates that the height and width of the arc are nearly identical. The ratio of the slender canal length to the canal arc radius of the posterior semicircular canal is the greatest (5.20; ratio of anterior equals 4.37; ratio of lateral equals 4.56).

The ancestor of Chiroptera retained ancestral placental features, including a lateral semicircular canal that was positioned high compared to the posterior canal and that opened into the vestibule directly, as well as the anterior semicircular canal arc as the largest among the three arcs. The ancestral chiropteran cochlea had a high aspect ratio (a condition shared with Carnivora), coiled 763.8°, and contributed 61% to the overall volume of the inner ear cavities (also shared with Carnivora). The labyrinth of *Pteropus* retains all discrete character states from its chiropteran ancestor, but the cochlea of *Pteropus* coils to a lesser degree (656.0°).

Microchiroptera

Among the microchiropteran species examined in the present study, *Nycteris grandis* (Figures 5.44-5.45), *Rhinolophus ferrumequinum* (Figures 5.46-5.47), and *Tadarida brasiliensis* (Figures 5.48-5.49), the species with the largest body mass (as reported in Silva and Downing, 1995) is *Nycteris* (29.3 g; mass of *Rhinolophus* equals 17.2 g; mass of *Tadarida* equals 12.1 g). However, the bony labyrinth of *Rhinolophus* is the largest, both in terms of gross volume of the inner ear cavities (5.90 mm^3; volume of *Nycteris* equals 2.13 mm^3; volume of *Tadarida* equals 3.86 mm^3), as well as the total length of the labyrinth (3.76 mm; length of *Nycteris* equals 3.39 mm; length of *Tadarida* equals 3.22 mm). Likewise, the volume of the cochlea of *Rhinolophus* (2.80 mm^3) is greater than that measured for both *Nycteris* (1.42 mm^3) and *Tadarida* (2.80 mm^3).

The cochleae of the three species comprise over half of the total inner ear volume. The cochlea of *Nycteris* contributes 66.5% of the total volume, which is similar to the percentage calculated in *Canis* (66.1%) and *Felis* (68.0%). The cochlea comprises 72.5% of the labyrinthine volume in *Tadarida*, which is similar to the percentage calculated in the afrotherians *Chrysochloris* (71.3%), *Macroscelides* (71.7%), and *Trichechus* (71.1%). The largest volumetric contribution among the bats examined was calculated for *Rhinolophus* (88.8%). The only other mammals that have a larger contribution than *Rhinolophus* are the cetaceans (contribution in *Tursiops* equals 93.5%; contribution in the balaenopterid equals 90.6%).

The cochlea of *Rhinolophus* (Figure 5.46) completes just over three complete turns (1114°), whereas the cochlea of *Nycteris* (Figure 5.44) and *Tadarida* (Figure 5.48) complete around two and one quarter turns (795° and 752° respectively). Likewise, the length of the cochlear canal of *Rhinolophus* (11.57 mm) is greater than that measured in either *Nycteris* (6.66 mm) or *Tadarida* (6.95 mm). A secondary bony lamina is present in

FIGURE 5.44. Bony labyrinth of *Nycteris grandis*. **A**, stereopair and labeled line drawing of digital endocast in anterior view; **B**, stereopair and labeled line drawing of digital endocast in dorsal view; **C**, stereopair and labeled line drawing of digital endocast in lateral view; **D**, line drawing of cochlea viewed down axis of rotation to display degree of coiling; **E**, line drawing of cochlea in profile. Abbreviations: **aa**, anterior ampulla; **ac**, anterior semicircular canal; **ant**, anterior direction; **cc**, canaliculus cochleae for aqueduct of cochlea; **co**, cochlea; **cr**, common crus; **dor**, dorsal direction; **fc**, fenestra cochleae; **fv**, fenestra vestibuli; **la**, lateral ampulla; **lc**, lateral semicircular canal; **med**, medial direction; **pa**, posterior ampulla; **pc**, posterior semicircular canal; **pos**, posterior direction; **ps**, outpocketing for perilymphatic sac; **sl**, secondary bony lamina.

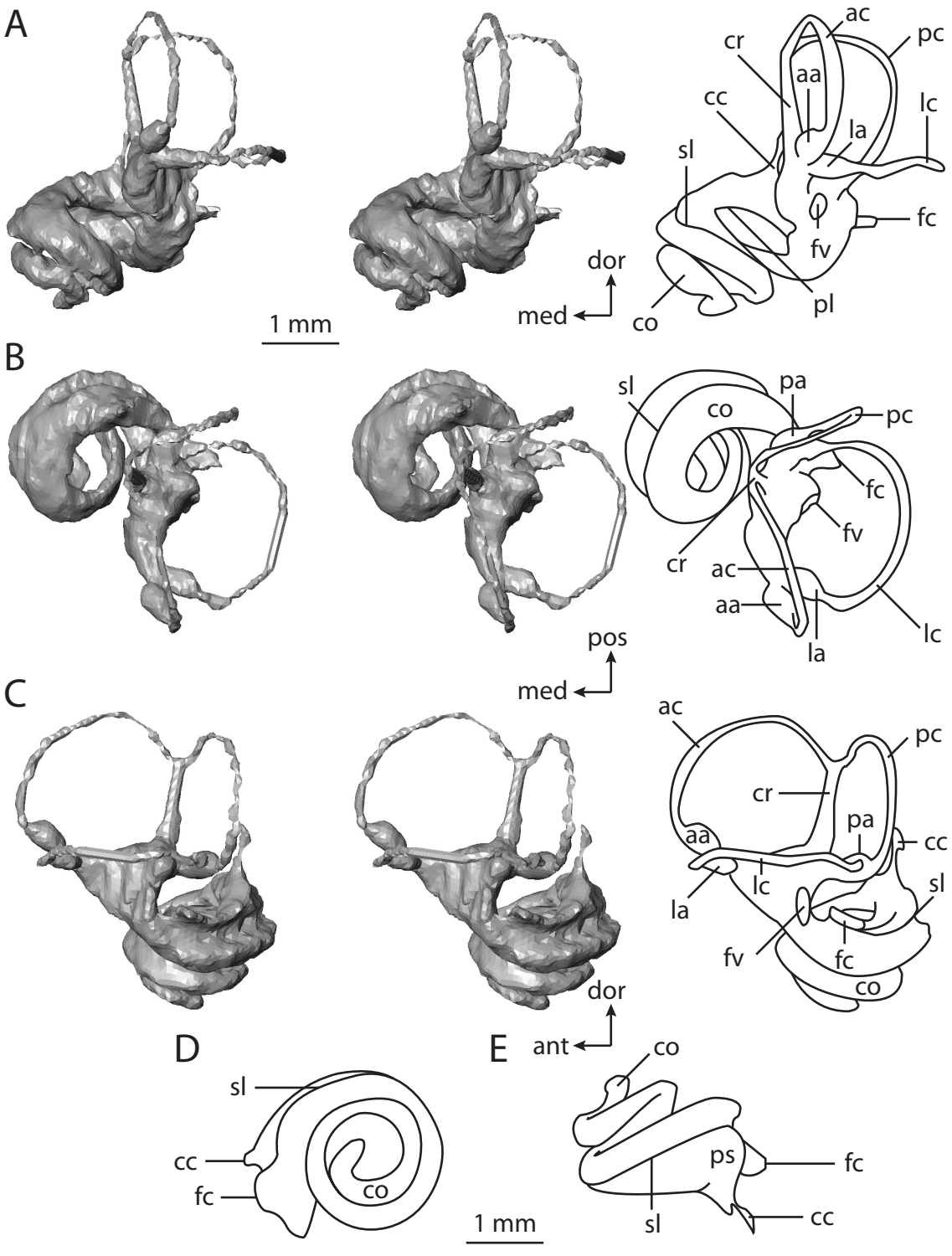
A
ac
pc
cr
aa
cc
lc
la
sl
fc
fv
dor
med
pl
co
1 mm
B
sl
pa
co
pc
fc
fv
cr
ac
aa
lc
la
pos
med
C
ac
pc
cr
pa
aa
cc
lc
sl
la
fv
fc
co
dor
ant
D
sl
cc
fc
co
1 mm
E
co
ps
fc
sl
cc

FIGURE 5.45. CT slices through ear region of *Nycteris grandis*. Abbreviations: **aa**, anterior ampulla; **ac**, anterior semicircular canal; **cc**, canaliculus cochleae for aqueduct of cochlea; **cn**, canal for cranial nerve VIII; **co**, cochlea; **fc**, fenestra cochleae; **fv**, fenestra vestibuli; **la**, lateral ampulla; **lc**, lateral semicircular canal; **med**, medial direction; **pa**, posterior ampulla; **pc**, posterior semicircular canal; **pl**, primary bony lamina; **pos**, posterior direction; **sa**, subarcuate fossa; **sl**, secondary lamina; **vb**, vestibule; **ven**, ventral direction.

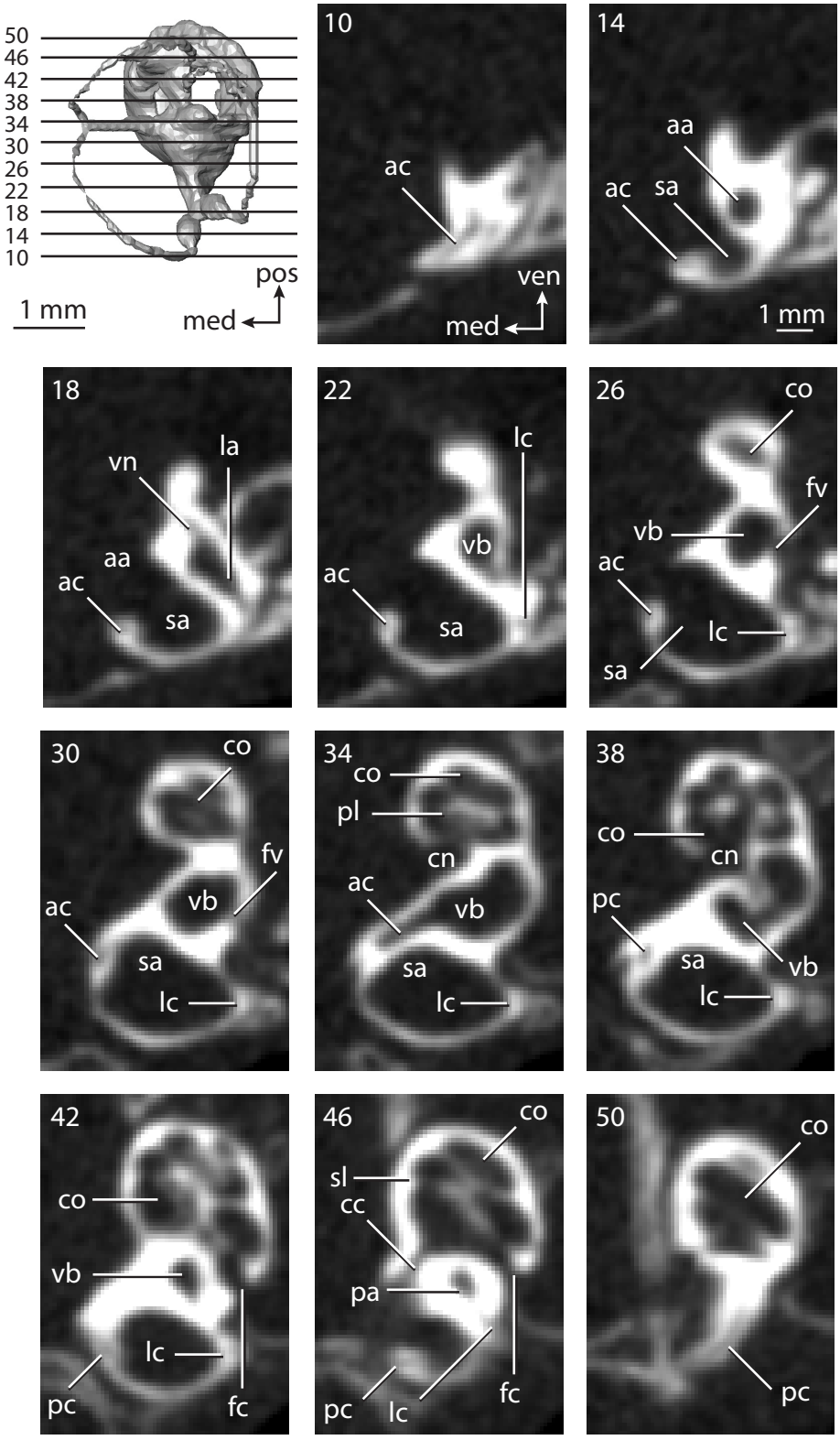
50
46
42
38
34
30
26
22
18
14
10
pos
1 mm
med
10
ac
ven
med
14
aa
ac
sa
1 mm
18
vn
la
aa
ac
sa
22
lc
vb
ac
sa
26
co
fv
vb
ac
lc
sa
30
co
fv
ac
vb
sa
lc
34
co
pl
cn
ac
vb
sa
lc
38
co
cn
pc
sa
vb
lc
42
co
vb
lc
pc
fc
46
co
sl
cc
pa
pc
lc
fc
50
co
pc

FIGURE 5.46. Bony labyrinth of *Rhinolophus ferrumequinum*. **A**, stereopair and labeled line drawing of digital endocast in anterior view; **B**, stereopair and labeled line drawing of digital endocast in dorsal view; **C**, stereopair and labeled line drawing of digital endocast in lateral view; **D**, line drawing of cochlea viewed down axis of rotation to display degree of coiling; **E**, line drawing of cochlea in profile. Abbreviations: **aa**, anterior ampulla; **ac**, anterior semicircular canal; **ant**, anterior direction; **av**, bony channel for aqueduct of vestibule; **cc**, canaliculus cochleae for aqueduct of cochlea; **co**, cochlea; **cr**, common crus; **dor**, dorsal direction; **er**, elliptical recess of vestibule; **fc**, fenestra cochleae; **fv**, fenestra vestibuli; **la**, lateral ampulla; **lc**, lateral semicircular canal; **med**, medial direction; **pa**, posterior ampulla; **pc**, posterior semicircular canal; **pl**, primary bony lamina; **pos**, posterior direction; **sl**, secondary bony lamina.

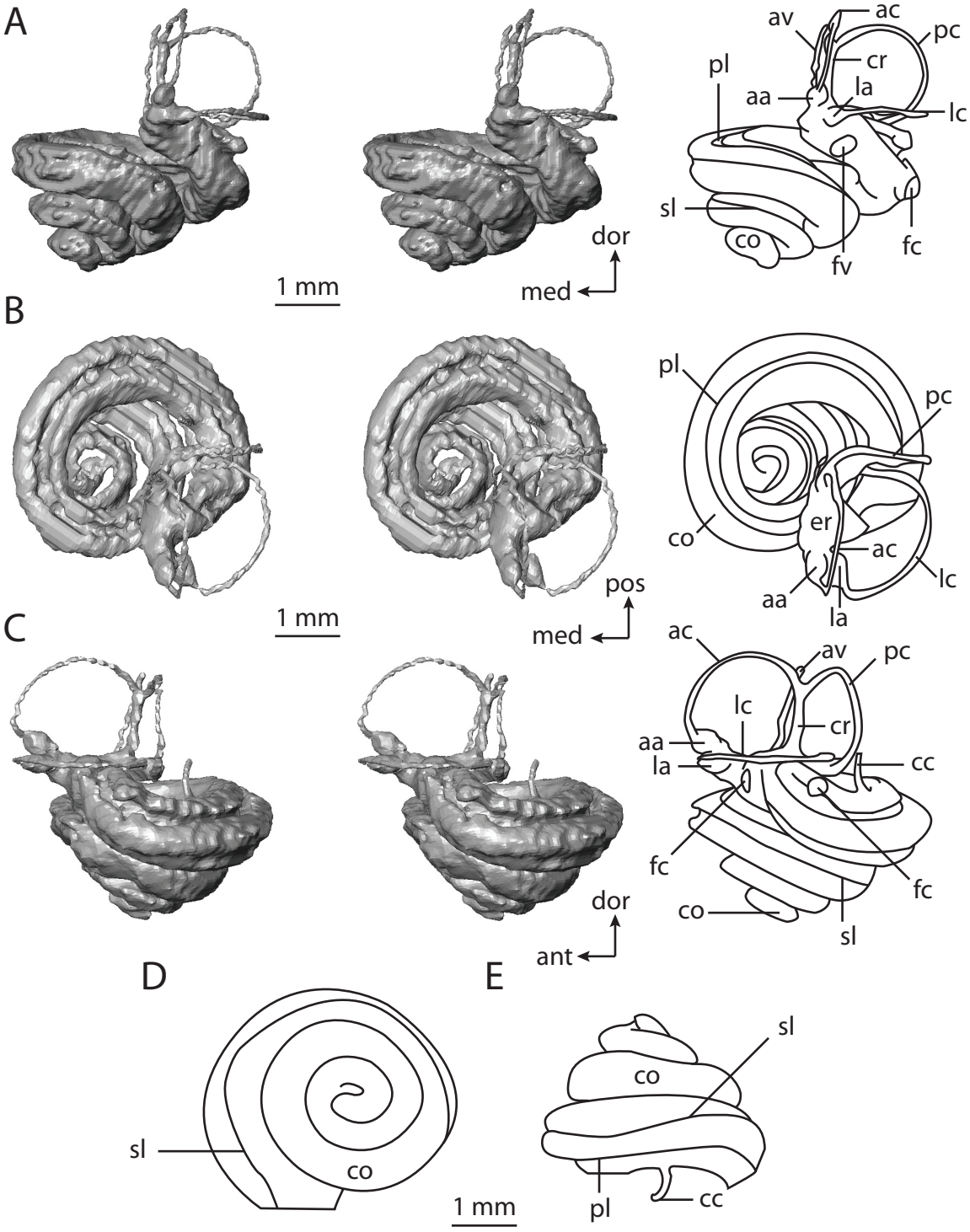
A
av
ac
pc
cr
pl
la
aa
lc
sl
co
fv
fc
dor
med
1 mm
B
pl
pc
co
er
ac
lc
aa
la
pos
med
1 mm
C
ac
av
pc
lc
cr
aa
la
cc
fc
fc
co
sl
dor
ant
D
sl
co
1 mm
E
sl
co
pl
cc

FIGURE 5.47. CT slices through ear region of *Rhinolophus ferrumequinum*. Abbreviations: **aa**, anterior ampulla; **ac**, anterior semicircular canal; **av**, bony channel for aqueduct of vestibule; **cn**, canal for cranial nerve VIII; **co**, cochlea; **cr**, common crus; **dor**, dorsal direction; **fc**, fenestra cochleae; **fn**, canal for cranial nerve VII; **fv**, fenestra vestibuli; **la**, lateral ampulla; **lc**, lateral semicircular canal; **med**, medial direction; **pa**, posterior ampulla; **pc**, posterior semicircular canal; **pl**, primary bony lamina; **pos**, posterior direction; **sa**, subarcuate fossa; **sg**, canal for spiral ganglion within primary lamina; **sl**, secondary lamina; **vb**, vestibule; **ven**, ventral direction; **vn**, canal for vestibular branch of cranial nerve VIII.

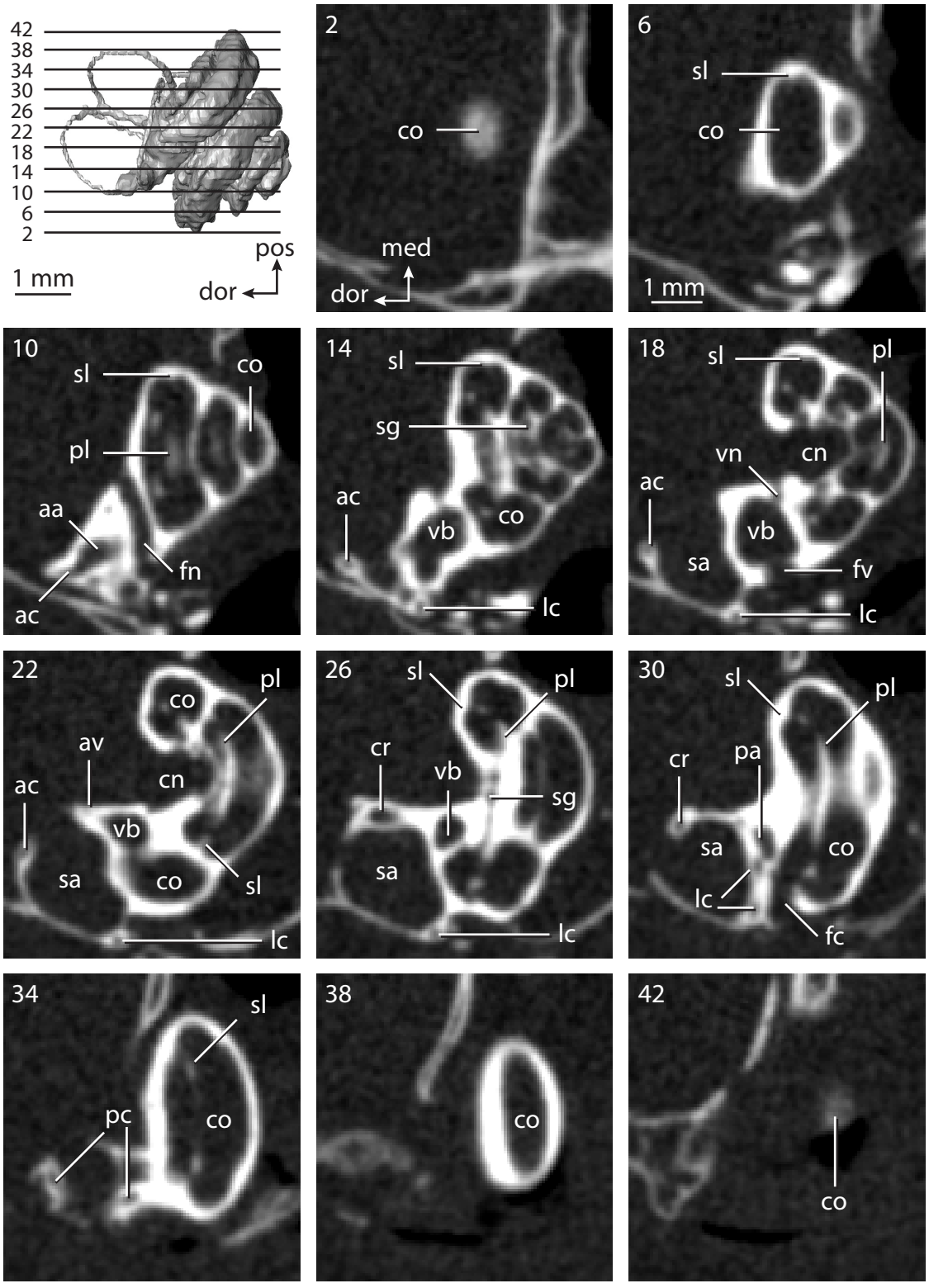
42
38
34
30
26
22
18
14
10
6
2
pos
dor
1 mm
2
co
med
dor
6
sl
co
1 mm
10
sl
co
pl
aa
fn
ac
14
sl
sg
ac
vb
co
lc
18
sl
pl
vn
cn
ac
vb
sa
fv
lc
22
co
pl
av
ac
cn
vb
sa
co
sl
lc
26
sl
pl
cr
vb
sg
sa
lc
30
sl
pl
cr
pa
sa
co
lc
fc
34
sl
pc
co
38
co
42
co

FIGURE 5.48. Bony labyrinth of *Tadarida brasiliensis*. **A**, stereopair and labeled line drawing of digital endocast in anterior view; **B**, stereopair and labeled line drawing of digital endocast in dorsal view; **C**, stereopair and labeled line drawing of digital endocast in lateral view; **D**, line drawing of cochlea viewed down axis of rotation to display degree of coiling; **E**, line drawing of cochlea in profile. Abbreviations: **aa**, anterior ampulla; **ac**, anterior semicircular canal; **ant**, anterior direction; **av**, bony channel for aqueduct of vestibule; **cc**, canaliculus cochleae for aqueduct of cochlea; **co**, cochlea; **cr**, common crus; **dor**, dorsal direction; **er**, elliptical recess of vestibule; **fc**, fenestra cochleae; **fv**, fenestra vestibuli; **la**, lateral ampulla; **lc**, lateral semicircular canal; **med**, medial direction; **pa**, posterior ampulla; **pc**, posterior semicircular canal; **pl**, primary bony lamina; **pos**, posterior direction; **ps**, outpocketing for the perilymphatic sac; **sl**, secondary bony lamina; **sr**, spherical recess of vestibule.

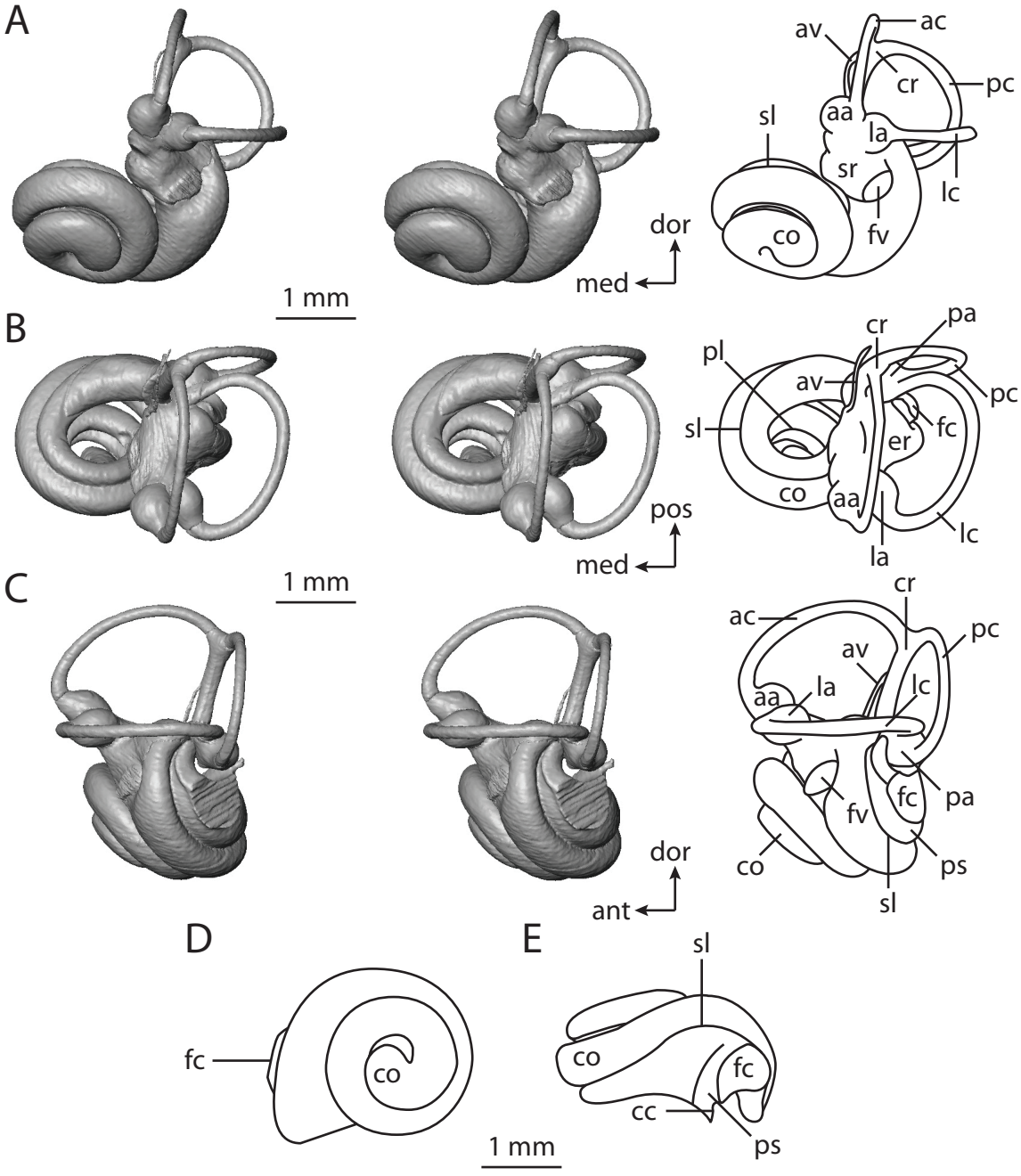
A
av
ac
cr
pc
sl
aa
la
sr
lc
co
fv
dor
med
1 mm
B
cr
pa
pl
av
pc
sl
fc
er
co
aa
lc
la
pos
med
1 mm
C
cr
ac
pc
av
aa
la
lc
fc
pa
fv
co
ps
sl
dor
ant
D
fc
co
1 mm
E
sl
co
fc
cc
ps

FIGURE 5.49. CT slices through ear region of *Tadarida brasiliensis*. Abbreviations: **aa**, anterior ampulla; **ac**, anterior semicircular canal; **ant**, anterior direction; **av**, bony channel for aqueduct of vestibule; **cf**, foramina within cribriform plate; **cn**, canal for cranial nerve VIII; **co**, cochlea; **cr**, common crus; **er**, elliptical recess of vestibule; **fc**, fenestra cochleae; **fn**, canal for cranial nerve VII; **fv**, fenestra vestibuli; **la**, lateral ampulla; **lat**, lateral direction; **lc**, lateral semicircular canal; **med**, medial direction; **pa**, posterior ampulla; **pc**, posterior semicircular canal; **pl**, primary bony lamina; **pos**, posterior direction; **sa**, subarcuate fossa; **sg**, canal for spiral ganglion within primary lamina; **sl**, secondary lamina; **sr**, spherical recess of vestibule; **ven**, ventral direction; **vn**, canal for vestibular branch of cranial nerve VIII.

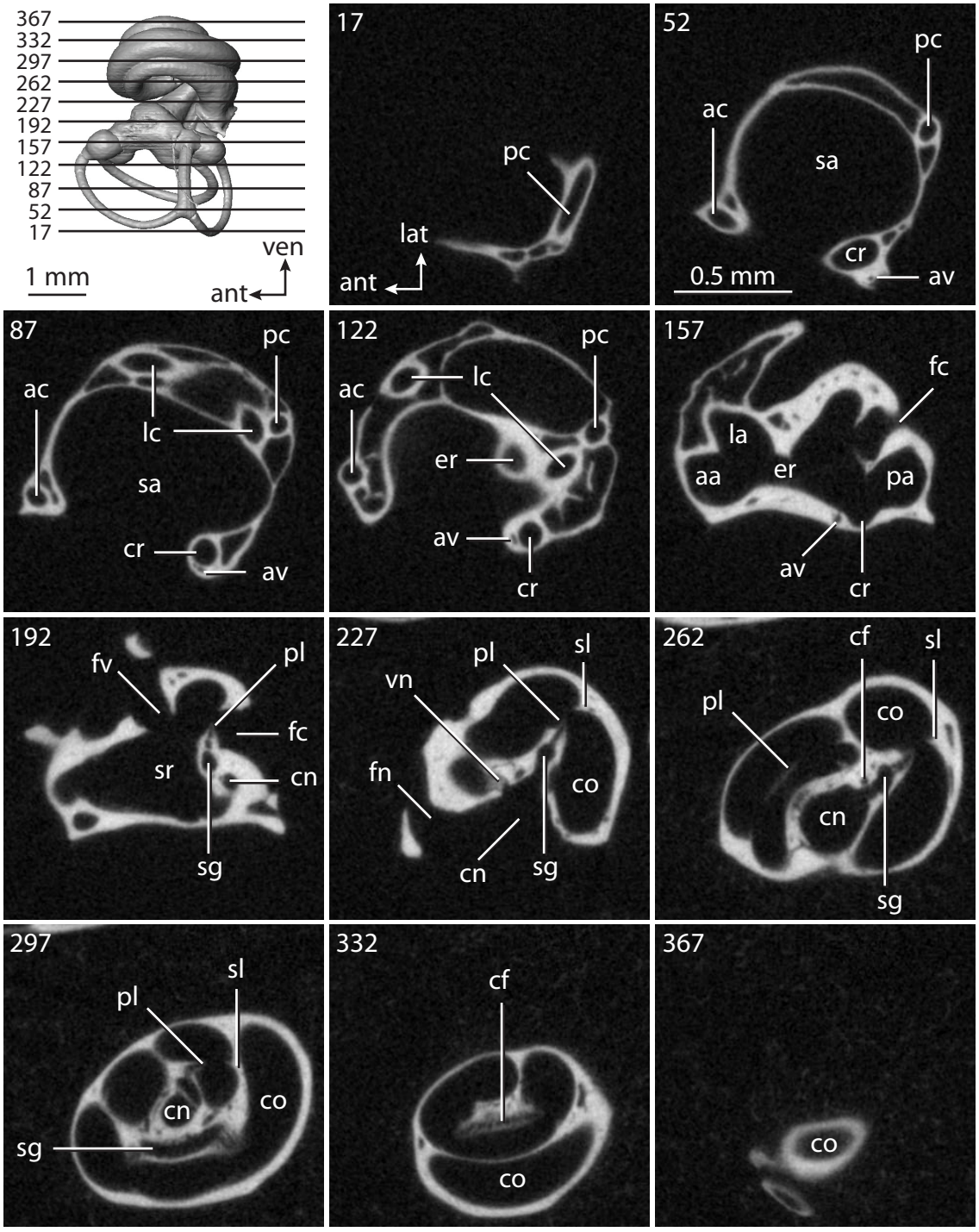
367
332
297
262
227
192
157
122
87
52
17
1 mm
ven
ant
17
pc
lat
ant
52
pc
ac
sa
cr
av
0.5 mm
87
pc
ac
lc
sa
cr
av
122
pc
ac
lc
er
av
cr
157
fc
la
aa
er
pa
av
cr
192
fv
pl
fc
sr
cn
sg
227
pl
sl
vn
fn
co
cn
sg
262
cf
sl
pl
co
cn
sg
297
pl
sl
cn
co
sg
332
cf
co
367
co

each of the chiropteran taxa examined. The secondary lamina of *Rhinolophus* (Figure 5.47), which is expressed as a groove on the endocast, persists for the greatest relative distance along the radial wall of the cochlear canal (935°), and the least in *Nycteris* (316°; Figure 5.45). The secondary lamina of *Tadarida* (Figure 5.49) extends for 659°, which is intermediate between the other two microchiropterans. The secondary laminae of *Rhinolophus* and *Tadarida* are the only laminae examined so far to extend beyond the basal turn, with the exception of the lamina in *Tursiops* (396°). The lamina of *Rhinolophus* completes more turns than that of any other mammal examined in this study (see also Staněk, 1933).

The aspect ratio of the cochlear spiral in profile is the smallest for *Tadarida* (0.52; 0.61 for *Nycteris*; 0.63 for *Rhinolophus*). The apical whorls of the cochlea of *Tadarida* sit upon the basal turn, whereas the apical whorls fit within the more basal turns in both *Rhinolophus* and *Nycteris*. A groove, which is expressed as a ridge on the endocast, situated on the axial wall of the cochlear canal opposite the fenestra cochleae, leads to the short canaliculus cochleae for the aqueduct of the cochlea in *Tadarida* (0.12 mm in length). A canaliculus is observed in both *Rhinolophus* (0.59 mm in length) and *Nycteris* (0.66 mm in length), although the groove opposite the fenestra cochleae is not observed in these latter species. The canaliculus is very straight in *Rhinolophus*, and it is oriented nearly perpendicular to the plane of the basal turn of the cochlea.

The plane of the basal turn of the cochlea of *Rhinolophus* forms an angle of 5.5° with the plane of the lateral semicircular canal, which is the smallest angle measured between the structures of any mammal described here (see Table 5.3). The angle in *Nycteris* (47.2°) is similar to that measured in *Felis* (45.8°) and the elephantoid (48.5°), and the angle in *Tadarida* (29.2°) is not much different from that observed in *Eumetopias* (31.6°) and *Orycteropus* (31.9°).

The fenestra vestibuli is elliptical in *Tadarida* (stapedial ratio equals 2.0), although the ratio calculated for *Nycteris* (1.0) indicates a circular fenestra. The stapedial ratio, as measured from the fenestra vestibuli, of *Rhinolophus* is 1.4. The spherical recess of *Tadarida* is separated from the elliptical recess by a mild constriction of the vestibule. The elliptical recess is elongated, with extensions at its anterior and posterior ends. The recesses are not distinguishable within the vestibule of either *Rhinolophus* or *Nycteris*, but as in *Tadarida*, the vestibule of the other two species possess an anterior excavation for the anterior and posterior ampullae, as well as a posterior excavation for the posterior ampulla and common crus. The posterior excavation is best developed in *Rhinolophus*.

The common crura of all three bats are tall and especially slender in *Rhinolophus* and *Nycteris*. The bony channel for the aqueduct of the vestibule leaves the inner ear medial and anterior to the vestibular aperture of the common crus in *Tadarida* and *Rhinolophus*, rather than directly medial to the crus as in *Pteropus*. The channel is straight and 1.40 mm in length in *Rhinolophus*, opening on the surface of the petrosal near the apex of the common crus, but the channel of *Tadarida* (1.42 mm in length) curves gently towards the posterior end of the labyrinth. The presence of a bony channel for the aqueduct of the vestibule cannot be determined for *Nycteris*, because the data were not adequate to resolve the structure (only 70 slices with an interpixel spacing of 0.0654 mm in *Nycteris* versus 380 slices with and interpixel spacing of 0.0097 mm in *Tadarida*; see Table 1). However, the CT dataset of the ear region of *Rhinolophus* contains fewer slices (45) than that of *Nycteris*, yet the channel for the aqueduct of the vestibule is observed, perhaps because the slices were of a higher resolution interpixel spacing of 0.043 mm).

The posterior limb of the lateral semicircular canal opens into the posterior ampulla in *Nycteris* and *Rhinolophus*, but the canal opens directly into the vestibule

anterior to the posterior ampulla in *Tadarida*. The lateral canals of *Tadarida* and *Rhinolophus* are positioned high with respect to the other vestibular constituents (sagittal labyrinthine indices 22.1 and 38.3 respectively), but the canal is comparatively lower in *Nycteris*, in which the lateral canal does not cross the space enclosed by the posterior semicircular canal.

The angle between the planes of the posterior and anterior semicircular canals is the largest measured in each of the microchiropteran taxa, especially in *Nycteris* (112°; angle equals 104° in *Rhinolophus*; angle equals 98.4° in *Tadarida*). The anterior and lateral semicircular canals express the smallest angle in all of the species, especially *Tadarida* (74.7°; angle equals 79.9° in *Rhinolophus*; angle equals 85.9° in *Nycteris*). The angle between the posterior and lateral semicircular canals of *Nycteris* (86.3°) is smaller than that measured for both *Rhinolophus* (87.9°) and *Tadarida* (98.4°).

The semicircular canals of *Tadarida* are the most planar among the microchiropterans, and none of them deviate significantly from their planes (ratios of total linear deviation over cross-sectional diameter of anterior, lateral, and posterior canals are 0.21, 0.36, and 0.00 respectively). The posterior canal does not deviate significantly from its plane in *Tadarida*, although the canal is the least planar in both *Rhinolophus* (total deviation equals 13.9°; ratio equals 2.09) and *Nycteris* (22.7°; ratio equals 2.77). The greatest total angular deviation in *Tadarida* was measured for the lateral semicircular canal (4.7°; deviation equals 4.1° in *Rhinolophus* with ratio of 0.54; deviation equals 6.6 in *Nycteris* with ratio of 0.74). The total angular deviation of the anterior semicircular canal is 8.3° in *Rhinolophus*, 4.1° in *Nycteris*, and 2.0° in *Tadarida*. The degree of deviation of the anterior semicircular canal is significant in *Rhinolophus* (ratio equals 1.66), but the canal does not deviate significantly in *Nycteris* (ratio equals 0.58).

The radius of the arc of the anterior semicircular canal is greater than the other canal radii in the three microchiropteran taxa examined here. Among the three species, the anterior arc radius is largest for *Nycteris* (0.97 mm; 0.83 mm for *Rhinolophus*; 0.85 mm for *Tadarida*). The smallest arc radius was measured for the lateral semicircular canal arc in *Rhinolophus* (0.69 mm; 0.87 mm for *Nycteris*; 0.74 mm for *Tadarida*). The radii of the arc of the posterior semicircular canal for *Rhinolophus*, *Nycteris*, and *Tadarida* are 0.74 mm, 0.79 mm, and 0.73 mm respectively.

The semicircular canals themselves are longer for *Nycteris* (4.35 mm for anterior; 3.40 mm for lateral; 4.36 mm for posterior) than either *Rhinolophus* (3.52 mm for anterior; 3.21 mm for lateral; 3.90 mm for posterior) or *Tadarida* (3.90 mm for anterior; 3.26 mm for lateral; 3.59 mm for posterior). However, the canals of *Tadarida* are larger in terms of cross-sectional diameter. The diameters of the anterior, lateral, and posterior canals, respectively, are 0.15 mm, 0.17 mm, and 0.14 mm for *Tadarida*, 0.07 mm, 0.09 mm, and 0.09 mm for *Rhinolophus*, and 0.12 mm, 0.14 mm, and 0.11 for *Nycteris*.

The aspect ratio of the arc of the lateral semicircular canal is the lowest among the three canals for the microchiropterans, particularly for *Rhinolophus* (0.46; 0.71 for *Nycteris*; 0.58 for *Tadarida*). Only the aspect ratio of the lateral canal in the balaenopterid (0.39) is smaller than that calculated for *Rhinolophus*. The highest aspect ratio among the microchiropteran canal arcs was measured for the posterior canal of *Rhinolophus* (0.98; 0.95 for *Nycteris*; 0.91 for *Tadarida*). The ratio of the slender canal length to arc radius for the posterior semicircular canal was the greatest ratio in *Nycteris* (5.51; anterior ratio equals 4.48; lateral ratio equals 3.91), *Rhinolophus* (5.25; anterior ratio equals 4.25; lateral equals 4.64), and *Tadarida* (4.88; anterior equals 4.62; lateral equals 4.45).

There are no unambiguous synapomorphies within the bony labyrinth uniting Chiroptera as a whole, nor is there evidence from the inner ear that *Rhinolophus* shares a

more recent common ancestor with *Pteropus* than the definitive microchiropterans *Nycteris* and *Tadarida*. However, the lateral semicircular canals of both *Nycteris* and *Rhinolophus* empty into the posterior ampulla, whereas the lateral canals of *Pteropus* and *Tadarida* open into the vestibule directly.

A secondary common crus is not observed in any of the bats examined. In this regard, the bony labyrinth of Chiroptera is derived from that of the ancestral eutherian, but retains this morphology from the ancestral placental. Most of the bats are derived from the ancestral eutherian condition in the position of the lateral semicircular canal in relation to the ampullar opening of the posterior canal, although *Nycteris* retains the ancestral condition. Because of this, the state in the ancestor of Microchiroptera is equivocal as reconstructed. *Tadarida* retains the ancestral therian state of a flattened cochlea, whereas the cochleae of all other bats have a high aspect ratio. Nonetheless, the ancestral microchiropteran condition is a cochlea with a high aspect ratio, which is retained from the ancestor to all of Chiroptera. The largest semicircular canal arc is observed in the anterior canal in all of the bats, although this feature is plesiomorphic and shared with most therian taxa. The cochlea of the microchiropteran ancestor coils 820.1° and contributes 68.0% of the total labyrinthine volume, both of which are greater values than those reconstructed for the ancestor of Chiroptera (763.7°; 61.0%).

The most recent common ancestor of *Rhinolophus* and *Tadarida* possessed a cochlea with a high aspect ratio, a lateral semicircular canal positioned high compared to the posterior canal, and an anterior semicircular canal arc that was the largest among the three arcs. All of these states also are present in the ancestor of Chiroptera. Because the lateral semicircular canal opened into the vestibule in *Tadarida* and into the posterior ampulla in *Rhinolophus*, the state in the most recent common ancestor of these taxa was reconstructed as equivocal. The cochlea of this ancestor coiled 895.6°, and contributed

76.0% of the entire labyrinthine volume. Although the cochlea contributed a great amount of the labyrinthine volume, it was not as great as that reconstructed for Cetacea (84.0%).

Eulipotyphla

The sister taxon to the Ungulata, Ferae, and Chiroptera polytomy is Eulipotyphla. The constituents of Eulipotyphla are Erinaceidae (hedgehogs), Soricidae (shrews), Talpidae (moles), *Solenodon*, and the extinct genus *Nesophontes* (following Asher, 2005). These taxa traditionally were grouped with the afrosoricid Tenrecidae and Chrysochloridae within the paraphyletic Lipotyphla (sensu McKenna and Bell, 1997), which in turn was a subset of Insectivora (sensu Simpson, 1945), that also included Macroscelidea. Although most recent phylogenetic analyses fail to support either insectivoran or lipotyphlan monophyly, a monophyletic Eulipotyphla often is recovered (e.g., Stanhope et al., 1998; Murphy et al., 2001a, b; Asher et al., 2003; Grenyer and Purvis, 2003; Nikaido et al., 2003; Bininda-Emonds et al., 2007). However, eulipotyphlan monophyly is not always found, even among molecular studies that group the afrosoricids with other afrotherians (e.g., Emerson et al., 1999; Mouchaty et al., 2000).

The eulipotyphlans form the third most speciose clade of placental mammals (Wilson and Reeder, 1993; Reeder et al., 2007), most of which belong to the subclade Soricomorpha (shrews, moles, solenodons, and nesophontids). The sister taxon to the soricomorphs are the hedgehogs, which belong to the group Erinaceomorpha. Both major subclades of eulipotyphlan are represented - the hedgehog *Atelerix albiventris* (Figures 5.50-5.51) and the shrew *Sorex monticolus* (Figures 5.52-5.53).

Atelerix is significantly larger than *Sorex*, with a body mass of 866 grams versus 6.1 grams for the shrew (Silva and Downing, 1995). Likewise, the bony labyrinth of

FIGURE 5.50. Bony labyrinth of *Atelerix albiventris*. **A**, stereopair and labeled line drawing of digital endocast in anterior view; **B**, stereopair and labeled line drawing of digital endocast in dorsal view; **C**, stereopair and labeled line drawing of digital endocast in lateral view; **D**, line drawing of cochlea viewed down axis of rotation to display degree of coiling; **E**, line drawing of cochlea in profile. Abbreviations: **aa**, anterior ampulla; **ac**, anterior semicircular canal; **ant**, anterior direction; **cc**, canaliculus cochleae for aqueduct of cochlea; **co**, cochlea; **cr**, common crus; **dor**, dorsal direction; **er**, elliptical recess of vestibule; **fc**, fenestra cochleae; **fv**, fenestra vestibuli; **la**, lateral ampulla; **lc**, lateral semicircular canal; **med**, medial direction; **pa**, posterior ampulla; **pc**, posterior semicircular canal; **pl**, primary bony lamina; **pos**, posterior direction; **sl**, secondary bony lamina; **sr**, spherical recess of vestibule.

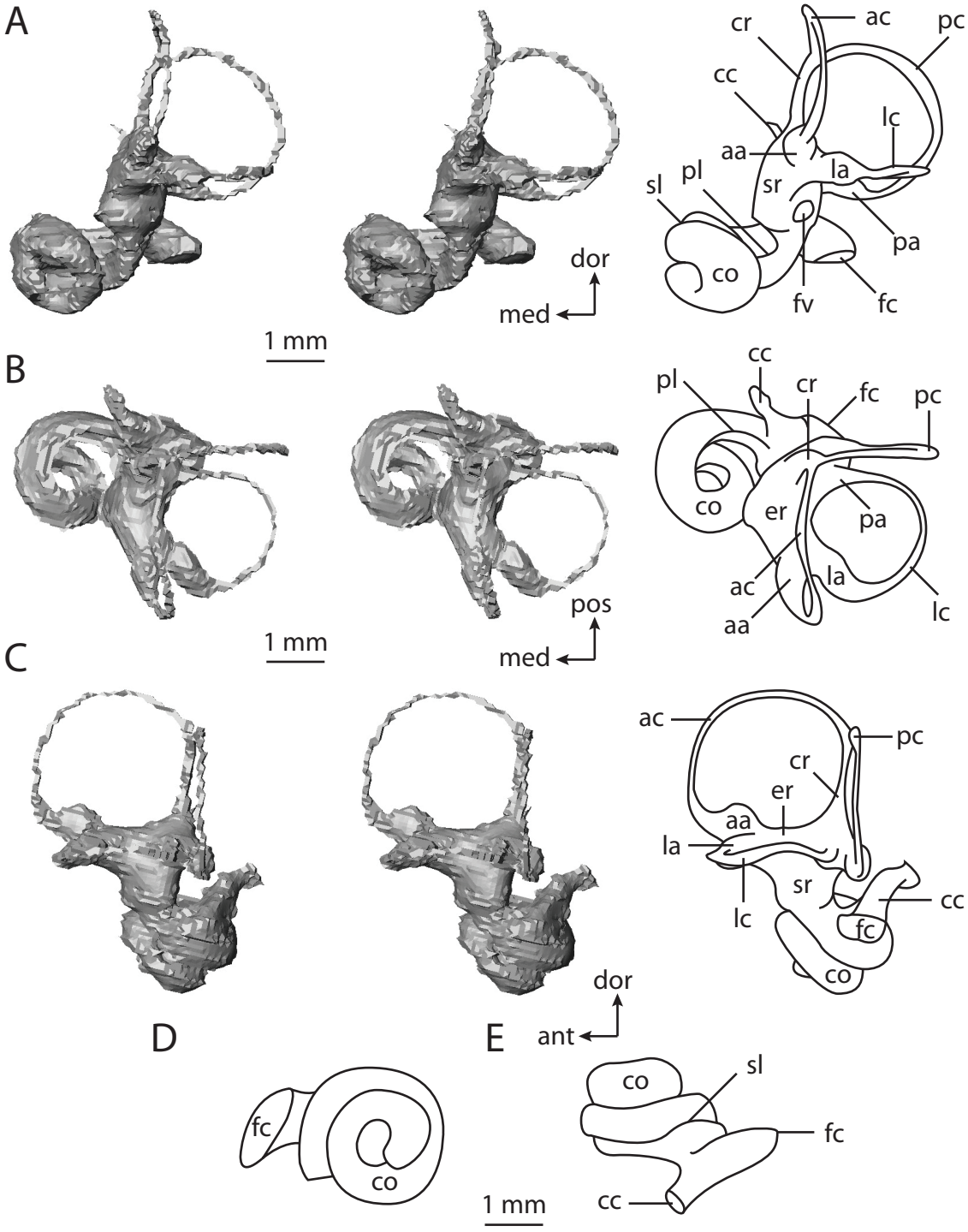
A
cr
ac
pc
cc
lc
aa
la
sl
pl
sr
pa
co
fv
fc
dor
med
1 mm
B
cc
pl
cr
fc
pc
co
er
pa
ac
la
lc
aa
pos
med
1 mm
C
ac
pc
cr
er
aa
la
sr
cc
lc
fc
co
dor
ant
D
fc
co
E
co
sl
fc
cc
1 mm

FIGURE 5.51. CT slices through ear region of *Atelerix albiventris*. Abbreviations: **aa**, anterior ampulla; **ac**, anterior semicircular canal; **cn**, canal for cranial nerve VIII; **co**, cochlea; **cr**, common crus; **dor**, dorsal direction; **fc**, fenestra cochleae; **fn**, canal for cranial nerve VII; **fv**, fenestra vestibuli; **la**, lateral ampulla; **lc**, lateral semicircular canal; **med**, medial direction; **pa**, posterior ampulla; **pc**, posterior semicircular canal; **pl**, primary bony lamina; **pos**, posterior direction; **vb**, vestibule; **vn**, canal for vestibular branch of cranial nerve VIII.

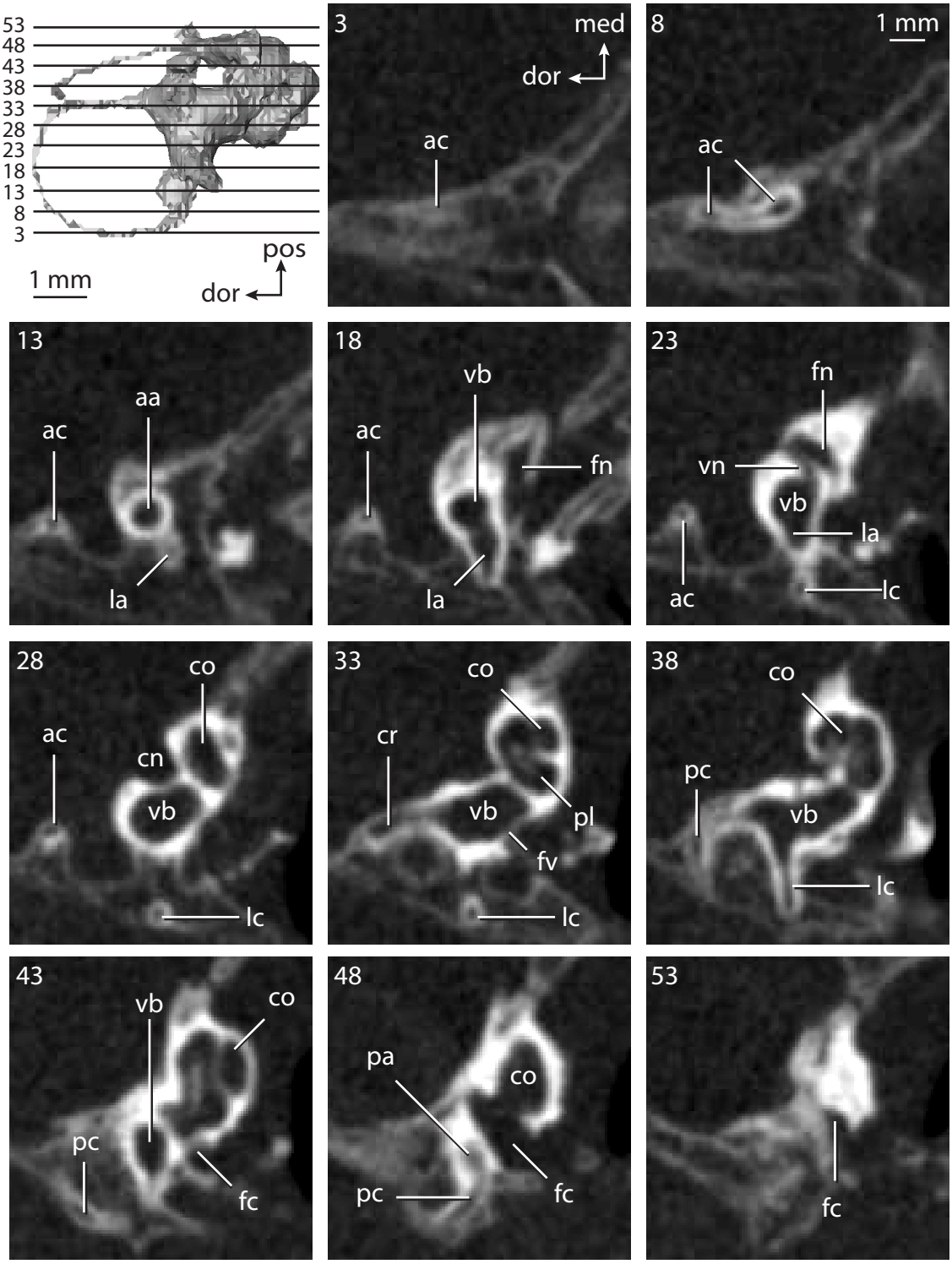
53
48
43
38
33
28
23
18
13
8
3
1 mm
pos
dor
3
med
dor
ac
8
1 mm
ac
13
aa
ac
la
18
vb
ac
fn
la
23
fn
vn
vb
la
ac
lc
28
co
ac
cn
vb
lc
33
co
cr
vb
pl
fv
lc
38
co
pc
vb
lc
43
vb
co
pc
fc
48
pa
co
pc
fc
53
fc

FIGURE 5.52. Bony labyrinth of *Sorex monticolus*. **A**, stereopair and labeled line drawing of digital endocast in anterior view; **B**, stereopair and labeled line drawing of digital endocast in dorsal view; **C**, stereopair and labeled line drawing of digital endocast in lateral view; **D**, line drawing of cochlea viewed down axis of rotation to display degree of coiling; **E**, line drawing of cochlea in profile. Abbreviations: **aa**, anterior ampulla; **ac**, anterior semicircular canal; **ant**, anterior direction; **av**, bony channel for aqueduct of vestibule; **cc**, canaliculus cochleae for aqueduct of cochlea; **co**, cochlea; **cr**, common crus; **dor**, dorsal direction; **er**, elliptical recess of vestibule; **fc**, fenestra cochleae; **fv**, fenestra vestibuli; **la**, lateral ampulla; **lc**, lateral semicircular canal; **med**, medial direction; **pa**, posterior ampulla; **pc**, posterior semicircular canal; **pl**, primary bony lamina; **pos**, posterior direction; **sl**, secondary bony lamina; **sr**, spherical recess of vestibule.

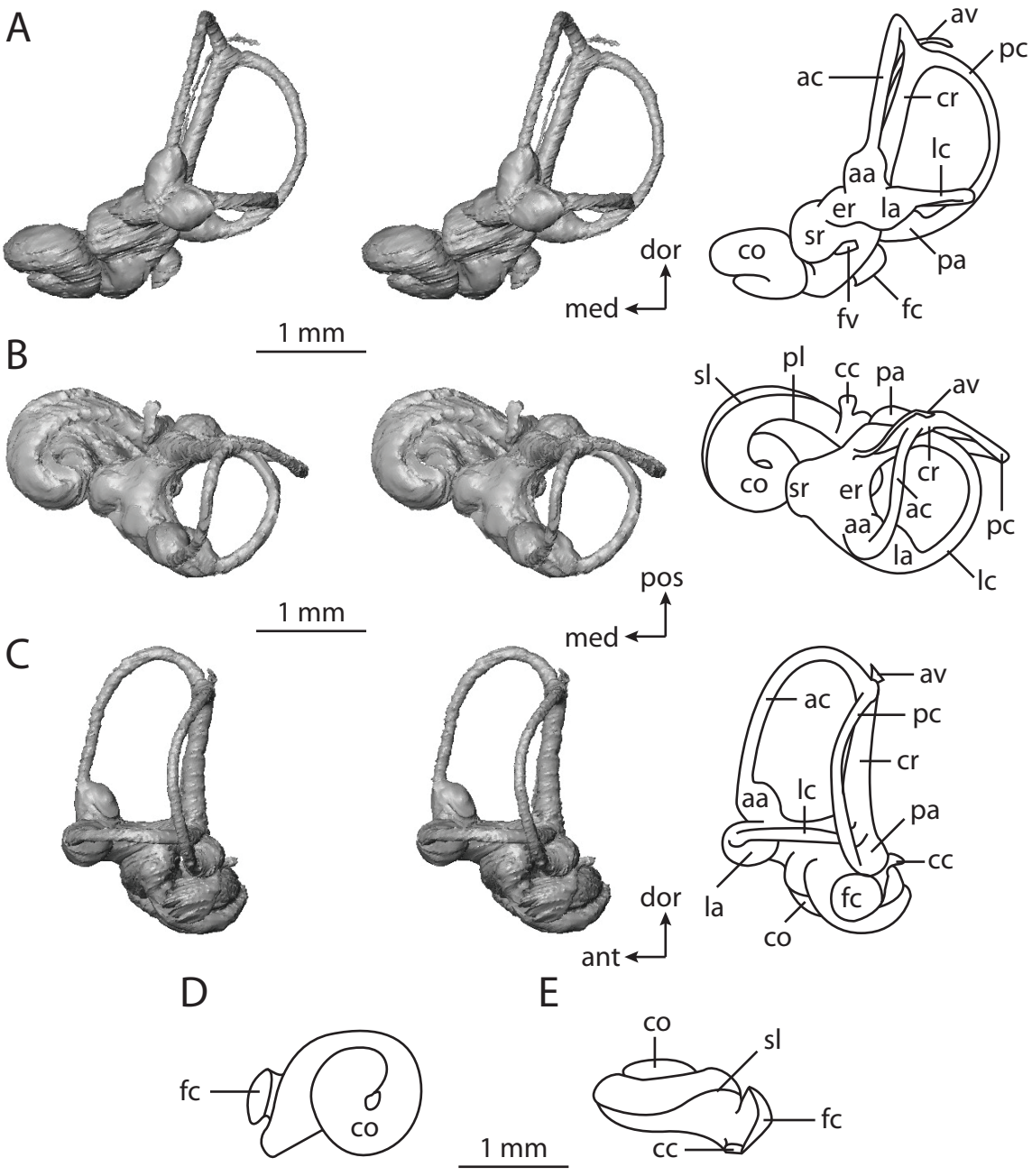
A
av
pc
ac
cr
lc
aa
er
la
sr
co
pa
fv
fc
dor
med
1 mm
B
sl
pl
cc
pa
av
co
sr
er
cr
ac
aa
pc
la
lc
pos
med
1 mm
C
av
ac
pc
cr
aa
lc
pa
cc
la
fc
co
dor
ant
D
fc
co
E
co
sl
fc
cc
1 mm

FIGURE 5.53. CT slices through ear region of *Sorex monticolus*. Abbreviations: **aa**, anterior ampulla; **ac**, anterior semicircular canal; **av**, bony channel for aqueduct of vestibule; **cn**, canal for cranial nerve VIII; **co**, cochlea; **cr**, common crus; **dor**, dorsal direction; **er**, elliptical recess; **fc**, fenestra cochleae; **la**, lateral ampulla; **lat**, lateral direction; **lc**, lateral semicircular canal; **pc**, posterior semicircular canal; **pl**, primary bony lamina; **pos**, posterior direction; **sr**, spherical recess of vestibule; **st**, stapes within fenestra vestibuli; **vb**, vestibule.

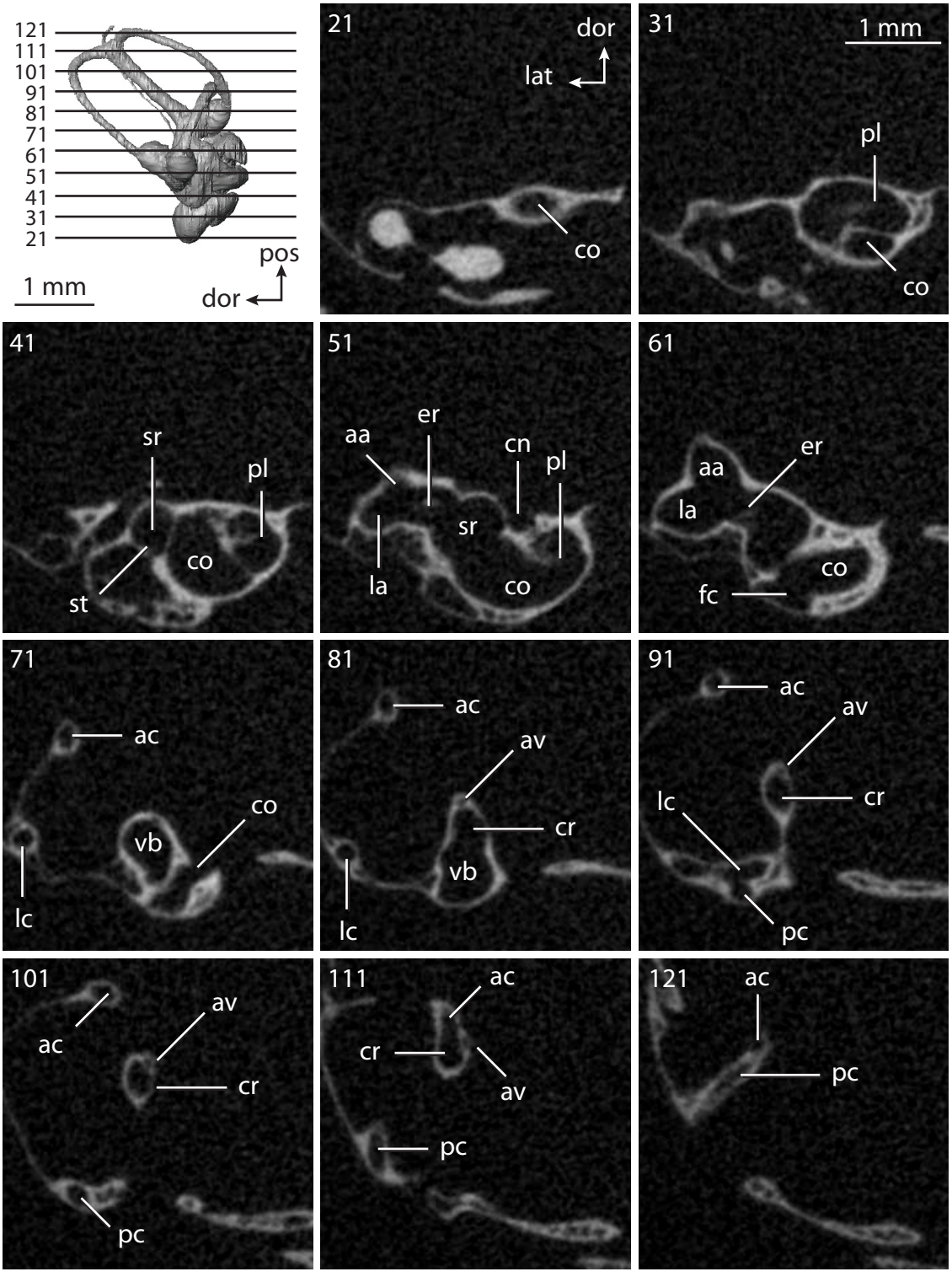
121
111
101
91
81
71
61
51
41
31
21
pos
dor
1 mm
21
dor
lat
co
31
1 mm
pl
co
41
sr
pl
co
st
51
aa
er
cn
pl
sr
la
co
61
er
aa
la
co
fc
71
ac
co
vb
lc
81
ac
av
cr
vb
lc
91
ac
av
cr
lc
pc
101
ac
av
cr
pc
111
ac
cr
av
pc
121
ac
pc

Atelerix is larger than that of *Sorex* (Figure 5.17), both in terms of length (5.46 mm versus 2.81 mm respectively) and volume (4.58 mm versus 0.81 mm^3 respectively). The volume of the cochlear canal of *Atelerix* (2.28 mm^3) is greater than that measured for *Sorex* (0.37 mm^3), although the respective contributions of the cochlea to total inner ear volume (49.7% versus 45.5%) are similar.

Not only is the length of the cochlear canal of *Atelerix* (4.99 mm) longer than that of *Sorex* (2.52 mm), the cochlea of the hedgehog completes a greater degree of coiling (624°) than the shrew (493°). The secondary bony lamina of *Sorex* persists for the first half of the basal turn of the cochlea (179°), whereas the lamina persists for two thirds of the basal turn in *Atelerix* (240°). The aspect ratio of the spiral of the cochlea in profile of *Atelerix* (0.69) is greater than the ratio calculated for *Sorex* (0.47).

The plane of the basal turn of the cochlea forms an angle of 53.8° with the plane for the lateral semicircular canal in *Atelerix*, but an angle of only 9.4° was measured for *Sorex*. The canaliculus cochleae for the aqueduct of the cochlea is 0.77 mm in length in *Atelerix* versus 0.23 mm in *Sorex*. The scala tympani of the cochlea is expanded internal to the fenestra cochleae, leading to the canaliculus in both eulipotyphlan taxa. The expansion in *Atelerix* is elongated, and curves ventrally, forming a hook on the endocast that terminates with the fenestra cochleae. Elongation of the expansion is not observed in *Sorex*.

The fenestra vestibuli of both eulipotyphlan taxa are elliptical, with stapedial ratios (calculated from dimensions of the fenestra) of 1.8 for *Atelerix* and 1.7 for *Sorex*. The vestibules of both taxa are constricted, separating the spherical and elliptical recesses, the latter with anterior and posterior excavations in both *Atelerix* and *Sorex*. The bony channel for the aqueduct of the vestibule opens medial to the vestibular aperture of the common crus in *Atelerix*, but the channel exits the inner ear cavities anterior to the

crus in *Sorex*. The relative lengths of the channels are different between the eulipotyphlans. The channel is very short (0.38 mm in length) and straight in *Atelerix*, although the channel extends for a greater distance in *Sorex*, where the delicate canal parallels the common crus for much of its length before turning posteriorly to open on the external surface of the petrosal. The absolute length of the channel for the aqueduct of the vestibule is 1.58 mm in *Sorex*.

The posterior limb of the lateral semicircular canal opens directly into the vestibule in both taxa, although the vestibular aperture of the canal of *Atelerix* is further separated from the base of the posterior ampulla than the canal in *Sorex*. The lateral canal is positioned high relative to the posterior semicircular canal in both the hedgehog and shrew, particularly in *Atelerix* (sagittal labyrinthine index equals 26.4; index equals 11.9 in *Sorex*).

The angle between the planes of the posterior and lateral semicircular canals (92.1°) is the greatest between canals in *Atelerix*, although the angle between the anterior and posterior canals in the hedgehog labyrinth is not much different (91.7°). The angle between the anterior and lateral canals is significantly more acute (82.2°). The greatest angle in *Sorex* was measured between the anterior and posterior canals (89.6°), but as was measured for *Atelerix*, the angle between the posterior and lateral canals is similar (89.3°). The angle between the anterior and lateral semicircular canals in *Sorex* is 75.3°.

Among the semicircular canals of both eulipotyphlan taxa, the posterior canal *Sorex* deviates the most from its plane (total angular deviation equals 21.2°; deviation in *Atelerix* equals 14.6°). The least planar canal of *Atelerix* is the lateral semicircular canal (18.9°), which does not deviate significantly from its plane in the shrew. The total angular deviation of the anterior canal is 10.6° in *Atelerix* and 7.9° in *Sorex*. The degrees of deviation for the anterior, lateral, and posterior semicircular canals are significant for

Atelerix (ratios of total linear deviation over cross-sectional diameter equal 1.40, 2.00, and 2.22 respectively), but only the posterior canal of *Sorex* exhibits significant deviation (ratio is 1.87; anterior is 0.78; lateral is 0.00).

The arc radius of curvature of the anterior semicircular canal is largest in both *Atelerix* (1.24 mm) and *Sorex* (0.65 mm), although the radius of the posterior arc is similar to that of the anterior in both taxa (1.22 mm for *Atelerix*; 0.63 mm for *Sorex*). The radius of the arc of the lateral semicircular canal is 0.88 mm for *Atelerix* and 0.48 mm in *Sorex*. The anterior semicircular canal of *Atelerix* (5.88 mm) is greater than either the lateral (3.67 mm) or posterior canals (5.80 mm), although the longest canal in *Sorex* is the posterior semicircular canal (3.42 mm; anterior equals 3.20 mm; lateral equals 1.63 mm). The anterior and posterior semicircular canal volumes are the same in *Atelerix* (0.04 mm^3 each), which is a greater value than the lateral canal (0.03 mm^3). The volumes of all of the canals in *Sorex* are identical (0.02 mm^3). The cross-sectional diameters of the anterior and posterior semicircular canals are the same in *Sorex* (0.12 mm), which is a smaller value than that measured for the lateral canal (0.14 mm). The diameter of the anterior canal is largest in *Atelerix* (0.16 mm; lateral and posterior both equal 0.14 mm).

The lateral and posterior semicircular canal arcs of *Atelerix* approach perfect circles (height and width nearly identical) with respective aspect ratios of 0.99 and 0.97 (versus 0.88 and 0.72 in *Sorex*). The ratio of slender canal length to arc radius of the posterior semicircular canal is the greatest in *Sorex* (5.44), and the ratio of the lateral canal is the smallest in the shrew (3.38). The ratio of the lateral canal in *Atelerix* is the smallest (4.15), and the ratio is identical for the anterior and posterior canals (4.74).

No features of the bony labyrinth support monophyly of Eulipotyphla, nor are there any unambiguous characters that unite the eulipotyphlans with the afrosoricids (*Chrysochloris* and *Hemicentetes*). Both *Sorex* and *Atelerix* are derived from the ancestral

eutherian condition in that the lateral semicircular canal enters the vestibule directly rather than forming a secondary common crus with the posterior canal, as well as a high position of the plane of the lateral canal in relation to the ampullar opening of the posterior semicircular canal. Vestibular entry of the lateral canal is inherited from the ancestor of Placentalia. The cochlea of *Atelerix* is derived from the ancestral eutherian in that the aspect ratio of the spiral is high, whereas the cochlea of *Sorex* retains the primitive flattened condition reconstructed for the ancestor of Theria.

The ancestral states of Eulipotyphla include a lateral semicircular canal that opens into the vestibule directly (retained from placental ancestor) and is positioned high compared to the ampullar entrance of the posterior canal (retained from boreoeutherian ancestor), and an anterior semicircular canal arc with the largest radius among the three arcs (retained from therian ancestor). The state of the aspect ratio is reconstructed as equivocal for the ancestor of Eulipotyphla. The cochlea of the most recent common ancestor of *Atelerix* and *Sorex* contributes 50.0% of labyrinthine volume and the cochlear canal coils 622.6°. The low degree of coiling of the ancestral eulipotyphlan either is a retention from its therian ancestor, or else a reversal to a more ancestral morphology.

Euarchontoglires

Euarchontoglires contains the remaining placental mammal clades. Among these are the highly speciose Rodentia, Primates, Lagomorpha, Dermoptera, and Scandentia. Gross dimensions of the bony labyrinths of Euarchontoglires are provided in Table 5.2. Dimensions of the cochlea are provided in Table 5.3, and dimensions and orientations of the semicircular canals are reported in Tables 5.4-5.6.

The states reconstructed for the bony labyrinth of the most recent common ancestor of Euarchontoglires are the same as those for Boreoeutheria. That is, the lateral semicircular canal opens into the vestibule directly in the absence of a secondary common crus, the lateral semicircular canal is positioned high compared to the posterior semicircular canal, and the anterior canal arc is the largest in terms of radius of curvature among the three arcs. The cochlea of the ancestral euarchontoglire coils 956.9°, which is over a quarter of a turn greater than that reconstructed for the ancestral boreoeutherian (815.4°), and the cochlea of Euarchontoglires contributes 53.0% of the total inner ear volume (retained from the ancestor of Boreoeutheria, which had a cochlea contributing 55.0%). An unequivocal state of the aspect ratio of the cochlea could not be reconstructed.

Recognition of a close relationship between rodents and lagomorphs can be traced back to the seminal classification of Linnaeus (1758), in which he also included the rhinoceros (although before 1758, he restricted Glires to rodents and lagomorphs; Linnaeus, 1748). Monophyly of Glires persisted in several later classifications, most notably those of Flower (1883), Gregory (1910), Simpson (1945), and McKenna and Bell (1997). That is not to say that a monophyletic Glires has been free from controversy (see Wood, 1957; Meng and Wyss, 2005). Both morphological (Gidley, 1912; Wood, 1957, 1962; Van Valen, 1971; McKenna, 1975) and molecular investigations (Moody et al., 1949; Easteal, 1990; Stanhope et al., 1992; Porter et al., 1996; Arnason et al., 2002; Misawa and Janke, 2003) have either allied Rodentia or Lagomorpha with various other placental mammal taxa, or else render the groups within Glires paraphyletic with varying levels of robusticity. Despite the ambiguity of rodent and lagomorph affinites in earlier studies, a unified Glires is supported by many recent phylogenetic analyses (Liu et al., 2001; Meng and Wyss, 2001; Murphy et al., 2001a, b; Lin et al., 2002; de Jong et al.,

2003; Meng et al., 2003; Springer et al., 2003; Douzery and Huchon, 2004; Meng, 2004; Asher et al., 2005; Asher, 2007; Bininda-Emonds, 2007; Wible et al., 2007).

The most recent common ancestor of Rodentia and Lagomorpha (Glires) retained a lateral semicircular canal that opened into the vestibule directly in absence of a secondary common crus from Placentalia, a position of the lateral canal high compared to the posterior canal from Boreoeutheria, and the highest arc radius of curvature measured for the anterior semicircular canal arc from Theria. Although the euarchontoglire ancestral state of the aspect ratio of the cochlea was equivocal, the ancestral glire possessed a cochlea with a high aspect ratio, which was shared with Scandentia among the members of Euarchontoglires. The cochlea of the ancestral Glires coiled 923.6°, and the cochlea contributed 55% of the total labyrinthine volume, which was inherited from the ancestral boreoeutherian.

Primates, dermopterans, and scandentians together form the clade Euarchonta (following Beard, 1993; Waddell et al., 1999). However, the results of Bininda-Emonds do not recover a monophyletic Euarchonta. Rather, Scandentia is placed in a polytomy with Glires and a Dermoptera plus Primates clade, which is referred to as Primatomorpha (Figure 5.2). The ancestral labyrinth of Primatomorpha retained an anterior semicircular canal with the greatest arc radius of curvature among the three canal arcs from the ancestral therian, a high position of the lateral semicircular canal from the ancestral boreoeutherian, and a direct vestibular entrance of the lateral semicircular canal from the ancestral placental. The aspect ratio of the cochlea was low for Primatomorpha, which is a unique state within Euarchontoglires.

Rodentia

Rodents make up the most speciose clade of mammals, contributing over 40% of all named extant mammal species (Reeder et al., 2007). The supertree of Bininda-Emonds et al. (2007) depicts Rodentia as a natural clade, although rodent monophyly has been questioned. The results of some phylogenetic analyses based on molecular sequence data support the hypothesis that guinea pigs do not share a common ancestry with other rodent taxa, but rather with Primates and ungulates (Graur et al., 1991, 1992; Li et al., 1992; Ma, 1993; D'Erchia et al., 1996). Despite these analyses, the majority of data, both morphological (Luckett and Hartenberger, 1993; Asher et al., 2003; Meng et al., 2003) and molecular (Cao et al., 1994; Frye and Hedges, 1995; Cao et al., 1997; Huchon et al., 1999; Adkins et al., 2001; Murphy et al., 2001a, b; Huchon et al., 2002), support a monophyletic Rodentia.

The rodents examined in this study are the mouse *Mus musculus* (Figures 5.54-5.55) and the guinea pig *Cavia porcellus* (Figures 5.56-5.57). The bony labyrinth of *Cavia* is larger than that of *Mus*, both in terms of labyrinthine length (22.22 mm versus 1.47 mm) and volume (7.13 mm^3 versus 2.71 mm^3). The dimensions of the inner ear cavities are mirrored by the average body masses of the two species (728 g for *Cavia* and 15.5 g for *Mus*; Silva and Downing, 1995). The volume of the cochlea of *Cavia* (12.26 mm^3) is significantly greater than that measured for *Mus* (0.86 mm^3), although the cochlea forms a greater proportion of the bony labyrinth in the mouse (58.6%) than in the guinea pig (55.2%).

The most noticeable aspect of the bony labyrinth of *Cavia* is the sharp cone formed by the cochlea (Figure 5.56). Not only is the aspect ratio of the cochlea (1.29) twice what is observed in *Mus* (0.62), the ratio of the guinea pig is greater than that calculated for any other mammal discussed here (closest is *Macroscelides* with a ratio of

FIGURE 5.54. Bony labyrinth of *Mus musculus*. **A**, stereopair and labeled line drawing of digital endocast in anterior view; **B**, stereopair and labeled line drawing of digital endocast in dorsal view; **C**, stereopair and labeled line drawing of digital endocast in lateral view; **D**, line drawing of cochlea viewed down axis of rotation to display degree of coiling; **E**, line drawing of cochlea in profile. Abbreviations: **aa**, anterior ampulla; **ac**, anterior semicircular canal; **ant**, anterior direction; **av**, bony channel for aqueduct of vestibule; **cc**, canaliculus cochleae for aqueduct of cochlea; **co**, cochlea; **cr**, common crus; **dor**, dorsal direction; **er**, elliptical recess of vestibule; **fc**, fenestra cochleae; **fv**, fenestra vestibuli; **la**, lateral ampulla; **lc**, lateral semicircular canal; **med**, medial direction; **pa**, posterior ampulla; **pc**, posterior semicircular canal; **pl**, primary bony lamina; **pos**, posterior direction; **ps**, outpocketing for the perilymphatic sac; **sl**, secondary bony lamina; **sr**, spherical recess of vestibule.

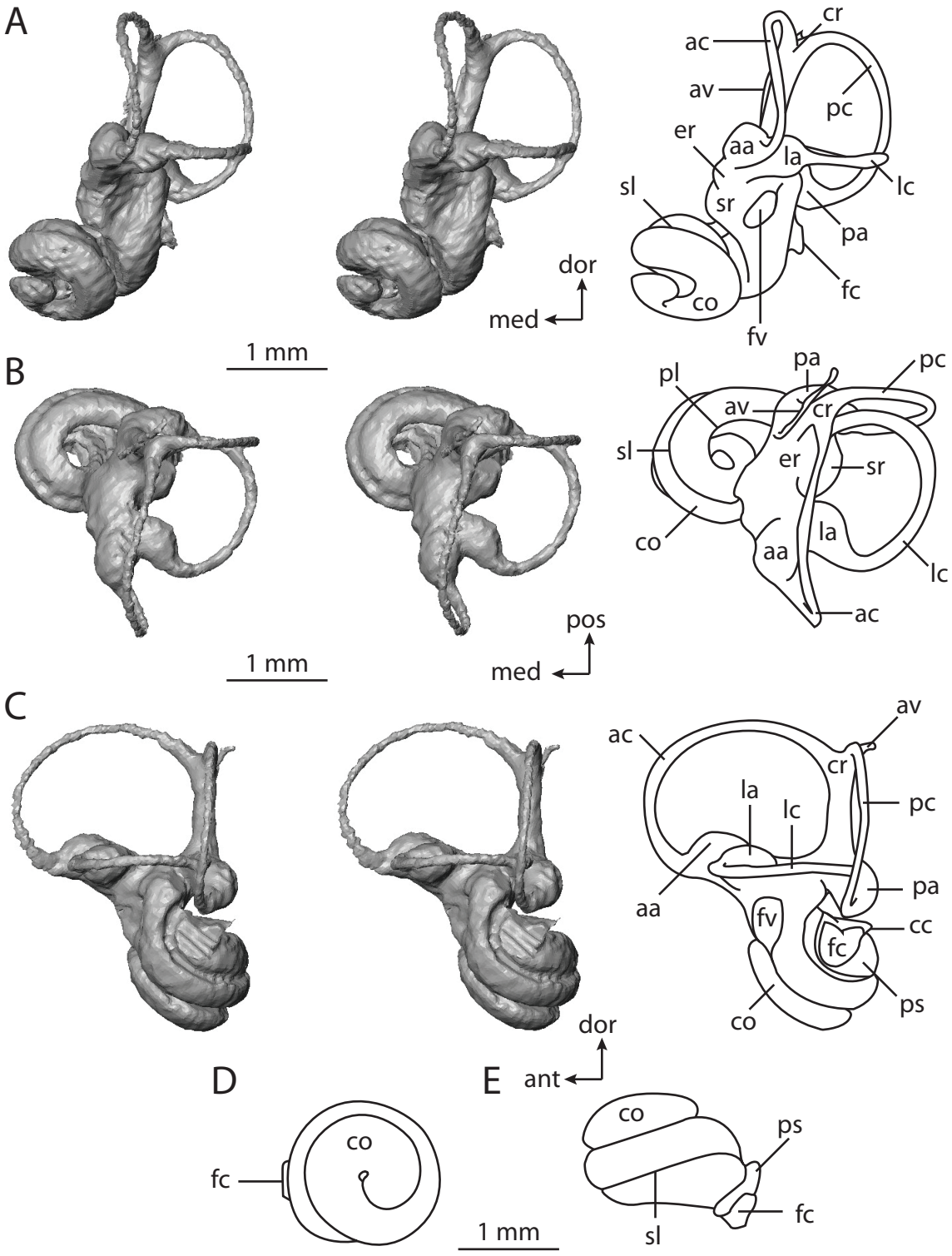
A
cr
ac
av
pc
er
aa
la
lc
sl
sr
pa
fc
co
fv
dor
med
1 mm
B
pa
pc
pl
av
cr
sl
er
sr
co
la
aa
lc
ac
pos
med
1 mm
C
av
ac
cr
la
lc
pc
pa
aa
fv
cc
fc
ps
co
dor
ant
D
co
fc
1 mm
E
co
ps
fc
sl

FIGURE 5.55. CT slices through ear region of *Mus musculus*. Abbreviations: **aa**, anterior ampulla; **ac**, anterior semicircular canal; **av**, bony channel for aqueduct of vestibule; **cn**, canal for cranial nerve VIII; **co**, cochlea; **cr**, common crus; **fc**, fenestra cochleae; **fn**, canal for cranial nerve VII; **fv**, fenestra vestibuli; **la**, lateral ampulla; **lat**, lateral direction; **lc**, lateral semicircular canal; **med**, medial direction; **pa**, posterior ampulla; **pc**, posterior semicircular canal; **pos**, posterior direction; **sa**, subarcuate fossa; **sg**, canal for spiral ganglion within primary bony lamina; **sl**, secondary bony lamina; **vb**, vestibule; **vn**, canal for vestibular branch of cranial nerve VIII.

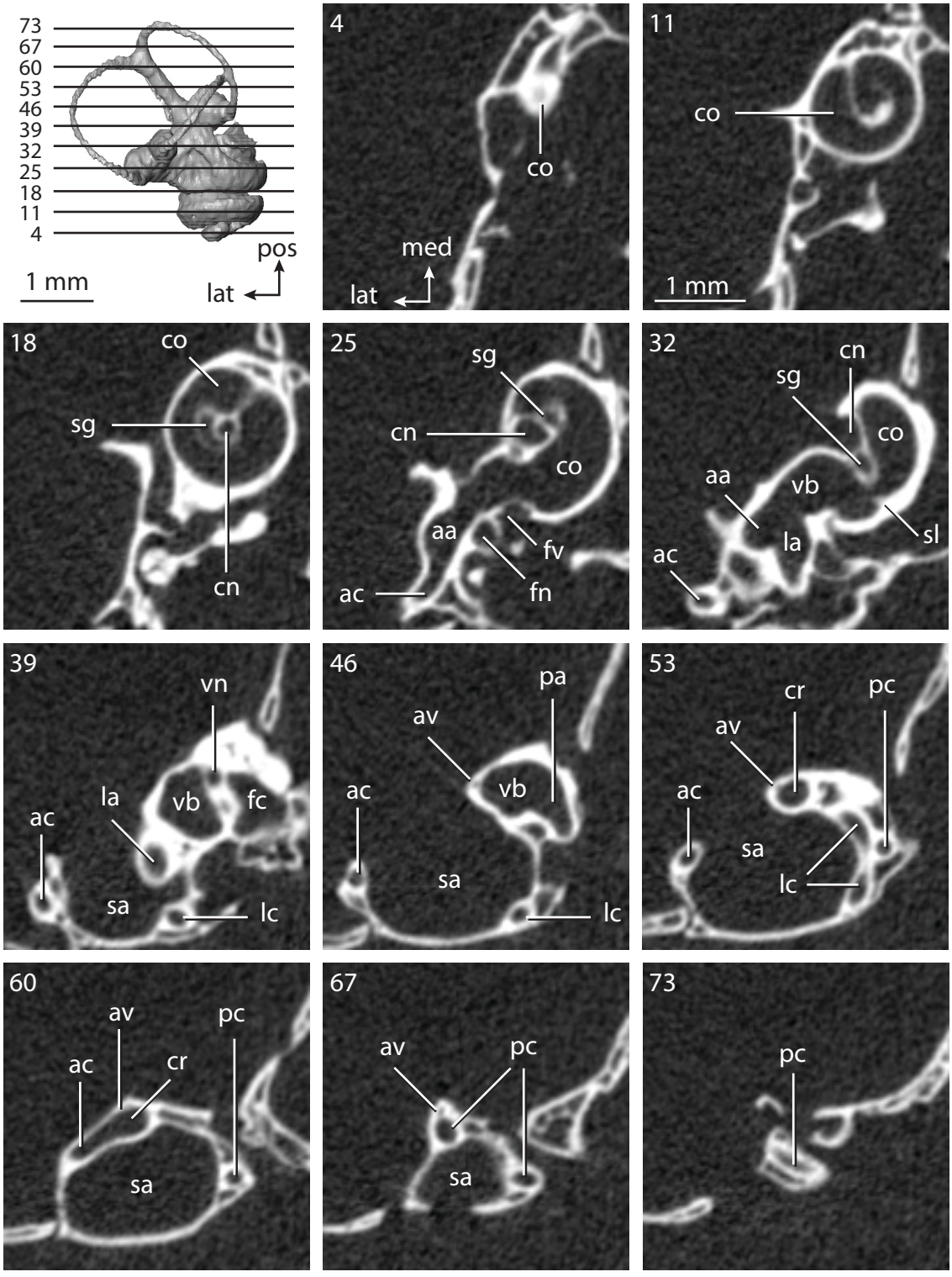
73
67
60
53
46
39
32
25
18
11
4
pos
1 mm
lat
4
co
med
lat
11
co
1 mm
18
co
sg
cn
25
sg
cn
co
aa
fv
ac
fn
32
cn
sg
co
aa
vb
la
sl
ac
39
vn
la
vb
fc
ac
sa
lc
46
pa
av
ac
vb
sa
lc
53
cr
pc
av
ac
sa
lc
60
av
pc
ac
cr
sa
67
av
pc
sa
73
pc

FIGURE 5.56. Bony labyrinth of *Cavia porcellus*. **A**, stereopair and labeled line drawing of digital endocast in anterior view; **B**, stereopair and labeled line drawing of digital endocast in dorsal view; **C**, stereopair and labeled line drawing of digital endocast in lateral view; **D**, line drawing of cochlea viewed down axis of rotation to display degree of coiling; **E**, line drawing of cochlea in profile. Abbreviations: **aa**, anterior ampulla; **ac**, anterior semicircular canal; **ant**, anterior direction; **av**, bony channel for aqueduct of vestibule; **cc**, canaliculus cochleae for aqueduct of cochlea; **co**, cochlea; **cr**, common crus; **dor**, dorsal direction; **er**, elliptical recess of vestibule; **fc**, fenestra cochleae; **fv**, fenestra vestibuli; **la**, lateral ampulla; **lc**, lateral semicircular canal; **med**, medial direction; **pa**, posterior ampulla; **pc**, posterior semicircular canal; **pl**, primary bony lamina; **pos**, posterior direction; **ps**, outpocketing for the perilymphatic sac; **sl**, secondary bony lamina; **sr**, spherical recess of vestibule.

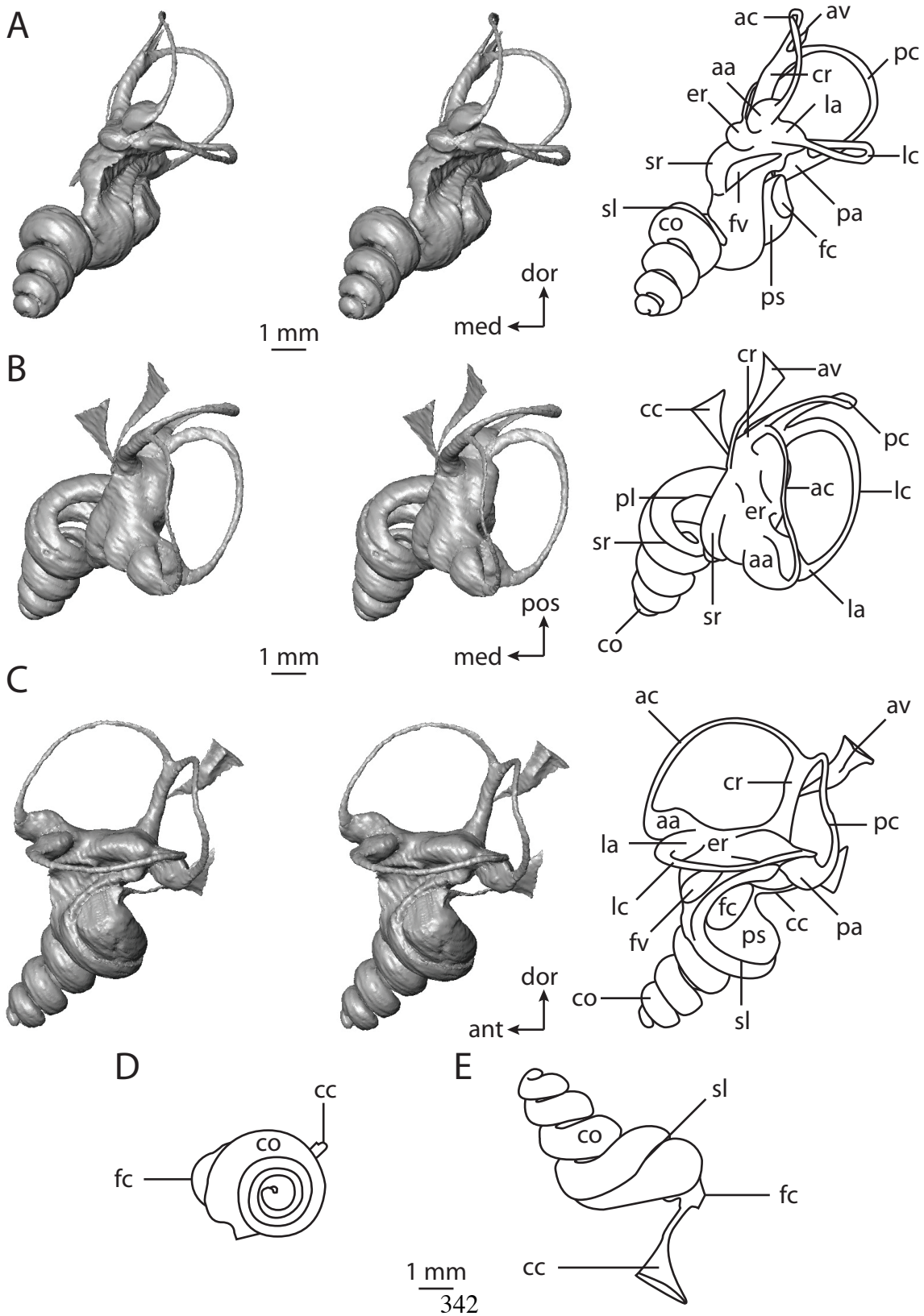
A
ac
av
pc
aa
cr
er
la
lc
sr
sl
co
fv
pa
fc
ps
dor
med
1 mm
B
cr
av
cc
pc
pl
ac
lc
er
sr
aa
la
sr
co
pos
med
1 mm
C
ac
av
cr
aa
pc
la
er
lc
fc
cc
pa
fv
ps
co
sl
dor
ant
D
cc
co
fc
E
sl
co
fc
cc
1 mm

FIGURE 5.57. CT slices through ear region of *Cavia porcellus*. Abbreviations: **aa**, anterior ampulla; **ac**, anterior semicircular canal; **av**, bony channel for aqueduct of vestibule; **cc**, canaliculus cochleae for aqueduct of cochlea; **cn**, canal for cranial nerve VIII; **co**, cochlea; **cr**, common crus; **dor**, dorsal direction; **fc**, fenestra cochleae; **fn**, canal for cranial nerve VII; **la**, lateral ampulla; **lc**, lateral semicircular canal; **med**, medial direction; **pa**, posterior ampulla; **pc**, posterior semicircular canal; **pl**, primary bony lamina; **pos**, posterior direction; **sa**, subarcuate fossa; **sg**, canal for spiral ganglion within primary bony lamina; **sr**, spherical recess of vestibule; **st**, stapes within fenestra vestibuli; **vn**, canal for vestibular branch of cranial nerve VIII.

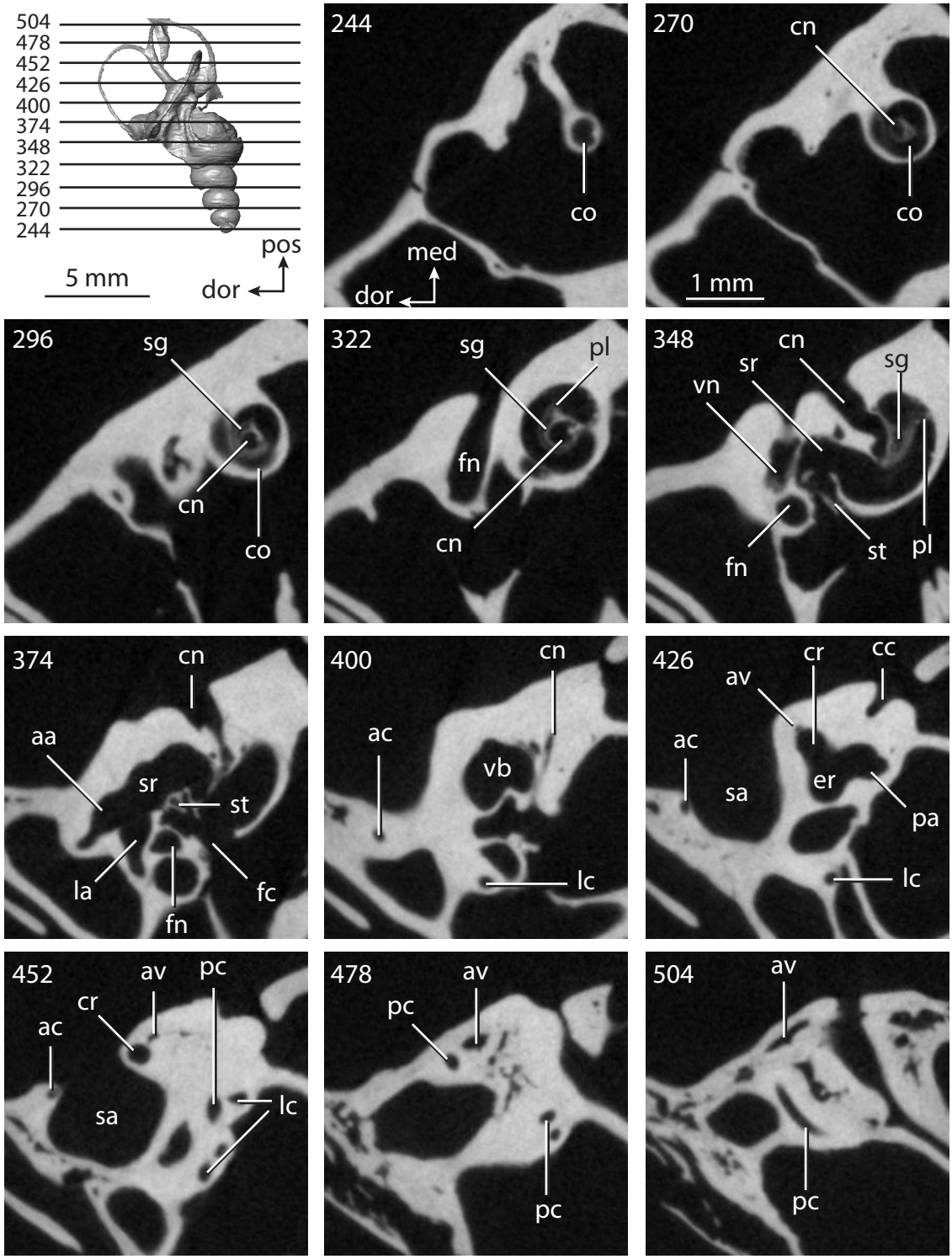
504
478
452
426
400
374
348
322
296
270
244
pos
5 mm
dor
244
co
med
dor
270
cn
co
1 mm
296
sg
cn
co
322
sg
pl
fn
cn
348
cn
sr
sg
vn
fn
st
pl
374
cn
aa
sr
st
la
fc
fn
400
cn
ac
vb
lc
426
av
cr
cc
ac
sa
er
pa
lc
452
av
pc
cr
ac
sa
lc
478
av
pc
pc
504
av
pc

0.80). The cochlea of *Cavia* coils to a much greater degree than any other mammal studied here (1457.1°), completing over four whorls. Even the highly coiled cochlea of *Procavia capensis* only coils three and three quarters turns (see Figure 5.16). The cochlea of *Mus* coils to 627.7°, and the length of the cochlear canal is 3.87 mm (13.43 mm for *Cavia*).

The scala tympani is expanded interior to the fenestra cochleae in both taxa. The expansion leads to the canaliculus cochleae for the aqueduct of the cochlea. The canaliculus is a short and straight tube in *Mus* (0.17 mm in length), but the slender canal of *Cavia* (2.52 mm in length) is gently curved and ends in a triangular shaped fissure. The plane of the basal turn of the cochlea deviates from the plane of the lateral semicircular canal to a greater degree in *Cavia* (35.1°) than in *Mus* (10.8°).

The bony vestibule of *Mus* is not divided into the spherical and elliptical recesses, although an excavation at the anterior end of the vestibule, which is expressed as a bulbous pedestal in the endocast, for the posterior ampulla, common crus, and posterior limb of the lateral semicircular canal is present in the mouse. The vestibule is subdivided into the spherical and elliptical recesses by a constriction interior to the fenestra vestibuli in *Cavia*. The fenestra vestibuli is elliptical in the guinea pig, with a stapedial ratio of 2.9 (ratio in *Mus* equals 1.9), which is expressed as an oblong depression in the spherical recess on the endocast. Both the spherical and elliptical recesses are elongate cavities.

Unlike *Mus*, the common crus and posterior ampulla of *Cavia* do not empty into a posterior extension of the vestibule. The bony channel for the aqueduct of the vestibule exits the inner ear anterior to the medial edge of the vestibular aperture of the common crus in both taxa (length equals 3.82 mm in *Cavia*; 1.28 mm in *Mus*). The posterior limb of the lateral semicircular canal opens directly into the vestibule anterior to the posterior ampulla in both rodents. The plane of the lateral canal is positioned dorsal relative to the

posterior semicircular canal, in both *Cavia* and *Mus* (sagittal labyrinthine indices equal 25.3 and 25.8 respectively).

The planes of the anterior and posterior semicircular canals in *Cavia* form an angle of 105° (angle equals 94.4° in *Mus*), which is the greatest angle measured between any two canals measured for both rodent species. The planes of the anterior and lateral semicircular canals in *Cavia* form an angle of 77.2° (88.8° for *Mus*), which is the smallest angle measured between any two canals measured for both rodents. The angle measured between the posterior and lateral semicircular canals is 85.5° for *Cavia* and 95.6° for *Mus*. The semicircular canals of *Cavia* are less planar than the canals of *Mus*, especially the posterior canal, which deviates from its plane by a total of 30.7° in *Cavia* (ratio of total linear deviation over cross-sectional diameter is 3.13; angular deviation is 3.4° and ratio is 1.16 in *Mus*). The lateral semicircular canal of *Mus* is the most planar canal in either taxon, with a total angular deviation of 1.9° (ratio is 0.13; angular deviation is 15.8° and ratio is 1.49 for *Cavia*). The total angular deviation of the anterior semicircular canal from its plane is 19.1° for *Cavia* (ratio is 0.31) and 13.3° for *Mus* (ratio is 3.10).

The anterior semicircular canal is the largest in terms of arc radius of curvature and slender canal length for both rodents (1.88 mm and 9.01 mm respectively for *Cavia*; 0.78 mm and 3.86 mm for *Mus*), and the lateral canal is the smallest for the same dimensions (1.57 mm and 6.49 mm for *Cavia*; 0.60 mm and 2.48 mm for *Mus*). The arc radius and length of the posterior semicircular canal are 1.63 mm and 8.18 mm respectively for *Cavia*, and 0.67 mm and 3.60 mm for *Mus*. The cross-sectional diameter of the anterior semicircular canal of *Mus* (0.16 mm) is greater than the lateral (0.15 mm) and posterior canals (0.13 mm), but the diameter of the lateral canal of *Cavia* (0.29 mm) is greater than the anterior (0.21 mm) and posterior semicircular canals (0.28 mm).

Both the largest and smallest semicircular canal arc aspect ratios were measured for the arcs of *Cavia*. The largest semicircular canal arc aspect ratio in *Cavia* is observed in the posterior canal (0.99; ratio equals 0.75 in *Mus*), and the smallest ratio is observed in the lateral semicircular canal for the guinea pig (0.49; ratio equals 0.92 in *Mus*). The aspect ratio of the anterior semicircular canal is 0.75 in *Cavia* and 0.67 in *Mus*. The ratio of the slender canal length to arc radius of the posterior semicircular canal is the greatest for both species (5.02 for *Cavia*; 5.39 for *Mus*), and the ratio is the smallest in the lateral canal (4.13 for *Cavia*; 4.12 for *Mus*). The canal length to arc radius ratio of the anterior semicircular canal is 4.79 for *Cavia* and 4.98 for *Mus*.

The labyrinths of *Cavia* and *Mus* retain the ancestral condition reconstructed for Theria in that the largest semicircular arc radius is observed in the anterior canal. Further, the labyrinth of the ancestor of Rodentia retained the ancestral placental entry of the lateral canal (into the vestibule directly), the ancestral boreoeutherian position of the lateral semicircular canal (high compared to the posterior canal), and the ancestral glire cochlear aspect ratio (high). The cochlea of the rodent ancestor coiled 1002.8° (close to 1013.1° reconstructed for the most recent common ancestor of Cetacea plus *Sus*) and contributed 56.0% of the total labyrinthine volume (close to 55.0% contribution of the cochlea of Boreoeutheria).

Lagomorpha

Lagomorphs (rabbits and pikas) are classically allied with rodents (proposed as far back as Linnaeus, 1748) and the majority of recent phylogenetic analyses support this hypothesis (e.g., Liu et al., 2001; Murphy et al., 2001a, b; Meng et al., 2003; Wible et al., 2007). However, Lagomorpha has been united with ungulates (Gidley, 1912; Moody et al., 1949; Wood, 1957) and other placental clades (Misawa and Janke, 2003). Given the

predominance of data supporting a clade exclusive to rodents and lagomorphs (Glires), such a relationship is accepted here.

Two lagomorph species examined here were *Lepus californicus* (Figures 5.58-5.59) and *Sylvilagus floridanus* (Figures 5.60-5.61). The bony labyrinth of *Lepus* is the most voluminous (24.27 mm^3 versus 11.32 mm^3) and longest (7.39 mm versus 5.82 mm). The black-tailed jackrabbit (*Lepus*) is a larger species overall than the eastern cottontail (*Sylvilagus*), with an average body mass of 2.35 kg for the species, versus 1.16 kg for *Sylvilagus* (Silva and Downing, 1995). The volume of the cochlea of *Lepus* (13.07 mm^3) is over twice that measured for *Sylvilagus* (6.26 mm^3), although the relative contribution that the cochlea of each species to total labyrinthine volume is comparable between the species (53.9% for *Lepus*; 55.3% for *Sylvilagus*).

The length of the cochlear canal of *Lepus* (8.80 mm) is slightly larger than that of *Sylvilagus* (8.75 mm), although the cochlea of the cottontail coils to a greater degree than the jackrabbit (817° versus 693°). Likewise, the secondary bony lamina extends a greater relative distance along the radial wall of the of the cochlea in *Sylvilagus* (200°) than in *Lepus* (147°), and the aspect ratio of the cochlea of *Sylvilagus* (0.71) is greater than that calculated for *Lepus* (0.64). The apical turns of the cochleae of both lagomorphs sit upon the basal whorl, as is observed in *Mus musculus* and *Cavia porcellus*, and the plane of the basal turn of the cochlea forms a similar angle with the plane of the lateral semicircular canal in both *Lepus* (40.6°) and *Sylvilagus* (40.3°). The scala tympani of the cochlea is expanded internal to the fenestra cochleae, which leads to a robust canaliculus cochleae in each species. The canaliculus of *Lepus* (4.80 mm in length) forms a straight tube that is subcircular in cross-section, but the bony canal is flattened and curves ventrally in *Sylvilagus*.

FIGURE 5.58. Bony labyrinth of *Lepus californicus*. **A**, stereopair and labeled line drawing of digital endocast in anterior view; **B**, stereopair and labeled line drawing of digital endocast in dorsal view; **C**, stereopair and labeled line drawing of digital endocast in lateral view; **D**, line drawing of cochlea viewed down axis of rotation to display degree of coiling; **E**, line drawing of cochlea in profile. Abbreviations: **aa**, anterior ampulla; **ac**, anterior semicircular canal; **ant**, anterior direction; **av**, bony channel for aqueduct of vestibule; **cc**, canaliculus cochleae for aqueduct of cochlea; **co**, cochlea; **cr**, common crus; **dor**, dorsal direction; **er**, elliptical recess of vestibule; **fc**, fenestra cochleae; **fv**, fenestra vestibuli; **la**, lateral ampulla; **lc**, lateral semicircular canal; **med**, medial direction; **pa**, posterior ampulla; **pc**, posterior semicircular canal; **pl**, primary bony lamina; **pos**, posterior direction; **ps**, outpocketing for the perilymphatic sac; **sl**, secondary bony lamina; **sr**, spherical recess of vestibule.

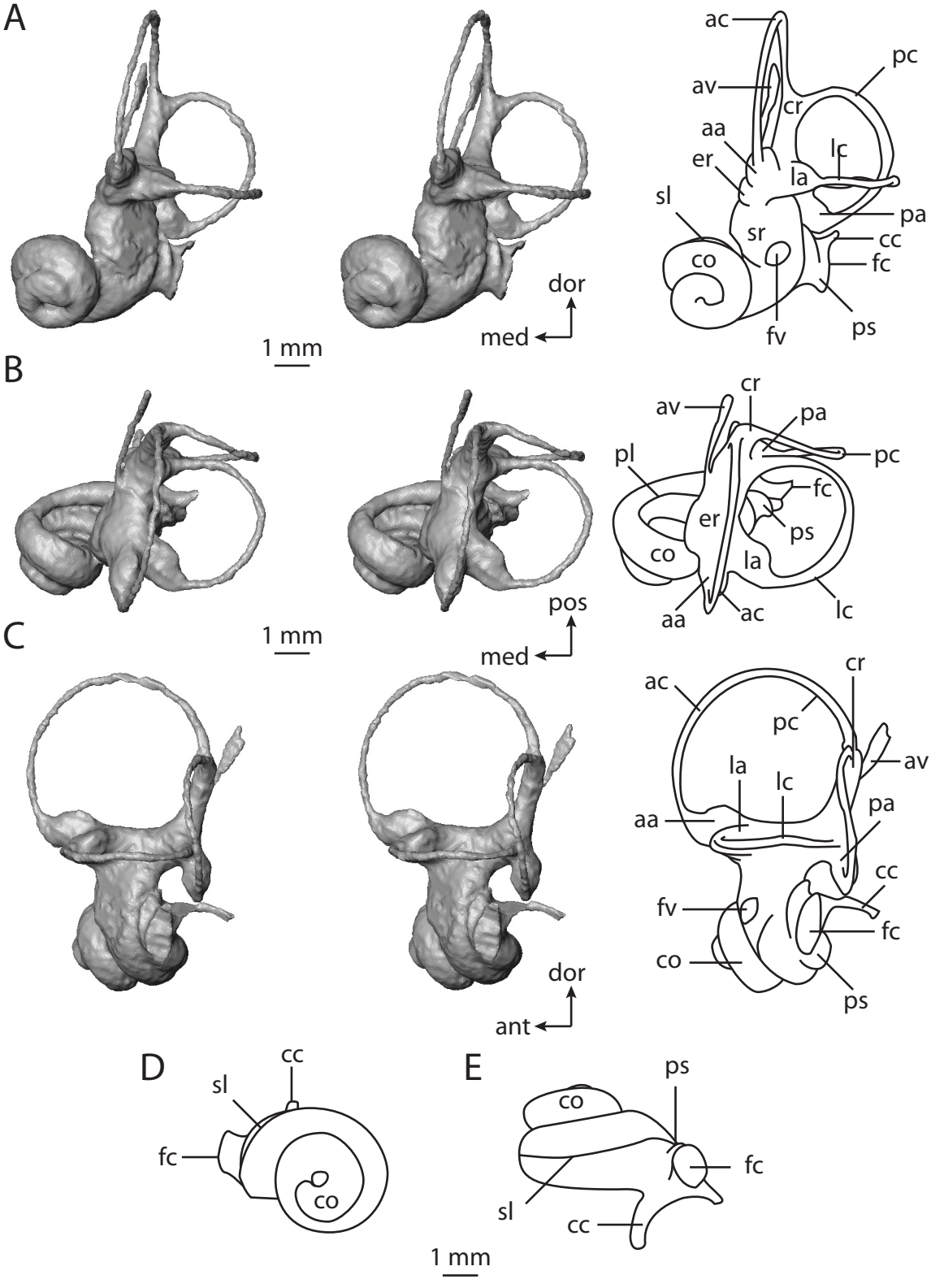
A
ac
pc
av
cr
aa
er
lc
la
sl
pa
sr
cc
co
fc
fv
ps
dor
med
1 mm
B
cr
av
pa
pl
pc
fc
er
ps
co
la
aa
ac
lc
pos
med
1 mm
C
cr
ac
pc
av
la
lc
aa
pa
cc
fv
fc
co
ps
dor
ant
D
cc
sl
fc
co
E
ps
co
fc
sl
cc
1 mm

FIGURE 5.59. CT slices through ear region of *Lepus californicus*. Abbreviations: **aa**, anterior ampulla; **ac**, anterior semicircular canal; **av**, bony channel for aqueduct of vestibule; **cc**, canaliculus cochleae for aqueduct of cochlea; **cn**, canal for cranial nerve VIII; **co**, cochlea; **cr**, common crus; **dor**, dorsal direction; **fc**, fenestra cochleae; **fn**, canal for cranial nerve VII; **la**, lateral ampulla; **lc**, lateral semicircular canal; **med**, medial direction; **pa**, posterior ampulla; **pc**, posterior semicircular canal; **pl**, primary bony lamina; **pos**, posterior direction; **sa**, subarcuate fossa; **sl**, secondary bony lamina; **st**, stapes within fenestra vestibuli; **vb**, vestibule.

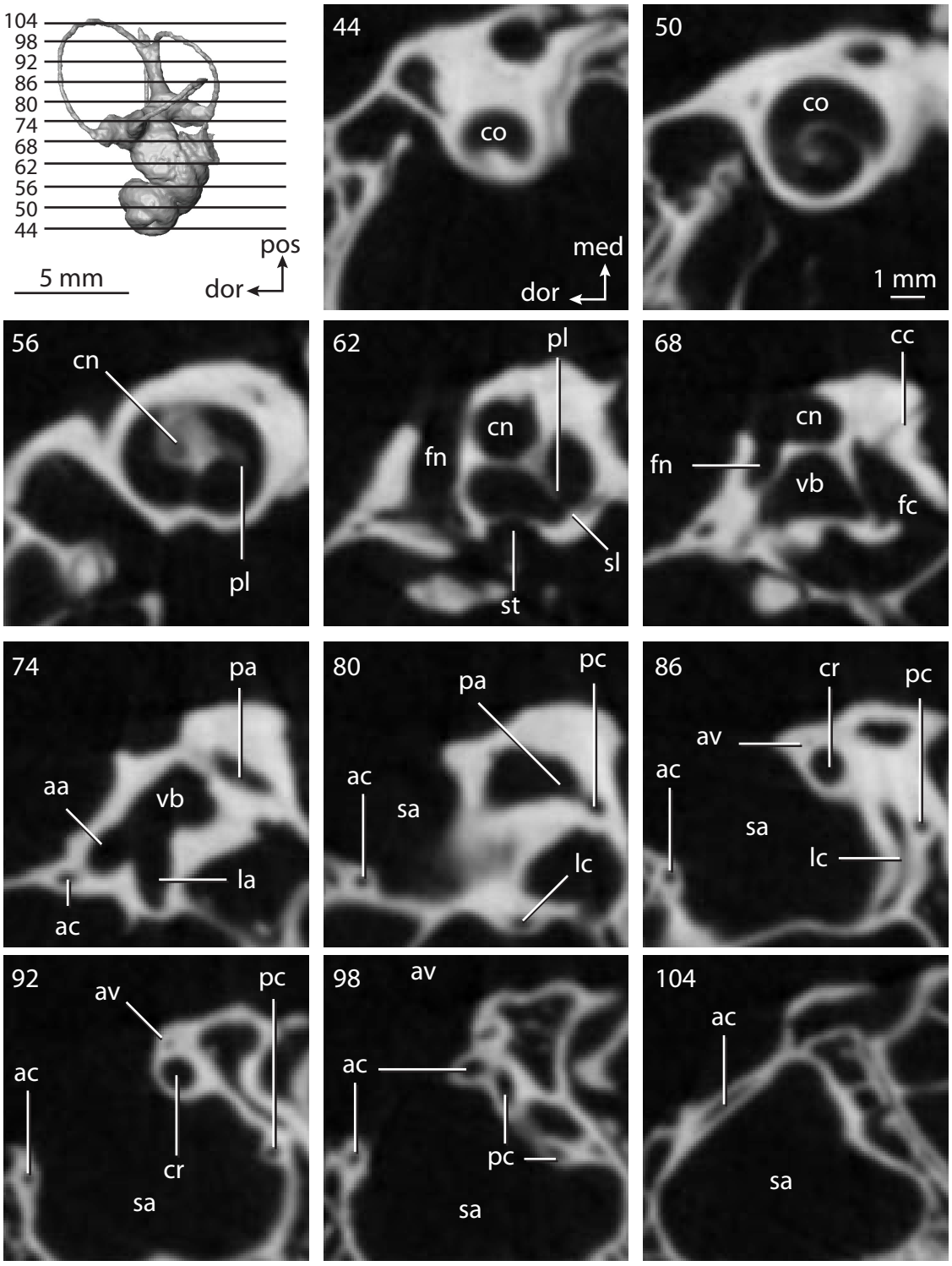
104
98
92
86
80
74
68
62
56
50
44
5 mm
pos
dor
44
co
med
dor
50
co
1 mm
56
cn
pl
62
pl
cn
fn
sl
st
68
cc
cn
fn
vb
fc
74
pa
aa
vb
la
ac
80
pa
pc
ac
sa
lc
86
cr
pc
av
ac
sa
lc
92
av
pc
ac
cr
sa
98
av
ac
pc
sa
104
ac
sa

FIGURE 5.60. Bony labyrinth of *Sylvilagus floridanus*. **A**, stereopair and labeled line drawing of digital endocast in anterior view; **B**, stereopair and labeled line drawing of digital endocast in dorsal view; **C**, stereopair and labeled line drawing of digital endocast in lateral view; **D**, line drawing of cochlea viewed down axis of rotation to display degree of coiling; **E**, line drawing of cochlea in profile. Abbreviations: **aa**, anterior ampulla; **ac**, anterior semicircular canal; **ant**, anterior direction; **av**, bony channel for aqueduct of vestibule; **cc**, canaliculus cochleae for aqueduct of cochlea; **co**, cochlea; **cr**, common crus; **dor**, dorsal direction; **er**, elliptical recess of vestibule; **fc**, fenestra cochleae; **fv**, fenestra vestibuli; **la**, lateral ampulla; **lc**, lateral semicircular canal; **med**, medial direction; **pa**, posterior ampulla; **pc**, posterior semicircular canal; **pl**, primary bony lamina; **pos**, posterior direction; **ps**, outpocketing for the perilymphatic sac; **sl**, secondary bony lamina; **sr**, spherical recess of vestibule.

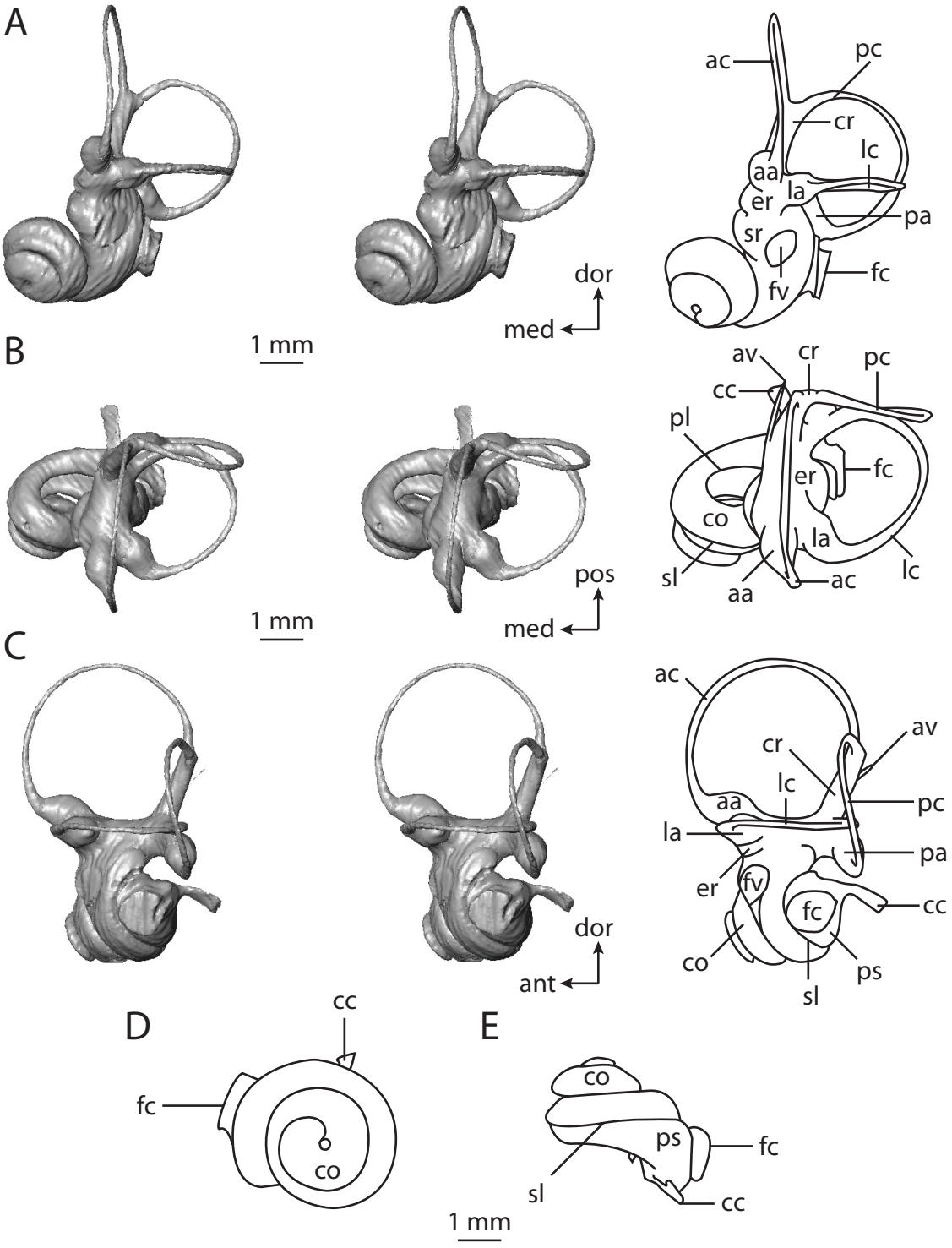
A
ac
pc
cr
lc
aa
la
er
pa
sr
fc
fv
dor
med
1 mm
B
av
cr
pc
cc
pl
fc
er
co
la
sl
aa
ac
lc
pos
med
1 mm
C
ac
av
cr
lc
pc
aa
la
pa
er
fv
fc
cc
co
ps
sl
dor
ant
D
cc
fc
co
E
co
ps
fc
sl
cc
1 mm

FIGURE 5.61. CT slices through ear region of *Sylvilagus floridanus*. Abbreviations: **aa**, anterior ampulla; **ac**, anterior semicircular canal; **av**, bony channel for aqueduct of vestibule; **cc**, canaliculus cochleae for aqueduct of cochlea; **cn**, canal for cranial nerve VIII; **co**, cochlea; **cr**, common crus; **dor**, dorsal direction; **fc**, fenestra cochleae; **fn**, canal for cranial nerve VII; **fv**, fenestra vestibuli; **la**, lateral ampulla; **lc**, lateral semicircular canal; **med**, medial direction; **pa**, posterior ampulla; **pc**, posterior semicircular canal; **pl**, primary bony lamina; **pos**, posterior direction; **sa**, subarcuate fossa; **sg**, canal for spiral ganglion within primary bony lamina; **sl**, secondary bony lamina; **sr**, spherical recess of vestibule; **st**, stapes within fenestra vestibuli; **vb**, vestibule; **vn**, canal for vestibular branch of cranial nerve VIII.

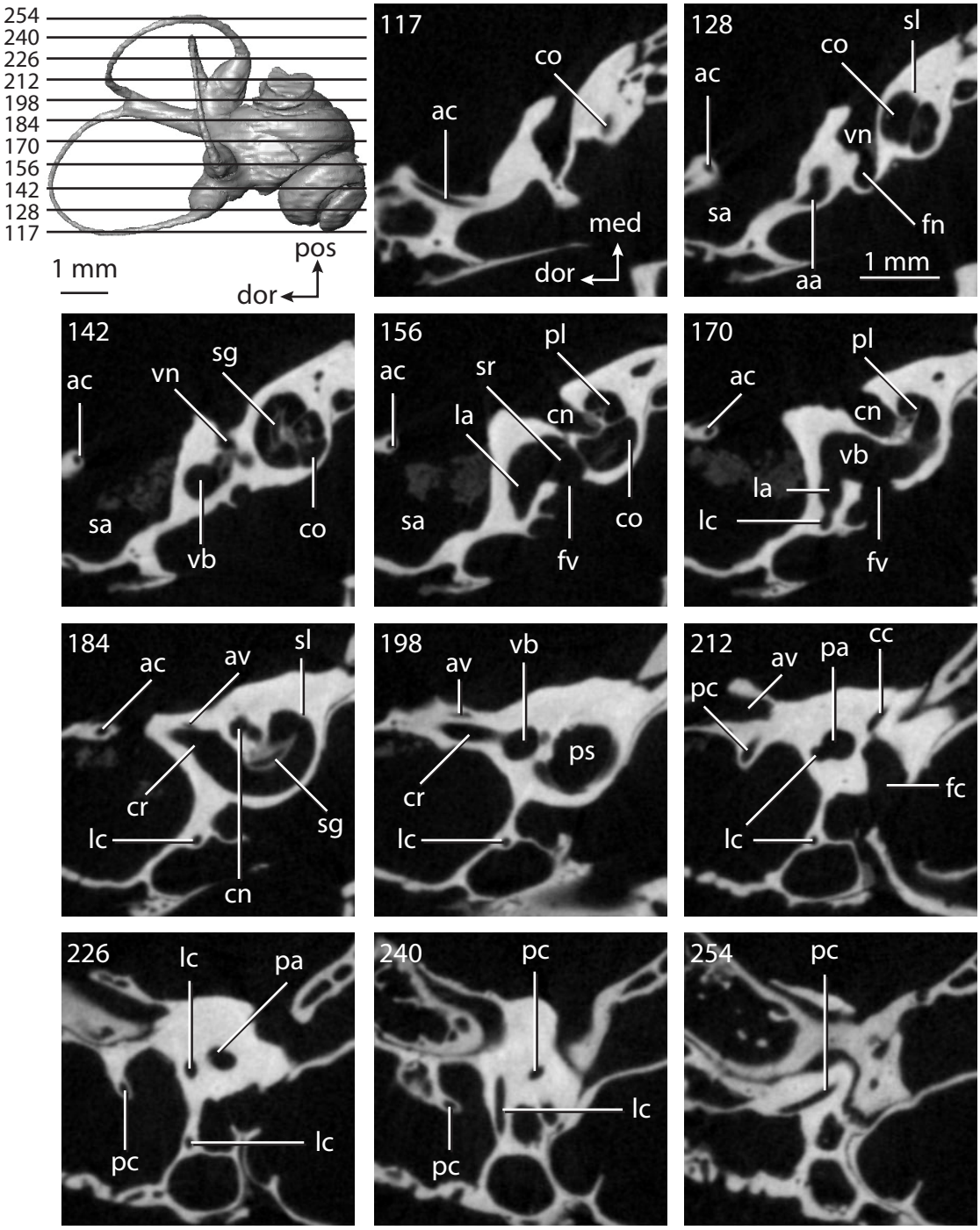
254
240
226
212
198
184
170
156
142
128
117
1 mm
pos
dor
117
co
ac
med
dor
128
sl
co
ac
vn
sa
fn
aa
1 mm
142
sg
vn
ac
sa
co
vb
156
pl
sr
ac
la
cn
sa
co
fv
170
pl
ac
cn
vb
la
lc
fv
184
ac
av
sl
cr
sg
lc
cn
198
av
vb
ps
cr
lc
212
av
pa
cc
pc
fc
lc
226
lc
pa
pc
lc
240
pc
lc
pc
254
pc

The fenestrae vestibuli are less elliptical in the lagomorphs (stapedial ratio equals 1.7 for *Lepus*; ratio equals 1.5 for *Sylvilagus*) than for the rodents (*Mus* equals 1.9; *Cavia* equals 2.9), but they are not as round as the fenestra of the microchiropteran bat *Nycteris grandis* (1.0). A gentle constriction of the vestibule divides the spherical and elliptical recesses in both *Lepus* and *Sylvilagus*, where the elliptical recesses of the lagomorphs are elongated with distinct excavations at the anterior and posterior ends (expressed as pedestals for the ampullae of the semicircular canals on the endocasts).

The bony channel for the aqueduct of the vestibule exits the inner ear cavities medial to the vestibular aperture of the common crus. The channel is a delicate passage in *Sylvilagus*, and it does not end as a flattened fissure as in most other mammals, including *Lepus*. The channel is longer in *Lepus* than it is in *Sylvilagus*, both in terms of absolute length (3.71 mm versus 2.08 mm) and length relative to the common crus (channel terminates ventral to the apex of the common crus in *Sylvilagus*, but dorsal to the top of the crus in *Lepus*).

The lateral semicircular canal opens directly into the vestibule dorsal to the posterior ampulla in both lagomorphs, giving the plane of the lateral canal a dorsal position in relation to the posterior semicircular canal (sagittal labyrinthine index equals 32.4 in *Lepus*; index equals 33.9 in *Sylvilagus*). The level of the lateral semicircular canal compared to the posterior canal in the lagomorphs is similar to that observed in *Macroscelides proboscideus* (index equals 32.7), where the lateral canal divides the arc of the posterior canal when the labyrinth is viewed anteriorly.

The planes of the anterior and posterior semicircular canals form the greatest angle between canals in both *Lepus* (94.0°) and *Sylvilagus* (97.5°). The smallest angle between canals in *Lepus* was measured between the anterior and lateral semicircular canals (84.2°; angle equals 92.7° in *Sylvilagus*), and the smallest angle measured within

the labyrinth of *Sylvilagus* is between the posterior and lateral canals (77.9°; angle equals 88.6° in *Lepus*). The posterior semicircular canal is the least planar canal in both taxa, where the canal of *Sylvilagus* deviates from its plane to a greater degree than that of *Lepus* (25.3° versus 10.9°). The posterior canal of *Sylvilagus* deviates to a significant degree (ratio of linear deviation over cross-sectional diameter is 3.79), as does the posterior canal of *Lepus* (ratio is 1.09). The lateral semicircular canal of *Lepus* is the most planar among all of the canals between the two species, with a total angular deviation of only 2.1° (canal deviates by 5.3° in *Sylvilagus*). The deviation is not significant for either species (ratio of 0.24 for *Lepus*; 0.51 for *Sylvilagus*). The anterior semicircular canal deviates from its average plane by a total of 3.9° in *Lepus* and 5.0° in *Sylvilagus*. However, only the anterior canal of *Sylvilagus* deviates to a significant degree (ratio is 1.28; 0.59 for *Lepus*).

The arc of the anterior semicircular canal not only has the greatest radius of curvature in both *Lepus* (2.34 mm; radius of lateral equals 1.66 mm; radius of posterior equals 1.69 mm) and *Sylvilagus* (1.86 mm; radius of lateral equals 1.29; radius of posterior equals 1.44 mm), but the slender canal length of the anterior semicircular canal in both *Lepus* (11.45 mm) and *Sylvilagus* (8.98 mm) is greater than either the lateral (6.86 mm and 5.65 mm respectively) or posterior canal (8.10 mm and 7.38 mm respectively). Likewise, the volume of the anterior semicircular canal of *Lepus* (0.32 mm^3) is greater than either the lateral (0.25 mm^3) or posterior canals (0.24 mm^3), although the most voluminous canal within the labyrinth of *Sylvilagus* is the lateral semicircular canal (0.19 mm^3 versus 0.16 mm^3 for the anterior and 0.14 mm^3 for the posterior canals). The cross-sectional diameter of the posterior semicircular canal of *Lepus* (0.30 mm; diameter equals 0.16 mm in *Sylvilagus*) is greater than either the anterior (0.27 mm; 0.13 for *Sylvilagus*) or lateral semicircular canal (0.26 mm; 0.24 mm for *Sylvilagus*).

The aspect ratios of the anterior and posterior canals are greater in *Sylvilagus* (0.97 and 0.94 respectively) than in *Lepus* (0.86 and 0.81 respectively), but the ratio calculated for the arc of the lateral canal is greater in *Lepus* than *Sylvilagus* (0.87 versus 0.84). As in the majority of mammals described so far, the ratio of the slender canal length to arc radius for the posterior semicircular canal of *Sylvilagus* (5.13) is greater than that computed for the anterior (4.84) and lateral semicircular canals (4.38). However, the greatest ratio among the canals of *Lepus* was calculated for the anterior semicircular canal (4.89; 4.13 for the lateral canal; 4.80 for the posterior canal).

There are no unambiguous synapomorphies that support monophyly of Lagomorpha within Glires or Euarchontoglires. The states reconstructed for the ancestor of Lagomorpha are the same as those for both Rodentia and Glires, as the lagomorphs retain the ancestral therian condition of the largest radius of curvature measured for the anterior semicircular canal arc, the placental condition of the direct vestibular entrance of the lateral semicircular canal, the ancestral boreoeutherian condition of the high position of the lateral semicircular canal compared to the ampullar opening of the posterior canal, and the glire condition of the high aspect ratio of the cochlea. The cochlea of the most recent common ancestor of lagomorphs coils 751.0° and contributes 53.0% to the total volume of the inner ear cavities.

Primates

Primates consists of two major groups, Strepsirhini which includes the lemurs and lorises, and Haplorhini which includes monkeys and apes. The haplorhines are divided further into three groups, which are Tarsiidae (tarsiers), Platyrhini (New World monkeys), and Catarhini (Old World monkeys and apes). Monophyly of all of these clades is supported by numerous phylogenetic analyses (e.g., Shoshani et al., 1996; Kay

et al., 1997; Goodman et al., 1998; Poux and Douzery, 2004; Bininda-Emonds, 2007; Janečka et al., 2007).

The two primate species examined here are the rhesus monkey, *Macaca mulatta* (Figures 5.62-5.63), and the human being, *Homo sapiens* (Figures 5.64-5.65). The average body mass of adult humans (74-86 kg; Ogden et al., 2004) is significantly greater than that of rhesus monkeys (4.7 kg; Silva and Downing, 1995), and this pattern is mirrored by the volume (164.73 mm^3 versus 41.64 mm^3) and length (16.31 mm versus 11.23 mm) of the bony labyrinth. The human cochlea is larger than that of *Macaca* in absolute volume (71.49 mm^3 versus 20.96 mm^3) and canal length (22.49 mm versus 16.94 mm), but the cochlea of *Homo* contributes a lesser amount to the entire bony labyrinth than does the cochlear cavity of *Macaca* (50.3% and 43.4% respectively). Only the cochlea of the elephantoid proboscidean contributes less (30.6%) to the bony labyrinth among the mammal species discussed so far.

The cochlea of *Macaca* completes a greater degree of coiling than the cochlea of *Homo* (1088° versus 889°; see Figures 5.62 and 5.64), and the secondary bony lamina persists to a greater relative distance in the rhesus monkey than the human (81° versus 22°; see Figures 5.63 and 5.65). The aspect ratios of the cochlea in profile for *Macaca* and *Homo* are 0.48 and 0.36 respectively. The scala tympani is expanded internal to the fenestra cochleae. The canaliculus cochleae for the aqueduct of the cochlea exits the inner ear from this excavation, and the canaliculus forms a long tunnel (10.86 mm in length) ending in a triangular cavity in *Homo*. The canaliculus forms a flattened, ever-expanded passage in *Macaca* (3.53 mm in length).

The apical turns of the cochlea are separated from the basal whorl (fitting inside of the basal whorl when the cochlea is viewed down its axis of rotation), and the apical turns sit on top of one another. A difference between the angle formed by the planes of

FIGURE 5.62. Bony labyrinth of *Macaca mulatta*. **A**, stereopair and labeled line drawing of digital endocast in anterior view; **B**, stereopair and labeled line drawing of digital endocast in dorsal view; **C**, stereopair and labeled line drawing of digital endocast in lateral view; **D**, line drawing of cochlea viewed down axis of rotation to display degree of coiling; **E**, line drawing of cochlea in profile. Abbreviations: **aa**, anterior ampulla; **ac**, anterior semicircular canal; **ant**, anterior direction; **av**, bony channel for aqueduct of vestibule; **cc**, canaliculus cochleae for aqueduct of cochlea; **co**, cochlea; **cr**, common crus; **dor**, dorsal direction; **er**, elliptical recess of vestibule; **fc**, fenestra cochleae; **fv**, fenestra vestibuli; **la**, lateral ampulla; **lc**, lateral semicircular canal; **med**, medial direction; **pa**, posterior ampulla; **pc**, posterior semicircular canal; **pl**, primary bony lamina; **pos**, posterior direction; **sl**, secondary bony lamina; **sr**, spherical recess of vestibule.

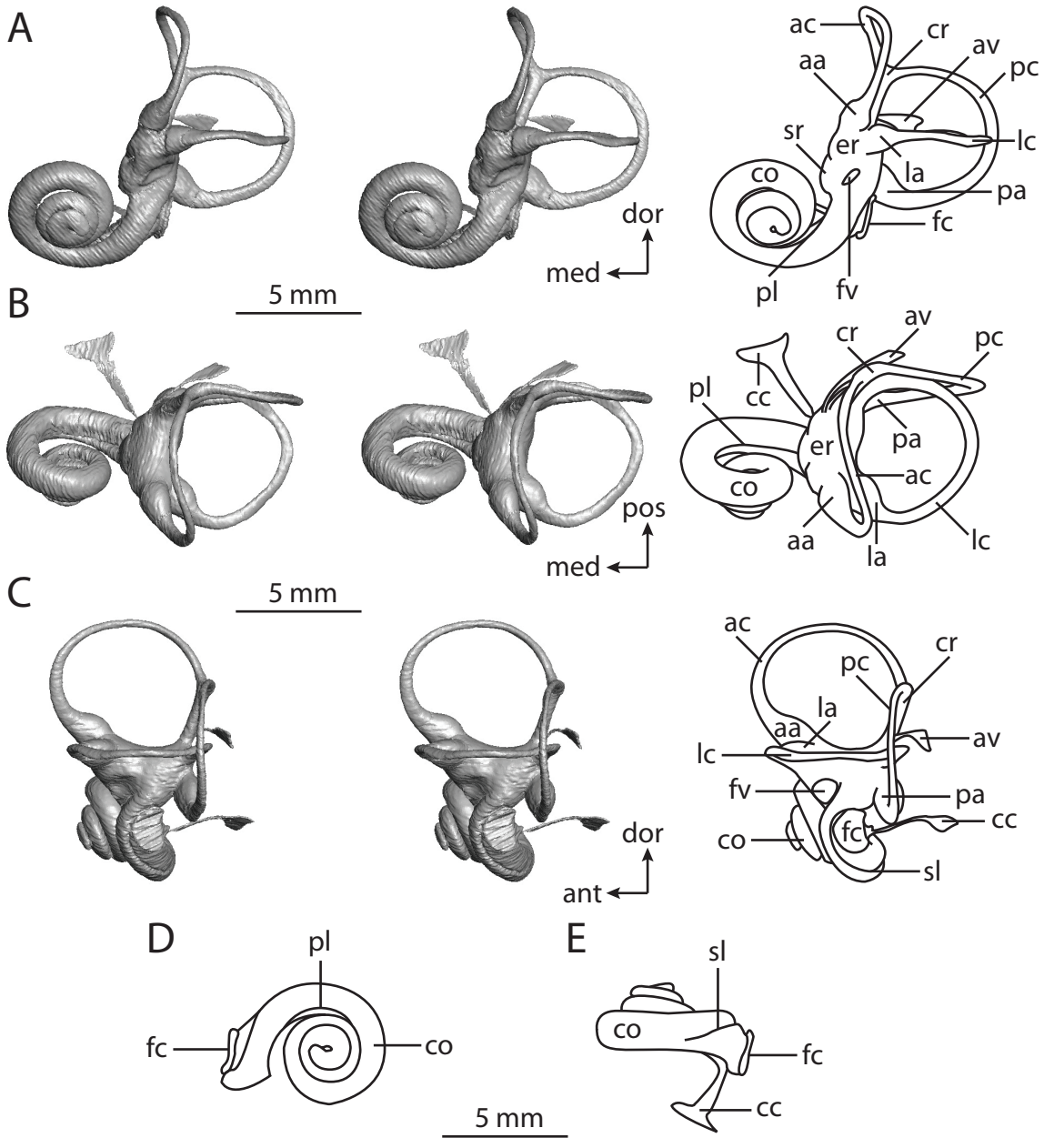
A
ac
cr
av
aa
pc
sr
er
lc
co
la
pa
fc
pl
fv
dor
med
5 mm
B
cr
av
pc
pl
cc
er
pa
co
ac
aa
la
lc
pos
med
C
5 mm
ac
cr
pc
la
aa
av
lc
fv
pa
cc
co
fc
sl
dor
ant
D
pl
fc
co
5 mm
E
sl
co
fc
cc

FIGURE 5.63. CT slices through ear region of *Macaca mulatta*. Abbreviations: **aa**, anterior ampulla; **ac**, anterior semicircular canal; **ant**, anterior direction; **av**, bony channel for aqueduct of vestibule; **cc**, canaliculus cochleae for aqueduct of cochlea; **cf**, foramina within cribriform plate; **cn**, canal for cranial nerve VIII; **co**, cochlea; **cr**, common crus; **dor**, dorsal direction; **er**, elliptical recess of vestibule; **fc**, fenestra cochleae; **fn**, canal for cranial nerve VII; **fv**, fenestra vestibuli; **in**, incus; **la**, lateral ampulla; **lat**, lateral direction; **lc**, lateral semicircular canal; **ma**, malleus; **med**, medial direction; **pa**, posterior ampulla; **pc**, posterior semicircular canal; **pl**, primary bony lamina; **sa**, subarcuate fossa; **sl**, secondary bony lamina; **st**, stapes within fenestra vestibuli; **vb**, vestibule; **vn**, canal for vestibular branch of cranial nerve VIII.

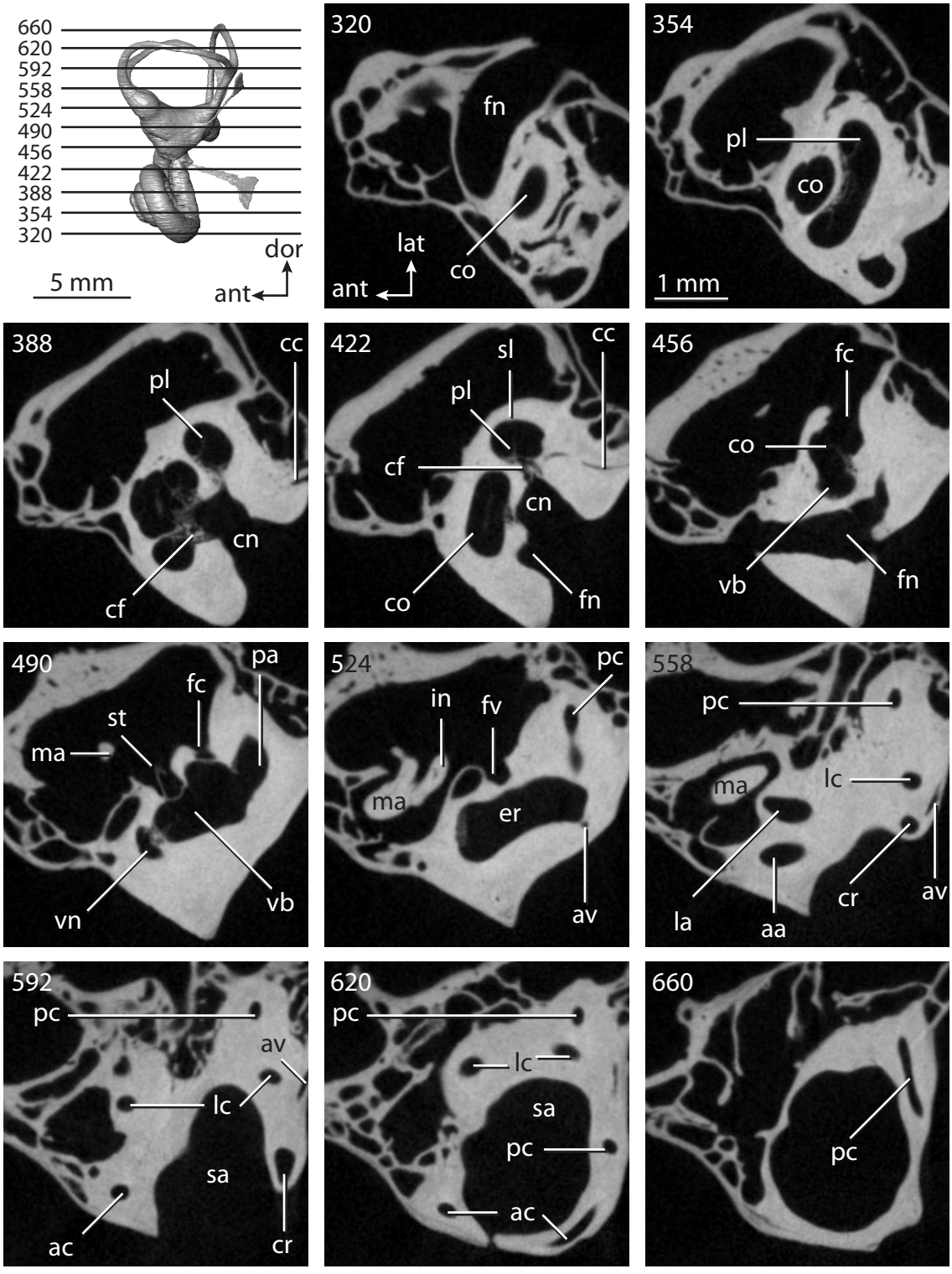
660
620
592
558
524
490
456
422
388
354
320
5 mm
dor
ant
320
fn
lat
ant
co
354
pl
co
1 mm
388
cc
pl
cn
cf
422
sl
cc
pl
cf
cn
co
fn
456
fc
co
vb
fn
490
pa
fc
st
ma
vn
vb
524
pc
in
fv
ma
er
av
558
pc
lc
ma
la
aa
cr
av
592
pc
av
lc
sa
ac
cr
620
pc
lc
sa
pc
ac
660
pc

FIGURE 5.64. Bony labyrinth of *Homo sapiens*. **A**, stereopair and labeled line drawing of digital endocast in anterior view; **B**, stereopair and labeled line drawing of digital endocast in dorsal view; **C**, stereopair and labeled line drawing of digital endocast in lateral view; **D**, line drawing of cochlea viewed down axis of rotation to display degree of coiling; **E**, line drawing of cochlea in profile. Abbreviations: **aa**, anterior ampulla; **ac**, anterior semicircular canal; **ant**, anterior direction; **av**, bony channel for aqueduct of vestibule; **cc**, canaliculus cochleae for aqueduct of cochlea; **co**, cochlea; **cr**, common crus; **dor**, dorsal direction; **er**, elliptical recess of vestibule; **fc**, fenestra cochleae; **fv**, fenestra vestibuli; **la**, lateral ampulla; **lc**, lateral semicircular canal; **med**, medial direction; **pa**, posterior ampulla; **pc**, posterior semicircular canal; **pl**, primary bony lamina; **pos**, posterior direction; **sr**, spherical recess of vestibule.

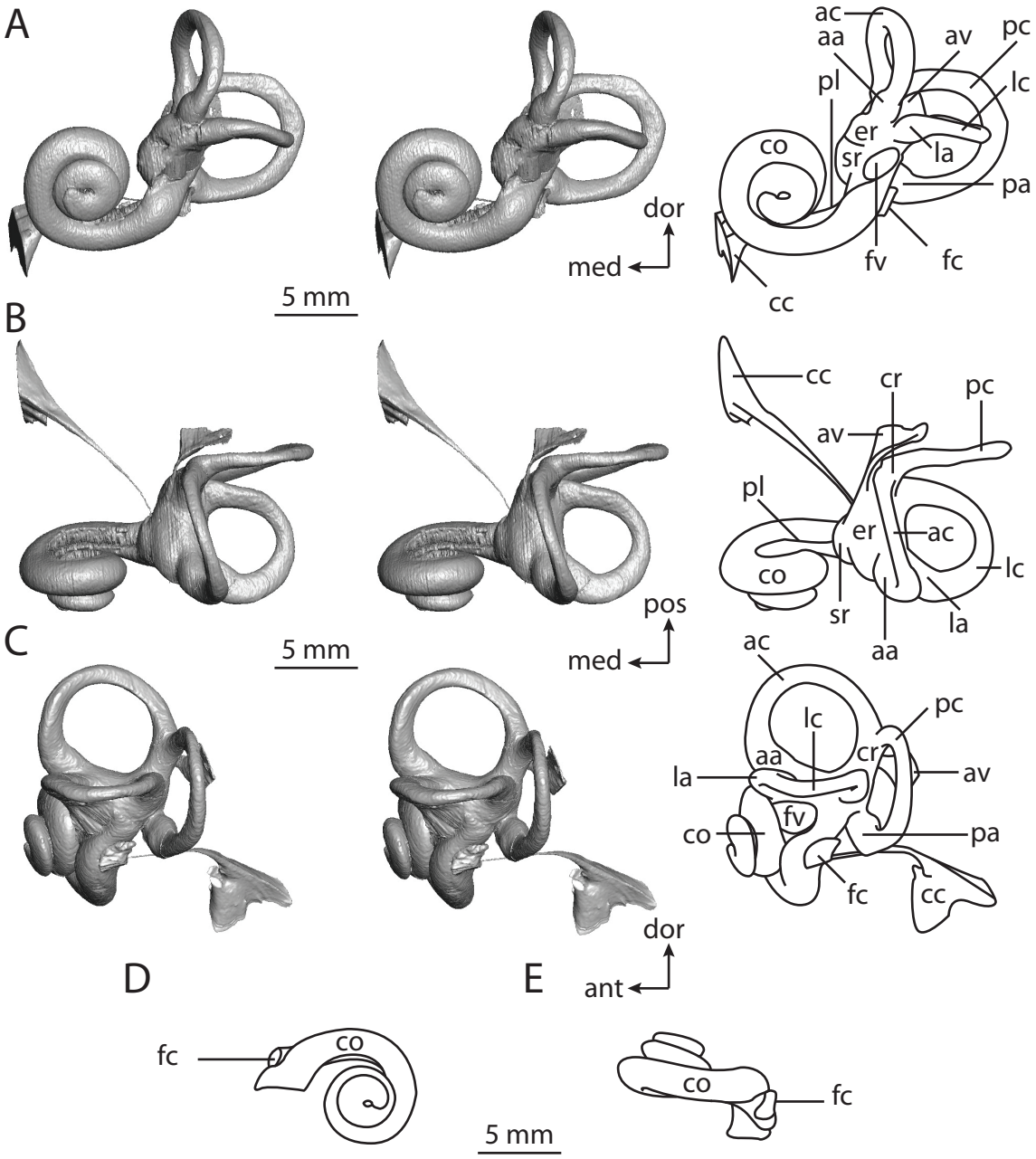
A
ac
aa
av
pc
pl
lc
er
co
sr
la
pa
fv
fc
cc
dor
med
5 mm
B
cc
cr
pc
av
pl
er
ac
co
lc
sr
la
aa
pos
med
5 mm
C
ac
lc
pc
aa
cr
la
av
fv
co
pa
fc
cc
dor
ant
D
E
fc
co
co
fc
5 mm

FIGURE 5.65. CT slices through ear region of *Homo sapiens*. Abbreviations: **aa**, anterior ampulla; **ac**, anterior semicircular canal; **ant**, anterior direction; **av**, bony channel for aqueduct of vestibule; **cc**, canaliculus cochleae for aqueduct of cochlea; **cf**, foramina within cribriform plate; **cn**, canal for cranial nerve VIII; **co**, cochlea; **cr**, common crus; **fc**, fenestra cochleae; **fn**, canal for cranial nerve VII; **fv**, fenestra vestibuli; **la**, lateral ampulla; **lat**, lateral direction; **lc**, lateral semicircular canal; **pa**, posterior ampulla; **pc**, posterior semicircular canal; **pl**, primary bony lamina; **sg**, spiral ganglion within primary lamina; **sr**, spherical recess of vestibule; **st**, stapes within fenestra vestibuli; **vb**, vestibule; **ven**, ventral direction; **vn**, canal for vestibular branch of cranial nerve VIII.

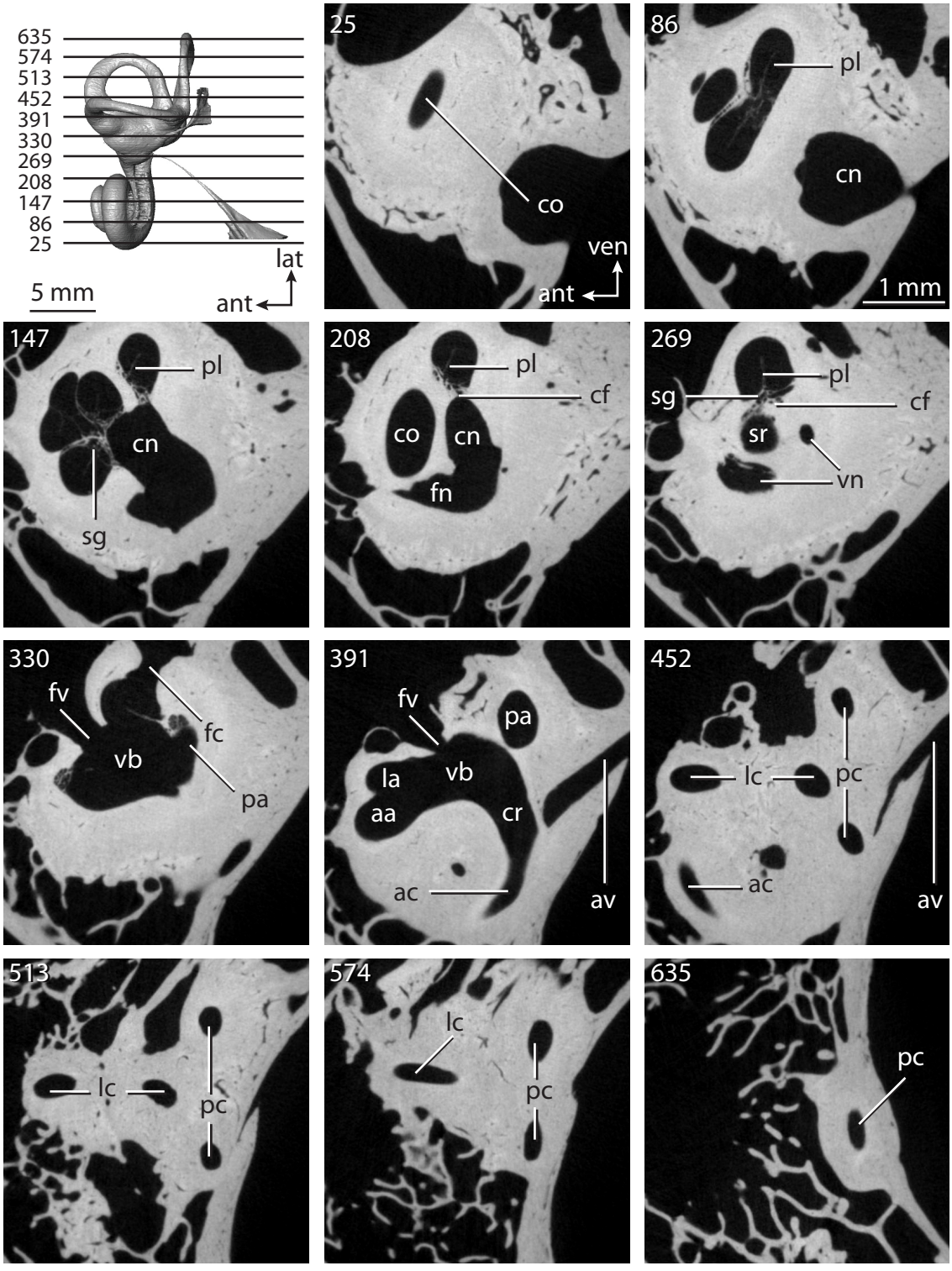
635
574
513
452
391
330
269
208
147
86
25
lat
5 mm
ant
25
co
ven
ant
86
pl
cn
1 mm
147
pl
cn
sg
208
pl
cf
co
cn
fn
269
pl
sg
cf
sr
vn
330
fv
fc
vb
pa
391
fv
pa
la
vb
aa
cr
ac
av
452
lc
pc
ac
av
513
lc
pc
574
lc
pc
635
pc

the basal turn of the cochlea and lateral semicircular canal was measured between the primate species, where the angle was much larger in *Homo* (62.4°) than measured in *Macaca* (47.8°). The angle between the cochlea and lateral canal of *Macaca* is similar to that observed in the elephantoid proboscidean (48.5°), *Procavia* (45.4°), and *Felis* (45.8°), but the angle in *Homo* is greater than that in any other mammal.

The fenestrae vestibuli of the primates are among the most elliptical fenestrae among the mammals examined here (stapedial ratio equals 2.5 in *Macaca*; ratio equals 3.0 in *Homo*), similar to *Cavia porcellus* (ratio equals 2.9). The vestibule is constricted internal to the fenestra vestibuli, thereby defining the border between the spherical and elliptical recesses. The bony channel for the aqueduct of the vestibule leaves the inner ear dorsal to the medial edge of the common crus. The channel, which is robust in *Homo* (5.47 mm in length; length equals 3.76 mm in *Macaca*), terminates as a fissure in both species,. The semicircular canals of *Homo* are relatively thick compared to the canals of *Macaca*, and the common crus of *Homo* is short and stout, similar to the crus in *Manis tricuspis*.

The greatest angle between the planes of any two semicircular canals in primates was measured between the anterior and posterior semicircular canals, totaling 100° for both *Macaca* and *Homo*. The planes of the anterior and lateral semicircular canals of *Homo* form a similar angle (98.9°; 83.1° for *Macaca*), and the angle between the posterior and lateral semicircular canals is 89.8° for *Homo* and 89.0° for *Macaca*.

The anterior semicircular canal is the least planar canal in each primate, with a total angular deviation of 26.4° in *Macaca* and 19.5° in *Homo*. The total deviation of the lateral semicircular canal in *Macaca* (7.7°) is less than that measured for the posterior canal (11.8°), and the posterior semicircular canal is the most planar within the labyrinth of *Homo* (total deviation of 6.3° versus 7.1° calculated for the lateral canal). The degree

of deviation of the anterior canal is significant for both primates (ratio of total linear deviation to cross-sectional diameter is 1.08 for *Homo*; 3.75 for *Macaca*), but only the posterior canal of *Macaca* deviates significantly (ratio is 1.11; 0.6 for *Homo*). The degree of deviation of the lateral canal is not significant in either species (ratio is 0.34 for *Homo*; 0.66 for *Macaca*).

The posterior limb of the lateral semicircular canal opens directly into the vestibule, nearly equidistant between the vestibular apertures of the common crus and posterior ampulla, in both primate species. The sagittal labyrinthine indices of *Macaca* (50.1) and *Homo* (55.8) are greater than that calculated for any other mammal discussed here. The closest non-primate to approach this index is *Procavia* (44.9).

The posterior semicircular canal of *Homo* is the largest in all dimensions explored in this study, including the arc radius (3.10 mm; 2.94 mm for anterior; 2.35 mm for lateral), for which the anterior canal has the greatest value in most mammals. In fact, the radius of the anterior semicircular canal (2.70 mm) is greater than either the lateral (2.47 mm) or posterior canal (2.54 mm) in *Macaca*. The slender canal lengths of the posterior semicircular canals of both *Homo* and *Macaca* (14.73 mm and 13.05 mm respectively) are greater than either the anterior (13.55 mm and 12.79 mm respectively) or lateral canals (10.31 mm and 10.57 mm). The posterior semicircular canal of *Homo* has a cross-sectional diameter of 1.12 mm (0.92 mm for anterior; 0.86 mm), which is over twice as large as the diameter measured in *Macaca* (0.47 mm; 0.33 mm for anterior; 0.50 mm for lateral).

The aspect ratios of the arcs of the semicircular canals are similar between the two primate taxa. The ratios of the anterior semicircular canals are 0.87 and 0.86 for *Macaca* and *Homo* respectively, while the ratios for the lateral canals are 0.89 and 0.85 respectively. The highest aspect ratio in each species was calculated for the posterior

canal arc (0.98 in *Macaca*; 1.08 in *Homo*), where the heights and widths of the canal arcs are nearly identical. The ratio of the slender canal length to arc radius of the posterior semicircular canal is larger than the other canals in both *Macaca* (5.13; 4.74 for anterior; 4.29 for lateral) and *Homo* (4.76; 4.61 for anterior; 4.39 for lateral).

There are no unambiguous synapomorphies in the bony labyrinth to support monophyly of Primates, and the clade retains the ancestral primatomorphan morphology of the cochlear spiral in that the cochlea has a low aspect ratio in profile. The anterior semicircular canal arc has the largest radius of curvature, which is retained from the ancestor to Theria, although the greatest radius in *Homo* was measured for the posterior canal arc. The arc of the posterior semicircular canal of no other euarchontoglire is the largest in terms of radius of curvature, and the only mammals for which the posterior canal arc is the greatest are *Manis* (only member of Laurasiatheria with the posterior canal the greatest), *Dasypus* (the distribution within Xenarthra beyond this taxon is unknown), and *Orycteropus* and *Procavia* among afrotherians.

The ancestral primate retained the ancestral placental condition of the direct vestibular entrance of lateral semicircular canals in the absence of a secondary common crus, and the plane of the lateral canal was high relative to the ampullar entrance of the posterior canal, which was retained from the ancestor of Boreoeutheria, if not earlier (state is equivocal for Placentalia). The cochlea of the ancestor of Primates coiled 980.2°, and the cochlea contributed 48.0% of the total labyrinthine volume.

Dermoptera

The colugos are gliding mammals divided into two extant species, *Cynocephalus volans* and *Galeopterus variegatus* (Wilson and Reeder, 2005), and the bony labyrinth of *Cynocephalus* is used as a representative of Dermoptera. Phylogenetic analyses based on

molecular data reconstruct a close relationship between Primates and Dermoptera (Schmitz and Zischler, 2003; Bininda-Emonds et al., 2007; Janečka et al., 2007), with the occasional result of Dermoptera nested within Primates (Murphy et al., 2001a; Schmitz et al., 2002)

Although the average body mass of *Cynocephalus volans* is less than *Sylvilagus floridanus* (1.0 versus 1.2 kg; Silva and Downing, 1995), the dimensions of the inner ear of the colugo are greater than that for the rabbit. The gross volume of the bony labyrinth of *Cynocephalus* is 20.32 mm^3 (versus 11.32 mm^3 for *Sylvilagus*), and the anterior-posterior length of the labyrinth is 7.17 mm (versus 5.82 mm for *Sylvilagus*). The cochlear canal of *Cynocephalus* contributes 48.4% of the total labyrinthine volume (9.83 mm^3), which is similar to the contribution calculated for *Homo sapiens* (50.3%). The cochlear spiral completes nearly two and two thirds whorls (954°), and the secondary bony lamina persists for around one fifth of the basal turn of the cochlea (65.4°), as is illustrated in Figures 5.66-5.67.

The cochlear canal is 12.20 mm in length, and the apical turns of the cochlea fit within the basal coils when the cochlea is viewed down its axis of rotation. The bony canaliculus cochleae (0.90 mm in length) is developed as a delicate tube that curves along its course. A second channel, which likely carried a blood vessel in life, extends away from the bony labyrinth alongside the canaliculus cochleae. The planes of the basal turn of the cochlea and lateral semicircular canal form an angle of 34.6°.

The fenestra vestibuli is elliptical, with a stapedial ratio of 2.0 (the same value calculated for *Tadarida brasiliensis*), and a constriction of the vestibule internal to the fenestra vestibuli can be used to distinguish between the spherical and elliptical recesses. The ampullae are very round in *Cynocephalus*, and the posterior limb of the lateral semicircular canal opens directly into the vestibule immediately dorsal to the vestibular

FIGURE 5.66. Bony labyrinth of *Cynocephalus volans*. **A**, stereopair and labeled line drawing of digital endocast in anterior view; **B**, stereopair and labeled line drawing of digital endocast in dorsal view; **C**, stereopair and labeled line drawing of digital endocast in lateral view; **D**, line drawing of cochlea viewed down axis of rotation to display degree of coiling; **E**, line drawing of cochlea in profile. Abbreviations: **aa**, anterior ampulla; **ac**, anterior semicircular canal; **ant**, anterior direction; **av**, bony channel for aqueduct of vestibule; **cc**, canaliculus cochleae for aqueduct of cochlea; **co**, cochlea; **cr**, common crus; **er**, elliptical recess of vestibule; **dor**, dorsal direction; **fc**, fenestra cochleae; **fv**, fenestra vestibuli; **la**, lateral ampulla; **lc**, lateral semicircular canal; **med**, medial direction; **pa**, posterior ampulla; **pc**, posterior semicircular canal; **pl**, primary bony lamina; **pos**, posterior direction; **sl**, secondary bony lamina; **sr**, spherical recess of vestibule.

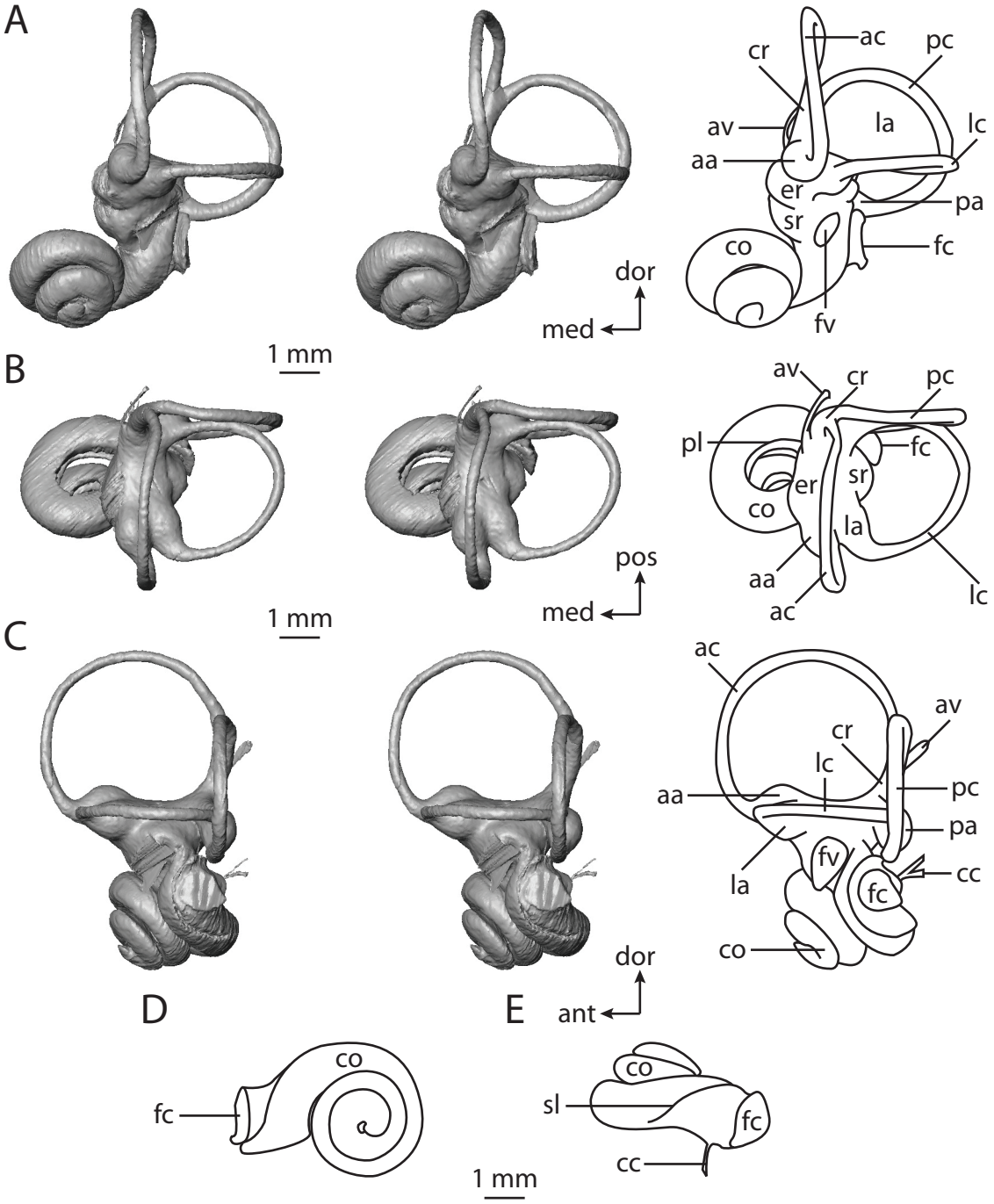
A
ac
pc
cr
av
la
lc
aa
er
pa
sr
co
fc
fv
dor
med
1 mm
B
av
cr
pc
pl
fc
sr
er
co
la
aa
ac
lc
pos
med
1 mm
C
ac
av
cr
lc
aa
pc
pa
fv
cc
la
fc
co
dor
ant
D
co
fc
E
co
sl
fc
cc
1 mm

FIGURE 5.67. CT slices through ear region of *Cynocephalus volans*. Abbreviations: **aa**, anterior ampulla; **ac**, anterior semicircular canal; **av**, bony channel for aqueduct of vestibule; **cn**, canal for cranial nerve VIII; **co**, cochlea; **cr**, common crus; **dor**, dorsal direction; **fc**, fenestra cochleae; **fn**, canal for cranial nerve VII; **fv**, fenestra vestibuli; **in**, incus; **la**, lateral ampulla; **lc**, lateral semicircular canal; **ma**, malleus; **med**, medial direction; **pa**, posterior ampulla; **pc**, posterior semicircular canal; **pl**, primary bony lamina; **pos**, posterior direction; **sa**, subarcuate fossa; **sg**, spiral ganglion within primary lamina; **sl**, spiral bony lamina; **sr**, spherical recess of vestibule; **st**, stapes fallen into vestibule; **vb**, vestibule; **vn**, canal for vestibular branch of cranial nerve VIII.

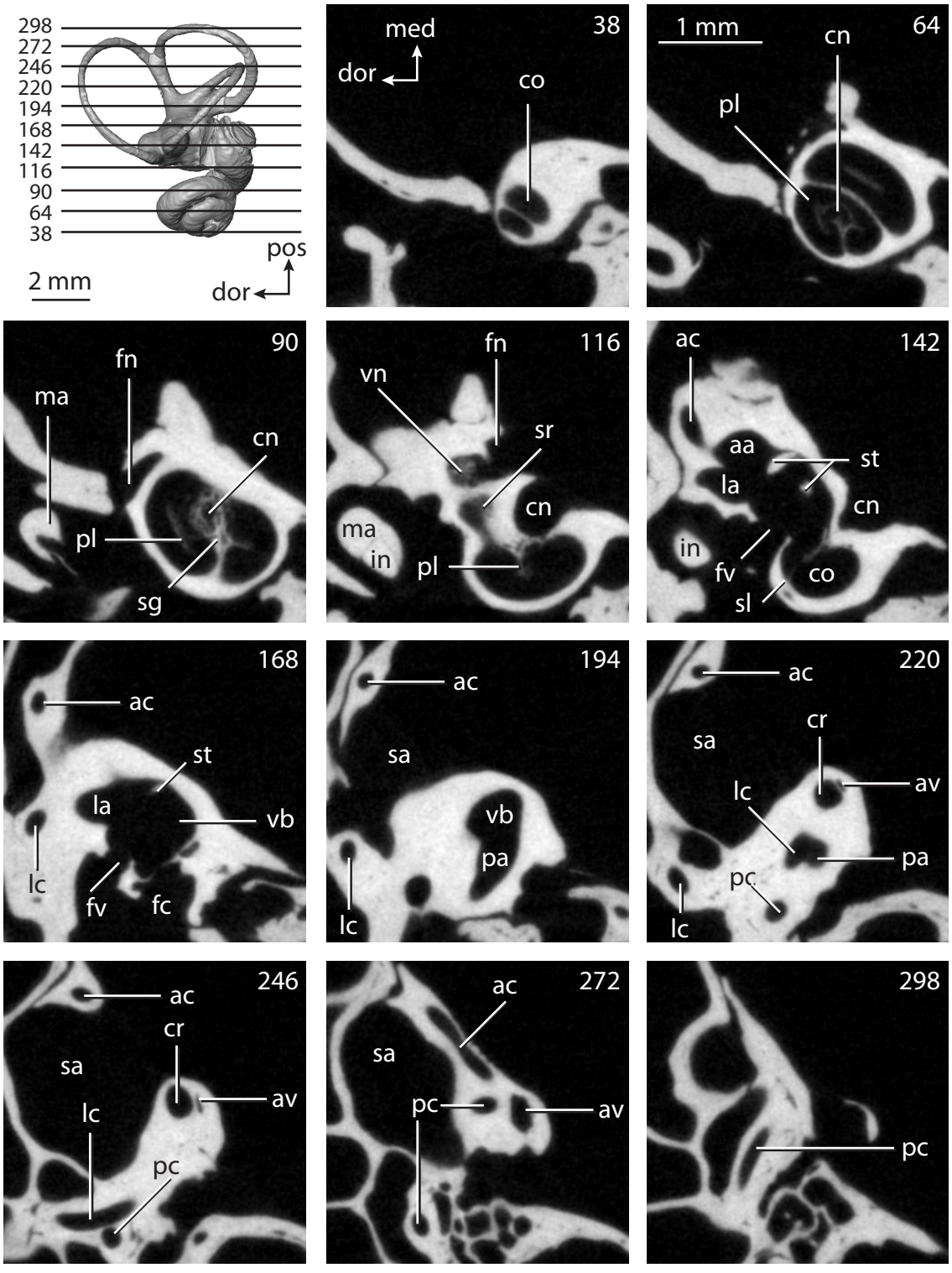
298
272
246
220
194
168
142
116
90
64
38
2 mm
pos
dor
med
dor
38
co
1 mm
64
cn
pl
90
fn
ma
cn
pl
sg
116
fn
vn
sr
cn
ma
in
pl
142
ac
aa
st
la
cn
in
fv
co
sl
168
ac
st
la
vb
lc
fv
fc
194
ac
sa
vb
pa
lc
220
ac
cr
sa
av
lc
pa
pc
lc
246
ac
cr
sa
av
lc
pc
272
ac
sa
pc
av
298
pc

aperture of the posterior ampulla (sagittal labyrinthine index equals 30.8). The bony channel for the aqueduct of the vestibule (1.80 mm in length) is a straight tube that exits the inner ear cavities medial to the vestibular aperture of the common crus.

The planes of the anterior and posterior semicircular canals of *Cynocephalus* form a 90° angle with each other, and the other angles between semicircular canals are not far off. The angle between the anterior and lateral canals is 92.2°, and an angle of 91.8° was measured between the posterior and lateral semicircular canals. The anterior canal is the least planar of the three semicircular canals with a total angular deviation from its plane of 13.5°, compared to 3.5° and 3.0° calculated for the lateral and posterior semicircular canals respectively. Likewise, the anterior canal deviates to a significant degree (ratio of total linear deviation over cross-sectional canal diameter is 1.64), but the deviations of the lateral and posterior canals are not significant (ratios are 0.24 and 0.28 respectively).

The anterior semicircular canal is the largest in terms of arc radius (1.93 mm versus 1.47 and 1.70 mm for the lateral and posterior canals respectively) and slender canal length (9.93 mm; 6.99 mm for lateral; 8.38 mm for posterior). This pattern is observed in most of the mammals considered for this study. However, the lateral semicircular canal is the largest in terms of cross-sectional diameter (0.37 mm; 0.27 mm for anterior; 0.32 for posterior).

The arcs of the semicircular canals are graceful and circular, particularly the arc of the posterior canal, which has an aspect ratio of 1.05 (similar to the ratio of 1.08 calculated for *Homo*). The aspect ratios of the anterior and lateral semicircular canals are 0.82 and 0.85 respectively. The ratio of the slender canal length to arc radius of the anterior semicircular canal of *Cynocephalus* (5.15) is greatest among the canals (ratio of lateral equals 4.75; ratio of posterior equals 4.94), which is different than the condition in

most of the mammals examined here, where the greatest ratio is observed in the posterior semicircular canal.

The bony labyrinth of *Cynocephalus* retains all states reconstructed in the most recent common ancestor of Primatomorpha (Primates plus Dermoptera). The aspect ratio of the cochlea is low (retained from Primatomorpha), the lateral semicircular canal is high compared to the ampullar opening of the posterior semicircular canal (retained from Boreoeutheria), the lateral canal opens into the vestibule directly in the absence of a secondary common crus (retained from Placentalia), and the greatest arc radius of curvature was measured for the anterior semicircular canal (retained from Theria). The contribution of the cochlea calculated for *Cynocephalus* (48.0%) is retained from the ancestor of Primatomorpha (50.0%), and the coiling of the cochlea (953.7°) is similar to that reconstructed for the ancestor of Euarchontoglires (956.9°).

Scandentia

The final species to be considered here is the tree shrew, *Tupaia glis* (Figures 5.68-5.69). Scandentians were considered to have "insectivoran" affinities in early classifications (e.g., Flower, 1883), as well as close associations with Macroscelidea (Gregory, 1910). The results of later studies have been used to remove tree shrews from Lipotyphla and to postulate a closer relationship between Scandentia and Primates, at times with tree shrews included within Primates (Carlsson, 1922; Simpson, 1945). Most mammalian systematists today agree that Scandentia is a clade exclusive of Primates (Van Valen, 1965; Campbell, 1966; Butler, 1972), and the majority of anatomical and molecular evidence supports the monophyly of Euarchonta (Primates, Dermoptera, Scandentia), even if the relationships within the clade remain unresolved (Adkins and

FIGURE 5.68. Bony labyrinth of *Tupaia glis*. **A**, stereopair and labeled line drawing of digital endocast in anterior view; **B**, stereopair and labeled line drawing of digital endocast in dorsal view; **C**, stereopair and labeled line drawing of digital endocast in lateral view; **D**, line drawing of cochlea viewed down axis of rotation to display degree of coiling; **E**, line drawing of cochlea in profile. Abbreviations: **aa**, anterior ampulla; **ac**, anterior semicircular canal; **ant**, anterior direction; **av**, bony channel for aqueduct of vestibule; **cc**, canaliculus cochleae for aqueduct of cochlea; **co**, cochlea; **cr**, common crus; **dor**, dorsal direction; **er**, elliptical recess of vestibule; **fc**, fenestra cochleae; **fv**, fenestra vestibuli; **la**, lateral ampulla; **lc**, lateral semicircular canal; **med**, medial direction; **pa**, posterior ampulla; **pc**, posterior semicircular canal; **pl**, primary bony lamina; **pos**, posterior direction; **sl**, secondary bony lamina; **sr**, spherical recess of vestibule.

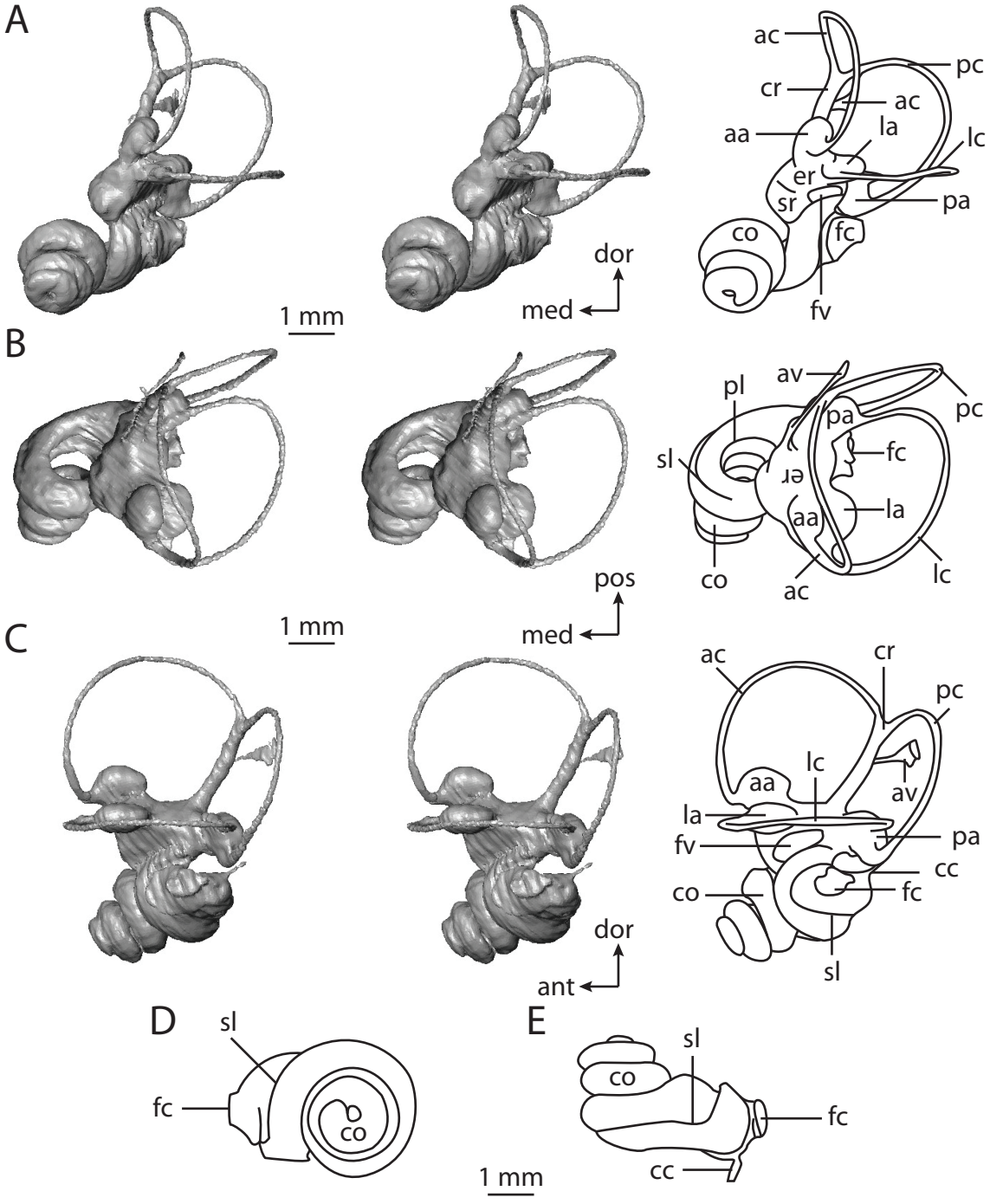
A
1 mm
dor
med
ac
pc
cr
ac
aa
la
lc
er
sr
pa
co
fc
fv
B
1 mm
pos
med
pl
av
pc
pa
sl
fc
la
aa
co
ac
lc
C
1 mm
dor
ant
ac
cr
pc
lc
aa
av
la
fv
pa
cc
co
fc
sl
D
sl
fc
co
E
sl
co
fc
cc
1 mm

FIGURE 5.69. CT slices through ear region of *Tupaia glis*. Abbreviations: **aa**, anterior ampulla; **ac**, anterior semicircular canal; **av**, bony channel for aqueduct of vestibule; **cn**, canal for cranial nerve VIII; **co**, cochlea; **cr**, common crus; **la**, lateral ampulla; **lat**, lateral direction; **lc**, lateral semicircular canal; **pa**, posterior ampulla; **pc**, posterior semicircular canal; **pl**, primary bony lamina; **pos**, posterior direction; **sa**, subarcuate fossa; **st**, stapes within fenestra vestibuli; **vb**, vestibule; **ven**, ventral direction.

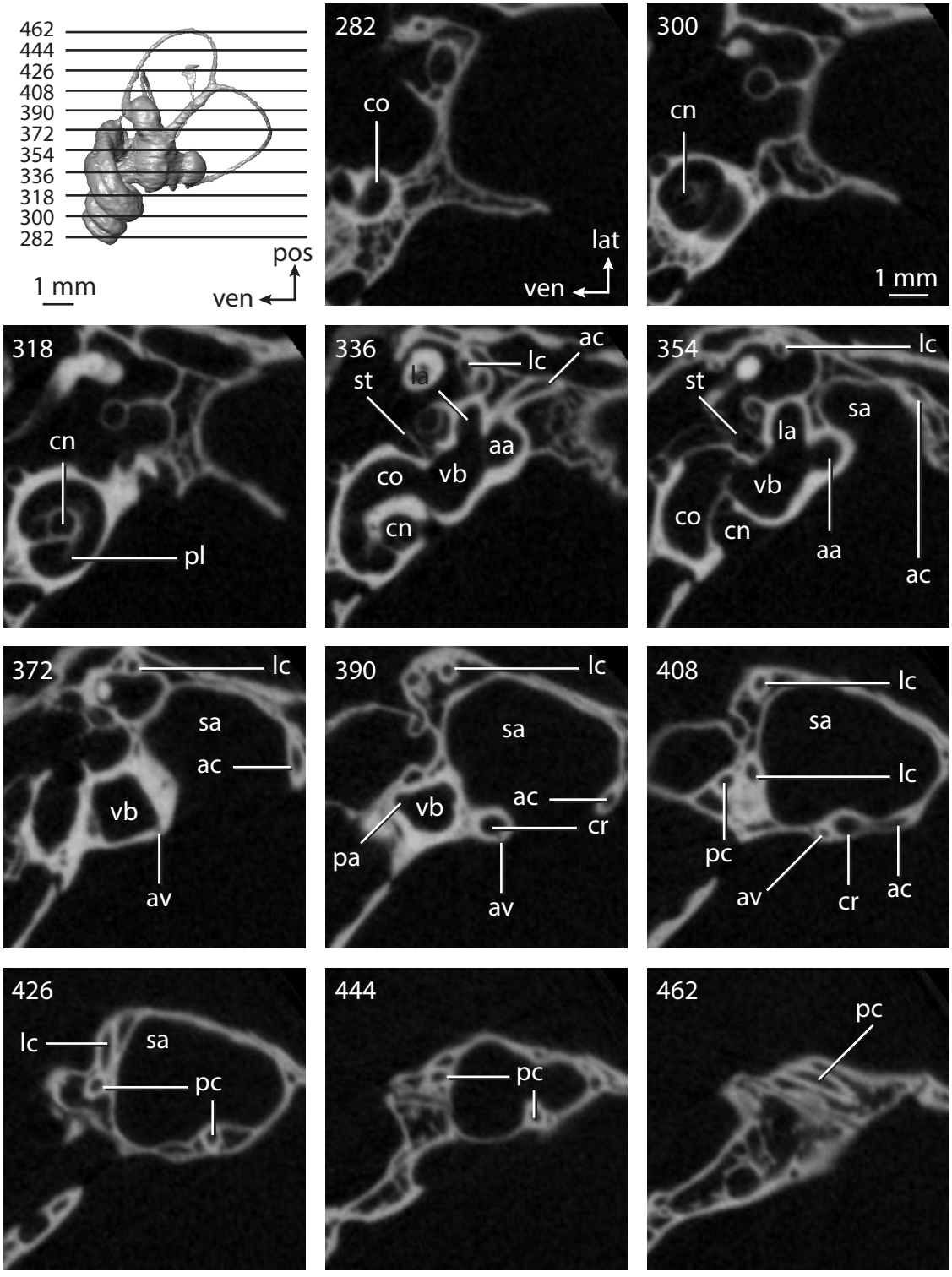
462
444
426
408
390
372
354
336
318
300
282
pos
ven
1 mm
282
co
lat
ven
300
cn
1 mm
318
cn
pl
336
ac
lc
st
la
aa
co
vb
cn
354
lc
st
sa
la
vb
co
cn
aa
ac
372
lc
sa
ac
vb
av
390
lc
sa
ac
vb
cr
pa
av
408
lc
sa
lc
pc
av
cr
ac
426
lc
sa
pc
444
pc
462
pc

Honeycutt, 1991; Murphy et al., 2001a, b; Silcox et al., 2005; Bininda-Emonds et al., 2007).

The gross volume of the inner ear cavities of *Tupaia* is 9.83 mm^3, and the anterior-posterior length of the bony labyrinth is 6.67 mm. The length of the labyrinth of *Tupaia* is similar to that measured for the dermopteran *Cynocephalus volans* (7.17 mm), despite a body mass of *Cynocephalus* (1 kg; Silva and Downing, 1995) that is one order of magnitude larger than that of *Tupaia* (131 g; Silva and Downing, 1995). The volume of the cochlea of *Tupaia* is 5.43 mm^3, which is 55.2% of the total inner ear volume.

The cochlea of the tree shrew completes over three turns (1125°), and the secondary bony lamina extends beyond half of the basal coil (220°). The length of the cochlear canal is 10.51 mm, and the aspect ratio of the cochlear spiral in profile is 0.66, which is among the highest calculated among the mammal sample. The scala tympani of the cochlea is expanded internal to the fenestra cochleae, from which the canaliculus cochleae exits the cochlea. The canaliculus is a straight tube that extends posterodorsally from the scala tympani. The canaliculus is 0.66 mm in length. The planes of the basal turn of the cochlea and lateral semicircular canal form an angle of 29°.

The shape of the fenestra vestibuli of *Tupaia* is elliptical, with a stapedial (aspect) ratio of 2.6, similar to the rhesus monkey, *Macaca mulatta* (2.53). A slight constriction of the vestibule internal to the fenestra vestibuli separates the spherical and elliptical recesses. The bony channel for the aqueduct of the vestibule opens immediately anterior to the medial edge of the vestibular aperture of the common crus. The channel, which is 2.61 mm in length, curves posteriorly and terminates in a triangular fissure. The posterior limb of the lateral semicircular canal does not open directly into the vestibule, but rather into the anterior aspect of the posterior ampulla. A groove extends from the entry point of the lateral canal to the vestibule across the anterior wall of the posterior ampulla (the

groove is expressed as a rounded ridge on the endocast). The lateral semicircular canal does not join with the posterior canal, and a secondary common crus is not formed.

The planes of the anterior and posterior semicircular canals form an angle of 106°, and the planes of the posterior and lateral canals form an angle of 102°. The angle between the planes of the anterior and lateral semicircular canals is significantly smaller (82°). The anterior semicircular canal is the least planar among the three canals with a total deviation of 23.1°. The lateral and posterior semicircular canals deviate from their planes by a total of 8.4° and 5.4° respectively. Both the anterior and posterior semicircular canals deviate from their planes by a significant degree (ratios of total linear deviation over cross-sectional diameter are 3.76 and 1.54 respectively). The lateral semicircular canal does not deviate from its plane significantly (ratio is 0.97), although nearly so.

The semicircular canals form delicate arcs, and the canals themselves are slender compared to the rest of bony labyrinth (as opposed to the thick canals observed in *Homo*). The radius of the arc of the anterior semicircular canal of *Tupaia* (1.73 mm) is greater than either the lateral (1.44 mm) or posterior canals (1.50 mm). Similarly, the slender canal length of the anterior semicircular canal is the greatest (9.24 mm; 7.84 mm for lateral; 8.07 mm for posterior). The lateral semicircular canal is largest in terms of cross-sectional diameter (0.22 mm; anterior and posterior canals have a diameter of 0.22 mm each).

The arc of the anterior semicircular canal appears more circular than the lateral and posterior canal arcs (Figure 5.63), although the aspect ratio of the posterior canal arc (0.96) is higher than that calculated for the anterior canal (0.85). This is a result of the method employed to measure the height and width of the posterior semicircular canal arc, which does not reflect the shape of the arc in this situation. The aspect ratio of the lateral

semicircular canal is 0.71, which more accurately represents the ellipse formed by the lateral canal arc. The ratio of the slender canal length to arc radius of the anterior semicircular canal (5.35) is not the greatest, as is observed in most of the mammals examined here, but rather the smallest. The ratio for the lateral canal (5.46) is the largest, and the ratio for the posterior canal falls in between (5.40).

The bony labyrinth of *Tupaia* is derived from the ancestral eutherian condition in that the plane of the lateral semicircular canal is high in relation to the ampullar entrance of the posterior canal, although this state was inherited from the most recent common ancestor of boreoeutherians. The lateral semicircular canal opens into the posterior ampulla separate from the posterior canal (a secondary common crus is not formed), a condition that is unique to *Tupaia* among euarchontoglires, but shared by *Hemicentetes*, Cetacea, *Equus*, Carnivora (except *Canis*), and the bats *Nycteris* and *Rhinolophus*. The greatest arc radius of curvature was measured for the anterior semicircular canal in *Tupaia*, which is consistent for most of the therian mammals considered here.

The high aspect ratio of the cochlea of *Tupaia* is derived from the ancestral eutherian condition, which the taxon shares with Glires within Euarchontoglires. The shape of the cochlear spiral may be a synapomorphy supporting a *Tupaia* plus Glires clade, although the ancestral state of Euarchontoglires is equivocal with respect to this character. The cochlea coils to a greater degree (1125.0°) than that reconstructed for the ancestor of Euarchontoglires (956.9°), but not more than a quarter turn. The cochlea of Scandentia contributes 55.0% of the total labyrinthine volume, which is he same percentage calculated for the cochlea of Boreoeutheria.

RESULTS – DIMENSION COMPARISONS

Large-bodied animals tend towards large inner ears. For example, the labyrinths of large-bodied *Homo sapiens* and *Equus caballus* are among the most voluminous, while the inner ears of *Mus musculus* and *Sorex monticolus* are the smallest. In order to test if there is a correlation between body size and inner ear dimensions, the coefficient of correlation was calculated between specific measurements and body mass (Table 5.7). The total size of the bony labyrinth, both in terms of the total volume of the cavities and length of the inner ear, are related strongly to body mass across the sample when the data are transformed using the natural logarithm (Figure 5.70). A coefficient of correlation (r; not to be confused by the slender canal radius of Jones and Spells, 1963) of 0.94 was calculated between labyrinth length and body mass, and a coefficient of 0.95 between total labyrinthine volume and body mass.

Because the size of the bony labyrinth is closely correlated to the overall size of the animal, the dimensions of the bony labyrinth can be used to estimate the body mass of fossil species. The length of the bony labyrinth rather than its volume is used here to make this estimate, because it is less prone to error. Volumes of the inner ear constituents are calculated from the segmented endocast, where boundaries between the middle and inner ear cavities, or else between the cochlea and vestibule, can be ambiguous for some species. Consistent boundaries are maintained as much as possible, but the longitudinal measure of the length of the bony labyrinth is less ambiguous.

The equation for the regression line between the length of the bony labyrinth and body mass is y=0.151x+0.8212, where “x” equals the body mass and “y” equals the length of the bony labyrinth. The accuracy of the equation can be tested by estimating the body mass was of *Canis familiaris* specimen, which was not incorporated in the correlations with body mass (see discussion in the materials and methods section). Using

TABLE 5.7. Coefficients of correlation (r) calculates for dimensions over body mass[a]

Measurement	Coefficient of Correlation - r
Labyrinth	
Volume	**0.95**
Length	**0.94**
Cochlea	
Volume	**0.93**
Percent of Total Volume	0.13
Canal Length	**0.84**
Aqueduct Length	**0.91**
Coiling	0.02
2° Lamina Extension	0.36
Angle with Lateral Canal	0.36
Aspect Ratio	0.19
Vestibule	
Aqueduct Length	**0.70**
Stapedial Ratio	0.26
Semicircular Canal Orientation	
Anterior-Lateral	0.15
Anterior-Posterior	0.07
Lateral-Posterior	0.33
Semicircular Canal Dimensions	
Anterior Radius	**0.85**
Lateral Radius	**0.88**
Posterior Radius	**0.84**
Anterior Length	**0.79**
Lateral Length	**0.83**
Posterior Length	**0.83**
Anterior Diameter	**0.83**
Lateral Diameter	**0.81**
Posterior Diameter	**0.82**
Anterior Linear Deviation	0.33
Lateral Linear Deviation	0.64
Posterior Linear Deviation	0.35
Anterior Angular Deviation	0.17
Lateral Angular Deviation	0.19
Posterior Angular Deviation	0.08
Anterior Aspect Ratio	0.19

TABLE 5.7. (Continued)

Measurement	Coefficient of Correlation - r
Lateral Aspect Ratio	0.50
Posterior Aspect Ratio	0.61

[a] Data logarithmically transformed using the natural logarithm. Values over 0.70 (in bold) are considered significant.

FIGURE 5.70. Bivariate plots of labyrinth dimensions over body mass. All data logarithmically transformed using the natural logarithm (ln). **A**, total labyrinth volume over body mass; **B**, total length of labyrinth over body mass; **C**, volume of cochlea over body mass; **D**, length of canaliculus cochleae for aqueduct of cochlea over body mass; **E**, length of bony channel for aqueduct of vestibule over body mass; **F**, length of cochlear canal over body mass; **G**, length of slender anterior semicircular canal over body mass; **H**, length of slender lateral semicircular canal over body mass; **I**, length of slender posterior semicircular canal over body mass; **J**, arc radius of curvature of anterior semicircular canal over body mass; **K**, arc radius of curvature of lateral semicircular canal over body mass; **L**, arc radius of curvature of posterior semicircular canal over body mass. The outlier that falls well below regression line in G-L is *Tursiops truncatus*.

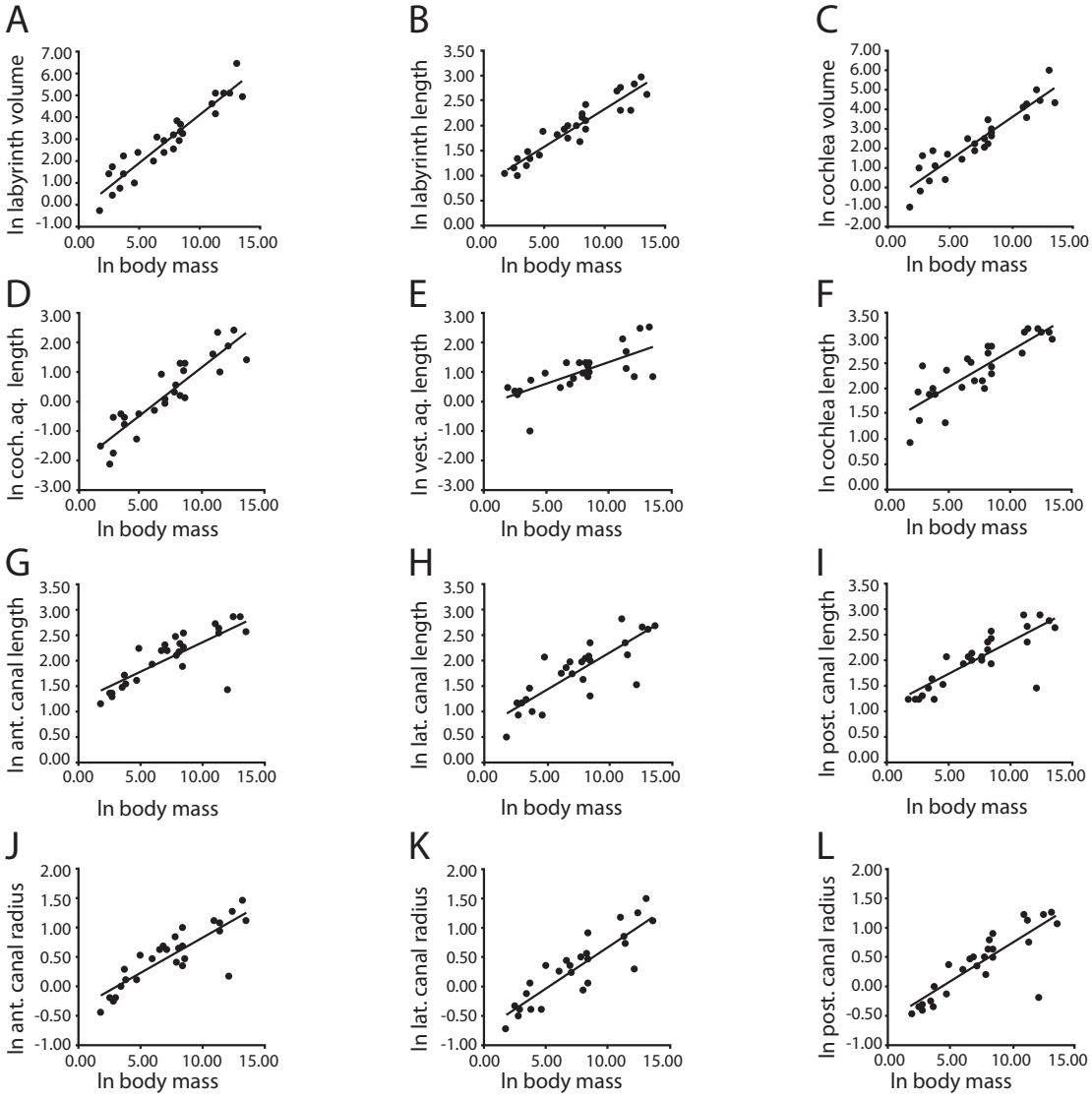
A
ln labyrinth volume
7.00
6.00
5.00
4.00
3.00
2.00
1.00
0.00
-1.00
0.00
5.00
10.00
15.00
ln body mass
B
ln labyrinth length
3.50
3.00
2.50
2.00
1.50
1.00
0.50
0.00
0.00
5.00
10.00
15.00
ln body mass
C
ln cochlea volume
7.00
6.00
5.00
4.00
3.00
2.00
1.00
0.00
-1.00
-2.00
0.00
5.00
10.00
15.00
ln body mass
D
ln coch. aq. length
3.00
2.00
1.00
0.00
-1.00
-2.00
-3.00
0.00
5.00
10.00
15.00
ln body mass
E
ln vest. aq. length
3.00
2.00
1.00
0.00
-1.00
-2.00
-3.00
0.00
5.00
10.00
15.00
ln body mass
F
ln cochlea length
3.50
3.00
2.50
2.00
1.50
1.00
0.50
0.00
0.00
5.00
10.00
15.00
ln body mass
G
ln ant. canal length
3.50
3.00
2.50
2.00
1.50
1.00
0.50
0.00
0.00
5.00
10.00
15.00
ln body mass
H
ln lat. canal length
3.50
3.00
2.50
2.00
1.50
1.00
0.50
0.00
0.00
5.00
10.00
15.00
ln body mass
I
ln post. canal length
3.50
3.00
2.50
2.00
1.50
1.00
0.50
0.00
0.00
5.00
10.00
15.00
ln body mass
J
ln ant. canal radius
2.00
1.50
1.00
0.50
0.00
-0.50
-1.00
0.00
5.00
10.00
15.00
ln body mass
K
ln lat. canal radius
2.00
1.50
1.00
0.50
0.00
-0.50
-1.00
0.00
5.00
10.00
15.00
ln body mass
L
ln post. canal radius
2.00
1.50
1.00
0.50
0.00
-0.50
-1.00
0.00
5.00
10.00
15.00
ln body mass

the equation above, the estimated body mass of the specimen is 4.5 kg, which is at the low range of dog body masses (3.4 to 31.3 kg as reported by Galvão, 1947). In fact, the breed of dog used in this study is from a Chihuahua, which is among the smallest breeds of domestic dog. This equation can be used to calculate body masses for extinct taxa. For example, the estimated body masses of the oreodont *Bathygenys reevesi* and the fossil balaenopterid whale are 2.5 kg and 1608.3 kg respectively.

Additional dimensions significantly scale with body mass (see Table 5.7), including the length and volume of the cochlear canal (r equals 0.84 and 0.93 respectively), lengths of the bony channels for the aqueducts of the cochlea (canaliculus cochleae; r equals 0.91) and vestibule (r equals 0.70), slender canal lengths of the anterior (r equals 0.79), lateral (r equals 0.83), and posterior semicircular canals (0.83), as well as the radii of curvature of the semicircular canal arcs (r equals 0.85 for anterior; 0.88 for lateral; 0.84 for posterior). In all cases, the mammals with the largest inner ear dimensions are large-bodied animals (see Figure 5.70). Alternatively, the aspect ratios of the cochlea (r equals 0.19) and semicircular canal arcs (0.19 for anterior; 0.50 for lateral; 0.61 for posterior) do not correlate with body mass.

The degree of coiling exhibited by the cochlea and body mass do not correlated with one another (r equals 0.02). That is, large animals, such as *Equus caballus*, do not have a significantly more or less coiled cochlea than smaller species. Species with a large number of cochlear whorls do not have significantly more voluminous cochleae (r equals 0.07), longer cochlear canals (r equals 0.36), or cochlear spirals with higher aspect ratios (r equals 0.44), as summarized in Table 5.8. Likewise, a long cochlear canal does not signify a high-spired cochlea (r equals 0.10), as observed in *Cavia porcellus*. Table 5.9 summarizes correlations among dimensions of the semicircular canals.

TABLE 5.8. Coefficients of correlation (r) calculated for dimensions of the cochlea[a]

	Degree of Coiling	Canal Volume	Canal Length	Aspect Ratio
Degree of Coiling	-	0.07	0.36	0.44
Canal Volume	0.07	-	**0.94**	0.22
Canal Length	0.36	**0.94**	-	0.10
Aspect Ratio	0.44	0.22	0.10	-

[a] Data logarithmically transformed using the natural logarithm. Values over 0.70 (in bold) are considered significant.

TABLE 5.9. Coefficients of correlation (r) calculated for dimensions of the semicircular canals[a]

	Ant			Lat			Post		
	Radius	Length	Ratio	Radius	Length	Ratio	Radius	Length	Ratio
Radius	-	**0.98**	0.26	-	**0.98**	0.26	-	**0.99**	0.40
Length	**0.98**	-	0.31	**0.98**	-	0.29	**0.99**	-	0.39
Ratio	0.26	0.31	-	0.26	0.29	-	0.40	0.39	-

[a] Data logarithmically transformed using the natural logarithm. Values over 0.70 (in bold) are considered significant.

In short, strong correlations were observed between the semicircular canal arc radii of curvature and slender canal length (r ranging from 0.98 to 0.99). The correlations between the aspect ratio of a canal arc and respective length or arc radius are not significant (Table 5.9).

DISCUSSION

General Patterns

That variation was observed across the sample of bony labyrinths of placental mammals is not surprising, and it has been a long-recognized phenomenon, even before the seminal works of Gustaf Retzius in the late 19th Century (for example, see Retzius, 1884). However, the nature of this variation has received only a superficial treatment in the scientific literature; exceptions include Caix and Outrequin (1979), Dimopoulos and Muren (1990), and Chapter 4 of this dissertation. Variation in the degree of coiling in the cochlea in particular is related to phylogeny (e.g., Meng and Fox, 1995) and function (West, 1985). The broad range of over 1,400° (nearly 3 turns) within the placental sample examined here may be a reflection of taxonomic diversity, where at least 5,421 extant mammal species are recognized (Wilson and Reeder, 2005; Reeder et al., 2007), as well as physiological diversity, where a range of auditory sensitivities extend from subsonic (in proboscideans and cetaceans; Payne et al., 1986; Poole et al., 1988; Ketten, 1997) to ultrasonic frequencies (in some chiropterans, soricid lipotyphlans, and tenrecs; Gould, 1965; Tomasi, 1979; Simmons et al., 1979).

Other general patterns in the bony labyrinth anatomy include the arc radius of curvature of the anterior semicircular canal being the largest among the three canals in

the majority of the mammals examined here (24 out of 32 species). This pattern has been observed in most mammal species (Curthoys et al., 1977a, b; Blanks et al., 1985; Muren et al., 1986; Spoor and Zonneveld, 1998; Jeffery and Spoor, 2004; Calabrese and Hullar, 2006; Spoor et al., 2007), and a large anterior semicircular canal arc signifies that the majority of mammals are most sensitive to rotational head movement in the pitch (anterior-posterior) direction (Yang and Hullar, 2007). Exceptions include *Dasypus novemcinctus*, where the posterior canal is the most sensitive, or *Eumetopias jubatus* where the lateral canal would be most sensitive.

The posterior semicircular canal is the least planar of the three canals in most of the bony labyrinths studied here (15 out of 32 species), and the lateral canal is the most planar for the majority of taxa (18 out of 32 species). The ratio of the total linear deviation to the cross-sectional diameter of the semicircular canal is used in the present study to describe the degree of planar deviation of a semicircular canal, where a ratio above 1 (linear deviation greater than diameter) is considered substantial. Any physiological importance of planar deviation has yet to be explored in a rigorous sense, and such substantial deviation may not have any basis in function. The ratio is used for descriptive and comparative purposes only. Although the ratio is arbitrary, evidence suggests that, even in species with broad ranges of planarities (such as in *Monodelphis domestica*; Chapter 2), there is not much variation in whether or not the ratio is substantial (Table 5.10). The degree of deviation exhibited both by the anterior and posterior semicircular canals is considered substantial in half of the taxa examined here (16 out of 32), although the deviations of the two canals are not always significant within the same labyrinth. The deviation of the lateral semicircular canal is significant in only one quarter of the mammals.

TABLE 5.10. Linear deviations of the semicircular canals of *Monodelphis domestica*[a]

	Specimens (TMM M)											
	7595	8261	8265	7536	8266	7539	7542	8267	7545	8268	8273	7599
Linear Deviations												
Anterior	0.00	0.08	0.05	0.11	0.11	0.00	0.08	0.07	0.10	0.11	0.11	0.07
Lateral	0.00	0.00	0.00	0.05	0.05	0.00	0.00	0.05	0.05	0.04	0.07	0.06
Posterior	0.00	0.08	0.08	0.07	0.07	0.10	0.06	0.06	0.09	0.09	0.09	0.07
Canal Diameters												
Anterior	0.20	0.21	0.29	0.19	0.19	0.21	0.23	0.17	0.17	0.17	0.23	0.18
Lateral	0.27	0.24	0.25	0.19	0.19	0.19	0.22	0.19	0.25	0.20	0.20	0.20
Posterior	0.26	0.18	0.22	0.24	0.19	0.22	0.25	0.22	0.27	0.20	0.24	0.26
Ratios												
Anterior	0.00	0.38	0.17	0.58	0.58	0.00	0.35	0.41	0.59	0.65	0.48	0.39
Lateral	0.00	0.00	0.00	0.26	0.26	0.00	0.00	0.26	0.20	0.20	0.35	0.30
Posterior	0.00	0.44	0.36	0.29	0.37	0.45	0.24	0.27	0.33	0.45	0.38	0.27

[a] Scanning parameters provided in Chapter 3. All specimens housed at the Texas Natural Sciences Center, Austin Texas (TMM M). Linear dimensions expressed in millimeters.

Functional Considerations

A strong relationship between the size of the bony labyrinth and body mass is to be expected. This phenomenon causes a tricky situation when morphologies within the inner ear are used to make functional interpretations. A clear positive correlation between the arc radius of curvature and sensitivity is evident (Yang and Hullar, 2007), with absolutely larger canals being more sensitive to rotational movement than smaller canals. Additionally, the size of the canals has been related to locomotor behavior (e.g., Spoor et al., 1994, 2002), but this relationship has yet to be tested experimentally.

The size of a semicircular canal arc appears to be correlated with agility (Spoor et al., 2007). In theory, agile (coded as "fast" by Spoor et al., 2007) mammals will have a larger semicircular canal arc radius (averaged over the three canals within a labyrinth) than slower animals of the same body size. The average radius of the anterior, lateral, and posterior semicircular canals was calculated for each taxon examined in this study, and the average was divided by body mass in order to normalize the data (Table 5.11). No correlation is recovered when the ratios of arc radius over body mass are plotted over agility (based on a six point scoring system developed by Spoor et al., 2007). All data were logarithmically transformed using the natural log.

Although the radius of curvature does not correlate to the agility scores of Spoor et al. (2007) when the radius is divided by body mass, the ratios of aquatic taxa are nearly an order of magnitude smaller than the ratios calculated for terrestrial animals, regardless of their evolutionary relationships (see Table 5.11). This suggests that bony labyrinth morphology can be used to identify aquatic tendencies (Spoor et al., 2002; Boyer and Georgi, 2007; Georgi and Sipla, 2008). For example, the size ratio between the cochlea and vestibular apparatus of cetaceans is greater than that observed in most mammals, and

TABLE 5.11. Ratios of Semicircular Canal Arc Radius of Curvature over Average Body Mass and Slender Canal Length[a]

Taxon[b]	Radius / Average Body Mass				Length[c] / Radius		
	Ant	Lat	Post	Average	Ant	Lat	Post
Marsupialia							
Didelphis	0.0523	0.0331	0.0440	0.0361	5.63	5.47	6.11
Eutheria							
Kulbeckia	NA	NA	NA	NA	4.80	4.29	4.75
Ukhaatherium	NA	NA	NA	NA	4.55	4.28	4.88
Zalambdalestes	NA	NA	NA	NA	4.77	4.36	4.53
Zhelestid	NA	NA	NA	NA	4.96	4.40	5.15
Afrotheria							
Chrysochloris	2.4675	1.5184	1.5980	1.8613	4.30	3.89	5.07
Hemicentetes	0.9977	0.6182	0.8045	0.8068	4.52	3.59	5.41
Macroscelides	3.4387	2.7400	2.6670	2.9490	4.25	4.00	5.10
Elephantoidea	NA	NA	NA	NA	4.93	4.70	4.41
Orycteropus	0.0052	0.0054	0.0060	0.0055	4.96	5.03	.5.39
Procavia	0.0524	0.0470	0.0570	0.0520	5.14	4.28	4.90
Trichechus	0.0009	0.0009	0.0010	0.0008	4.02	3.18	4.67
Xenarthra							
Dasypus	0.0345	0.0336	0.0400	0.0362	5.91	4.63	5.88
Laurasiatheria							
Atelerix	0.1431	0.1021	0.1410	0.1288	4.74	4.15	4.74
Balaenopteridae	NA	NA	NA	NA	4.19	4.05	4.94
Bathygenys	NA	NA	NA	NA	5.08	4.68	5.59
Canis	NA	NA	NA	NA	4.97	4.50	5.14
Equus	0.0014	0.0014	0.0010	0.0014	4.79	4.02	5.32
Eumetopias	0.0004	0.0004	0.0004	0.0004	4.33	4.72	4.92
Felis	0.0563	0.0494	0.0559	0.0539	4.57	4.45	4.93
Manis	0.0324	0.0236	0.0369	0.0310	4.52	3.49	4.23
Nycteris	3.3118	2.9696	2.7014	2.9942	4.48	3.91	5.51
Pteropus	0.3604	0.2951	0.3106	0.3221	4.37	4.56	5.20
Rhinolophus	4.8121	4.0187	4.3210	4.3839	4.25	4.64	5.25
Sorex	10.7230	7.9496	10.3611	9.6780	4.91	3.38	5.44
Sus	0.0028	0.0024	0.0025	0.0026	4.86	3.87	4.89
Tadarida	6.9670	6.0395	6.0601	6.3556	4.62	4.45	4.88
Tursiops	0.0007	0.0008	0.0005	0.0006	3.47	3.38	5.17
Euarchontoglires							

TABLE 5.11. (Continued)

Taxon[b]	Radius / Average Body Mass				Length[c] / Radius		
	Ant	Lat	Post	Average	Ant	Lat	Post
Cavia	0.2581	0.2156	0.2240	0.2325	4.79	4.13	5.02
Cynocephalus	0.1930	0.1471	0.1695	0.1699	5.15	4.75	4.94
Homo	0.0037	0.0029	0.0039	0.0035	4.61	4.39	4.76
Lepus	0.0996	0.0707	0.0718	0.0807	4.89	4.13	4.80
Macaca	0.0578	0.0528	0.0545	0.0550	4.74	4.29	5.13
Mus	5.0069	3.8899	4.3126	4.4032	4.98	4.12	5.39
Sylvilagus	0.1600	0.1111	0.1241	0.1317	4.84	4.38	5.13
Tupaia	1.3157	1.0953	1.1412	1.1840	5.35	5.46	5.40

[a] Taxonomy and systematic arrangement follows Bininda-Emonds et al. (2007).Institutional abbreviations: AMNH, American Museum of Natural History, New York, NY; MSW, Mortality South West; SDSNH, San Diego Society of Natural History, San Diego, CA; TMM, Texas Natural Science Center, Austin, TX.
[b] Body mass data from Loughlin et al. (1987) for *Eumetopias*, Ogden et al (2004) for *Homo*, and Silva and Downing (1995) for remaining taxa. Ratio multiplied by 100.
[c] Slender canal length defined as length of the semicircular canal minus its ampullated end.

this led to a hypothesis that a reduced vestibular system is an evolutionary response to the rapid body movements within an aquatic environment exhibited by extant cetaceans (Spoor et al, 2002). Because the mobility of the head and neck in cetaceans nearly is eliminated owing to fusion of cervical vertebrae in some taxa, the vestibulo-collic and vestibulo-ocular reflexes that stabilize the head and eyes during rapid rotations of the body are no longer effective (see Cox and Jeffery, 2008). Thus, larger, more sensitive semicircular canals may no longer compensate for agile movements when the head is unable to move. A reduced vestibular apparatus would reduce sensitivity of the system (see Yang and Hullar, 2007 for a discussion of canal arc size and sensitivity), and lessen any ill effects of an agile lifestyle with cervical fusion.

Although a fully aquatic lifestyle, increased agility, and reduced vestibular systems are observed individually within many mammal taxa, cetaceans are unique in having the full suite of these characteristics. For example, the vestibule and its associated semicircular canals contribute a significantly smaller proportion of the entire bony labyrinth in *Rhinolophus ferrumequinum*, similar to that observed in cetaceans, but *Rhinolophus* does not inhabit an aquatic environment at all. Likewise, sirenians are fully aquatic, but they are among the least agile mammals (as scored by Spoor et al., 2007) and their cervical vertebrae are not fused (see Kaiser, 1974).

The low contribution of the vestibule (or inversely, the high contribution of the cochlea) might be related to an aquatic lifestyle nonetheless. To investigate this hypothesis, the relative contributions of the cochlea and vestibule are compared between terrestrial and aquatic taxa. Because the bats are the only true volant mammals and their ears likely are specialized for aerial locomotion, Chiroptera was not incorporated into this comparison. The vestibular contribution of *Tursiops* and the balaenopterid (6.5% and 9.4% respectively) are less than that observed in terrestrial mammals (range of 28.3% for

Macroscelides to 69.4% for the elephantoid). The vestibular contribution of *Trichechus* (28.9%) is on the low end of the entire mammal range, but it is still greater than the vestibular apparati of both *Macroscelides* (28.3%) and *Chrysochloris* (28.7%), which are strictly terrestrial. Furthermore, the vestibular apparatus of *Eumetopias* contributes 46.5% of total labyrinthine volume, which is only slightly larger than the mean for terrestrial mammals (43.7%). This suggests that aquatic behavior alone cannot explain a reduced vestibular system.

Although the ranges of vestibular contribution overlap between the terrestrial and aquatic samples, the means of each group may differ significantly. The small number of aquatic species used here limits the effectiveness of statistical analysis. The hypothesis that the mean contribution of the vestibule differs significantly between terrestrial and aquatic mammals was tested, with a two-tailed *t*-test assuming unequal variances (determined through an *F*-test). An *a priori* significance level of 0.05 was selected (following Hammer and Harper, 2006), and the null hypothesis is that the mean contributions of the vestibule are equal between the aquatic and terrestrial samples. The results of the analysis ($p=0.007$, which is less than the significance level of 0.05) reject the null hypothesis and suggest that the vestibular contribution of aquatic mammals is significantly greater than that of terrestrial mammals. However, a more thorough analysis incorporating larger sample sizes is needed before a formal conclusion can be made. The aquatic sample is very small, and cetaceans are overrepresented (50.0% of the aquatic taxa) within the sample, which potentially skews the analysis.

Nonetheless, the ratio of semicircular canal arc over body mass is significantly reduced compared to terrestrial species. Furthermore, the vestibules of the two aquatic species *Trichechus manatus* and *Eumetopias jubatus* appear as though they have been

compressed (see Figures 5.18 and 5.36). The deflation may, in essence, reflect a reduction of the membranous utricle and saccule within the bony vestibule.

Further aspects of bony labyrinth morphology are thought to be related to aquatic behavior, namely dimensions of the semicircular canals and their respective arcs. The ratio between the length of the slender semicircular canal over arc radius reflects the frequencies of neural impulses transduced from mechanoreceptors within the membranous labyrinth during rotation of the canal (Boyer and Georgi, 2007). Differences in the ratio might indicate different locomotor abilities, such as semiaquatic versus fully terrestrial. The only pattern observed in the data presented here is that the ratios of length to radius of the anterior semicircular canal of aquatic species tends to be less than that calculated for their close terrestrial relatives (Table 5.11). Although a pattern is observed, the sample size and taxonomic resolution of the current study is insufficient to postulate a formal connection between the ratio of slender duct length to arc radius and locomotor behavior.

The aspect ratios of the arcs of the anterior and posterior semicircular canals of aquatic non-mammalian amniotes tend to be significantly lower than their close terrestrial relatives (Georgi and Sipla, 2008). However, an opposite situation is observed across the mammalian sample examined here, where the radii of the arcs of the two vertical canals (anterior and posterior) are greater for every case in which the canals were compared between aquatic and closely related terrestrial species (see Table 5.4). Methodological differences in the calculation of aspect ratios between the present investigation and that of Georgi and Sipla (2008) might account for the discrepancy in the pattern, or else mammals may in fact exhibit the opposite pattern from other amniotes.

Phylogenetic Considerations

There are major structural differences within the membranous labyrinth that likely contain a phylogenetic signal (Gray 1906, 1907). Two particular features identified by Gray (1906), pigmentation within the membranes and size of the perilymphatic space surrounding the membranous semicircular ducts (which are filled with endolymph themselves). Unfortunately, neither can be assessed from the morphology of the bony labyrinth alone. Gray (1906) considered the perilymphatic space to be an important character in regard to mammal phylogeny, and he argued that a large space is ancestral for mammals (given that he observed a large space within the semicircular canals of reptiles, including birds). Unfortunately, the caliber of the bony canal approximates the shape of the membranous duct within, but not necessarily the size (Curthoys et al., 1977b).

Additional features that may have an importance in determining evolutionary relationships that can be observed within the bony labyrinth include the size of otoliths within the vestibular apparatus, coiling of the cochlea, and shape of the cochlear spiral. The otoliths are tiny in most mammal species, although Gray (1906, 1907, 1908) observed sizeable otoliths within the labyrinths of the marsupial *Petrogale penicillata*, the cetaceans *Balaena australis* and *Phocaena communis*, the sirenian *Dugong dugon*, and the pinniped carnivorans *Phoca vitulina*, *Halichoerus grypus*, and *Otaria pulsilla*. However, otoliths were not observed in the CT imagery of any specimen examined in the present study, including investigated members of Cetacea, Sirenia, and Carnivora.

There are several reasons for the absence of otoliths on the CT scans. The composition and density of otoliths makes it virtually impossible that they would have been missed in CT data if present. Indeed, CT scans of many non-mammalian vertebrates (see scans of fish and squamate reptiles at www.digimorph.org; Maisano and Rieppel,

2007) reveal otoliths. Alternatively, otoliths may be lacking within the bony labyrinth at the time of scanning, either because large otoliths do not occur in life in these species, or else through loss during skeletal preparation. The latter cannot be ruled out, because specimens representing the taxa in which Gray observed large otoliths that were used in this study are dried skulls, and it is conceivable that the otoliths fell out of the ear cavity once the membranes holding them decayed. Even so, otoliths were not observed in specimens that were preserved in alcohol, such as *Chrysochloris* and *Atelerix*, thereby preserving the membranous labyrinths with the otoliths supposedly intact.

Two cochlear shapes termed "sharp-pointed" (observed in rodents, lagomorphs, and non-pinniped carnivorans) and "flattened" (observed in pinnipeds, primates, cetartiodactyls and perissodactyls) were identified by Gray (1906). The distinction between the two morphotypes is not clear, although they roughly correspond to the aspect ratios of the cochlea reported in the present investigation. That is, the taxa with the "sharp-pointed" condition tend towards high aspect ratios, above 0.55, whereas the aspect ratios calculated for species with "flattened" cochleae are 0.55 or less. A couple of exceptions to the generality are *Eumetopias*, which has a cochlear aspect ratio of 0.68 similar to other carnivorans, and *Sus*, which has an aspect ratio of 0.71. However, Gray (1907) described the cochlea of *Sus* as intermediate between "flattened" and "sharp-pointed", but he described the cochleae of pinnipeds as "flattened".

The cochlea of *Cavia porcellus* has the highest aspect ratio (1.29), and it is the only species in this study in which the height of the cochlea is greater than the width. Similar high-spired cochleae are observed within other caviomorph rodents, including *Hydrochoerus capybara* (Gray, 1908), *Dolichotis patagonum* (http://digimorph.org), *Myocastor coypu* (Solntseva, 2007), and *Chinchilla laniger* (personal observation). A high-spired cochlea is likely a synapomorphy for caviomorph rodents, although the

cochlea of the North American porcupine, *Erethizon dorsatum* (which is nested well within Caviomorpha; Huchon and Douzery, 2001; Huchon et al., 2007), is low spired in *Mus musculus* and non-caviomorph rodents (Gray, 1907, 1908; personal observation). Absence of the high-spired cochlea might retention of the ancestral state in *Erethizon*, but it more likely is a reversal. A more thorough investigation of the bony labyrinths of caviomorph and closely related non-caviomorph rodents is needed to fully explore the issue.

The coiling of the cochlea is phylogenetically informative (suggested by Gray, 1907), and can be used to distinguish therian and non-therian mammals (Rowe, 1988), where all extant therian cochleae are coiled to at least 360°. One fossil exception *Uchkudukodon nessovi* from the Cretaceous of Uzbekistan, which has a cochlea that completes less than 360° (McKenna et al., 2000). A single turn likely is plesiomorphic for Eutheria (Meng and Fox, 1995; Chapter 4), and coiling beyond a single turn developed more than once within placental lineages. The number of cochlear whorls was not phylogenetically informative in the present study, however, and could not be used to distinguish major clades within Placentalia. For example, *Mus musculus* and *Pteropus lyelli* both possess a low degree of coiling (628° and 656° respectively), but other members of their clades possess high degrees of coiling (e.g., 1457° in *Cavia porcellus* and 1115° in *Rhinolophus ferrumequinum*).

The stapedial ratio is an index commonly used in phylogenetic analyses to explore the relationships between Mesozoic therians (Wible, 1990; Rougier et al., 1998; Archibald et al., 2001; Ladevèze, 2007). Use of the stapedial ratio in phylogenetic analyses is perpetuated by the assumption that (with a few exceptions; Segall, 1970; Ekdale et al., 2004) marsupials tend to have fenestra vestibuli that are more circular (with a height to width ratio of the stapedial footplate below 1.8; dimensions of the fenestra

vestibuli are used as a proxy in the absence of the stapes) than placentals (based on observations of Segall, 1970). The only marsupial considered here (*Didelphis virginiana*) does, in fact, possess a fenestra vestibuli that falls below the 1.8 cut-off (ratio of 1.6). Among the placentals examined here, however half of the taxa (15; note that no ratio was calculated for *Bathygenys*) exhibit the 'marsupial condition' (below 1.8) of Segall (1970). In fact, the ratio for *Nycteris* is 1.0, which is the observed condition among monotremes (Segall, 1970). This result indicates that a thorough exploration of the stapedial ratio across a broad range of marsupial and placental taxa is necessary before using the ratio in phylogenetic studies.

A further example of the phylogenetic significance of the bony labyrinth of mammals is the relative contribution of the vestibule to the entire labyrinth. The size of the vestibular apparatus certainly is correlated to function (as discussed above), but a reduced vestibule is also a synapomorphy for Cetacea, if only among cetartiodactyls. The contribution of the vestibule of *Rhinolophus* is similar to that observed in cetaceans, but the vestibular (or inversely, cochlear) contribution calculated for other bats fall within the range of other mammals. Because a large cochlea is phylogenetically informative for Cetacea, the phenomenon may also be informative within Chiroptera, upon which a denser sampling of taxa might shed light.

The secondary common crus between the lateral and posterior semicircular canals is an ancestral feature for Theria. All Cretaceous therians possess the secondary crus (Meng and Fox, 1995; Chapter 4), although the structure is lost within most extant placental groups. In fact, the only extant mammals considered in this study having the secondary crus are the marsupial *Didelphis virginiana*, as well as the placentals *Canis familiaris* and *Orycteropus afer*. The lateral semicircular canal opens directly into the

vestibule at its posterior end in the vast majority of the species examined here (20 out of 32), and absence of a secondary common crus is a synapomorphy for crown Placentalia.

A third state is entry of the lateral semicircular canal into the posterior ampulla rather than the vestibule, but separate from the posterior canal (a secondary common crus is not developed). Although the entry of the posterior limb of the lateral semicircular canal does not express any major pattern with the taxonomic sampling employed by the current study, potential for informativeness at lower levels is apparent. For example, the lateral canal opens into the posterior ampulla in the cetaceans, but it opens into the vestibule in their closest terrestrial relatives. Even so, entry of the lateral canal into the posterior ampulla is reconstructed as a synapomorphy of Cetacea, as well as Carnivora. A denser sampling at lower taxonomic levels within these groups, as well as Perissodactyla and Chiroptera, may reveal phylogenetic patterns that are lost at the coarse resolution of this study.

CONCLUSIONS

Variation is a naturally occurring phenomenon that is observable at all levels of morphology, from anatomical variations of DNA molecules to gross variations between whole organisms. The structure of the otic region is no exception. The present paper documents the broad morphological diversity exhibited by the inner ear region of placental mammals. Not surprisingly, many of the individual dimensions of the inner ear correspond with each other, as well as with overall body size of the individual animal.

Great advancements have been made in our understanding of the physiological role played by the inner ear labyrinth over the past 50 years, and this information has been used to make functional and phylogenetic interpretations of fossil vertebrate taxa.

Certainly the morphology of the inner ear cavities has physiological correlates, and it appears that the ratio of the average semicircular canal radius over body mass indeed can distinguish aquatic from terrestrial mammals. Moreover, a generally reduced vestibular system may indicate aquatic lifestyles among closely related taxa.

Phylogenetic patterns are preserved within the ear region. The reduced vestibular apparatus of cetaceans may be rooted in physiology, but the condition, at least when compared to their terrestrial relatives, is a synapomorphy for Cetacea, and such a character state can be used to place fossil cetartiodactyls into a phylogenetic framework. Additionally, the high aspect ratio of the cochlea of caviomorph rodents (excepting *Erethizon dorsatum*) appears to be a synapomorphy for Caviomorpha.

The morphology of the bony labyrinth is phylogenetically informative at the ordinal level, but the morphology of the inner ear does not support any superordinal relationships. In order to fully understand the functional and evolutionary implications within the structure of the bony labyrinth, both physiology and phylogeny must be considered, as these two phenomena are not necessarily mutually exclusive. Future detailed studies of the inner ear among closely related species will increase our knowledge of the phylogenetic and functional implications of the inner ear, and foster the application of bony labyrinth morphology to the biological interpretation of fossil vertebrates.

Appendix 1

Specific CT scanning parameters employed during scanning and post-scanning image processing. Definitions of parameters are as follows: **FR**, field of reconstruction is the dimensions of an individual CT slice, expressed in millimeters; **Pixel**, interpixel spacing, or vertical and horizontal dimensions of an individual pixel, expressed in millimeters, and calculated as FR/Size; **Size**, number of pixels in a CT slice, either 512X512, or 1024X1024 pixels; **Side**, perusal from left or right side of skull; **Slices**, number of CT slices through inner ear collected in the coronal (original) slice plane; **Space**, interslice spacing, or distance between consecutive slices, expressed in millimeters.

Taxon and Specimen No.	Side	Slices	Space	FR	Pixel	Size
Cretaceous Eutheria						
Zhelestid						
URBAC 99-02	left	379	0.0128	11.5	0.0112	1024
URBAC 99-41	right	336	0.0127	15.0	0.0146	1024
URBAC 99-73	right	530	0.0128	10.5	0.0103	1024
URBAC 03-39	left	536	0.0158	14.9	0.0146	1024
URBAC 04-233	right	536	0.0158	14.9	0.0146	1024
ZIN C. 85511	right	397	0.0127	12.0	0.0117	1024
ZIN C. 85512	left	333	0.0128	11.5	0.0112	1024
Kulbeckia kulbeke						
URBAC 98-113	left	126	0.0128	10.0	0.00977	1024
URBAC 00-16	left	446	0.0128	10	0.00977	1024
URBAC 02-56	right	377	0.0128	10.0	0.00977	1024
URBAC 04-36	right	387	0.0157	14.9	0.0146	1024
Ukhaatherium nessovi						
PSS-MAE 110	left	59	0.0800	15.0	0.0293	512
Zalambdalestes lechei						
PSS-MAE 108	left	66	0.113	24.5	0.0479	512
PSS-MAE 108	right	66	0.113	24.5	0.0479	512
PSS-MAE 130	left	127	0.111	28.0	0.0547	512
PSS-MAE 130	right	127	0.111	28.0	0.0547	512

Appendix 1. (Continued).

Taxon and Specimen No.	Side	Slices	Space	FR	Pixel	Size
Extant Placentalia						
Dasypus novemcinctus						
TMM M-152	left	494	0.0291	25.0	0.0244	1024
TMM M-1065	left	494	0.0291	25.0	0.0244	1024
TMM M-1880	left	494	0.0291	25.0	0.0244	1024
TMM M-1885	left	494	0.0291	25.0	0.0244	1024
TMM M-7417	left	97	0.0371	38.0	0.0371	1024
Tadarida brasiliensis						
TMM M-3030	left	380	0.0104	9.9	0.00967	1024
TMM M-3030	right	315	0.0104	9.9	0.00967	1024
TMM M-3110	left	393	0.0104	9.9	0.00967	1024
TMM M-3110	right	388	0.0104	9.9	0.00967	1024
TMM M-6421	left	396	0.0104	9.9	0.00967	1024
TMM M-6653	left	450	0.0104	9.9	0.00967	1024
TMM M-6653	right	351	0.0104	9.9	0.00967	1024
Extant Marsupialia						
Monodelphis domestica						
TMM M-7536	left	81	0.0625	14.0	0.0273	512
TMM M-7539	left	76	0.0676	14.9	0.0291	512
TMM M-7542	left	96	0.0608	17.9	0.0350	512
TMM M-7545	left	81	0.0682	19.0	0.0371	512
TMM M-7595	left	116	0.0371	10.8	0.0211	512
TMM M-8261	left	69	0.0483	16.5	0.0161	1024
TMM M-8265	left	108	0.0338	13.0	0.0127	1024
TMM M-8266	left	119	0.0355	17.0	0.0166	1024
TMM M-8267	left	91	0.0480	22.0	0.0215	1024
TMM M-8268	left	109	0.0480	22.0	0.0215	1024
TMM M-8273	right	61	0.1170	55.7	0.0543	1024

Appendix 2

Extant placentals taken from published material for variation comparisons.

Carnivora

Felis catus (Curthoys et al., 1977a)

Primates

Alouatta seniculus (Spoor and Zonneveld, 1998)

Gorilla gorilla (Spoor and Zonneveld, 1998)

Homo sapiens (Blanks et al., 1975; Curthoys et al., 1977a; Muren et al., 1986; Curthoys and Oman, 1987; Jeffery and Spoor, 2004)

Hylobates syndactylus (Spoor and Zonneveld, 1998)

Macaca fascicularis (Spoor and Zonneveld, 1998)

Macaca mulatta (Blanks et al., 1985)

Pan paniscus (Spoor and Zonneveld, 1998)

Pan troglodytes (Spoor and Zonneveld, 1998)

Pongo pygmaeus (Spoor and Zonneveld, 1998)

Saimiri sciureus (Blanks et al., 1985)

Rodentia

Cavia porcellus (Curthoys et al., 1975, 1977a; Curthoys and Oman, 1986)

Chinchilla laniger (Hullar and Williams, 2006)

Mus musculus (Calabrese and Hullar, 2006)

Rattus rattus (Curthoys and Oman, 1986).

References

Adkins, R. M., and R. L. Honeycutt. 1991. Molecular phylogeny of the superorder Archonta. Proceedings of the National Academy of Sciences of the United States of America 88:10317-10321.

Adkins, R. M., E. L. Gelke, D. Rowe, and R. L. Honeycutt. 2001. Molecular phylogeny and divergence time estimates for major rodent groups: evidence from multiple genes. Molecular Biology and Evolution 18:777-791.

Aitkin, L., S. Cochran, S. Frost, A. Martsi-McClintock, and B. Masterton. 1997. Features of the auditory development of the short-tailed Brazilian opossum, *Monodelphis domestica*: evoked responses, neonatal vocalizations and synapses in the inferior colliculus. Hearing Research 113:69-75.

Alexander, R. M. 2002. Stability and maneuverability of terrestrial vertebrates. Integrative and Comparative Biology 42:158-164.

Alonso, P. D., A. C. Milner, R. A. Ketcham, M. J. Cookson, and T. B. Rowe. 2004. The avian nature of the brain and inner ear of *Archaeopteryx*. Nature 430:666-669.

Amrine-Madsen, H., K. –P. Koepfli, R. K. Wayne, and M. S. Springer. 2003. A new phylogenetic marker, apolipoprotein B, provides compelling evidence for eutherian relationships. Molecular Phylogenetics and Evolution 28:225-240.

Archibald, J. D. 1979. Oldest known eutherian stapes and a marsupial petrosal bone from the Late Cretaceous of North America. Nature 281:669-670.

Archibald, J. D. 1996. Fossil evidence for a Late Cretaceous origin of "hoofed" mammals. Science 272:1150-1153.

Archibald, J. D., and A. O. Averianov. 2003. The Late Cretaceous placental mammal *Kulbeckia*. Journal of Vertebrate Paleontology 23:404-419.

Archibald, J. D., and A. O. Averianov. 2005. Mammalian succession in the Cretaceous of the Kyzylkum Desert. Journal of Mammalian Evolution 12:9-22.

Archibald, J. D., and A. O. Averianov. 2006. Late Cretaceous asioryctitherian eutherian mammals from Uzbekistan and phylogenetic analysis of Asioryctitheria. Acta Palaeontologica Polonica 51:351-376.

Archibald, J. D., and A. O. Averianov. 2007. Zhelestids: stem eutherians or basal laurasiatherians, but no evidence for placental orders in the Cretaceous. Journal of Vertebrate Paleontology 27(3, Supplement):41A.

Archibald, J. D., A. O. Averianov, and E. G. Ekdale. 2001. Late Cretaceous relatives of rabbits, rodents, and other extant eutherian mammals. Nature 414:62-65.

Arnason, U., J. A. Adegoke, K. Bodin, E. W. Born, Y. B. Esa, A. Gullberg, M. Nilsson, R. V. Short, X. Xu, and A. Janke. 2002. Mammalian mitogenomic relationships

and the root of the eutherian tree. Proceedings of the National Academy of Sciences 99:8151-8156.

Asher, R. J. 2001. Cranial anatomy in tenrecid insectivorans: character evolution across competing phylogenies. American Museum Novitates 3352:1-54.

Asher, R. J. 2005. Insectivoran-grade placentals; pp. 50-70 in K. D. Rose and J. D. Archibald (eds), The rise of placental mammals: origins and relationships of the major extant clades. The Johns Hopkins University Press, Baltimore.

Asher, R. J. 2007. A web-database of mammalian morphology and a reanalysis of placental phylogeny. BMC Evolutionary Biology 7(108):1-10.

Asher, R. J., M. J. Novacek, and J. H. Geisler. 2003. Relationships of endemic African mammals and their fossil relatives based on morphological and molecular evidence. Journal of Mammalian Evolution 10:131-194.

Asher, R. J., J. Meng, J. R. Wible, M. C. McKenna, G. W. Rougier, D. Dashzeveg, and M. J. Novacek. 2005. Stem Lagomorpha and the antiquity of Glires. Science 307:1091-1094.

Averianov, A. O., and J. D. Archibald. 2005. Mammals from the mid-Cretaceous Khodzhakul Formation, Kyzylkum Desert, Uzbekistan. Cretaceous Research 26:593-608.

Beard, K. C. 1993. Phylogenetic systematics of the Primatomorpha, with special reference to Dermoptera; pp 129-150 in F. S. Szalay, M. J. Novacek, and M. C. McKenna (eds.), Mammal Phylogeny: Placentals. Springer-Verlag, New York.

Beck, R. M. D., H. Godthelp, V. Weisbecker, M. Archer, and S. J. Hand. 2008. Australia's oldest marsupial fossils and their biogeographical implications. PLoS One 3(3):e1858.

Bever, G. S. 2006. Studies on post-natal variation and variability in the skeleton and its paleontological implications. Unpublished PhD Dissertation, The University of Texas at Austin, 719 p.

Bever, G. S., C. J. Bell, and J. A. Maisano. 2005. The ossified braincase and cephalic osteoderms of *Shinisaurus crocodilurus* (Squamata, Shinisauridae). Palaeontologia Electronica 8(4A):1-36.

Bininda-Emonds, O. R. P., J. L. Gittelman, and A. Purvis. 1999. Building large trees by combining phylogenetic information: a complete phylogeny of the extant Carnivora (Mammalia). Biological Reviews 74:143-175.

Bininda-Emonds, O. R. P., M. Cardilla, K. E. Jones, D. E. Ross, R. M. D. Beck, R. Grenyer, S. A. Price, R. A. Voss, J. L. Gittleman, and A. Purvis. 2007. The delayed rise of present-day mammals. Nature 446:507-512.

Blair, P. 1710-1712a. Osteographia elephantina: or, a full and exact description of all the bones of an elephant, which died near Dundee, April the 27th, 1706. With their several dimensions. Communicated in a letter to Dr. Hans Sloane, R. S. Secr. By Mr Patrick Blair, &c. Philosophical Transactions (1683-1775) 27:53-116.

Blair, P. 1710-1712b. A continuation of the osteographia elephantina: or, a description of the bones of an elephant, which died near Dundee, April the 27th, 1706. By Mr. Patrick Blair. Philosophical Transactions (1683-1775) 27:117-168.

Blair, P. 1717-1719. A description of the organ of hearing in the elephant, with the figures and situation of the ossicles, labyrinth and cochlea in the ear of that large animal. Communicated to the Royal Society by Dr. Patrick Blair, R. S. S. Philosophical Transactions (1683-1775) 30:885-898.

Blanks, R. H. I., I. S. Curthoys, and C. H. Markham. 1972. Planar relationships of semicircular canals in the cat. American Journal of Physiology 223:55-62.

Blanks, R. H. I., I. S. Curthoys, and C. H. Markham. 1975. Planar relationships of the semicircular canals in man. Acta Oto-Laryngolica 80:185-196.

Blanks, R. H. I., I. S. Curthoys, M. L. Bennett, and C. H. Markham. 1985. Planar relationships of the semicircular canals in rhesus and squirrel monkeys. Brain Research 340:315-324.

Boisvert, C. A. 2005. The pelvic fin and girdle of Panderichthys and the origin of tetrapod locomotion. Nature 438:1145-1147.

Boulter, M. C., D. Gee, and H. C. Fisher. 1998. Angiosperm radiations at the Cenomanian/Turonian and Cretaceous/Tertiary boundaries. Cretaceous Research 19:107-112.

Boyden A, Gemeroy D. 1950. The relative position of the Cetacea among the orders of Mammalia as indicated by precipitin tests. Zoologica 35:145-151.

Boyer, D. M. and J. A. Georgi. 2007. Cranial morphology of a pantolestid eutherian mammal from the Eocene Bridger Formation, Wyoming, USA: implications for relationships and habitat. Journal of Mammalian Evolution 14:239-380.

Brinkman, D. 1988. Size-independent criteria for estimating relative age in *Ophiacodon* and *Dimetrodon* (Reptilia, Pelycosauria) from the Admiral and Lower Belle Plains formations of west-central Texas. Journal of Vertebrate Paleontology 8:172-180.

Brochu, C. A. 1996. Closure of neurocentral sutures during crocodilian ontogeny: implications for maturity assessment in fossil archosaurs. Journal of Vertebrate Paleontology 16:49-62.

Bugge, J. 1978. The cephalic arterial system in carnivores, with special reference to the systematic classification. Acta Anatomica 101:45-61.

Butler, P. M. 1972. The problem of insectivore classification; pp. 253-265 in K. A. Joysey, and T. S. Kemp (eds), Studies in vertebrate evolution. Winchester Press, New York, New York.

Caix, M., and G. Outrequin. 1979. Variability of the bony semicircular canals. Anatomia Clinica 1:259-265.

Calabrese, D. R., and T. E. Hullar. 2006. Planar relationships of the semicircular canals in two strains of mice. Journal for the Association for Research in Otolaryngology 7:151-159.

Campbell CBG. 1966. The relationships of the tree shrews: the evidence of the nervous system. Evolution 20:276-281.

Cao, Y., N. Okada, and M. Hasegawa. 1997. Phylogenetic position of guinea pigs revisited. Molecular Biology and Evolution 14:461-464.

Cao Y., J. Adachi , T. Yano, and M. Hasegawa. 1994. Phylogenetic place of guinea pigs: no support of the rodent-polyphyly hypothesis from maximum-likelihood analyses of multiple protein sequences. Molecular Biology and Evolution 11:593-604.

Cao Y., K. S. Kim, J. H. Ha, and M. Hasegawa. 1999. Model dependence of the phylogenetic inference: relationship among carnivores, perissodactyls and cetartiodactyls as inferred from mitochondrial genome sequences. Genes and Genetic Systems 74:211-217.

Carlsson, A. 1922. Über die Tupaiidae und ihre beziehungen zu den Insectivora und den Prosimiae. Acta Zoologica 3:227-270.

Carrasco, M. A. 1998. Variation and its implication in a population of *Cupidinimus* (Heteromyidae) from Hepburn's Mesa, Montana. Journal of Vertebrate Paleontology 18:391-402.

Chester, S., E. Sargis, E. Szalay, J. D. Archibald, and A. Averianov. 2007. Functional analysis of mammalian humeri from the Late Cretaceous of Uzbekistan. Journal of Vertebrate Paleontology 27(3, Supplement):58A.

Chester, S., E. Sargis, F. Szalay, J. D. Archibald, and A. O. Averianov. 2008. Therian femora from the Late Cretaceous of Uzbekistan. Journal of Vertebrate Paleontology 28(3, Supplement):63A.

Christiansen, P. 2004. Body size in proboscideans, with notes on elephant metabolism. Zoological Journal of the Linnean Society 140:523-549.

Cifelii, R. L. 1982. The petrosal structure of *Hyopsodus* with respect to that of some other ungulates, and its phylogenetic implications. Journal of Paleontology 56:795-805.

Cifelli, R. L. 1990. Cretaceous mammals of southern Utah. IV. Eutherian mammals from the Wahweap (Aquilan) and Kaiparowits (Judithian) formations. Journal of Vertebrate Paleontology 10:346-360.

Clack, J. A. 2002. Patterns and processes in the early evolution of the tetrapod ear. Journal of Neurobiology 53:251-264.

Clark, C. T. and K. K. Smith. 1993. Cranial osteogenesis in *Monodelphis domestica* (Didelphidae) and *Macropus eugenii* (Macropodidae). Journal of Morphology 215:119-149.

Clarke, A. H. 2005. On the vestibular labyrinth of *Brachiosaurus brancai*. Journal of Vestibular Research 15:65-71.

Clarke, J. A., C. P. Tambussi, J. I. Noriega, G. M. Erickson, and R. A. Ketcham. 2005. Definitive fossil evidence for the extant avian radiation in the Cretaceous. Nature 433:305-308.

Clemens, W. A. 1968. Origin and early evolution of marsupials. Evolution 22:1-18.

Colbert, M. W., and T. Rowe. 2008. Ontogenetic sequence analysis: using parsimony to characterize developmental sequences and sequence polymorphism. Journal of Experimental Zoology (Molecular and Developmental Evolution) 310B:398-416.

Coleman, M. N., and M. W. Colbert. 2007. Technical note: CT thresholding protocols for taking measurements on three-dimensional models. American Journal of Physical Anthropology 133:723-725.

Cooper, A., and D. Penny. 1997. Mass survival of birds across the Cretaceous-Tertiary boundary: molecular evidence. Science 275:1109-1113.

Cope, D. A., and M. G. Lacy. 1995. Comparative application of the coefficient of variation and range-based statistics for assessing the taxonomic composition of fossil samples. Journal of Human Evolution 29:549-576.

Court N. 1990. Periotic anatomy of *Arsinotherium* (Mammalia, Embrithopoda) and its phylogenetic implications. Journal of Vertebrate Paleontology 10:170-182.

Court N. 1992a. The skull of *Arsinotherium* (Mammalia, Embrithopoda) and the higher order interrelationships of ungulates. Palaeovertebrata 22:1-43.

Court, N. 1992b. Cochlea anatomy of *Numidotherium koholense*: auditory acuity in the oldest known proboscidean. Lethaia 25:211-215.

Court, N. 1994. The periotic of *Moeritherium* (Mammalia, Proboscidea): homology or homoplasy in the ear region of Tethytheria McKenna, 1975?. Zoological Journal of the Linnean Society 112:13-28.

Court, N. and J. –J. Jaeger. 1991. Anatomy of the periotic bone in the Eocene probsoidean *Numidotherium koholense*: an example of parallel evolution in the inner ear of tethytheres. Comptes Rendus de l'Académie des Sciences. Série II,

Mécanique, Physique, Chimie, Sciences de l'Univers, Sciences de la Terre, 312:559-565.

Cox, P. G., and N. Jeffery. 2008. Geometry of the semicircular canals and extraocular muscles in rodents, lagomorphs, felids and modern humans. Journal of Anatomy 213:583-596.

Cracraft, J. 1986. The origin and early diversification of birds. Paleobiology 12:383-399.

Curthoys, I. A., and C. M. Oman. 1986. Dimensions of the horizontal semicircular duct, ampulla and utricle in rat and guinea pig. Acta Oto-laryngolica 101:1-10.

Curthoys, I. A., and Oman. 1987. Dimensions of the horizontal semicircular duct, ampulla and utricle in the human. Acta Oto-laryngolica 103:254-261.

Curthoys, I. S., R. H. I. Blanks, and C. H. Markham. 1977a. Semicircular canal radii of curvature (R) in cat, guinea pig and man. Journal of Morphology 151:1-16.

Curthoys, I. S., C. H. Markham, and E. J. Curthoys. 1977b. Semicircular duct and ampulla dimensions in cat, guinea pig and man. Journal of Morphology 151:17-34.

Curthoys, I. S., E. J. Curthoys, R. H. I. Blanks, and C. H. Markham. 1975. The orientation of the semicircular canals in the guinea pig. Acta Otolaryngolica 80:197-205.

de Beer, G. R. 1947. How animals hold their heads. Proceedings of the Linnean Society of London 159:125-139.

de Jong, W. W., A. Zweers, and M. Goodman. 1981. Relationship of aardvark to elephants, hyraxes and sea cows from α-crystallin sequences. Nature 292:538-540.

de Jong, W. W., M. A. M. van Dijk, C. Poux, G. Kappé, T. van Rheede, and O. Madsen. 2003. Indels in protein-coding sequences of Euarchontoglires constrain the rooting of the eutherian tree. Molecular Phylogenetics and Evolution 28:328-340.

D'Erchia, A. M., C. Gisso, G. Pesole, C. Saccone, and U. Arnason. 1996. The guinea-pig is not a rodent. Nature 381:597-600.

Dercum, F. 1879. On the morphology of the semicircular canals. American Naturalist 13:366-374.

Dimopoulos, P., and C. Muren. 1990. Anatomic variations of the cochlea and relations to other temporal bone structures. Acta Radiologica 31:439-444.

Douzery, E. J. P., and D. Huchon. 2004. Rabbits, if anything, are likely Glires. Molecular Phylogenetics and Evolution 33:922-935.

Eales, N. B. 1926. The anatomy of the head of a foetal African elephant, *Elephas africanus* (*Loxodonta africana*). Transactions of the Royal Society of Edinburgh 54:491-551.

Easteal, S. 1990. The pattern of mammalian evolution and the relative rate of molecular evolution. Genetics 124:165-173.

Eizirik, E., W. J. Murphy, and S. J. O'Brien. 2001. Molecular dating and biogeography of the early placental mammal radiation. Journal of Heredity 92:212-219.

Ekdale, E. G. 2005. Ontogeny of the inner ear of mammals: implications for the phylogenetic assessment of fossils. Journal of Vertebrate Paleontology (3, Supplement) 25:53A.

Ekdale, E. G., J. D. Archibald, and A. O. Averianov. 2004. Petrosal bones of placental mammals from the Late Cretaceous of Uzbekistan. Acta Palaeontological Polonica 49:161-176.

Emerson, G. L., C. W. Kilpatrick, B. E. McNiff, J. Ottenwalder, M. W. Allard. 1999. Phylogenetic relationships of the order Insectivora based on complete 12S rRNA sequences from mitochondria. Cladistics 15:221-230.

Eugenín, J. and J. G. Nicholls. 1997. Chemosensory and cholinergic stimulation of fictive respiration in isolated CNS of neonatal opossum. Journal of Physiology 501:425-437.

Evans, G. L. 1961. The Friesenhahn Cave. Bulletin of the Texas Memorial Museum 2:7-22.

Evans, H. E. 1993. Miller's Anatomy of the Dog (third edition). Saunders, Philadelphia, 1113 p.

Fadem, B. H., G. L. Trupin, E. Maliniak, J. L. VandeBerg, and V. Hayssen. 1982. Care and breeding of the gray, short-tailed opossum (*Monodelphis domestica*). Laboratory Animal Science 32:405-409.

Fischer, M. S. 1990. Un trait unique de l'orielle des elephants et des siréniens (Mammalia): un paradoxe phylogénétigue. Comptes Rendus de l'Académie des Sciences. Série II, Sciences de la Vie 311:157-162.

Fischer, M. S. and P. Tassy. 1993. The interrelation between Proboscidea, Sirenia, Hyracoidea, and Mesaxonia: the morphological evidence; pp. 217-234 in F. S. Szalay, M. J. Novacek, and M. C. McKenna (eds.), Mammal Phylogeny: Placentals. Springer-Verlag, New York.

Fleischer, G. 1976. Hearing in extinct cetaceans as determined by cochlear structure. Journal of Paleontology 50:133-152.

Flower, W. H. 1883. On the arrangement of the orders and families of existing Mammalia. Proceedings of the Zoological Society of London 1883:178-186.

Flynn, J. J., and G. D. Wesley-Hunt. 2005. Carnivora; pp 175-198 in K. D. Rose, and J. D. Archibald (eds.), The rise of placental mammals: origins and relationships of the major extant clades. The Johns Hopkins University Press, Baltimore.

Fox, R. C. 1989. The Wounded Knee local fauna and mammalian evolution near the Cretaceous-Tertiary boundary, Saskatchewan, Canada. Palaeontographica Abteilung A 208:11-59.

Frye, M. S., and S. B. Hedges. 1995. Monophyly of the order Rodentia inferred from mitochondrial DNA sequences of the genes for 12S rRNA, 16S rRNA, and tRNA-valine. Molecular Biology and Evolution 12:168-176.

Galvão, P. E. 1947. Heat production in relation to body weight and body surface. Inapplicability of the surface law on dogs of the tropical zone. American Journal of Physiology 148:478-489.

Gatesy, J., C. Hayashi, M. A. Cronin, and P. Arctander. 1996. Evidence from milk casein genes that cetaceans are close relatives of hippopotamid artiodactyls. Molecular Biology Evolution 13:954-963.

Gatesy, J., M. Milinkovitch, V. Waddell, and M. Stanhope. 1999. Stability of cladistic relationships between Cetacea and higher-level artiodactyl taxa. Systematic Biology 48:6-20.

Gaudin, T. J., and A. A. Biewener. 1992. The functional morphology of xenarthrous vertebrae in the armadillo *Dasypus novemcinctus* (Mammalia, Xenarthra). Journal of Morphology 214:63-81.

Geisler, J.H. 2001. New morphological evidence for the phylogeny of Artiodactyla, Cetacea, and Mesonychidae. American Museum Novitates 3344:1-53.

Geisler, J. H. and Z. Luo. 1996. The petrosal and inner ear of *Herpetocetus* sp. (Mammalia: Cetacea) and their implications for the phylogeny and hearing of archaic mysticetes. Journal of Paleontology 70:1045-1066.

Geisler, J. H., and Z. Luo. 1998. Relationships of Cetacea to terrestrial ungulates and the evolution of cranial vasculature in Cete; pp. 163-212 in J. G. M Thewissen (ed.), The Emergence of Whales. Plenum Press, New York.

Geisler, J. H., and J. M. Theodor. 2009. Hippopotamus and whale phylogeny. Nature 458:E1-E4.

Geisler, J. H., M. D. Uhen. 2003. Morphological support for a close relationship between hippos and whales. Journal of Vertebrate Paleontology 23:991-996.

George, C. O., E. L. Lundelius, Jr., L. Meissner, R. S. Toomey, III, and R. W. Graham. 2007. Late Quaternary cave sites of central Texas: field trip guidebook. Prepared for the Society of Vertebrate Paleontology, Austin,TX, Oct. 15-16, 67th Annual Meeting, 48 p.

Georgi, J. A., and J. S. Sipla. 2008. Comparative and functional anatomy of balance in aquatic reptiles and birds; pp. 233-256 in J. G. M. Thewissen and S. Numella (eds.), Sensory Evolution on the Threshold: Adaptations in Secondarily Aquatic Vertebrates. University of California Press, Berkeley, California.

Gheerbrant, E., and H. Astibia. 1994. Un nouveau mammifère du Maastrichtien de Laño (Pays Basque espagnol). Comptes Rendus de l'Académie des Sciences, Série II , Sciences de la Terre et des Planètes 318:1125-1131.

Gheerbrant, E., D. P. Domning, and P. Tassy. 2005. Paenungulata (Sirenia, Proboscidea, Hyracoidea, and Relatives), pp. 84-105 in K. D. Rose, and J. D. Archibald (eds.), The Rise of Placental Mammals: Origins and Relationships of the Major Extant Clades. The Johns Hopkins University Press, Baltimore.

Gidley, J. W. 1912. The lagomorphs an independent order. Science 36:285-286.

Gingerich, P. D. 2005. Cetacea; pp. 234-252 in K. D. Rose, and J. D. Archibald JD (eds.), The Rise of Placental Mammals: Origins and Relationships of the Major Extant Clades. The Johns Hopkins University Press, Baltimore.

Gingerich, P. D., M. ul Haq, I. S. Zalmout, I. H. Khan, and M. S. Malkani. 2001. Origin of whales from early artiodactyls: hands and feet of Eocene Protocetidae from Pakistan. Science 293:2239-2242.

Goodman, M., C. A. Porter, J. Czelusniak, S. L. Page, H. Schneider, J. Shoshani, G. Gunnell, and C. P. Groves. 1998. Toward a phylogenetic classification of Primates based on DNA evidence complemented by fossil evidence. Molecular Phylogenetics and Evolution 9:585-598.

Gosman, J. H., and R. A. Ketcham. 2009. Patterns in ontogeny of human trabecular bone from SunWatch Village in the prehistoric Ohio Valley: general features of microarchitectural change. American Journal of Physical Anthropology 138:318-332.

Gosselin-Ildari, A. D. 2006. Functional morphology of the bony labyrinth in Primates. Unpublished Undergraduate Honors Thesis, The University of Texas at Austin, 52 p.

Gosselin-Ildari, A. D., and E. C. Kirk. 2007. Functional morphology of the primate cochlea. American Journal of Physical Anthropology 132(S44):118.

Gould, E. 1965. Evidence for echolocation in the Tenrecidae of Madagascar. Proceedings of the American Philosophical Society 109:352-360.

Graham, R. W. 1976. Pleistocene and Holocene mammals, taphonomy, and paleoecology of the Friesenhahn Cave local fauna, Bexar County, Texas. Unpublished Ph.D. Dissertation, The University of Texas at Austin, 233 p.

Graur, D., and D. G. Higgins. 1994. Molecular evidence for the inclusion of cetaceans within the order Artiodactyla. Molecular Biology and Evolution 11:357-364.

Graur, D., W. A. Hide, and W. –H. Li. 1991. Is the guinea-pig a rodent? Nature 351:649-652.

Graur, D., W. A. Hide, A. Zharkikh, and W. –H. Li. 1992. The biochemical phylogeny of guinea-pigs and gundis, and the paraphyly of the order Rodentia. Comparative Biochemistry and Physiology 101B:495-498.

Gray, A. A. 1903. On a method of preparing the membranous labyrinth. Journal of Anatomy and Physiology 37:379-381.

Gray, A. A. 1905. A demonstration of specimens prepared by the author's method to show the membranous labyrinth in man and lower animals. Transactions of the Otological Society of the United Kingdom 6:9-13.

Gray, A. A. 1906. Observations on the labyrinth of certain animals. Proceedings of the Royal Society of London. Series B, Containing Papers of a Biological Character 78:284-296.

Gray, A. A. 1907. The labyrinth of animals: including mammals, birds, reptiles and amphibians. Volume 1. J. and A. Churchill, London, 98 pp.

Gray, A. A. 1908. The labyrinth of animals: including mammals, birds, reptiles and amphibians. Volume 2. J. and A. Churchill, London, 252 pp.

Graybeal, A., J. J. Rosowski, D. R. Ketten, and A. W. Crompton. 1989. Inner-ear structure in *Morganucodon*, an early Jurassic mammal. Zoological Journal of the Linnean Society 96:107-117.

Gregory, W. K. 1910. The orders of mammals. Bulletin of the American Museum of Natural History 27:1-524.

Grenyer, R., and A. Purvis. 2003. A composite species-level phylogeny of the 'Insectivora' (Mammalia: Order Lipotyphla Haeckel, 1866). Journal of Zoology, London 260:245-257.

Guild, S. R. 1921. A graphic reconstruction method for the study of the organ of Corti. Anatomical Record 22:141-157.

Halpern, M., Y. Daniels, and I. Zuri. 2005. The role of the vomeronasal systemin food preferences of the gray short-tailed opossum, *Monodelphis domestica*. Nutrition and Metabolism 2(6):1-6.

Hammer, Ø., and D. Harper. 2006. Paleontological Data Analysis. Blackwell Publishing, Malden, Massachussets, 351 pp.

Harvati, K. A. and T. D. Weaver. 2006. Human cranial anatomy and the differential preservation of population history and climate signatures. Anatomical Record 288A:1225-1233.

Hawkins, J. E. 2004. Sketches of otohistory. Part 1: otoprehistory: how it all began. Audiology and Neuro-otology 9:66-71.

Hedges, S. B., P. H. Parker, C. G. Sibley, and S. Kumar. 1996. Continental breakup and the ordinal diversification of birds and mammals. Nature 381:226-229.

Heusner, A. A. 1991. Body mass, maintenance and basal metabolism in dogs. Journal of Nutrition 121:S8-S17.

Holroyd, P. A., J. C. Mussell. 2005. Macroscelidea and Tubulidentata; pp. 71-83 in K. D. Rose, J. D. Archibald (eds.), The Rise of Placental Mammals: Origins and Relationships of the Major Extant Clades. The Johns Hopkins University Press, Baltimore.

Honeycutt, R. L., and R. M. Adkins. 1993. Higher level systematics of eutherian mammals: an assessment of molecular characters and phylogenetic hypotheses. Annual Reviews in Ecology and Systematics 24:279-305.

Hooker, J. J. 2005. Perissodactyla; pp. 199-214 in K. D. Rose, and J. D. Archibald (eds.), The Rise of Placental Mammals: Origins and Relationships of the Major Extant Clades. The Johns Hopkins University Press, Baltimore.

Hoyte, D. A. N. 1961. The postnatal growth of the ear capsule in the rabbit. American Journal of Anatomy 108:1-16.

Hublin, J. –J, F. Spoor, M. Braun, F. Zonneveld, and S. Condemi. 1996. A late Neanderthal associated with Upper Paleaeolithic artifacts. Nature 381:224-226.

Huchon, D., and J. P. Douzery. 2001. From the Old World to the New World: a molecular chronicle of the phylogeny and biogeography of hystricognath rodents. Molecular Phylogenetics and Evolution 20:238-251.

Huchon, D., F. M. Catzeflis, and E. J. P. Douzery. 1999. Molecular evolution of the nuclear von Wollebrand factor gene in mammals and the phylogeny of rodents. Molecular Biology and Evolution 16:577-589.

Huchon, D., P. Chevret, U. Jordan, C. W. Kilpatrick, V. Ranwez, P. D. Jenkins, J. Brosius, and J. Schmitz. 2007. Multiple molecular evidences for a living mammalian fossil. Proceedings of the National Academy of Sciences of the United States of America 104:7495-7499.

Huchon, D., O. Madsen, M. J. J. B. Sibbald, K. Ament, M. J. Stanhope, F. Catzeflis, W. W. de Jong, and E. J. P. Douzery. 2002. Rodent phylogeny and a timescale for the evolution of Glires: evidence from an extensive taxon sampling using three nuclear genes. Molecular Biology and Evolution 19:1053-1065.

Hullar, T. E. 2006. Semicircular canal geometry, afferent sensitivity, and animal behavior. Anatomical Record 288A:466-472.

Hullar, T. E. and C. D. Williams. 2006. Geometry of the semicircular canals of the chinchilla (*Chinchilla laniger*). Hearing Research 213:17-24.

Hunt, R. M., Jr. 1987. Evolution of the aeluroid Carnivora: significance of auditory structure in the nimravid cat *Dinictis*. American Museum Novitates 2886:1-74.

Hunt, R. M., Jr. 1989. Evolution of the aeluroid Carnivora: significance of the ventral promontorial process of the petrosal, and the origin of basicranial patterns in living families. American Museum Novitates 2930: 1-32.

Hyrtl, J. 1845. Verleichende-anatomische Untersuchungen über das innere Gehörorgan des menschen und der Säugethiere. Prague, 139 pp.

Igarashi, M. 1967. Dimensional study of the vestibular apparatus. Laryngoscope 77:1806-1817.

Janečka, J. E., W. Miller, T. H. Pringle, F. Wiens, A. Zitzmann, K. M. Helgen, M. S. Springer, W. J. Murphy. 2007. Molecular and genomic data identify the closest living relative of Primates. Science 318:792-794.

Jeffery, N., and F. Spoor. 2004. Prenatal growth and development of the modern human labyrinth. Journal of Anatomy 204:71-92.

Jeffery, N. and F. Spoor. 2006. The primate subarcuate fossa and its relationship to the semicircular canals part I: prenatal growth. Journal of Human Evolution, 51:537-549.

Jones, G. M. and K. E. Spells. 1963. A theoretical and comparative study of the functional dependence of the semicircular canal upon its physical dimensions. Proceedings of the Royal Society of London B 157:403-419.

Kaiser, H. E. 1974. Morphology of the Sirenia: a macroscopic and X-ray atlas of the osteology of recent species. S. Karger, Basel, Switzerland, 75 pp.

Kay, R. F., C. Ross, and B. A. Williams. 1997. Anthropoid origins. Science 275:797-804.

Ketten, D. R. 1997. Structure and function in whale ears. Bioacoustics 8:103-135.

Kielan-Jaworowska, Z. 1984. Evolution of the therian mammals in the Late Cretaceous of Asia. Part VI. Endocranial casts of eutherian mammals. Palaeontologica Polonica 46:157-171.

Kielan-Jaworowska, Z., R. Cifelli, and Z. –X. Luo. 2004. Mammals from the Age of Dinosaurs. Columbia University Press, New York, 630 pp.

Kirk, E. C., and A. D. Gosselin-Ildari. 2009. Cochlear labyrinth volume and hearing abilities in Primates. Anatomical Record 292:765-776.

Kleineidam, R. G., G. Pesole, H. L. Breukelman, J. J. Beintema, and R. A. Kastelein. 1999. Inclusion of cetaceans within the order Artiodactyla based on phylogenetic analysis of pancreatic ribonuclease genes. Journal of Molecular Evolution 48:360-368.

Kumar, S., and S. B. Hedges. 1998. A molecular timescale for vertebrate evolution. Nature 392:917-920.

Kusewitt, D. F., T. A. Sherburn, K. B. Miska, G. B. Tafoya, J. M. Gale, and R. D. Miller. 1999. The *p53* tumor suppressor gene of the marsupial *Monodelphis domestica*:

cloning of exons 4-11 and mutations in exons 5-8 in ultraviolet radiation-induced corneal sarcomas. Carcinogenesis 20:963-968.

Ladevèze, S. 2004. Metatherian petrosals from the late Paleocene of Itaboraí, Brazil, and their phylogenetic implications. Journal of Vertebrate Paleontology 24:202-213.

Ladevèze, S. 2007. Petrosal bones of metatherian mammals form the Late Palaeocene of Itaboraí (Brazil), and a cladistic analysis of petrosal features in metatherians. Zoological Journal of the Linnean Society, 150:85-115.

Larsell, O., E. McCrady, Jr, and A. A. Zimmermann. 1935. Morphological and functional development of the membranous labyrinth in the opossum. Journal of Comparative Neurology 63:95-118.

Lambert, W. D. and J. Shoshani. 1998. Proboscidea, pp. 606-621 in C. M. Janis, K. M. Scott, and L. L. Jacobs (eds.), Evolution of Tertiary Mammals of North America, Volume 1: Terrestrial Carnivores, Ungulates, and Ungulatelike Mammals. Cambridge University Press, Cambridge.

Lavergne, A., E. Douzery, T. Stichler, F. M. Catzeflis, and M. S. Springer. 1996. Interordinal mammalian relationships: evidence for paenungulate monophyly is provided by complete mitochondrial 12S rRNA sequences. Molecular Phylogenetics and Evolution 6:245-258.

Lawrence, D. R. 1968. Taphonomy and information losses in fossil communities. Geological Society of America Bulletin 79:1315-1330.

Laws, R. M. 1966. Age criteria for the African elephant, *Loxodonta a. africana*. East African Wildlife Journal 4:1-37.

Lee, F. S. 1898. Functions of the ear and the lateral line in fishes. American Journal of Physiology 1:128-144.

Li W-H, Hide WA, Graur D. 1992. Origin of rodents and guinea-pigs. Nature 359:277-278.

Lillegraven, J. A. 1976. A new genus of therian mammal from the Late Cretaceous "El Gallo Formation," Baja California, Mexico. Journal of Paleontology 50:437-443.

Lin, Y. –H., P. J. Waddell, and D. Penny. 2002. Pika and vole mitochondrial genomes increase support for both rodent monophyly and glires. Gene 294:119-129.

Linnaeus, C. 1748. Systema Naturae sistens Regna tria Naturae, in Classes et Ordines, Genera et Species. Sixth Edition. Kiesewetteri, Stockholm, 224 pp.

Linnaeus C. 1758. Systema Naturae per Regna tria Naturae, secundum Classes, Ordines, Genera, Species, cum Characteribus, Differentiis, Synonymis, Locis. Volume 1. Tenth Edition. Laurentius Salvius, Stockholm, 376 pp.

Liu, F. –G., M. M. Miyamoto, N. P. Freire, P. Q. Ong, M. R. Tennant, T. S. Young, and K. F. Gugel. 2001. Molecular and morphological supertrees for eutherian (placental) mammals. Science 291:1786-1789.

Loughlin, T. R., M. A. Perez, R. L. Merrick. 1987. *Eumetopias jubatus*. Mammalian Species 283:1-7.

Luckett, W. P., and J. –L. Hartenberger. 1993. Monophyly or polyphyly of the order Rodentia: possible conflict between morphological and molecular interpretations. Journal of Mammalian Evolution 1:127-147.

Lundelius, E. L., Jr. and M. B. Collins. 1999. Speleological contexts of micromammal assemblages from caves and rockshelters in the Texas Hill Country: retrospects and prospects. International Union of Quaternary Research, XV International Congress Book of Abstracts :112.

Luo, Z., and E. R. Eastman. 1995. Petrosal and inner ear of a squalodontid whale: implications for the evolution of hearing in odontocetes. Journal of Vertebrate Paleontology 15:431-442.

Luo, Z., and P. D. Gingerich. 1999. Terrestrial Mesonychia to aquatic Cetacea: transformation of the basicranium and evolution of hearing in whales. University of Michigan Papers in Paleontology 31:1-98.

Luo, Z., and D. R. Ketten. 1991. CT scanning and computerized reconstructions of the inner ear of multituberculate mammals. Journal of Vertebrate Paleontology 11:220-228.

Luo, Z., and K. Marsh. 1996. Petrosal (periotic) and inner ear of a Pliocene kogiine whale (Kogiinae, Odontoceti): implications on relationships and hearing evolution of toothed whales. Journal of Vertebrate Paleontology 16:328-348.

Ma, D. –P., A. Zharkikh, D. Graur, J. L. Vandeberg, and W. –H. Li. 1993. Structure and evolution of opossum, guinea pig, and porcupine cytochrome *b* genes. Journal of Molecular Evolution 36:327-334.

MacFadden, B. J., and G. S. Morgan. 2003. New oreodont (Mammalia, Artiodactyla) from the Late Oligocene (Early Arikareean) of Florida. Bulletin of the American Museum of Natural History 279:368-396.

MacIntyre, G. T. 1972. The trisulcate petrosal pattern of mammals, pp. 275-303 in T. Dobzhansky, M. K. Hecht, and W. C. Steere (eds.), Evolutionary Biology, Vol. 6. Appleton-Century-Crofts, New York.

MacPhee, R. D. E. 1981. Auditory regions of primates and eutherian insectivores: morphology, ontogeny, and character analysis; in F. S. Szalay (ed.), Contributions to Primatology, Volume 18. S. Krager, Basel, 282 pp.

Macrini, T.E. 2004. *Monodelphis domestica*. Mamm Species 760:1-8.

Maddison, W. P., and D. R. Maddison. 2008. Mesquite: a modular system for evolutionary analysis. Version 2.5 http://mesquiteproject.org.

Madsen, O., M. Scally, C. J. Douady, D. J. Kao, R. W. DeBry, R. Adkins, H. M. Amrine, M. J. Stanhope, W. W. de Jong, M. S. Springer. 2001. Parallel adaptive radiations in two major clades of placental mammals. Nature 409:610-614.

Maisano, J. A., and O. Rieppel. 2007. The skull of the Round Island boa, *Casarea dussumieri* Schlegel, based on high-resolution X-ray computed tomography. Journal of Morphology 268:371-384.

Maisano, J. A., C. J. Bell, J. A. Gauthier, and T. Rowe. 2002. The osteoderms and palpebral in *Lanthanotus borneensis* (Squamata: Anguimorpha). Journal of Herpetology 36:678-682.

Malia, M. J., R. M. Adkins, and M. W. Allard. 2002. Molecular support for Afrotheria and the polyphyly of Lipotyphla based on analyses of the growth hormone receptor gene. Molecular Phylogenetics and Evolution 24:91-101.

Manley, G. A. 1972. A review of some current concepts of the functional evolution of the ear in terrestrial vertebrates. Evolution 26:608-621.

Manley, G. A. 2000. Cochlear mechanisms from a phylogenetic viewpoint. Proceedings of the National Academy of Sciences of the United States of America 97:11736-11743.

Manoussaki, D., E. K. Dimiriadis, and R. S. Chadwick. 2006. Cochlea's graded curvature effect on low frequency waves. Physical Review Letters 96(088701):1-4.

Manoussaki, D., R. S. Chadwick, D. R. Ketten, J. Arruda, E. K. Dimitriadis, and J. T. O'Malley. 2008. The influence of cochlear shape on low-frequency hearing. Proceedings of the National Academy of Sciences of the United States of America 105:6162-6166.

Martins, E. P. 1999. Estimation of ancestral states of continuous characters: a computer simulation study. Systematic Biology 48:642-650.

McBee, K., and R. J. Baker. 1982. *Dasypus novemcinctus*. Mamm Spec 162:1-9.

McCrady, E., Jr. 1938. The embryology of the opossum. American Anatomical Memoirs Number 16, 228 p.

McKenna, M. C. 1975. Toward a phylogenetic classification of the Mammalia; pp. 21-46 in W. P. Luckett, and F. S. Szalay (eds.), Phylogeny of the Primates, Plenum Publishing Company, New York.

McKenna, M. C. 1992. The alpha crystalline A chain of the eye lens and mammalian phylogeny. Annales Zoologici Fennici 28:349-360.

McKenna, M. C., and S. K. Bell. 1997. Classification of Mammals. Columbia University Press, New York, 631 pp.

McKenna, M. C., Z. Kielan-Jaworowska, and J. Meng. 2000. Earliest eutherian mammal skull, from the Late Cretaceous (Coniacian) of Uzbekistan. Acta Palaeontologica Polonica 41:1-54.

McLaren, I. A. 1960. Are the Pinnipedia biphyletic? Systematic Zoology 9:18-28.

Meade, G. E. 1961. The saber-toothed cat, *Dinobastis serus*. Bulletin of the Texas Memorial Museum 2:27-60.

Meng, J. 2004. Phylogeny and divergence of basal Glires. Bulletin of the American Museum of Natural History 285:93-109.

Meng, J., and R. C. Fox. 1995. Osseous inner ear structures and hearing in early marsupials and placentals. Zoological Journal of the Linnean Society 115:47-71.

Meng, J. and A. R. Wyss. 1995. Monotreme affinities and low-frequency hearing suggested by multituberculate ear. Nature 377:141-144.

Meng, J, and A. R. Wyss. 2001. The morphology of *Tribosphenomys* (Rodentiaformes, Mammalia): phylogenetic implications for basal Glires. Journal of Mammalian Evolution 8:1-71.

Meng, J., and A. R. Wyss. 2005. Glires (Lagomorpha, Rodentia); pp. 145-158 in K. D. Rose, and J. D. Archibald (eds.), The Rise of Placental Mammals: Origins and Relationships of the Major Extant Clades. The Johns Hopkins University Press, Baltimore.

Meng, J., Y. Hu, and C. Li. 2003. The osteology of *Rhombomylus* (Mammalia, Glires): implications for phylogeny and evolution of Glires. Bulletin of the American Museum of Natural History 275:1-247.

Mercury Computer Systems. 2003. Amira 3.1. Konrad-Zuse-Zentrum für Infromationstechnik, Berlin.

Mess, A., and A. M. Carter. 2006. Evolutionary transformations of fetal membrane characters in Eutheria with special reference to Afrotheria. Journal of Experimental Zoology (Moleular Development and Evolution) 306B:140-163.

Miao, D. 1988. Skull morphology of Lambdopsalis bulla (Mammalia, Multituberculata) and its implications to mammalian evolution. Contributions to Geology, University of Wyoming Special Paper 4:1-104.

Miller, M. R. 1966a. The cochlear duct of lizards. Proceedings of the California Academy of Sciences 33:255-359.

Miller, M. R. 1966b. The cochlear ducts of *Lanthanotus* and *Anelytropsis* with remarks on the familial relationship between *Anelytropsis* and *Dibamus*. Occasional Papers of the California Academy of Sciences 60:1-15.

Miller, M. R. 1968. The cochlear duct of snakes. Proceedings of the California Academy of Sciences 35:425-475.

Misawa, K., and A. Janke. 2003. Revisiting the Glires concept – phylogenetic analysis of nuclear sequences. Molecular Phylogenetics and Evolution 28:320-327.

Miyamoto, M. M., and M. Goodman. 1986. Biomolecular systematics of eutherian mammals: phylogenetic patterns and classification. Systematic Zoology 35:230-240.

Moody, P. A., V. A. Cochran, H. Drugg H. 1949. Serological evidence on lagomorph relationships. Evolution 3:25-33.

Morsli, H., D. Choo, A. Ryan, R. Johnson, and D. K. Wu. 1998. Development of the mouse inner ear and origin of its sensory organs. Journal of Neuroscience 18:3327-3335.

Mouchaty, S. K., A. Gullber, A. Janke, and U. Arnason. 2000. Phylogenetic position of the tenrecs (Mammalia: Tenrecidae) of Madagascar based on analysis of the complete mitochondrial genome sequence of *Echinops telfairi*. Zoologica Scripta 29:307-317.

Murata, Y., M. Nikaido, T. Sasaki, Y. Cao, Y. Fukumoto, M. Hasegawa, N. Okada. 2003. Afrotherian phylogeny as inferred from complete mitochondrial genomes. Molecular Phylogenetics and Evolution 28:253-260.

Muren, C., G. Ruhn, and H. Wilbrand. 1986. Anatomic variations of the human semicircular canals: a radioanatomic investigation. Acta Radiologica Diagnosis 27:157-163.

Murphy, W. J., E. Eizirik, W. E. Johnson, Y. P. Zhang, O. A. Ryder, S. J. O'Brien. 2001a. Molecular phylogenetics and the origins of placental mammals. Nature 409:614-617.

Murphy, W. J., E. Eizirik, S. J. O'Brien, O. Madsen, M. Scally, C. J. Douady, E. Teeling, O. A. Ryder, M. J. Stanhope, W. W. de Jong, M. S. Springer. 2001b. Resolution of the early placental mammal radiation using Bayesian phylogenetics. Science 294:2348-2351.

Naylor, G. J. P., and D. C. Adams. 2001. Are the fossil data really at odds with the molecular data? Morphological evidence for cetartiodactyla phylogeny reexamined. Systematic Biology 50:444-453.

Nessov, L. A. 1985. [New mammals from the Cretaceous of Kyzylkum]. Vestnik Leningradskogo Universiteta 17:8-18. [Russian]

Nessov, L. A. 1993. [New Mesozoic mammals of middle Asia and Kazakhstan, and comments about evolution of theriofaunas of Cretaceous coastal plains of ancient Asia]. Trudy Zoologicheskogo Instituta 249:105-133. [Russian 105-132; English 132-133]

Nessov, L. A., J. D. Archibald, and Z. Kielan-Jaworowska. 1998. Ungulate-like mammals from the Late Cretaceous of Uzbekistan and a phylogenetic analysis of Ungulatomorpha. Bulletin of Carnegie Museum of Natural History 34:40-88.

Nikaido, M., Y. Cao, M. Harada, N. Okada, and M. Hasegawa. 2003. Mitochondrial phylogeny of hedgehogs and monophyly of Eulipotyphla. Molecular Phylogenetics and Evolution 28:276-284.

Nilsson, M. A., A. Gullberg, A. E. Spotorno, U. Arnason, and A. Janke. 2003. Radiation of extant marsupials after the K/T boundary: evidence from complete mitochondrial genomes. Journal of Molecular Evolution 57:3-12.

Norman, J. E., and M. V. Ashley. 2000. Phylogenetics of Perissodactyla and tests of the molecular clock. Journal of Molecular Evolution 50:11-21.

Norris, C. A. 1994. The periotic bones of possums and cuscuses: cuscus polyphyly and the division of the marsupial family Phalangeridae. Zoological Journal of the Linnean Society 111:73-98.

Novacek, M. J. 1977. Aspects of the problem of variation, origin and evolution of the eutherian auditory bulla. Mammal Review 7:131-150.

Novacek, M. J. 1986. The skull of leptictid insectivorans and the higher-level classification of eutherian mammals. Bulletin of the American Museum of Natural History 183:1—111.

Novacek, M. J. 1992a. Fossils, topologies, missing data, and the higher level phylogeny of eutherian mammals. Systematic Biology 41:58-73.

Novacek, M. J. 1992b. Mammalian phylogeny: shaking the tree. Nature 356:121-125.

Novacek, M. J. 1993. Reflections on higher mammalian phylogenetics. Journal of Mammalian Evolution 1:3-30.

Novacek, M. J. and A. Wyss. 1986a. Origin and transformation of the mammalian stapes. Contributions to Geology, University of Wyoming, Special Paper 3:35-53.

Novacek, M. J. and A. Wyss. 1986b. Higher-level relationships of the Recent eutherian orders: morphological evidence. Cladistics 2:257-287.

Novacek, M. J., A. R. Wyss AR, M. C. McKenna. 1988. The major groups of eutherian mammals; pp. 31-71 in M. J. Benton MJ (ed.), The Phylogeny and Classification of the Tetrapods, Volume 2: Mammals. Clarendon Press, Oxford.

Ogden, C. L., C. D. Fryar, M. D. Carroll, and K. M. Flegal. 2004. Mean body weight, height, and body mass index, United States 1960-2002. Advance Data from Vital and Health Statistics; no 347. Hyattsville, Maryland. 20 p.

O'Leary, M. A. 1999. Parsimony analysis of total evidence from extinct and extant taxa and the cetacean-artiodactyl question (Mammalia, Ungulata). Cladistics 15:315-330.

O'Leary, M. A, and J. H. Geisler. 1999. The position of Cetacea within Mammalia: phylogenetic analysis of morphological data from extinct and extant taxa. Systematic Biology 48:455-490.

O'Leary, M. A, and M. D. Uhen. 1999. The time of origin of whales and the role of behavioral changes in the terrestrial-aquatic transition. Paleobiology 25:534-556.

Owen, R. 1848. Description of teeth and portions of jaws of two extinct anthracotheroid quadrupeds (*Hyopotamus vectianu* and *Hyop. bovinus*) discovered by the Marchioness of Hastings in the Eocene deposits on the N.W. coast of the Isle of Wight: with an attempt to develop Cuvier's idea of the classification of pachyderms by the number of their toes. Quarterly Journal of the Geolological Society 4:103-141.

Olson, E. C. 1944. Origin of mammals based upon cranial morphology of the therapsid suborders. Geological Society of America Special Papers 55: 1-136.

Payne, K. B., W. R. Langbauer, and E. M. Thomas. 1986. Infrasonic calls of the Asian elephant (Elephas maximus). Behavioral Ecology and Sociology 18:297-301.

Pol, C., A. D. Buscalioni, J. Carballeira, V. Francés, N. L. Martinez, B. Marandat, J. J. Moratalla, J. L. Sanz, B. Sigé, and J. Villatte. 1992. Reptiles and mammals from the Late Cretaceous new locality Quintanilla del Coco (Burgos Province, Spain). Neues Jahrbuch für Geologie und Paläontologie, Abhandlungen 184:279-314.

Poole, J. H., K. B. Payne, W. R. Langbauer, and C. J. Mos. 1988. Social contexts of some very low frequency calls of African elephants. Behavioral Ecology and Sociobiology 22:385-392.

Porter, C. A., M. Goodman, and M. J. Stanhope. 1996. Evidence on mammalian phylogeny from sequences of Exon 28 of the von Willebrand Factor gene. Molecular Phylogenetics and Evolution 5:89-101.

Poux, C., and E. J. P. Douzery. 2004. Primate phylogeny, evolutionary rate variations, and divergence times: a contribution from the nuclear gene IRBP. American Journal of Physical Anthropology 124:1-16.

Prothero, D. R., and R. J. Emry. 2004. The Chadronian, Orellan, and Whitneyan North American land mammal ages; pp. 156-168 in M. O. Woodburne (ed.), Late Cretaceous and Cenozoic Mammals of North America: Biostratigraphy and Geochronology. Columbia University Press, New York.

Quiroga, J. C. 1979. The inner ear of two cynodonts (Reptilia – Therapsida) and some comments on the evolution of the inner ear from pelycosaurs to mammals. Gegenbauers Morphologisches Jahrbuch 2:178-190.

Radinsky, L. B. 1964. *Paleomoropus*, a new Early Eocene chalicothere (Mammalia, Perissodactyla), and a revision of Eocene chalicotheres. American Museum Novitates 2179:1-28.

Ramprashad, F., J. P. Landolt, K. E. Money, D. Clark, AND J. Laufer. 1979. A morphometric study of the cochlea of the little brown bat (*Myotis lucifugus*). Journal of Morphology 160:345-358.

Rasmussen, D. T., M. Gagnon M, and E. L. Simons EL. 1990. Taxepody in the carpus and tarsus of Oligocene Pliohyracidae (Mammalia: Hyracoidea) and the phyletic position of hyraxes. Proceedings of the Nationall Academy of Sciences of the United States of America 87:4688-4691.

Raup, D. M., and J. J. Sepkoski, Jr. 1982. Mass extinctions in the marine fossil record. Science 215:1501-1503.

Reeder, D. M., K. M. Helen KM, and D. E. Wilson. 2007. Global trends and biases in new mammal species discoveries. Occasional Papers, Museum of Texas Tech University 269:1-35.

Reimer, K. 1996. Ontogeny of hearing in the marsupial, *Monodelphis domestica*, as revealed by brainstem auditory evoked potentials. Hearing Research 92:143-150.

Retzius, G. 1884. Das Gehörorgan der Wirbelthiere: morphologisch-histologische studien. II. Das Gehörorgan der Reptilien, der Vögel und der Säugethiere. Samson and Wallin, Stockholm, 368 pp.

Rogers, S. W. 1998. Exploring dinosaur neuropaleobiology: computed tomography scanning and analysis of an *Allosaurus fragilis* endocast. Neuron 21:673-679.

Rogers, S. W. 1999. *Allosaurus*, crocodiles, and birds: evolutionary clues from spiral computed tomography of an endocast. Anatomical Record Part B – New Anatomist 257:162-173.

Rose, K. D., R. J. Emry, T. J. Gaudin, and G. Storch. 2005. Xenarthra and Pholidota; pp. 106-126 in K. D. Rose, and J. D. Archibald (eds.), The rise of placental mammals: origins and relationships of the major extant clades. The Johns Hopkins University Press, Baltimore.

Rougier, G. W., J. R. Wible, and M. J. Novacel. 1998. Implications of *Deltatheridium* specimens for early marsupial history. Nature 396:459-463.

Rowe, T. 1986. Osteological diagnosis of Mammalia, L. 1758, and its relationship to extinct Synapsida. Ph.D. dissertation, University of California, Berkeley, CA, 446 pp.

Rowe, T. 1988. Definition, diagnosis, and origin of Mammalia. Journal of Vertebrate Paleontology 8:241-264.

Rowe, T. 1996. Coevolution of the mammalian middle ear and neocortex. Science 273:651-654.

Rowe, T. 1997. Response to "Comparative rates of development in *Monodelphis* and *Didelphis*. Science 275:684.

Rowe, T., W. Carlson, and W. Bottorf. 1995. *Thrinaxodon*: Digital atlas of the skull. CD-ROM (Second Edition for Windows and Macintosh platforms). University of Texas Press, Austin.

Rowe, T., J. Kappelman, W. D. Carlson, R. A. Ketcham, and C. Denison. 1997. High-resolution computed tomography: a breakthrough technology for earth scientists. Geotimes 42:23-27.

Ruf, I., Z. –X. Luo, J. R. Wible, and T. Martin. 2009. Petrosal anatomy and inner ear structures of the Late Jurassic *Henkelotherium* (Mammalia, Cladotheria, Dryolestoidea): insight into the early evolution of the ear region in cladotherian mammals. Journal of Anatomy 214:679-693.

Ryals, B. M., H. B. Creech, and E. W. Rubel. 1984. Postnatal changes in the size of the avian cochlear duct. Acta Otolaryngolica 98:93-97.

Sánchez-Villagra, M. R., and T. Schmelzle. 2007. Anatomy and development of the bony inner ear in the woolly opossum, Caluromys philander (Didelphimorphia, Marsupialia). Mastozoología Neotropical 14:53-60.

Sánchez-Villagra, M. R., Y. Narita, and S. Kuratani. 2007. Thoracolumbar vertebral number: the first skeletal synapomorphy for afrotherian mammals. Systematics Biodiversity 5:1-7.

Sanderson, M. J., A. Purvis, and C. Henze. 1998. Phylogenetic supertrees: assembling the trees of life. Trends in Ecology and Evolution 13:105-109.

Saunders, J. J. 1977. Late Pleistocene vertebrates of the Western Ozark Highland, Missouri. Illinois State Museum Reports of Investigations 33:1-118.

Schmidt, R. S. 1964. Phylogenetic significance of lizard cochlea. Copeia 1964:542-549.

Schmitz, J., and H. Zischler. 2003. A novel family of tRNA-derived SINEs in the colugo and two new retrotransposable markers separating dermopteras from primates. Molecular Phylogenetics and Evolution 28:341-349.

Schmitz, J., M. Ohme, B. Suryobroto, and H. Zischler. 2002. The colugo (*Cynocephalus variegates*, Dermoptera): the primates' gliding sister? Molecular Biology and Evolution 19:2308-2312.

Schuknecht, H. F. 1953. Techniques for study of cochlear function and pathology in experimental animals. Archives of Otolaryngology 58:377-397.

Segall, W. 1970. Morphological parallelisms of the bulla and auditory ossicles in some insectivores and marsupials. Fieldiana Zoology 51:169-205.

Seiffert, E. R. 2007. A new estimate of afrotherian phylogeny based on simultaneous analysis of genomic, morphological, and fossil evidence. BMC Evolutionary Biology 7(224):1-13.

Sheehan, P. M. and D. E. Fastovsky. 1992. Major extinctions of land-dwelling vertebrates at the Cretaceous-Tertiary boundary, eastern Montana. Geology 20:556-560.

Shoshani, J. 1986. Mammalian phylogeny: comparison of morphological and molecular results. Molecular Biology and Evolution 3:222-242.

Shoshani, J., M. C. McKenna M. 1998. Higher taxonomic relationships among extant mammals based on morphology, with selected comparisons of results from molecular data. Molecular Phylogenetics and Evolution 9:572-584.

Shoshani, J., C. P. Groves, E. L. Simons, and G. F. Gunnell. 1996. Primate phylogeny: morphological vs molecular results. Molecular Phylogenetics and Evolution 5:102-154.

Shubin, N. H., E. B. Daeschler, and M. I. Coates. 2004. The early evolution of the tetrapod humerus. Science 304:90-93.

Shute, C. C. D., and A. D'A. Bellairs. 1953. The cochlear apparatus of Geckonidae and Pygopodidae and its bearing on the affinities of these groups of lizards. Proceedings of the Zoological Society of Lond 123:695-709.

Silcox, M. T., J. I. Bloch, E. J. Sargis, D. M. Boyer. 2005. Euarchonta (Dermoptera, Scandentia, Primates); pp. 127-144 in K. D. Rose, and J. D. Archibald (eds.), The Rise of Placental Mammals: Origins and Relationships of the Major Extant Clades. The Johns Hopkins University Press, Baltimore.

Silva, M., and J. A. Downing. 1995. CRC Handbook of Mammalian Body Masses. CRC Press, Boca Raton, Florida, 359 pp.

Simmons, J. A., M. B. Fenton, and M. J. O'Farrell. 1979. Echolocation and pursuit of prey by bats. Science 203:16-21.

Simmons, N. B., K. L. Seymour, J. Habersetzer, and G. F. Gunnell. 2008. Primitive Early Eocene bat from Wyoming and the evolution of flight and echolocation. Nature 451:818-821.

Simpson, G. G. 1945. The principles of classification and a classification of mammals. Bulletin of the American Museum of Natural History 84:1-350.

Sisson, S. and J. D. Grossman. 1938. The Anatomy of the Domestic Animals (third edition, revised). W. B. Saunders Company, Philadelphia, 972 pp.

Solntseva, G. N. 2007. Morphology of the Auditory and Vestibular Organs in Mammals, with Emphasis on Marine Species. Pensoft and Brill, Sofia, 244 pp.

Spoor, F. and F. Zonneveld. 1995. Morphometry of the primate bony labyrinth: a new method based on high-resolution computed tomography. Journal of Anatomy 186:271-286.

Spoor, F., and F. Zonneveld. 1998. Comparative review of the human bony labyrinth. Yearbook of Physical Anthropology 41:211-251.

Spoor, F., B. Wood, and F. Zonneveld. 1994. Implications of early hominid labyrinthine morphology for evolution of human bipedal locomotion. Nature 369:645-648.

Spoor, F., B. Wood, and F. Zonneveld. 1996. Evidence for a link between human semicircular canal size and bipedal behaviour. Journal of Human Evolution 30:183-187.

Spoor, F., S. Bajpai, S. T. Hussain, K. Kumar, and J. G. M. Thewissen. 2002. Vestibular evidence for the evolution of aquatic behavior in early cetaceans. Nature 417:163-166.

Spoor, F., T. Garland, Jr., G. Krovitz, T. M. Ryan, M. T. Silcox, and A. Walker. 2007. The primate semicircular canal system and locomotion. Proceedings of the National Academy of Sciences of the United States of America 104:10808-10812.

Springer, M. S., H. M. Amrine, A. Burk, M. J. Stanhope. 1999. Additional support for Afrotheria and Paenungulata, the performance of mitochondrial versus nuclear genes, and the impact of data partitions with heterogeneous base composition. Systematic Biology 48:65-75.

Springer, M. S., W. J. Murphy, E. Eizirik, S. J. O'Brien. 2003. Placental mammal diversification and the Cretaceous-Tertiary boundary. Proceedings of the National Academy Sciences 100:1056-1061.

Springer, M. S., G. C. Cleven, O. Madsen, W. W. de Jong, V. G. Waddell, H. M. Amrine, and M. J. Stanhope. 1997. Endemic African mammals shake the phylogenetic tree. Nature 388:61-64.

Springer, M. S., M. Westerman, J. R. Kavanagh, A. Burk, M. O. Woodburne, D. J. Kao, and C. Krajewski. 1998. The origin of the Australasian marsupial fauna and the phylogenetic affinities of the enigmatic monito del monte and marsupial mole. Proceedings of the Royal Society of London B 265:2381-2386.

Staněk, V. J. 1933. K topografické a srovnávací anatomii sluchového orgánu našich chiropter. Nákladem České Akademie věd a Umění, Praze (Prague), 67 pp.

Stanhope, M. J., J. Czelusniak, J. –S. Si, J. Nickerson, and M. Goodman M. 1992. A molecular perspective on mammalian evolution from the gene encoding interphotoreceptor retinoid binding protein, with convincing evidence for bat monophyly. Molecular Phylogenetics and Evolution 1:148-160.

Stanhope, M. J., V. G. Waddell, O. Madsen, W. de Jong, S. B. Hedges, G. C. Cleven, D. Kao, and M. S. Springer. 1998. Molecular evidence for multiple origins of Insectivora and for a new order of endemic African insectivore mammals. Proceedings of the National Academy of Sciences of the United States of America 95:9967-9972.

Tedford, R. H. 1976. Relationship of pinnipeds to other carnivores (Mammalia). Systematic Zoology 25:363-374.

Teeling, E. C., M. Scally, D. J. Kao, M. L. Romagnoll, M. S. Springer, and M. J. Stanhope. 2000. Molecular evidence regarding the origin of echolocation and flight in bats. Nature 403:188-192.

Teeling, E. C., M. S. Springer, O. Madsen, P. Bates, S. J. O'Brien, and W. J. Murphy. 2005. A molecular phylogeny for bats illuminates biogeography and the fossil record. Science 307:580-584.

Theodor, J. M, and S. E. Foss SE. 2005. Deciduous dentitions of Eocene cebochoerid artiodactyls and cetartiodactyl relationships. Journal of Mammalian Evolution 12:161-181.

Theodor, J. M., K. D. Rose, and J. Erfurt. 2005 Artiodactyla; pp. 215-233 in K. D. Rose, and J. D. Archibald (eds.), The Rise of Placental Mammals: Origins and Relationships of the Major Extant Clades. The Johns Hopkins University Press, Baltimore.

Thewissen, J. G. M., and S. I. Madar. 1999. Ankle morphology of the earliest cetaceans and its implications for the phylogenetic relations among ungulates. Systematic Biology 48:21-30.

Thewissen, J. G. M., E. M. Williams, L. J. Roe, and S. T. Hussain ST. 2001. Skeletons of terrestrial cetaceans and the relationship of whales to artiodactyls. Nature 413:277-281.

Tomasi, T. E. 1979. Echolocation by the short-tailed shrew *Blarina brevicauda*. Journal Mammal 60:751-759.

Tykoski, R. S. 2005. Anatomy, ontogeny, and phylogeny of coelophysoid theropods. Unpublished Ph.D. Dissertation, The University of Texas at Austin, 572 pp.

Tykoski, R. S., T. B. Rowe, R. A. Ketcham, and M. W. Colbert. 2002. *Calsoyasuchus valliceps*, a new crocodyliform from the Early Jurassic Kayenta Formation of Arizona. Journal of Vertebrate Paleontology 22:593-611.

Tomasi, T. E. 1979. Echolocation by the short-tailed shrew Blarina brevicauda. Journal of Mammalogy 60:751-759.

Ursing, B. M., and U. Arnason. 1998. Analyses of mitochondrial genomes strongly support a hippopotamus-whale clade. Proceedings of the Royal Society of London B 265:2251-2255.

Vaughn, T. A., J. M. Ryan, and N. J. Czaplewski. 2000. Mammalogy, Fourth Edition. Saunders College, Philadelphia, 565 pp.

van der Klaauw, C. J. 1931. The auditory bulla in some fossil mammals: with a general introduction to this region of the skull. Bulletin of the American Museum of Natural History 67:1-352.

van Dijk, M. A. M., O. Madsen, F. Catzeflis, M. J. Stanhope, W. W. de Jong, and M. Pagel. 2001. Protein sequence signatures support the African clade of mammals. Proceedings of the National Academy of Sciences 98:188-193.

Van Kampen, P. N. 1904. De Tympanaalstreek van den Zoogdierschedel. P. N. Van Kampen and Zoon, Amsterdam, 378 pp.

Van Valen, L. 1965. Treeshrews, primates, and fossils. Evolution 19:137-151.

Van Valen, L. 1971. Adaptive zones and the orders of mammals. Evolution 25:420-428.

Volume Graphics. 2004. VGStudio Max 1.2. Heidelberg, Germany.

Waddell, P. J., N. Okada, M. Hasegawa. 1999. Towards resolving the interordinal relationships of placental mammals. Systematic Biology 48:1-5.

Wang, Z., G. B. Hubbard, S. Pathak, and J. L. VandeBerg. 2003. *In vivo* opossum xenograft maodel for cancer research. Cancer Research 63:6121-6124.

Watson, M. 1874. Contributions to the anatomy of the Indian elephant, Part IV. Muscles and blood-vessels of the face and head. Journal of Anatomy and Physiology 9:118-133.

West, C. D. 1985. The relationship of the spiral turns of the cochlea and the length of the basilar membrane to the range of audible frequencies in ground dwelling mammals. Journal of the Acoustical Society of America 77:1091-1101.

Wever, E. G., J. G. McCormick, J. Palin, and S. H. Ridgway. 1971a. The cochlea of the dolphin, *Tursiops truncatus*: general morphology. Proceedings of the National Academy of Sciences, USA 68:2381-2385.

Wever, E. G., J. G. McCormick, J. Palin, and S. H. Ridgway. 1971b. Cochlea of the dolphin, *Tursiops truncatus*: the basilar membrane. Proceedings of the National Academy of Sciences, USA 68:2708-2711.

Wible, J. R. 1987. The eutherian stapedial artery: character analysis and implications for superordinal relationships. Zoological Journal of the Linnean Society 91:107-135.

Wible, J. R. 1990. Petrosals of Late Cretaceous marsupials from North America, and a cladistic analysis of the petrosal in therian mammals. Journal of Vertebrate Paleontology 10:183-205.

Wible, J. R. 2003. On the cranial osteology of the short-tailed opossum *Monodelphis brevicaudata* (Didelphidae, Marsupialia). Annals of the Carnegie Museum 72:137-202.

Wible, J. R. and D. L. Davis. 2000. Ontogeny of the chiropteran basicranium, with reference to the Indian false vampire bat, *Megaderma lyra*, pp. 214-246 in R. A.

Adams, S. C. Pedersen (eds.), Ontogeny, Functional Ecology, and Evolution of Bats. Cambridge University Press, Cambridge.

Wible, J. R. and J. R. Martin. 1993. Ontogeny of the tympanic floor and roof in archontans, pp. 111-148 in R. D. E. MacPhee (ed.), Primates and Their Relatives in Phylogenetic Perspective. Plenum Press, New York.

Wible, J. R. and M. J. Novacek. 1988. Cranial evidence for the monophyletic origin of bats. American Museum Novitates, Number 2911:1-19.

Wible, J. R., M. J. Novacek, and G. W. Rougier. 2004. New data on the skull and dentition in the Mongolian Late Cretaceous eutherian mammal *Zalambdalestes*. Bulletin of the American Museum of Natural History 281:1-144.

Wible, J. R., G. W. Rougier, and M. J. Novacek. 2005. Anatomical evidence for superordinal eutherian taxa in the Cretaceous, pp. 15-36 in K. D. Rose and J. D. Archibald (eds.), The Rise of Placental Mammals: Origins and Relationships of the Major Extant Clades. Johns Hopkins University Press, Baltimore.

Wible, J. R., G. W. Rougier, M. J. Novacek, and R. J. Asher. 2007. Cretaceous eutherians and Laurasian origin for placental mammals near the K/T boundary. Nature 447:1003-1006.

Wible, J. R., G. W. Rougier, M. J. Novacek, and M. C. McKenna. 2001. Earliest eutherian ear region: a petrosal referred to *Prokennalestes* from the Early Cretaceous of Mongolia. American Museum Novitates 3322:1-44.

Wiens, J. J., R. M. Bonett, and P. T. Chippindale. 2005. Ontogeny discombobulates phylogeny: paedomorphosis and higher-level salamander relationships. Systematic Biology 54:91-110.

Wilson, D. E., D. M. Reeder. 2005. Mammal Species of the World: A Taxonomic and Geographic Reference (Third Edition). The Johns Hopkins University Press, Baltimore, 2142 pp.

Wilson, J. A. 1971. Early Tertiary vertebrate faunas, Vieja Group, Trans-Pecos Texas: Agrichoeridae and Merycoidontidae. Bulletin of the Texas Memorial Museum 18:1-83.

Witmer, L. M., S. Chatterjee, J. Franzosa, and T. Rowe. 2003. Neuroanatomy of flying reptiles and implications for flight, posture and behaviour. Nature 425:950-953.

Wood, A. E. 1957. What, if anything, is a rabbit? Evolution 11:417-425.

Wood, A. E. 1962. The Early Tertiary rodents of the family Paramyidae. Transactions of the American Philosophical Society 52:3-261.

Wyss, A. R. 1987. The walrus auditory region and the monophyly of pinnipeds. American Museum Novitates 2871:1-7.

Yang, A. and T. E. Hullar. 2007. Relationship of semicircular canal size to vestibular-nerve afferent sensitivity in mammals. Journal of Neurophysiology 98:3197-3205.

Vita

Eric Gregory Ekdale was born in Salt Lake City, UT. He attended Judge Memorial Catholic High School, and he graduated in 1995. He matriculated at Augustana College in Rock Island, IL, and he received a Bachelor of Arts degree in Biology and Scandinavian Studies (separate majors) in the spring of 1999. During his education at Augustana College, he also enrolled in summer courses at the University of Utah in Salt Lake City, UT, but no degree was conferred from that institution. In the fall of 1999, he attended classes at San Diego State University in San Diego, CA, where he earned a Masters of Science degree in Biology (with an emphasis in Systematics, Evolutionary and Organismal Biology) in May 2002. He entered the graduate school at The University of Texas at Austin in 2002, where he immediately began work towards a Doctor of Philosophy degree in Geological Sciences. During his time at The University of Texas, Eric presented at the annual meetings of the Society of Vertebrate Paleontology and Texas Academy of Sciences, almost on a yearly basis. During the 2008-2009 academic year, he was awarded the Hogg Fellowship from The University of Texas at Austin. The Hogg Fellowship is one of the highest honors awarded by the university to graduates students.

Permanent address: 3816 South Lamar Blvd, Apt. #1804, Austin, TX 78704

This dissertation was typed by the author.